FINAL REPORT

Project Title: S1 Measurement of Bridge - Vehicle Interaction Under Live Load (2013/14 - 2015/16)

Project No: 010571

Author/s: Torill Pape

Client: Queensland Department of Transport and Main Roads

Date: September 2016

AN INITIATIVE BY:

SUMMARY

The Queensland Department of Transport and Main Roads (TMR) is responsible for approximately 3000 bridges and 4000 major culverts, with a gross replacement asset value in excess of $11 billion. Of this number, there are several bridges that are subject to load and permit restrictions, with estimated costs to upgrade or maintain these structures in the order of $120 million.

In the assessment of these structures, the dynamic effects on bridge components due to dynamic vehicle loading remains a key consideration. To account for the amplification of dynamic wheel loads imposed on a structure due to the passage of vehicles, the application of numerous published and codified load factors is required, to ensure that acceptable factors of safety are maintained. This is particularly important where assessments indicate that maintenance and strengthening of structures may be required and funding is limited. One such factor is the dynamic load allowance (DLA), as specified in the AS 5100 Bridge Design Code. Current codes adopted by TMR in its Tier 1 bridge assessment guidelines specify a generic and constant DLA factor of 0.4 to be applied, regardless of vehicle, structure or component type. However, TMR is looking to develop an improved understanding of a family of bridges for higher-order bridge assessments when adopting DLA factors, accounting for various vehicle and structure types and dynamic influences. In particular, TMR is investigating whether the DLA can be reduced for substructure components in assessments.

To investigate this hypothesis, load testing of three representative bridges of different substructure types was conducted with a focus on investigating interactions between vehicles and bridges, and the degree of variance that occurs with different parameters such as structure type, road profile conditions, vehicle and suspension type. The determination and comparison of dynamic increments were compared for superstructure and substructure components, which is unique, and there has been limited information published or documented in relation to this aspect.

The research highlighted that substructure components (such as headstocks and columns) were more likely to yield dynamic increments equal to or greater than superstructure components (e.g. girders). The degree of variation between components was dependent on vehicle type, suspension characteristics, as well as speed and direction of travel and the transverse location of the test vehicle. The inherent frequency responses of the bridge and the vehicle were both influential in the response of each bridge to controlled loads, as was the condition of the road profile leading up to the bridge. Evidence of frequency matching between vehicles, superstructure and substructure components was noted.

Dynamic increments varied in magnitude. On average, all values determined for the superstructure were less than 0.4, with approximately than 5% of outliers. An increased percentage of DI values exceeded 0.4 for substructure components, with some values approaching or exceeding 1.0 in critical cases. The determination of dynamic increments was subjected to a sensitivity review, and the process was found to be sensitive to the selection of components to determine values, with questions raised about the objectivity of the current process.

If certain network, analysis and structural condition caveats are met, the current research supports consideration for the reduction of DLA factor for superstructure components under operational network conditions. This is in keeping with international best practice, particularly for structures where higher traffic volumes exist. However, no reduction in DLA factors for substructure components is recommended, and it is recommended that further research be conducted to verify the current results and investigate whether the value of 0.4 is appropriate, or whether higher values are required. Caution is advised where high DI values

coincide with poor component condition and theoretical limits that indicate structural deficiencies.

It is not clear to what extent the results for these structures can be extended to other similar bridges as the presence of existing defects/cracks in the substructure may influence these results. Further research would be required to determine whether the research findings should be applied to other similar structures.

CONTENTS

TABLES

FIGURES

GLOSSARY OF TERMS

AADT	Average Annual Daily Traffic
Axle-hop frequency	frequency response of truck suspension system when in motion
Body-bounce frequency	Frequency response of vibration of the truck body in motion; varies depending on vehicle and suspension type
CR1	4-axle hydro-pneumatic all-terrain crane (48 t)
CR2	4-axle steel-leaf suspension truck-mounted crane (40 t) – Dawson and Neerkol bridges only
DI	Dynamic Increment; quantifies the load amplification due to dynamic loading
DLA	Dynamic Load Amplification factor, as defined in AS 5100.2 and AS 5100.7. Applied to assessment and design calculations to account for the dynamic load effects of the vehicle
dynamic	Measured response of a component to vehicle loading at higher speeds
GML	General Mass Limits
HLP	Heavy Load Platforms
HML	Higher Mass Limits
In-service	Response of structure to normal traffic loading
IRI	International Roughness Index, used in determining roughness of a road section; measured in mm/m or m/km
NACoE	National Asset Centre of Excellence
OSOM	Over-size, over-mass vehicles
PBS	Performance-based Standards for heavy vehicles
quasi-resonance	Frequency matching between two or more structural components vibrating at the same frequency, causing increased loading
RT1	Roadtrain (steel leaf or mechanical suspension)
RT2	Roadtrain (air-bag suspension)
ST1	Semi-trailer (steel leaf or mechanical suspension) – Canal Creek Bridge only
ST2	Semi-trailer (air-bag suspension) – Canal Creek Bridge only
static	Measured response of a component to vehicle loading at crawl speeds (5 km/h or less)
Substructure	Incorporates bridge components that are placed below the bearings
Superstructure	Incorporates bridge components that are placed above the bearings
Tandem axle	Two wheel groups per axle
TMR	Queensland Department of Transport and Main Roads
Tri-axle	Three wheel groups per axle
VBI	Vehicle-Bridge Interaction model
WIM	Weigh-in-Motion data; records axle loads of in-service traffic

1 INTRODUCTION

1.1 Background

Queensland Department of Transport and Main Roads (TMR) is responsible for over 3 000 bridges and 4 000 major culverts. The gross replacement value of these structures exceeds $11 billion. A number of these bridges are subject to load and permit restrictions. The cost to upgrade or maintain these structures in order to address these limitations is in the order of $120 million.

A significant amount of national and international research has been conducted over the last few decades regarding dynamic bridge-vehicle interactions and the amplification of dynamic wheel loads on pavements and bridges, of which various Dynamic Load Allowance (DLA) factors have been identified and discussed. With the evolution of 'road-friendly' suspension-type vehicles, improved vehicle design/technology, and the move towards the introduction of performance-based standards for heavy vehicles (PBS) vehicles in recent times, the understanding of the dynamic interactions between bridges and these 'improved' vehicle types requires review.

The amplification of dynamic live loads on bridge structures due to the passage of heavy vehicles is a significant factor to be incorporated into the assessment of structurally-deficient in-service bridges. To account for such loads, the current Australian Bridge Design Code AS 5100.7 defines a DLA factor to be applied in addition to existing live load factors. It stipulates that this factor should be 0.4 for typical design and assessment vehicles. This factor is historically based on empirical dynamic load test data predominantly carried out in Ontario in the mid-1980s and subsequently adopted by the Canadian design codes (CSA S6). TMR has adopted the AS 5100.7 DLA value in its base level *Tier 1 Bridge Heavy Load Assessment Criteria* (TMR 2013). However, it is looking to strengthen its understanding of bridge-vehicle interactions leading to improved approaches for higher-order bridge assessments which account for various vehicle and structure types and dynamic influences.

Strict speed restrictions and permit requirements exist across the TMR network for certain vehicle types (particularly cranes and PBS vehicles) and for a number of at-risk structures, based on load assessments incorporating the current DLA factor. A review of the actual dynamic bridge-vehicle interactions induced by such vehicle types, and subsequent applicability of the adopted DLA factors, may result in the alleviation of travel restrictions across these structures. Specifically, an improved understanding of vehicle/bridge dynamic interactions of heavy vehicles would enable TMR to:

- make informed decisions regarding the provision of appropriate access for heavy vehicles over structures at risk of overload
- eliminate conservative restrictions on existing bridges on key routes and support increased freight movement, leading to increased productivity
- reduce or eliminate the need to undertake strengthening or replacement of bridges
- improve risk management in conjunction with health monitoring to prevent damage to bridges.

At present, only limited testing and information exists regarding the dynamic influence of newer vehicle types on bridges, particularly regarding the DLA factors that might be associated with such vehicles and particular bridge types. Furthermore, whilst detailed models have been developed nationally and internationally with respect to bridge-vehicle interactions, no predictive tools have been established to provide an estimation of anticipated DLA factors for certain vehicle-bridge combinations, a key factor in the assessment of at-risk structures. To address these challenges, a detailed program of review, testing, and numerical modelling has been commissioned. The outcomes and recommendations are contained within the current report.

1.2 Project Aims

The objective of this project was to review the dynamic interaction of bridges with the passage of heavy vehicles, particularly all-terrain cranes and road trains, and the resulting applicability of DLA factors in the structural assessment of existing bridges.

The predominant aims were to:

- investigate the dynamic effects induced in a structure due to the passage of heavy vehicles (particularly cranes and road trains)
- review the DLA factors obtained from testing and a literature review, and investigate the viability of factor reduction for certain vehicle types
- investigate the influence of heavy vehicles and dynamic interactions on substructure components
- investigate the influence of road profile on the amplification on dynamic loads
- investigate the influence of various suspension types (steel, air, pneumatic, other technologies)
- improve in-house skills and capabilities.

1.3 Project Scope

This was a three year project. The tasks conducted over the life of the project were as follows.

1.3.1 Year 1

- project scoping and literature review
- desktop study for bridge-vehicle interaction models
- development of draft vehicle instrumentation specification
- development of scope, instrumentation plan and vehicle selection for load testing
- selection of instrumentation subcontractor
- load testing – Canal Creek Bridge
- collation of historical dynamic load test data
- preparation of interim report.

1.3.2 Year 2

- development of scope, instrumentation plan and vehicle selection for loading test
- selection of instrumentation subcontractor
- load testing – Dawson River Bridge and Neerkol Creek Bridge
- preparation of interim report.

1.3.3 Year 3

- analysis, calibration, and reporting.

1.4 Overview of Report

The structure of this report is presented in Table 1.1.

Table 1.1: Report structure

Section	Title	Description
1	Introduction	
2	Literature review	
3	Test program	Details of the test program, including the bridges, vehicles, instrumentation
4	Influence of bridge characteristics	Presentation of bridge findings
5	Influence of vehicle characteristics	Presentation of vehicle findings
6	Influence of road profile	Presentation of road profile findings
7	Additional findings	Presentation of additional result observations
8	Discussion	Discussion of findings presented and presentation of recommendations
9	Conclusion	Summary of report
10	Appendices	Provision of key supporting information; inclusion of electronic data.

1.5 Supporting Project Documents

1.5.1 Previous Project Reports

The following interim reports were prepared during the course of this project:

- Year 1: Interim contract report (July 2014)
- Year 2: Measurement of bridge-vehicle dynamic interactions: Dawson River Bridge & Neerkol Creek (No. 1) Bridge load tests report (October 2015).

Relevant information from these reports has been incorporated into the current report.

1.5.2 Concurrent NACoE Projects

The following NACoE projects ran concurrent to this project and provided some relevant input:

- S2: Guidelines for monitoring of existing structures (completed 2015)
- S3: Deck unit bridge deck analysis under live load (completed 2017)
- R34: Review of in-service test for road friendly suspensions (on hold).

1.5.3 Additional Projects

The following Austroads project is also recognised:

- AT1733: Analysing dynamic wheel loads and its effects on the network.

1.6 Project Team

The planning, preparation, coordination and facilitation of the field testing was carried out by ARRB and TMR Engineering & Technology (E&T) project staff, who also provided technical input/advice as required. Instrumentation and data acquisition services were provided by SLR Consulting, engaged and managed by ARRB. RoadTek provided all site and traffic management services under instruction from TMR E&T staff, including provisions for safety, on-site power and security. Test vehicles were coordinated by ARRB and TMR and procured from a local hire company.

Data review, manipulation, analysis, interpretation and reporting were completed collaboratively between SLR Consulting, ARRB and TMR staff.

Relevant permits regarding unrestricted access for the 48 t crane to access the test bridges for the duration of the load test were obtained by TMR.

2 LITERATURE REVIEW

2.1 Background

The dynamic interaction between a moving vehicle and a supporting structure continues to facilitate strong interest in various engineering and transport sectors. Historically, research into this topic was purportedly initiated by researchers investigating the collapse of several railway bridges in Great Britain in 1849, where, after carrying out laboratory trials, it was concluded that the dynamic response of the bridges to heavy vehicles was likely to have been influential in the collapses (R Willis as cited by Cantieni (1983, p. 7)). The first documented dynamic field trial on a highway bridge is purported to have occurred on the Pont de Pontoise near Paris (Roš 1921) and Bühler (1924) as cited by Cantieni (1983, p .7)). Since that time, ongoing research has provided improved understanding of dynamic loading on structures. The predominant focus of the research has been on vehicle and superstructure dynamic interactions for transport infrastructure (for example highway and rail bridges), but in recent times this has extended to pavement, seismic, collision and geotechnical areas. For the purposes of this project, the focus of this report will be on dynamic interactions between moving heavy vehicles and road bridges.

Despite this research, the dynamic response of a bridge to vehicular loading remains complex. With the advent of increasing mass limits on bridges, increased freight movements, increasing pressure to extend the service life of existing structures, and the evolution of new vehicle designs and technology, there are still many unknowns that require quantification and further research in this area. Increased knowledge of bridge-vehicle dynamic interactions will enable asset owners to improve their understanding of the dynamic implications such live loads pose on existing structures, as well as how vehicles and structures interact dynamically to enable the development of appropriate management procedures and permit requirements (Bakht & Pinjarkar 1989; McLean & Marsh 1998).

The following literature review provides an overview of vehicle-bridge dynamic interactions and influential factors. A discussion on the historical development of national and international codes to account for dynamic loading is provided, along with a review of the methods used to quantify dynamic load effects and to compare them against codified values. A summary of recent and relevant work into bridge-vehicle interaction models is also provided.

2.1.1 Reference Literature

An extensive literature review of both historic and recent sources was conducted. All relevant citations referred to are noted in the references. A listing of the most significant or influential literature is as follows.

A number of large and detailed national and international studies have previously been conducted into dynamic bridge-vehicle interactions, which include:

- ARCHES project (and associated publications) (González et al. 2010; González, Canteno & O'Brien 2009; González 2009a; González et al. 2008; O'Brien et al. 2009; O'Brien, Li & González 2006; O'Brien; Rattigan, O'Brien & Gonzalez 2005)
- work by Szurgott et al. 2011 and Li et al. 2008
- Austroads project report AP-T23-03 (Austroads 2003) 'Dynamic Interaction of Vehicles and Bridges' and associated publications (Prem et al. 1998a; Heywood, Roberts & Boully 2001; Austroads 2002a).

Other historical research programs include:

- Swiss Federal Laboratories for Materials Testing and Research (EMPA) (Cantieni 1983, Cantieni et a. 2010).
- Ontario Ministry of Transportation and Communications (MTC) in Canada (Billing 1984; Billing & Green 1984; Billing & Agarwal 1990).
- OECD Dynamic Interaction between Vehicles and Infrastructure Experiment (DIVINE) project (Cantieni et al. 2010; Davis & Bunker 2009; Heywood et al. 2001; OECD 1999; Sweatman, Woodrooffe & McFarlane 1997).
- Dynamic loads research conducted at the University of Queensland (O'Connor & Pritchard 1985; O'Connor & Pritchard 1984; Pritchard & O'Connor 1984).

Detailed literature reviews on dynamic effects and interactions in bridges included are:

- Deng, Wang & He (2015)
- NCHRP Synthesis Report 266 "Dynamic Impact Factors for Bridges" (McLean & Marsh 1998)
- Paultre et al. (1992)
- Bakht and Pinjarkar (1989)
- work by Nowak and colleagues (Hwang & Nowak 1991; Kim & Nowak 1997; Nassif & Nowak 1995; Nowak, Kim & Szerszen).

Other relevant national studies include:

- Senthilvasan, Brameld & Thambiratnam (1997) and Senthilvasan, Thambiratnam & Brameld 2002)
- Various works by Dr Lloyd Davis (Davis 2010; Davis & Bunker 2009; Davis & Bunker 2008).

The following sections further elaborate on these topics.

2.2 Vehicle-Bridge Interactions

Bridge-vehicle dynamic interactions centres around the moving load concept, i.e. where a mass moves across a supported element and subsequent load actions are determined. To account for the load affects via dynamic interaction, both the gravitational and inertial actions relating to the mass of the moving load needs to be considered in conjunction with the mass of the supporting structure. It is widely recognised that the concept of dynamic structural response is complex and requires careful consideration in order to adequately characterise all the resulting dynamic actions and forces within the structure (McLean & Marsh 1998).

The relationship between a static and dynamic vehicle load imposed on a bridge, and the resulting dynamic interaction between them, is demonstrated graphically in Figure 2.1 for a (a) simply supported and (b) continuous structure respectively. The overall dynamic response of a structural system comprises the sum of the individual dynamic responses of its components, which can respond in various states of natural and excitation frequencies. For a bridge-vehicle interaction system, these components are the bridge, the vehicle and the condition of the road surface (leading up to and over the bridge, acting as the interfacial surface between the bridge and vehicle). The dynamic response of the structural system globally and locally and the resulting load amplification can be influenced by several factors. An extensive amount of literature exists which investigates the influences of these factors (Austroads 2003; Billing & Agarwal 1990; González

2009a; McLean & Marsh 1998; O'Connor & Pritchard 1985; Paultre et al. 1992; Li et al. 2008), and a brief summary of these findings is provided in the following sections.

Figure 2.1: Dynamic and static deflections induced in a bridge from a crossing vehicle

(a) Simply-supported span

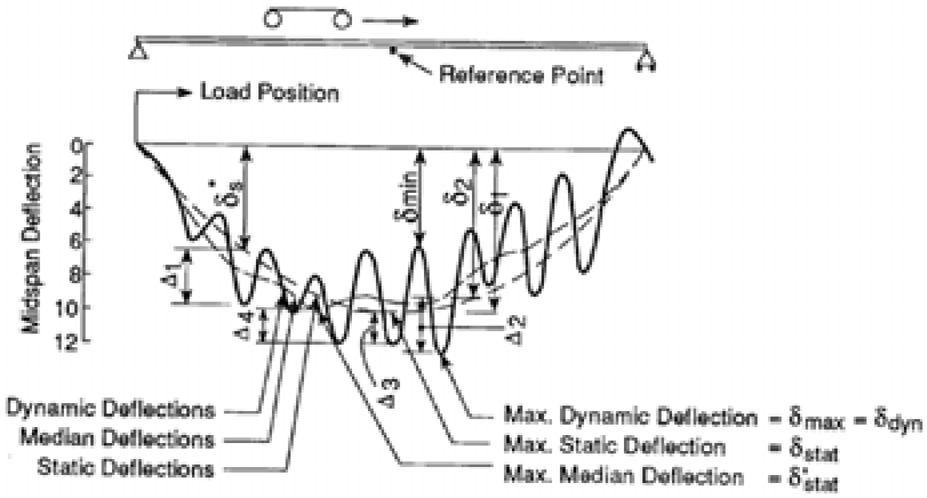

Source: Figure 1 from Bakht & Pinjarkar (1989a).

(b) Continuous spans

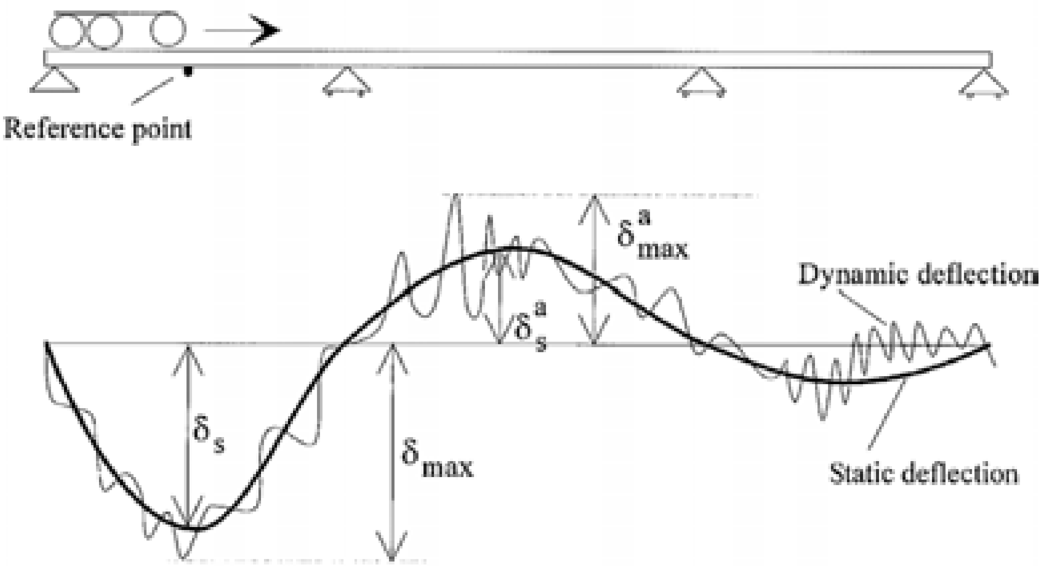

Source: Figure 7 from Senthilvasan et al. (2002).

2.2.1 Influence of Bridge Inherent Dynamic Characteristics

The extent of bridge dynamic response is dependent on factors pertaining to the geometric, material, and natural dynamic characteristics of the bridge itself. These factors and their influences are now summarised.

Natural/fundamental frequency of a bridge

- The natural frequency of a bridge is a measure of the inherent stiffness and strength. It has been shown to be related to the span length (see Figure 2.2 from Heywood (2000)).
- Typically, bridges with shorter spans have been shown to be more dynamically sensitive, with significant amplification of dynamic loads. Conversely, structures with longer spans are expected to exhibit lower dynamic amplification (González 2009a; Hwang & Nowak 1991).
- Pre-existing vibrations on bridges due to prior vehicle loading may contribute to the overall dynamic effects induced, with the possibility of frequency matching occurring (and subsequent load amplification) with following traffic (O'Brien et al. 2009; Rattigan, Gonzalez & O'Brien 2009). This is considered to be more likely to occur for longer span structures that are subject to multiple vehicle events.

Figure 2.2: Natural bridge frequency versus span length

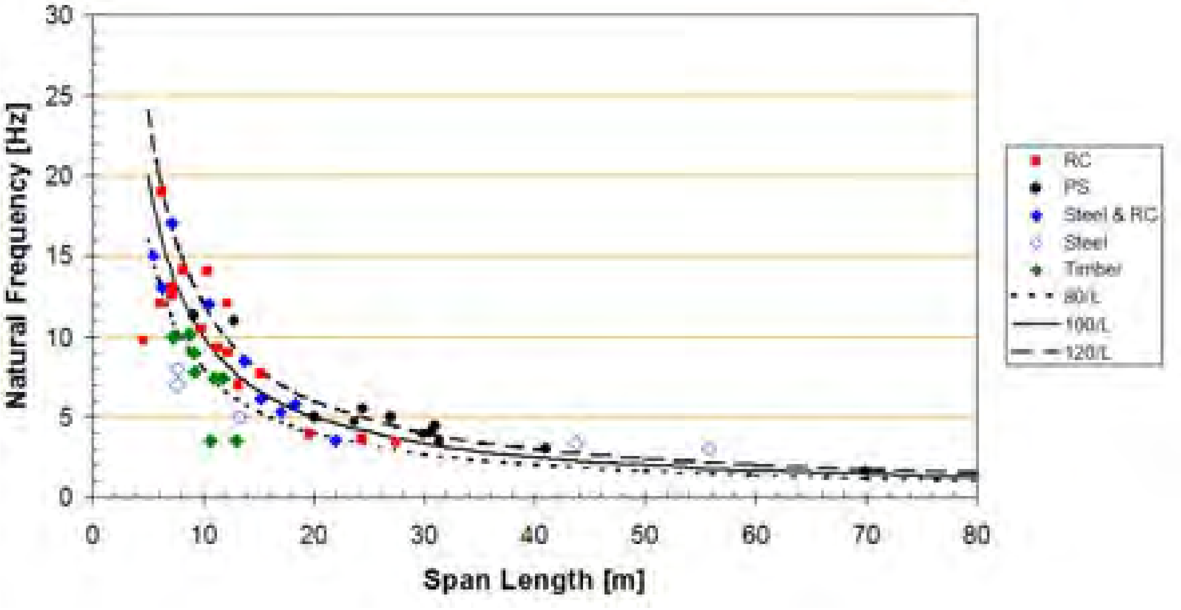

Source: Heywood (2000).

Bridge type

- Certain types of structures (such as deck/girder, box girder, prestressed concrete, slender structures) can result in greater dynamic amplification or provide greater damping characteristics (Cantieni 1983; Paultre, Chaallal & Proulx 1992). An example of the measured dynamic response of various types of structures is shown in Figure 2.3.
- Simply supported structures with multiple girders are not significantly affected by peak load amplification for each girder (Wang et al. (1996) as cited by McLean and Marsh (1998)). In contrast, continuous multi-girder structures are more likely to yield higher load amplification at interior supports.
- The dynamic response of continuous structures is known to be significantly influenced by road profile and vehicle speed (McLean & Marsh 1998).
- Cantilevered structures are known to be sensitive to dynamic loading and produce various levels of load amplification, predominantly due to the inherent dynamic characteristics of the cantilever (Huang et al. as cited by McLean and Marsh (1998)).

- Cable-stay and suspension structures have been shown to result in lower dynamic load amplification. However this is highly dependent on the quality of the road surface (McLean and Marsh 1998).
- The Japan Road Association (JRA) provides guidance on Impact Coefficients in accordance with bridge type (*The Specification for Highway Bridges* (JRA 1996) as cited by Deng, Yan & Zhu (2015, p. 4) – see Table 2.1).

Figure 2.3: Natural bridge frequency versus span length, shown by bridge type

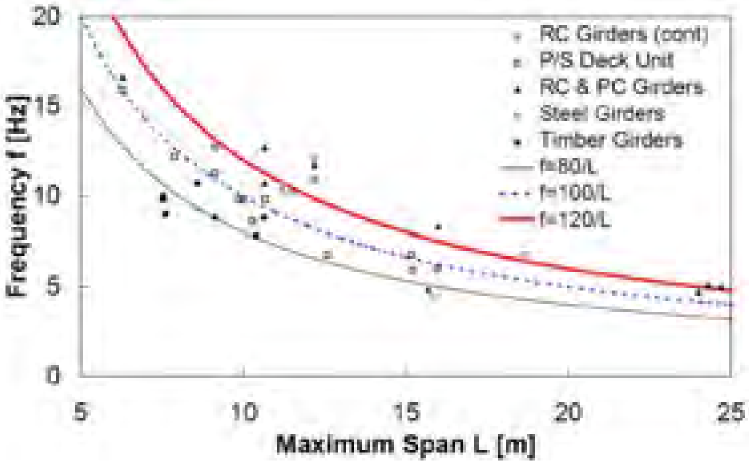

Source: Figure 5, Cantieni et al. (2010).

Table 2.1: JRA impact coefficient specification according to bridge type

Bridge type	Loading type	IM
Steel	Truck and lane	$20/(50+L)$
RC	Truck	$20/(50+L)$
	Lane	$7/(20+L)$
Prestressed concrete	Truck	$20/(50+L)$
	Lane	$10/(25+L)$

Note: L = span length (in meters).

Source: Table 6, Deng et al. (2015).

Bridge material type

- Contradictory findings are noted in relation to the inherent material type of a bridge. McLean and Marsh (1998) stated that similar dynamic responses were likely for various materials (e.g. prestressed and reinforced concrete, and steel girders). However, significant load amplification has been recorded for timber structures (Ritter et al. (1995) as cited by McLean and Marsh (1998)).

Bridge geometry

- Cantieni (1983) suggested that skewed bridges or bridges with extreme curvature were less likely to produce elevated dynamic responses compared to straight beam-type bridges (Figure 2.4). This was attributed to the flexural and torsional modes.
- In contrast, research carried out by Senthilvasan et al. (2002) and Ashebo et al. (2007) identify skewed or curved structures as being influential on dynamic response.

- Frequency matching between vehicles and skewed/curved structures may mask the actual cause for dynamic amplification (Paultre, Chaallal & Proulx 1992).
- Cantieni (1983) noted that bridge geometry was closed linked with the damping capability of the structure, which influences dynamic response (see following section).

Figure 2.4: Dynamic amplification of load with respect to straight or skewed/curved structures

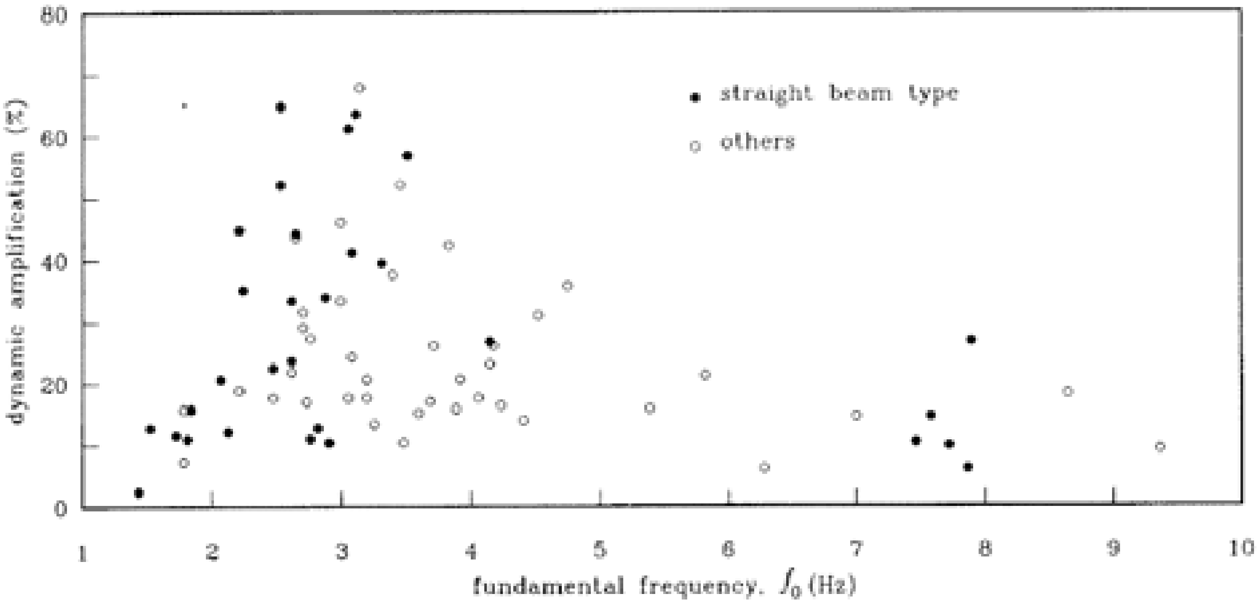

Source: Cantieni (1983) as adapted by Paultre et al. (1992).

Damping capability of the bridge

- Cantieni (1983) noted that, based on empirical data collected by EMPA, the damping capability was closely linked to the bridge type, material type, geometry and boundary conditions of a structure. This subsequently influences the dynamic response of the structure.
- Damping values measured in the field have been noted to be variable. Gonzalez (2009a) noted that natural damping levels for bridges were more likely to be between 1% and 5%, whereas values less than 1% and greater than 10% have been observed from field tests (McLean & Marsh 1998 – see Table 2.2).
- Billing (1984) and Paultre et al. (1992) noted that dynamic load amplification was likely to be smaller if the damping characteristics of a structure were great. Bez, Cantieni & Jacquemoud (1987) agreed with these conclusions, stating that bridges were more likely to have low levels of damping; as such, their dynamic response is subsequently influenced by the coincidence of vehicle and bridge fundamental or excitation frequencies.
- Conversely, Gonzalez (2009a) argued that damping did not influence dynamic effects significantly.
- Damping was noted to be less significant for short- to medium-span bridges in terms of their maximum dynamic response (Moghimi & Ronagh 2008).
- Heywood et al. (2001) noted that enabling high levels of damping on a short-span structure will reduce the likelihood of dynamic load amplification and minimise quasi-resonance.
- Gonzales (2009a) noted that damping capabilities were more likely to be critical for successive loadings/multiple vehicles.

Table 2.2: Damping measured for various structure types

Type of Bridge	Span Length (m)	Number of Bridges Tested	Average Damping Value	Lowest Damping Measured
Concrete in Switzerland, Great Britain, and Belgium (Tilly 1986)	10–85	213	0.079	0.020
Composite, steel-concrete in Great Britain (Tilly (1986)	28–41	12	0.084	0.055
Prestressed concrete (Billing 1984)	8–42	4	0.022	0.008
Steel (Billing 1984)	4–122	14	0.013	0.004

Source: McLean and Marsh (1998).

Boundary conditions on a structure

- Boundary conditions are known to be influential on the dynamic response of a structure (Wang et al. 1992 as cited by González 2009a); however, minimal research has been conducted in this area.
- Barr, Halling & Womack (2008) found that changes in boundary conditions altered dynamic moments by approximately 5% and modal frequencies by 34%, resulting in changes to stiffness which changes the physical response of the structure.
- Seismic tests conducted by Chegini and Palermo (2014) identified that the dynamic response of a bridge could be altered due to skew, which was attributed to boundary conditions.
- A numerical model study conducted by Carey, O'Brien & González (2010) noted that rotational restraint at bridge supports (i.e. boundary restraints) resulted in changes to the frequency response of a structure, which ultimately governs the resulting dynamic amplification. Carey et al. also recognised that significant assumptions are typically made when accounting for boundary conditions in relation to dynamic load amplification and that, in reality, field trials actually show the resistance of rotation at bearing locations which highlight the contribution of boundary conditions.

2.2.2 Influence of the Condition of the Road Surface

The condition of the road surface across the bridge and on either approach has consistently been identified as the most important factor influencing the dynamic response of a bridge to live loading (Austroads 2003; Austroads 2002b; Bakht & Pinjarkar 1989; Cantieni 1992; González 2009a; Heywood 2000; O'Brien et al. 2006). With the passage of a vehicle over a road surface, the quality of the road profile may introduce additional vibrations to the vehicular system, which may result in the amplification of dynamic wheel loads. These introduced vibrations are related to two inherent dynamic characteristics of the vehicle: body bounce and axle, or wheel, hop (Austroads 2002b; Cantieni 1983). Body-bounce vibration relates to the movement of the body or sprung mass of the heavy vehicle, with natural frequencies typically between 1.5-5 Hz. Axle-hop is associated with the independent axle vibrations between the road surface and the supported body (see Figure 2.5). It is influenced by the tyre and suspension characteristics of the vehicle, and typically observed at natural frequencies between 8 and 15 Hz (OECD 1999; Paultre, Chaallal & Proulx 1992).

With decreasing road profile quality, the dynamic wheel loads imparted to the bridge increase, thus increasing the potential for structural damage. This is further exacerbated when poor vehicle suspension/damping characteristics exist. Heywood et al. (2001) showed that the dynamic effects were greater where road profiles were classified with an International Roughness Index (IRI) greater than 4 mm/m (i.e. an older pavement with some surface imperfections, see Figure 2.6).

Figure 2.5: Illustration of axle-hop and body-bounce movements and resulting wheel forces induced on the supporting structure due to poor road profile

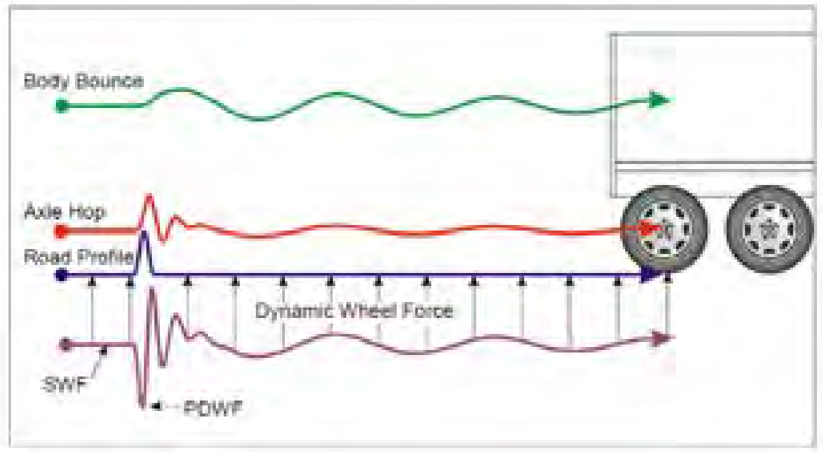

Source: Austroads (2002b).

Note: SWF: static wheel force; PDWF: peak dynamic wheel force.

Figure 2.6: Road roughness characteristics and relative road pavement condition

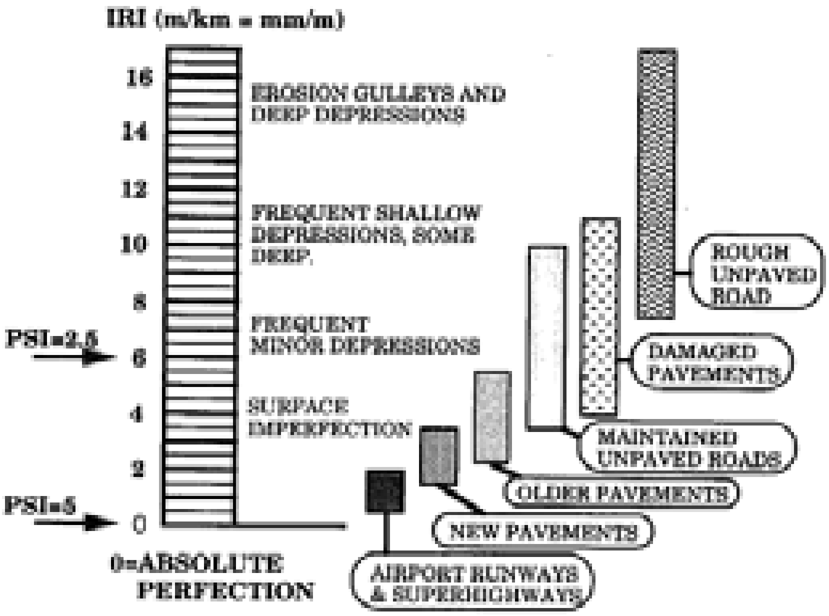

Source: Hwang and Nowak (1992).

Prem and Heywood (2000) presented research results of two short-span bridges (Swamp Creek Bridge and Chiltern/Beechworth Overpass) that highlighted the differences in measured dynamic load amplification for roads that were pre- and post-treatment. The research confirmed that, by altering the road profile, the dynamic response of the bridge could be changed, with 20% reductions in DI values observed. However, the results were dependent on vehicle type and the frequency characteristics of each bridge.

It is also known that, in addition to a poor road profile, irregularities associated with expansion joints, poor abutment profiling and periodic road corrugations will accentuate dynamic effects. These are known as damaging discrete road features, with examples shown in Figure 2.7 from Austroads (2002b).

Figure 2.7: Discrete road profile features that contribute to dynamic effects on bridges

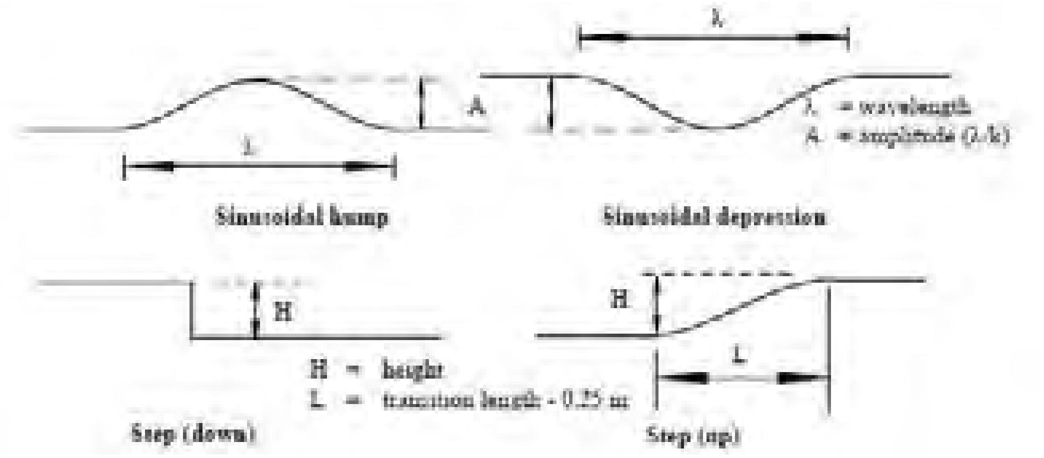

Source: Austroads (2002b).

Significant research has been, and is continuing to be, conducted into dynamic load effects due to and subjected to pavement profiles. Recent examples include Austroads (2002); Constanzi & Cebon (2006); O'Brien and González (2006); Steinauer & Ueckermann (2002); and Sweatman, Woodrooffe & McFarlane (1997).

2.2.3 Influence of Vehicle Dynamic Characteristics

Similar to the bridge dynamic properties, vehicles have their own inherent dynamic properties that individually contribute to dynamic loading on a supporting structure. Factors typically considered include the vehicle geometric and load details, dynamic control factors (such as suspension systems and shock absorbers), the travel of the vehicle (speed and lateral travel position), and the influence of multiple vehicles. These variables are now discussed.

Vehicle speed

- Older research supports the thought that high velocities result in higher dynamic forces, yet recent research suggests the relationship between velocity and dynamic amplification is more unclear.
- Vehicle speed becomes more influential on the road profile for load amplification (Wang et al. 1992 cited by González (2009a), McLean and Marsh (1998) and et al. (1992), where vehicles travelling at high speed are more likely to produce greater load effects than one travelling at the same speed over a smoother surface (Figure 2.8).
- Results from the SAMARIS research study found an unclear relationship between vehicle speed and load amplification; however, this study incorporated multiple vehicle events which leads to additional disrupting frequencies (Žnidarič et al. 2006).
- The amplification of load at axle-hop frequencies (i.e. between 2 and 5 Hz) is known to be speed dependent (McLean & Marsh 1998).
- Recent research suggests that certain critical velocities will result in dynamic amplification; however, it is dependent on span length and the natural frequency of the bridge (O'Brien and González et al. 2006; Senthilvasan, Thambiratnam & Brameld 2002).
- Acceleration/deceleration has not been studied in depth to date. Preliminary studies show rapid braking may promote greater dynamic amplification (González 2009a and 2009b).

Figure 2.8: Dynamic Impact factors when compared to vehicle speed and road profile condition

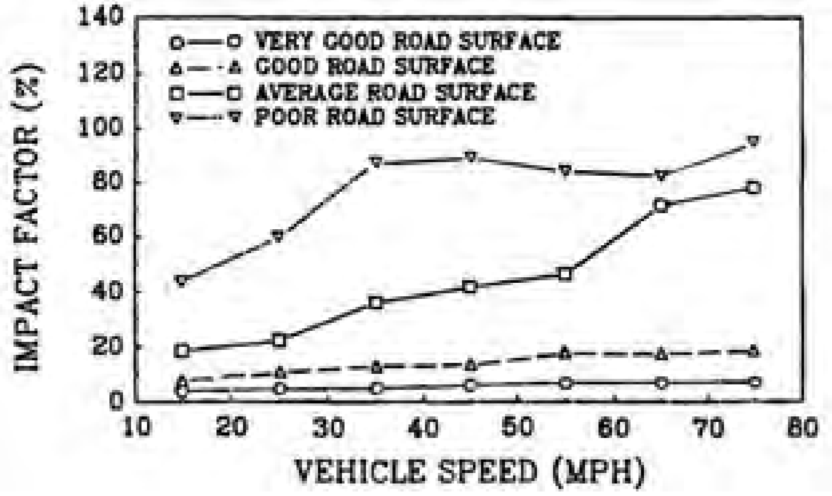

Source: Wang et al. (1993) as cited by McLean and Marsh (1998).

Vehicle mass

- There is general agreement in the literature that dynamic amplification decreases with increasing vehicle mass, based on field and analytical studies (Billing & Green 1984; Heywood, Roberts & Boully 2001; Hwang & Nowak 1991).
- Where multiple vehicles are present (i.e. increased load), dynamic load amplification has been noted to be less than for a single-vehicle event mass (Ashebo, Chan & Yu 2007; Hwang & Nowak 1991).
- Relatively greater load amplification can occur for light vehicles (when compared to dynamic strains/deflections recorded for such vehicles) (Bakht & Pinjarkar 1989; McLean & Marsh 1998; O'Connor & Pritchard 1984 and 1985).
- The greater the load carried by part of the bridge, the lower the dynamic amplification (González 2009a and 2009b).

Suspension & shock absorber types

- Dynamic loading has been found to be sensitive to the stiffness and damping characteristics of the vehicle suspension system (OECD 1999).
- Steel suspensions are more likely to result in greater dynamic amplification than air-bag systems, due to lower natural frequencies and heavier damping in air sprung systems (Austroads 2003; Heywood 2000).
- The type of suspension highly influences the dominating body bounce frequency. For example, vehicles with steel suspensions are more likely to exhibit body bounce frequencies of approximately 3 Hz, whereas vehicles with air bag suspensions are more likely to fall between 1.5 and 1.8 Hz. There is no apparent distinction between the two suspension types at axle-hop frequencies of 8-20 Hz (Cantieni et al. 2010).
- Reductions in dynamic load amplification are more likely to occur when vehicle shock absorbers are in good condition, limiting the maximum dynamic response of the vehicle. However, shock absorbers that have deteriorated affording little or no damping capability may result in large load amplification, manifesting as body bounce frequencies (McLean & Marsh 1998). This concept is further validated by Heywood et al. (2001), where it is noted that air-bag suspension vehicles with deteriorated or non-existent damping have the potential to inflict significant damage to structure.

- Using ‘bridge-friendly’ vehicle suspensions and dampers can limit the level of dynamic excitation by crossing vehicles. However, bridge-friendly suspensions are not the same as road friendly suspensions (González 2009b).
- Very little has been published in regard to the dynamic influence of the hydro-pneumatic suspension system used in mobile all-terrain cranes. Research conducted by Heywood (1998) showed that the dynamic effect of the crane on the bridge was less than that recorded for air and steel suspension semi-trailers. Similar results were achieved where an axle-hop plank was used to induce maximum dynamic effects (OECD 1999).

Axle spacing and configuration

- Studies have shown that dynamic load amplification is related to the number and configuration of the vehicle axle groups, where the axle groups interact with each other locally and with the bridge and vehicle globally (McLean & Marsh 1998).
- Research by O’Connor and Pritchard (1985) identified that a dual axle suspension systems with load sharing capabilities can be strongly influential on load amplification.
- An analytical study by Hwang and Nowak (1991) noted that single truck configurations were more likely to produce greater load amplification when compared to a vehicle with a tractor-trailer configuration.
- Similarly, vehicles with shorter axle configurations have been shown to produce an increased dynamic response in bridges (Billing & Agarwal 1990; Sweatman et al. 1997).
- Single or tandem axle configurations are more likely to result in greater load amplification loading than tri-axle configurations (Cantieni et al. 2010; O’Connor & Pritchard 1985).
- Nowak (1994) concluded that load amplification was more likely to be lower as the number of axle groups increased (Figure 2.9). However contradictory research conducted by Nassif and Nowak (1995) found that increased load amplification occurred in two, four and five axle trucks.

Figure 2.9: Amplification of load for a single and two-axle truck

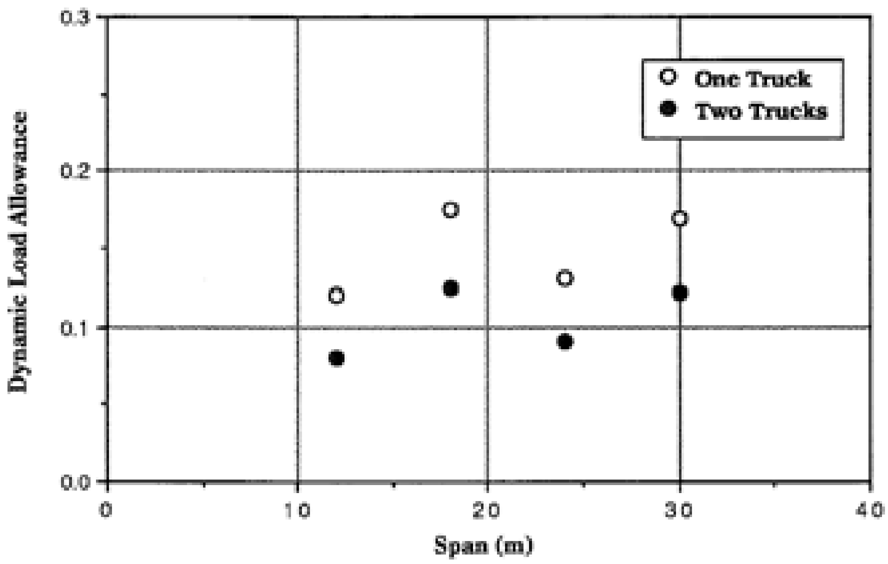

Source: Nowak (1994).

Vehicle position

- The transverse position of vehicle across the bridge deck is known to be influential on dynamic loads transferred to the supporting structure (Bakht & Pinjarkar 1989; Cantieni 1983; Rattigan et al. 2005; Senthilvasan, Thambiratnam & Brameld 2002). Deck and girder bridges are particularly sensitive to vehicle location, with Huang (1993, as cited by González (2009a)) stating 'the impact of each girder in multi-girder concrete bridges is closely related to the lateral position of vehicles'.
- When the transverse static load distribution increases, dynamic influences decrease i.e. the more load-sharing across girders, the dynamic amplification is likely to be less. Thus dynamic amplification is greater in unloaded lanes than loaded lanes (González 2009b).
- The location of the vehicle transversely across the deck will cause the establishment of 'zones of direct influence', as shown in Figure 2.10 (Bakht & Pinjarkar 1989) . This ultimately determines the girders that need to be considered in the assessment of dynamic load amplification. Similarly, Nassif and Nowak (1995) recommended that only girders exhibiting maximum stress values should be considered when determining amplification factors.

Figure 2.10: Zones of influence across the superstructure from vehicle loading

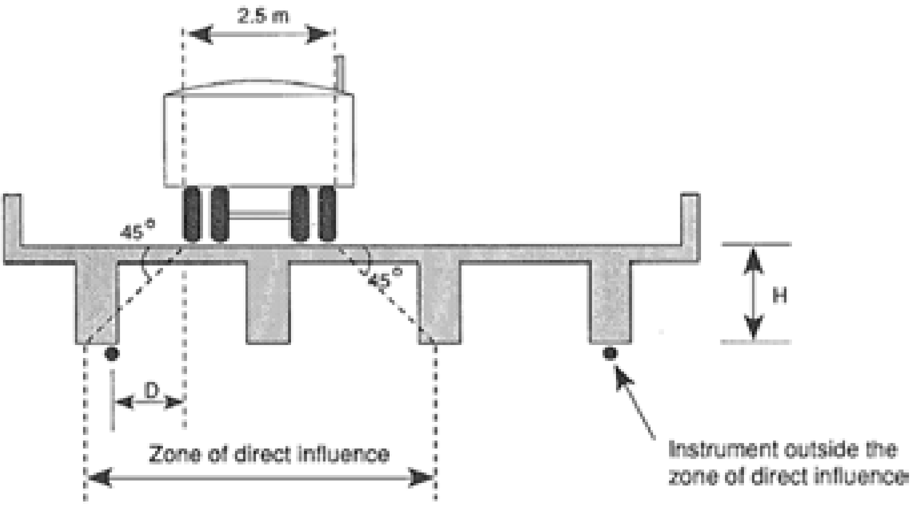

Source: Bakht and Pinjarkar (1989).

Presence of multiple vehicles

- Several publications state that the presence of multiple vehicles along a bridge can result in reduced dynamic load amplification (Arun, Menon & Prasad 2011; Bakht & Pinjarkar 1989). This is due to the dynamic response of each vehicle having a high probability of being out of phase with each other.
- The simultaneous encounter of vehicles on a bridge deck may also be influential, typically resulting in a reduced dynamic effect due to cancellation (González 2009b; Rattigan, Gonzále & O'Brien 2009).
- Pre-existing vibrations of the bridge prior to vehicular loading can be a contributory factor for load amplification (González 2009a; Rattigan et al. 2009). It has been noted by O'Brien and Gonzáles (2006) that sufficient gap between vehicles will enable free vibration of a bridge after the last crossing. It was also noted that certain combinations and gaps could be lead to peak dynamic load amplification.

2.2.4 Quasi-resonance – Frequency Matching Between Vehicles and Bridges

As stated previously, the overall response of a dynamic system and the amplification of load is dependent on the combined dynamic responses of the individual components, i.e. the bridge, the vehicle and the road interface. If the fundamental frequency of the bridge is close to the natural or excitation frequency of the passing vehicle, then large dynamic load amplification is possible. This is otherwise known as 'quasi-resonance' (Austroads 2003; Cantieni 1983). The degree of resonance will depend on the damping capability of the system, as demonstrated in Figure 2.9 , where increasing load amplification occurs with reducing damping. This is most critical for frequencies between 1.5 and 5 Hz (i.e. vehicle body bounce frequencies); however, frequencies relating to vehicle axle hop have also been noted to result in significant dynamic load amplification (Austroads 2002a).

Figure 2.11: Demonstration of resonance for a single degree of freedom system

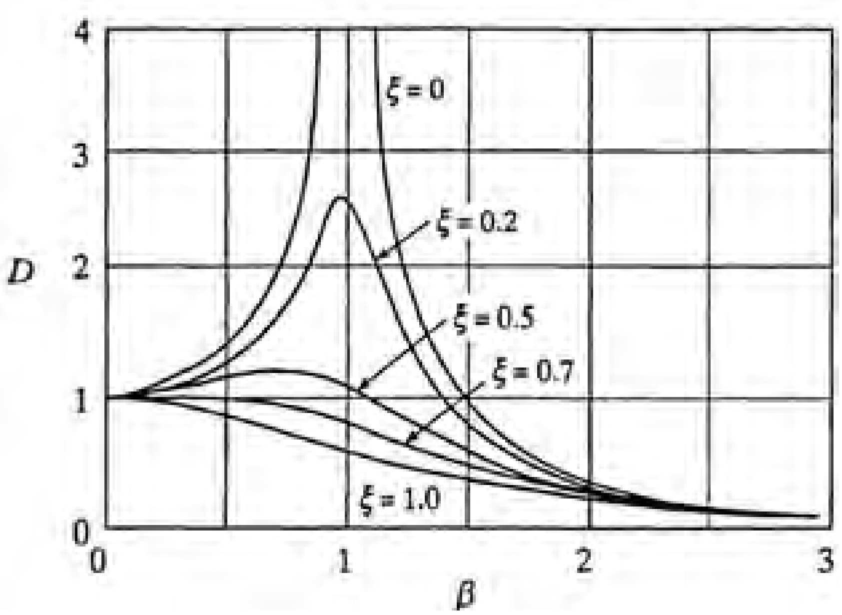

Source: Clough and Penzien (1993) as cited by McLean and Marsh (1998)

Legend: D: magnification factor of dynamic load

β: ratio of loading frequency to system frequency (1 = resonance)

ξ: damping ratio (compared to critical damping).

2.3 Quantifying Dynamic Load Effects: Dynamic Increment

As shown in Figure 2.1, differences exist between the static and dynamic response of a bridge when subjected to a moving load, of which the degree of difference depends on the factors discussed in Section 2.2. The ratio between measurable peak static and dynamic responses has traditionally defined the quantifiable increase in load on a structure due to a moving load. The terminology originates from the early 1930s, when Fuller et al. (cited by Bakht and Pinjarkar (1989, p. 1) defined the 'impact increment of dynamic force' as being 'the amount of force, expressed as a fraction of the static force, by which the dynamic force exceeds the static force'.

This ratio is known most commonly as the Dynamic Increment (DI) or impact fraction. However, as McLean and Marsh (1998) note, the term 'impact' has limitations and that 'dynamic load allowance' is known to be a more appropriate term, encompassing all vehicular dynamic effects and not just impact. DI is the terminology generally adopted in Australia, and will be adopted in this report herein when quantifying dynamic load effects from load tests.

There are a variety of methods that have been published and utilised over the last few decades. Bakht and Pinjarkar (1989) conducted an extensive and well-known review into the various numerical methods used historically and in current-day applications. It was noted that many methods were without justification for the adoption of a consistent methodology. The review included a comparison of DI values calculated using the different methods, showcasing the significant variations that can be obtained depending on the definition adopted. The study also highlighted inconsistencies and lack of uniformity in the approach to present DLA factors.

Cantieni (1983), in an attempt to normalise results from the extensive EMPA field test database, also provided a small review of DI formula historically adopted by EMPA. From both reviews, a preferred numerical method was identified, which is shown in Equation 1, defining the DI. The relationship is also shown graphically in Figure 2.12 .

$$\phi = \frac{A_{dynamic} - A_{static}}{A_{static}}.100\ [\%] \qquad 1$$

where

ϕ	=	DI (expressed as %)
$A_{dynamic}$	=	peak dynamic strain, deflection, or stress in relation to live load at elevated speeds
A_{static}	=	peak static strain, deflection, or stress in relation to live load at speeds less than 5 km/h

This method has traditionally been implemented in the majority of Australian field tests and other similar investigations (e.g. Senthilvasan et al. (1997)), which also adopted the term DI. Peak DI values for a specific bridge are subsequently compared to DLA values specified in AS 5100.2. This methodology has been adopted for the current project.

Figure 2.12: Determination of Dynamic Increment (ϕ or DI)

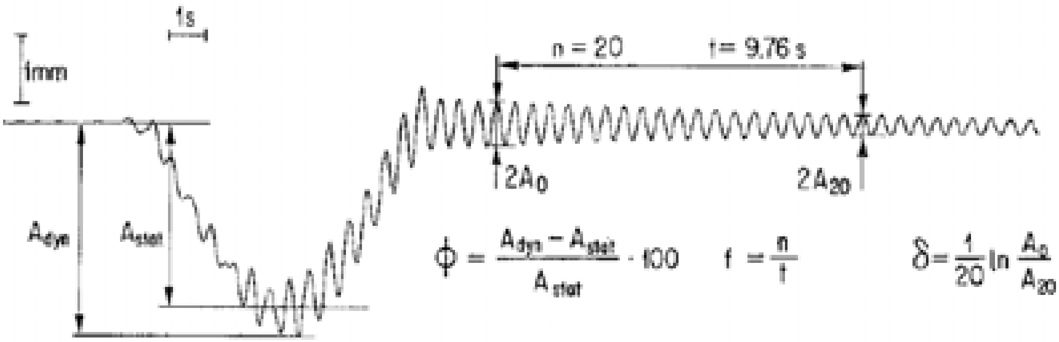

Source: Cantieni (1983).

2.4 Provisions for Dynamic Load Effects in Bridge Assessments: Dynamic Load Allowance

Accounting for dynamic load effects and the possibility of load amplification in structures remains a key consideration in the assessment of new and existing structures. Quantifying these complex effects on the overall structural system is generally simplified by a factored static load based on peak loads, with the factor being representative of the ratio between static and dynamic loads

(Bakht & Pinjarkar 1989; Deng et al. 2015; Nassif & Nowak 1995). This basic concept (originating from the 1930s as noted in Section 2.2) forms the basis of the majority of bridge design and assessment codes, specifying the dynamic factor to be applied in such instances. However, due to the variety of influential factors in and on a dynamic structural system and the seemingly conflicting field test results (which have historically had direct input into codified factors), there are significant variations in assessment methodologies and no singular dynamic factor exists for all codes and guidelines. It is also recognised that improved risk management processes have been influential with these developments (Heywood 2000).

Terminology for the dynamic factor is also varied across the various codes, such as dynamic load factor (DLF), dynamic amplification factor (DAF), dynamic load allowance (DLA), impact factor (IF) and impact coefficient (IC). McLean and Marsh (1998) noted that the term 'impact' has been found to have limitations and that 'dynamic load allowance' is a more appropriate term, encompassing all vehicular dynamic effects and not just impact). 'DLA factor' is the terminology adopted in Australian codes and will be referred to herein. This terminology is not to be confused with the DI, terminology defining the quantification of dynamic load effects determined from field measurements (as noted in Section 2.3). The DI value has traditionally been used to compare against codified values accounting for acceptable limits of dynamic load amplification in structures.

The following sections provide a summarised account of the historical development of the dynamic load allowance factor in an Australian context, the various factors currently adopted by national and international codes, and how DI values are determined to compare against codified dynamic load allowances.

2.4.1 Historical Development of Australian Code Requirements for Dynamic Load Effects

Detailed reviews regarding the development of DLA requirements around the world have previously been conducted (Austroads 2003; Bakht & Pinjarkar 1989; Billing 1984; Cantieni 1983; Deng et al. 2015; González et al. 2009a; McLean & Marsh 1998; Paultre et al. 1992). A brief review is now provided, with specific focus on the development of the DLA factor specified in Australian bridge design and assessment codes.

The first significant report on the subject of dynamic load amplification factor recommendations for bridges was conducted in 1931 by a committee of the American Society of Civil Engineers (cited by (Paultre et al. 1992). From this report, a number of amplification factors were recommended for various superstructure elements for application to similar structures. Several dynamic field tests followed across a number of international jurisdictions in response to dynamic behaviour of structures, with the appreciation that limits on deflections were not always appropriate when accounting for vibrational behaviour of bridges and that the amplification of dynamic loads required further research and quantification. Results from several significant research programs were published, of which the findings have been thoroughly reviewed by Paultre et al. (1992).

The DLA factors currently adopted by AS 5100.2-2004 (and by default most state and territory road jurisdictions) are founded on empirical data obtained from field trials (predominantly dynamic load tests) conducted by several transport and research institutions. These include research programs carried out by the Ontario Ministry of Transportation and Communications (OMTC) (Billing 1984; Billing & Green 1984), the Swiss Federal Laboratories for Material Testing and Research (EMPA) (Cantieni 1983), the OECD DIVINE project (Austroads 2003; Heywood 1995b; OECD 1999), and investigations carried out by Austroads (Austroads 2003; Austroads 2002a; Austroads 2002b; Heywood 2000). These programs and their influences are now discussed.

Ontario Ministry of Transportation and Communications (OMTC)

Billing and Green (1984) conducted a significant program of research and review on behalf of OMTC, where the current-day approach to account for dynamic loads specified in the Ontario Highway Bridge Design Code (OHBDC) was queried (Billing 1984; Billing 1982; Billing & Green 1984). The authors provide an overview of the historical development in methodology for the calculation of dynamic increment in bridges, referred to as an impact factor. The establishment of these methods were based on early railroad and highway experience (c. 1920s), of which the majority of materials were outdated at the time the review was conducted. This, combined with the motivation to improve understanding of bridge response to dynamic loading, led to full-scale dynamic load testing of 27 highway bridges in 1980. Interpretation of results allowed for the definition of a DLA factor related to the fundamental frequency of the bridge (Figure 2.13), which is considered to be the first instance which makes this connection. Note the downgrade of DLA factors recommended for the second edition of the OHBDC, of which the maximum DLA specified (for bridges with frequencies between 2.5 and 5 Hz) is 0.4. An upper limit of 0.25 was recommended for bridges exhibiting frequencies greater than 6 Hz. This work is seen as providing the first code to provide DLA values with respect to bridge frequency. This method was subsequently adopted by the superseded 1992 Australian Bridge Design Code (ABDC) (Austroads 1992). The upper bound of 0.4 has also informed the AS 5100.2 requirement for the DLA factor.

Figure 2.13: Summary of field test information and DLA recommendations (according to bridge fundamental frequency)

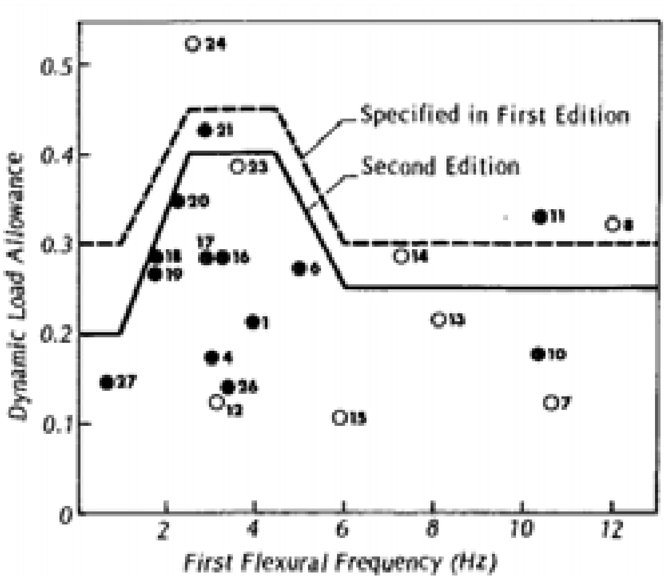

Source: Billing (1984).

Swiss Federal Laboratories for Material Testing and Research (EMPA)

In a similar vein, extensive dynamic testing was carried out by Cantieni and colleagues under the auspices of EMPA (Cantieni 1992; Cantieni 1984; Cantieni 1983). These records date back to 1841, although results from tests prior to 1960 were predominantly for rail bridges. The findings of the research were extensive and thorough, with dynamic load amplification results documented in terms of fundamental bridge frequency as per the results from the previous OMTC study (see sample shown in Figure 2.14). The findings of this research were submitted for recommendations as input into the pending Swiss Bridge Design Code (SIA 160) for DLA factors, with an upper bound of dynamic coefficient values of 1.8 (or 0.8 when translated to the Australian DLA factor) for predominant loads (load model 1) for bridge frequencies of 2–4 Hz or greater than 8 Hz (Bez, Cantieni & Jacquemoud, 1987). However the published method is shown in Figure 2.16 , which shows a constant dynamic coefficient of 1.4 (or a DLA of 0.4) for frequencies greater than 5 Hz. The constant value of 0.4 validates the currently adopted DLA factor in AS 5100.7.

Figure 2.14: Dynamic increments recorded for 73 concrete bridges (with no axle-hop plank)

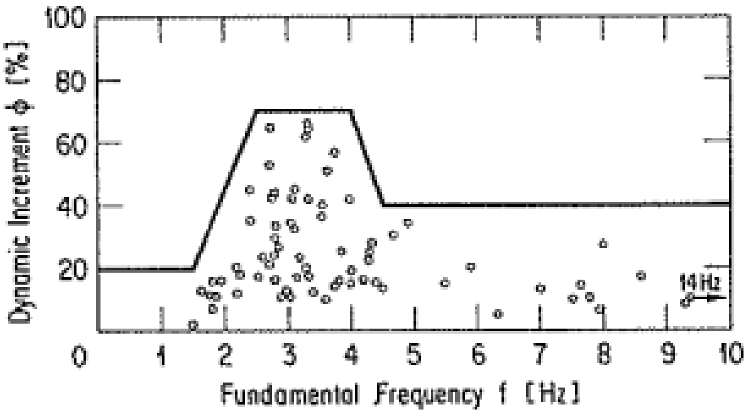

Source: Cantieni (1983).

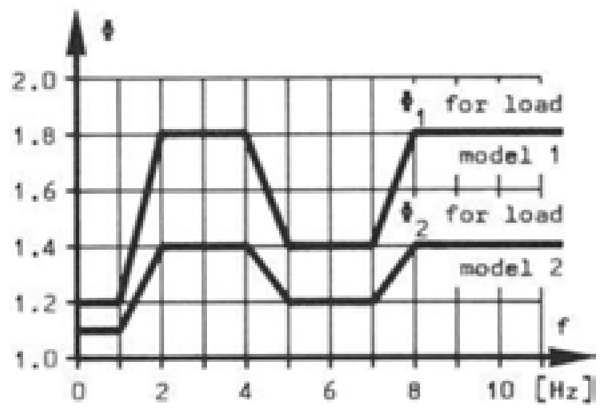

Figure 2.15:DLA factors recommended for adoption in SIA 160

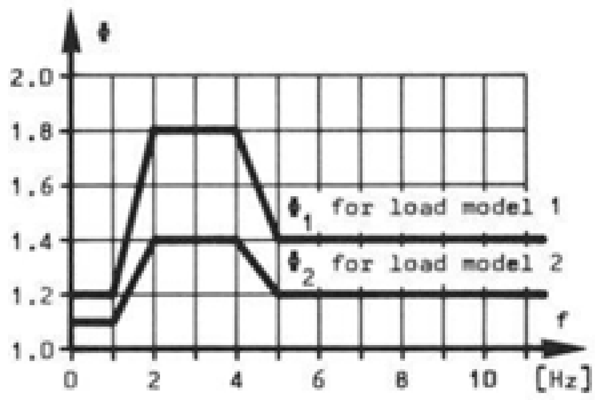

Figure 2.16: Published DLA factors adopted in SIA 160 (1988)

Source: Bez et al. (1987).

Legend: X-axis: Bridge frequency (f)

Y-axis: Dynamic coefficient (Φ)

OECD DIVINE Project & Austroads Project AP–T23/03

A review of bridge-vehicle dynamic interactions was conducted in 2003 (Austroads 2003). The conclusions and recommendations made from this report regarding dynamic load allowances were mostly incorporated into AS 5100. Recommended code updates were summarised as follows:

- Where the road profile on bridges and approaches is well maintained (with IRI less than 4.0) or well managed, there is sufficient evidence to support a reduction in the dynamic load allowance to 0.30 independent of bridge span.
- Where maintaining road profile is not economic or preferred, dynamic load allowance recommendations (relating to first frequency) should be implemented. This relationship has been developed from the extensive research conducted by Cantieni (Cantieni 1983), which related the DLA to the fundamental frequency of the bridge, rather than the span length.

Further to these recommendations, additional research was identified:

- Suspension characteristics and vehicle configurations/mass on vehicle-bridge interactions require further investigation in relation to the DLA recommendations for SM1600 (AS 5100).
- Investigate load sharing between axles.
- Investigate changes in stiffness of steel suspensions with increasing load.
- Expand vehicle-based model to accommodate full vehicle configurations.
- In relation to body-bounce behaviour for short-span bridges (especially for air suspensions):
  - Improvements are required in bridge deflection model.
  - A model needs to be developed to accommodate multi-span simple support and continuous bridges.
  - There is a need to investigate the behaviour of more sophisticated steel suspension models with respect to increasing mass.
  - A revision of accompanying lane factors may be required to account for multiple vehicle events, leading to less conservative and simpler design procedures.

Generally, the recommended DLA was in accordance with Austroads (1996), where the DLA is dependent on the first flexural frequency of the bridge, or as a function of span length. Figure 2.15 sets out the DLA recommendations for various flexural frequencies, based on the relationship derived by Billing (1984) and Cantieni (1984). Note this approach does not account for air suspensions in heavy vehicles.

Figure 2.17: ABDC 1996 Dynamic load allowance recommendations

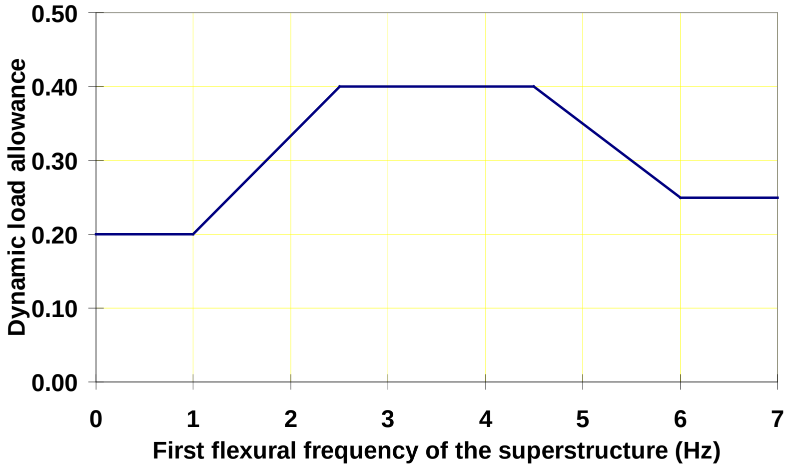

Source: Austroads (1996).

An overview of how the various Australian bridge codes have accounted for dynamic load effects in bridge design more recently in existing structure assessments is provided in Table 2.3. It highlights the recommended code requirements for the updated bridge design code AS 5100.

Table 2.3: Summary of DLA factor evolution in Australian bridge design codes

Code	Year	Allowance for dynamic load effects
AS 5100.2 Design loads	2017	▪ Very similar provisions to previous editions ▪ DLA factor remains a constant, with additional factors provided for other vehicle types and loading scenarios. General vehicle access 0.40 T44/L44 0.40 Cranes 0.40 Livestock 0.40 Restricted access 0.40 M1600 load 0.30 W80 wheel load 0.40 A160 axle load 0.40 M1600 tri-axle group 0.35 HLP load 0.10
AS 5100.7 Bridge assessment	2017	▪ DLA in accordance with AS 5100.2. ▪ Provisions for DLA reductions due to low speed and vehicle location (subject to authority approval). ▪ Provisions for DLA reduction for HLP or other specific loads possible (with restrictions) (subject to authority approval). ▪ Provisions for DLA reduction to 0.3 where road profile is low (supporting documentation required, timeframe restrictions, subject to authority approval). ▪ Provisions for DLA revision based on load testing, investigations (subject to authority approval).
AS 5100.8 Rehabilitation and Strengthening	2017	▪ Additional exceptions provided for timber bridges as follows: Timber bridges ≤ 0.20 Stress Laminated Timber deck ≤ 0.25
AS 5100.2	2004	▪ Provides a range of constant DLA factors for various vehicles and wheel/axle group configurations. This is a fundamental shift from the previous code (Australian Bridge Design Code 1996). ▪ Additional wheel load requirements added (W80, A160) added, with DLA factors of 0.4 recommended due to empirical data on short span structures and individual components (Taplin et al. 2013). M1600 load 0.30 W80 wheel load 0.40 A160 axle load 0.40 M1600 triaxle group 0.35 HLP load 0.10
AS 5100.7	2004	▪ DLA in accordance with AS 5100.2. ▪ No specific requirement for general or other loads. ▪ Engineering judgement encouraged in DLA application in AS 5100.7. ▪ Provisions for DLA revision based on load testing, investigations (subject to authority approval). ▪ Provisions for DLA reduction for HLP or other specific loads possible (with restrictions) (subject to authority approval).
Australian Bridge Design Code (1996)	1992	▪ DLA varies between 0.2 and 0.4, dependent on bridge fundamental frequency as per Figure 2.17 . ▪ DLA for Wheel loads: 0.25.

Code	Year	Allowance for dynamic load effects
NAASRA Bridge Design Specification	1976, 1970, 1965	▪ Similar method to early AASHO requirements. Impact (%) = $\frac{1600}{L+40}$, 0.10 ≤ I ≤ 0.30.

2.4.2 Current International Code Requirements for Dynamic Load Effects

Table 2.4 provides a summary of requirements when accounting for dynamic load effects from recent editions of various key international codes (summary information has been obtained from McLean and Marsh (1998), Deng et al. (2015) and Heywood (2000)).

Table 2.4: Summary of International Code factors and requirements for dynamic load effects

Country	Code	Year	Allowance for dynamic load effects
New Zealand	NZTA Bridge Manual (NZ Transport Agency 2016)	2016	▪ Dynamic load factor (DLF) varies depending on span length, the location of the structural element and the material. Maximum DLF is 1.3. See Figure 2.18 . Figure 2.18: NZTA Bridge Manual DLF requirements 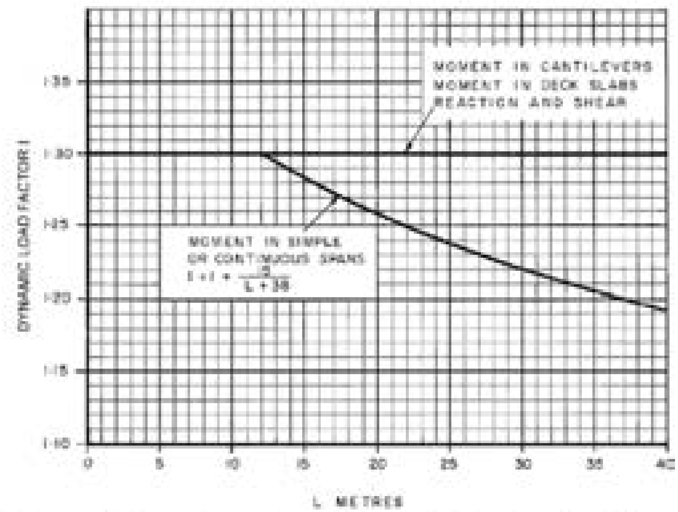 L is the span length for positive moment and the average of adjacent span lengths for negative moment. Source: NZTA Bridge Manual (NZ Transport Authority 2016) ▪ DLF used in moment calculations subscribes to superseded AASHTO methodology: $\text{DLF} = \begin{cases} 1.30 & L \le 12\text{ m} \\ 1+\frac{15}{L+38} & L > 12\text{ m} \end{cases}$ ▪ A recent research report by Taplin et al.(2013) recommends this methodology remain in the Bridge Manual ▪ Reductions for specific circumstances permitted – Timber bridges: DLF (revised) = $1.0 + (DLF - 1.0) \times 1.7$ – Specific heavy vehicles (HPMV, 50MAX) – A specific value determined from load testing or site measurements

Country	Code	Year	Allowance for dynamic load effects
USA	AASHTO Bridge Design Specification	2014	▪ Constant DLA factor provided, independent of span length (unlike previous editions). General 0.33 Fatigue, fracture limit 0.15 Deck joints 0.75 ▪ DLA same for design load rating, legal load rating. ▪ Permit load rating allows DLA of 0.33 for moving vehicles only. ▪ Reductions in DLA permissible as per following guidelines: – AASHTO Guide Manual for Condition Evaluation and Load and Resistance Factor Rating (LRFR) of Highway Bridges (2003) – AASHTO Manual for Bridge Evaluation (2011). Smooth riding surface at approaches, bridge deck, and expansion joints 0.10 Minor surface deviations or depressions 0.20
Canada	CSA-S6-14 Canadian Highway Bridge Design Code	2014	▪ DLA dependent on number of axles on design truck (CL-W). ▪ Recognition of influence of road profile, bridge joints on dynamic loading. ▪ Has moved away from previous edition (i.e. DLA based on bridge frequency (Billing & Green 1984)). One Axle (CL-W truck) 0.33 Two axles (CL-W truck) 0.15 Three or more axles (CL-W truck) 0.75 Deck joints 0.50
Europe	EN 1990: Basis for Structural Design EN 1991-2 Actions on Structures – Part 2: traffic loads on bridges	2005 2003	▪ Dynamic amplification factor (DAF) is integrated into the loading models, with exception of load model #3. ▪ DAF is defined in each model according to moment and shear capacity. For Bending: $\text{DLA} = \begin{cases} 1.7 & L \leq 5\text{ m} \\ 0.85 - 0.03L & 5\text{ m} \leq L \leq 15\text{ m} \\ 1.4 & L \geq 25\text{ m} \end{cases}$ For Shear $\text{DLA} = \begin{cases} 1.4 & L \leq 5\text{ m} \\ 1.45 - 0.01L & 5\text{ m} \leq L \leq 15\text{ m} \\ 1.2 & L \geq 25\text{ m} \end{cases}$ ▪ For Load model #3: DAF = $\varphi = 1.40 - \frac{L}{500}$, $\varphi \geq 1$

Country	Code	Year	Allowance for dynamic load effects
United Kingdom	BS EN 1991-2	2003	▪ DAF incorporated into the loading models as per previous, with exception of Load model #3. ▪ For Load model #3, the following factors are recommended: Basic axle load — DAF 100 kN — 1.20 130 kN — 1.16 165 kN — 1.12 180 kN — 1.10 225 kN — 1.07
Japan	Specifications for Highway Bridges (Japan Road Association 2012)	2012	▪ The Dynamic Impact Factor (IM) expressed as a function of span length. Bridge type — Dynamic impact factor Steel — $\frac{20}{L+50}$ RC — $\frac{20}{L+50}$ Prestressed concrete — $\frac{20}{L+50}$
China	General Code for Design of Highway Bridges and Culverts, JTG D60-2004	2004	▪ The Dynamic Impact Factor (IM) is a function of bridge fundamental frequency. ▪ There are no provisions for material or structure type, as per the previous edition. $IM = \begin{cases} 0.05 & f \leq 1.5\text{ Hz} \\ 0.176\ln[f] - 0.0157 & 1.5\text{ Hz} \leq f \leq 14\text{ Hz} \\ 0.45 & f \leq 1.5\text{ Hz} \end{cases}$

2.4.3 TMR Requirements

TMR has developed the *Tier 1 Bridge Heavy Load Assessment Criteria* (TMR 2013) to provide guidance to those conducting bridge assessments for structures on the TMR network. It is underpinned by AS 5100. To account for dynamic load effects, TMR has adopted a constant dynamic load allowance (DLA) factor of 0.4 to be applied to all assessment vehicles travelling at speeds greater than 10 km/h (refer to Table 10 of TMR 2013). This is regardless of the structure type, the vehicle type and the condition of the road profile. TMR considers this to be a more accurate reflection of the condition of the approaches on many structures across the network, particularly after recent flood events.

2.4.4 DLA Factors Adopted by Other Jurisdictions

As part of a survey distributed to members of the Austroads Bridge Task Force in 2011, members provided information on the DLA factors adopted by the various jurisdictions for standard bridge assessment procedures. A summary of the findings provided is shown in Table 2.5.

Table 2.5: DLA factors adopted by national jurisdictions (summarised from national survey results)

Jurisdiction	Standard	DLA factor	Comments
MRWA	AS 5100.7	0.4	▪ Limited test information available

Jurisdiction	Standard	DLA factor	Comments
DPTI	ABDC 1992	Max 0.4	▪ Uses 'Heywood model' (DI vs. frequency) for bridges with frequency between 9-17.5 Hz ▪ Actual DLAs adopted where available
VicRoads	AS 5100.2	Max 0.4	▪ Uses 'Heywood model' (DI vs. frequency) for bridges with frequency between 9-17.5 Hz
RMS (formerly RTA)	AS 5100.7	0.4	▪ Limited dynamic testing done for concrete, steel and timber bridges with varying suspension types

Note that none of the jurisdictions identified specific DLA factors according to vehicle or axle type. The DLA factors provided would be influenced by the current review of AS 5100.7 and jurisdictional endorsement.

The survey concluded that additional review was required into the relevance of DLA levels currently adopted, as these are based on older research and do not incorporate improved vehicle technologies. Recommendations for the application of reduced DLA factors would depend on the vehicle and axle type, and would not be recommended for extreme events.

2.5 Research Gaps

Based on this literature review, a number of areas have been identified that require further investigation or have no supporting literature to date. Of these items, the following were identified as key areas for consideration under the current project. Subsequently, the research carried out as part of this project aims to address these gaps.

2.5.1 Substructure Components

Research into the dynamic response of bridges has predominantly focussed on superstructure components such as girders or decks. However, TMR has identified that substructure components are critical members in most structural assessments. With minimal literature providing guidance or research outcomes on substructure dynamic responses and its contribution to the amplification of dynamic loads, this was identified as a key area for research.

2.5.2 Different Vehicle Types

The majority of load tests conducted nationally and internationally have provided dynamic results for truck and trailer arrangements with several tandem and triaxle groups. Conversely, minimal information exists for other vehicles types such as over-size over-mass (OSOM) vehicles, heavy load platforms (HLP), PBS vehicles and cranes.

Four- or five-axle cranes with hydro-pneumatic suspensions have become increasingly popular in Australia due to their mobility, lane width compliance, and 'road friendly' status. Despite their wide acceptance in their European continent of origin, they are currently subject to access restrictions on the network due to the higher axle loads of 12 t per group, with concerns surrounding shear capacity. Alternatively, there are industry claims that the dynamic effects on bridges resulting from these cranes are significantly less than older or steel-suspension cranes, with pressure from industry to provide a reduced DLA factor to be applied to such cranes in recognition of this fact.

Minimal objective information is available to TMR to enable them to provide an informed decision for hydro-pneumatic crane access based on reduced factors. Therefore additional research into the dynamic behaviour of bridges in response to these crane types and the dynamic load amplification is required.

2.5.3 Vehicle Suspension Type

As noted in Section 2.2.3 ‘Suspension and shock absorbers’, the suspension characteristics of vehicles plays a key role in the amplification of dynamic loads in a bridge. Some research has been conducted previously investigating these effects (Cantieni et al. 2010; Heywood 1998), which has highlighted the different responses between steel and air-bag suspension semi-trailers. However, additional research is required to further validate these findings. Of particular interest to TMR are the differences in dynamic responses between steel and air-bag suspension road trains and steel and hydro-pneumatic cranes.

2.5.4 Vehicle Length

Research previously conducted into vehicle length has predominantly focussed on axle groups (single, tandem and triaxle), with the suggestion that with an increasing number of wheels per axle group a reduction in dynamic load effects may be realised (see Section 2.2.3 ‘Axle spacing and configuration’). Also noted is the commonly-held view in the literature that longer vehicles will produce lower dynamic load effects. However, with contradictory research by Nassif and Nowak (1995) suggesting that load amplification may be possible with more axle groups (up to five) and the event of road trains and PBS vehicles on the TMR road network, it is important to investigate whether load amplification is possible for longer vehicles.

2.5.5 Quasi-resonance (Frequency Matching) Between Vehicles and Bridges

Quasi-resonance has previously been identified as a key factor in the amplification of dynamic loads on bridges (Section 2.2.4). However, whether this translates to reality – and for what bridge or vehicle components needs to be clarified and documented. Reviewing the dynamic response of a bridge and the vehicle in the frequency domain will provide additional insights into this phenomenon, as well as providing additional information relating to the interaction relationship between these components.

3 TEST PROGRAM DETAILS

3.1 Overview

In order to fulfil the data collection requirements for this project, the following testing was undertaken:

- modal impact test
- controlled load test
- periodic in-service monitoring.

The following sections provide summary details of the test programs, including an overview of the test bridges, the final instrumentation plan, selected test vehicles, the final test schedule, and other information relevant to the project objectives.

The following three bridges were tested:

- Canal Creek Bridge
- Dawson River Bridge
- Neerkol Creek (No. 1) Bridge.

The testing of the Canal Creek Bridge was carried out in conjunction with NACOE project S3: *Deck Unit Bridge Deck Analysis under Live Load*.

More detailed information regarding the test programs can be found in the following TMR progress reports:

- BIS 7703 Canal Creek Bridge: Load Test and In-service Monitoring, Final Contract Report, Project 008286 (Ngo & Pape 2015).
- Measurement of Bridge-Vehicle Dynamic Interactions: Dawson River Bridge & Neerkol Creek (No. 1) Bridge Load Tests Report, NACOE Interim Report (Final), Project 007203 (Pape, Kotze & Ngo 2015).

3.2 Test Bridges

3.2.1 Canal Creek Bridge

General information

The Canal Creek Bridge (BIS ID 7703) is a two-span precast prestressed concrete deck unit bridge. It is located at chainage 93.845 km on the Flinders Highway, approximately 40 km east of Cloncurry. This route is designated by TMR as an RT2 heavy vehicle route with HML loading. The bridge services approximately 400 vehicles per day with approximately 30% heavy vehicles.

The bridge was designed in late 1969 for H20-S16 vehicle loading. It is representative of a family of deck unit bridges designed pre-1969 which have been identified as being at-risk structures by TMR. Its construction was completed in 1970. An overview of the structure details according to TMR's Bridge Asset Management (BAM) data is provided in Figure 3.1.

Figure 3.1: Bridge asset management (BAM) data for the Canal Creek Bridge

Structure Id	7703	Name	Canal Creek	
Crossing Name	Canal Creek	Alt. Name		
Structure Type	Bridge	Owner	MR	Department Of Main Roads
Construction Ty	Deck Unit	District	10	North Western District
Construction Materia	Pre-Stressed Concrete	LGA Id	036	Cloncurry Shire Council

Road Section					Start		End		TDist	
Id	Description	S	Cway	S	RPC	Dist	RPC	Dist	Start	End
14E	JULIA CREEK - CLC	C	1	C	8	7.435	8	7.451	93.845	93.861

Source: TMR Level 2 inspection report BIS 7703 Canal Creek 14-03-12.

An elevation of the bridge is shown in Figure 3.2 and assembly details from the as-constructed drawings are shown in Figure 3.3. The structure comprises two simply-supported spans, each 8.23 m in length, and a two-lane, two-way carriageway 6.7 m wide. The bridge has no skew, longitudinal gradient or horizontal curvature of significance.

The superstructure comprises 11 internal deck units (rectangular hollow section of 597 mm wide and 280 mm in high and 2 x 150 mm diameter voids) and two upright external units (rectangular solid section 305 mm wide and 650 mm high) which simultaneously act as bridge kerbs (Figure 3.3-b). The units are transversely stressed using bonded post-tensioned tendons at four locations along the span, with a mortar layer 25 mm thick between each unit. The design details of the deck and kerb units are shown in Figure 3.4. The wearing surface is an asphalt layer with an average thickness of 100 mm. The deck has a crossfall of 1.5% from the centerline to both edges of the deck.

The substructure consists of two abutments and a pier, each comprised of a cast-in situ reinforced concrete headstock and four precast concrete driven piles (356 mm square in cross-section).

Figure 3.2: Canal Creek Bridge – elevation

Source: TMR.

Figure 3.3: Bridge details (not to scale)

(a) Elevation

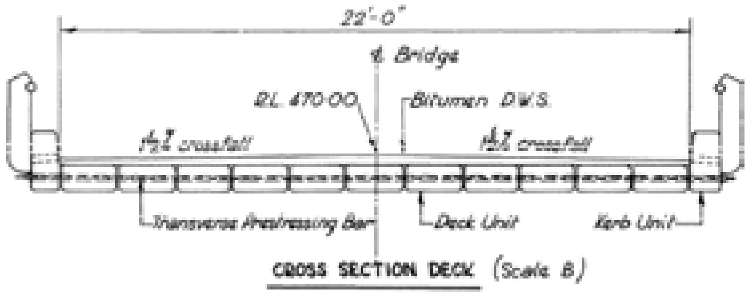

(b) Cross-section

Source: TMR drawing plan no. 98570 and standard drawing no. S926.

Bridge condition

The most recent Level 2 inspection took place on 14 March 2012 and was conducted by RoadTek. Previous Level 2 and 3 inspections noted that the bridge was generally in good condition, having an overall condition state of CS2. There was no evidence of visible cracking, spalling, delamination or signs of structural distress across all deck units, abutments and the central pier. There was also no evidence of settlement of the central pier.

Prior to testing, the bridge was inspected by TMR staff. The bridge was confirmed to be in good condition with no evidence of significant defects or structural distress. At the time of testing, access to the bridge was excellent; the deck soffit was within arm's reach and the river bed was flat and dry at the time of testing.

Figure 3.4: Deck and kerb unit details (not to scale)

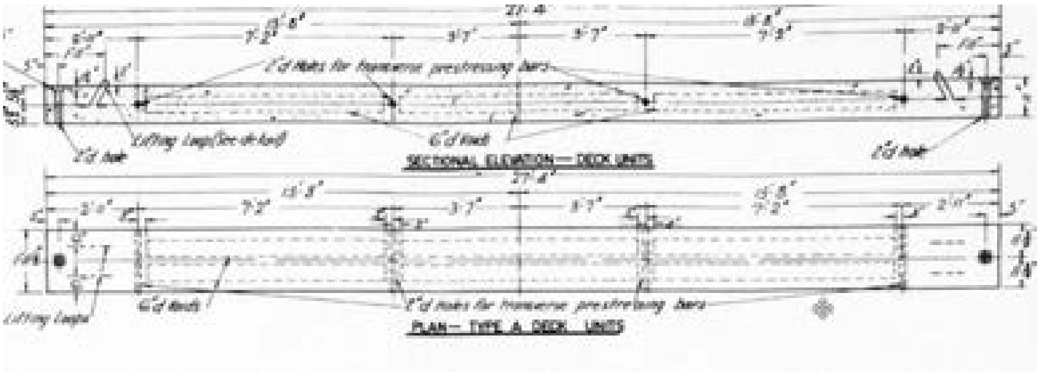

(a) Deck unit elevation

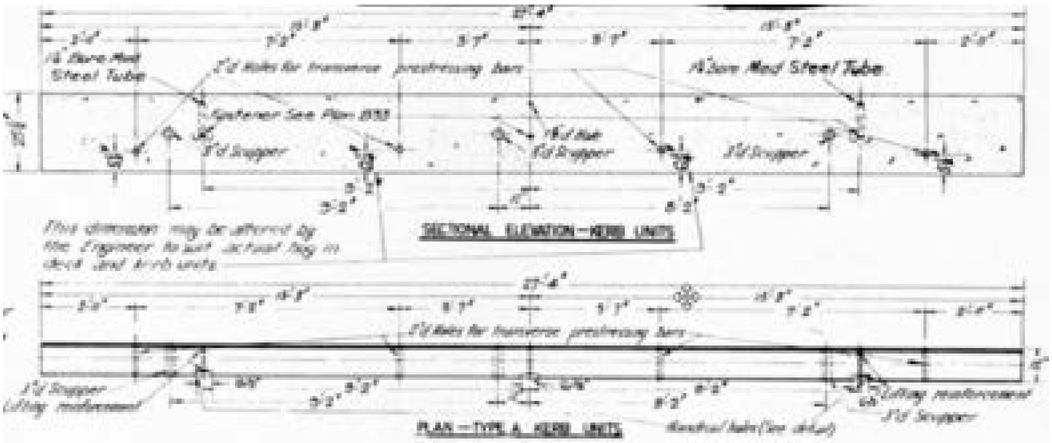

(b) Kerb unit elevation

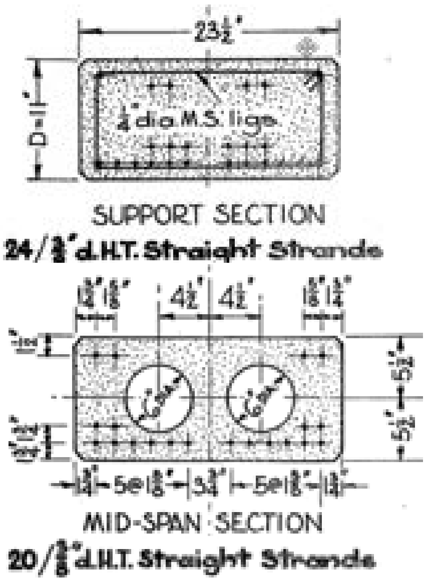

(c) Deck unit cross-section

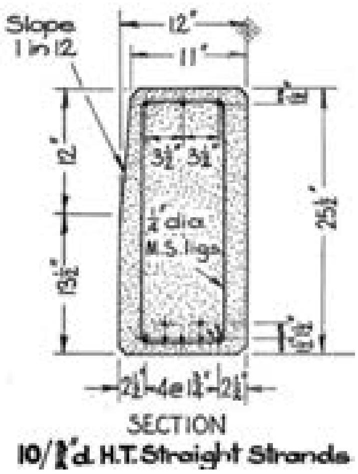

(d) Kerb unit cross-section

Source: TMR drawing plan no. 98570 and standard drawing no. S926.

Recent structural assessment results

A Tier 1 structural assessment of the bridge was conducted by Arup in 2011 using TMR's *Heavy Load Assessment: Project Brief for External Consultants* (TMR 2011), and in 2013 using TMR's *Tier 1 Bridge Heavy Load Assessment Criteria* (TMR 2013), with the latter assessment focussing on the substructure only. The assessments were based on linear elastic grillage models using methodologies, factors and reference vehicles provided within the TMR's corresponding guideline and AS 5100.5 (2004). The condition of the structure was also taken into account in the assessment.

A summary of the findings of the assessment, including Equivalence Ratio Bridge (ERB) values, is presented in Table 3.1. The original superstructure assessment (2011) identified structural deficiencies in the deck units for bending and recommended limitation of access to HML semi-trailers, road trains, 48 t cranes and 79.5 t cranes for unrestricted travel for centreline and coexisting vehicle load cases.

A preliminary substructure assessment identified the piles as being potentially structurally deficient due to geotechnical conditions, based on geotechnical working loads specified on the drawings. A Tier 2 assessment was conducted in 2013 on the headstocks due to insufficient shear reinforcement to satisfy minimum requirements as dictated by TMR documentation. However, headstock capacities were found to be sufficient. It was recommended that a qualitative analysis be conducted on the piles to review for signs of overloading or structural distress.

Table 3.1: Summary of the Canal Creek Bridge Tier 1 structural assessment

Component	ERB (worst case)	Comment
Deck unit	<1	Governed by bending capacity
Kerb unit	>1	
Headstock	>1	
Piles	<1	Insufficient geotechnical capacity (based on drawings)

Source: ARUP Tier 1 Assessment Report.

A preliminary analysis was carried out by ARRB and TMR prior to conducting the load test in order to confirm the anticipated and maximum allowable strains for the duration of testing. These results are summarised in Table 3.2 and Table 3.3. Limiting tensile strains for the kerb and deck units determined for live load based on concrete design tensile stress limits specified in Clause 8.6.2(a) of AS 5100.5 were used to monitor the bridge during the test for overloading. More detailed information on this analysis is contained within the S3 project documentation.

Table 3.2: Maximum estimated bending strains for kerb and deck units for 48 t crane

Load case	Deck unit (με)	Kerb unit (με)
Dead load only (DL + 1.3 SDL + prestress) [1]	–363	–199
Dead load + live load (centreline travel)	–89	–144
Dead load + live load (lane travel)	–104	+19

1 Values used in combination with measured live load strains for bridge monitoring (see Table 3.3).

Table 3.3: Strain and deflection limits for on-site monitoring

Design tensile crack stress limit (Cl 8.6.2(a), AS 5100.5-2004	Deck unit	Kerb unit
Strain (με)	317	248
Deflection (mm)	16.2	11.4

Road profile

The road profile was generally smooth on the bridge except for two areas above each abutment joint caused by the depression of the wearing surface (due to the transition from the road to the bridge deck). The depression at Abutment 2 was the greatest (Figure 3.5). An undulating, sinusoidal profile was also noted on some sections of the road on the approach to Abutment 2.

Figure 3.5: Depression of wearing surface at both abutments

(a) Abutment 1

(b) Abutment 2

Source: ARRB.

3.2.2 Dawson River Bridge

General information

The Dawson River Bridge (BIS ID 8233), also known as the Harold Hinchcliffe Bridge, is an eight-span simply-supported, precast prestressed concrete (PSC) I-girder bridge. It is located at chainage 93.249 km on the Capricorn Highway (16A) 12 km east of the township of Duaringa (Figure 3.6). The bridge is located on a TMR-designated road train/heavy vehicle route with GML loading. The bridge services approximately 3 400 vehicles per day with an estimated 20% heavy vehicles.

The bridge was designed in 1975 for vehicle class MS 18 and constructed in 1977. It is documented to have a high level of redundancy. Summary geometric and structural information on the bridge is presented in Table 3.4 and a general arrangement of the bridge is shown in Figure 3.7. The bridge has a two-lane, two-way carriageway 8.6 m wide. It has no significant skew, longitudinal gradient or horizontal curvature. The deck has a crossfall of 3% from the centerline to both edges of the deck and no bituminous deck wearing surface (which has been taken into account in the original design).

Figure 3.6: Dawson River Bridge

Source: ARRB Group Ltd.

Each superstructure span comprises six precast PSC I-girders, 1118 mm high and 23 m long. They act compositely with a cast-in situ reinforced concrete (RC) deck slab 155 mm thick and with 300 mm x 464 mm kerbs. The I-girders are provided with lateral and torsional restraints in the form of cast-in situ RC cross-girder infills at each abutment and pier support at two equally-spaced points along the span. The superstructure is supported by piers comprising single columns 1700 mm in diameter and cantilevered angled headstocks 1100 mm wide. The original design of the piers called for a piled foundation with an RC pile cap and twelve 450 mm wide PSC raked octagonal piles. It has since been noted that 450 mm (ID) steel tubes were adopted as piles in lieu of the PSC piles. The abutments consist of an RC headstock, 1100 mm wide and 850 mm deep, with a ballast wall and seven PSC raked octagonal piles. The abutment wingwalls are composed of rubble masonry.

Table 3.4: Dawson River Bridge – geometric and structural information

Geometric Information	
Number of Spans	8
Span Lengths	22750 mm (Spans 1 and 8) 23000 mm (Spans 2 – 7)
Bridge Total Length	183500 mm
Skew	0°
Carriageway Width	8600 mm which supports two traffic lanes
Superstructure Information	
Number of Girders	8 PSC I-girders to Project Drawings 131684 (deflected strand)
Spacing of Girders	1550 mm
Deck	155 mm minimum thick in situ RC slab with 300 mm x 464 mm kerbs
Barrier	Bridge Handrail Type 1 to Standard Drawing S1059
Substructure Information	
Abutments	RC Headstock, 7 No. 450 mm Octagonal PSC Raked Piles
Piers	RC Headstock, 1 No. 1700 mm diameter RC column, RC Pile Cap and 12 No. 450 mm Octagonal PSC Raked Piles (Piers 2 to 5) or 10 No. 450 mm Octagonal PSC Raked Piles (Piers 1, 6 and 7)

Source: Aurecon Tier 1 Bridge Heavy Load Assessment Report, Project number 236871, Rev. 2. 10-12-2013.

Bridge condition

The latest Level 2 inspection was undertaken in October 2011. The structure condition report documents an overall structure condition rating of CS4 (Very Poor) due to the settlement of pier P1 and the recommendation for bearing replacement.

Previous inspection reports had noted that the founding level of the pier P1 piles had settled; this was based on the observation that the level of the deck had dropped 65 mm to 70 mm over the pier. However, the latest report documented that the pier had not settled further since the last inspection. The bearings were reported to show signs of bulging, distortion or rolling. A Structure Scour Sounding Report (17 October 2011) documented changes in scour sounding depths of up to 3.1 m at spans 1 and 2 on the downstream side of the bridge. The most recent scour survey (1 February 2013) shows that these areas had not experienced additional scour.

Other issues documented for the structure include:

- Tension cracking was observed along the top of some of the headstock cantilevers.
- Settlement had occurred in the approaches behind the abutments.
- Pier P1 headstock had minor spalling on the top edge.
- Pier P1 bearing pedestal had minor spalling.
- Several restraint angles were missing or had loose bolts.
- Forward movement on all wingwalls of up to 50 mm was evident and Wingwall 2 at Abutment 2 showed signs of rotation.
- Abutment 2 and pier P6 joints were leaking. Joints on piers P1, 5 and 7 were missing seals and had gravel obstructing movement of the joints. Pier P2 joint had separation of the sealant and there was evidence of leakage. Pier P3 joint had deteriorated and there was evidence of leakage.

- The bridge rail had impact damage and an intermediate post in span S1 had spalling with exposed reinforcement.

Results of recent structural assessments

A Tier 1 structural assessment of the bridge was conducted by Aurecon in 2013 using TMR (2013). The assessment results showed that, while the superstructure was not overstressed, the piles had very low values of Equivalence Ratio Bridge (ERB) factor (e.g. as low as 0.14 on pier P4). Some other structural components were also flagged including insufficient capacity for bending moment of the pier P7 column, settlement at pier P1 and abutments, and critical buckling load of piers P1, P3 and P4, which limits the axial capacity (Table 3.5).

Table 3.5: Summary of Tier 1 structural assessment

Component	ERB/SAR (worst case)	Comment
Driven piles, P1, P3 and P4	ERB = 0.14	Insufficient axial capacity
Pile cap, P2 to 5	ERB = 0.98	Insufficient tie capacity
Pier column, P7	ERB = 0.93	Insufficient design capacity for moment due to 6G (GML AAB Quad Road Train)
Pier P1 and abutments		Settlement
Pier headstock, P7	SAR = 1.05	Due to 6G, travel restriction TR1 (in lane, >10 km/h, with accompanying vehicle)
Cross girders	ERB = 0.74	Due to reference vehicle 5 (HLP)
Girders		Shear at changes in ligature spacing was not assessed

Source: Aurecon Tier 1 Bridge Heavy Load Assessment Report, Project number 236871, Rev. 2. 10-12-2013.

More recently, a preliminary analysis undertaken by TMR prior to testing determined the theoretical strain and deflection values to provide an upper limit to on-site testing (see Table 3.6).

Table 3.6: Summary of theoretical strains and deflections for the Dawson River Bridge (based on 79.5 t crane)

Parameter	Upper limit for on-site testing
Top headstock flexural strain between G2 & G3 ($\mu\varepsilon$)	35
Base column compressive strain at loaded side ($\mu\varepsilon$)	111
Base column compressive strain at non-loaded side ($\mu\varepsilon$)	87
Maximum shear strain of internal girder at d0 ($\mu\varepsilon$)	56
Maximum shear strain of internal girder at quarter-span ($\mu\varepsilon$)	34
Pier headstock deflection at loaded side (mm – downwards)	
Pier headstock deflection at non-loaded side (mm – upwards)	

Note: us = microstrain ($\mu\varepsilon$).
Source: TMR.

Road profile

Generally the road profile was observed to be in good condition (based on the latest Level 2 inspection report), with the exception of the depression noted behind both abutments (more prominent behind abutment 2). There was no road surfacing across the deck of the bridge.

Figure 3.7: General arrangement – Dawson River Bridge

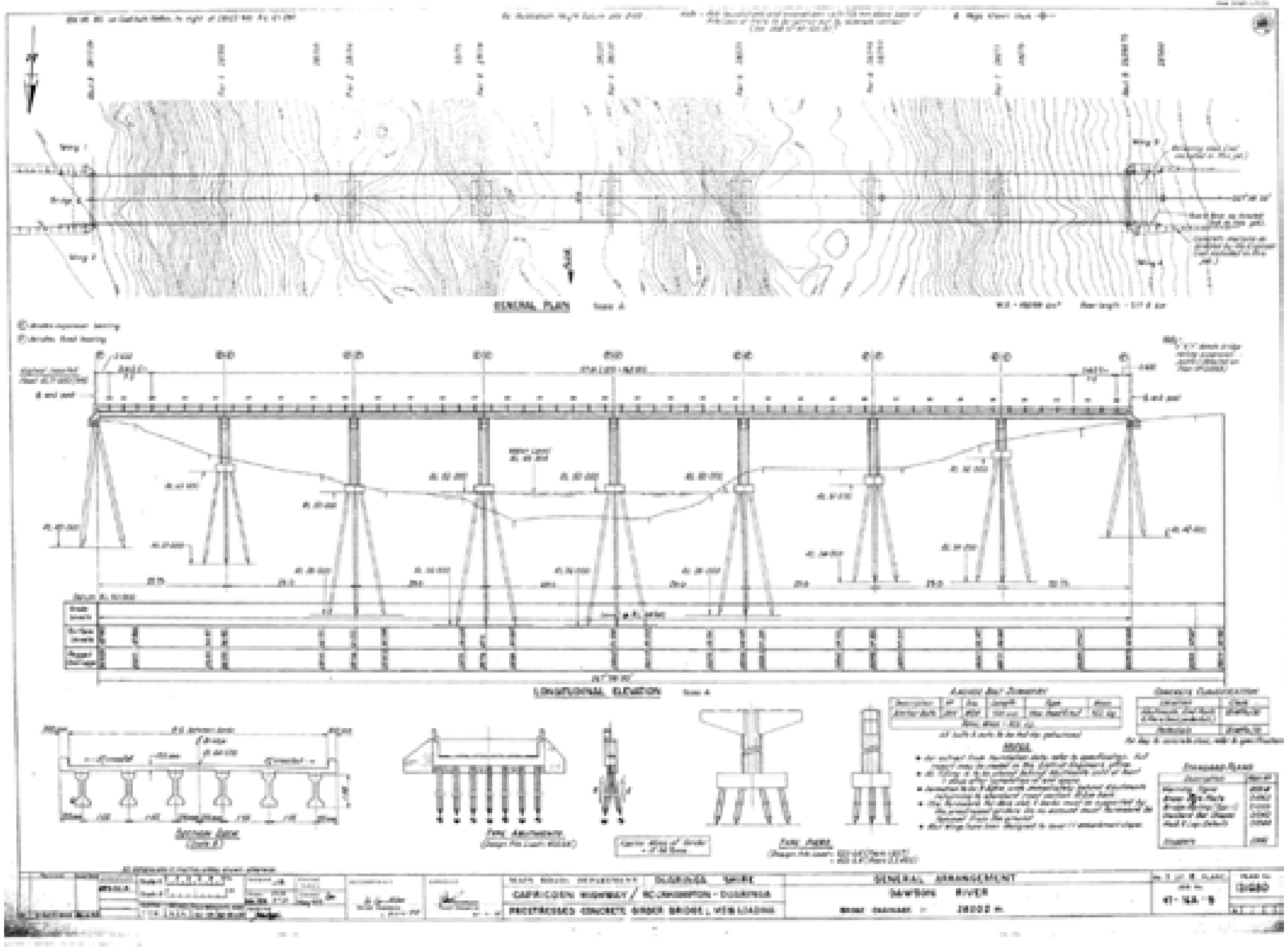

Source: TMR.

3.2.3 Neerkol Creek No. 1 Bridge

General information

The Neerkol Creek Bridge (No.1) (BIS ID 675) is a three span simply-supported, precast prestressed concrete I-girder bridge. It is located at chainage 18.813 km on Capricorn Highway (16A) 2 km east of Stanwell and approximately 20 km southwest of Rockhampton (Figure 3.8). The bridge is on a TMR-designated road train/heavy vehicle route with HML loading. The bridge services approximately 3 500 vehicles per day with an estimated 23% heavy vehicles.

The bridge was designed and constructed in 1974 for vehicle class HS20 and was considered to have a high level of redundancy. Summary geometric and structural information is presented in Table 3.7 and a general arrangement of the bridge is shown in Figure 3.9. The bridge has a two-lane two-way carriageway 7.9 m wide. It has no significant skew, longitudinal gradient or horizontal curvature. The deck has a crossfall of 2% from the centerline to both edges of the deck with no bituminous deck wearing surface.

Each superstructure span comprises five PSC I-girders which are 1118 mm high, 24.4 m long, acting compositely with a cast-in situ RC deck slab at least 165 mm thick and 300 mm x 300 mm kerbs. The girders are provided with lateral and torsional restraints in the form of cast-in situ RC cross-girder infills at each abutment and pier support and at two equally-spaced points along each span. The piers are portal frames with cast-in situ RC columns which are 1435 mm in diameter and cast-in situ RC headstocks which are 914 mm wide and 1524 mm high. The columns were sunk into rock at the time of construction. The abutment at either end of the bridge comprises an RC headstock with a ballast wall and seven precast RC 400 mm x 400 mm raked piles. The abutment wingwalls and batter protection consist of rock, placed after the January 2012 floods.

Figure 3.8: Neerkol Creek (No. 1) Bridge

Source: ARRB.

Table 3.7: Neerkol Creek Bridge – geometric and structural information

Parameter	Value
Number of spans	3
Span length	24 x 150 mm (span 1 and 3), 24 x 380 (span 2)
Skew	0 °
Carriageway width (mm)	7 928 (between kerbs)
Number of girders	5
Spacing of girders (mm)	1 980
Deck	165 mm thick in situ RC slab with 2% crossfall
Barrier	300 mm x 300 mm in situ concrete kerbs
Abutments	RC headstock on 7 No. 400 mm x 400 mm driven RC piles
Piers	RC headstock on 2 No. 1500 mm diameter RC cast-in place piles

Source: TMR BR675 as built drawings.

Bridge condition

TMR provided inspection reports for three previous Level 2 bridge inspections and one Level 3 inspection. The Level 2 inspections took place in 2000, 2002 and 2008. The inspection carried out in 2000 indicated that the bridge was rated in CS4 condition (Very Poor) due to the severe shear cracking observed on the pier P1 headstock. A Level 3 inspection was subsequently carried out and the cracks have since been repaired. Inspections carried out in 2002 and 2008 rated the bridge in CS2 condition (Fair); however, issues affecting the serviceability of the bridge were identified. Specifically, the Abutment 2 protection has scoured somewhat due to natural erosion. The most recent Level 2 inspection was undertaken in November 2012. The condition report documented an overall structure condition rating of CS3 (Poor), relating to cracks in the concrete of a non-structural element under the abutment. Cracking of the headstocks of all piers remains a concern. Crack maps can be found in the relevant inspection records.

Since 1990, the Neerkol Creek Bridge has had as many as 15 flooding events where the creek height has exceeded 5 m, coinciding with periods of heavy rainfall. The bridge has been subjected to high-velocity flow during each of these events, and it suffered significant scour damage behind both abutments during the 2011 floods. The bridge has since been repaired and the abutments reinforced with rock-boulder batter protection. Both road approaches have also been reinstated.

Recent structural assessment results

A Tier 1 structural assessment of the bridge was conducted by Parsons Brinckerhoff in 2013 using TMR's *Heavy Load Assessment: Project Brief for External Consultants* (QTMR 2013). Assessment results show that for the reference vehicles 2H – HML Road Train (6H – HML AAB-Quad). It was found that the:

- external girder was under-capacity due to sagging moment; ERB = 0.71 (0.69); SAR = 0.83 (0.81)
- external girder was under-capacity due to shear; ERB = 0.75 (0.72); SAR = 0.85 (0.82)
- internal girder is under-capacity due to shear; ERB = 0.67 (0.67); SAR = 0.81 (0.81).

More recently, a preliminary analysis undertaken by TMR prior to testing to determine the theoretical strain and deflection values in the substructure to provide an upper limit or guidance to on-site testing (Table 3.8).

Figure 3.9: General arrangement – Neerkol Creek Bridge

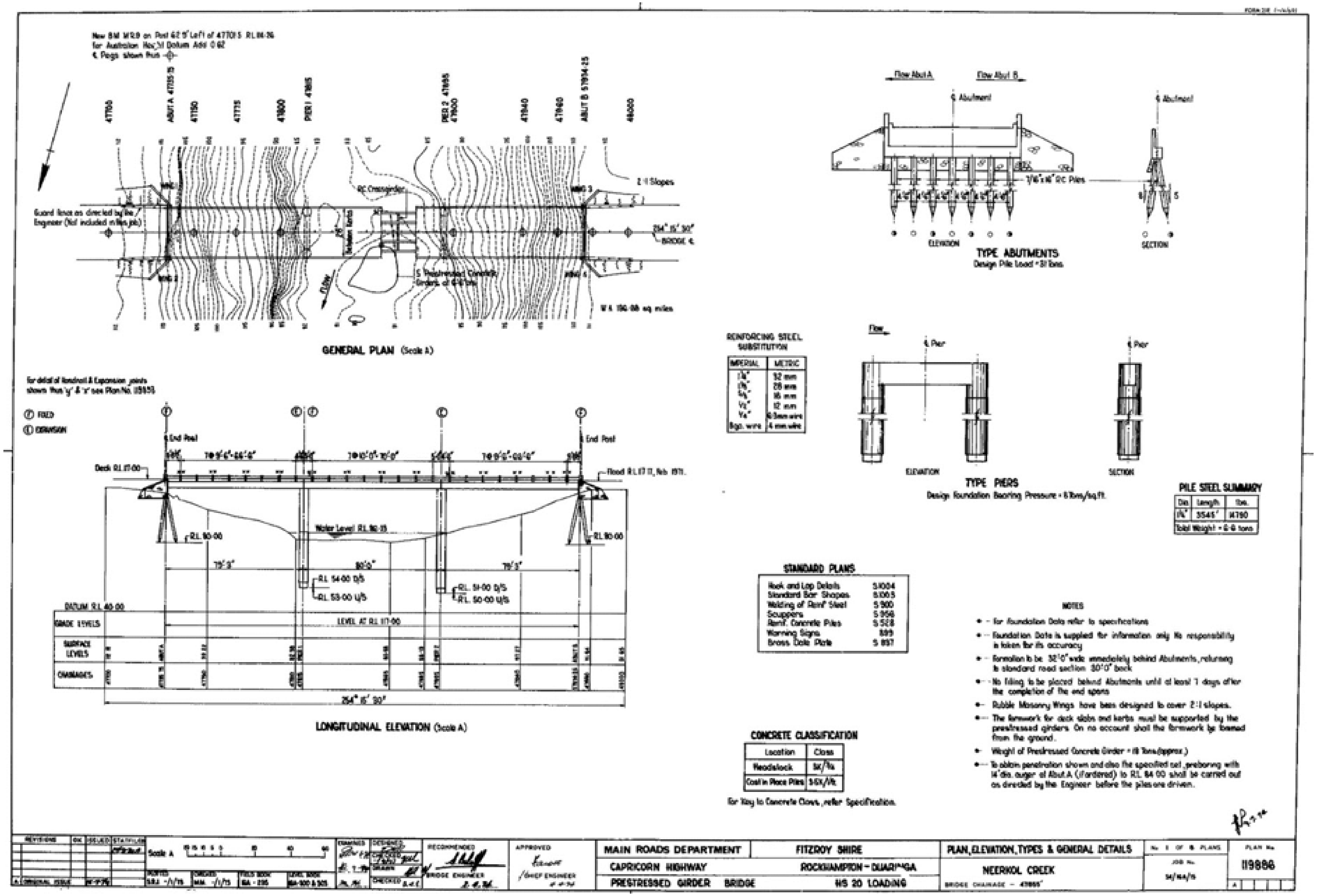

Source: TMR.

Table 3.8: Summary of theoretical strains and deflections for the Neerkol Creek Bridge (for various vehicles)

Parameter	Theoretical strains and deflections
Pier headstock mid-span strain	▪ 30 $\mu\varepsilon$ for C48 , C79.5 and Type1 road train
Pier column strain	▪ 22 $\mu\varepsilon$ for C48 ▪ 28 $\mu\varepsilon$ for C79.5 ▪ 27 $\mu\varepsilon$ for Type 1 road train
External girder deflection	▪ 10 mm for C48 ▪ 12 mm for C79.5 ▪ 11 mm for Type 1 road train
First fundamental frequency	▪ 4.3 Hz, vertical bending

Source: TMR.

Road profile

Despite the installation of a new road surfacing after the 2011 floods, the road profile on the approach to Abutment 1 (from Rockhampton) was in poor condition, with several potholes and delamination in the road seal along the wheel path. The approach to Abutment 2 was in good condition. There was no road surfacing across the deck of the bridge.

3.3 Test Vehicles

In keeping with the original research objectives, a suite of test vehicles with different specifications and characteristics was required. More specifically, the following attributes were identified for the test vehicles:

- a hydro-pneumatic four-axle crane
- maximum legal loading
- different suspension characteristics (e.g. steel-leaf vs air bag suspension)
- a longer vehicle, i.e. type 1 or 2 road train.

The following test vehicles were used for the controlled test programs.

3.3.1 Canal Creek Bridge

The following four test vehicles were used in the load testing of the bridge:

- a 4-axle 48 t all-terrain crane (Figure 3.10) (CR)
- a steel-leaf suspension articulated semi-trailer of 1-2-3 axle configuration (Figure 3.11) (ST1)
- an air-bag suspension articulated semi-trailer of 1-2-3 axle configuration (Figure 3.12) (ST2)
- a steel-leaf suspension road train with two trailers (Figure 3.13) (RT).

The semi-trailers had a legal limit of 45.5 t while the road train had an 85 t legal limit.

Figure 3.10: Hydro-pneumatic crane (CR) (Canal Creek Bridge)

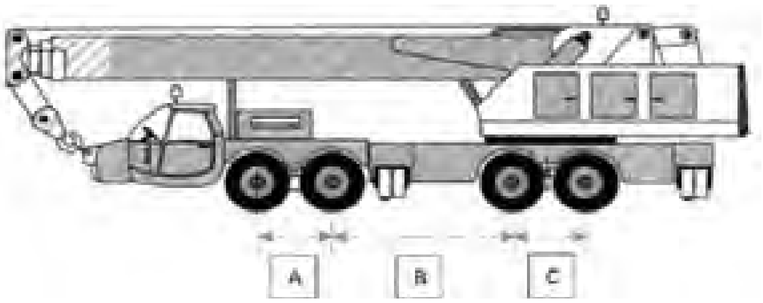

Axle spacing (m)

	A	B	C	Total
Standard	1.65	2.35	1.65	5.65
Measured	1.7	2.05	1.71	5.46

Axle weight (t)

	1	2	3	4	Total
Standard	12	12	12	12	48
Measured	11.64	11.84	11.86	11.62	46.96

Vehicle track and tyre width:

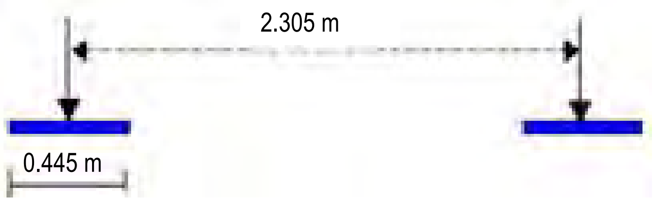

Figure 3.11: Steel-suspension semi-trailer (ST1) (Canal Creek Bridge)

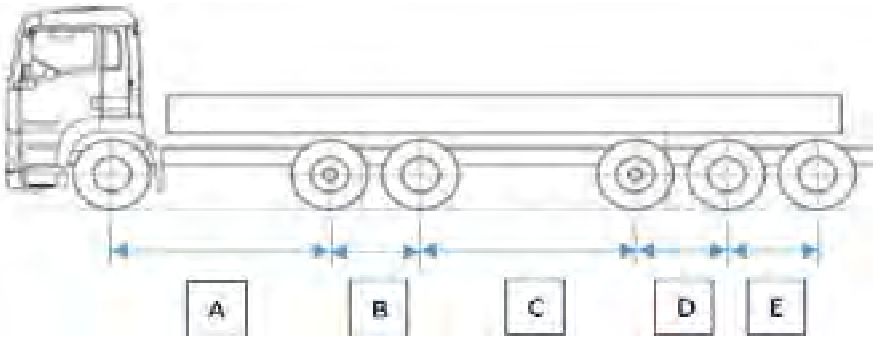

Axle spacing (m)

	A	B	C	D	E	Total
Standard	3	1.2	4.4	1.2	1.2	11
Measured	4.7	1.4	7	1.2	1.2	15.5

Axle weight (t)

	1	2	3	4	5	6	Total
Standard	6	8.5	8.5	7.5	7.5	7.5	45.5
Measured	5.46	17.44		17.12			40.02

Note: weights are not equally distributed between axles in the tandem and tri-axle groups. No exact axle weights are available. Vehicle track and tyre width are the same for the road train in Figure 3.13.

Figure 3.12: Air-suspension semi-trailer (ST2) (Canal Creek Bridge)

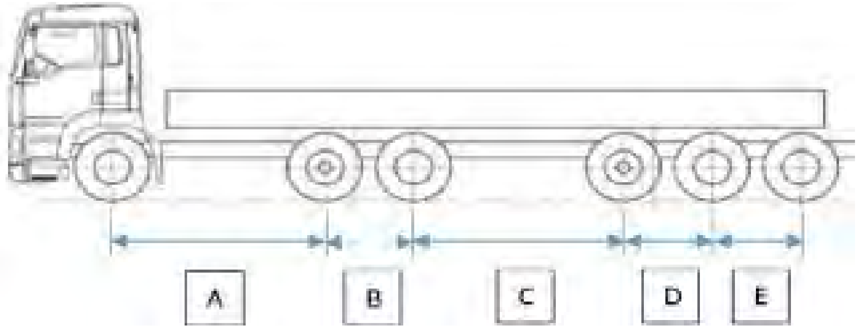

Axle spacing (m)

	A	B	C	D	E	Total
Standard	3	1.2	4.4	1.2	1.2	11
Measured	3.3	1.4	7.7	1.4	1.4	15.2

Axle weight (t)

	1	2	3	4	5	6	Total
Standard	6	8.5	8.5	7.5	7.5	7.5	45.5
Measured	6.14	7.14	6.88	7.68	8.14	8.04	44.02

Note: Vehicle track and tyre width are the same for the road train in Figure 3.13.

Figure 3.13: Road train (RT) (Canal Creek Bridge)

Axle spacing (m)

	A	B	C	D	E	F	G	H	I	J	Total
Standard	3	1.2	4.4	1.2	1.2	4.4	1.2	4.4	1.2	1.2	23.4
Measured	4.7	1.4	7	1.2	1.2	4.4	1.2	6.5	1.2	1.2	30

Axle weight (t)

	1	2	3	4	5	6	7	8	9	10	11	Total
Standard	6	8.5	8.5	7.5	7.5	7.5	8.5	8.5	7.5	7.5	7.5	85
Measured	5.46	17.44		17.12			14.06		19.38			73.46

Vehicle track and tyre width (rear tyres):

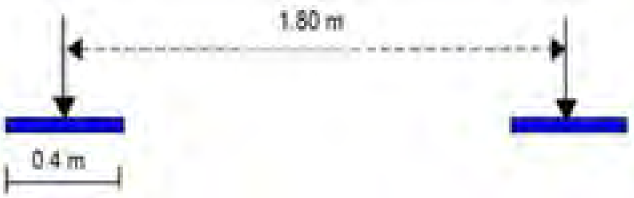

Note: weights are not equally distributed between axles in the tandem and tri-axle groups. No exact axle weights are available.

3.3.2 Dawson River Bridge and Neerkol Creek No. 1 Bridge

Four test vehicles were selected as the test vehicles for both Dawson River Bridge and Neerkol Creek Bridge:

- a 4-axle 48 t mobile crane (Figure 3.14) (CR1)
- a steel-leaf suspension 40 t t mobile crane (CR2)
- a steel-leaf suspension articulated type 1 road train of 1-2-3-3 axle configuration (Figure 3.16) (RT1)
- an air-bag suspension articulated type 1 road train of 1-2-3-3 axle configuration (Figure 3.16) (RT2).

RT1 and RT2 differed slightly from the original TMR vehicle specification in terms of axle groups and spacing. However, loads per axle group were consistent with GML loading. Weighbridge certificates were provided for RT1 and RT2.

Figure 3.14: Hydro-pneumatic crane details (CR1) (Dawson and Neerkol tests)

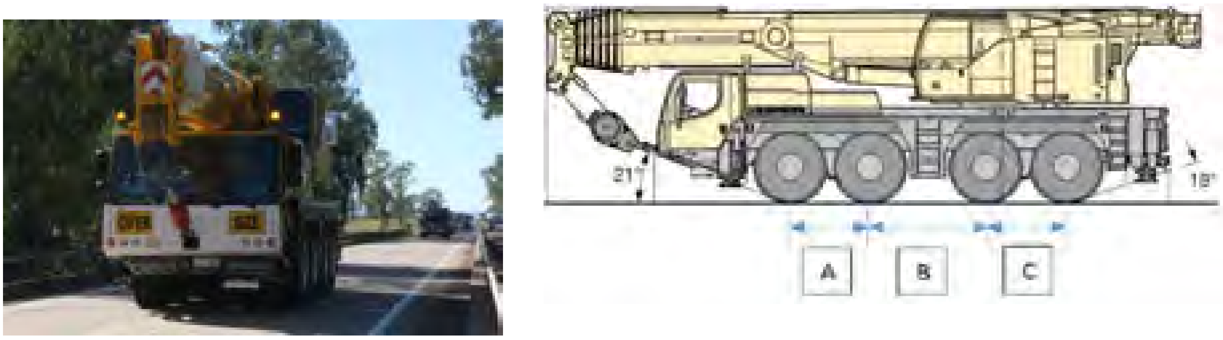

Axle spacing (m)

	A	B	C	Total	Track width (m)	Tyre width (m)
Standard	1.65	2.35	1.65	5.65	2.175	0.525
Measured	1.7	2.05	1.71	5.46	2.1	0.525

Axle weight (t)

	1	2	3	4	Total
Standard	12	12	12	12	48
Measured	11.625	11.625	11.97	11.97	47.19

Figure 3.15: Steel suspension crane details (CR2) (Dawson and Neerkol tests)

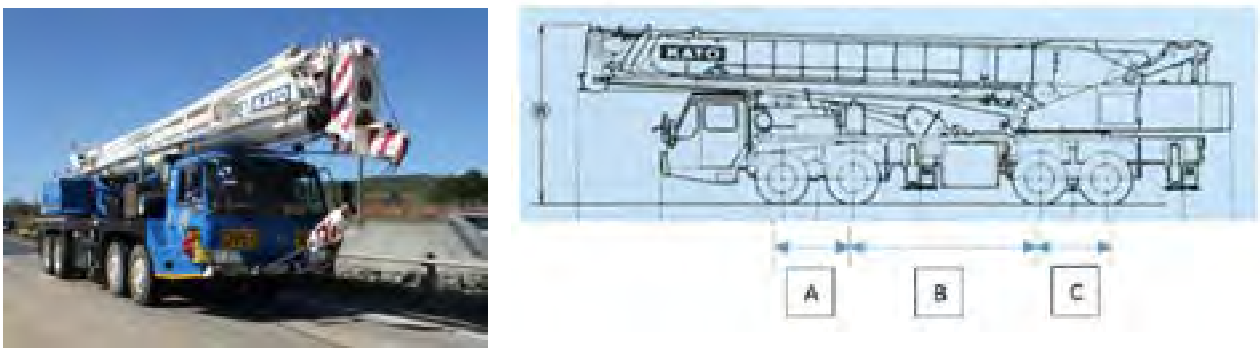

Axle spacing (m)

	A	B	C	Total	Tyre width (m)	Track width (m)	
Measured	1.45	3.9	1.35	6.7	0.356	2.58	Front
					3.00	2 x 0.300	Rear

Axle weight (t)

	1	2	3	4	Total
Measured	8	8	12	12	40

Figure 3.16: Road train details (RT1 and RT2) (Dawson and Neerkol tests)

RT1: Steel-suspension road train

RT2: Air-suspension road train

Axle spacing (m)

	A	B	C	D	E	F	G	H	I	J	K	Total
Standard	3	1.2	4.4	1.2	1.2	4.4	1.2	-	4.4	1.2	1.2	23.4
RT1-Measured	4.5	1.4	4.8	1.2	1.2	4.3	1.2	1.2	4.25	1.2	1.2	26.45
RT2-Measured	5.1	1.4	4.5	1.2	1.2	3.5	1.2	1.2	3.7	1.2	1.2	25.4

	Track width (m)		Tyre width (m)		Tyre patch (m)			
	steer	*trailer*	*steer*	*trailer*	*trailer only*			
	X1	X2	Y1	Y2	Zlength	Zwidth, total	Gap	Area
RT1	2.13	1.83	0.27	0.24	0.3	0.57	0.09	0.144
RT2	2.16	1.85	0.24	0.22	0.3	0.55	0.11	0.132

Axle weight (t)

Wheel No.	1	2	3	4	5	6	7	8	-	10	11	12	Total
Standard	6	16.5		20			20		-	20			82.5

Wheel No.	1	2	3	4	5	6	7	8	9	10	11	12	Total
RT1-Measured	6.06	16.35		19.91			19.93			19.92			82.17
RT2-Measured	6.72	15.86		19.96			19.94			19.91			82.39
	steer	tandem		triaxle			triaxle			triaxle			

3.4 Instrumentation

3.4.1 General Overview

Individual plans for each bridge were developed by the Working Group (WG) based on the research priorities identified. These priorities included:

- dynamic performance of the superstructure and substructure
- comparison of dynamic increment of superstructure and substructure
- dynamic responses of superstructure and substructure (based on accelerometer data)

- the movement of each bridge when loaded and unloaded
- transverse load distribution on the main span.

Other important factors for inclusion relating to the overall project objectives were:

- influence of vehicle details (i.e. type, suspension and damping characteristics)
- influence of vehicle dynamic characteristics
- influence of bridge and vehicle damping
- influence of bridge geometry and boundary conditions
- influence of road profile (e.g. local, global, and approaches)
- torsional effects
- bridge responses to live traffic
- frequency matching between bridge and vehicle (holistically and on a component level).

Based on these objectives, the following instrumentation sensors and transducers were selected to fulfil these requirements:

- strain gauges: bending and compressive strains for girders, headstocks and columns
- string potentiometers/LVDTs: mid-span and substructure vertical deflections
- accelerometers: three-dimensional vibrations for girders (mid-span and ends) and headstock where applicable; also to be used to measure the modal response of the structure for impact tests
- tilt meters: global and local 3D rotations of superstructure and substructure components (as required)
- proximity probes: bearing compression based on gap opening/shortening (Dawson and Neerkol only).

The following sections summarise the instrumentation selection and layout of selected and installed for each test bridge, as well as the test vehicles for Dawson and Neerkol bridges.

3.4.2 Bridges

Instrumentation plans can be found in Figure 3.17 Figure 3.17 for the Canal Creek Bridge, Figure 3.18 to Figure 3.20 for the Dawson River Bridge and Figure 3.21 to Figure 3.23 for the Neerkol Creek Bridge. Additional details regarding the instrumentation and specifications can be found in the specific test reports.

Figure 3.17: General instrumentation layout for superstructure – Canal Creek Bridge

(a) General instrumentation layout for superstructure – Canal Creek Bridge

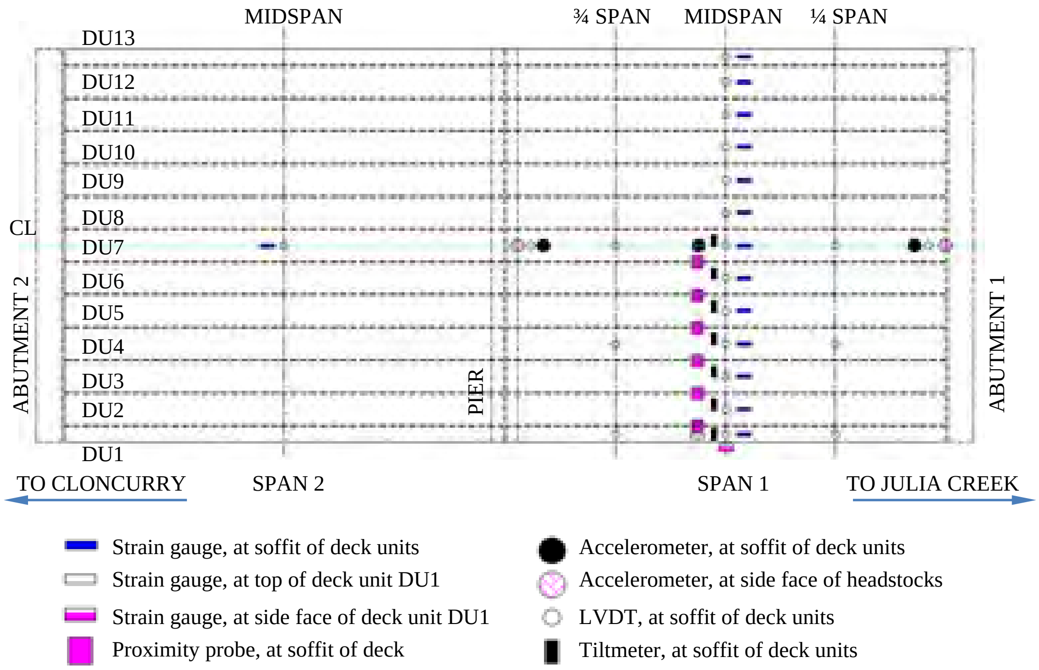

(b) strain gauge placement on kerb unit

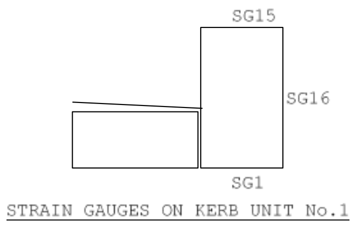

(c) Accelerometer placement on substructure

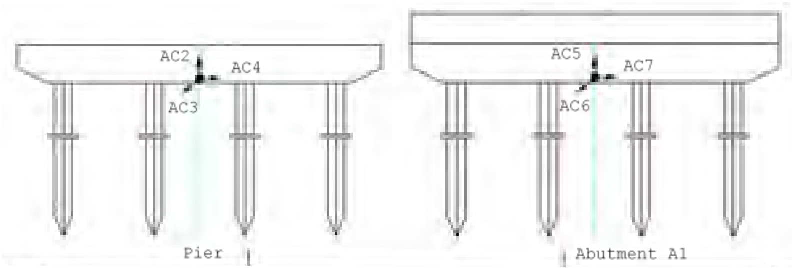

Source: ARRB Group Ltd.

Figure 3.18: General instrumentation layout for superstructure – Dawson River Bridge

Source: ARRB Group Ltd.

Figure 3.19: General instrumentation layout for substructure – Dawson River Bridge

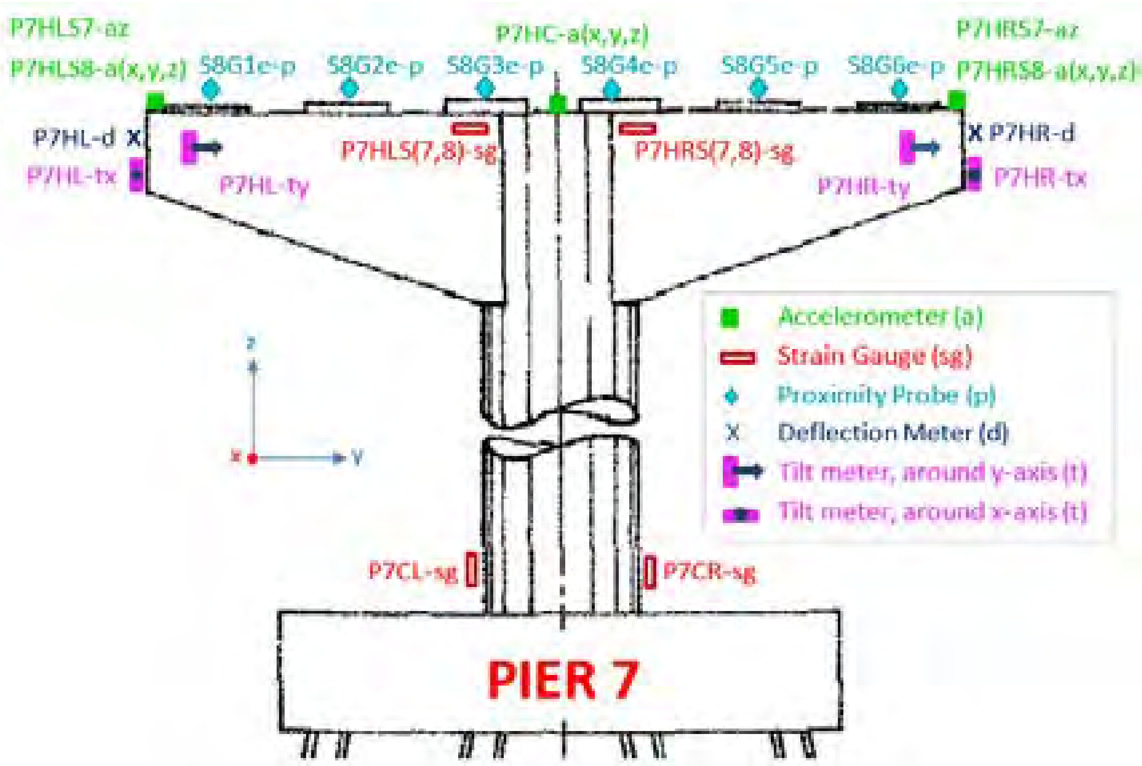

Source: ARRB Group Ltd.

Figure 3.20: Layout for proximity probes (left) and accelerometers (right) – Dawson River Bridge

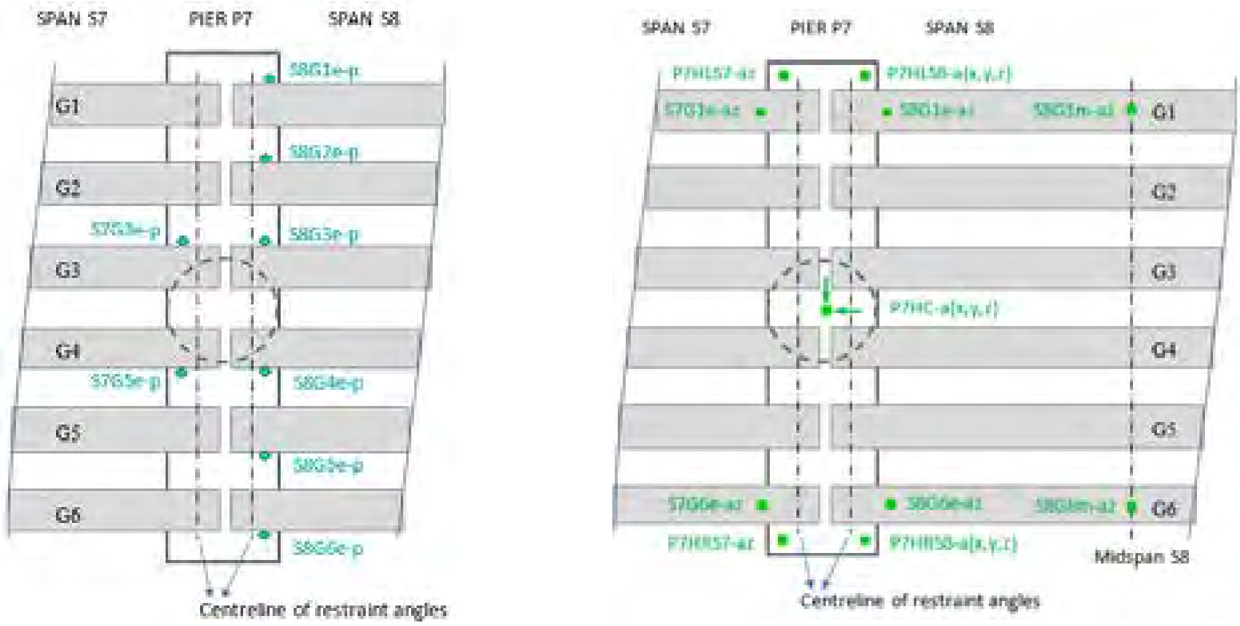

Notes:

1 Proximity probes were installed at the side of girders.
2 Girders' accelerometers were installed at the soffit of girders and in upward direction.
3 Headstock's accelerometers were installed on top surface of the headstock. The vertical accelerometers were in upward direction.

Source: ARRB Group Ltd.

Figure 3.21: General instrumentation layout for superstructure – Neerkol Creek Bridge

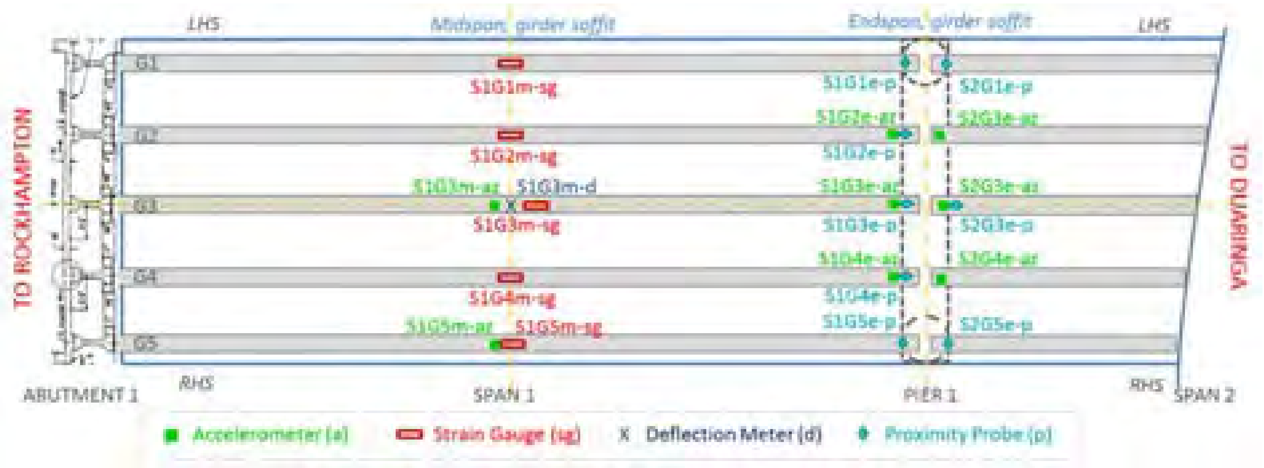

Source: ARRB Group Ltd.

Figure 3.22: General instrumentation layout for substructure – Neerkol Creek Bridge

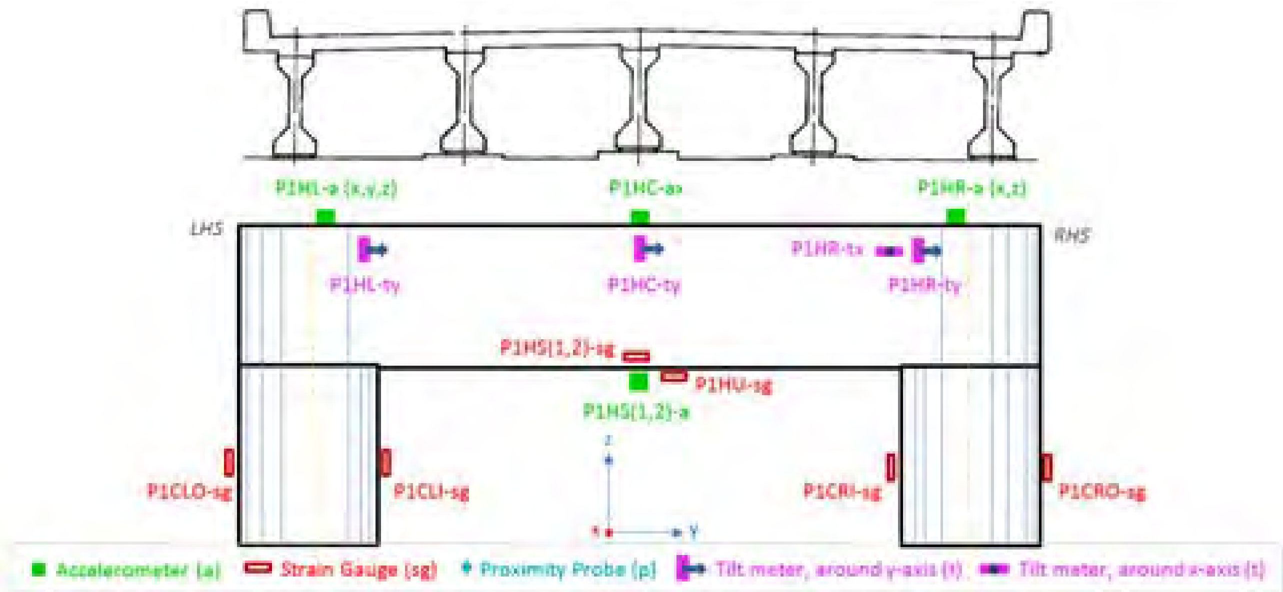

Source: ARRB Group Ltd.

Figure 3.23: Layout for proximity probes (left) and accelerometers (right) – Neerkol Creek Bridge

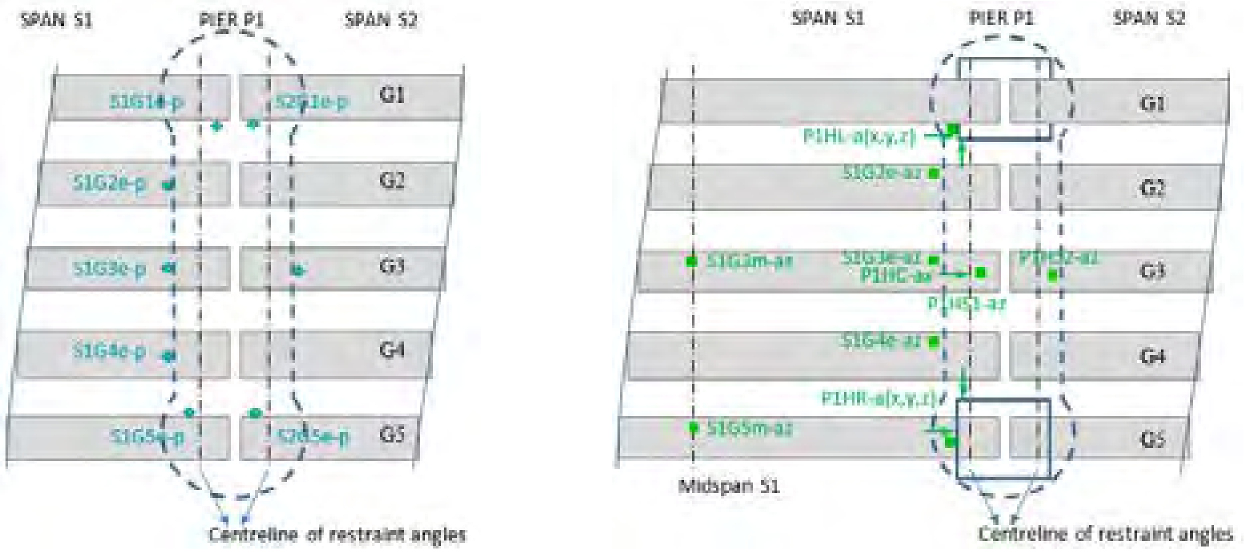

Notes:

1 Proximity probes were installed at the soffit of girders or at side of girders.
2 Girders' accelerometers were installed at the soffit of girders and in upward direction.
3 P1HL-az and P1HR-az were installed in downward direction.
4 P1HS1-az and P1HS2-az were installed at the soffit of the headstock and in upward direction.

Source: ARRB Group Ltd.

3.4.3 Vehicles

In addition to bridge instrumentation, the instrumentation of test vehicles was discussed due to the future requirement to develop a Vehicle-Bridge Interaction (VBI) model. Key variables of interest were vertical deflection and acceleration, wheel/axle load, load distribution across the axle groups, and the frequency response of the vehicle (investigating axle hop and body bounce of the test vehicles). Dr Lloyd Davis was subcontracted to develop a vehicle instrumentation specification to address these requirements.

The instrumentation of the vehicles was implemented in Year 2 of the project, with the selection of the road trains for instrumentation on the Dawson River Bridge and Neerkol Creek Bridge tests. Cranes were excluded due to the complex nature of the required instrumentation, which had implications in terms of timing and budget. A simple instrumentation plan was subsequently implemented, with the focus on the deflections above each axle group (excluding the steer axle) and the body bounce frequencies of the vehicles. The representative layout of the instrumentation for each road train is shown in Figure 3.24. Four accelerometers were placed on the body of the vehicle above each tandem or triaxle group to measure vertical vibrations of the vehicle for the duration of the controlled tests.

Figure 3.24: Vehicle instrumentation layout for RT1 and RT2

Source: ARRB.

3.5 In-Service Monitoring

To gain an understanding of the performance of each bridge under in-service conditions, a program of continuous monitoring was conducted. The monitoring priorities included:

- peak mid-span girder strains and deflections
- peak strains and deflections of substructure elements
- traffic using each bridge, i.e. count, mix of traffic, trends in traffic movement
- identification of any risks posed to each bridge due to high-load traffic events.

In-service monitoring of each bridge took place at the completion of the controlled testing program.

Full instrumentation was used for the Canal Creek Bridge and the Neerkol Creek Bridge. A selection of sensors were used for in-service monitoring of the Dawson River Bridge (four channels for bending strains, four channels for deflection, see Figure 3.25).

At the completion of all in-service monitoring, all instrumentation was removed from both bridges.

Figure 3.25: Instrumentation selected for in-service monitoring – Dawson River Bridge

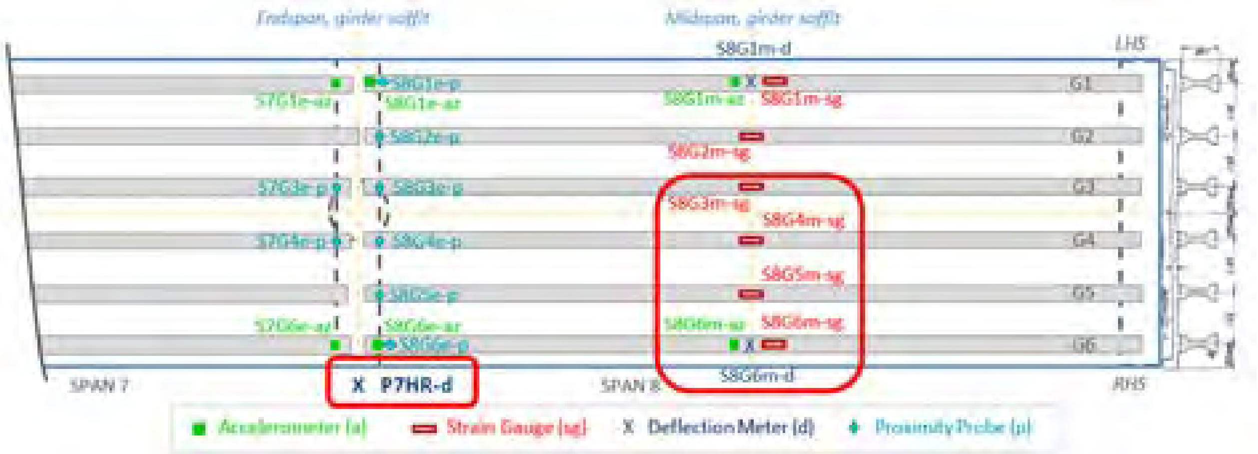

Source: ARRB Group Ltd.

3.6 Test Schedule

The test vehicles crossed the bridges at speeds between crawling speed (approximately 5 km/h) and the speed limit (110 km/h) in both directions and in different transverse locations on each bridge. For the crawl tests, vehicles travelled down the centre of the bridge as well as in the marked lane (the outside face of the wheel was approximately located 0.6 m from the face of the kerb). Additional crawl runs were conducted for all test vehicles travelling closer to the kerb for the Canal Creek and Dawson River Bridges to investigate edge beam and headstock loading effects.

For higher speeds, each vehicle crossed the bridge in the designated lane at 20, 40, 60 and 80 km/h and free speed up to the speed limit. For higher-speed runs, vehicles tended to travel slightly away from the kerb towards the centre of the bridge.

A detailed schedule of individual vehicle runs at each test bridge can be found in the individual test reports. These schedules provide details on vehicle type, vehicle speed, direction of travel, and transverse location on the deck.

The dates when the load testing and subsequent in-service monitoring was carried out are shown in Table 3.9.

Table 3.9: Dates of load testing

	Controlled tests	In-service monitoring
Canal Creek Bridge	29 April–2 May 2014	2–8 May 2014
Dawson River Bridge	13 May 2015	14–19 May 2015
Neerkol Creek Bridge	15 May 2015	15–20 May 2015

3.7 Additional Information

3.7.1 Specific Test Logistics

Specific details regarding the organisation and coordination of the logistics for each test event can be found in the relevant test reports listed in Section 3.1. A summary of key items follows.

Instrumentation subcontractor

A subcontractor, SLR Consulting, was engaged to carry out all instrumentation installation, data collection and preliminary presentation of results and reporting. Additional test activities carried out by SLR were modal impact tests, vehicle instrumentation and data collection (for Dawson and Neerkol only), and imaging of vehicles during test runs to confirm the transverse locations of wheel loads across the deck (for Dawson and Neerkol only).

Site management

Site and facilities management was carried out by RoadTek under instruction from TMR.

Traffic management

A local traffic management subcontractor was engaged by RoadTek.

Vehicle hire

Vehicle hire was coordinated by ARRB and TMR, with TMR directly engaging local heavy haulage contractors to provide the specified test vehicles. Weighbridge certificates were obtained for all test vehicles.

Permits

An individual trip permit was required for the 48 t crane to travel to and traverse the Canal Creek Bridge for the purposes of the test. This was coordinated by TMR.

3.7.2 Modal Impact Tests

To determine the bridge's natural dynamic frequency responses and modal shapes, a modal impact test was conducted prior to the controlled load tests. An overview of the test is shown in Figure 3.26. Impact tests were conducted using a 6 kg hammer to impact the soffit of the deck at predetermined grid points on the deck. The response of the deck to the impact was recorded using accelerometers attached to the deck at various locations. Analysis of the results was conducted by SLR Consulting.

Further details regarding the background of the method, how the results are interpreted and the findings from site measurements can be found in the relevant test reports noted in Section 3.1.

3.7.3 Vehicle Transverse Positions

Due to the sensitivity of results to the transverse location of the vehicle, the location of each test vehicle was recorded at various positions along the test span. To accommodate this, the bridge deck surface was marked up in a series of lines at 100 mm spacing from the kerbs and at key locations (e.g. centreline of bridge, centreline of lane) at the abutment, pier and mid-span using high-visibility paint (Figure 3.27). To record the location of the vehicle during each test, the position of the vehicle in relation to the line markers was visually noted during the passage of the vehicle. High-speed images were also taken using a GoPro camera mounted on the guardrail prior to the tests.

Figure 3.26: Overview of modal test equipment

(a) Overview of modal test equipment

Source: ARRB Group Ltd.

(a) Modal test in progress

Source: ARRB Group Ltd.

Figure 3.27: Example of transverse location markers on deck at the Neerkol Creek Bridge

Source: ARRB Group Ltd.

4 INFLUENCE OF BRIDGE CHARACTERISTICS

4.1 Introduction

As discussed in Section 2.2.1, the dynamic response of bridges plays a significant role in the potential amplification of live load. The various influential factors relating to bridge specific characteristics and their influence on dynamic load amplification are summarised in Table 4.1. The following sections presents and discusses the research findings from the current project in context of these various factors. All discussion will be discussed in terms of frequency and dynamic response as required and make reference to the dynamic increment values quantifying the amplification of live load for representative vehicles (such as 48 t hydro-pneumatic crane, CR1, steel suspension road train, RT1) travelling at 80 km/h (which was a vehicle common to each test bridge and consistently resulted in peak results). Understanding these concepts and their influence on load amplification will then provide a platform to discuss dynamic interaction processes and learnings for TMR.

Table 4.1: Factors influencing dynamic load amplification

Scenario	Effect	Implication on dynamic load amplification (DLA)
Damping/Stiffness	Low levels of damping Increase in stiffness	Increase
Span length	Short spans	Increase
Bridge & component type	Slender structures (e.g. PSC girders)	Increase
	Increasing number in girders superstructure)	Decrease
	Substructure influence	Unknown
Fundamental frequency	Coincidence with fundamental frequency Governs dynamic response	Increase
Fixture & boundary conditions at piers/ abutments	Changes in frequency response Increase in stiffness	Decrease

4.2 Fundamental Responses

4.2.1 Fundamental Frequency

The fundamental frequencies of a bridge are a significant contributor to the amplification of load as it governs the structural dynamic response of the bridge. It incorporates the span length, geometric form, stiffness and boundary conditions (González 2009a). Prior to reviewing the dynamic frequency response of each test bridge under live load, a review of the fundamental frequency data was conducted based on modal analysis tests carried out for each bridge, summarised in Table 4.2. Each bridge exhibited fundamental bending and torsion frequencies. Fundamental bending and torsion responses for Dawson and Neerkol bridges were similar, with bending frequencies between 4 and 6 Hz and torsional frequencies between 13 and 15 Hz. This is expected for PSC girder bridges of similar geometric design and span length. The Canal Creek Bridge exhibited a stiffer response in bending, but a similar torsional response for the superstructure. Also of significance was the influence of the transverse stressing bars (TSB) for the Canal Creek Bridge at 12.3 Hz, which was close to the fundamental bending frequency but invokes a distinct frequency response.

Table 4.2: Fundamental frequency results for each test bridge (from modal impact tests)

Canal Creek Bridge (8 m span)		Dawson River Bridge (23 m span)		Neerkol Creek Bridge (24.5 m span)	
Fundamental frequency (Hz)[1]		Fundamental frequency (Hz)		Fundamental frequency (Hz)	
12.3	Bending (superstructure): ▪ influenced by transverse stressing bar ▪ similar to fundamental bending	5.9[2]	Bending (superstructure)	4.6[2]	Bending (superstructure)
14.6[2]	Bending (superstructure)	15.0[3]	Torsion (superstructure)	13.3[3]	Torsion (superstructure)
19.2[3]	Torsion (superstructure)	35.5	Longitudinal rotation of pier (parallel with road)	2.5	Longitudinal rotation of pier (parallel with road)
29.0	Higher-order torsion (superstructure)	1.7	Rigid body rotation of headstock		
> 35	Bridge not influenced by vehicles				

5 Substructure modal response not determined for the Canal Creek Bridge.

6 Fundamental frequency for bending.

7 Fundamental frequency for torsion.

Modal analysis was also carried out on the substructure components for the Dawson and Neerkol bridges. Fundamental substructure dynamic responses were noted to be inherently different. For the Dawson River Bridge, the torsional mode of the superstructure was intrinsically linked with the single column and cantilever headstock design, which showed greater propensity for transverse rotation about the direction of travel (transverse rotation), pivoting cyclically about the base of the column. The rigid body rotation of the cantilevers at a frequency of 1.7 Hz was also noted to influence the rotation and overall dynamic response of the pier. A fundamental frequency of 35.5 Hz was identified for the pier in a longitudinal direction (parallel to direction of traffic); however, the high frequency level indicates the relative stiffness of the pier in this direction. Fundamental transverse rotations were not identified for the Neerkol Creek Bridge, which highlights the significant stiffness of the piers in this direction due to the portal frame design, but a low frequency response at 2.5 Hz was determined for pier rotations in the direction of travel (longitudinal rotations).

Whilst no specific modal data was obtained for the Canal Creek Bridge, the piers and abutment components were anticipated to respond more rigidly in vertical and transverse directions due to the configuration of the headstocks and the nature of the driven piles. Some longitudinal rotation of the piers was expected but anticipated to be restricted due to the shorter span length and inherent stiffness characteristics of the superstructure, which contributes to the relative freedom of pier rotation (in terms of boundary conditions and fixtures, see Section 2.2.1).

4.2.2 Critical Damping

Various views exist in the literature regarding the influence of damping characteristics on the dynamic structural response. Some state that dynamic load amplification is less likely for structures with higher levels of damping (Bezet al. 1987; Billing 1984; Paultre et al. 1992), whereas others argue damping is an insignificant consideration and more likely to be influential for multiple loading events (González 2009).

In order to review the contribution of damping characteristics to the amplification or suppression of dynamic load, critical damping results from the modal analysis for each bridge are presented in Table 4.3 (in relation to the superstructure only). In relation to fundamental frequencies, the Dawson and Neerkol bridges exhibited similar low levels of damping of 4.6% and 4.5% of critical damping respectively for the superstructure. In comparison, the damping levels for the Canal

Creek Bridge were higher at 6.5%, indicating lower stiffness in bending. The influence of the transverse stressing bars improves the damping capability of the superstructure to 4.0%. Note that the modal masses for the Dawson and Neerkol bridges are similar. Substructure damping capabilities were not determined for all bridges.

Table 4.3: Critical damping and modal mass results for bridge superstructure (from modal impact tests)

(a) Canal Creek Bridge

Fundamental Frequency (Hz)	Mode	Critical Damping (%)
12.3	Bending (with TSB)	4.0
14.6	Bending (fundamental)	6.5
19.2	Torsion (fundamental)	4.8
29.0	Higher-order torsion	3.4

(b) Dawson River Bridge

Fundamental Frequency (Hz)	Mode	Modal Mass (t)	Critical Damping (%)
5.9	Bending	78	4.6

(c) Neerkol Creek Bridge

Fundamental Frequency (Hz)	Mode	Modal Mass (t)	Critical Damping (%)
4.6	Bending	73	4.5

4.3 Dynamic Response of Structure to Load

4.3.1 Overview

The contribution of previously-identified factors (see Section 2) on the dynamic response of each bridge under live load is of interest. For example, bridge or component types and geometric configurations are noted to also be influential for load amplification, in particular slender structures, box girder or prestressed concrete girder structures have previously been documented to yield greater dynamic responses (Cantieni et al. 2010; McLean & Marsh 1998; Paultre et al. 1992). To this end, some international jurisdictions have provided specific load allowances to accommodate for structure type, as well as material type. The boundary and fixture conditions of various components have also been noted to influence the overall response of the structure. Notably absent from the literature is the influence and contribution of the substructure on dynamic response and load amplification in isolation and in interaction with the superstructure.

In order to investigate these influences in relation to the TMR network, the results from the current project were reviewed and they are presented in the following sections. The test results will be discussed based on the influence of the fundamental characteristics of the structure globally and the contributions of the superstructure and substructure individually, the geometric configurations of each structure type, span lengths, and boundary conditions and fixtures. Material type shall not be considered herein due to all test bridges comprising reinforced and prestressed concrete components. Discussions are ultimately related to dynamic load amplification.

4.3.2 Superstructure

For the current project, two types of bridge superstructures were investigated; the first being a short-span deck unit bridge (Canal Creek Bridge) and the second being a longer-span prestressed concrete (PSC) girder and in situ slab bridge (applicable to Dawson and Neerkol bridges). Of the latter structure type, each test bridge had different substructure forms, with the Dawson River Bridge having a single-column cantilever pier and a portal frame pier for the Neerkol Creek Bridge.

Initial comparison is made to the frequency responses of the superstructures to dynamic loading, commencing with a review of mid-span accelerometer data using a representative case for the steel suspension road train (RT1) travelling at 80 km/h.

The mid-span acceleration response of each bridge is shown in Figure 4.1. All three acceleration patterns for each bridge were unique; however, the longer-spanned PSC bridges (Dawson and Neerkol) showing prolonged vibration after the passage of RT1 compared to the Canal Creek Bridge, indicative of the length of the span, the lower stiffness and the level of damping afforded by these superstructure types. The inherent frequency characteristics of the PSC bridges in a loaded and unloaded state is evident in the waveforms, particularly in the resonant responses after the passage of the vehicle.

Figure 4.1: Mid-span vibration for each test bridge for RT1 travelling in the lane at 80 km/h

(a) Canal Creek Bridge

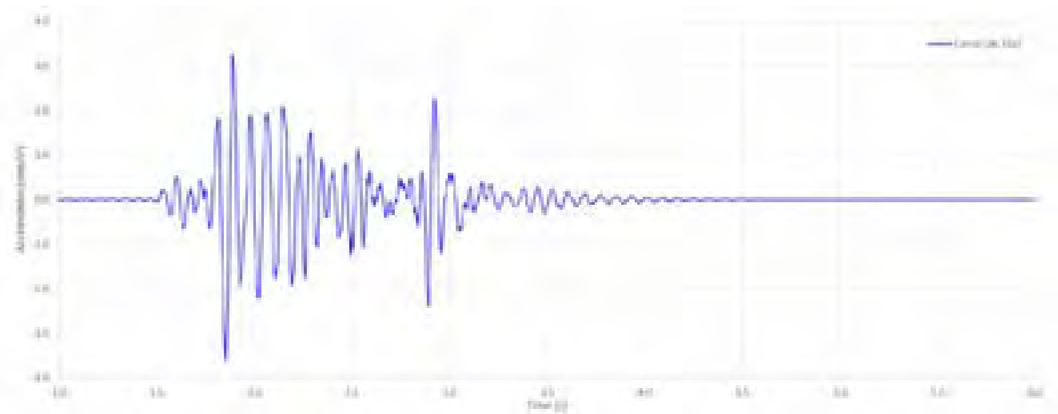

(b) Dawson River Bridge

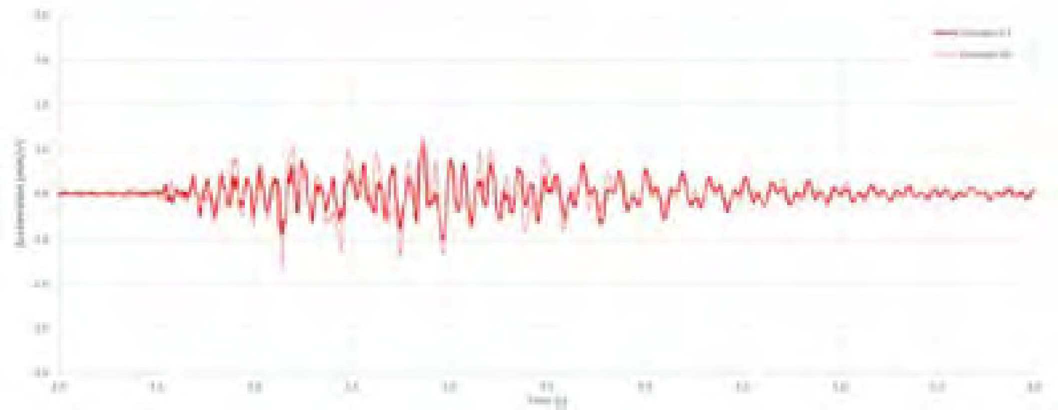

(c) Neerkol Creek Bridge

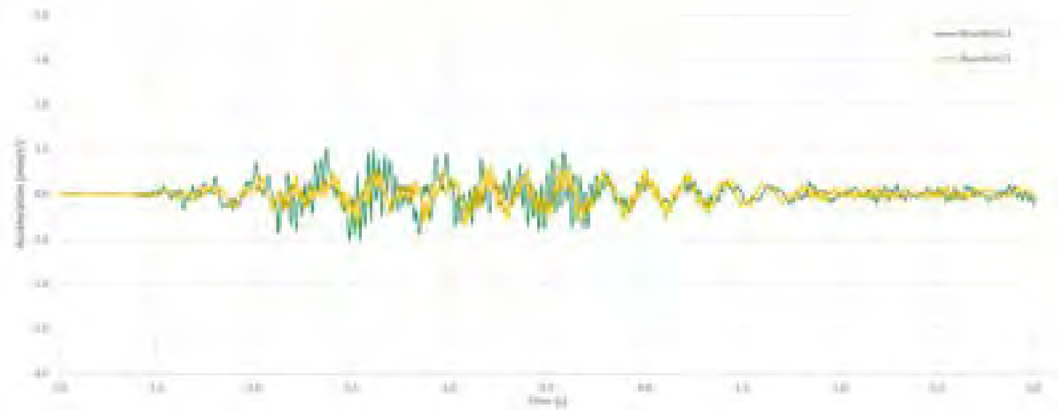

In comparison, the amplitude of the response for the Canal Creek Bridge was greater than for the Dawson and Neerkol bridges, indicative of the shorter span of this bridge. However signal decay was more rapid and resonant responses restricted, demonstrating the higher stiffness and damping characteristics this bridge compared to the more-flexible PSC bridges.

For the Neerkol Creek Bridge, the influence of direct wheel loading and load amplification was also evident, particularly for Girders 3 and 5 (Figure 4.1 (b)), with Girder 3 directly influenced and showing higher vibratory response when under load but returning to a similar resonant response of Girder 5. The resonant response of the girders after the passage of the vehicle highlights the contribution of the cross-girders and the facilitation of live load distribution. Almost harmonious responses between Girders 1 and 6 for the Dawson River Bridge (Figure 4.1(a)) highlight the influence of the superstructure frequency characteristics and the contribution of the cross-girders, facilitating the distribution of load.

To further analyse the dynamic bridge response, accelerometer data was transformed into frequency data using the Fast Fourier Transformation (FFT) analysis function. This transformation enables a review of energy distribution over a range of frequencies based on each instrumented component, and to identify the key frequency responses. Accelerations were considered in order to correlate results with load (in accordance with Newton’s second law of motion, F = ma) and the direct derivative of deflections from these results.

Key frequency peaks for each bridge based on peak girder acceleration responses (based on measurements from accelerometers) are shown in Figure 4.2. Significant peaks were observed for all bridges close to their respective fundamental bending frequencies. Discrete frequency peaks noted for the Dawson and Neerkol bridges had shifted higher than the fundamental bending frequency. A broad range of frequency peaks was noted around the fundamental bending frequency for the Canal Creek Bridge, ranging from 9 to 14 Hz, with limited response noted across the remaining frequency spectrum. Additional peaks were noted between 12 and 16 Hz for the Dawson River Bridge. Similar but less significant peaks were also observed for the Neerkol Creek Bridge. These peaks were close to the fundamental torsional frequency. Collectively, these observations highlight the influence fundamental frequencies on the dynamic response of the superstructure. The differences in key frequency responses between the longer span PSC bridges (Dawson and Neerkol) and the shorter span deck unit bridge (Canal Creek) are also apparent.

Figure 4.2: FFT for girder responses recorded for each test bridge from RT1 travelling in the lane at 80 km/h

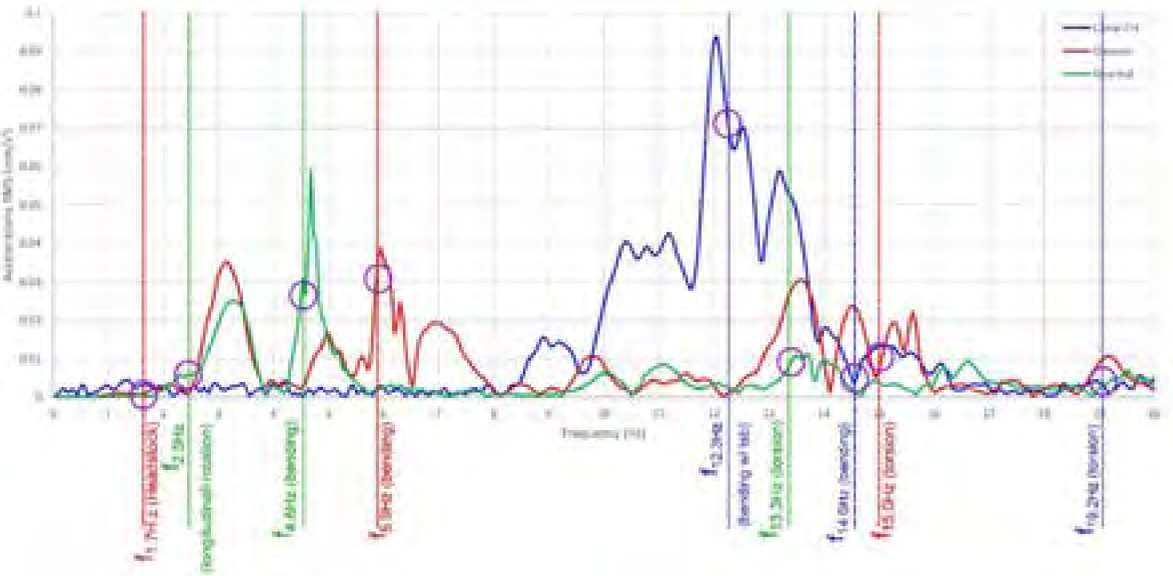

Attention is finally drawn to coincidental peaks at approximately 3.2 Hz for both the Dawson and Neerkol bridges. This is unrelated to the headstock and longitudinal fundamental frequencies noted for the Dawson and Neerkol bridges respectively, but appears to be related to the frequency characteristics of the vehicle itself. This is discussed further in Section 6.

In order to investigate the influence of the superstructure further, a review was carried out on mid-span bending and deflection data obtained for the same test vehicle travelling at the same speed and similar road profile conditions. Figure 4.3 shows the peak mid-span bending strains recorded for critical girder(s) in each bridge superstructure induced from RT1. A number of distinguishing features can be observed between the deck unit bridge and the PSC bridges. Firstly, the number of girders has been influential in load distribution and ultimately the dynamic response of the bridge. The mid-span bending strains are lowest for the Canal Creek Bridge, followed by Dawson and then Neerkol bridges, correlating to the decreasing number of girders respectively.

Figure 4.3: Mid-span bending strains for each test bridge for RT1 travelling in the lane at 80 km/h

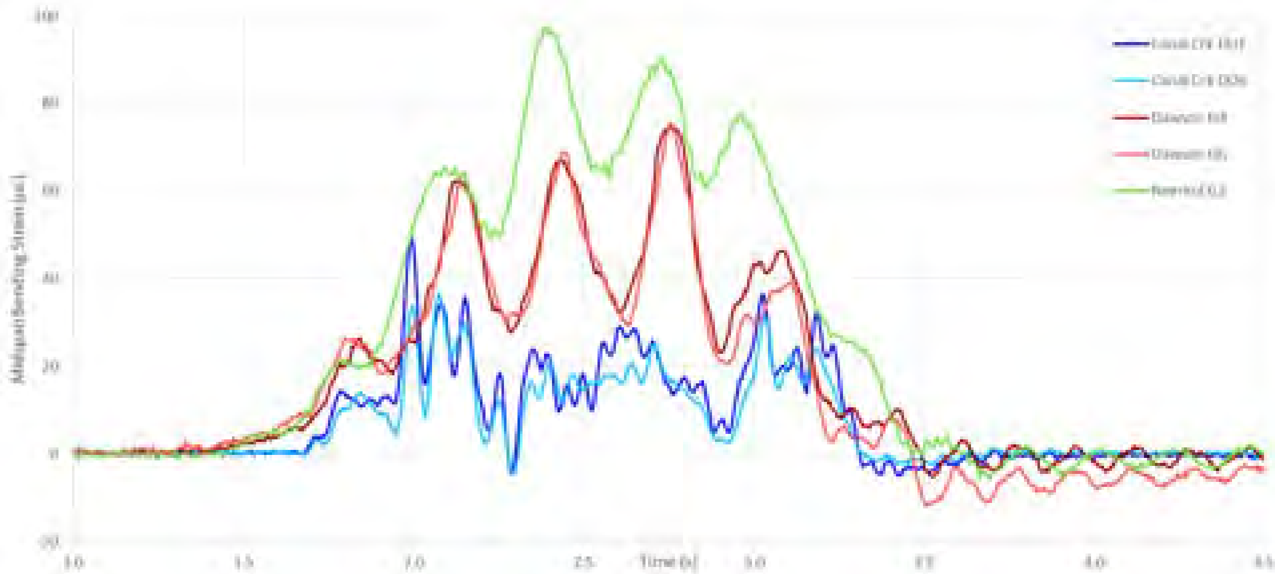

The bending strain waveform for the deck unit bridge was also significantly different to the PSC superstructure of similar span length, with clearly defined axle groups evident in the latter, and an irregular but cyclic response noted for the former. This exemplifies the superstructure type, as well as stiffness characteristics for each structure. The cyclic response of the Canal Creek superstructure is in keeping with the fundamental frequency of the deck including the TSBs (at a frequency of 12.3 Hz).

Also worthy of note was the rapid increase in strain for the Canal Creek Bridge compared to the Dawson and Neerkol bridges. This was noted irrespective of vehicle type and was more evident with increasing vehicle speed. The smaller span length, higher stiffness characteristics, and increased distribution capability of the Canal Creek Bridge were influential factors in this observation. The design and configuration of the deck unit bridge has contributed to higher strains being attracted to the edge girders, which influences the stiffness of the structure, which has subsequently governed the dynamic response of this bridge. As load amplification is often determined from peak strains, this feature is distinct from the typical open girder structures and may have an impact on the quantification of load amplification. This is discussed further in Section 8.

Consider the mid-span deflections for each bridge measured for the same vehicle case shown in Figure 4.4. Again, the Dawson and Neerkol bridges yield greater deflections as expected for PSC superstructures and in keeping with the inherent stiffness characteristics. The cyclic behaviour of these bridges to the road train is evident in the waveforms which appears to correlate well to the axle groups of the vehicle, with the Dawson River Bridge showing a larger range between peaks. Note that these peaks occur at an approximate frequency of 3 Hz. The prolonged resonant behaviour of the PSC bridges highlights lighter levels of damping on these superstructures, particularly when compared to the negligible resonant response for the Canal Creek Bridge. The rapid increase and decrease in deflections for the Canal Creek Bridge further highlight the relatively greater damping capability and stiffness of this structure.

Figure 4.4: Mid-span deflections for each test bridge for RT1 travelling in the lane at 80 km/h

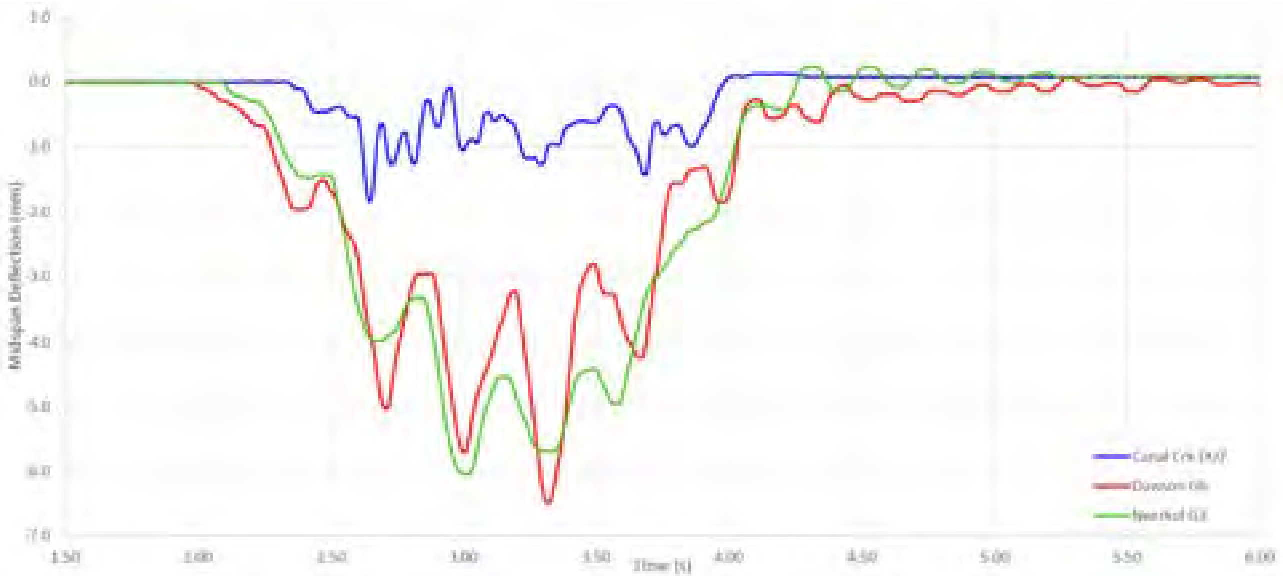

Mid-span deflection patterns recorded for the Canal Creek Bridge were irregular and partially cyclic, with no discernible pattern in relation to fundamental frequencies or vehicle axle groups. Magnitudes were suppressed, which is not unexpected for a short span structure, however it is evident that the stiffness of the deck has contributed to the repressed dynamic response of the structure.

To further explore the influence of damping capability on the frequency response for each test bridge, consider the accelerometer graphs shown for RT1 in Figure 4.5. The resonant response of the girders after the passage of the vehicle is of interest, as this highlights the damping characteristics of the bridge under load. The significant damping capacity of the Canal Creek Bridge and its suppression of dynamic load has been noted previously in Figure 4.1(a), as has the lighter damping observed for the Dawson and Neerkol bridges (Figure 4.1(b) and (c)). Of interest in Figure 4.5 is the evidence of the repeating and alternating pattern observed between girders for both bridges. This phenomenon is otherwise known as a ‘beat frequency, and is observed when two waveforms of similar frequency and amplitude combine to cause a resulting waveform. Where the two waveforms match frequency and amplitude, the signal is amplified. Alternatively, the waveform is diminished when the signals are out of phase. The phenomenon is common, and is often observed in industrial applications with a variety of machinery in operation. Whilst these observations are not uncommon for lightly-damped structures (in particular PSC girders) the physical application of this phenomenon is that amplification of load is possible after the vehicle event and thus sustained damage may occur. It is also considered to be a risk factor for fatigue if stress concentrations are significant at these locations, but this is unlikely in this instance (see Al-Zaid and Nowak (1988)). Ultimately, damage due to load amplification will be dependent on instances of frequency matching between various components and the passing vehicle and critical damping.

Consider the vibration response of girders from the Neerkol Creek Bridge due to RT1 travelling east along the centreline of the bridge Figure 4.6. Both girders were noted to be vibrating in phase, prolonging the response of the girders to live load, which is in contrast to the waveform observed in Figure 4.5(b). This contrast highlights the influence of vehicle location on the frequency response and how the structure is loaded over time after the passage of a vehicle, and will be discussed further in Section 6.

Figure 4.5: Resonant mid-span vibration response of girders due to RT1 travelling at 80 km/h

(a) Dawson River Bridge (in lane travelling east)

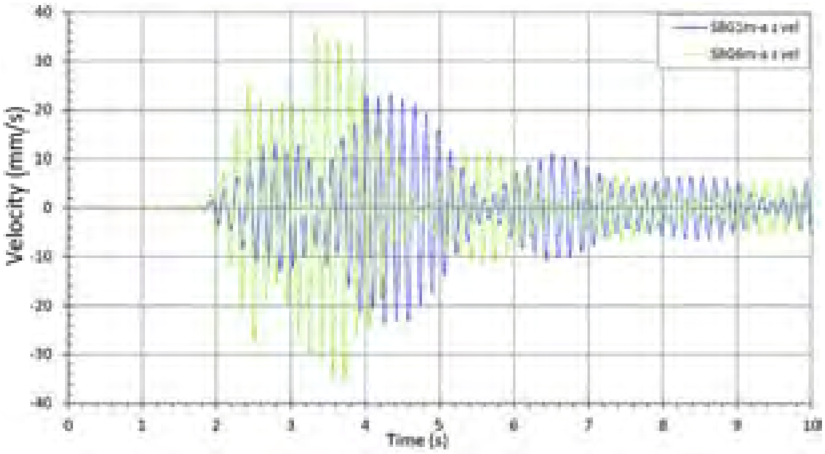

(b) Neerkol Bridge (in lane travelling east)

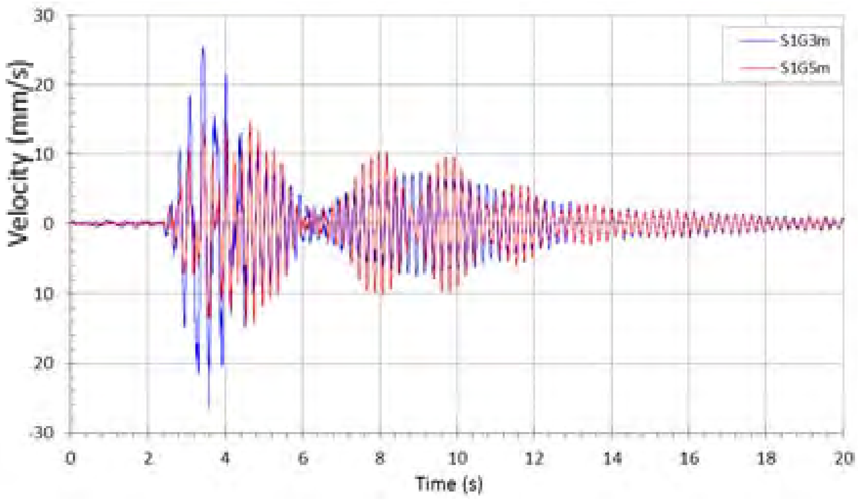

Figure 4.6: Superstructure vibrations and decay of signal for the Neerkol Creek Bridge for RT1 centreline travel at 80 km/h

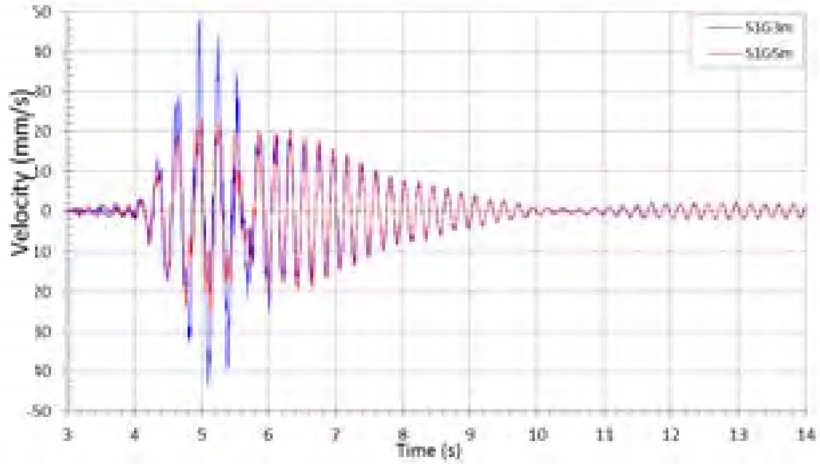

4.3.3 Substructure

In terms of substructure responses, Figure 4.7 shows accelerations recorded for substructure components in vertical, transverse and longitudinal directions. For comparison of magnitude, the mid-span accelerations recorded for peak girder responses in each bridge is also shown. Several distinct observations relating to the structure and geometric form is evident in each waveform.

The amplitude of response was greater for substructure components in the Dawson River Bridge, with similar magnitude responses for the Canal Creek and Neerkol Creek bridges. The length of response for Dawson is also significantly greater, with signals recorded in the substructure components for extended periods of time after the passage of RT1, indicative of the load transfer behaviour from adjacent spans, the resonant behaviour of each component and the inherent frequency, damping and stiffness characteristics of the bridge overall. A similar prolonged response was noted for the Neerkol Creek Bridge, however the amplitude of response was significantly less for all components in all directions. The Canal Creek Bridge exhibited the stiffest response and a rapid dissipation of load with minimal resonance, in keeping with responses expected for shorter span and slab-like structures. It also evidences the contribution of the transverse stressing bars in the distribution of load and the increased damping capability for this particular load case.

Figure 4.7: Substructure component accelerations measured for RT1 (steel suspension) for lane travel at 80 km/h

(a) Canal Creek Bridge

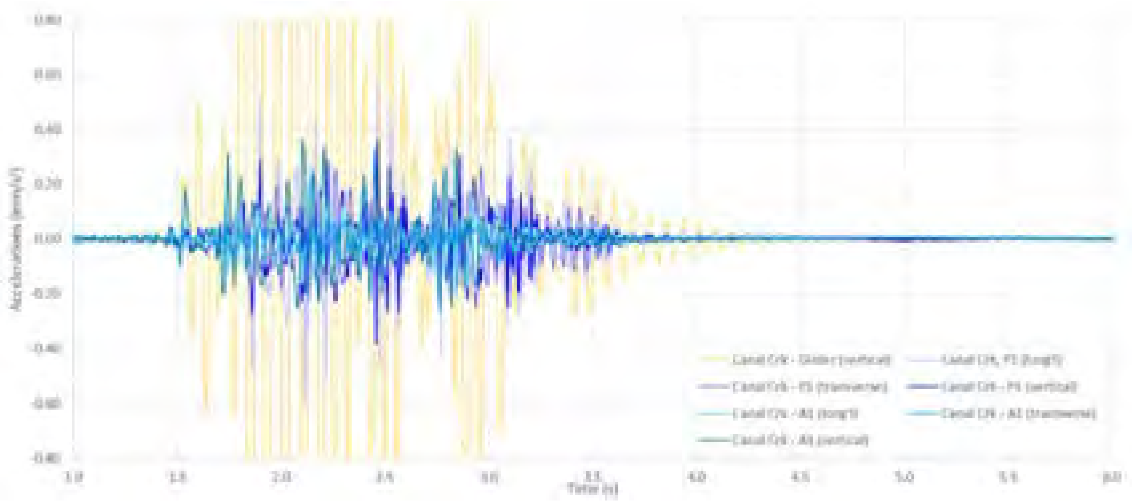

(b) Dawson River Bridge

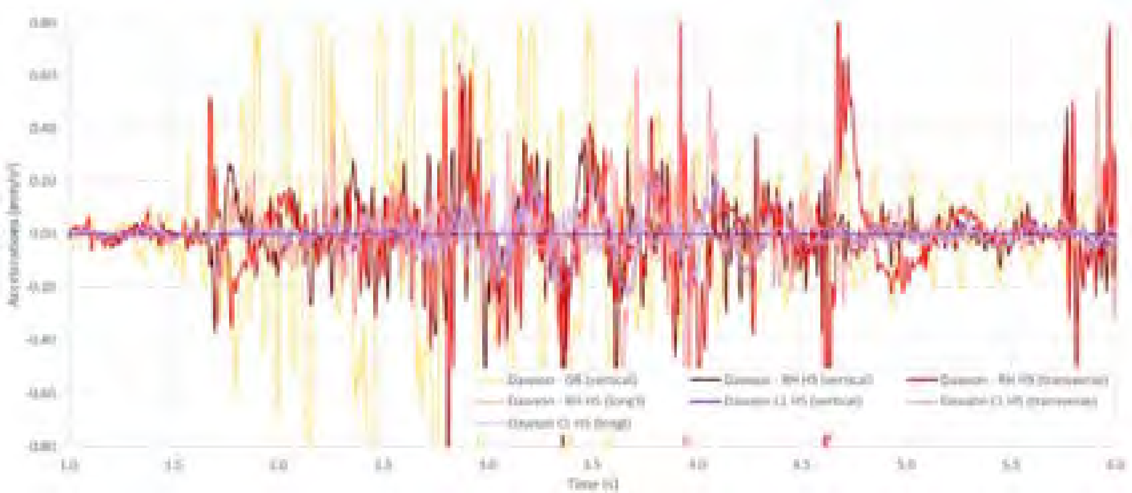

(c) Neerkol Creek Bridge

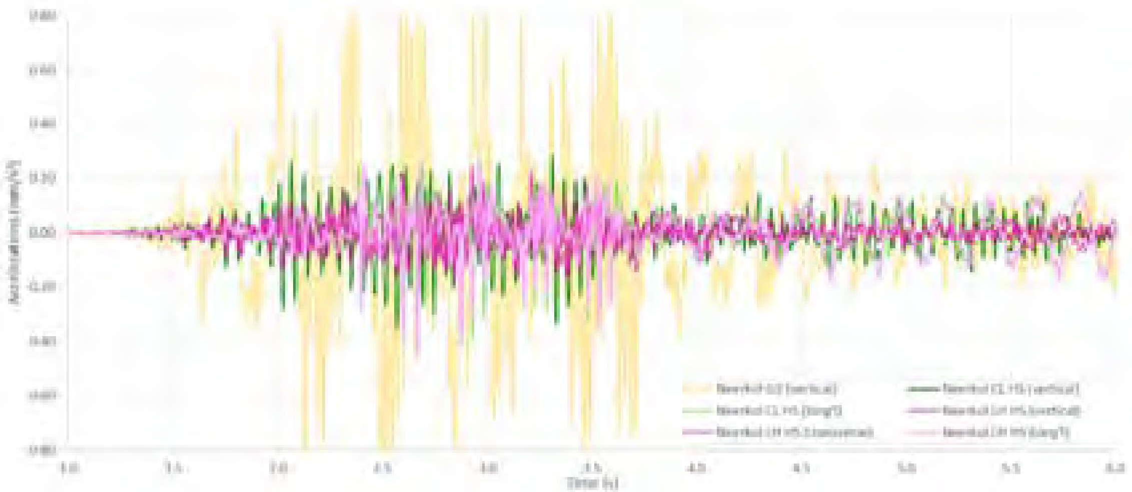

The contribution of substructure dynamic responses in multiple directions was also explored for these representative cases (Figure 4.7). Headstock accelerations recorded for transverse and longitudinal directions were equivalent to or less than vertical accelerations for the Neerkol and Canal Creek bridges, with magnitudes significantly less than mid-span girder accelerations, indicative of the higher stiffness and damping capability of the substructures in multiple directions. For the Neerkol Creek Bridge (Figure 4.7(c)), a low-amplitude cyclic response of the pier in the longitudinal direction was evident after the passage of the vehicle over the pier, highlighting the transfer of load from spans 2 and 3 as the vehicle continues across the bridge as well as the inherent resonant behaviour of the pier occurring at a low frequency of approximately 2.3 Hz (which correlates to the frequency peak observed for sensor P7-HC-a-x in Figure 4.7(c)), which aligns with the fundamental rotational frequency of 2.5 Hz identified in the modal analysis (Table 4.2).

Conversely for the Dawson River Bridge, a cyclic, significant response with an amplitude equivalent to mid-span girder accelerations under load was recorded for the cantilevered headstock in the transverse direction. Whilst the responses were predominantly cyclic, a large impulse response was observed for the right cantilever (under load) in the transverse direction which appears to be after the passage of the vehicle. This suggests an impact from the final axle or contributions from the adjacent span as the vehicle continues eastwards.

FFT frequency data based on accelerometer data obtained for bridge substructure components is shown in Figure 4.8 for multiple directions. For RT1, substructure frequency peaks for the Dawson River Bridge were mostly associated with low frequencies (i.e. less than 7 Hz) in all directions. Similarly, the majority of peaks determined for Canal Creek were typically observed at frequencies greater than 9 Hz. The pier for Neerkol demonstrated peaks over a range of frequencies, with vertical responses more likely to occur at higher frequencies(14-20 Hz) and transverse and longitudinal frequencies at lower frequencies (less than 6 Hz). However, a consistent peak at a frequency similar to the fundamental bending frequency (4.6 Hz) was observed in each direction, in particular the longitudinal response.

Similarly, coincidental peaks were also observed in all directions for the Canal Creek Bridge at 12.3 Hz (taking into account the influence of the TSBs). Such results were not observed for the Dawson River Bridge. The similarity of the substructure types for the Neerkol and Canal Creek bridges is likely to have been influential in this regard, particularly as results are based on sensors located at the centre soffit of the first pier headstock.

Some additional features to note include the peak alignment in the transverse direction with the torsional fundamental frequency for the Canal Creek Bridge. Similar observations were not noted for the Neerkol Bridge, which highlights the influence of the superstructure (i.e. combination and arrangement of the deck units) in this instance. Significant peaks between 3 and 4 Hz were observed for all three bridges and in most directions. This appears unrelated to a fundamental frequency, and is more likely to be related to the inherent frequency characteristics of the vehicle (i.e. RT1). The implications of these observations will be explored further in Section 6 and discussed in Section 8.

Figure 4.8: FFT for substructure components from each test bridge for RT1 travelling in the lane at 80 km/h (multi-directional)

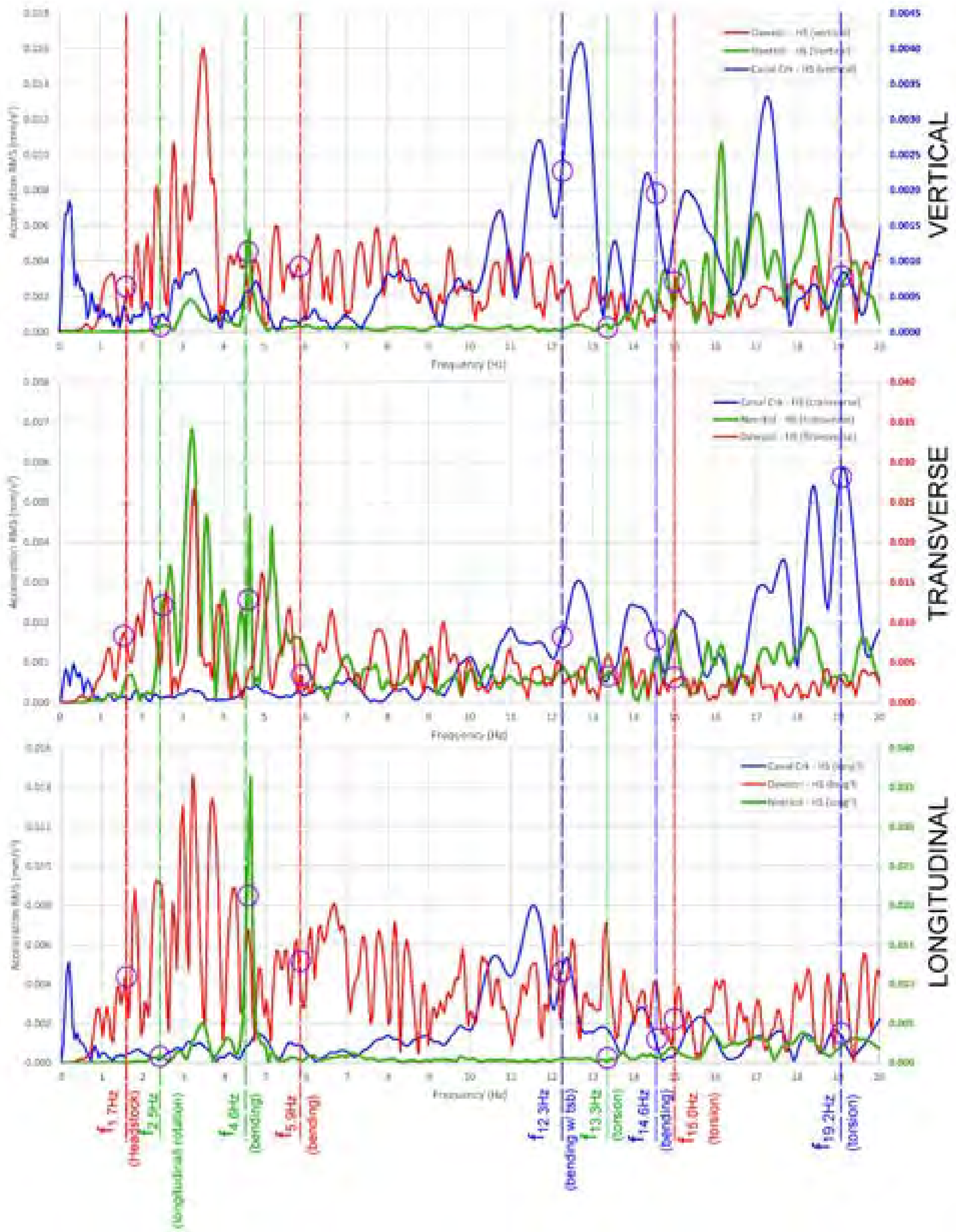

In terms of substructure load response, Figure 4.9 shows the bending strains recorded for the cantilever headstock and the soffit of the headstock for the Dawson River Bridge and the Neerkol Creek Bridge respectively. Despite the magnitude differences, the waveforms are similar, with the axle groups for RT1 clearly evident.

Figure 4.9: Bending strains measured on headstock for Dawson and Neerkol bridges induced by RT1 travelling in the lane at 80 km/h

Rotational effects of the headstock for the Dawson and Neerkol bridges in response to RT1 travelling 80 km/h are shown in Figure 4.10. The influence of stiffness is evident from the amplitude of rotations in the transverse and longitudinal direction for the Dawson River Bridge. Greater cyclic transverse rotations are in keeping with the rigid body rotation fundamental frequency identified for the headstock, which also significantly influences the torsional mode of the superstructure due to the connectivity of the cantilever to the girders via the restrain angles (see Section 4.4.4 for discussion on boundary conditions). The amplitude of rotations significantly decrease in this direction after the passage of the vehicle, indicating the likely damping capability of the headstock.

Rotations for the Neerkol Creek Bridge were significantly less in magnitude, which is not unexpected due to the stiffness of the headstock, and also due to the location of the sensors over the columns. There was a rapid decrease in rotational energy for the longitudinal direction after the passage of the road train, once again highlighting stiffness and higher damping capability. A prolonged resonant response was observed in the transverse direction, with all sensors recording in-phase simultaneous rotation. This observation was unique for this vehicle (refer to Section 4.4.2 in the S1 Year 2 report), and may be indicative of frequency matching between the vehicle and the substructure at this location.

Figure 4.10: Dynamic headstock rotations for RT1 travelling in lane at 80 km/h

(a) Dawson River Bridge

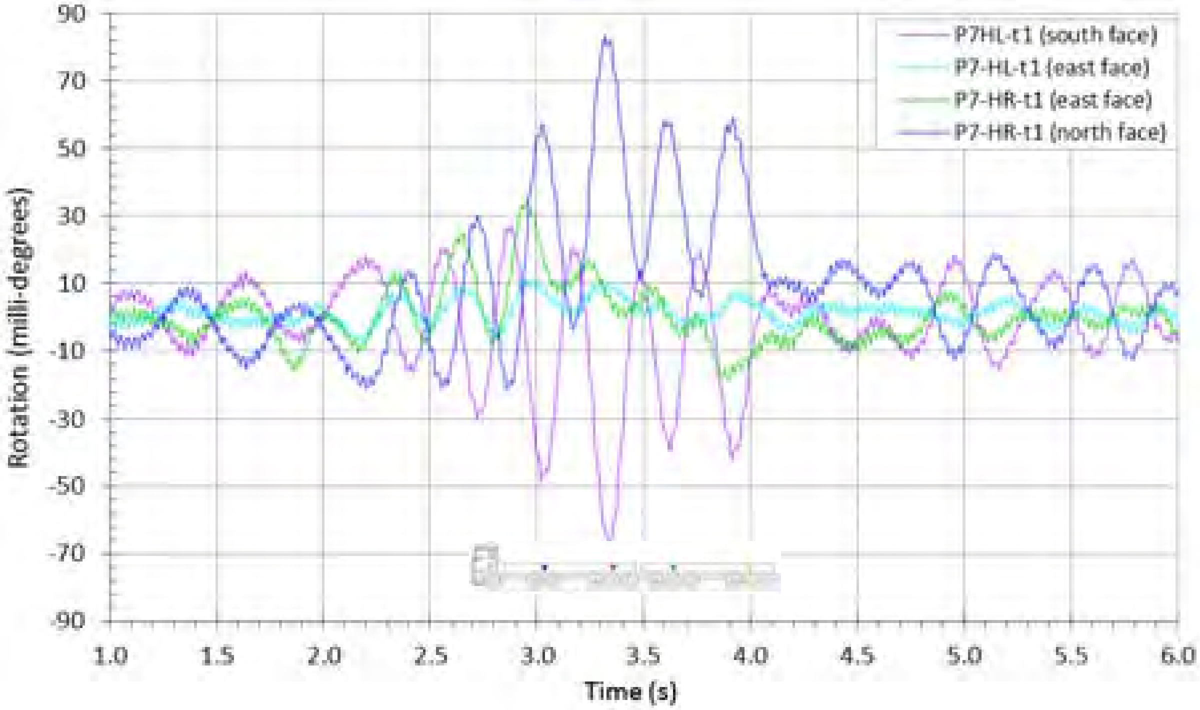

(a) Neerkol Creek Bridge

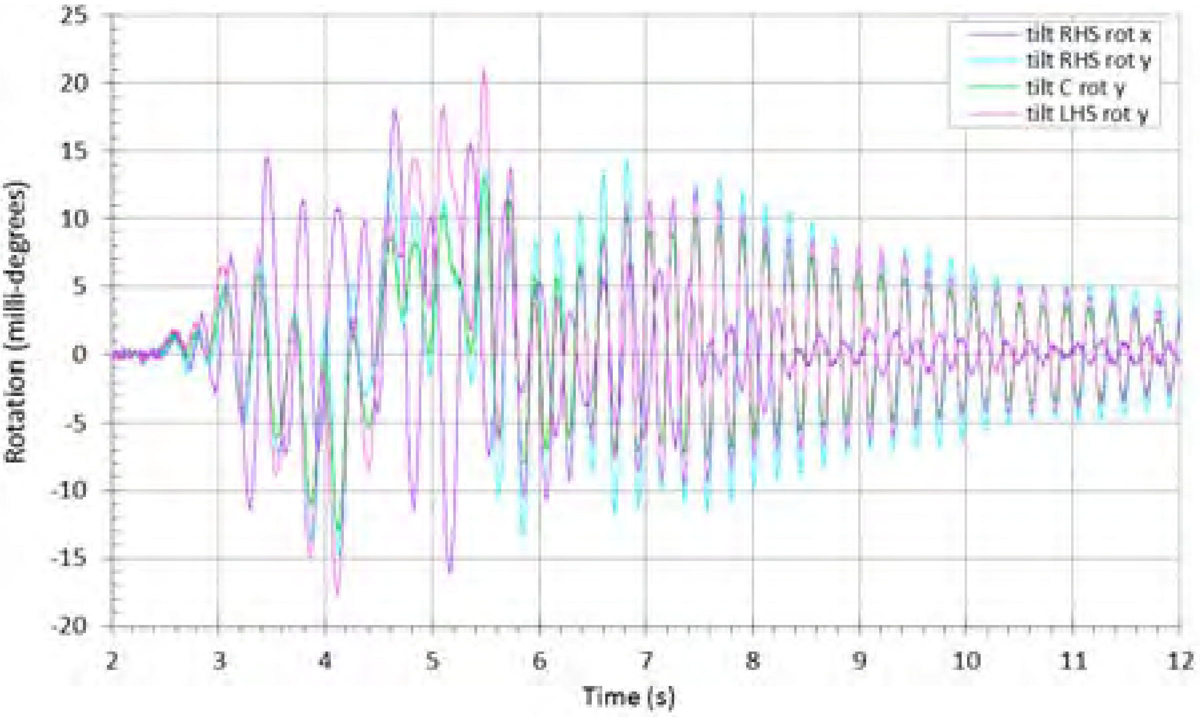

4.4 Resulting Dynamic Load Amplification

A review of DI diagrams for superstructure and substructure components was carried out to relate the dynamic response observations discussed in Sections 4.2 to Section 4.3 to implications on dynamic load amplification. A summary of DI values for superstructure and substructure components for each bridge is shown in Table 4.4 for the vehicle case discussed in this section, with an overview of DI graphs determined for RT1 at various speeds for representative superstructure and substructure components in each test bridge are presented in the following sections (Figure 4.11 and Figure 4.13).

Table 4.1 has been extended to correlate the results to load amplification observations made in the literature and the resulting summary is shown in Table 4.5. It is clear from the results that the fundamental frequency, damping capability, and stiffness characteristics are all influential on dynamic load amplification to some degree. Irrespective of speed, the stiffer and more heavily damped slab-like superstructure of the Canal Creek Bridge consistently yields lower DI values in comparison to the more slender and flexible PSC open-girder superstructure of the Dawson and Neerkol bridges. The influence of each of these factors on the resulting DI values is now discussed.

Table 4.4: DI values for superstructure and substructure components for RT1 travelling at 80 km/h

Bridge	Direction of Travel	DI Values(1, 2)			
		Superstructure	Substructure		
		Girders	Headstock	Columns (tension)	Columns (compression)
Canal Creek	West	-0.18	–	–	–
Dawson River	East	0.41 (0.30)(3)	0.85 (0.21) (3)	0.23	0.92
Neerkol Creek	West	0.17 (0.13) (3)	0.53	0.59	0.15

8 Correlates to circled values in Figure 4.11

9 Based on maximum DI values determined from peak bending strains recorded for components under direct load

10 DI values in brackets are based on peak deflections where available.

4.4.1 Structure Type

From the results presented in the previous sections, it is apparent that the structure type and form has proved influential in governing the dynamic structural response. This includes geometric considerations, construction material, multiple girders and configuration, and support conditions (Cantieni et al. 2010; McLean & Marsh 1998). Based on the factors identified in the literature and outlined in Table 4.5, elevated DI values are anticipated where there are lower number of girders and the structure is increasingly slender.

For the current report, two superstructure types and three substructure types can be reviewed and commented on in relation to correlation to DI values. These are:

- Superstructure:
  - short-span PSC deck units (similar to slab) (*Canal Creek Bridge*)
  - longer-span PSC I-girders and in situ RC deck) (*Dawson and Neerkol bridges*).
- Substructure:
  - short RC headstock on driven piles (*Canal Creek Bridge*)
  - tall RC portal-frame type pier (*Neerkol Creek Bridge*)
  - tall RC single column cantilevered headstock pier (*Dawson River Bridge*).

Table 4.5: Review of factors influencing dynamic load amplification in light of test results (based on RT1)

Scenario	Effect	Implication on dynamic load amplification (DLA)	Observations from project load tests (based on RT1)
Structure & component type	Increasing number in girders (superstructure)	Decrease	▪ Canal Creek Bridge (13 girders) lower DI values compared to Dawson (6 girders) and Neerkol (5 girders) ▪ Minimal difference between Dawson and Neerkol DI values
	Slender structures (e.g. PSC open girders)	Increase	▪ DI values greater for Dawson and Neerkol bridges (PSC open girders) ▪ Canal Creek (slab structure) mostly lower DI values, with exception of 20 & 40 km/h. TSB influential
Structure & component type	Substructure component type	Unknown	▪ DI values greater for substructure than superstructure in most cases ▪ Most DI values greater than 0.4 for speeds greater than 60 km/h (excludes westerly travel for Dawson – highest DI) ▪ Speed and road profile influential on substructure DI
Fundamental frequency	Coincidence with fundamental frequency Governs dynamic response	Increase	▪ Relative elevated DI values observed where bridge response matched fundamental frequencies ▪ Influence of inherent substructure characteristics has contributed to global load amplification ▪ Not always consistent in load amplification ▪ Vehicle frequency influence evident
Damping/Stiffness	Low levels of damping Increase in stiffness	Increase	▪ Stiffer bridge (Canal Creek) has mostly resulted in lower DI values ▪ Greater damping levels, lower DI values ▪ See Fixture & Boundary Conditions for additional comment
Span Length	Short spans	Increase	▪ Lower DI values recorded for shorter span structure (Canal Creek) ▪ Dependent on direction of travel
Fixture & boundary conditions at piers/ abutments	Changes in frequency response Increase in stiffness	Decrease	▪ Fixture of girders to substructure have influenced dynamic response of structure (esp. Dawson) ▪ Stiffer connections to substructure showed lower DI values ▪ Spans supported by piers (stiffer connections) more likely to yield lower DI values

Intrinsically linked to the structure type and its dynamic response is the stiffness and damping capability, fundamental frequency modes for the superstructure and substructure, and the span length. The following observations are made in relation to DI values.

Superstructure

From the results presented previously in Section 4.3.2, the superstructure dynamic response of the Canal Creek Bridge was less than the Dawson and Neerkol Bridges. These observations appear to correlate well to the lower DI values (less than 0.4) that can be observed for both directions of travel and irrespective of speed, with the exception of west travel at lower speeds (20–40 km/h) (Figure 4.11). It is suggested that the frequency and stiffness characteristics, the damping capability, and the wider distribution of load across several units has been influential in the suppressed result. Negative values for the Canal Creek Bridge at higher speeds may indicate the out-of-phase response of the bridge to the road train trailers, resulting in suppressed dynamic responses.

In comparison, DI values for the PSC bridges were similar where road profile was not influential. There was little difference in DI values recorded between 5 and 6 girders for the Neerkol and The Dawson bridges respectively. The DI values for the Dawson River Bridge were elevated where speeds exceeded 60 km/h when travelling east (0.41 at 80 km/h).

Figure 4.11: Superstructure DIs determined for RT1 (steel suspension) for lane travel at various speeds and direction of travel for each bridge (based on peak DI values determined from bending strains)

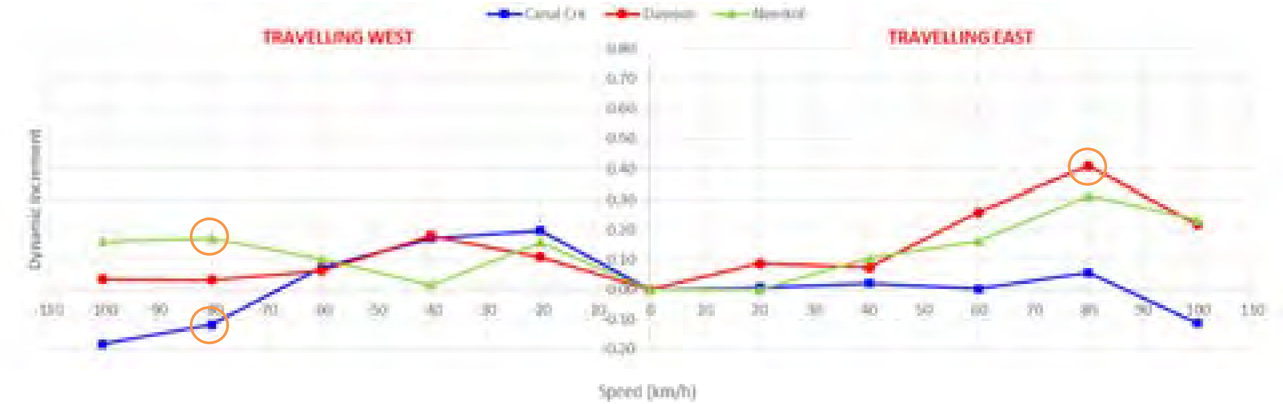

Note:

- Based on maximum DI values determined from peak bending strains recorded for components under direct load
- Circled points are referred to in the report discussion.

A comparative review of the DI values was conducted on results obtained for the 48 t hydro-pneumatic crane (CR1), as shown in Figure 4.12. The DI values for all three bridges were relatively similar for this vehicle, with values less than 0.4 irrespective speed and direction of travel. The Canal Creek Bridge yielded the greatest DI value at 80 km/h travelling west, which is in contrast to the road train. These results highlight the influence of the vehicle type on bridge dynamic response, and will be explored further in Section 5.

Figure 4.12: DIs determined for CR1 for lane travel at various speeds and direction of travel for each bridge (based on peak girder bending strains)

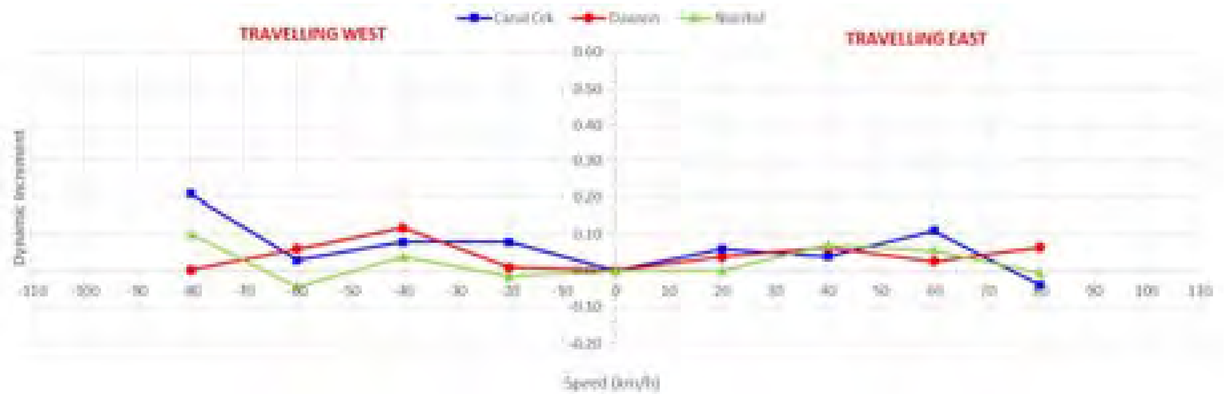

Substructure

At present, little or no data has been published that specifically quantifies the amplification of load between superstructure and substructure components. The results for the current case study for the Dawson Creek and Neerkol bridges are shown in Figure 4.13(a) and (b). Overall, the DI values were found to be significantly greater than 0.40 in most cases. Peak values of up to 0.85 for the headstocks and 0.25 and 0.92 columns for tensile and compressive strains respectively were determined at elevated speeds. In some instances, the DI values were equivalent to, or exceeded, the superstructure results. DI peaks coinciding with similar peaks for superstructure components were observed at 80 km/h for vehicles travelling east.

Substructure components for the Dawson River Bridge were most affected by the direction of travel, with suppressed DI values less than 0.2 obtained for all components when RT1 travelled west, in comparison to several values exceeding 0.4 when travelling east. In contrast, elevated DI values were evident at speeds exceeding 60 km/h for the Neerkol Creek Bridge irrespective of this, with both headstock and column results yielding similar waveforms.

Vehicle speed and direction of travel were notable influences on the resulting DI values; this is discussed further in Section 5 and Section 6 respectively. Also of significance is the difference in DI values determined from tensile or compressive strains for the columns, and the influence of the road profile condition is again evident.

Figure 4.13: Substructure DIs determined for RT1 (steel suspension) for lane travel at various speeds and direction of travel for each bridge (based on peak DI values determined from bending strains)

(a) Headstock

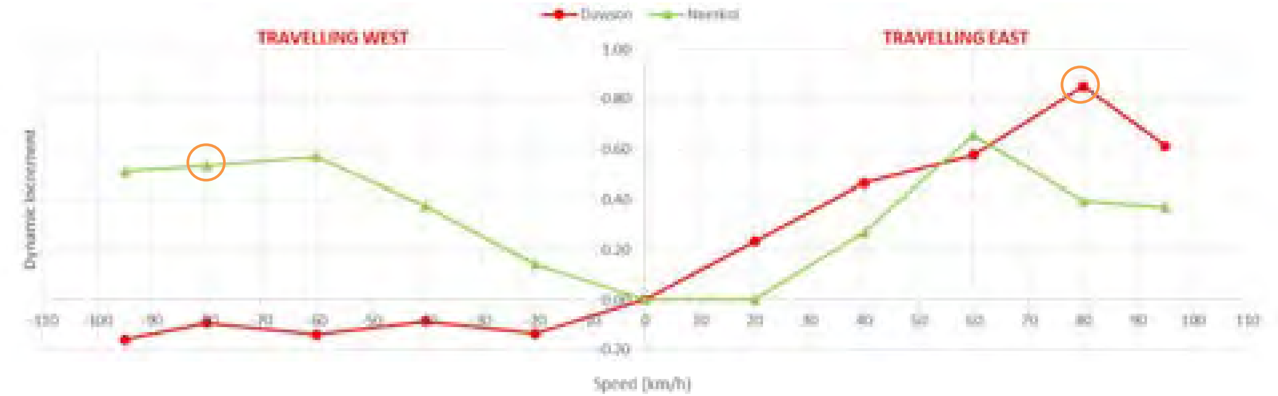

(b) Column

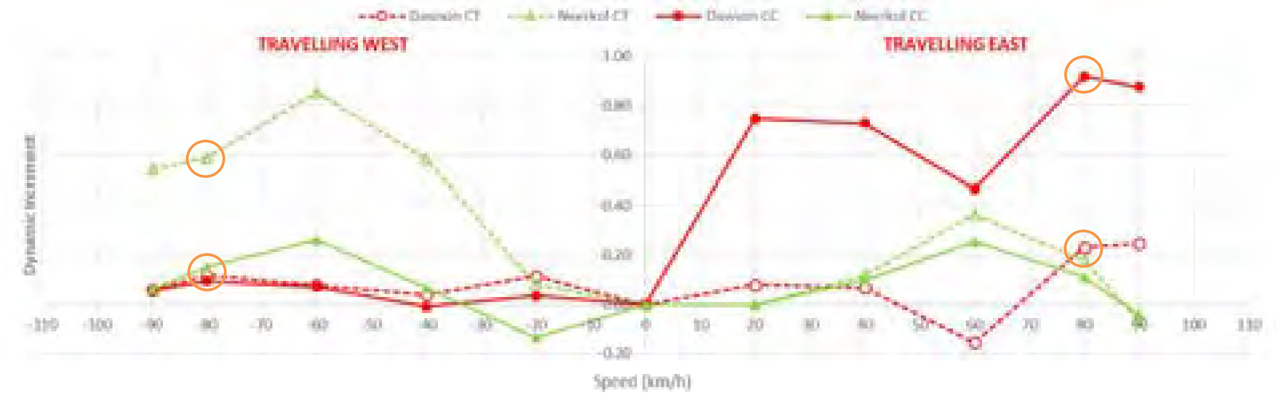

Note:

- Based on maximum DI values determined from peak bending strains recorded for components under direct load
- DI values shown for column were determined from either tensile strains (CT) (dashed line) or compressive strains (CC) (solid line)
- Circled points are referred to in the report discussion.

4.4.2 *Influence of Fundamental Frequency*

Load amplification can be significant where the components dynamically respond to live load at the same frequency as fundamental frequencies. This is otherwise known as frequency matching of 'quasi-resonance' (see Section 2). As previously discussed in Section 4.3.2 and Section 4.3.3, a number of frequency peaks (from FFT diagrams) were observed to coincide exactly or closely with fundamental frequencies for both superstructure and substructure components for the case of RT1 travelling at 80 km/h (see Figure 4.2 and Figure 4.8 respectively). Corresponding DI values for each component are shown in Table 4.6, along with corresponding matching fundamental frequency modes.

Table 4.6: Correlation of DI values with FFT frequency peaks matching fundamental modes (RT1 at 80 km/h)

(a) Superstructure

Bridge	DI value (Girders, bending strain)	Match with fundamental mode	Comment
Canal Creek	–0.18	Bending (with TSB) (12.3 Hz)	▪ Significant response, but exact match not at peak ▪ No matches exist with other fundamental modes
Dawson River	0.41	Bending (5.9 Hz)	▪ Significant response, match close to peak ▪ Slight match around torsional frequency mode
Neerkol Creek	0.17	Bending (4.6 Hz)	▪ Significant response, but exact match not at peak ▪ Slight match around torsional frequency mode

(a) Substructure

Bridge	DI values (bending strain)			Match with fundamental mode	Comment
	Headstock	Columns (tension)	Columns (compression)		
Canal Creek	–	–	–	Bending (w/- TSB) (12.3 Hz)	▪ Match in all directions, least in transverse direction
				Bending (no TSB) (14 Hz)	▪ Strong match in vertical direction ▪ Shift close to transverse and longitudinal directions
				Torsion (19.2 Hz)	▪ Strong match in transverse direction, and vertical direction to lesser degree
Dawson River	0.85	0.23	0.92	Bending (5.9 Hz)	▪ Match or shift for all directions ▪ Least response in transverse direction
				Torsion (15 Hz)	▪ Negligible response in all directions overall ▪ Low-level match in vertical direction
				Headstock (rigid body) (1.7 Hz)	▪ Match in transverse direction ▪ Shift close to longitudinal direction
Neerkol Creek	0.17	0.59	0.15	Bending (4.6 Hz)	▪ Narrow but strong match in all three directions ▪ Strongest in longitudinal direction, minimal response across rest of spectrum
				Longitudinal rotation (2.5 Hz)	▪ Match in transverse direction only

For superstructure components, strong frequency peaks aligning with the bending fundamental frequency correlated well with elevated DI values determined for the Dawson River Bridge. Conversely, a negative DI value exists for the Canal and Neerkol Creek Bridges despite significant coincidental frequency peaks. This result may indicate a suppression of dynamic response due to the coincidence of several simultaneous frequency responses, as demonstrated by the elevated peaks over a range of 9.5 Hz–14 Hz. Coincidentally, this frequency range is known to align with axle hop frequencies, and as such this result may also be indicative of an axle hop mode for this vehicle. These ideas will be explored further in Section 6.

For the substructure, correlation of DI values was only possible for the Dawson and Neerkol bridges. Here, elevated DI values were determined for most substructure components that exceeded 0.4. In particular, for the Dawson River Bridge, the significant DI value of 0.85 in the headstock correlates well to the coincidence of frequency peaks to fundamental modes, not least being a match to the rigid body rotation of the headstock cantilever at 1.7 Hz.

For the Neerkol Creek Bridge, clear and significant coincidental frequency peaks were noted in all directions corresponding with the fundamental bending frequency, with mostly minimal response across the remaining frequency spectrum. The most significant peak was recorded for the longitudinal direction, of which the fundamental frequency for longitudinal pier rotations was 2.5 Hz. Of note, there were no corresponding frequency matches for this frequency in this direction. However, DI values were based on bending strains on the soffit of the headstock and as such are unlikely to translate to elevated DI values in the longitudinal direction. Despite these observations, the resulting elevated DI value appears to coincide with the fundamental frequency response for the pier in this case.

The lower values of tension and compressive strain-based DI values for the Dawson and Neerkol bridges respectively is acknowledged, and this will be explored further in Section 6 and Section 8. Also of interest, the translation of frequency peaks away from fundamental frequencies, providing evidence of the influence of the inherent vehicle dynamic characteristics (also discussed in Section 6).

4.4.3 Influence of Span Length

Known to be related to the frequency response of a bridge, the span length has been documented in the literature as being influential. Longer spans are more likely to result in lower dynamic response in comparison to shorter spans, which are more likely to be more dynamically sensitive and result in high load amplification. For RT1, amplification of load is evident at speeds greater than 40 km/h for the longer spanned the Dawson and Neerkol bridges compared to the shorter, stiffer span of the Canal Creek Bridge, with maximum DI values of approximately 0.4 and 0.3 respectively. However, the amplification of load is not symmetrical or identical with respect to direction of travel.

To test the validity of these results and the claims in the literature, no clear trends relating to span length were evident for the hydro-pneumatic crane (CR1) for both speed and direction of travel (Figure 4.12). Elevated and almost identical DI values of approximately 0.3 and 0.4 were recorded for both the Neerkol and Canal Creek Bridges travelling west at speeds greater than and equal to 60 km/h. In the opposite direction for the same speeds, identical DI values were again recorded for the Neerkol and Canal Creek Bridges, with values less than 0.2.

To understand the response of each structure in terms of its fundamental frequencies in relation to its span length, the results of the modal analysis for each bridge were reviewed against test data collated of approximately 90 bridges tested as part of the OECD IR6 DIVINE Project (Figure 4.14). Deck unit bridges subscribe to the frequency relationship of 100/L, whereas prestressed concrete girder structures align more closely with the 120/L relationship. The modal results from each test bridge from the current program have been incorporated into Figure 4.14, and confirm these relationships.

Figure 4.14: Frequency response of bridges in relation to span length

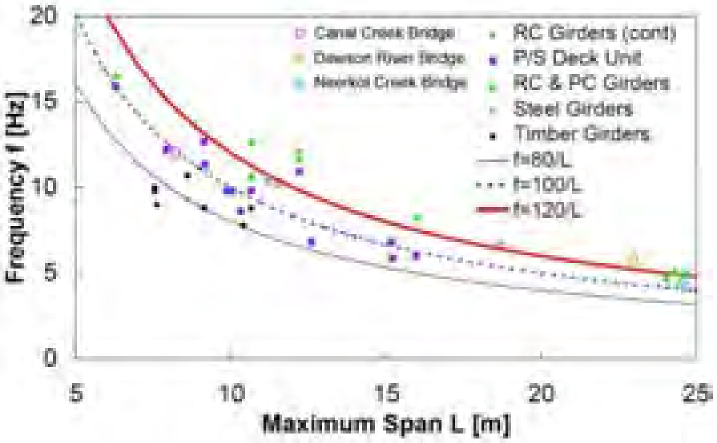

Source: Based on Figure 5 from OECD IR6 DIVINE Project: Element 6, Bridge Research (Final Report) (Cantieni et al. 2010).

The stiffness and damping capability, fundamental frequency modes for the superstructure and substructure, and the span length are intrinsically linked to the structure type and its dynamic response. The following observations are made in relation to DI values.

As noted in Section 4.3.2, the deck unit bridge, the Canal Creek Bridge, exhibited a suppressed dynamic mid-span response when compared to the Dawson and Neerkol bridges (see Figure 4.3 and Figure 4.4). Previous discussions have also recognised the contribution of a greater level of damping and stiffness in the restriction of dynamic response for the Canal Creek Bridge.

4.4.4 Influence of Fixture/Boundary Conditions

As noted in Section 2, boundary conditions are influential on the stiffness characteristics of a bridge, which influences the overall frequency response of a structure (Barr et al. 2008; Carey et al. 2010; Chegini & Palermo 2014; Kaliyaperumal, Imam & Righiniotis 2011). Ultimately this influences amplification of load, with greater stiffness resulting in a reduction in load amplification. Boundary conditions that are likely to be influential on bridge response and to be considered herein for the three test bridges under review include the role of restraint angles, the direction of travel and the relative degrees of freedom between the abutment and piers. These are now discussed.

Responses between simply supported and continuous structures are known to evoke different dynamic responses due to the inherently different boundary conditions. All three test bridges were noted to have simply supported superstructures, which is more likely to yield more significant dynamic amplification than those that are continuous. However, based on the distribution of load across the pier to adjacent spans evident in waveforms for all three bridges (as shown in Figure 4.15) due to the provision of restraint angles (for the Dawson and Neerkol bridges) and doweled hold-down bolts (for Canal Creek), a reduction in load amplification is likely to have occurred. The fixture conditions between each bridge is now reviewed in terms of its influence of stiffness and subsequent reduction in load amplification. Specific fixture details have been noted previously in Section 3.

Figure 4.15: Examples of load distribution over the pier to adjacent spans

(a) Canal Creek Bridge

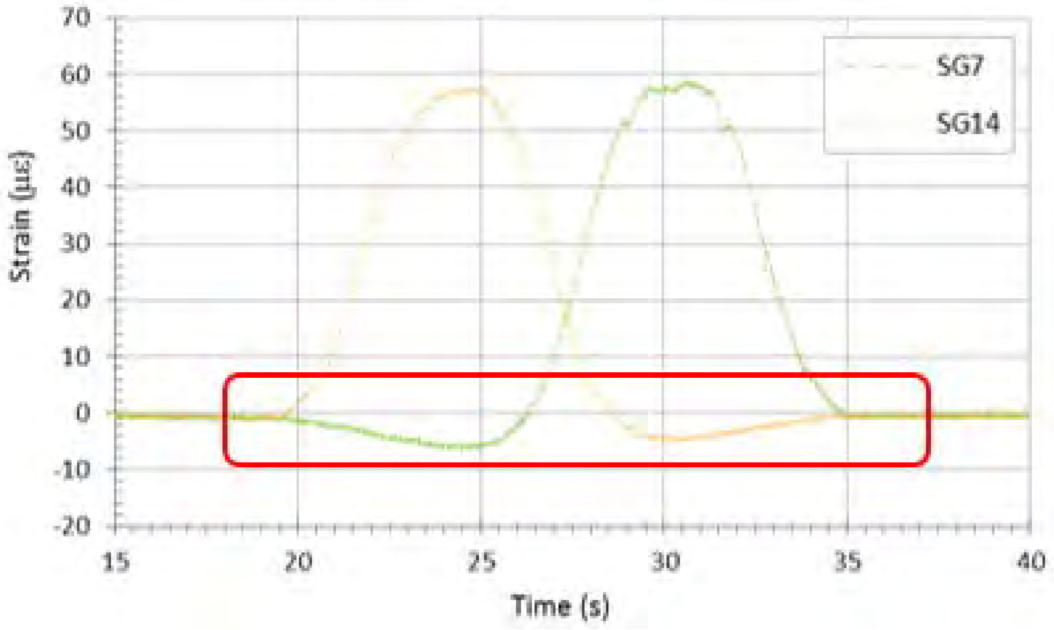

Note: Based on mid-span bending strains measured for deck unit DU7, Span 1 (SG7) and Span 2 (SG14) for RT1 travelling east at 60 km/h.

(b) Dawson River Bridge

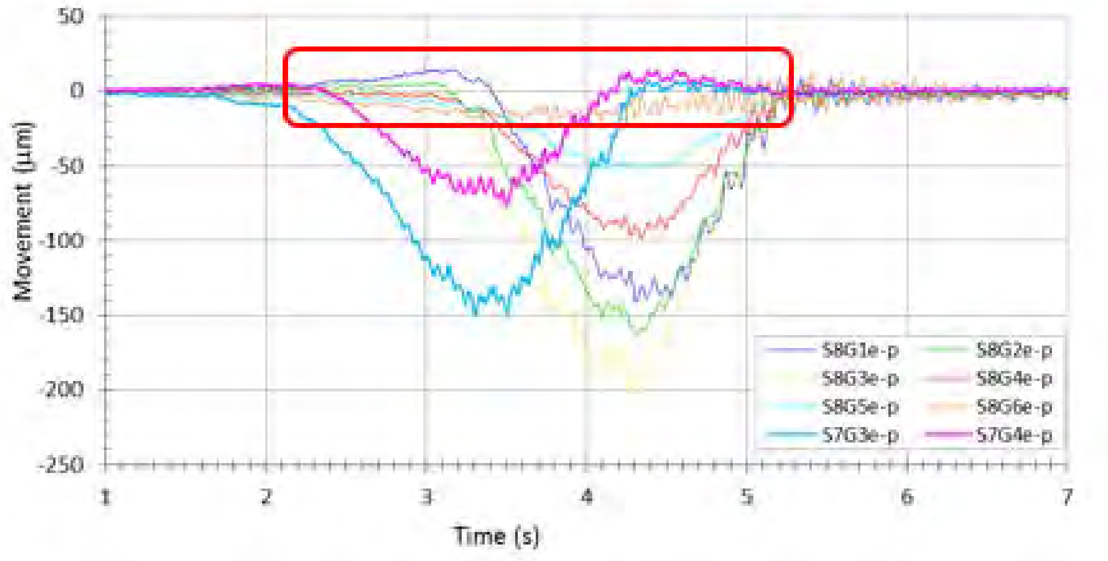

Note: Based on bearing compression measured at girder ends on Pier 7 due to passage of air-bag suspension road train (RT2) travelling west at 80 km/h.

Whilst all three bridges were found to have fundamental torsional frequency responses, the response of the Dawson River Bridge appears to have been particularly significant, with the global response of the bridge intrinsically linked to the contributions afforded by the substructure components. To explore this further, consider the torsional response of the superstructure as evidenced by the out-of-phase accelerometer mid-span response of girders 1 and 3 in Figure 4.5(a). Further consider the low-frequency sway response of the pier as evidenced in Figure 4.10(a) and the significant frequency response of the headstock in the transverse direction in Figure 4.7(b), including the impulse response due to the passage of the road train. From these observations, it is clear that the rotational dynamic response of the pier has been significantly influential on the dynamic response of the superstructure, which would not have been possible if not for the presence of the restraint angles connecting the girders to the headstock, driving the response of the girders. The corresponding high DI values of 0.85 and 0.92 in the headstock and column (compressive strain) respectively appear to correlate well with this (see Table 4.4).

In relation to fixture conditions, the type of fixture may be influential in terms of reducing rotations and therefore increasing stiffness (Carey et al. 2010). Due to the geometry of the Canal Creek Bridge superstructure and the design of the doweled hold-down bolts fixing the deck to the headstock, it is anticipated that this condition would be relatively stiff due to the restriction of significant rotations. This is also evidenced by the higher fundamental frequencies determined for this bridge. As such, lower load amplification is anticipated. In comparison and as discussed in the previous paragraph, the restrain angle fixtures at the ends of the girders for the Dawson River Bridge (and therefore also the Neerkol Creek Bridge) will likely permit relatively greater rotations and theoretically greater load amplification. Table 4.7 shows the DI values determined for each bridge for RT1 travelling at 80 km/h in equivocal directions of travel (obtained from Table 4.4). As can be observed, DI values for the Dawson River Bridge was 0.41, which is significantly greater than the DLA factor of 0.4. In comparison, the DI values for the Canal Creek and Neerkol Creek Bridges are –0.12 and 0.17 respectively. This appears to support the above-mentioned hypothesis for the current case. For comparison, DI values for the 48 t hydro-pneumatic crane travelling in the same direction and at the same speed are presented in Table 4.8. In this instance, DI values for the Dawson River Bridge are marginally lower than the Canal Creek and Neerkol Creek Bridges. Despite the fact that the influence of vehicle type is apparent, the DI values for these cases are the maximums for this speed irrespective of direction of travel. Therefore, it may be postulated that there is some merit in the influence of fixture conditions.

Table 4.7: DI values determined for each test bridge for RT1 travelling in lane at 80 km/h

Bridge	DI value (mid-span bending strain)	Direction of travel
Canal Creek	–0.12	West
Dawson River	0.41	East
Neerkol Creek	0.17	West

Table 4.8: DI values determined for each test bridge for CR1 travelling in lane at 80 km/h

Bridge	DI value (mid-span bending strain)	Direction of travel
Canal Creek	0.21	West
Dawson River	0.06	East
Neerkol Creek	0.10	West

To further review the influence of boundary conditions, the influence of abutment and pier fixture conditions has been reviewed. Due to the previously-identified load distribution across the piers for all bridges (Figure 4.15), it is anticipated that less rotation and therefore stiffer conditions are more likely to exist over the piers than at the abutments. In other words, a span supported by two piers may be more likely to produce a lower DI value than one supported by an abutment and a pier. To investigate this observation, mid-span bending strain and deflection waveforms were reviewed for both directions of travel for RT1 travelling at 80 km/h, which are presented in Figure 4.16 and Figure 4.17 for the Canal Creek and

Dawson River Bridges respectively. Corresponding DI values were subsequently analysed and summarised in

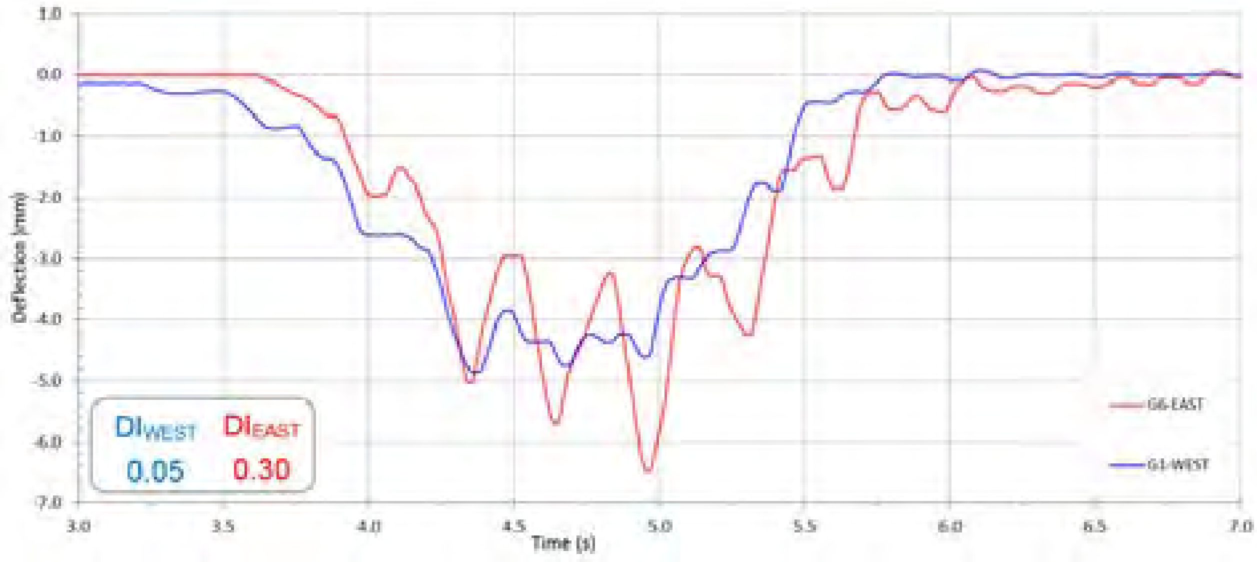

Table 4.9.

Figure 4.16: Dynamic response of the Canal Creek Bridge in both directions of lane travel for RT1 at 80 km/h

(a) Mid-span bending strains

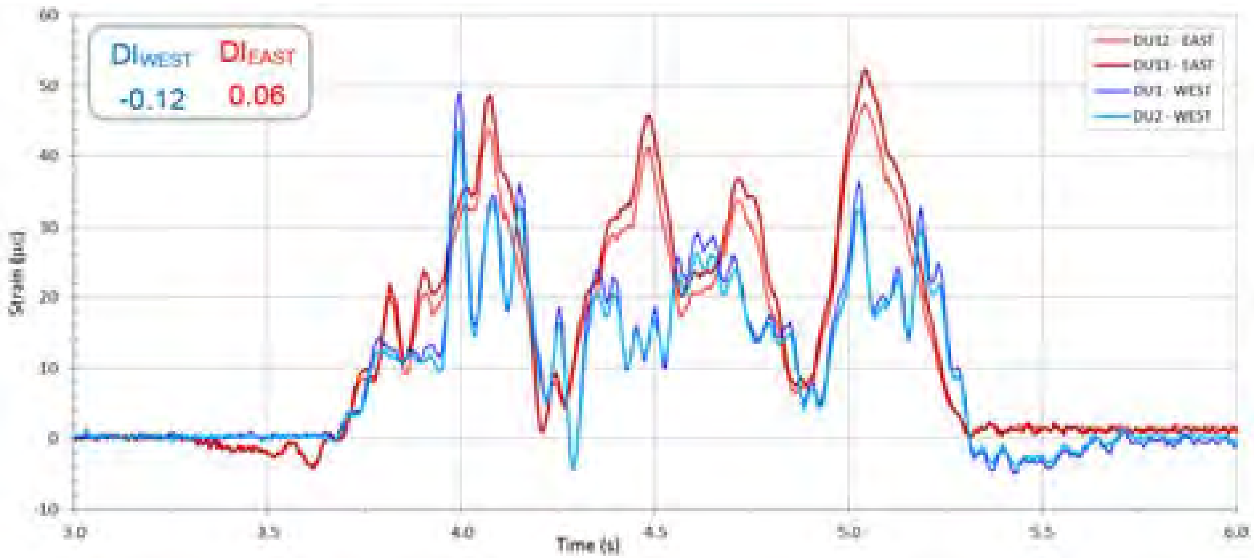

(b) Mid-span deflection

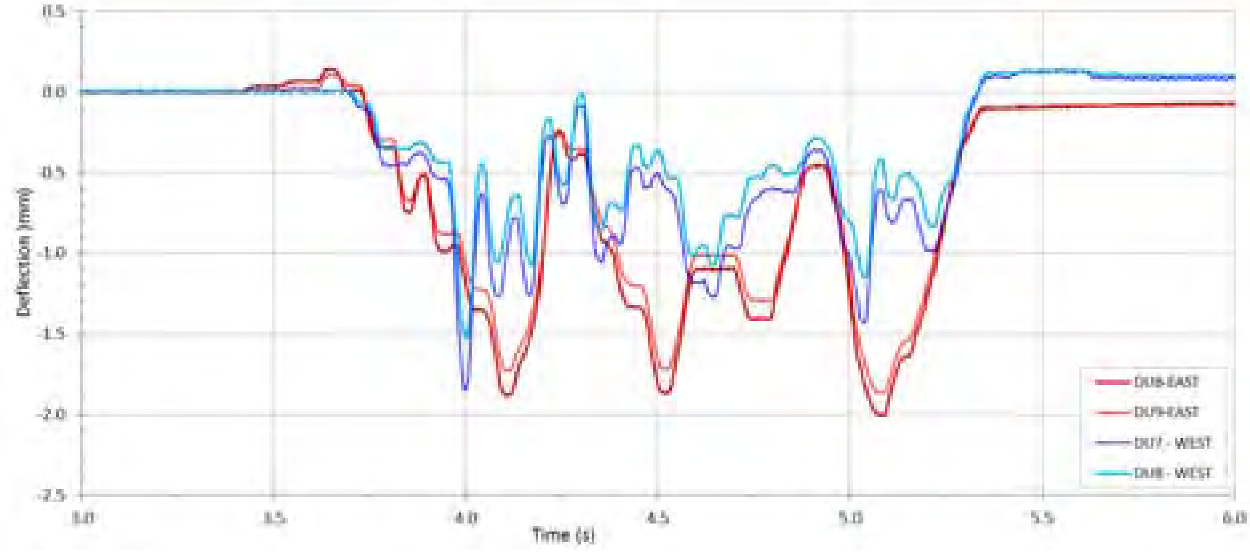

Figure 4.17: Dynamic response of the Dawson River Bridge in both directions of lane travel for RT1 at 80 km/h

(a) Mid-span bending strain

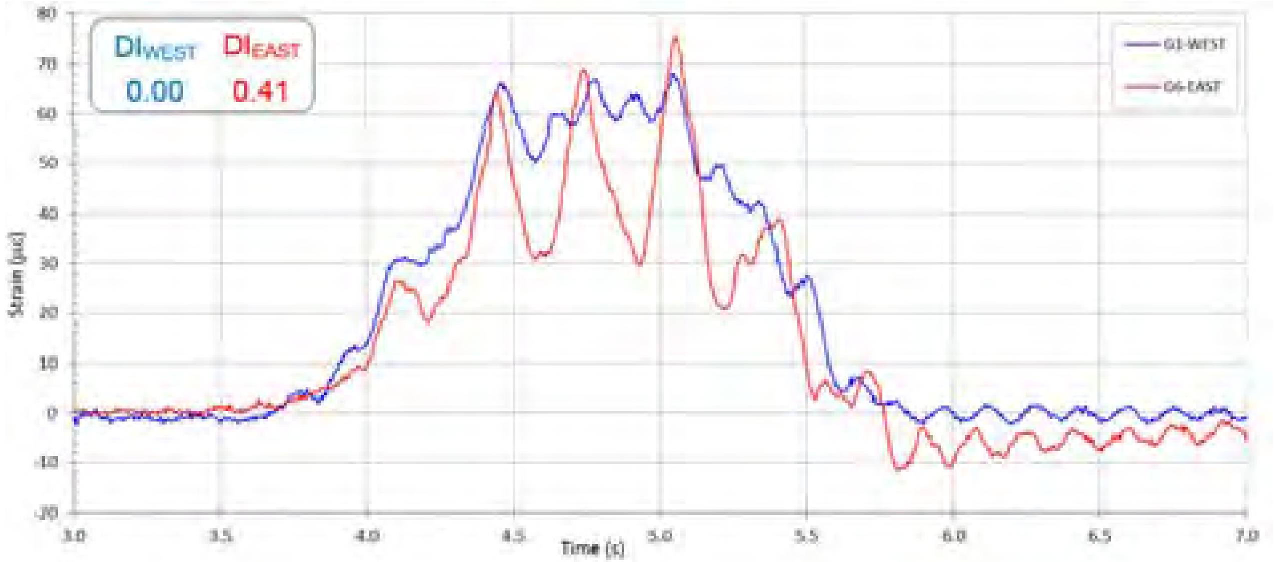

(b) Mid-span deflection

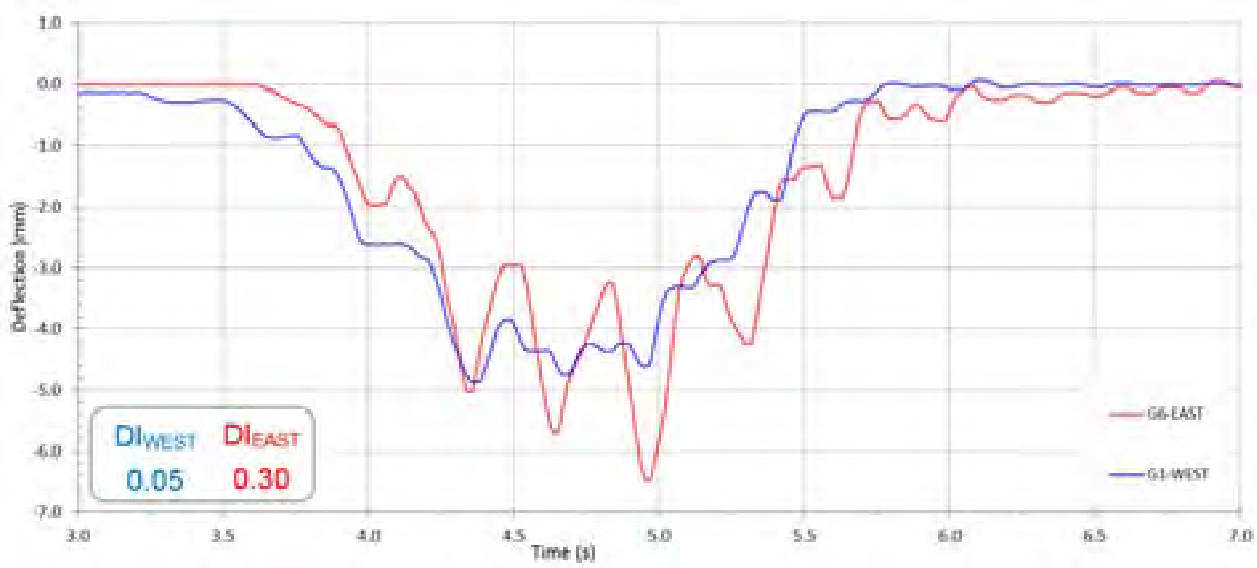

Table 4.9: DI values determined for each test bridge for RT1 travelling in each direction at 80 km/h

Bridge	DI Value (RT1, 80 km/h)			
	Travelling East		Travelling West	
	Bending strain	Deflection	Bending strain	Deflection
Canal Creek	0.06	–	–0.12	–
Dawson River	0.41	0.30	0.00	0.05
Neerkol Creek	0.31	0.22	0.17	0.13

Despite the evidence to suggest the significant influence of the road profile on the resulting dynamic response of the bridge (discussed in further detail in Section 6), the waveforms and DI values provide some insight into the influence of longitudinal boundary conditions, such as stiffer abutment structures and the contribution of longitudinal and transverse rotations from adjacent spans and piers. For the Canal Creek Bridge (Figure 4.16), the most significant response was recorded for RT1 travelling east, reaching the instrumented span prior to crossing the adjacent abutment. Well-defined peaks with minimal cyclic responses was recorded, which resulted in a corresponding peak DI value of 0.06 (mid-span bending strains). In contrast, when the same vehicle travelled west at the same speed, the dynamic response was supressed and more cyclic, with a corresponding lesser DI value of –0.12 (bending strains). In this direction, the road train approaches the instrumented span from abutment 1, and there is no contribution from adjacent spans to loading in this scenario.

The opposite was observed for the Dawson River Bridge (Figure 4.17). For westward travel, RT1 traversed the length of the bridge prior to reaching the instrumented span, resulting in load distributions and movements from adjacent spans influencing this span. This was evident from the resulting bending strain and deflection waveforms. Peaks recorded for westward travel were not as significant or severe as those recorded for travel east, despite the vehicle travelling in almost identical transverse locations in the lane. The influence of the axle groups was also evident in the eastward travel waveform. Corresponding DI values for mid-span bending strains were 0.03 and 0.70 for westward and eastward travel respectively. This is in direct contrast to the findings of Canal Creek. DI values for the Neerkol Creek Bridge appear to support the observations made for the Dawson River Bridge rather than the Canal Creek Bridge.

To verify these observations, a comparison is provided in Table 4.10 for the 48 t hydro-pneumatic crane (CR1) for each bridge. For the Dawson River Bridge, similar findings were observed as for RT1, with larger DI values occurring for travel when approaching the instrumented span first from the abutment. Conversely for the Neerkol and Canal Creek Bridges, the results oppose those determined for RT1.

Table 4.10: DI values determined for each test bridge for CR1 travelling in each direction at 80 km/h

Bridge	DI value (RT1, 80 km/h)			
	Travelling East		Travelling West	
	Bending strain	Deflection	Bending strain	Deflection
Canal Creek	–0.04		0.21	–
Dawson River	0.06	–0.04	0.00	–0.03
Neerkol Creek	–0.01	–0.04	0.10	–0.04

Based on these observations, it appears that boundary conditions may influence the resulting load amplification (supporting the theory that restriction of rotation will lead to suppression in dynamic load amplification). However, further investigation is warranted to quantify these effects for various vehicles and structural conditions. It is also postulated that the accumulating dynamic response of the adjacent spans and piers of numerous components may have contributed to the reduced dynamic response in the westerly direction, causing disruption rather than frequency matching to enable dynamic load amplification. The increased degrees of freedom in the transverse and longitudinal directions, and the influence of span length should also not be overlooked in this instance.

4.5 Summary/Key Findings

In summary, the current project results to mostly support the recommendations set out in the literature. More specifically:

- Increases to stiffness and damping characteristics were more likely to result in lower DI values.
- The slender superstructure and decreased number of girders for the PSC bridges appears to have resulted in higher DI values in comparison to the Canal Creek Bridge.
- Higher DI values were more likely to occur where dynamic responses identified by FFT analysis coincided with fundamental frequencies. Alternatively, where frequencies were out of phase, suppression of dynamic response was more likely. Frequency matching was evident.
- The fixture conditions of the girders to the superstructure have been influential in the amplification or suppression of dynamic load on each structure. The stiffer the connection, the less rotation and subsequently, lower DI values.

In contrast to the literature, the shorter-span bridge did not yield lower DI values in comparison to longer, slender spans. Rather, the response of the span was more likely to be influenced by the vehicle type.

Substructure responses were more likely to yield greater DI values than for the superstructure, often in excess of 0.4. The dynamic response and amplification of load was significantly influenced by the fundamental frequency modes and also the vehicle type.

5 INFLUENCE OF VEHICLE CHARACTERISTICS

5.1 Introduction

Previous publications summarised in Section 2.2.3 have identified the various vehicle characteristics that can influence the dynamic response of a bridge and ultimately the amplification of load. In keeping with the outline of Section 4, the following sections review the research results obtained from the current project in relation to the relevant literature review findings.

5.2 Speed

Early literature states that maximum speeds will invoke peak DI values (Frýba 1972), whereas more recent literature has associated peak DI values with a variety of critical speeds (Brady, O'Brien & Žnidarič 2006; González 2009a; Heywood 2000; Senthilvasan et al. 2002). To investigate for trends relating to vehicle speed, DI values for each test vehicle were collated and compared against each test bridge, as shown in Figure 5.1.

The results confirmed the more recent findings relating to speed, with peak DI values coinciding with a range of speeds. Of interest was that several peak DI values existed at lower speeds (for example 40 km/h for CR1, 60 km/h for CR2 and RT2, and 20 km/h for RT1). This appears to confirm observations from recent research which suggested that the vehicle's inherent body bounce and axle hop frequencies are more likely to be significantly influential on bridge response at lower speeds (Carey et al. 2010; Heywood 2000). At these speeds, however, resulting DI values were less than 0.4.

Overall, the Dawson River Bridge appeared to be most significantly affected by vehicle travelling speed, with significant variations observed in load amplification for CR2 and RT1. The most consistent and repeatable results were obtained for the RT2 for both bridges, which were not affected by road profile conditions, with DI values less than 0.2 irrespective of speed. For some vehicles, consistent DI peaks were observed for each vehicle type at critical speeds irrespective of the bridge. For example, a consistent DI peak at 40 km/h was observed for CR1 regardless of direction of travel. This demonstrates the influence that the vehicle type has on the resulting load amplification induced.

Other observations confirmed the influence that road profile plays on the amplification of load at high speeds (Cantieni 1983; McLean & Marsh 1998; Paultre et al. 1992; Sweatman et al. 1997). This is clearly evident in the DI values for RT1 and CR2 traveling east, with peak DI values occurring at 80 and 100 km/h (albeit a large scatter ranging between 0.05 and 0.41).

DI peaks between vehicles at coincidental speeds were noted for the following instances (Figure 5.1):

- Canal Creek Bridge:
  - RT1 and ST1 at 40 km/h travelling east
- Dawson River Bridge:
  - CR1 and RT1 at 40 km/h travelling west
  - RT1 at 80 km/h travelling east
- Neerkol Creek Bridge:
  - CR1 and RT1 at 80 km/h travelling west.

Figure 5.1: DI Values for various vehicle speeds and direction of travel – comparison between bridges

(a) CR1

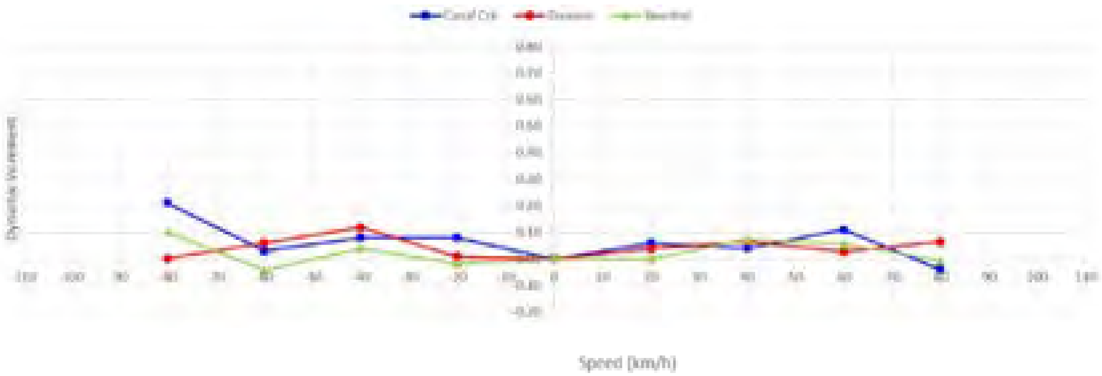

(b) CR2

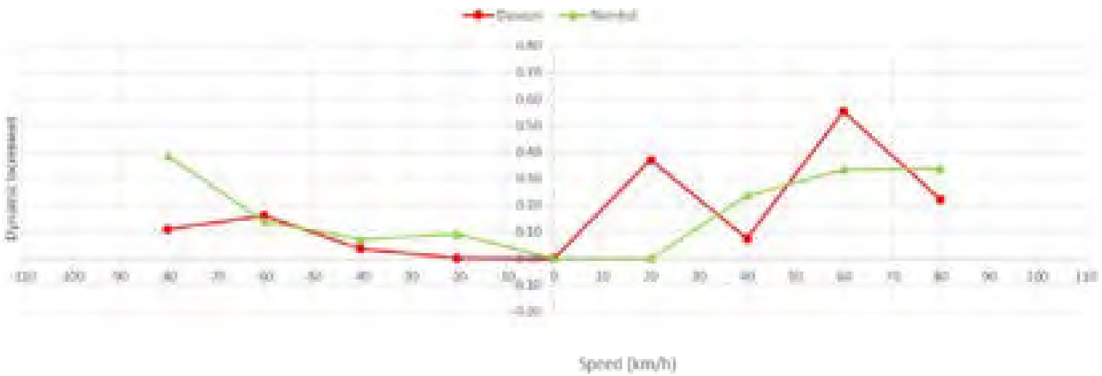

(c) RT1

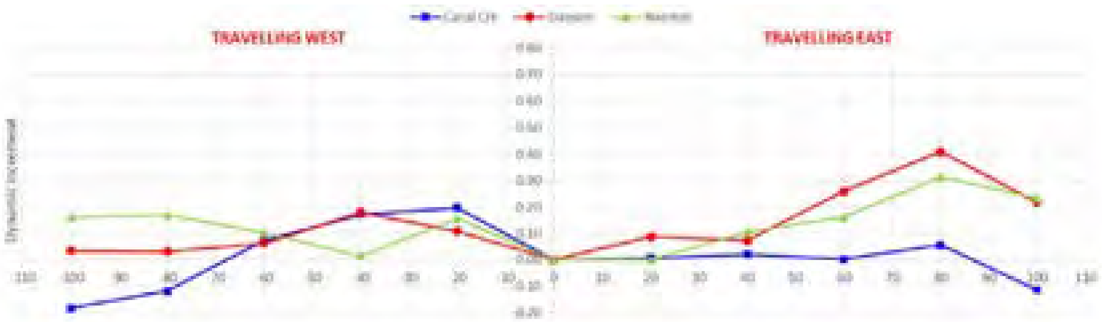

(d) RT2

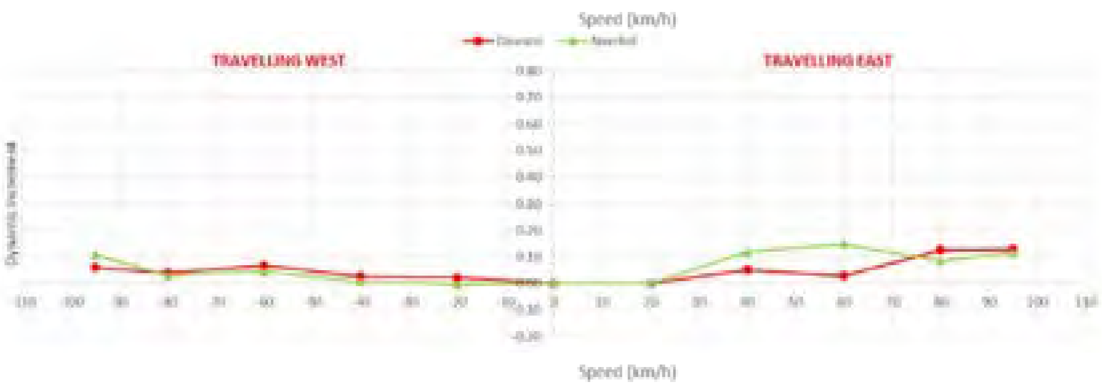

5.3 Gross Vehicle Mass

The mass of each test vehicle for each bridge is summarised in Table 5.1. The comparison of vehicle gross mass to resulting DI values is shown in Figure 5.2(a) (directly comparing mass), and in Figure 5.2(b) (relating the results to bridge frequency). It can be seen that no consistent trend is immediately evident. From Figure 5.2(a), all bridges show a very weak decreasing trend of DI values with increasing mass, which is consistent with recent observations in the literature (e.g. Cantero et al. 2014; Hwang & Nowak 1991; Nassif & Nowak 1995); however the scatter in the data is considerable. Due to the weak correlation, any trends are tenuous at best. It is apparent from these observations that vehicle type and characteristics are more likely to influence DI than the gross mass of individual vehicles.

It has been noted in the literature that single vehicle events are more likely to yield higher dynamic load amplification in comparison to multiple vehicles, despite the increase in mass on the bridge (e.g. Arun et al. 2011; Cantero et al. 2014; Caprani 2005; Rattigan et al. 2005). This is discussed further in Section 7 and Section 8 in relation to in-service monitoring data. However to date Australian field trials of this nature are yet to occur. It is recommended that this area be investigated in relation to the possible reductions in DI values.

Table 5.1: Certified mass of each test vehicle

Bridge	Mass (t)					
	CR1	CR2	ST1	ST2	RT1	RT2
Canal Creek	47	–	40	44	73.5	–
Dawson & Neerkol	47	40	–	–	82	82

Figure 5.2: Review of DI values in relation to vehicle mass

(a) Mass vs DI values

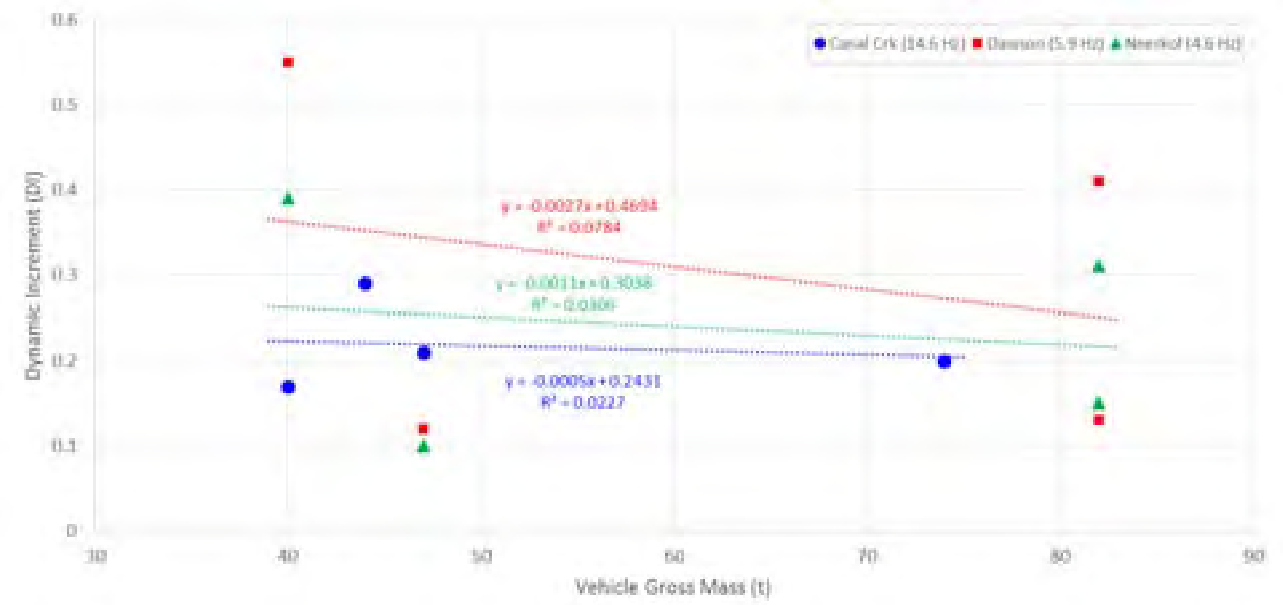

(b) Relating to bridge frequency, f

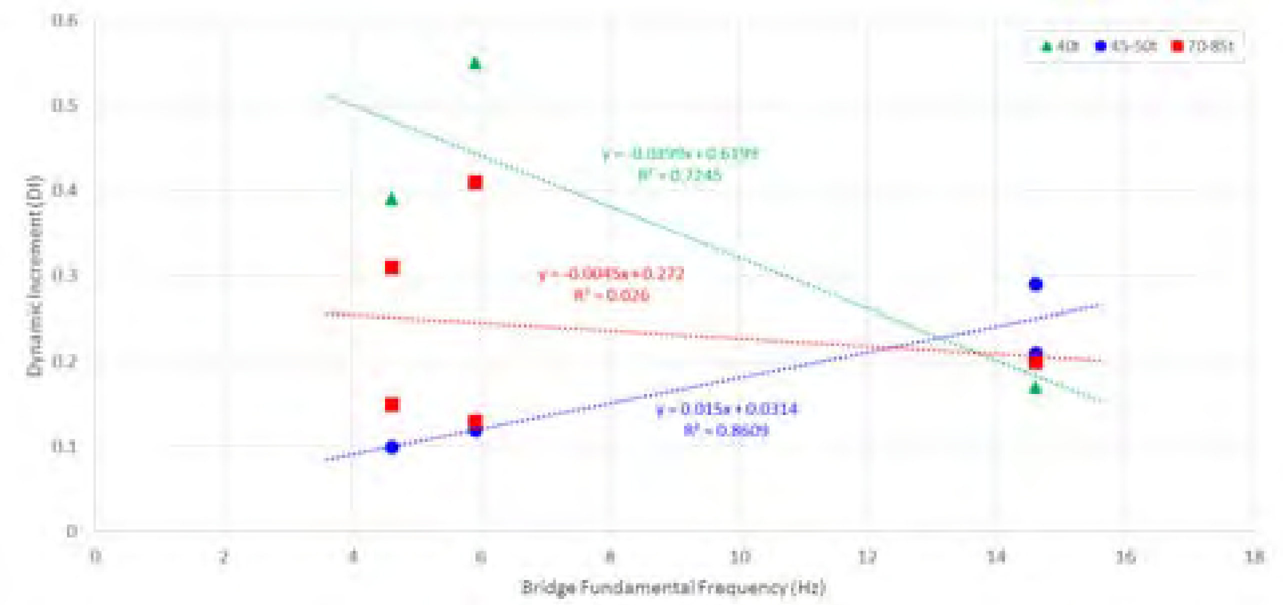

5.4 Vehicle Length, Axle Groups and Configuration

The variety of vehicles used for each bridge test enabled a review of various parameters noted to be influential in the literature. These include (Billing & Agarwal 1990; McLean & Marsh 1998; O'Connor & Pritchard 1985; Sweatman et al. 1997):

- number of axle groups (relating to the length of the vehicle)
- axle group configuration (e.g. single, tandem and triaxle groups, distance between groups).

In order to review these influences, the dynamic response of the bridge was reviewed as shown in Table 5.2.

Table 5.2: Methodology for comparison of vehicle length and configuration

Vehicle Comparison	Bridge	Demonstrated Parameter
CR1:RT1	Canal Creek, Dawson & Neerkol	▪ number of axle groups/vehicle length
CR2:RT1	Canal Creek, Dawson & Neerkol	▪ number of axle groups/vehicle length
CR1:RT2	Dawson and Neerkol	▪ number of axle groups/vehicle length ▪ axle group configuration
ST1:RT1	Canal Creek	▪ number of axle groups/vehicle length
CR1:ST2	Canal Creek	▪ number of axle groups/vehicle length
RT1:RT1	Canal Creek, Dawson & Neerkol	▪ axle group configuration

Representative cases of vehicles travelling at 80 km/h were reviewed and the results of the comparison are now discussed in light of load amplification (from DI values).

5.4.1 Vehicle Length

Hwang and Nowak (1991) noted that single truck configurations (such as short, rigid vehicles) were more likely to produce greater load amplification in comparison to a tractor-trailer-type configuration (such as an articulated semi-trailer). To investigate this claim, shorter test vehicles (such as CR1 and CR2) were compared against semi-trailers ST1 and ST2 (for Canal Creek) and RT1 (for all bridges), with vehicles being grouped and reviewed in accordance with similar suspension types. The peak DI values for the representative vehicle speed (80 km/h) and direction of travel for each vehicle case are summarised in Table 5.3, whilst relative vehicle sizes are shown in Figure 5.3. The graphical comparisons of vehicle waveforms are shown in Figure 5.4 to

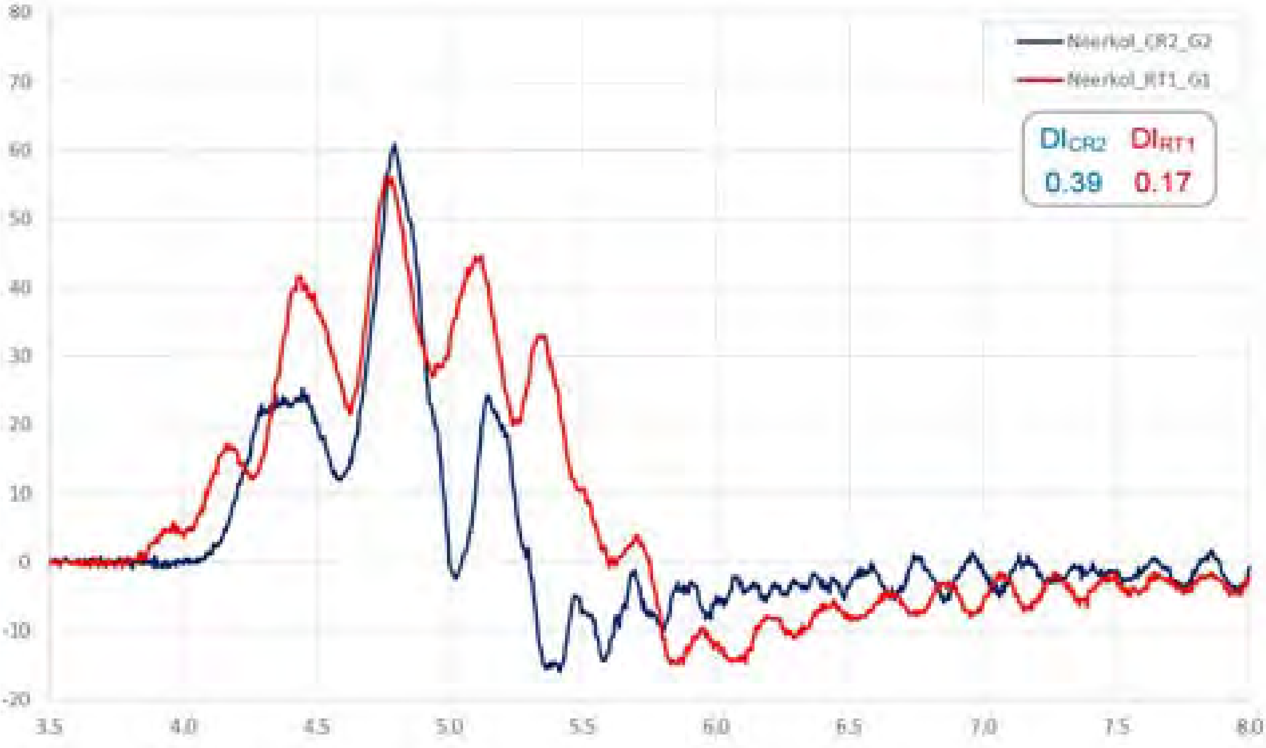

Figure 5.7. When comparing crane test vehicles to semi-trailers and road trains, no apparent trend is directly evident to support that shorter vehicles are more likely induce more elevated DI values. For example, the DI values for CR1 were less than those determined for RT2 for the Dawson River Bridge (Figure 5.5(a)), but the opposite was noted for the Neerkol Creek Bridge (

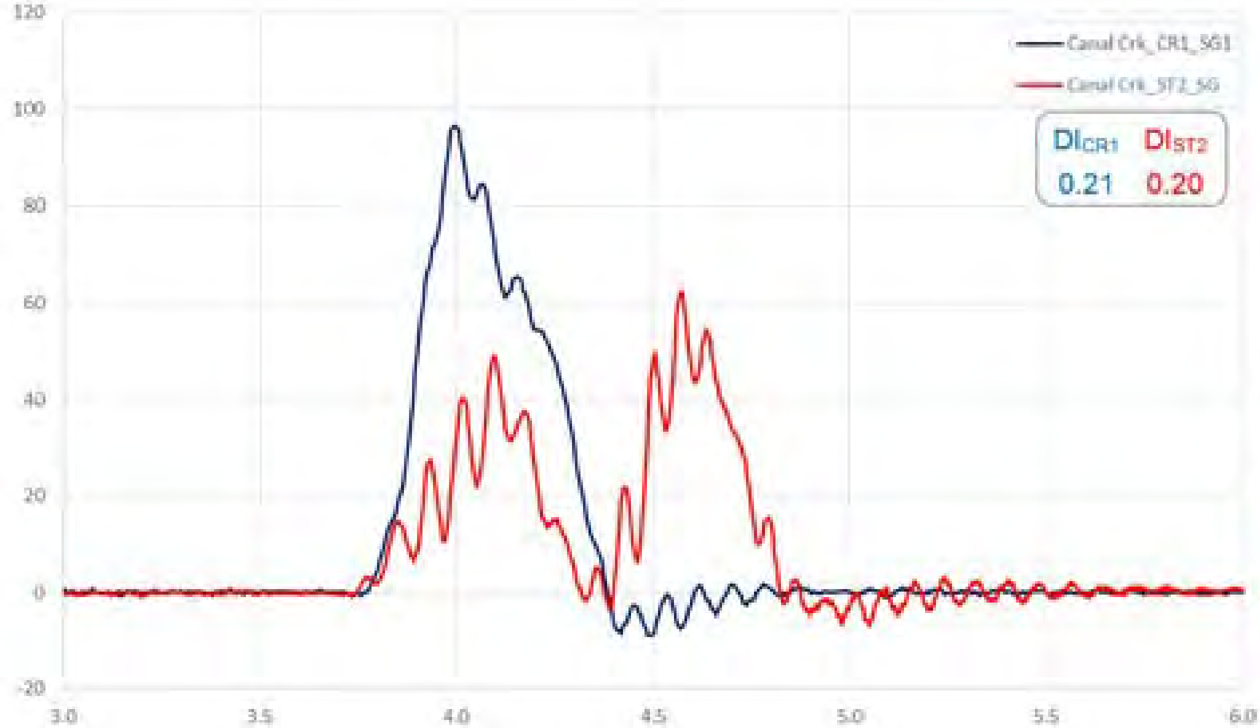

Figure 5.5(b)). It is likely that the axle spacing and configuration has been more influential rather than based purely on vehicle length. Similar opposing trends were observed between CR2 and RT1 (

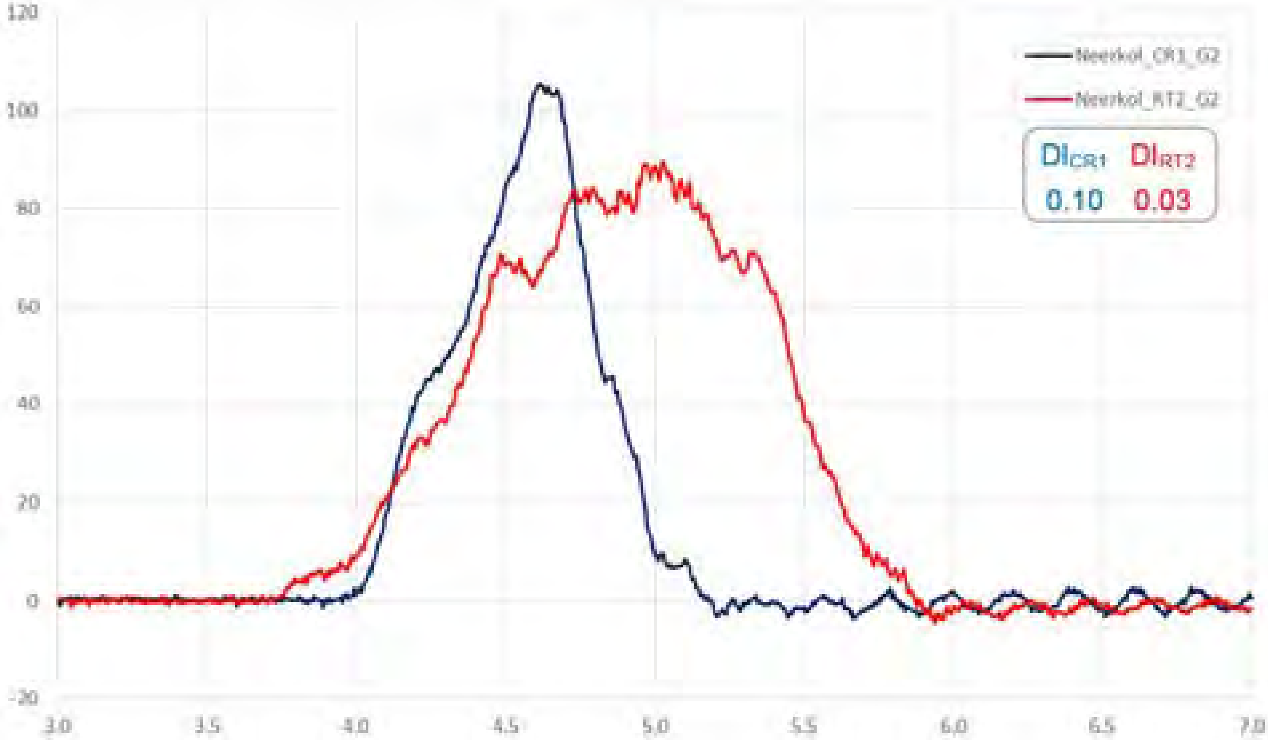

Figure 5.6Figure 5.6).

For a more direct comparison of vehicle length, attention is brought to Figure 5.7 which highlights the different responses between ST1 and RT1 for the Canal Creek Bridge. RT1 comprises the same prime mover and first trailer as ST1, and was approximately 14 m longer. The DI value for ST1 is greater than that recorded for RT1, which is in keeping with Hwang and Nowak's observations, with the DI value for RT1 less than 0, possibly indicating an out-of-phase response of the road train to the bridge. Note, however, that these peak values were less than 0.4.

It is of interest to note the identical nature of the ST1 and RT1 waveforms for the first trailer in Figure 5.7. Peak DI values were determined from peak strain values induced by the tandem axle group for both vehicles, indicating that in this instance the vehicle's centre of gravity is acting close to this location.

Table 5.3: Comparison of load amplification for shorter and longer vehicles (travelling at 80 km/h in the same direction)

Comparative case	Bridge	DI value		$DI_{short} > DI_{long}$?
		Shorter	Longer	
CR1:ST2	Canal Creek	CR1 0.21	ST2 0.20	True
CR1:RT2	Dawson River	CR1 0.06	RT2 0.13	False
	Neerkol Creek	CR1 0.10	RT2 0.03	True
CR2:RT1	Dawson River	CR2 0.22	RT1 0.41	False
	Neerkol Creek	CR2 0.39	RT1 0.17	True
ST1:RT1	Canal Creek	ST1 0.04	RT1 -0.12	False

Figure 5.3: Relative test vehicle size

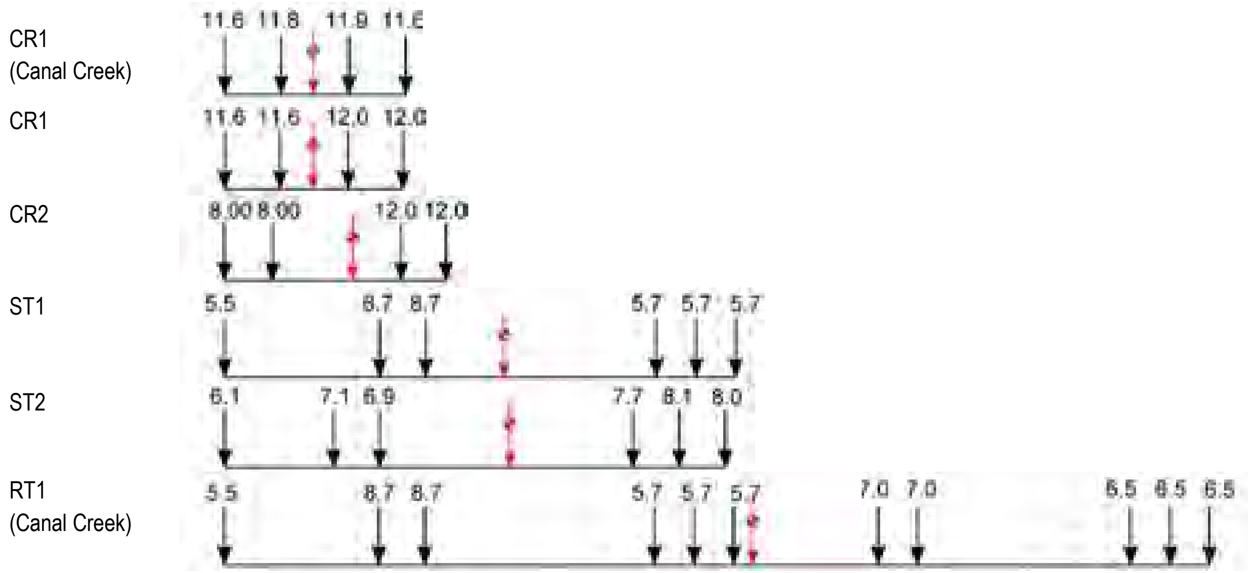

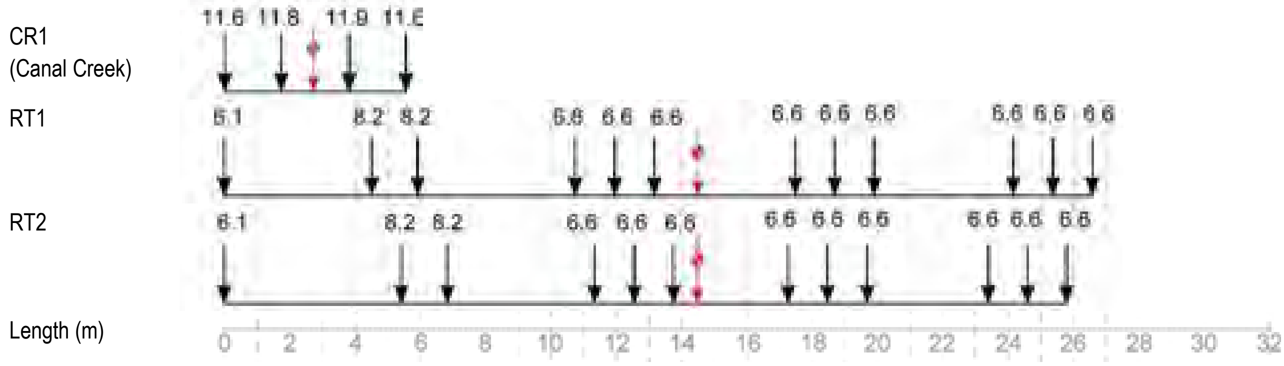

Figure 5.4: Comparison of mid-span bending strain waveform – CR1:ST2 (Canal Creek Bridge)

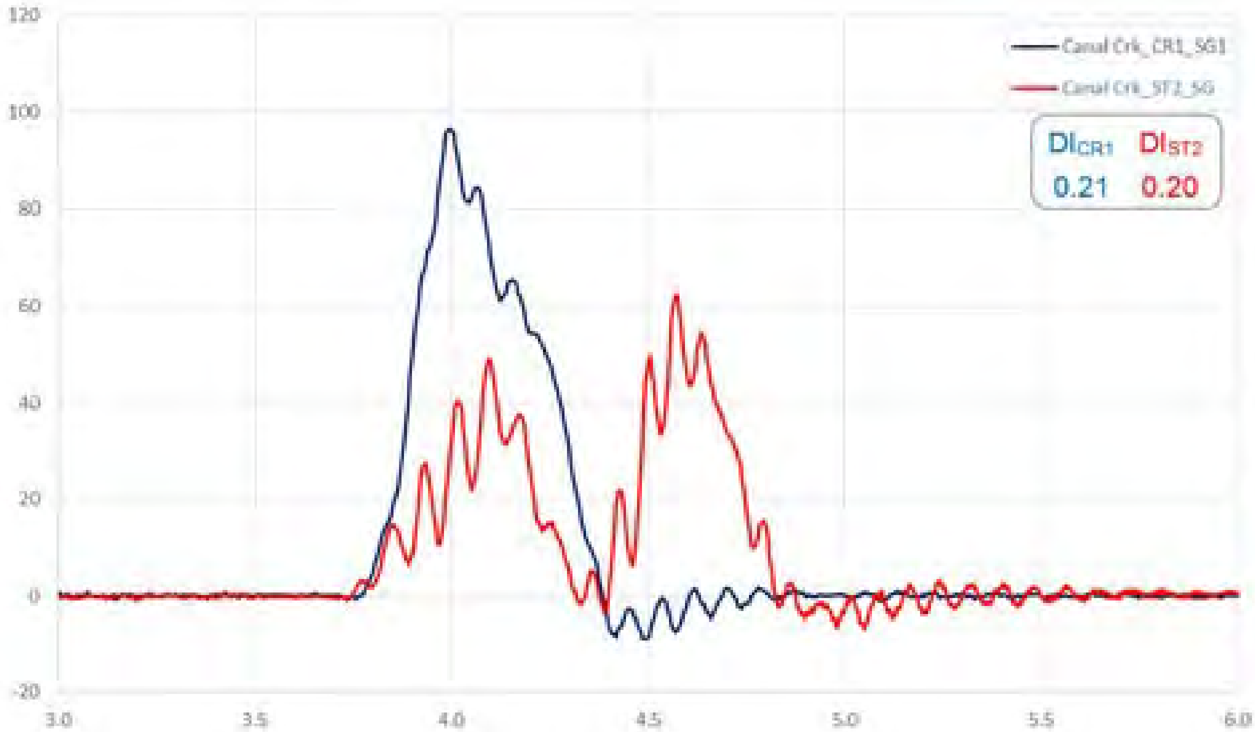

Figure 5.5: Comparison of mid-span bending strain waveform – CR1:RT2

(a) Dawson River Bridge

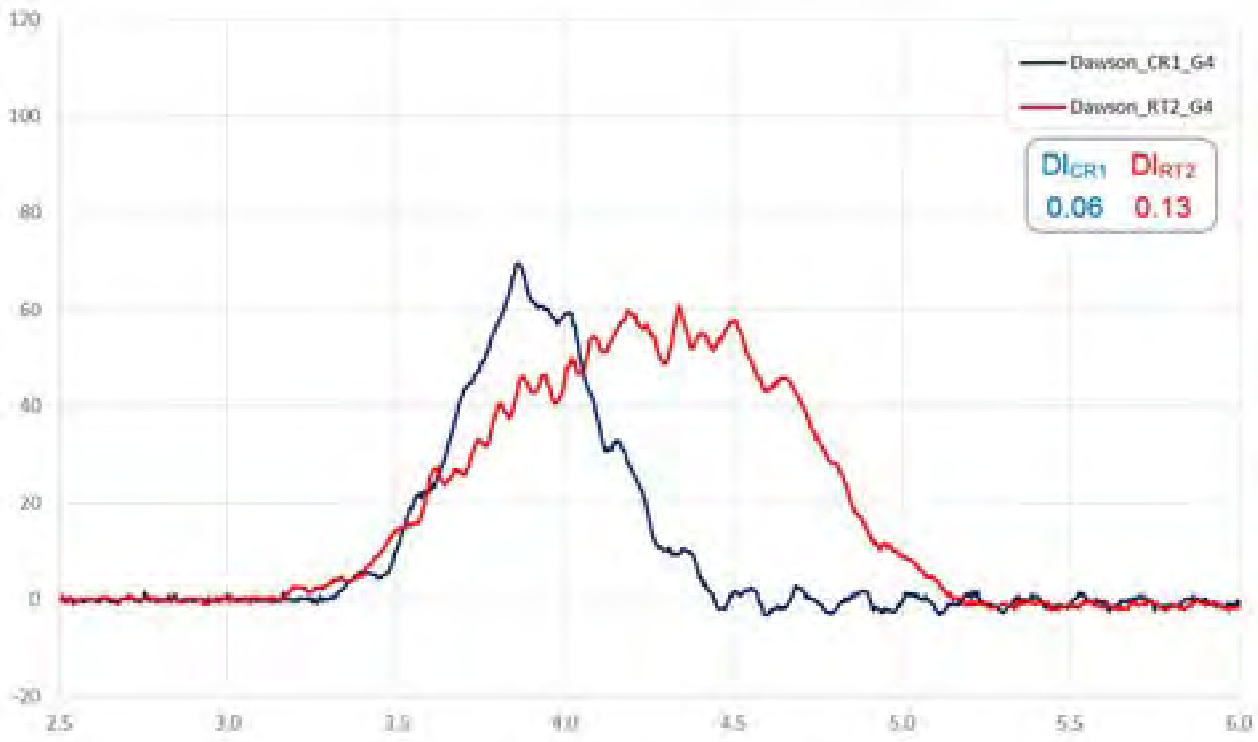

(b) Neerkol Creek Bridge

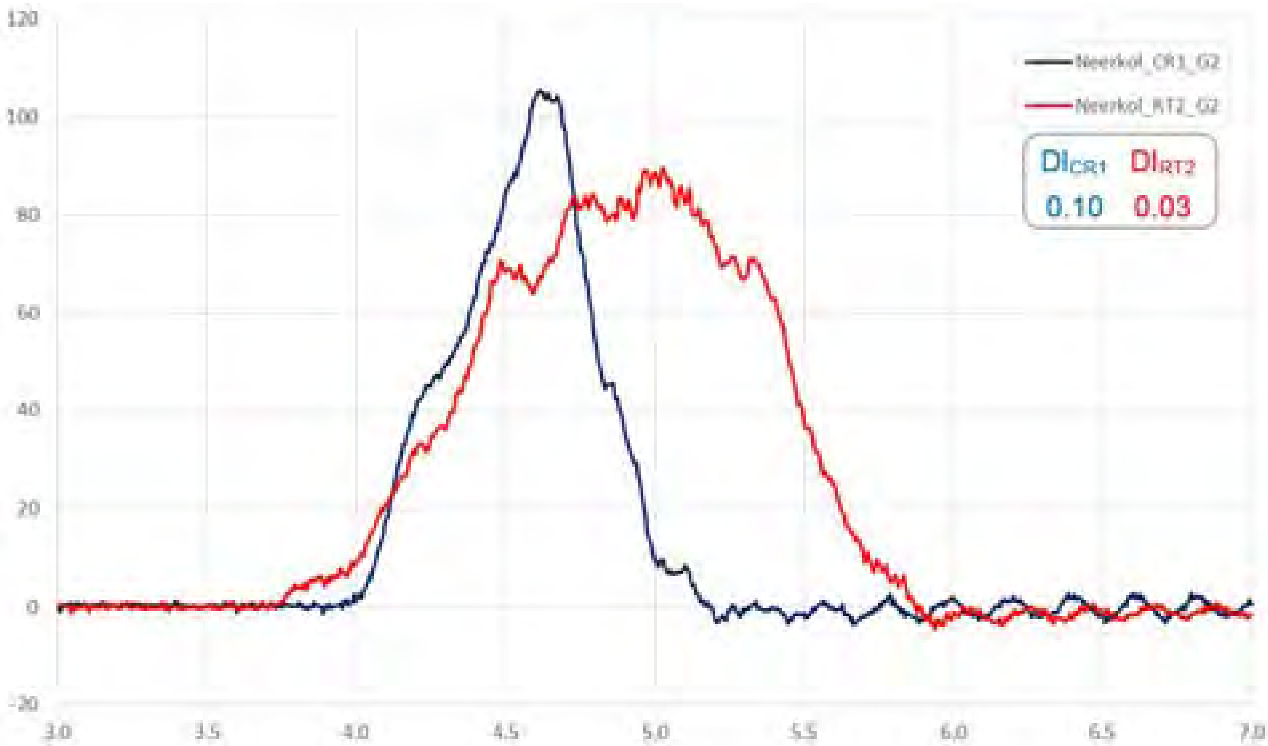

Figure 5.6: Comparison of mid-span bending strain waveform – CR2:RT1

(a) Dawson River Bridge

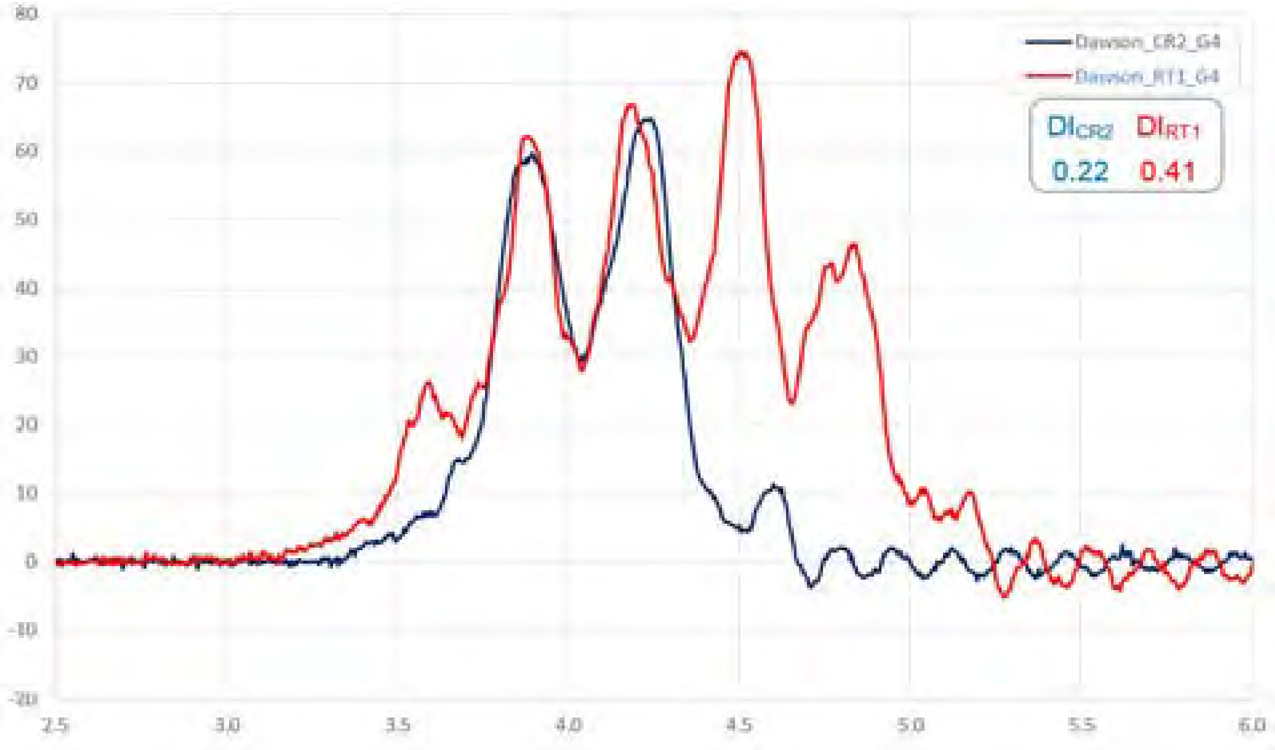

(b) Neerkol Creek Bridge

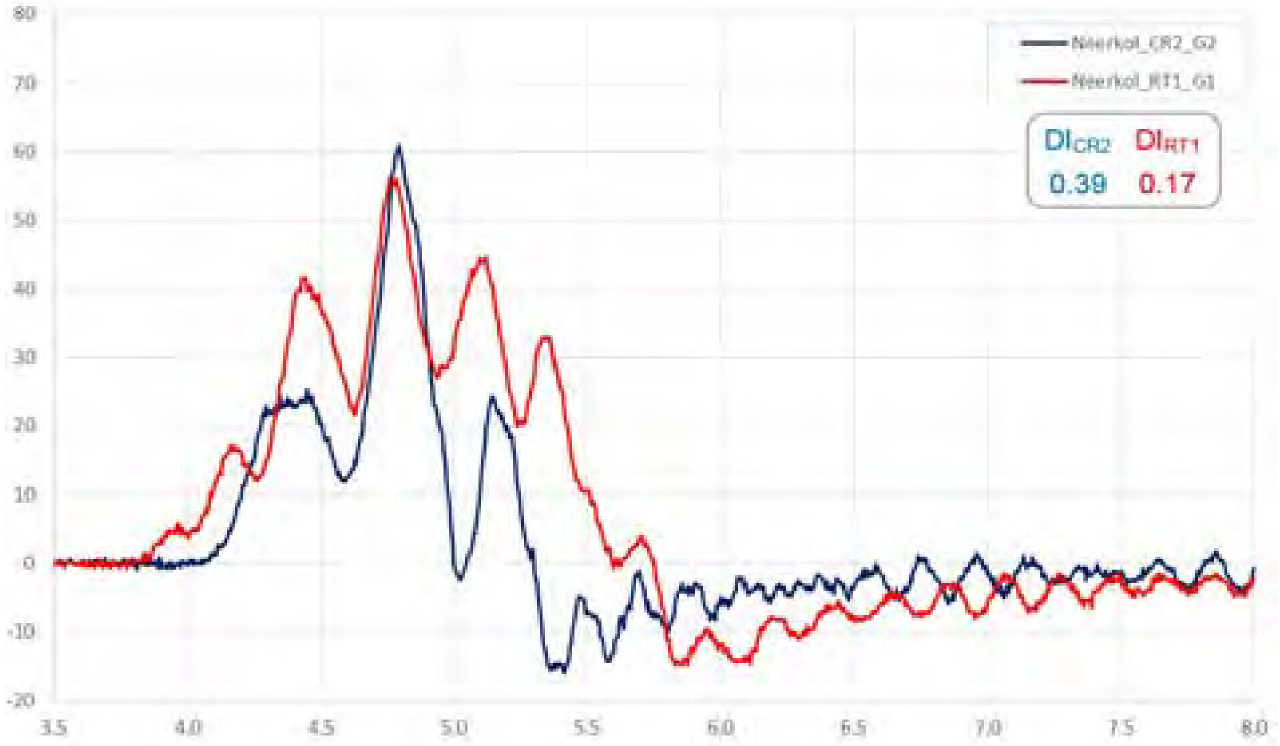

Figure 5.7: Comparison of mid-span bending strain waveform – ST1:RT1 (Canal Creek Bridge)

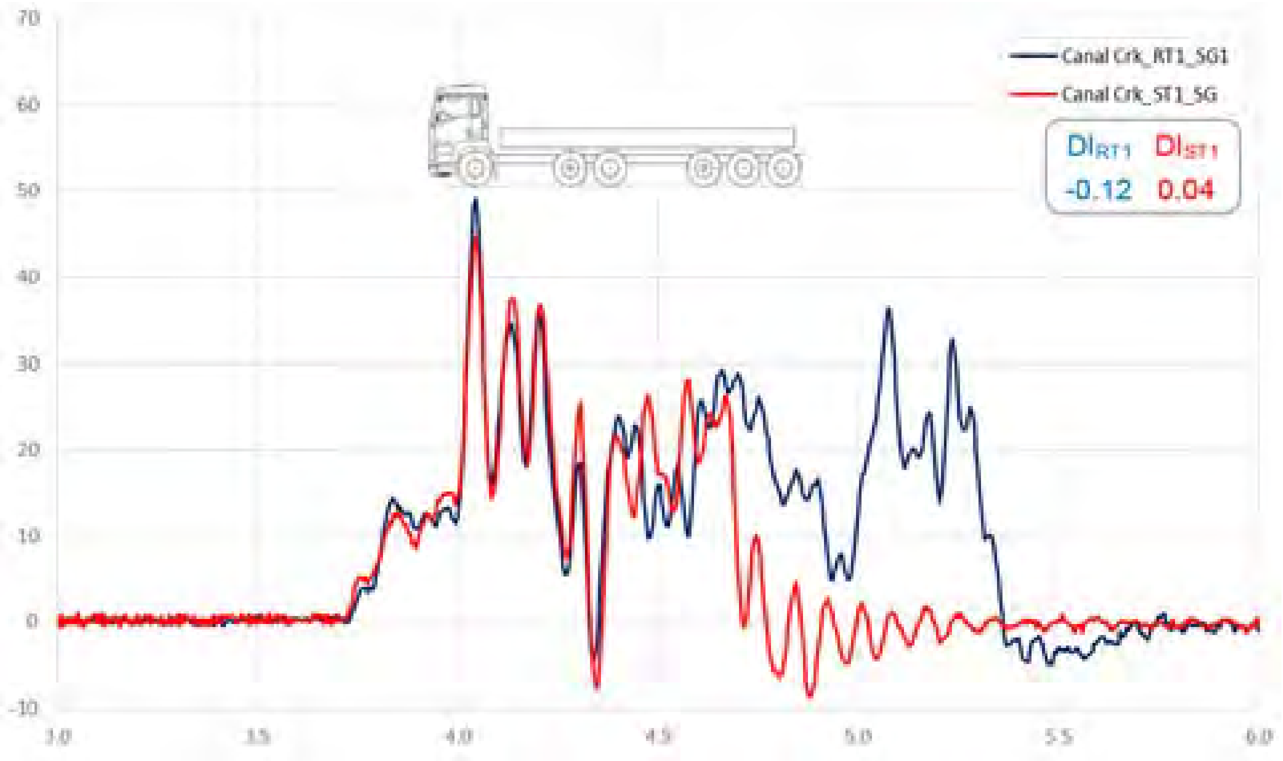

5.4.2 Axle Group Configuration

Various authors have noted that shorter axle configurations are more likely to produce greater load amplification in comparison to those with a longer wheel base (Baumgärtner 1998; Billing & Agarwal 1990; Gillmann 1999; Hwang & Nowak 1991). Of the various test vehicles, peak DI values corresponding to maximum superstructure bending strains were reviewed for single, tandem and triaxle group configurations, and the results are summarised in Table 5.4.

A review of the DI values for single axle points (i.e. CR1 and CR2), suggested that the peak DI values were relatively low for CR1 and approximately or higher than 0.4 for CR2. Axle spacings for CR2 were slightly longer than CR1, and as such, the DI results were not in keeping with the observations in the literature. For ST1 and ST2 for the Canal Creek Bridge, the DI values were similar despite different critical speeds, with ST2 being slightly higher. Axle spacings between groups three and four were longer for ST2 than ST1 and, based on the literature, DI values were anticipated to be greater for ST1. This was not the case.

Regarding the road trains, the largest DI values (exceeding 0.4) were recorded for the Dawson River Bridge, followed by the Neerkol Creek Bridge. Peak DI values occurred predominantly at the 3rd triaxle group at higher speeds, with the exception of RT1 for the Canal Creek Bridge which occurred at the tandem axle group at 20 km/h.

Table 5.4: Peak DI values and bending strains compared to corresponding axle group from each test vehicle

Test vehicle	Bridge	Peak DI	Corresponding peak strain (με)	Direction of travel	Speed (km/h)	Axle group	
CR1	Canal Creek	0.21	97	West	80	2nd	Single
	Dawson	0.12	83	West	40	Undefined	Single
	Neerkol	0.10	105	West	80	2nd, 3rd	Single

Test vehicle	Bridge	Peak DI	Corresponding peak strain ($\mu\varepsilon$)	Direction of travel	Speed (km/h)	Axle group	
CR2	Dawson	0.55	83	East	60	3rd	Single
	Neerkol	0.39	109	West	80	3rd	Single
ST1	Canal Creek	0.19	61	West	40	2nd	Tandem
ST2*	Canal Creek	0.29	70	West	100	3rd	Tri-axle
RT1 *	Canal Creek	0.20	67	West	20	2nd	Tandem
	Dawson	0.41	76	East	80	4th	Tri-axle
	Neerkol	0.31	87	East	80	3rd	Tri-axle
RT2	Dawson*	0.09	65, 65	East	80, 100	3rd or 4th	Tri-axle
	Neerkol*	0.15	75	East	60	4th	Tri-axle

Axle spacing for RT1 from Canal Creek were longer than those for RT1 and RT2 used for the Dawson and Neerkol Bridges. No clear trends agreeing with the findings of the literature regarding dynamic load amplification preferences could be identified from the current test results. As such, it is apparent that the vehicle type and the inherent dynamic characteristics of each bridge have been influential on the responses recorded.

For all vehicles, the centre of gravity (COG) has been influential on where peak DI values have occurred relating to axle groups, which is not unexpected. Contrary to this observation is the response recorded for ST1 and RT1 for the Canal Creek Bridge, where peak values resulted from the tandem axle group. The corresponding waveforms for these events are shown in Figure 5.9 and Figure 5.10 respectively. Note the frequency response of each waveform. For ST1 (Figure 5.9), a more dynamic response is noted for the prime-mover prior to the tandem axle passing mid-span. For RT1 (Figure 5.10), a similar response was recorded for both trailers and axle groups (with the exception of axle group 4), with axle group 5 yielding a significant dynamic response of similar amplitude to the tandem axle. An elevated strain response between axle groups 3 and 4 was evident, indicating the trailer connectivity constraints between these two groups. Very little exists in the structural engineering literature regarding trailer connection combinations, and it is recommended that further research be carried out to investigate the implications on dynamic load amplification.

5.4.3 Summary of Observations

In terms of the length of vehicle, inconsistent results were determined for most vehicle comparisons and they generally did not agree with the findings from the literature.

Figure 5.8: Mid-span bending strain waveform – ST2 travelling West at 40 km/h

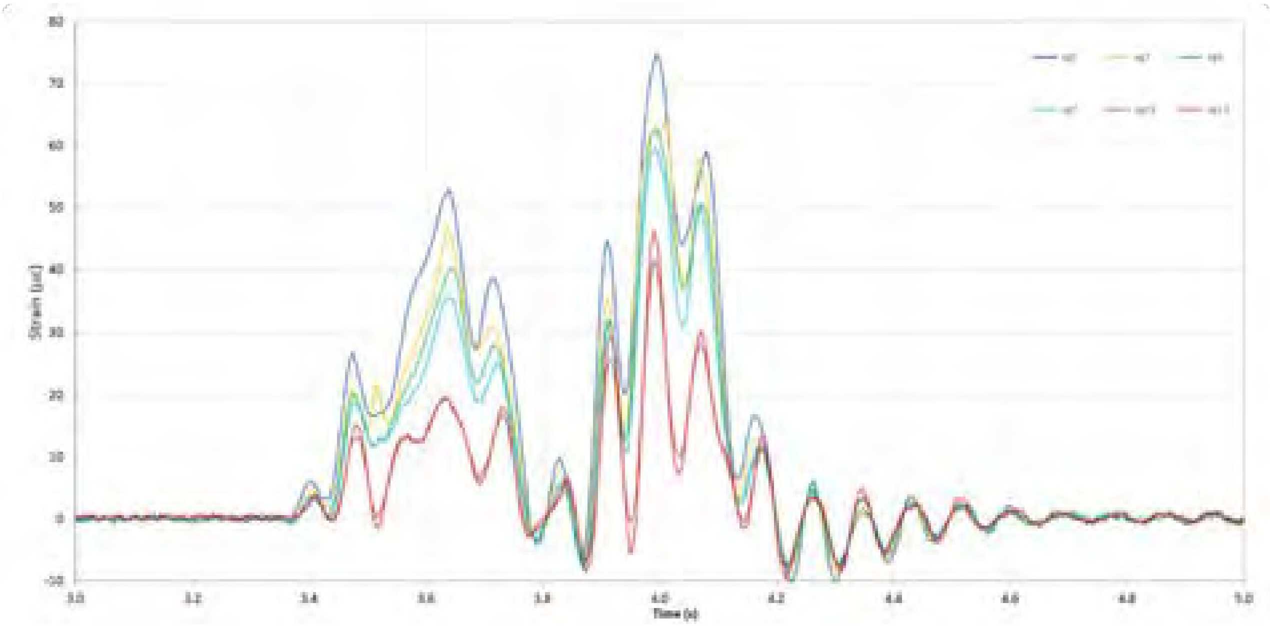

Figure 5.9: Mid-span bending strain waveform - ST1 travelling West at 40 km/h

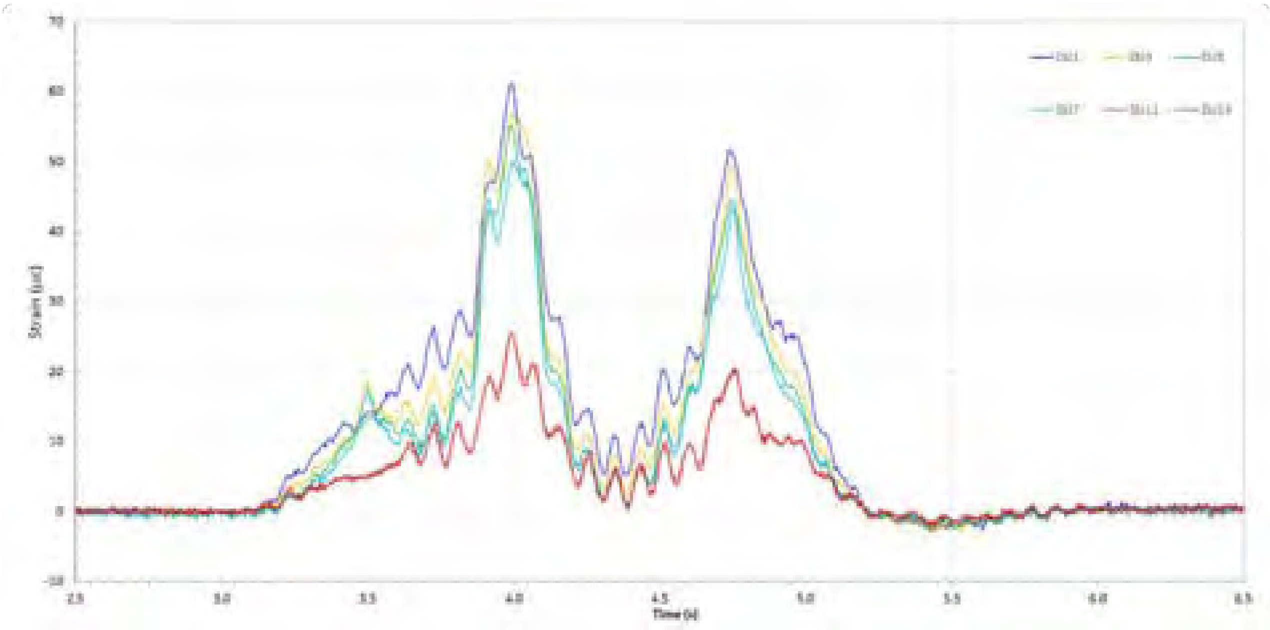

Figure 5.10: Mid-span bending strain waveform - RT1 travelling West at 20 km/h

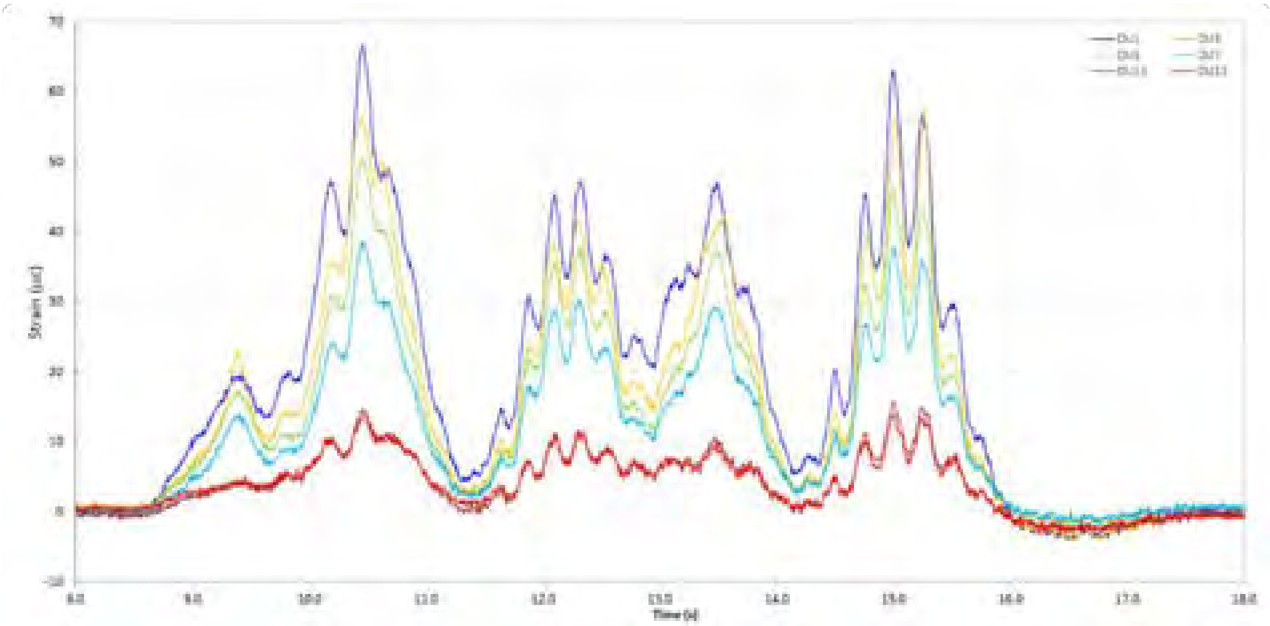

5.5 Vehicle Suspension Type

5.5.1 Introduction

It has been well documented in the literature that the suspension type of a vehicle can be a significant influence on the amplification of load (Austroads 2003; Green & Xie 1998; Heywood 2000; OECD 1999). In particular, the literature has noted that air-bag suspension vehicles are more likely to produce lower dynamic load amplification in comparison to steel suspension systems (Davis 2010; Green & Xie 1998; Heywood et al. 2001; Lambert, McLean & Li 2004). Limited research has been carried out in relation to load amplification of bridges in response to hydro-pneumatic cranes (Heywood 1998).

Results and direct comparisons of vehicle suspension types has been made using the following test vehicle combinations:

- ST1 vs ST2 (Canal Creek) (Section 5.5.2)
- RT1 vs RT2 (Dawson and Neerkol Bridges) (Section 5.5.3)
- CR1 vs CR2 (Dawson and Neerkol Bridges) (Section 5.5.4).

5.5.2 Comparison of Semi-trailer Performance (Canal Creek Bridge)

Figure 5.11 compares the mid-span bending strain waveforms for ST1 and ST2 travelling in the same direction at 80 km/h. Both waveforms exhibit cyclic responses in keeping with the fundamental bending frequency of this bridge, demonstrating the influential nature of such characteristics in governing dynamic behaviour. The influence of the vehicle's centre of gravity is evident in the dynamic response of the girders to the triaxle group. Note that despite the greater mass of ST2, the strain magnitude induced by ST1 under the tandem axle is similar to that of ST2 (44 $\mu\varepsilon$ in comparison to 52 $\mu\varepsilon$).

To compare load amplification, DI values are shown in Figure 5.12 for ST1 and ST2. Significant variation in load amplification exists for ST1 irrespective of speed and direction of travel. Peak values occur at lower speeds and do not exceed 0.2. In comparison, DI values for ST2 are insignificant for easterly travel. DI values increase linearly to 0.3 at maximum speed for westerly travel. The predominant comparative feature is the consistency of the results for an air-bag suspension heavy vehicle irrespective of speed (excluding the influence of road profile) in comparison to the sensitive and variable results for a steel suspension heavy vehicle.

These results highlight the differences between the two suspension types for a deck unit bridge. To investigate the repeatability of these observations, bridge responses to the road trains (RT1 and RT2) and the hydro-pneumatic crane (CR1) for various bridges are reviewed in the following sections.

Figure 5.11: Mid-span bending strains for ST1 and ST2 at the Canal Creek Bridge travelling west at 80 km/h (Superstructure only)

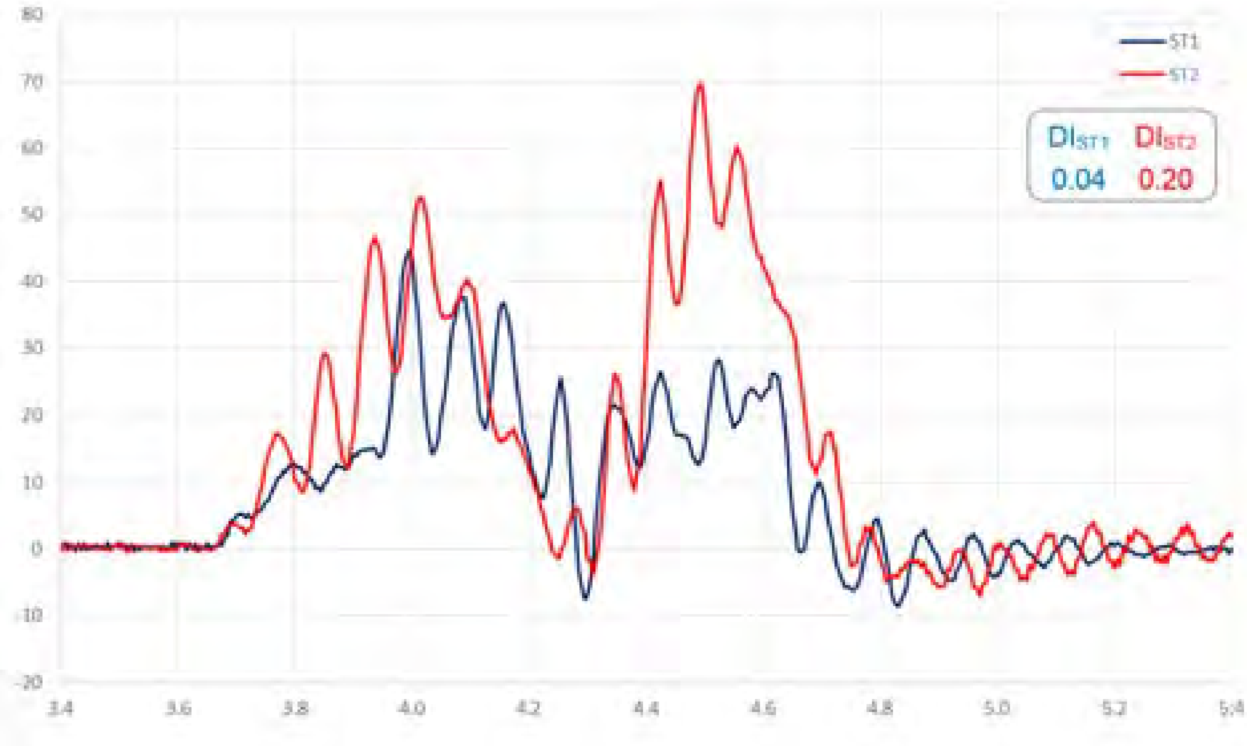

Figure 5.12: DI Values determined for ST1 and ST2 at the Canal Creek Bridge (Superstructure only)

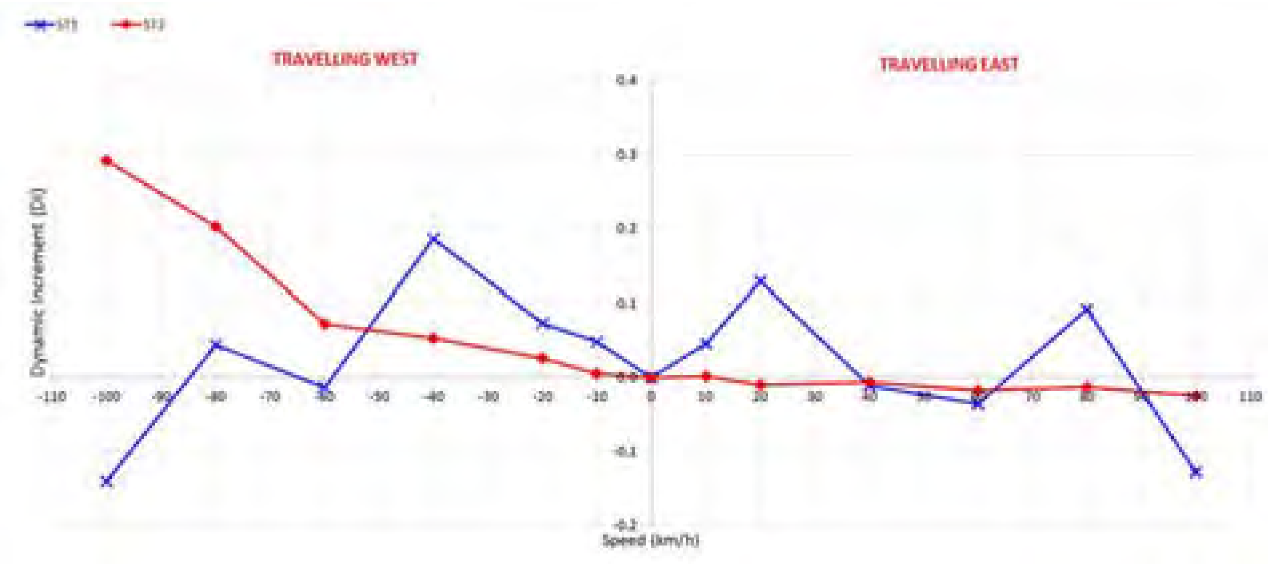

5.5.3 Road Train Performance Comparison (Dawson and Neerkol Bridges)

The mid-span dynamic response of the Dawson and Neerkol bridges to RT1 and RT2 travelling at 80 km/h is shown in Figure 5.13 and Figure 5.14 respectively for peak mid-span bending strains. For both bridges, different dynamic responses were induced by each vehicles. Distinctive and cyclic peaks were evident for RT1 at both bridge sites, with more prominent peaks noted for the Dawson River Bridge than recorded for Neerkol. In comparison, a more consistent and evenly distributed strain profile was recorded for RT2.

Figure 5.13: Mid-span bending strain comparison between RT1 and RT2 travelling west at 80 km/h (Dawson River Bridge)

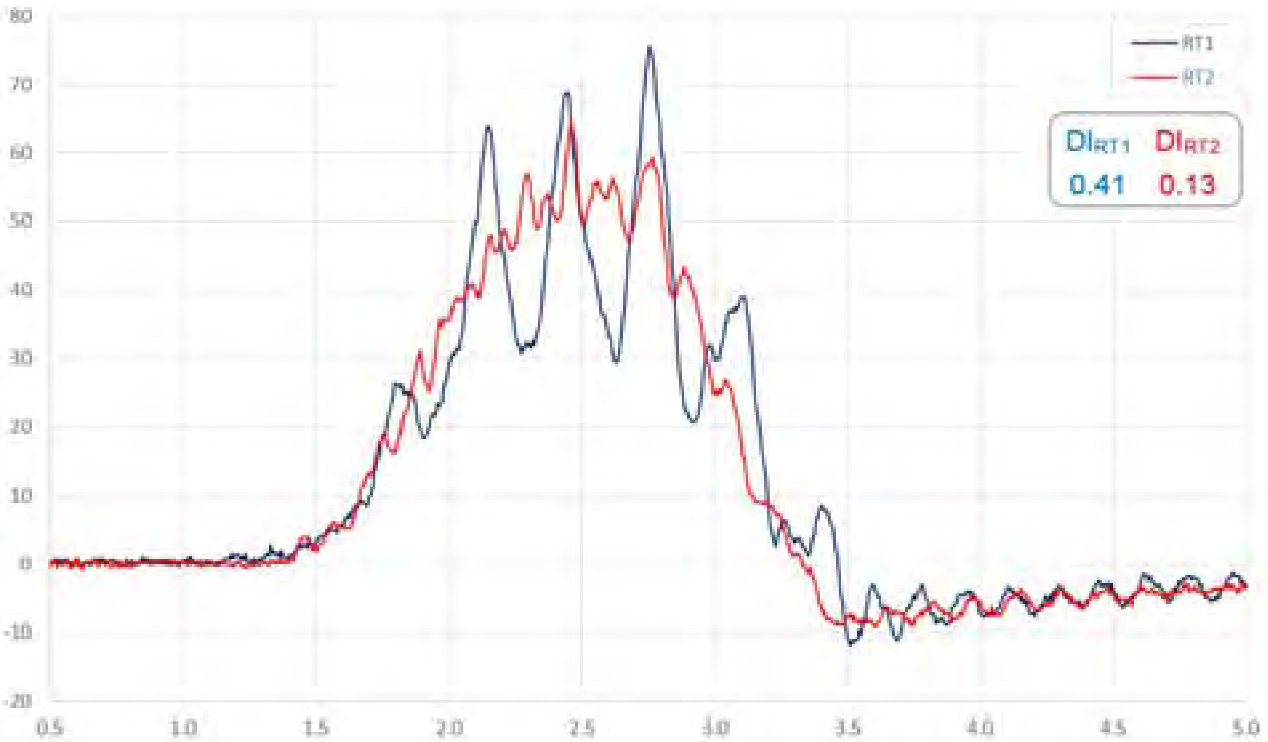

Figure 5.14: Mid-span bending strain comparison between RT1 and RT2 travelling west at 80 km/h (Neerkol Creek Bridge)

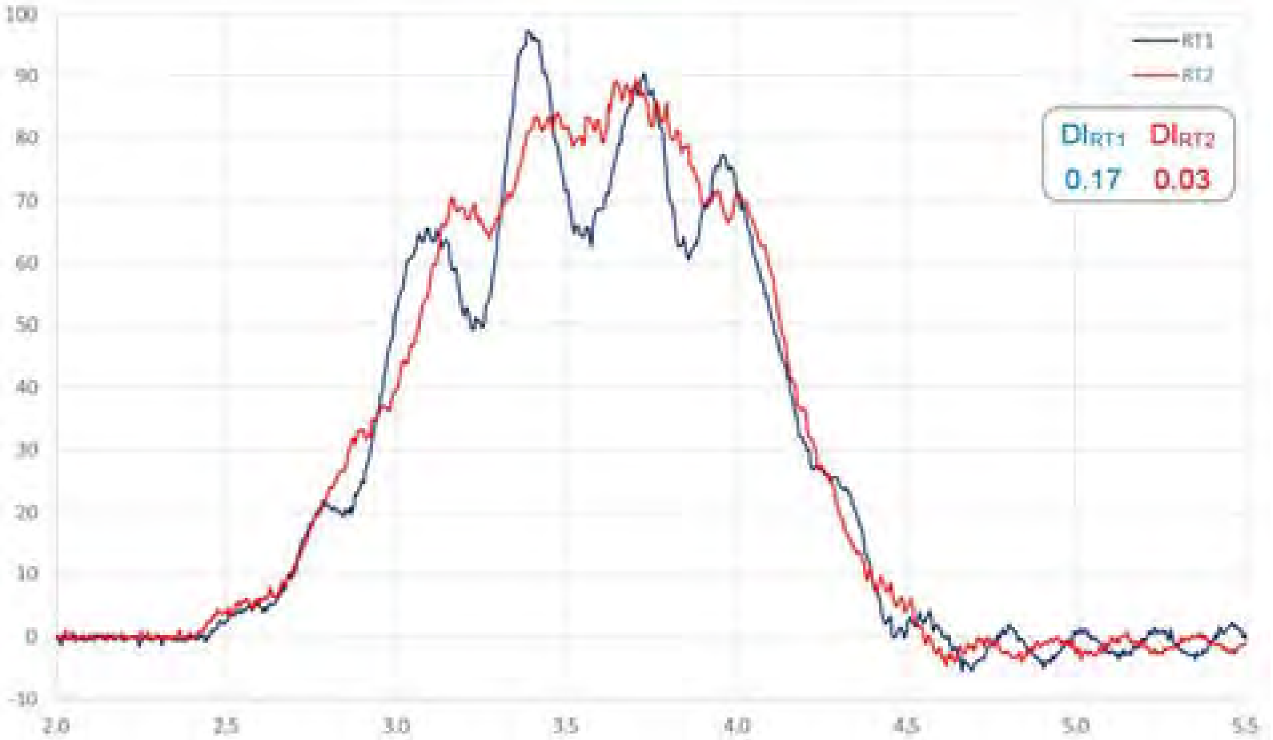

DI Value comparisons between RT1 and RT2 for the Dawson and Neerkol bridges are shown in Figure 5.15 and Figure 5.16 respectively, which have been further divided into superstructure and substructure responses. The superstructure results for the Dawson River Bridge show the response of RT1 was again more variable than RT2, with peaks occurring at lower speeds (20 and 40 km/h). RT2 yielded more consistent results less than 0.2. RT1 induced significant load amplification for easterly travel at higher speeds (peaking at 80 km/h). Whilst not significant in magnitude, DI values for RT2 increased with increasing speed for travel in the same direction, pointing to the influence of the road profile over Abutment 2.

Slightly different observations were made for substructure results for the Dawson River Bridge. DI values greater than 0.4 were determined in the headstock for RT1 travelling east, agreeing with the trend observed in the girders, with a similar trend noted for the column in tension and for RT2 travelling in the same direction. DI substructure values for RT1 were greater than those determined for RT2 travelling east, however the opposite was noted for travel west. For the cast of the column in tension, the road profile has been more influential on the increasing trend of DI values, and the suspension type has been influential on the magnitude of the load amplification where affected by road condition. Similar trends are noted for DI values determined for the column in compression, showing more distinct trends in relation to the road profile and vehicle speed.

For the Neerkol Creek Bridge, variable results for RT1 were also noted in superstructure, albeit to a lesser degree and lower magnitudes than Dawson (less than 0.3). Values increased with increasing vehicle speed irrespective of direction of travel. Consistent results were noted for RT2, with slight increases with increasing speed and similar magnitudes to RT1. For substructure components, different trends were observed, with peak DI values generally occurring at 60 km/h for both road trains and irrespective of direction of travel. Similar trends were observed between the two road trains, however DI values for RT1 were greater than RT2 values when travelling west, and vice versa for the opposing direction of travel. This may suggest the influence of inherent frequency characteristics of the substructure and boundary conditions for the Neerkol Creek

Bridge. It may also highlight the sensitivity of these substructure components to the vehicle suspension type exacerbated by the condition of the road profile.

Figure 5.15: DI Values determined for RT1 and RT2 at the Dawson River Bridge

(a) mid-span bending strains

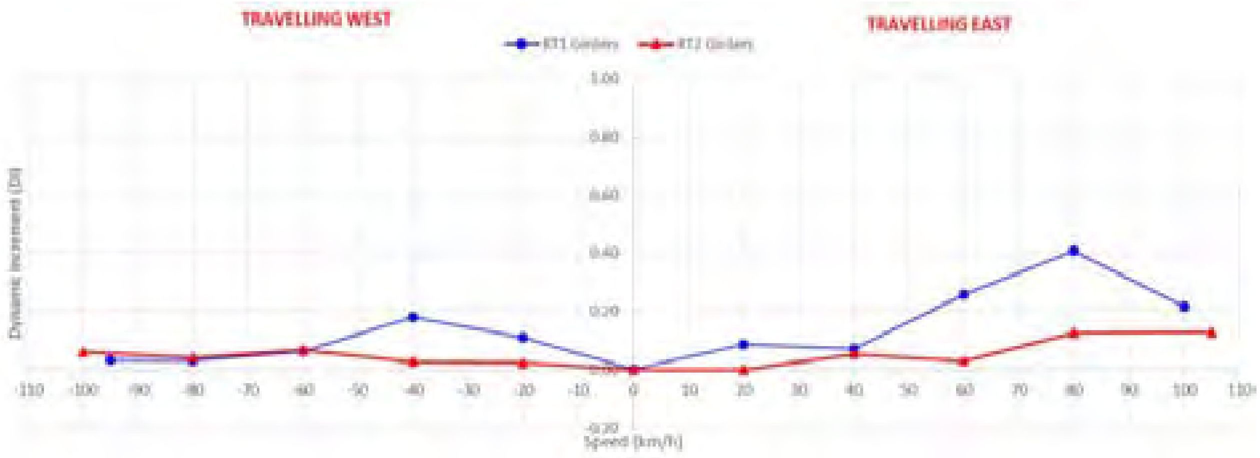

(b) substructure (tensile bending strains)

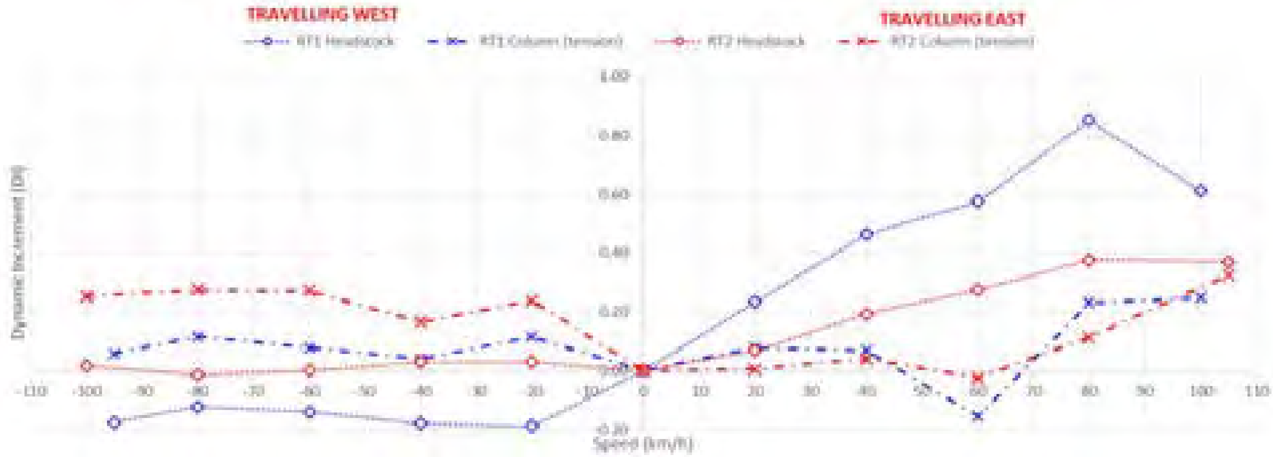

(c) substructure (compressive bending strains)

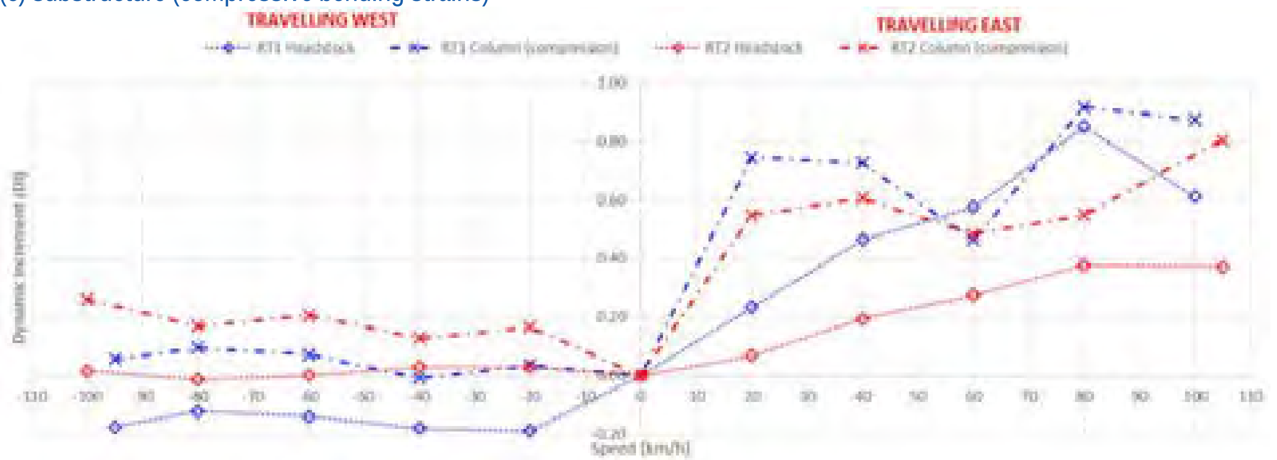

Figure 5.16: DI Values determined for RT1 and RT2 at the Neerkol Creek Bridge

(a) mid-span bending strains

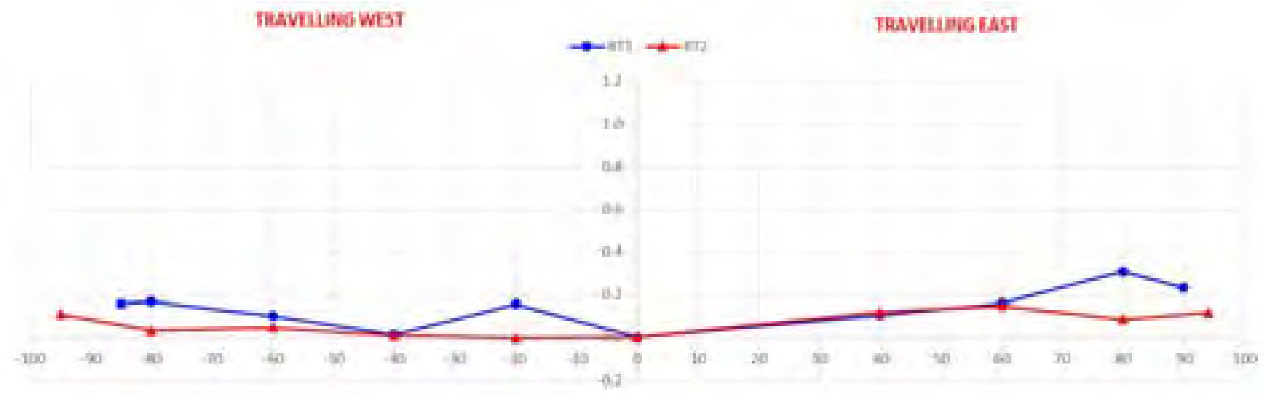

(b) substructure tensile bending strains

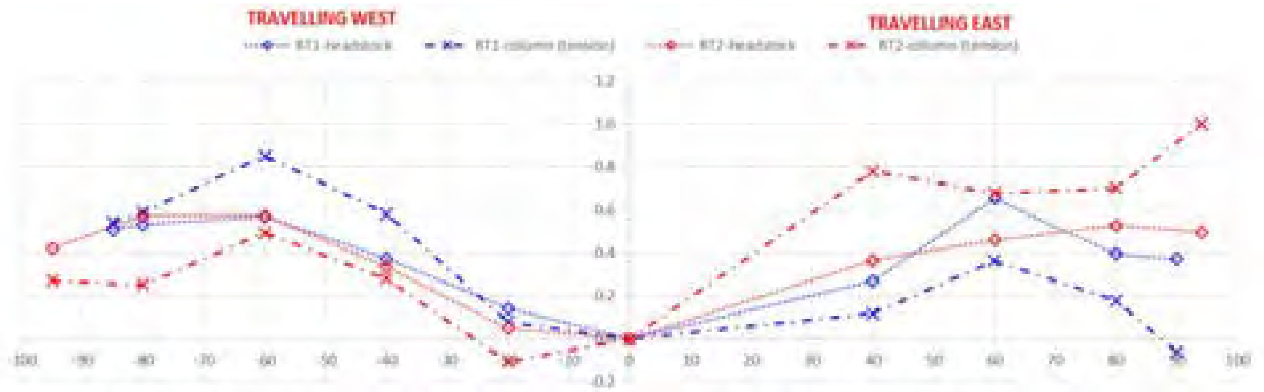

(c) substructure (compressive bending strains)

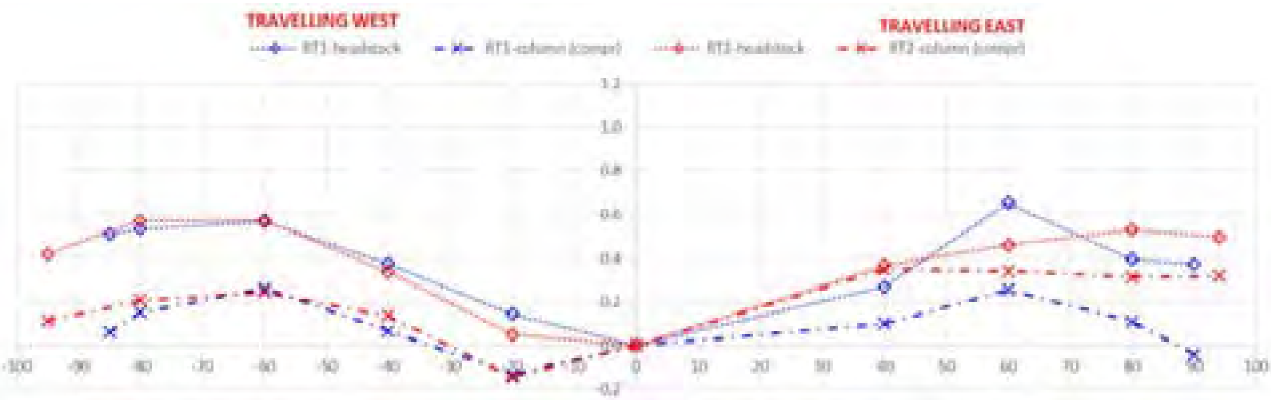

5.5.4 Comparison of Crane Performance (Dawson and Neerkol Bridges)

A comparison of superstructure dynamic response induced by the hydro-pneumatic crane (CR1) and the steel suspension truck-mounted crane (CR2) is shown in Figure 5.17 and

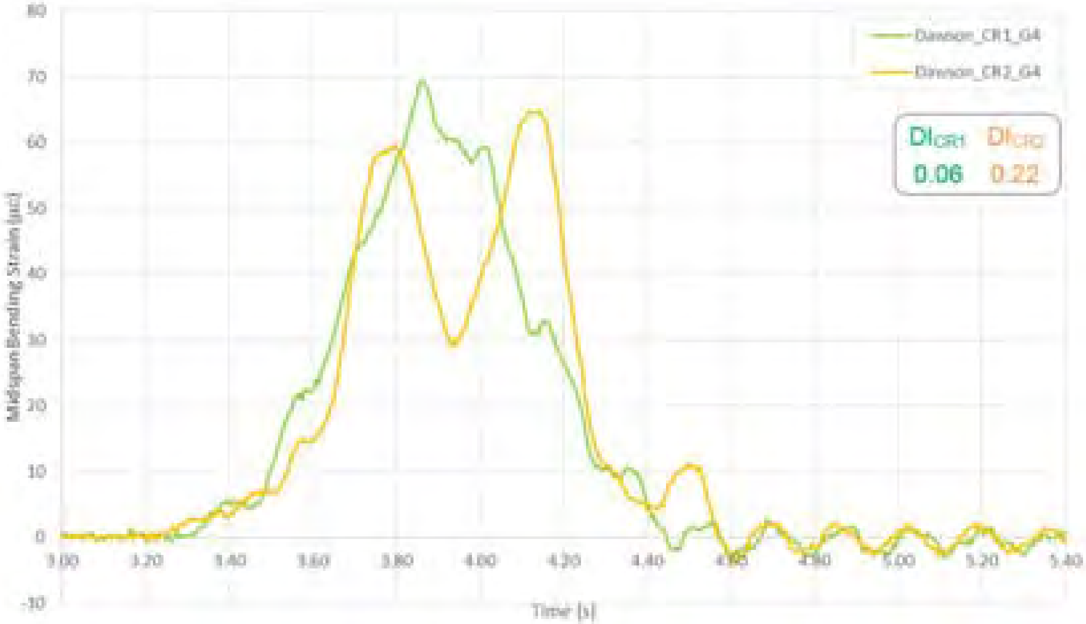

Figure 5.18 for the Dawson and Neerkol bridges respectively. A cyclic response for CR2 can be clearly identified for both bridges, in keeping with axle spacing, in comparison to the uniform and singular peak response of CR1. Note the similar strain magnitudes achieved by both cranes for Dawson, despite the differences in mass and axle spacing.

Figure 5.17: Mid-span bending strain comparison between CR1 and CR2 travelling east at 80 km/h (Dawson River Bridge)

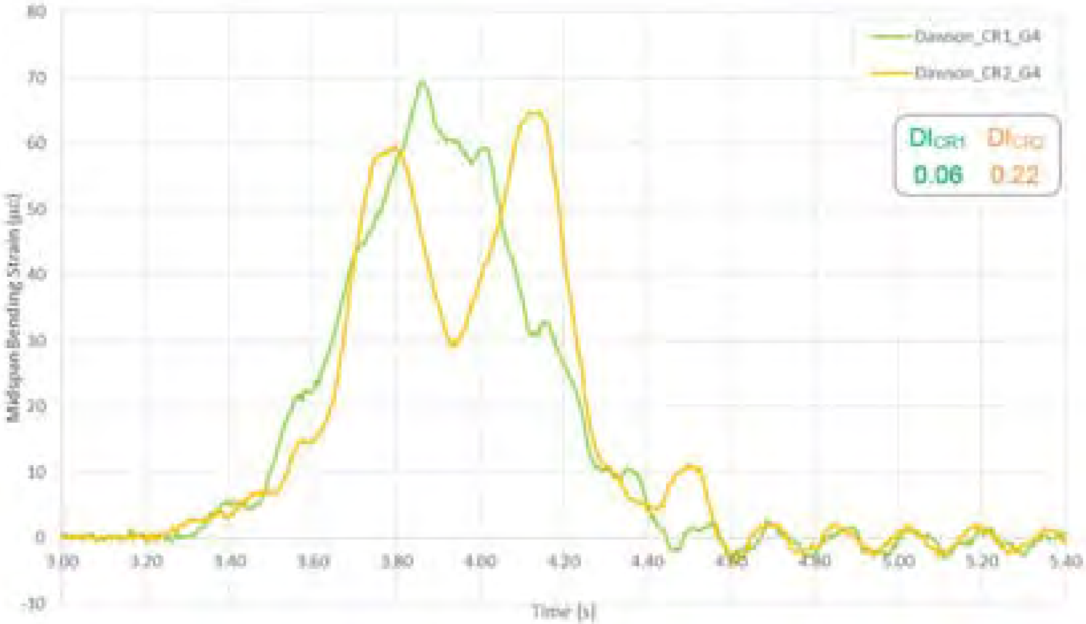

Figure 5.18: Mid-span bending strain comparison between CR1 and CR2 travelling west at 80 km/h (Neerkol Creek Bridge)

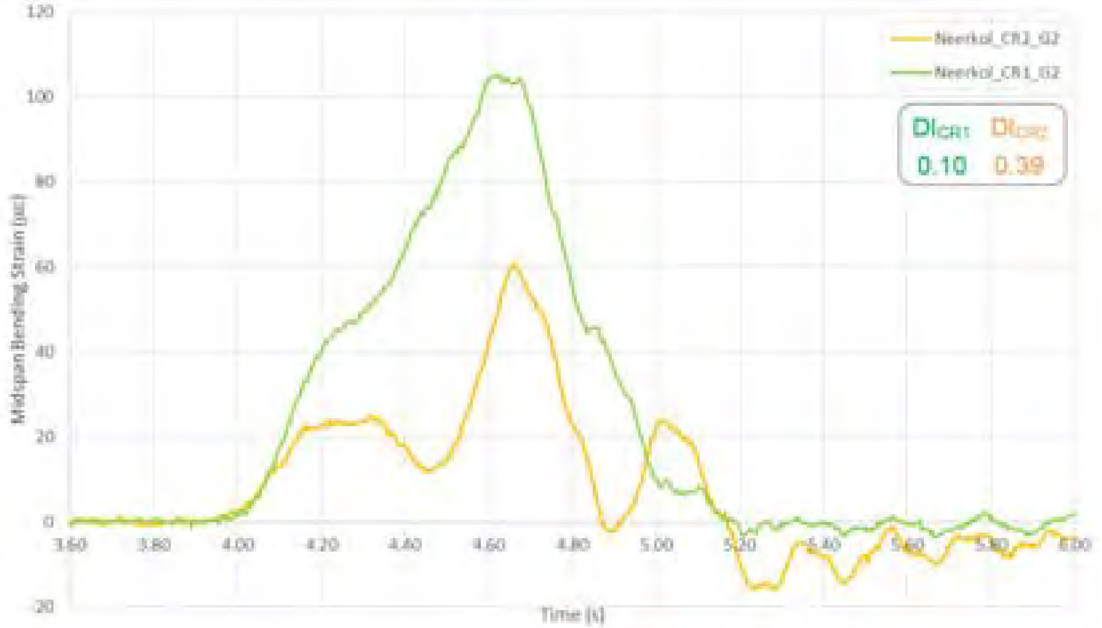

The superstructure and substructure DI values for each vehicle are compared in Figure 5.19 and Figure 5.20 for the Dawson and Neerkol bridges respectively. A similar variable waveform was noted for CR2 for both superstructure components in the Dawson River Bridge, with values peaking at 0.37 and 0.55 at 20 km/h and 60 km/h respectively. Road profile appears to have again been influential in the amplification of load; however, not at higher speeds. DI values were relatively consistent for CR1 irrespective of speed and direction of travel, with DI values not exceeding 0.15. Greater variability for both vehicles was observed in DI values determined for substructure components. However, the CR2 values were consistently greater than CR1 values irrespective of speed and direction of travel, and the CR1 DI values did not exceed 0.4 compared to those determined for CR2.

Figure 5.19: DI Values determined for CR1 and CR2 at the Dawson River Bridge

(a) Mid-span bending strains

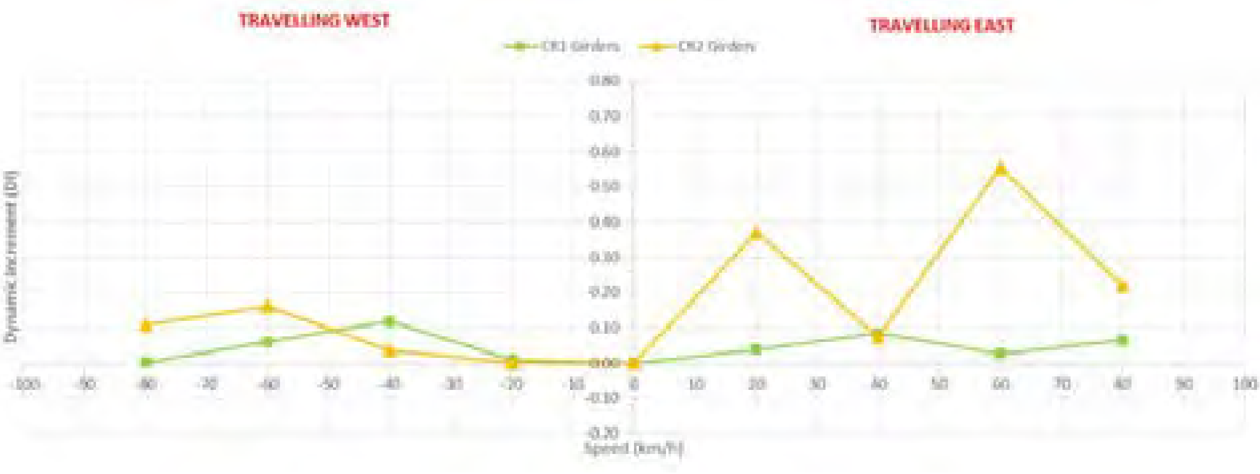

(b) Substructure tensile bending strains)

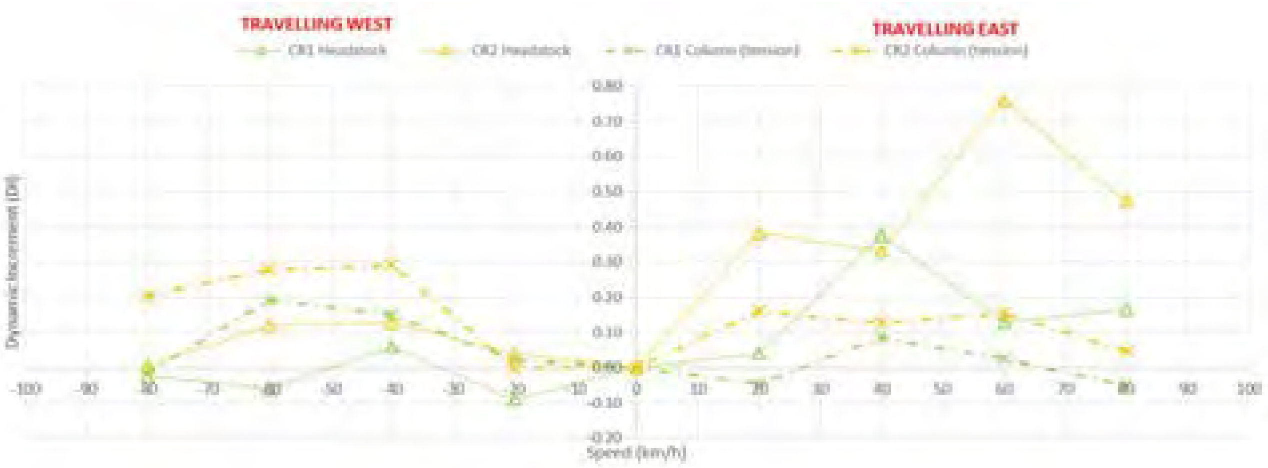

Figure 5.20: DI Values determined for CR1 and CR2 at the Neerkol Creek Bridge

(a) mid-span bending strains

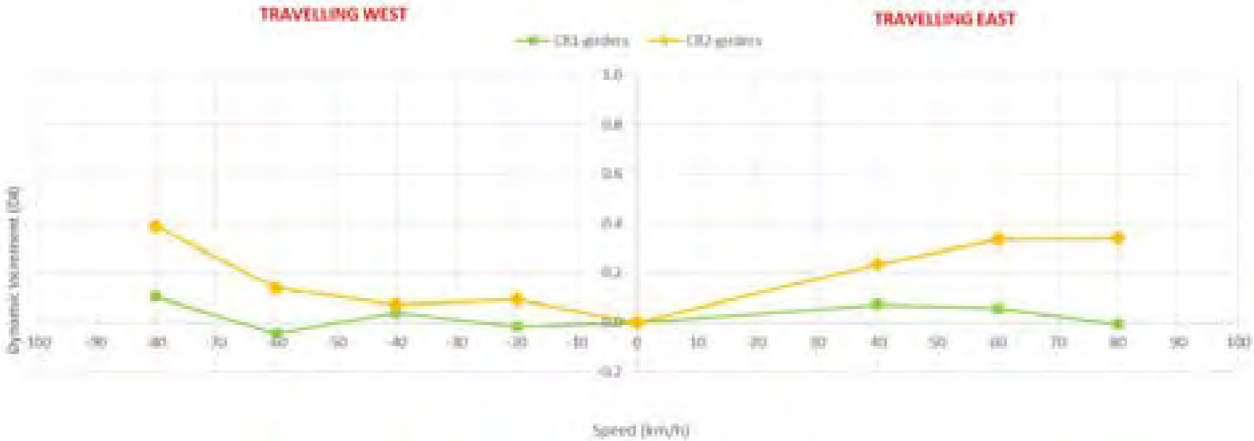

(b) Substructure tensile bending strains

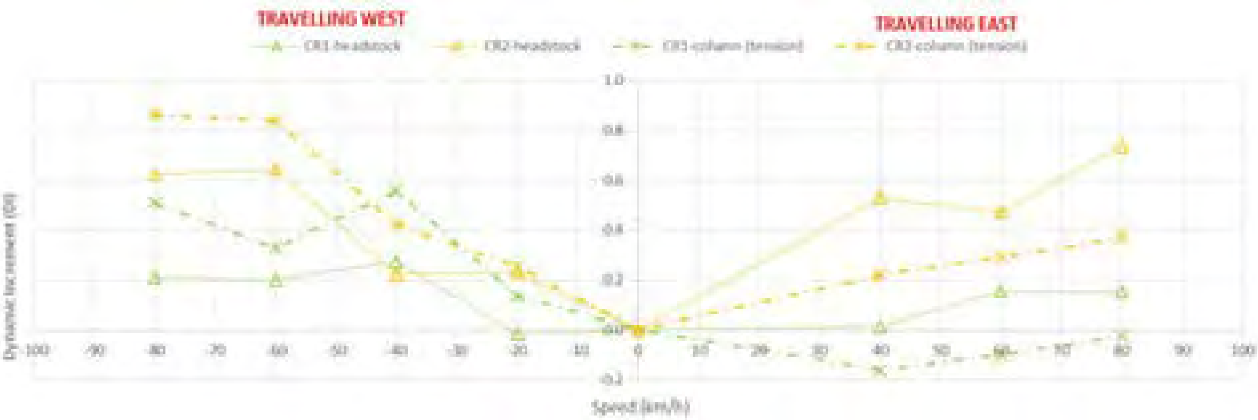

5.5.5 *Summary of Observations*

To summarise the observations of three sets of vehicles (semi-trailer, road train and cranes), it is apparent that steel-suspension vehicles were more likely to yield a greater degree of variability in DI values, particularly for shorter vehicles. Generally DI values were greater for steel suspension vehicles in comparison to air-bag and hydro-pneumatic suspension vehicles. However, increasing

DI values were recorded with increasing speed for air-bag and hydro-pneumatic vehicles for some directions of travel, suggesting that the condition of the road profile was likely to have been influential on the dynamic response of the bridge to these vehicles at higher speeds.

5.6 Frequency Characteristics (Dawson and Neerkol)

It has been previously noted in the literature that the inherent dynamic characteristics of the vehicle can be influential on resulting dynamic response of a bridge (González 2009; McLean & Marsh 1998). This was predominantly due to body-bounce and axle-hop frequencies induced in the vehicle. Body bounce frequencies range between 1.5 and 5 Hz, depending on suspension type. The frequencies in the steel-suspension vehicles were approximately 3-4 Hz whereas air-bag suspension vehicles were more likely to fall between 1.5 and 1.8 Hz (Austroads 2003; Davis 2010). There is no apparent distinction between the two suspension types at axle-hop frequencies (at 8-20 Hz) Cantieni et al. 2010; Paultre et al. 1992).

To further review the influence the test vehicles had on the dynamic response of the bridge, the dynamic response of the RT1 and RT2 were reviewed for various travel speeds in conjunction with the superstructure and substructure responses recorded for the corresponding vehicle passes on the Dawson and Neerkol bridges. A direct comparison was made by analysing accelerometer responses recorded for the test vehicle and each applicable bridge component, and interpreting the responses using a power spectrum analysis of each time series using a Fast-Fourier transformation (FFT) function. This enabled a comparative review of each component in the frequency domain, which is useful in relating observations back to fundamental frequency data of each bridge.

The influence of the two road trains (RT1 and RT2) on the response of each test bridge is demonstrated via FFT diagrams (Figure 5.21 to Figure 5.24) for representative cases. Dominant peaks have been matched between each Figure to observe any coincidental peaks. For both bridges and vehicles, all waveforms were predominantly low-frequency responses, i.e. less than 10 Hz. RT1 consistently induced peak responses in the superstructure and to a lesser degree the substructure for both bridges, with peaks predominantly coinciding between 2-4 Hz. Similarly for the Dawson River Bridge, coincidental peaks between the bridge and vehicle occurred between 1.5-2.5 Hz (lower than RT1).

Of interest are the recurring peak frequency responses for both vehicles and coincidental superstructure/substructure peaks. These responses are indicative of the influence that the vehicle body-bounce frequencies are capable of driving dynamic response of each bridge. Axle-hop frequencies were not evident in the road train vibration data due to the placement of the accelerometers above the axle groups. However, consistent observation of peaks in the superstructure between 13-15 Hz for RT2 (and in some places RT1) would suggest that axle-hop related frequencies were also influential. It is recommended that this area be investigated in the future to confirm this hypothesis.

Figure 5.21: FFT comparison between superstructure, substructure and RT1, travelling east at 80 km/h (Dawson River Bridge)

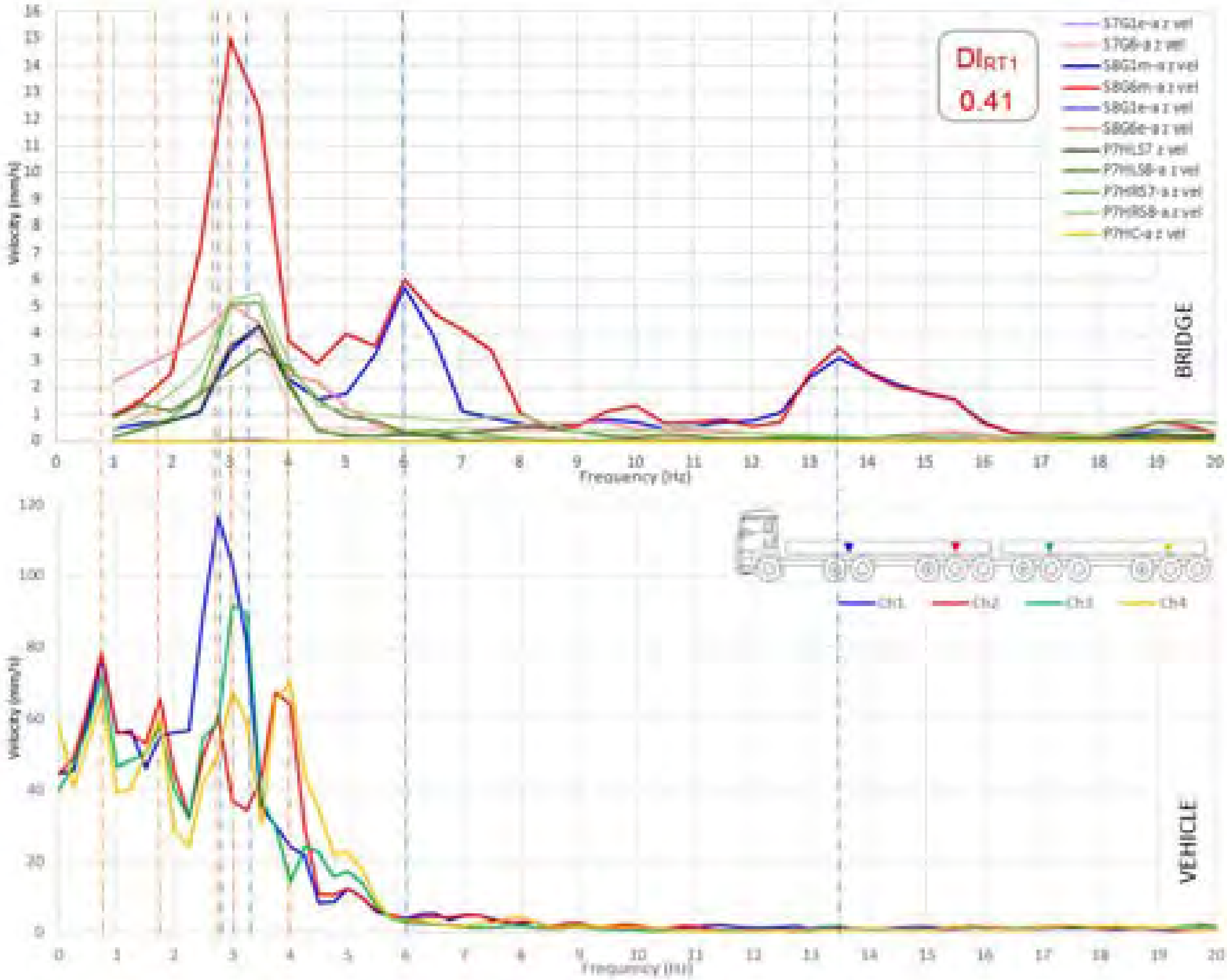

Figure 5.22: FFT comparison between superstructure, substructure and RT2, travelling east at 80 km/h (Dawson River Bridge)

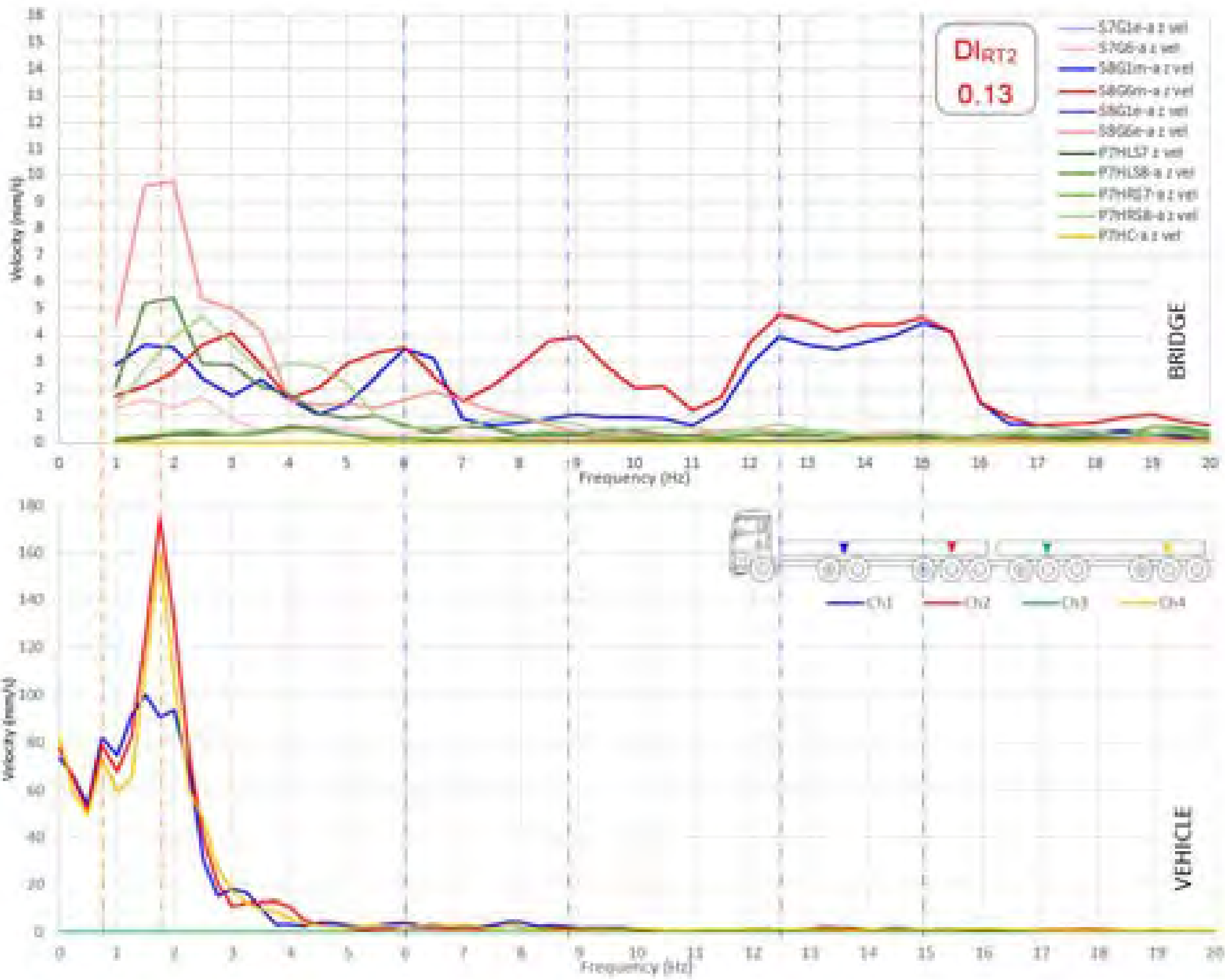

Figure 5.23: FFT comparison between superstructure, substructure and RT1, travelling west at 80 km/h (Neerkol Creek Bridge)

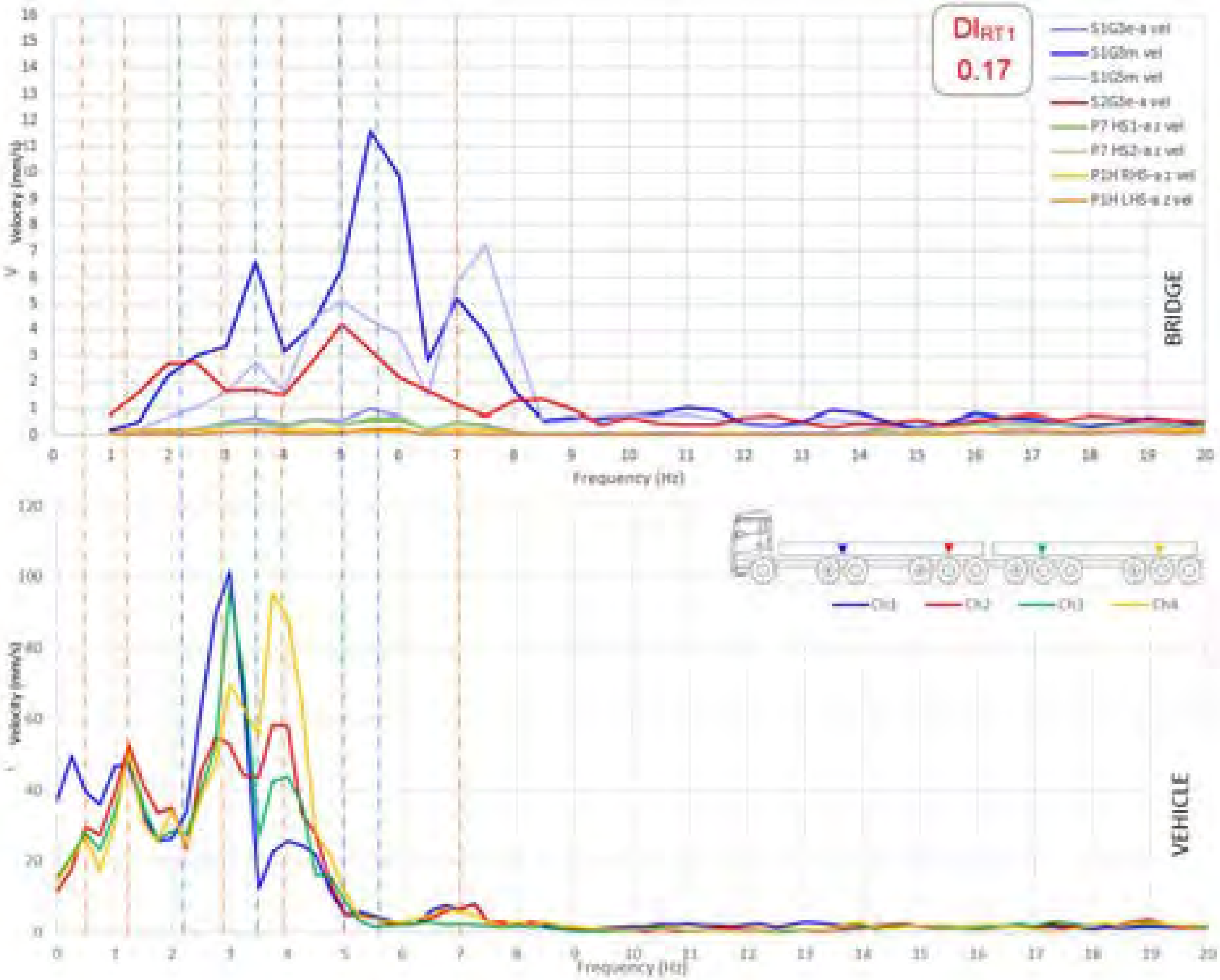

Figure 5.24: FFT comparison between superstructure, substructure and RT2, lane travel to Stanwell at 80 km/h (Neerkol Creek Bridge) (Run 13)

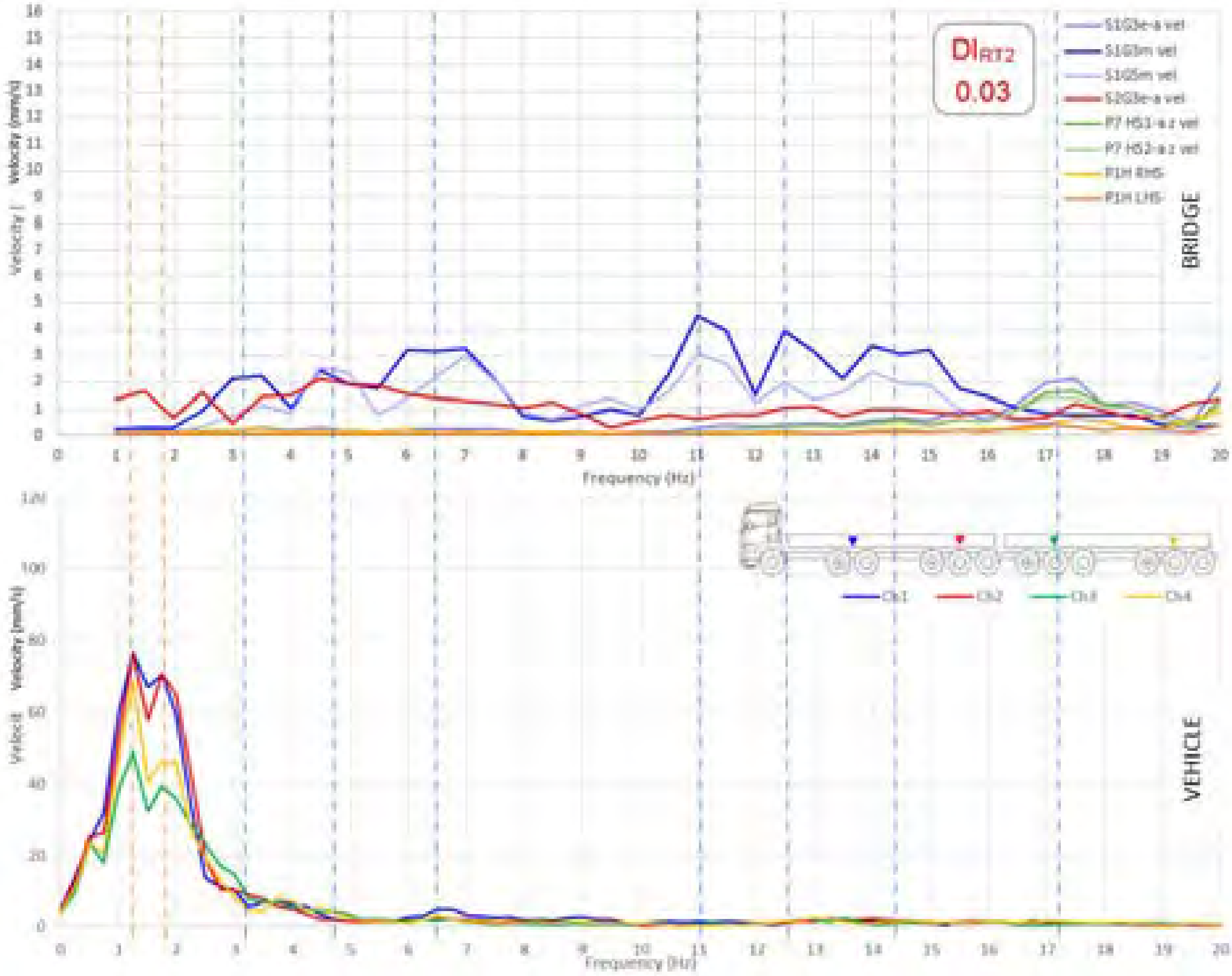

5.7 Summary

In summary, the following key items were observed from the test data:

- Various vehicle speeds were found to result in peak DI values, and did not always occur at high speeds. Where road profiles were poor, DI values were significantly greater at higher speeds, irrespective of vehicle type.
- No clear trend was confirmed relating to individual gross vehicle mass and amplification of dynamic load.
- Limited correlation was found between the length of vehicle and dynamic load amplification, with longer vehicles (such as road trains) capable of significant load amplification in comparison to shorter vehicles. However, a direct comparison between the steel suspension semi-trailer and road train for the Canal Creek Bridge supports the literature, despite values being lower than 0.4.
- Similar findings were identified regarding axle groups, with DI values determined for triaxle groups greater than or equivalent to DI values for single or tandem axles. The centre of mass of the vehicle is influential on the resulting DI values.

- Suspension type was found to be significantly influential on dynamic load amplification, with the following confirmed:
  - DI values were likely to be more variable across a range of speeds and greater in magnitude for steel-suspension vehicles.
  - DI values for hydro-pneumatic and air-bag suspension vehicles were less in magnitude and more consistent irrespective of speed where the road profile condition was not poor.
  - Substructure components appeared to be more influenced by suspension type and road profile than superstructure components.
  - Significant DI values for the air-bag suspension road train were recorded with increasing speed where the road profile was poor.
- Superstructure DI values for the hydro-pneumatic crane were less than 0.4 for all three test bridges; however, some substructure values exceeded this value at certain critical speeds. Speeds of 40 km/h appeared to result in relatively greater DI peaks in all components for both the Neerkol and Dawson bridges.
- To varying degrees, the inherent body-bounce frequency characteristics of the two road trains were noted to induce similar frequency responses in all the Dawson and Neerkol bridge components.

6 INFLUENCE OF ROAD PROFILE

6.1 Introduction

As discussed in Section 2.2, the condition of the road profile is known in the literature to be influential on dynamic load amplification experienced by bridges, and continues to be a source of research (Deng & Cai 2010; González 2009; McLean & Marsh 1998; Paultre et al. 1992). Previous work has been done to correlate the roughness of the road to dynamic load allowance factors (Austroads 2002; Constanzi & Cebon 2006; O'Brien et al. 2006; Prem & Heywood 2000; Steinauer & Ueckermann 2002), with the recent publication of AS 5100.7 recommending a revision to the DLA factor based the condition of the road. Specifically, Clause 11.3.6 states:

> Where the roughness of the road and bridge is controlled to ensure compliance with an international roughness index (IRI) of less than 4.0 for the length of the bridge plus a distance of 400 m on each approach to the bridge, the DLA may be reduced to 0.3. Conformity shall be formally documented with a management plan that documents frequency of road roughness measurements and timeframe for action where the road profile degrades to the required intervention level.

These recommendations are based on the research carried out by Heywood and colleagues (Austroads 2002; Austroads 2002a; Heywood 2000; OECD 1999; Prem & Heywood 2000).

Therefore, this section will focus on the influence of road profile on the dynamic response of each test bridge and the measured load amplification in key components. The measured roughness of the road profile (in terms of elevation vs. chainage and IRI) shall be presented for each bridge site as well as the adjacent approaches in each lane direction. The results will then be related to peak DI values determined for each approach and vehicle, and reviewed for trends in relation to the AS 5100.7 recommendations and general structural dynamic performance observations.

6.2 Actual Road Profile Data

6.2.1 Reviewed Data

To identify the condition of the road profile at each bridge site, various sources of visual and analytical information was reviewed, including:

- level 2 inspection reports and photographs
- site photographs taken during load test activities
- TMR road profile and condition data which includes[1]:
  - roughness data
  - road surface faults/defects detected
  - relative elevation of the road surface (per lane and wheel path)
  - International Roughness Index (IRI)
  - Hawkeye video and still images.

Details regarding the road profile data obtained for each bridge are shown in Table 6.1.

[1] Permission to retrieve and review data obtained from the Road Asset Data department, TMR (RoadAssetData@tmr.qld.gov.au)

Table 6.1: Road profile data details

Bridge	Road name	Road ID	Date of road profile data collection	Direction of travel	Chainage (Level 2 inspection report)		Chainage (TMR road condition database)	
					Start	Finish	Start	Finish
Canal Creek	Flinders Hwy	14E	5 April 2014	West	93.900	93.916	93.814	93.830
Dawson River	Capricorn Hwy	16A	22 September 2015	West	93.249	93.433	93.627	93.810
Neerkol Creek No. 1	Capricorn Hwy	16A	22 September 2015	West	18.813	18.886	18.866	18.938

6.2.2 *Visual Inspection*

From Level 2 condition inspection reports and Hawkeye imagery, observed pavement conditions for each bridge and approach in each direction of travel is summarised in Table 6.2, with visual records shown in Figure 6.1 to Figure 6.3 for each bridge respectively. Of these observations, the following significant or repeating defects were noted:

- Settlement behind abutment walls is common for all three bridges, with 'jumps' up or down to the bridge evident after the abutment in most cases.
  - For the Dawson River Bridge, a slight depression adjacent to the left wheel path behind Abutment 2 for the lane travelling east. This may be associated with the rotation of the abutment wing wall at this location and subsequent backfill movement (see Figure 6.2).
- The majority of the bituminous surfacings of the approaches exhibited flushing, particularly for the left wheel path. Wheel path demarcation was also observed across bridge spans adjacent to approach lanes.
  - Road and bridge cross-falls may have been influential in this pattern. Crossfall values were greatest for the Dawson River Bridge (3% from centreline), and least for the Canal Creek Bridge (1.5% from centreline).
- A sinusoidal pattern was evident in the road profile leading up to Approach 1 of the Canal Creek Bridge (travelling west).
- Some of the joints over the piers of the Dawson River Bridge were overlayed with asphalt, which raised the profile of the road surface in these locations.
- The presence of the relieving slab is evident in the road profile on Approach 1 for westerly travel over the Neerkol Creek Bridge.
- It is noted that, despite the seal for the Neerkol Creek Bridge being relatively new (i.e. it was replaced after the 2012 floods), significant potholing and deterioration was observed, predominantly along the left wheel path on Approach 1.

Table 6.2: Summary of pavement condition (based on visual observations)

Bridge	Visual condition of road						
	Approach 1		Over bridge			Approach 2	
	Travel West	Travel East	Travel West	Travel East	Abutment & joint features	Travel West	Travel East
Canal Creek	▪ Sinusoidal wave profile ▪ Some flushing along wheel paths (mostly LHS)	▪ Some flushing along wheel paths (mostly LHS)	▪ Some flushing along wheel paths (mostly LHS)	▪ Flushing along wheel paths (full span)	▪ A1: dip behind wall; seal damage evident ▪ A2: seal overlaps onto Span 8 ▪ Dips in seal over pier joints	▪ Some flushing along wheel paths (mostly LHS)	▪ Some flushing along wheel paths (mostly LHS)
Dawson River	▪ Some flushing prior to A1, wheel paths evident ▪ Seal damage behind A1 wall	▪ Some flushing prior to A1, wheel paths evident ▪ Seal damage behind A1 wall	▪ Concrete Surface ▪ In good condition ▪ No visible defects	▪ Concrete Surface ▪ In good condition ▪ No visible defects	▪ Some joints have asphalt overlay ▪ P7: smooth joint but dips down ▪ A1: dip in profile behind wall; seal damage evident ▪ A2: seal overlaps onto Span 8	▪ Good condition	▪ Some flushing in wheel paths prior to A2
Neerkol Creek	▪ Potholing, cracking and flushing along wheel paths prior to relieving slab (mostly LHS) ▪ Relieving Slab jump prior to bridge	▪ In better condition, no pot-holing	▪ Good condition ▪ Surface rough	▪ Good condition ▪ Surface rough	▪ P1: smooth joint but dips down ▪ A1: dip behind wall; seal build-up adds to height ▪ A2: seal overlaps onto Span 3	▪ Good condition	▪ Some rutting

Figure 6.1: Road profile condition for the Canal Creek Bridge (approach to Span 1, westerly travel)

(a) Looking west from Abutment 1

(b) Looking east from Abutment 2

Figure 6.2: Road profile condition for the Dawson River Bridge (approach to Span 8, westerly travel)

(a) Looking west from Abutment 1

(b) Looking east from Abutment 2

Figure 6.3: Road profile condition for the Neerkol Creek Bridge (Approach 1, westerly travel)

(a) Looking west from Abutment 1

(b) Looking east from Abutment 2

Figure 6.4: Summary of 2014 Level 2 Inspection information for wingwall defects noted at Abutment 2 of the Dawson River Bridge

O	AP2	PRO	53C	2	200.0	M2		190.0	10.0			UNCHANGED SINCE LAST INSPECTION SETTLEMENT UP TO 70MM ON SIDE 1 AND 2 PHOTO 5A MONITOR
O	A2	PRO	53C	2	60.0	M2		40.0		20.0		SCOURING ON SIDE 1 UP TO 1M IN DEPTH PHOTO 98 TYPICAL. INSTALL TYPE 2 BATTER PROTECTION FULL WIDTH
O	A2	WW	51C	2	2.0	EACH		1.0		1.0		WW1 HAS 35MM GAP PHOTO 98 WW2 HAS 15MM GAP PHOTO 105. FILL GAP WITH MORTAR MIX TO REDUCE FINES LOSS

Level 2 Inspection Report - Photos & Sketches Record B2/6 31 of 48

Structure Id 8233 Name Dawson River

Inspection Date 16-MAY-2014 Inspection Level 2 [X] Level 3 [ ] Underwater [ ]

Pictures ** All images printed for this report

Id [illegible] Date 16-MAY-2014

Film / Exposure Number PHOTO_58 Sketch No

Description GAP 35MM

Mod	Category	Number	Comp Code	Comp No
O	A	2	WW	1

6.2.3 Road Condition Data[2]

The road survey data for the west-bound lanes was reviewed for each bridge site to investigate the quantified condition of the approaches and bridge surface for each bridge site. The data was reviewed for road profile elevation and roughness in relation to the IRI, averaged for the lane, as well as Hawkeye video imagery.

Road profile information in terms of elevation is shown in Figure 6.5 for the westbound lane for each bridge. Vertical elevation is shown in centimetres and relative to the survey vehicle (being arbitrarily related to the height of the road). On average, the road surface profiles ranged between 10 and 20 mm in relative elevation, with approaches and the surface across the Canal Creek Bridge (Figure 6.5-a) exhibiting a relatively even profile in comparison to the Dawson and Neerkol bridges.

Profile data across the Dawson and Neerkol bridges highlights the relatively rough unsealed concrete surface. The largest magnitude elevation was recorded on the Dawson River Bridge (Figure 6.5-b), with a differential elevation of almost 40 mm at Abutment 2. Abutments and pier joints were evident from the profile data, with the most significant increases observed directly behind the abutments, or just after bridge passage. The run-on slab in approach 1 for the Neerkol Creek Bridge was evident in Figure 6.5-c; however, despite its presence, settlement behind abutment 1 was observed. Similar observations were made for the Dawson Bridge.

2 The authors would like to acknowledge the input provided by the ARRB Qld Systems team for their assistance in understanding, presenting and interpreting the road condition data in this section.

Figure 6.5: Road profile elevation for west-bound lane

(a) Canal Creek Bridge (+ 50 m approaches)

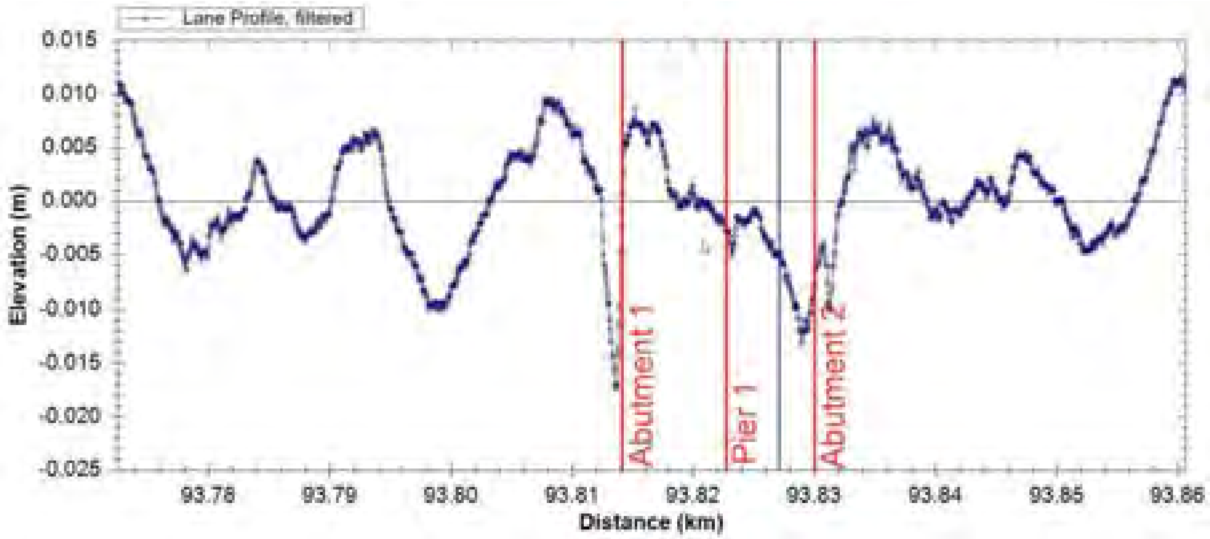

(b) Dawson River Bridge (+ 50 m approaches)

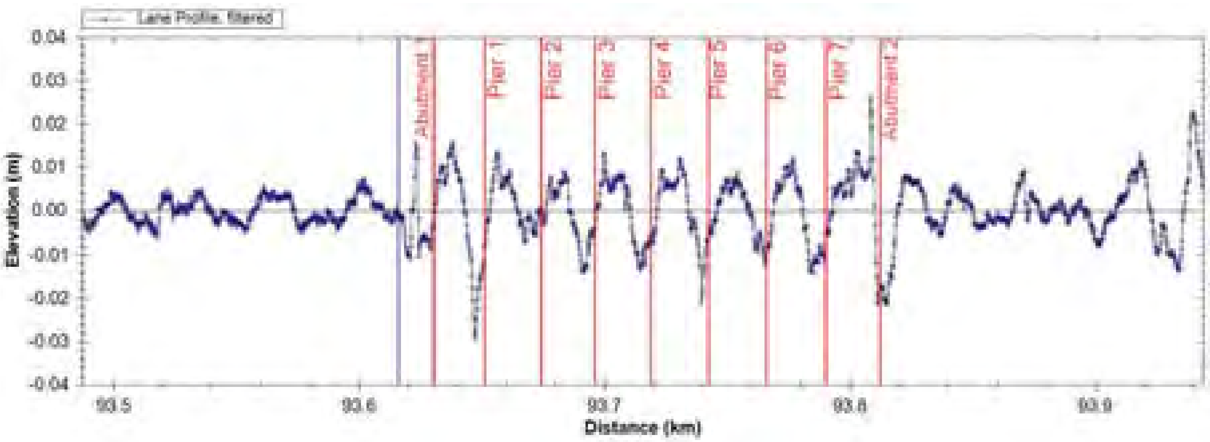

(c) Neerkol Creek Bridge (+ 50 m approaches)

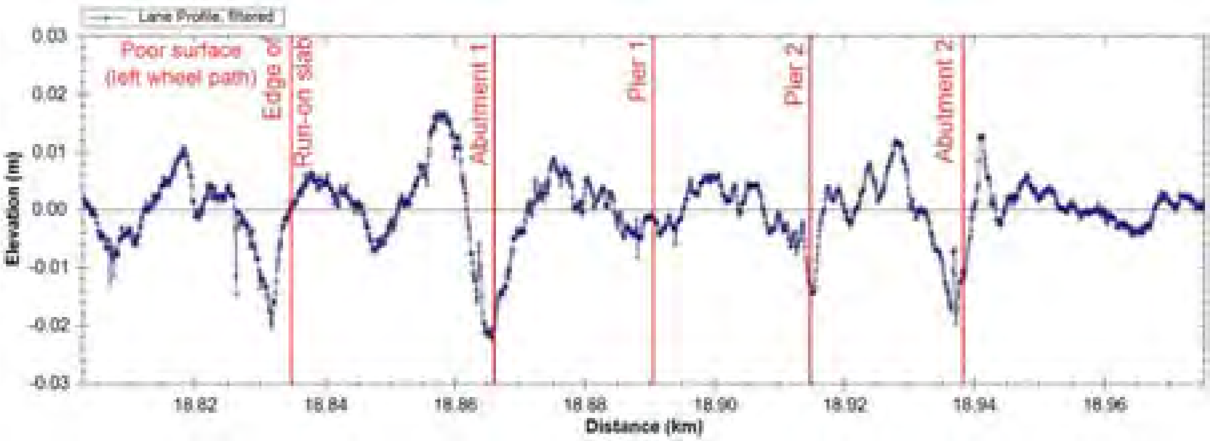

The roughness of the road approaches and over each bridge was assessed, and are shown in Figure 6.6 for each bridge in terms of IRI. Road section lengths of 100 m approaching each bridge were included in the review, which incorporated adjacent structures. The IRI data was obtained in 10 m steps in order to review localised effects such as joints, abutments and other road features that may influence the dynamic response of the vehicle. It should be noted that road roughness data has also been reviewed, indicating that it is typically averaged over 100 m steps.

In general, the IRI values were equal to or less than 4 for the majority of the westbound lanes in all bridges. Where the IRI exceeded this value, it was mostly associated with the poor condition of the road surface (as expected) and also bridge joints, most notably abutments.

On average, the IRI values for the Canal Creek Bridge were less than 4 and the least for all three bridges (Figure 6.6-a). There was evidence of sinusoidal road profile on the approach to Abutment 1 prior to the bridge. Note the elevation of IRI across the Dawson River Bridge, with an average of approximately 4, and the subsequent drop in roughness for the bridge approaches (averaging approximately 2-2.5, see Figure 6.6-b). Note also the prominent feature of the abutments in the adjacent bridge further west of the Dawson River Bridge. For the Neerkol Creek Bridge, the most significant IRI event was associated with the abutments (most notably Abutment 1), and the influence of the pier joints were not as significant (Figure 6.6-c). The average IRI values (excluding the abutments and joints) were mostly less than 4. Of interest is the fact that the edge of the run-on slab is evident in the IRI values and roughness values decrease after this point. However, localised settlement behind Abutment 1 has had a strong influence on the resulting IRI.

Figure 6.6: IRI measured against chainage (per span & 100 m approaches; based on 10 m step average)

(a) Canal Creek Bridge

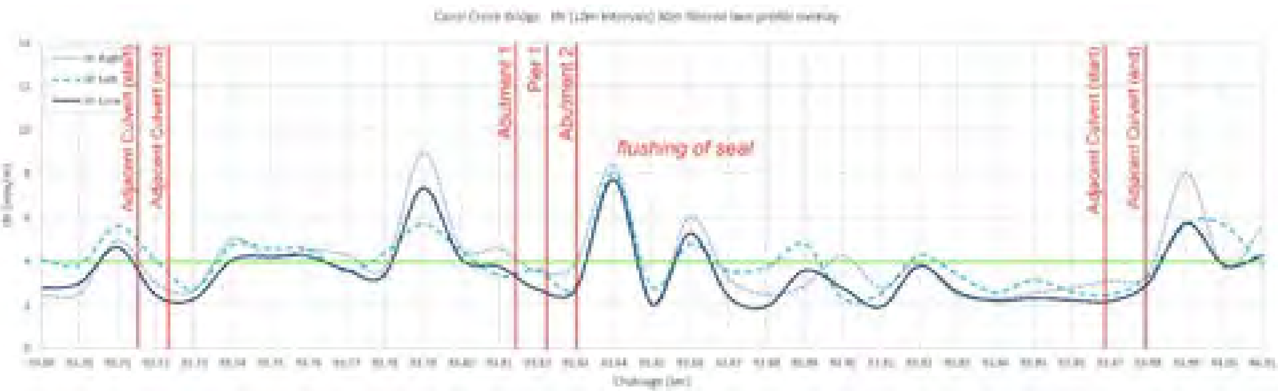

(b) Dawson River Bridge

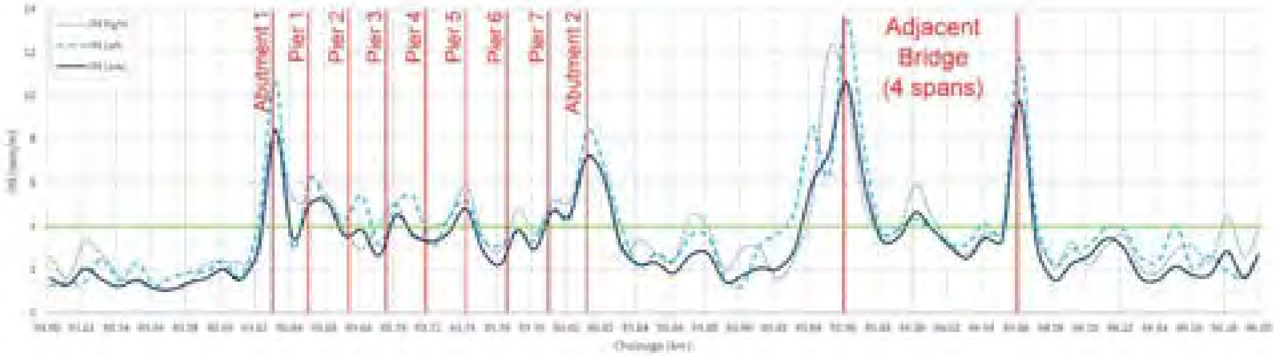

(c) Neerkol Creek Bridge

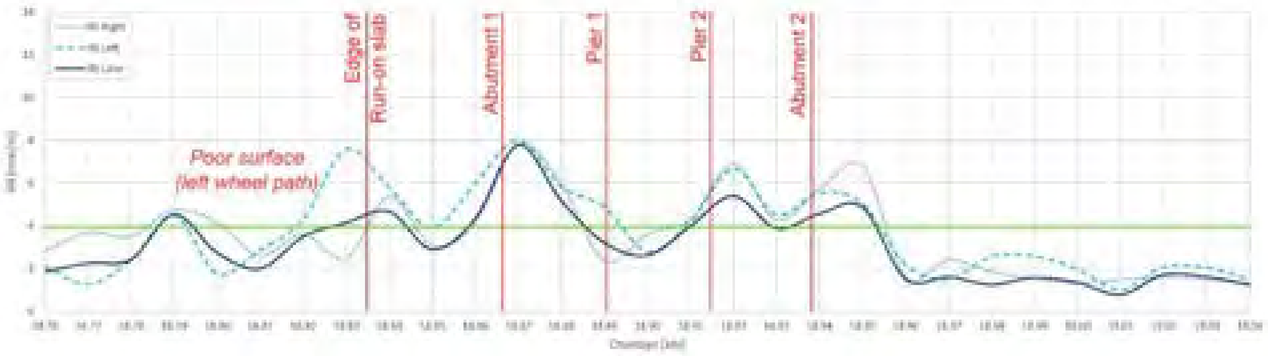

6.3 Correlation of Road Profile Condition to Dynamic Load Amplification (Dynamic Increment)

In order to review the degree of correlation between the condition of the road profile and the amplification of the load, the visual and survey data was compared to the DI values determined for the various test vehicles for each bridge. More specifically, IRI values were compared to DI values for vehicles travelling westbound. A summary of the DI values for each bridge is presented in Figure 6.7 to Figure 6.9 for superstructure and substructure components as applicable, whilst Table 6.3 provides a direct comparison between the peak DI and IRI values for westbound vehicles for each bridge. The following paragraphs summarise the test findings.

Based on the visual condition of the road profile, it is clear that there is a direct correlation between increasingly poor condition of the road and increasing DI values. This is particularly exacerbated with increasing vehicle speed. Despite no survey data being available for eastbound travel, the elevated DI values for both the superstructure and substructure components with increasing speed determined for the Dawson River Bridge highlight this correlation clearly, which is irrespective of vehicle type. The magnitude of the DI values may have been amplified due to the boundary conditions of the substructure responding to the direction of vehicle travel, and the inherent frequency characteristics of both the superstructure and the substructure components (as previously discussed in Section 4).

The road profile on the Canal Creek Bridge was relatively smooth, which correlates well with the reduced superstructure DI values determined for all vehicles, travelling speeds and direction of travel. Slightly greater DI values for vehicles travelling west were recorded compared to the vehicles travelling in the opposite direction, which is in keeping with the elevation of Abutment 1.

The relatively low superstructure DI values determined for the components of the Neerkol Creek Bridge also agree with the visual condition of the road profile, with the influence of the smooth profile of the run-on slab likely to have been influential in reducing body bounce effects (and subsequent load amplification) induced in the vehicles due to the poor condition of the road profile on approach to Abutment 1. However, consistently elevated DI values were observed for the substructure components (approaching or exceeding 0.4) with increasing vehicle speeds, which was contrary with the previous observation.

In reviewing the IRI values (Table 6.3), values less than 4 for the Canal Creek Bridge and the absence of an abutment feature in the approach road profile correlate well with the low DI values determined for westbound test vehicles. This is despite the significant elevation change at Abutment 1, as shown in Figure 6.6-a. However, the change relates to a drop rather than a step up to the bridge. This suggests that steps onto a bridge are more likely to be influential in the excitation of vehicle frequencies, which is supported in the literature (Austroads 2002; Heywood 1995b; Prem & Heywood 2000).

As with the Canal Creek Bridge, low DI and IR values were noted for westbound test vehicles for the Dawson River Bridge, with superstructure and substructure DI values consistently less than 0.4 correlating well with IRI values of 4 or less. Superstructure DI values for the Neerkol Creek Bridge also agreed with these observations; however, the results for the substructure do not. This may highlight the dominance of the geometric and frequency characteristics of the piers over road profile in this instance, based on longitudinal fundamental frequencies and the pre-existing cracked condition of the headstock (as noted in Section 4).

Table 6.3: DI and IRI values for westbound vehicle travel

Bridge	Test vehicle	Maximum DI		Average IRI		*Profile step before span*	
		Superstructure	*Substructure*	Approach to instrumented span (+100 m)	Instrumented span (length)	*Yes/No*	Localised IRI (from Figure 6.6)
Canal Creek	CR1	0.11	-	3.99	2.77	No	–
	ST1	0.13	-				
	ST2	0.00	-				
	RT1	0.10	-				
	Average	0.09	-				
Dawson River	CR1	0.12	*0.20*	3.49	4.58	Yes	4.5
	CR2	0.14	*0.30*				
	RT1	0.18	*0.15*				
	RT2	0.07	*0.27*				
	Average	0.13	*0.23*				
Neerkol Creek	CR1	0.10	*0.56*	3.21	6.47	Yes	7
	CR2	0.39	*0.87*				
	RT1	0.17	*0.85*				
	RT2	0.11	*0.49*				
	Average	0.19	*0.69*				

Figure 6.7: DI values for Canal Creek Bridge

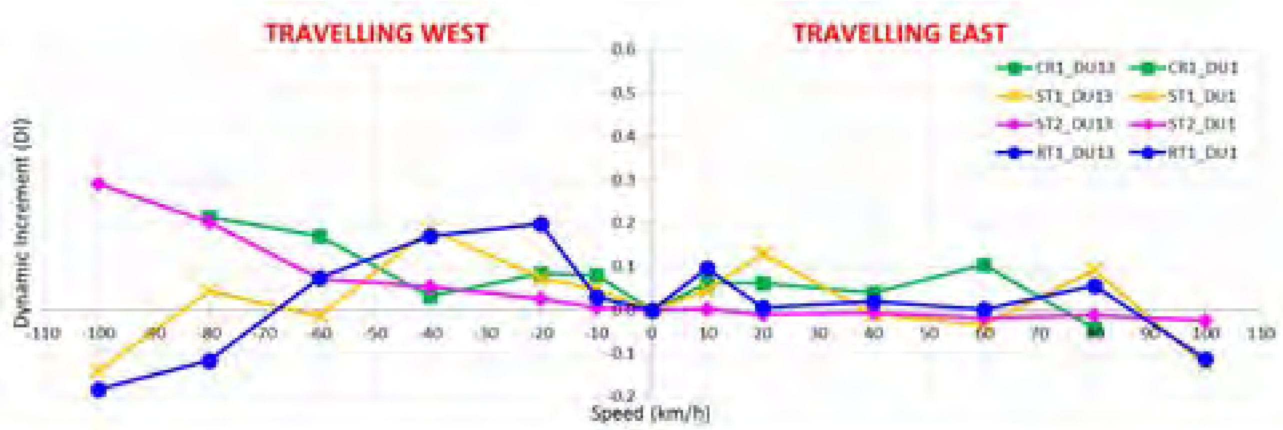

Note: DI values determined from maximum bending strains for kerb units attracting the greatest load

Figure 6.8: DI values for the Dawson River Bridge

(a) Girders

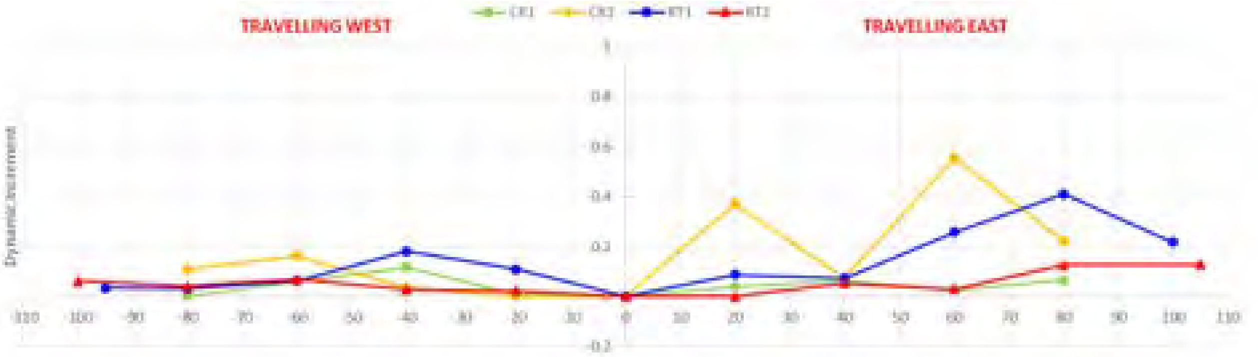

(b) Headstock

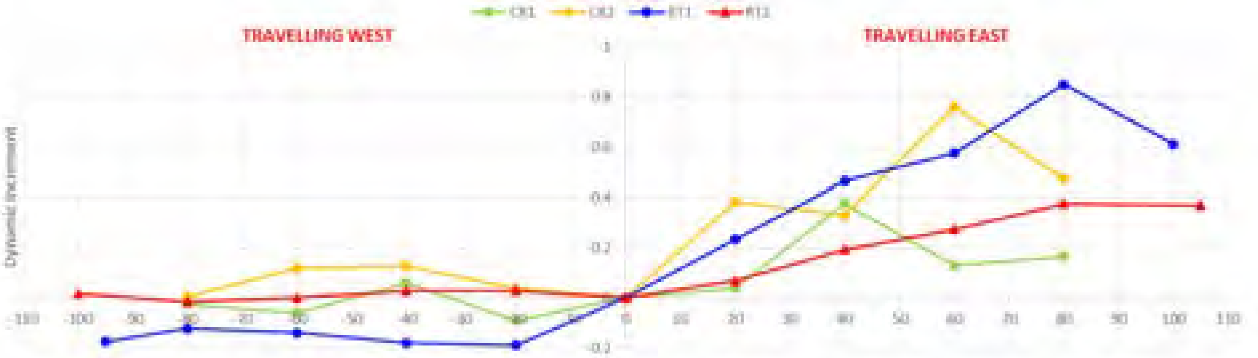

(c) Column

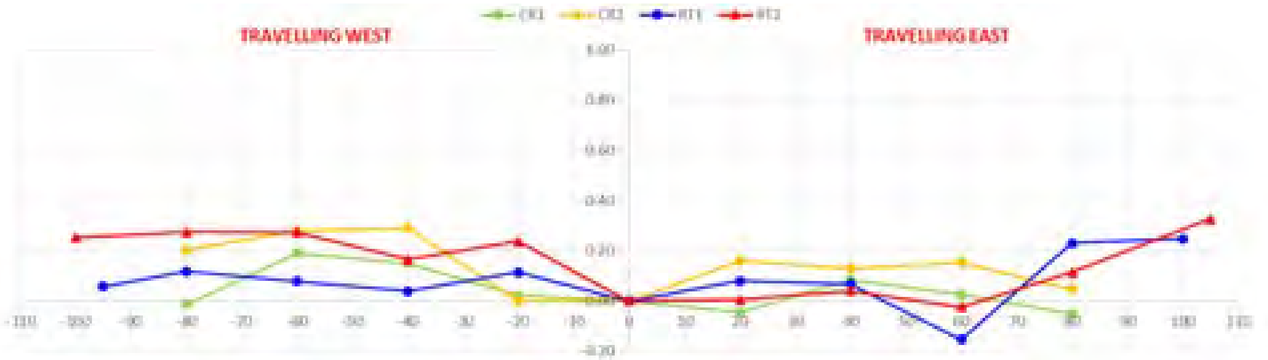

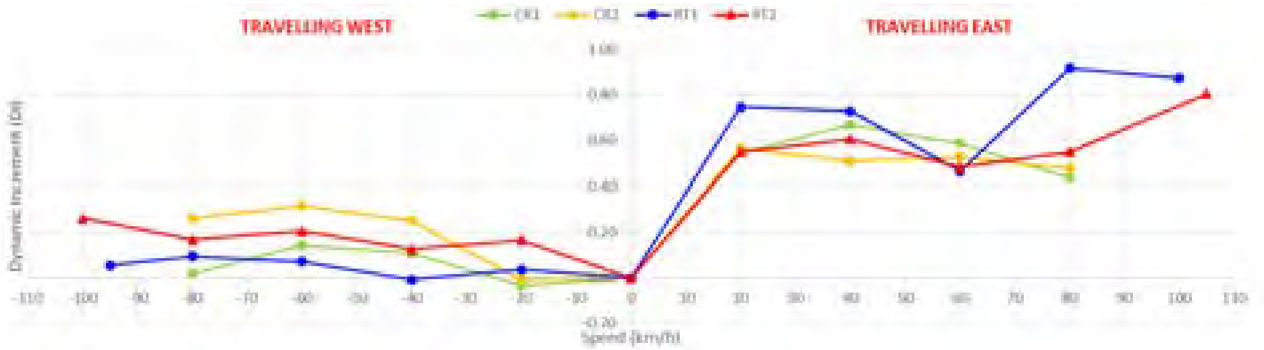

Note: Based on maximum DI values determined from peak bending strains recorded for components under direct load

Figure 6.9: DI values for the Neerkol Creek Bridge

(a) Girders

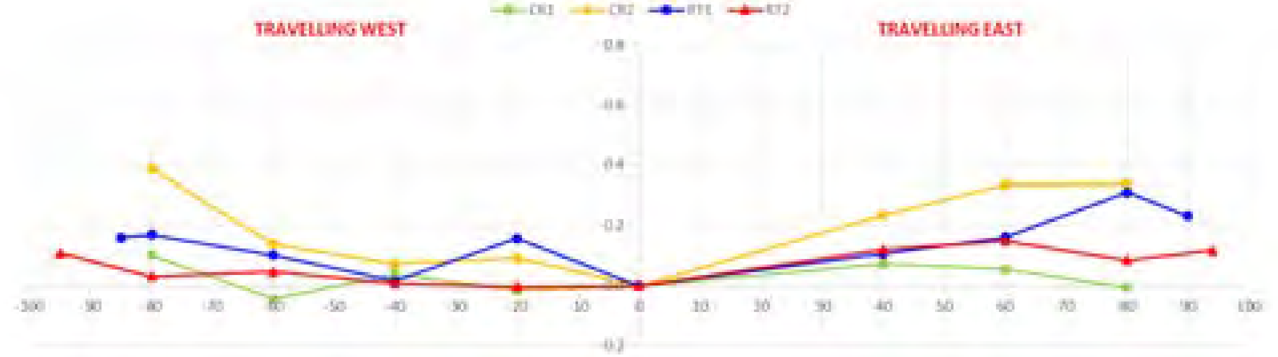

(b) Headstock

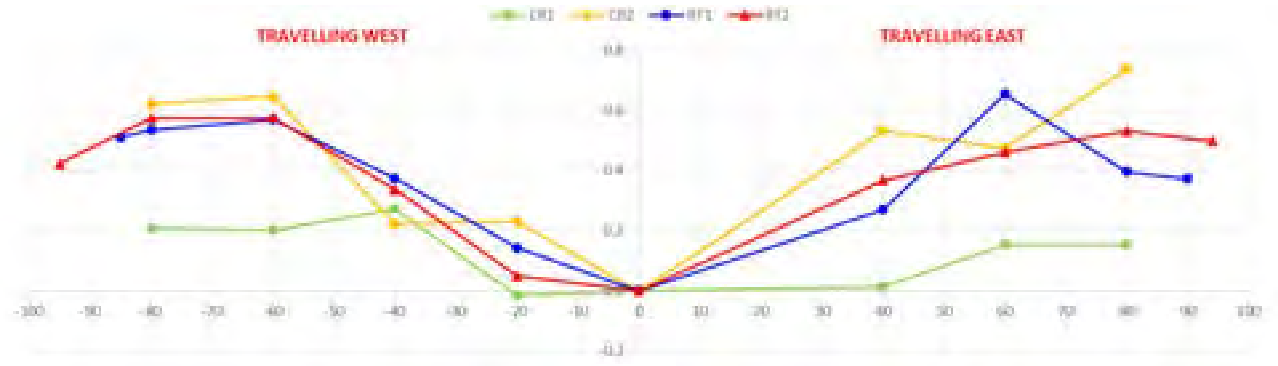

(c) Column

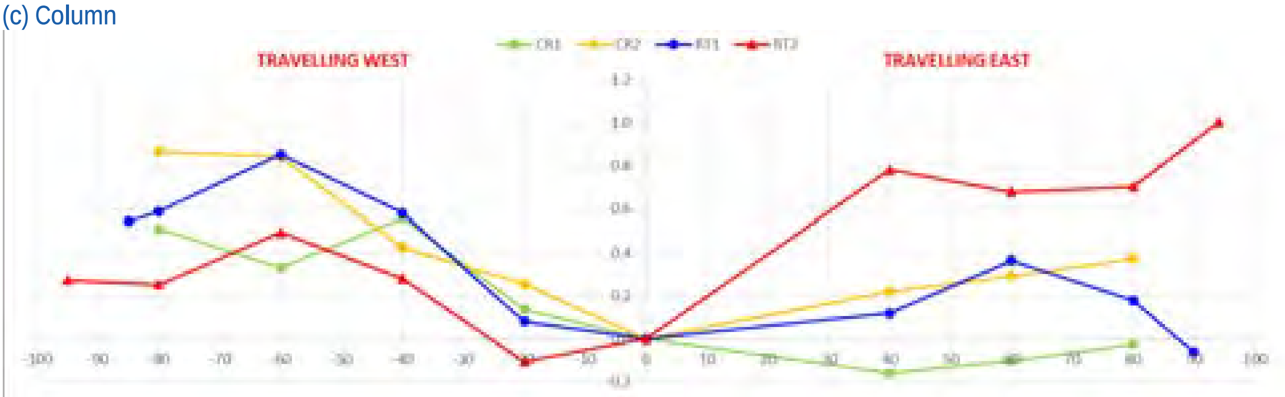

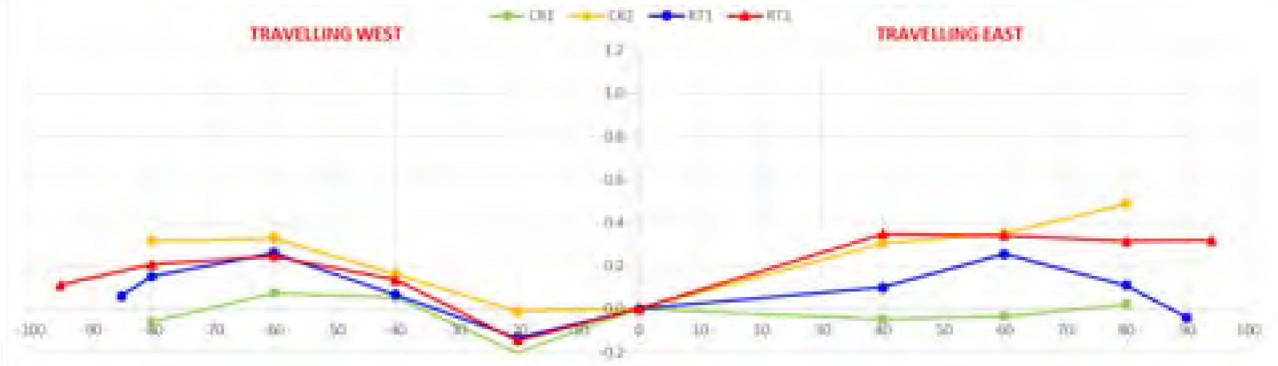

Note: Based on maximum DI values determined from peak bending strains recorded for components under direct load.
DI values shown for column were determined from either tensile strains or compressive strains.

6.4 Summary

In relation to the influence of the road profile on the interaction process and the dynamic amplification of the load, the following key points are noted:

- The elevation and condition of the road profile influenced the resulting DI values; however, the most influential factor appeared to be settlement behind abutments. The greater the step onto the bridge, the greater the dynamic loading for some vehicle types (see below).
- Road profile appeared to have the most influence on the dynamic load amplification at higher vehicle speeds.
- Steel=suspension vehicles were more likely to generate greater DI values where the road profile was poor.
- Excluding the IRI values pertaining to bridge abutments or pier joints, the greater the IRI value, the higher the DI value.
- Inconsistent results for substructure components were noted for load amplification due to road profile condition. Additional study is required to investigate these influences further.
- The Dawson River Bridge appeared to be most influenced by road profile condition for vehicles travelling east at higher speeds.
- To further validate IRI findings in relation to DI values, it is recommended that a road profile survey be conducted on the eastbound lanes.

7 ADDITIONAL FINDINGS

7.1 Introduction

Several additional concepts and observations were explored during the course of this project, relating to the concept of dynamic interactions and load amplification in bridges. These included:

- beat frequencies
- frequency matching between test vehicles and test bridge
- load distribution and the influence of vehicle transverse location
- distribution in relation to dynamic load amplification
- vehicle response to bridge and road profile contributions
- long-term monitoring observations.

The following sections discuss these findings and their potential implications on the overall outcomes of this research.

7.2 Beat Frequencies

For a number of high-speed runs for Dawson and Neerkol bridges, the resulting waveforms of some of the sensors show a repeating pattern of signal amplification and reduction after the passage of the vehicle as shown in Figure 4.5. This phenomenon is commonly known as a 'beat frequency' and is observed when two waveforms of similar frequency and amplitude combine to cause a resulting waveform. Where the two waveforms match frequency and amplitude, the signal is amplified. Alternatively, the waveform is diminished when the signals are out of phase. The phenomenon is common, and is often observed in industrial applications with a variety of machinery in operation.

These beat frequencies were often observed in waveforms for accelerometers, strain gauges and proximity probes for various vehicles travelling at medium to high speed. This was predominantly observed for Dawson and Neerkol bridges, which is likely to be due to the structural form of the superstructure, prestressed concrete I-girders with a low fundamental frequency response, as well as the contribution of torsional vibration modes.

Whilst the physical application of this phenomenon is likely to have little effect on the amplification of load, it does demonstrate that frequency matching is a possibility with these structures. There is also the consideration that prolonged, intermittent loading of a sustained nature may occur in these structures. With low levels of damping on these structures, and the transfer of these loads to the substructure components, long-term incremental damage may occur in the form of movement and possible fatigue scenarios, however fatigue in prestressed concrete girders is not known to be a significant issue (Al-Zaid & Nowak 1988). However, based on the cracking observed in the portal-frame of the Neerkol Creek Bridge and the cantilevered headstocks of the Dawson River Bridge, there could be cause for further investigation.

Figure 7.1: Example of a beat frequency observed for the Dawson River Bridge

(a) Dawson River Bridge

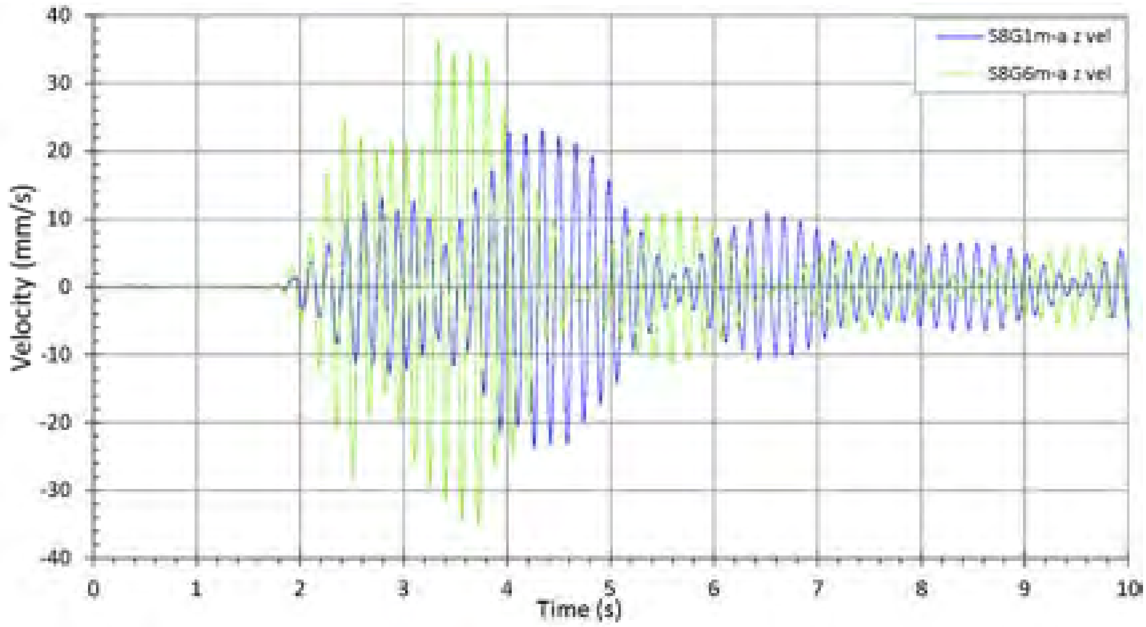

(a) Neerkol Creek Bridge

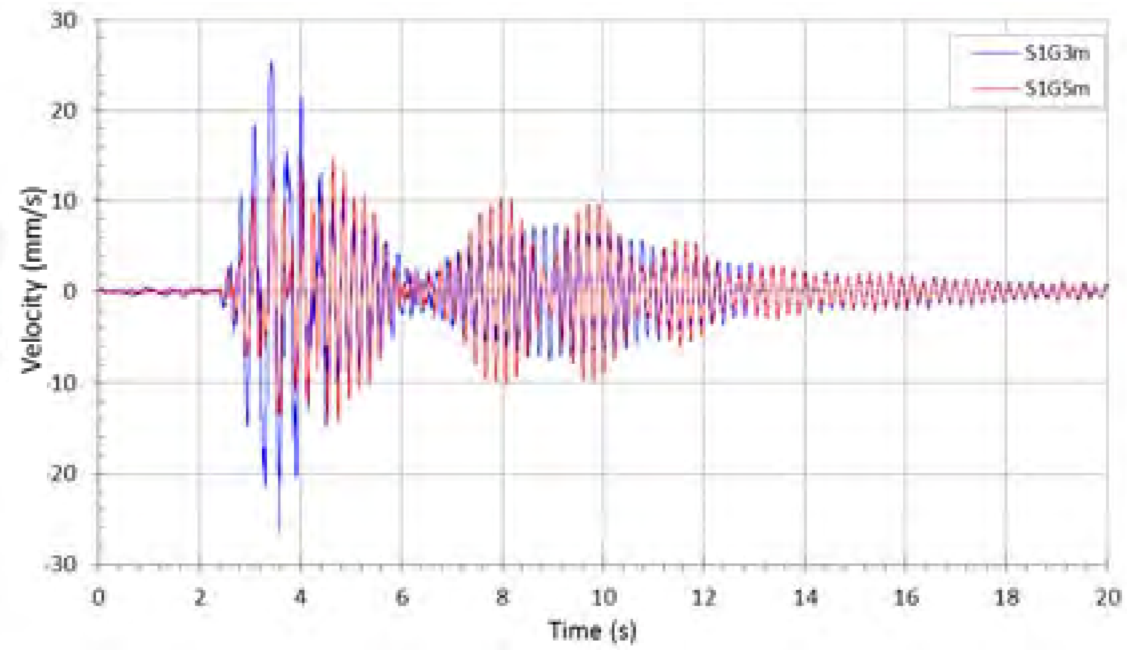

7.3 Frequency Matching/Quasi-resonance

The key risk for any interaction system is the amplification of load due to quasi-resonance, or frequency matching between systems. Quasi-resonance is an extension of the beat frequency phenomenon, but involves the harmonised vibration of bridge and vehicle components at their fundamental or induced frequencies, along with the road profile condition, which may result in significant amplification of dynamic load, particularly if damping levels are low.

For the purposes of this project, quasi-resonance was defined by coincidental peak events for superstructure and substructure components which included elevated DI values, alignment of FFT peak responses between bridge components and test vehicles (measured for Dawson and Neerkol bridges only) and significant responses observed from waveform for various key structural components.

Several instances of quasi-resonance were observed in all three bridges, which key events are summarised in Table 7.1 to Table 7.3 for each bridge respectively. Instances of quasi-resonance were not restricted to maximum speeds or specific vehicle types, rather it was observed to occur for all vehicles for speeds ranging between 40 km/h and 80 km/h. The greatest number of resonant cases was noted for the Dawson River Bridge.

In most cases, DI values did not exceed 0.4 for superstructure values, with the exception of RT1 and CR2 for the Dawson River Bridge. Conversely, substructure DI values for these cases mostly exceeded 0.4, with some approaching 1. RT1 and CR2 were most likely to produce cases of quasi-resonance, which indicates that suspension type has been influential in inducing resonant responses in the bridge. As will be discussed later in this section, the body bounce characteristics of these vehicles has been significantly influential in the amplification of load.

Table 7.1: Quasi-resonance examples for the Canal Creek Bridge

Vehicle	Speed (km/h)	Direction of travel	DI	Peak strain (με)
			DU1	Girders
ST2	100	West	0.29	75
RT1	20	West	0.20	67

Note:
- DI values determined from peak bending strains recorded for kerb unit directly affected by vehicle load
- Selection of quasi-resonance cases based on peak DI values for superstructure.

Table 7.2: Quasi-resonance examples for the Dawson River Bridge

Vehicle	Speed (km/h)	Direction of travel	DI			Peak strain (με)
			Girders	Headstock	Columns	Girders
RT1	80	East	0.41	0.85	0.23 (0.92)	76
CR2	60	East	0.55	0.76	0.15 (0.53)	83
CR1	40	West	0.12	0.06	0.15 (0.11)	83

Note:
- DI values determined from peak bending strains recorded for components under direct load
- Selection of quasi-resonance cases based on coincidental peak DI values for all structural components
- Column DI values in brackets are based on peak compression strains
- Values in red are those that exceed DLA factor of 0.4.

Table 7.3: Quasi-resonance examples for the Neerkol Creek Bridge

Vehicle	Speed (km/h)	Direction of travel	DI			Peak strain (με)
			Girders	Headstock	Columns	Girders
CR2	80	West	0.39	0.62	0.87 (0.32)	109
RT1	60	West	0.10	0.57	0.85 (0.26)	92

Note:
- DI values determined from peak bending strains recorded for components under direct load
- Selection of quasi-resonance cases based on coincidental peak DI values for all structural components
- Column DI values in brackets are based on peak compression strains
- Peak girder bending strain for CR2 was peak for all measurements
- Values in red are those that exceed DLA factor of 0.4.

The three cases of quasi-resonance will be reviewed in more detail below. Bending strain waveforms for the RT1 quasi-resonance case is shown in Figure 7.2. Significant and clearly defined cyclic response for all components can be observed, indicative of the excitation induced in response to this vehicle type. The vertical velocity of the girders and headstock validate this observation with responses of similar form and frequency to the bending strains.

The quasi-resonance case for CR2 is shown in Figure 7.3. Similar waveforms to RT1 have resulted, with the total mass and vehicle length distinguishing between the responses. Note that CR2 induces a greater bending strain in the mid-span girders than RT1 in this instance. The same is true for the corresponding superstructure DI values. This is despite the total mass of the vehicles, the length of the vehicles and the speed at which both are travelling at. Individual axle group loads are likely to be influential in this instance, with peak bending strains resulting the 3rd and 4th groups for CR2 and RT1 respectively, of which axle loading for these groups are 12 t and 6.7 t respectively.

Reviewing the DI peaks for this vehicle travelling in both directions (see Section 5 and 6), there is evidence to suggest that quasi-resonance has occurred for this vehicle travelling at 40 km/h, irrespective of direction of travel and road profile condition. For the case of CR1 travelling west, the resonant case is shown in Figure 7.4. Despite the DI values being less than 0.4, it is clear that a resonant response has been induced in the superstructure elements from the cyclic responses in the corresponding waveform, indicating excitation. Conversely, a subdued response for the substructure components was observed. This indicates that quasi-resonance occurred only between CR1 and the superstructure for this speed. In addition to the vertical acceleration data presented in Figure 7.4, headstock accelerations in three directions are shown in Figure 7.5 for comparison. For this vehicle run, it was observed that the left cantilever of the Pier 7 headstock under load recorded a significant impulse response in the longitudinal direction at 4.5 s, and in the transverse direction at approximately 4 and 9 s. These timestamps mark where CR1 crosses the pier and approaches Abutment 2 respectively. Similar impulses were observed for this vehicle travelling in the opposite direction at the same speed, and have previously been noted for a select number of speeds for various vehicles. It is likely that these impulses are due to the movement of the pier globally (due to the single column, cantilevered structure of the pier, causing the sway motion of the pier and torsional movements of the deck) and the localised rigid-body rotation of the headstock. It is unknown to what extent this action may have contributed to the current defects of the headstock and the dynamic amplification of load.

To further illustrate evidence of quasi-resonance, frequency data from accelerometers for all components was reviewed after transforming the data via Fast-Fourier Transformation (FFT) analysis. FFT graphs for the three quasi-resonance cases for the Dawson River Bridge are shown in Figure 7.6. Note the strong frequency response for girders 1 and 6 mid-span which coincides with a shifted fundamental bending frequency. This highlights the amplification of load in the superstructure, particularly RT1 and CR2.

For RT1 and CR2, there is a strong, coincidental peak frequency response recorded for all components between 2.5 and 3.5 Hz. This matches the body bounce frequencies previously identified in the literature (Austroads 2003; Cantieni, Krebs & Heywood 2010; Davis & Bunker 2008). To illustrate this point, a comparison of frequency data collected for the Dawson River Bridge components and the body response of RT1 for the same vehicle run is shown in Figure 7.7. It is evident that the frequency response of RT1 above the axle groups has been significantly influential in driving the frequency response in all components of the bridge. Specific vehicle response frequency data for CR2 was not collected during this test, however similar findings are anticipated. Combined with the elevated DI values in all components for both RT1 and CR2, the observations validate these instances of quasi-resonance at 80 km/h and 60 km/h respectively which has resulted in the amplification of live load.

A final observation is made for CR1 in Figure 7.6. Despite the significant response, the frequency response of the girders was not quite synchronised with the fundamental bending frequency of the superstructure which may explain the suppressed load amplification (i.e. less than 0.4). However, high DI values recorded for the headstock may subsequently be explained by a coincidental frequency response at approximately 1.5 - 2 Hz of both cantilevers of the headstock in the transverse and longitudinal direction. These responses are closely aligned with the fundamental rigid body rotation frequency recorded for the headstock cantilevers during modal tests (see Section 4). Also, whilst it is not known, it is postulated that the inherent body bounce frequency of CR1 may be close to this frequency (based on measured frequency responses from RT2). Interestingly, the strongest response was recorded in the cantilever not under load. It is not known why this is the case, however it may indicate a weakness in this headstock, or that the cantilevers have inherently different fundamental frequency responses. In any case, it is clear that the frequency data confirms evidence of quasi-resonance and that it has been predominantly driven by the inherent frequency characteristics of the test vehicle.

Figure 7.2: Example of quasi-resonance for RT1 travelling East at 80 km/h (Dawson River Bridge)

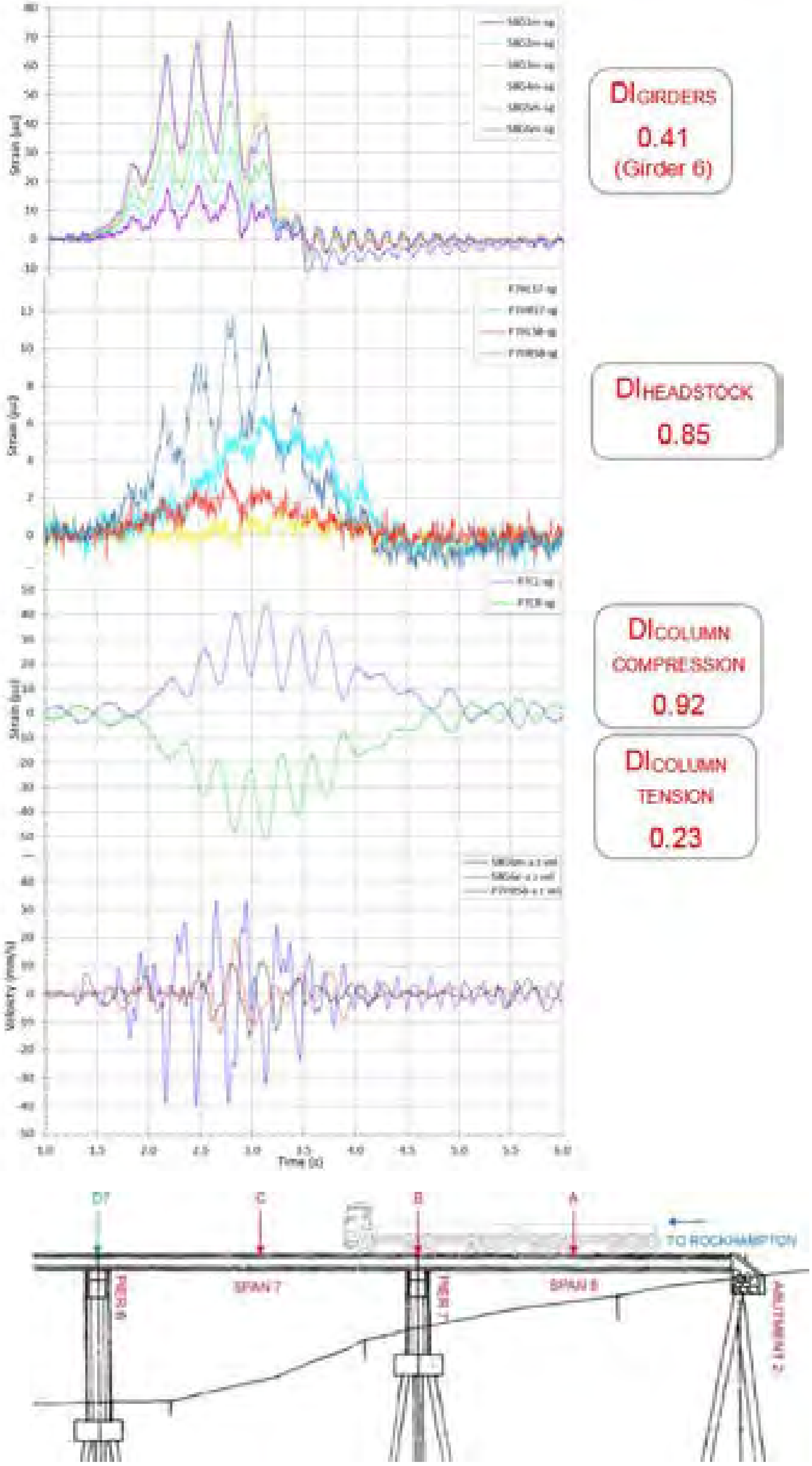

Figure 7.3: Example of quasi-resonance for CR2 travelling East at 60 km/h (Dawson River Bridge)

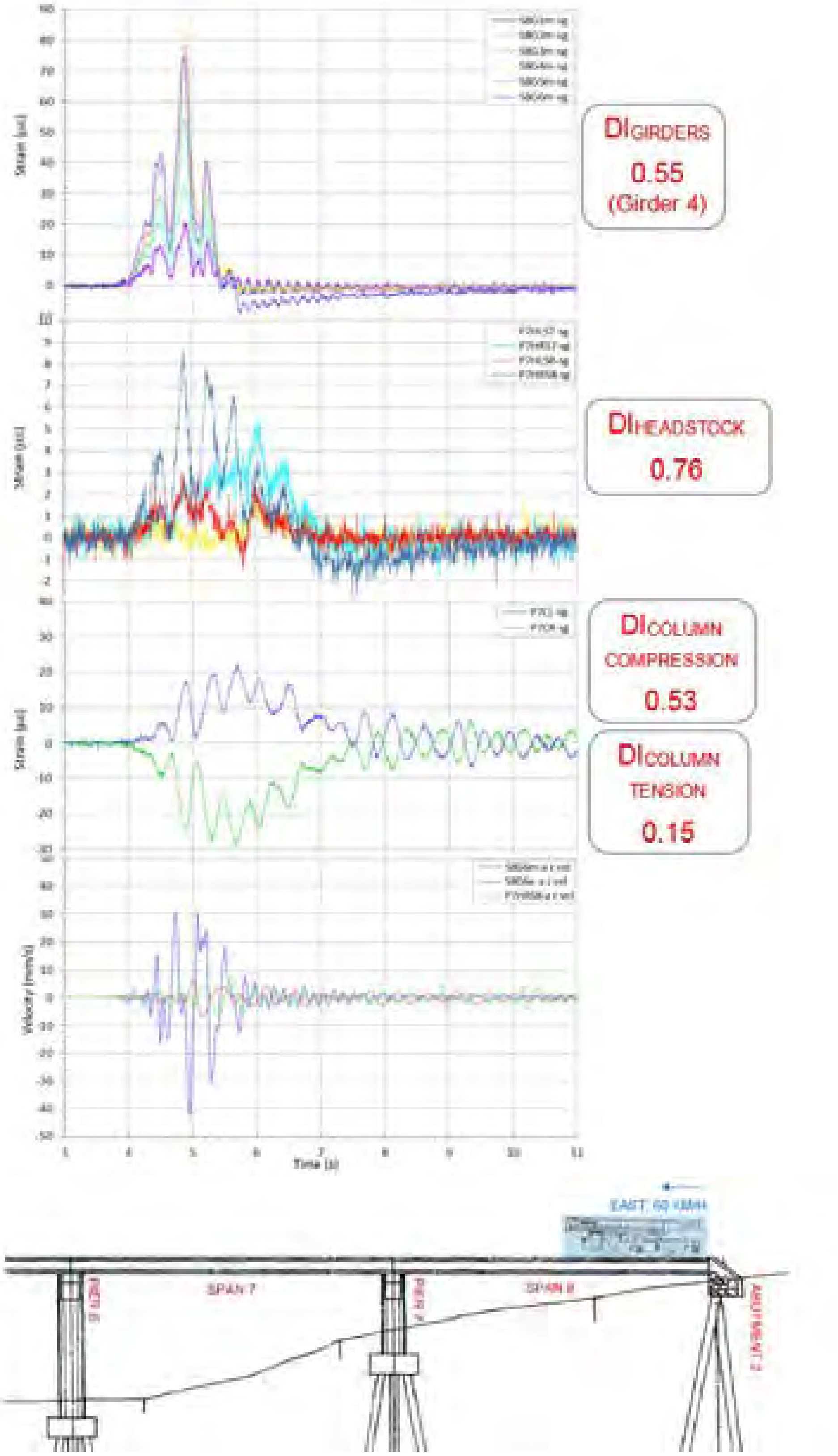

Figure 7.4: Example of quasi-resonance for CR1 travelling West at 40 km/h (Dawson River Bridge)

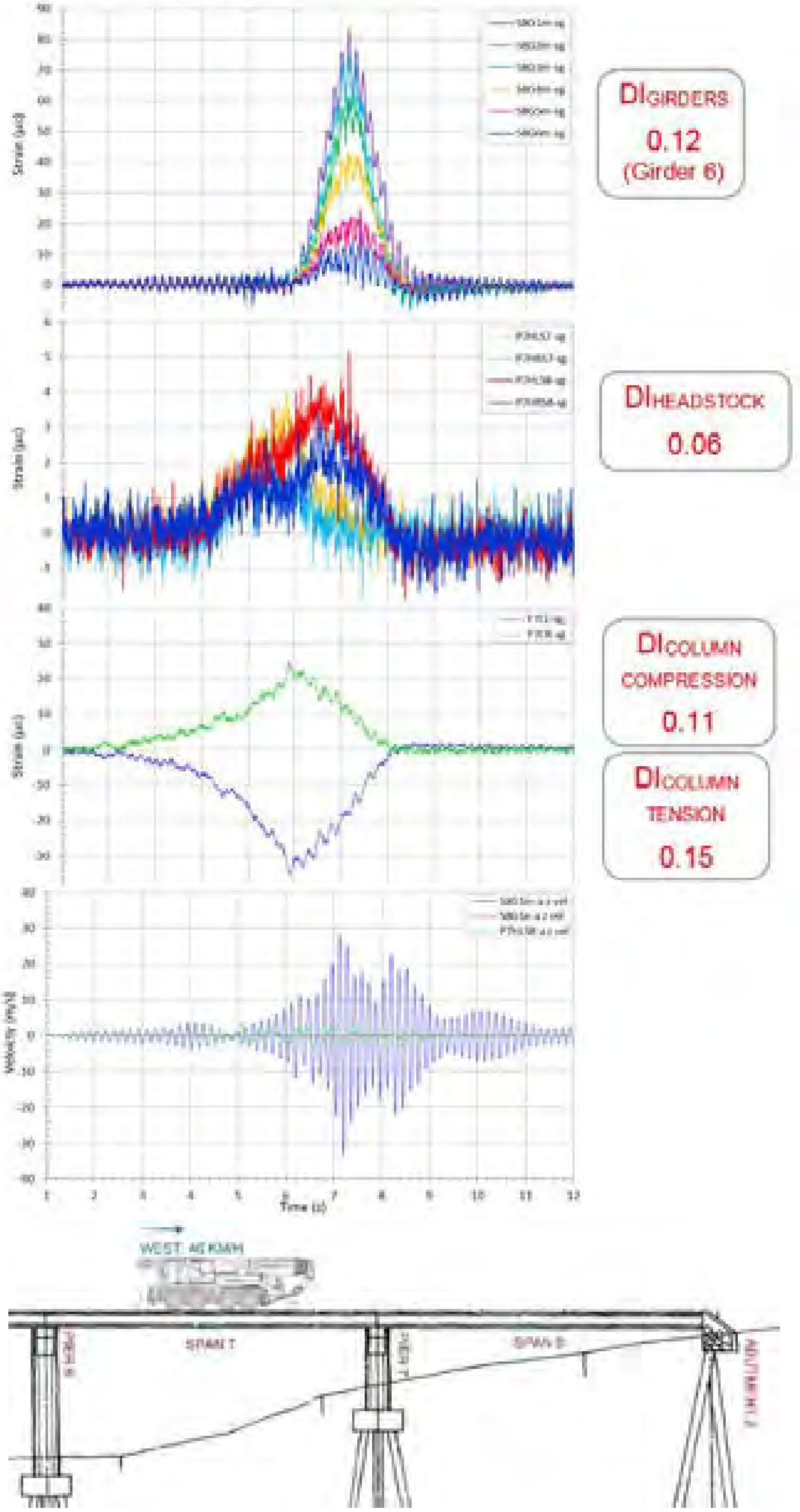

Figure 7.5: Three-dimensional accelerations recorded the loaded headstock left cantilever for the Dawson River Bridge (CR1 travelling west at 40 km/h)

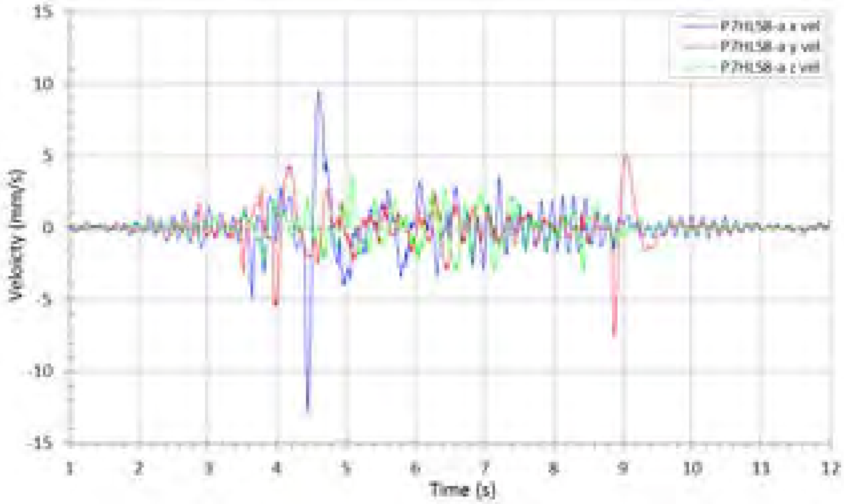

Figure 7.6: FFT analysis for quasi-resonance cases for the Dawson River Bridge (superstructure and substructure)

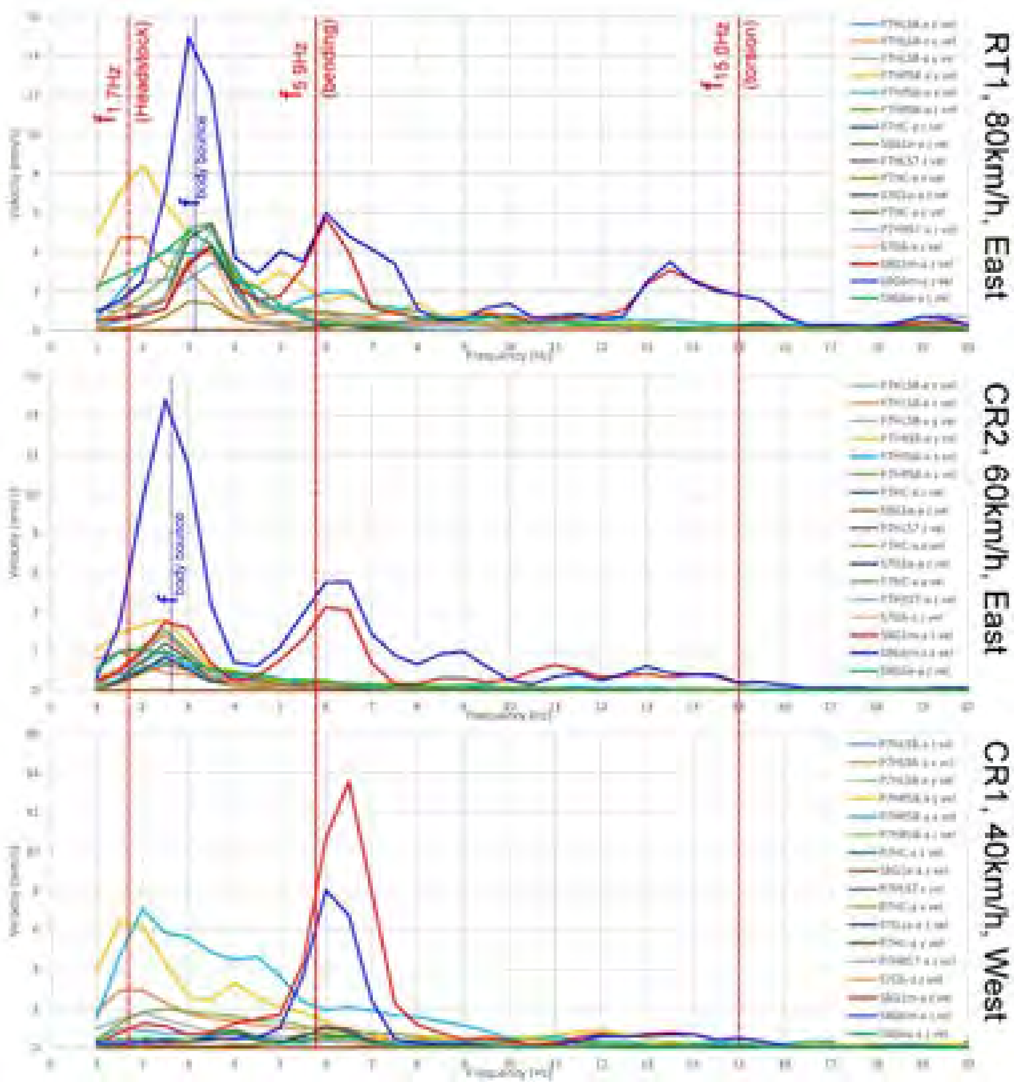

Figure 7.7: Comparison of frequency response of superstructure and substructure components for the Dawson River Bridge and RT1 (Travelling East at 80 km/h)

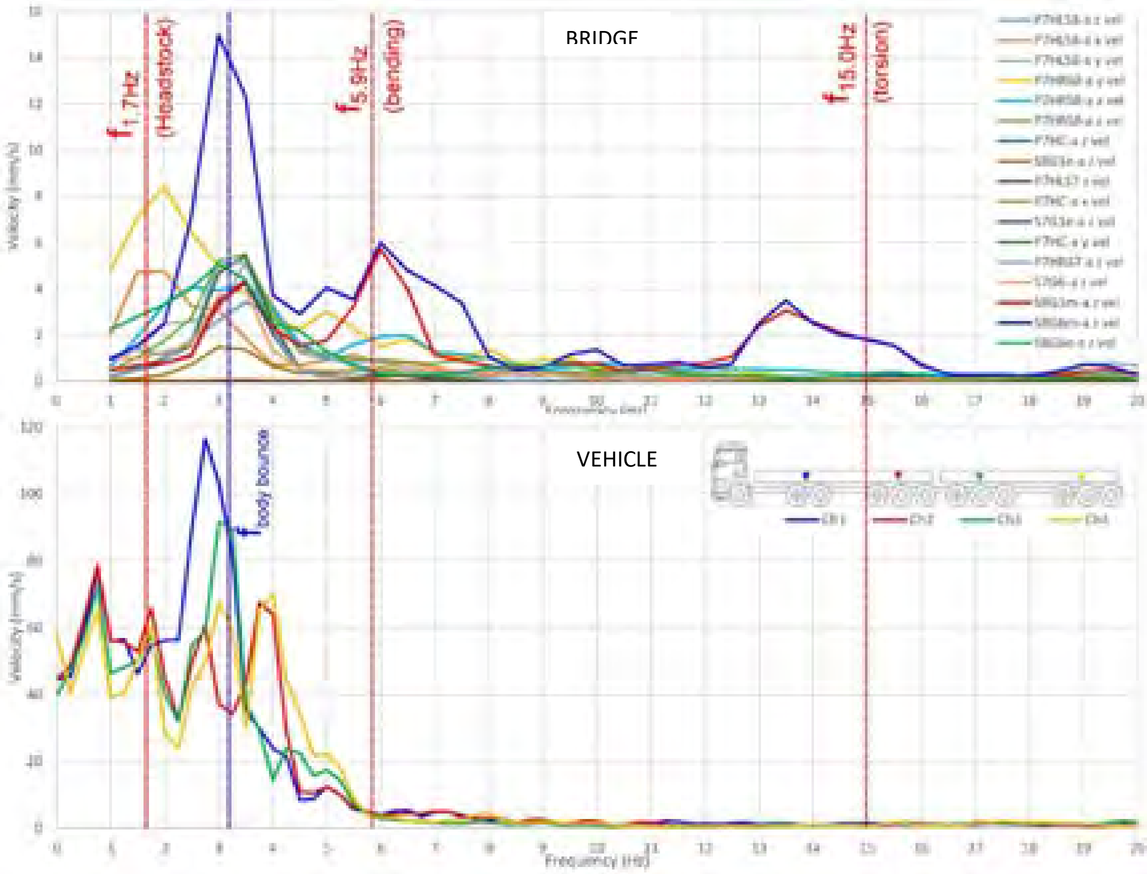

7.4 Load Distribution and Transverse Position of Vehicle

As the dynamic response of individual girders can be significantly influenced by the location of the vehicle wheel path (Bakht & Pinjarkar 1989; González 2009; Huang, Wang & Shahawy 1993; Zhou et al. 2015), each test vehicle run was investigated for transverse location across the deck. Of interest, the distribution of strains corresponding to the maximum bending strain recorded for selected runs was reviewed in conjunction with strains obtained from the corresponding crawl speed run. Investigation of the vehicle driveline also enables an integrity check of DI values determined previously.

To highlight the variability of driveline during testing, the location of each vehicle measured for each test run is shown in Table 7.4 for each test vehicle run and each bridge. An example of the identification of transverse vehicle location is shown in Figure 7.8. The results highlight the variability in the driveline between static and dynamic runs. Deviation from the static driveline was found to be related to increasing speed, the vehicle type and the personal driving habits of the driver. Trends show that as vehicle speed increases, there was a natural tendency for the driveline to drift towards the centre of the bridge. This also often highlighted the difference between vehicle location for static and dynamic runs. In some instances, deviations were due to traffic obstacles, such as parked vehicles, pedestrians, and interference from driving public, however these were minimal occurrences. As the peak static value was used in the determination of DI values, effects due to vehicle deviations were not considered to be significant, however this will be discussed further in Section 8.

To investigate the impact of vehicle deviation further, load distributions across the superstructure were reviewed for key vehicle runs for both static and dynamic runs, and are presented in Figure 7.9 to Figure 7.11. Full distribution results for all vehicles travelling at 80 km/h are included in Appendix A. A few key features can be noted in the distributions, which are summarised in the following paragraphs.

Load distribution patterns were reasonably reproducible between static and dynamic runs where the transverse location of the vehicle did not deviate significantly. Where deviations were in the order of 250 mm or more for the Canal Creek Bridge or 200 mm for Neerkol and Dawson bridges, a different form of load distribution was observed. For example, for CR1 travelling east over the Canal Creek Bridge (Figure 7.9a), a 250 mm deviation from the static run resulted in a different pattern of distribution, with static strains slightly exceeding dynamic strains when under load, but facilitating a greater and more even distribution of load across all units.

Distributions for the Canal Creek Bridge varied depending on vehicle track width and transverse location (Figure 7.9). For CR1, a 20 $\mu\varepsilon$ difference was observed between static and dynamic runs for the vehicle travelling West, with the vehicle running in the same transverse location on the bridge between runs. For CR1 travelling east, a 250 mm deviation from the static run resulted in a different pattern of distribution, with static strains slightly exceeding dynamic strains when under load, but facilitating a greater and more even distribution of load. Similar observations were made for other vehicles. The dynamic run for CR1 deviated 300 mm from the static run for the Dawson River Bridge, however minimal differences were observed in load distribution patterns for girders 4 to 6. Conversely, for a 250 mm deviation for RT1, a significant difference was recorded in the same girders.

For the Neerkol Creek Bridge (excluding the error in the Girder 3 strain gauge), centrally located girders were more likely to individually attract load (i.e. girders 2 to 4) (Figure 7.11). The differences between dynamic and static loading were more likely to be localised in lieu of the difference consistently distributed across all girders as observed in the Dawson River Bridge and Canal Creek Bridge (for example, static and dynamic strains for the edge girder in the opposite lane were relatively similar). Slightly different distribution patterns were observed where dynamic runs deviated significantly from static runs (i.e. more than 200 mm).

It was apparent that road profile had been a significant influence on the amplification of distributed load, particularly for CR2 and both roadtrains, although RT2 results exhibited slightly lower amplification. This is best demonstrated by distributions for the Dawson River Bridge in Figure 7.10, which show that vehicles travelling east exhibit larger load amplification under directly-loaded girders, with minimal differences between static and dynamic runs in the distributions for vehicles travelling in the opposite direction.

Figure 7.8: Identification of transverse vehicle location on site (Dawson River Bridge)

Table 7.4: Test vehicle transverse position in lane from adjacent kerb to outside wheel line

(a) Canal Creek

VEHICLE	Speed (km/h)	Travel to	Wheel location from kerb (mm)	Δ from static	Peak Strain	Based on Girder	Peak DI
CR1	Crawl	West	650	–	80.0	SG13	–
	20	West	600	-50	85.8	SG13	0.07
	40	West	1100	450	83.2	SG13	0.04
	60	West	700	50	88.4	SG13	0.11
	80	West	800	150	76.6	SG13	-0.04
	Crawl	East	700	–	79.6	SG1	–
	20	East	600	-100	86.3	SG1	0.08
	40	East	800	100	82.1	SG1	0.03
	60	East	650	-50	94.7	SG1	0.22
	80	East	700	0	96.7	SG1	0.22
ST1	Crawl	[illegible]	700	–	45.5	SG13	–
	20	West	700	0	51.4	SG13	0.13
	40	West	800	100	45.0	SG13	-0.01
	60	West	800	100	43.9	SG13	-0.04
	80	West	900	200	51.9	SG7	0.14
	max	West	600	-100	47.3	SG6	0.06
	Crawl	East	600	–	51.6	SG1	–
	20	East	650	50	56.5	SG3	0.11
	40	East	750	150	61.2	SG1	0.19
	60	East	700	100	53.7	SG1	0.05
	80	East	900	300	44.6	SG1	0.05
	max	East	600	0	47.0	SG8	0.07
ST2	Crawl	West	650	–	57.4	SG13	–
	20	West	600	-50	61.8	SG13	0.09
	40	West	1100	450	62.0	SG13	0.19
	60	West	750	100	61.3	SG13	0.21
	80	West	800	150	61.8	SG13	0.09
	max	West	600	-50	60.9	SG13	0.35
	Crawl	East	600	–	57.3	SG1	–
	20	East	600	0	59.4	SG1	0.03
	40	East	800	200	61.0	SG1	0.05
	60	East	650	50	62.1	SG1	0.07
	80	East	700	100	69.6	SG1	0.20
	max	East	600	0	74.6	SG1	0.29
ST3	Crawl	West	580	–	49.5	SG13	–
	20	West	650	70	58.5	SG13	0.18
	40	West	900	320	50.5	SG13	0.02
	60	West	900	320	49.6	SG13	0.00
	80	West	800	220	52.3	SG13	0.06
	max	West	900	320	53.0	SG7	0.09
	Crawl	East	600	–	55.6	SG1	–
	20	East	600	0	66.6	SG1	0.20
	40	East	600	0	65.1	SG1	0.17
	60	East	600	0	59.7	SG1	0.07
	80	East	900	300	49.1	SG1	-0.12
	max	East	900	300	45.5	SG6	-0.18

(b) Dawson River Bridge

VEHICLE	Speed (km/h)	Travel to	Wheel location from kerb (start) (mm)	Wheel location from kerb (finish) (mm)	Δ from static (start)	Δ from static (finish)	Peak Strain	Based on Girder	Peak DI
CR1	Crawl	West	1300	1400	–	–	74.6	G1	-
	20	West	1250	1300	-50	-100	75.2	G1	0.01
	40	West	1350	1450	50	50	83.4	G1	0.12
	60	West	1150	1100	-150	-300	79.0	G1	0.06
	80	West	1200	1200	-100	-200	74.7	G1	0.00
	Crawl	East	1200	1200	–	–	65.2	G4	–
	20	East	1400	1350	200	150	67.7	G4	0.04
	40	East	1250	1200	50	0	69.3	G5	0.05
	60	East	1350	1300	150	100	66.9	G4	0.03
	80	East	1500	1500	300	300	69.4	G4	0.06
CR2	Crawl	West	1450/1200	1300/1100	–	–	60.2	G1	
	20	West	1450/1200	1500/1250	0	200	60.4	G1	0.00
	40	West	1400/1150	1500/1250	-50	200	62.5	G1	0.04
	60	West	1450/1200	1600/1350	0	200	70.1	G1	0.16
	80	West	1550/1300	1650/1400	100	350	66.5	G1	0.11
	Crawl	East	1400/1150	1400/1150	–	–	53.2	G4	-
	20	East	1550/1300	1550/1300	150	150	72.9	G4	0.37
	40	East	1550/1300	1500/1250	150	100	67.1	G4	0.07
	60	East	1600/1350	1650/1400	200	250	82.6	G4	0.55
	80	East	1600/1350	1550/1300	200	150	64.9	G4	0.22
RT1	Crawl	West	1785	1500	-	-	66.0	G1	-
	20	West	1450	1500	-335	0	73.2	G1	0.11
	40	West	1450	1400	-335	-100	77.9	G1	0.18
	60	West	1500	1500	-285	0	70.1	G1	0.06
	80	West	1400	1400	-385	-100	68.1	G1	0.03
	95	West	1400	1400	-385	-100	68.3	G1	0.03
	Crawl	East	1600	1650	–	-	63.6	G4	
	20	East	1450	1550	-150	0	58.2	G4	0.09
	40	East	1400	1500	-200	-50	57.6	G4	0.07
	60	East	1650	1600	-50	-50	67.5	G4	0.26
	80	East	1750	1750	150	200	75.5	G6	0.41
	100	East	1600	1600	0	50	65.2	G6	0.22
RT2	Crawl	West	1775	1500	-	-	67.1	G1	-
	20	West	1400	1450	-375	-50	68.6	G1	0.02
	40	West	1400	1500	-375	0	68.9	G1	0.03
	60	West	1350	1400	-425	-100	71.8	G1	0.07
	80	West	1350	1400	-425	-100	69.9	G1	0.04
	105	West	1400	1400	-375	-100	71.2	G1	0.06
	Crawl	East	1800	1800	–	-	67.3	G4	-
	20	East	1500	1550	0	50	57.2	G4	0.00
	40	East	1450	1450	-50	-50	60.3	G4	0.05
	60	East	1550	1550	50	50	59.0	G4	0.03
	80	East	1700	1700	200	200	60.8	G4	0.13
	105	East	1400	1400	-100	-100	64.7	G6	0.17

(c) Neerkol Creek Bridge

VEHICLE	Speed (km/h)	Travel to	Wheel location from kerb (start) (mm)	Wheel location from kerb (finish) (mm)	Δ from static (start)	Δ from static (finish)	Peak Strain	Based on Girder	Peak DI
CR1	Crawl	East	1400	1300	-	-	77.2	G4	-
	40	East	1200	1200	-200	-100	82.8	G4	0.07
	60	East	1350	1300	-50	0	81.5	G4	0.06
	80	East	-	-	-	-	76.7	G4	-0.01
	Crawl	West	1400	1500	-	-	95.6	G2	-
	20	West	-	-	-	-	94.0	G2	-0.02
	40	West	1350	1400	-50	-100	99.3	G2	0.04
	60	West	1300	1300	-100	-200	91.3	G2	-0.04
	80	West	1300	1300	-100	-200	105.3	G2	0.10
CR2	Crawl	East	1400/1150	1450/1200	-	-	62.9	G4	-
	40	East	1450/1200	1450/1200	50	0	77.7	G4	0.24
	60	East	1350/1100	1400/1150	-50	-50	83.9	G4	0.34
	80	East	1500/1250	1450/1200	100	0	84.1	G4	0.34
	Crawl	West	1500/1250	1300/1150	-	-	78.3	G2	-
	20	West	-	-	-	-	85.5	G2	0.09
	40	West	1350/1100	1350/1100	-150	50	83.9	G2	0.07
	60	West	1500/1250	1500/1250	0	200	89.2	G2	0.14
	80	West	1450/1200	1450/1200	-50	150	108.7	G2	0.39
RT1	Crawl	East	1500	1500	-	-	66.0	G4	-
	40	East	1600	1500	100	0	73.0	G4	0.11
	60	East	1600	1550	100	50	76.7	G4	0.18
	80	East	1650	1500	150	0	86.8	G4	0.31
	90	East	-	-	-	-	81.4	G4	0.23
	Crawl	West	1500	1450	-	-	83.2	G2	-
	20	West	-	-	-	-	96.2	G2	0.16
	40	West	1750	1700	250	250	84.4	G2	0.02
	60	West	1600	1500	100	50	91.6	G2	0.10
	80	West	1500	1400	0	-50	97.3	G2	0.17
	86	West	1500	1500	0	50	96.6	G2	0.16
RT2	Crawl	East	1500	1450	-	-	65.2	G4	-
	40	East	1500	1500	0	50	73.0	G4	0.12
	60	East	1550	1600	50	150	75.0	G4	0.15
	80	East	1500	1500	0	50	70.8	G4	0.09
	94	East	-	-	-	-	72.8	G4	0.12
	Crawl	West	1550	1550	-	-	86.8	G2	-
	20	West	-	-	-	-	86.6	G2	0.00
	40	West	1550	1550	0	0	87.5	G2	0.01
	60	West	1500	1500	-50	-50	90.9	G2	0.06
	80	West	1500	1450	-50	-100	89.6	G2	0.03
	95	West	1500	1500	-50	-50	96.4	G2	0.11

Figure 7.9: Distribution of mid-span bending strains across girders for CR1 and RT1 for the Canal Creek Bridge (static vs. 80 km/h lane travel)

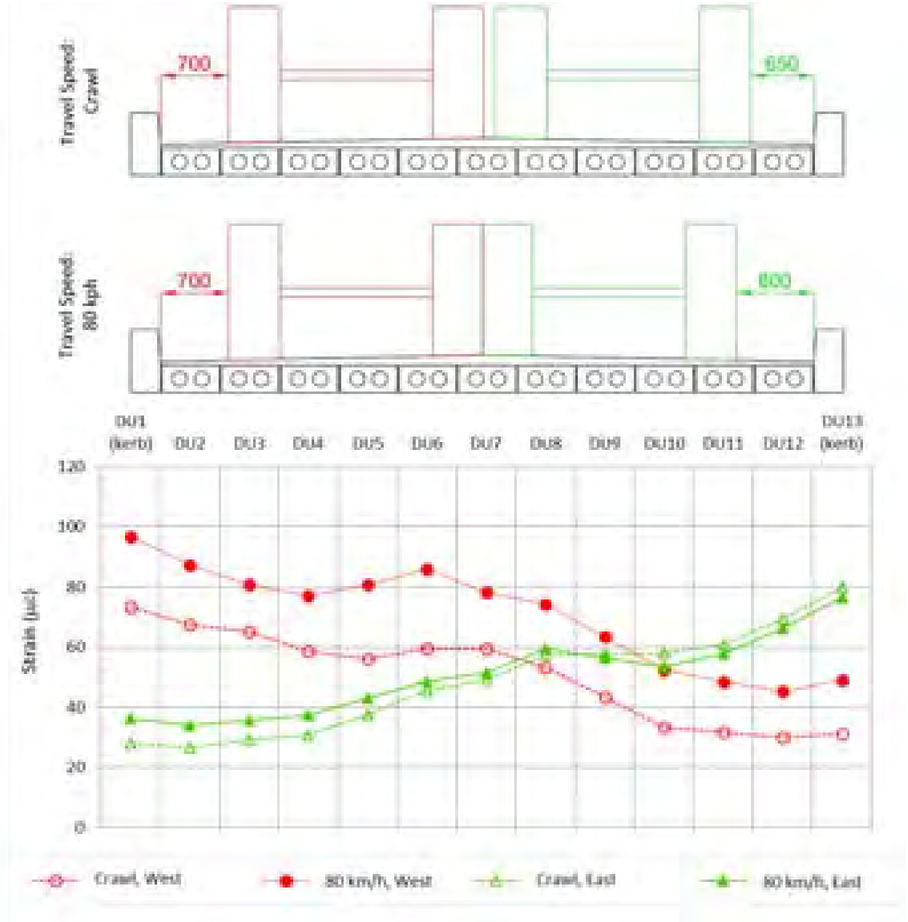

(a) CR1

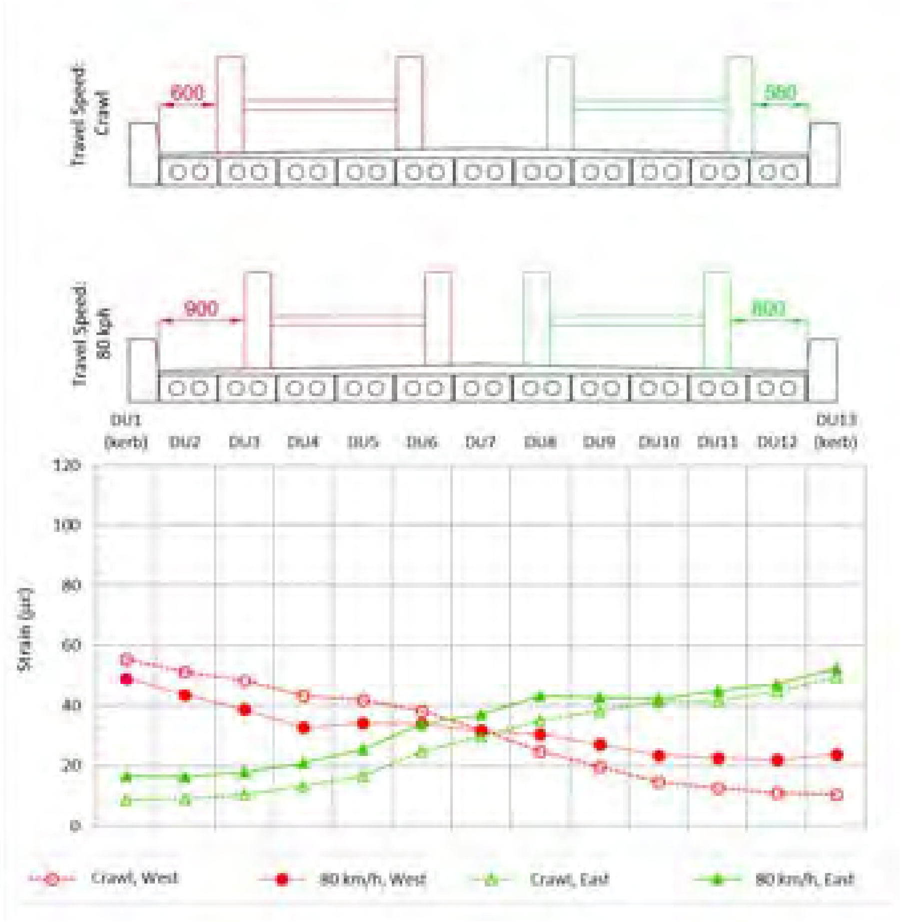

(b) RT1

Figure 7.10: Distribution of mid-span bending strains across girders for CR1 & RT1 for the Dawson River Bridge (static vs. 80 km/h lane travel)

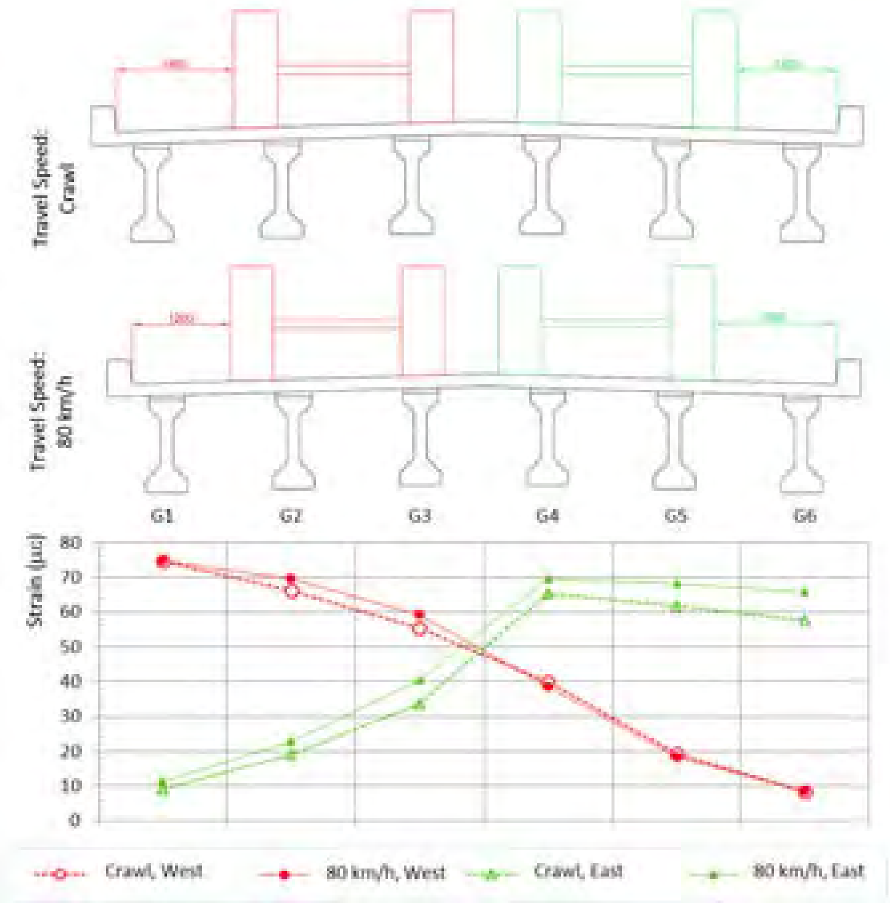

(a) CR1

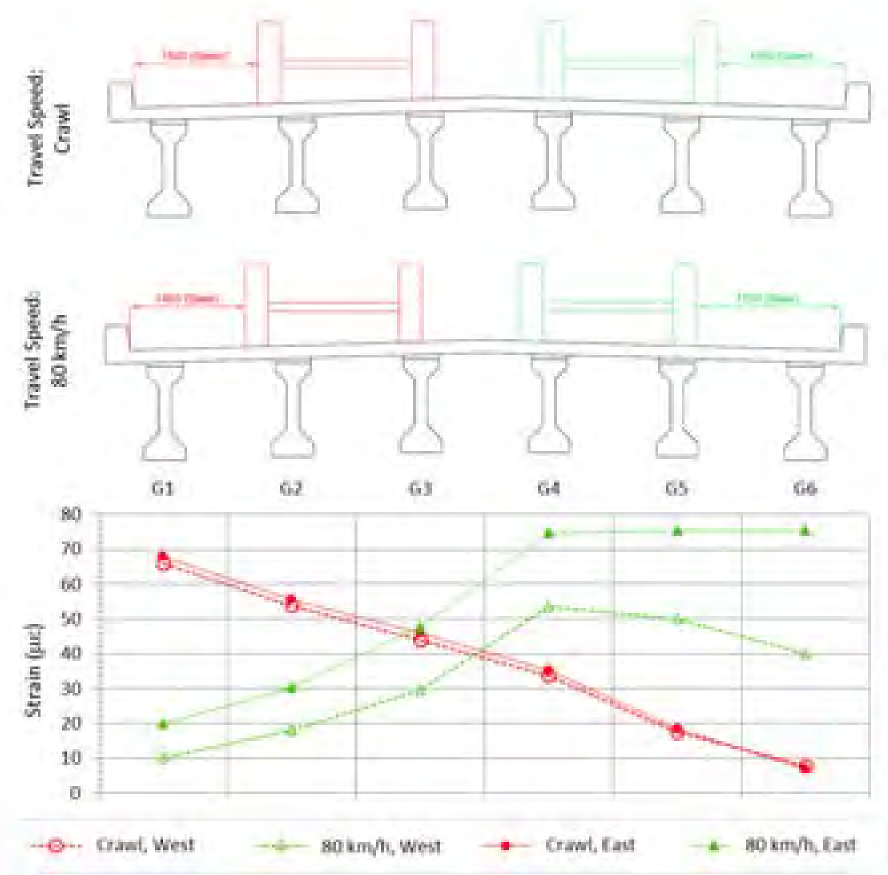

(b) RT1

Figure 7.11: Distribution of mid-span bending strains across girders for CR1 and RT21 for the Neerkol Creek Bridge (static vs. 80 km/h lane travel)

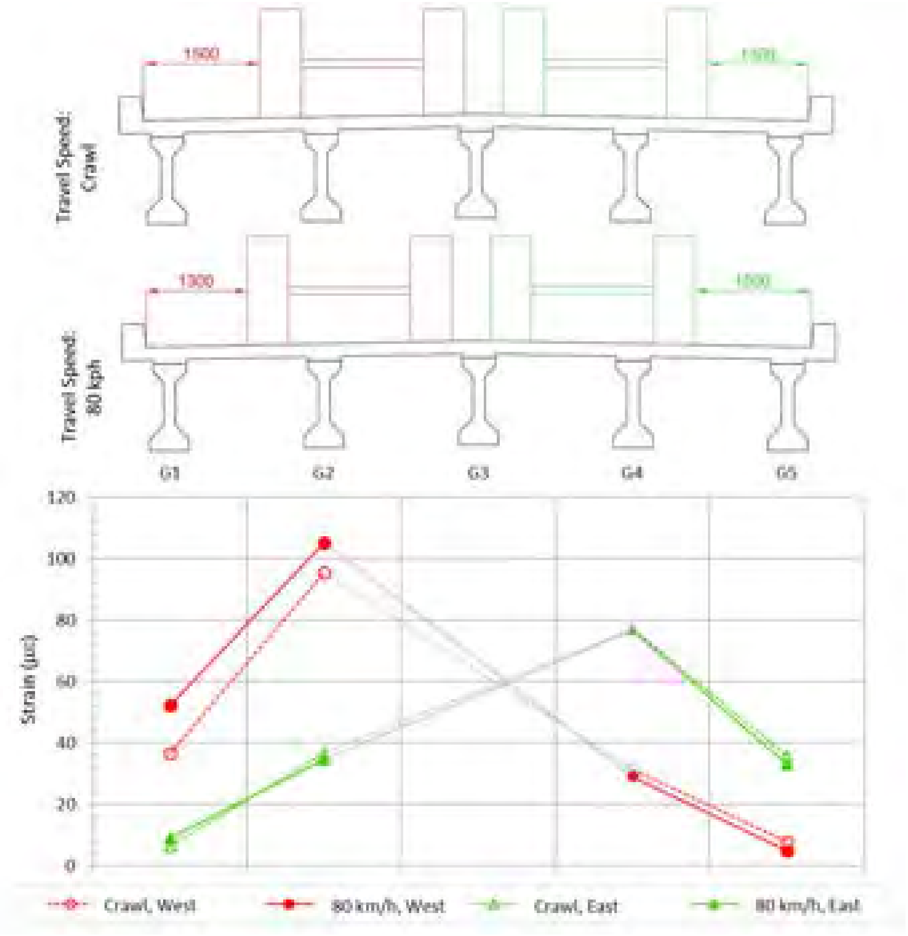

(a) CR1

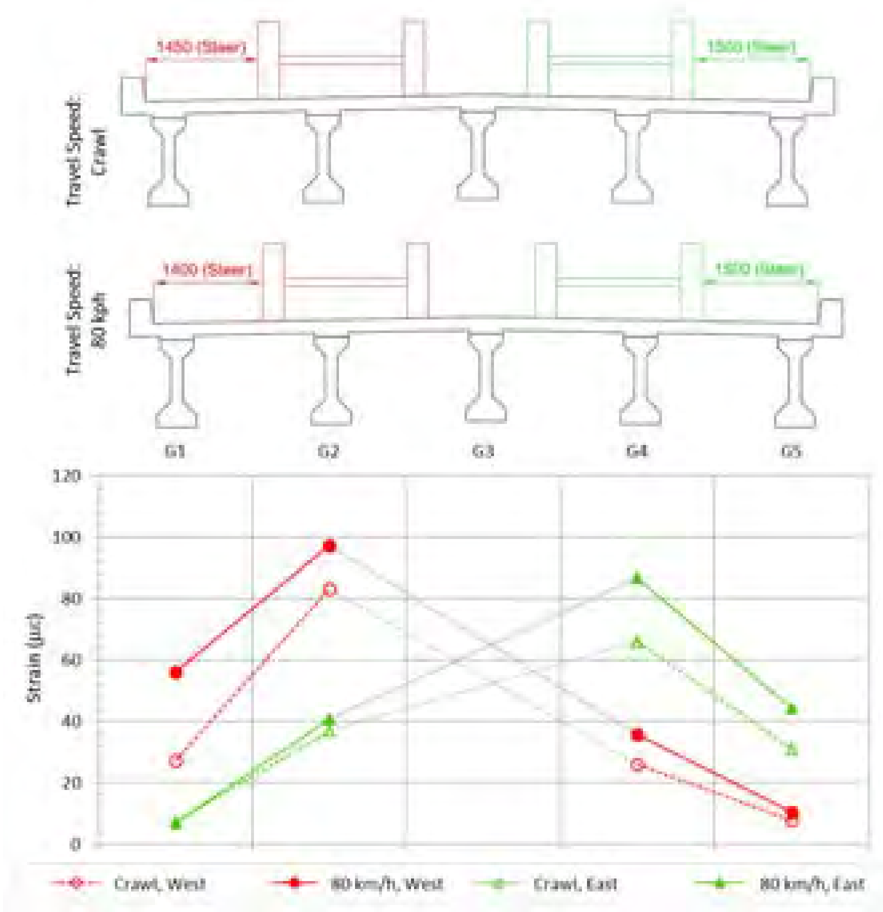

(b) RT1

7.5 Distribution Relating to Dynamic Load Amplification

As an extension of Section 7.4, the distribution of DI values corresponding to each test vehicle has been mapped according to girder position, as previously done by Nassif and Nowak (Nassif & Nowak 1995). These values were derived from the peak value recorded for one girder and the corresponding load distribution across the other girders for each test vehicle travelling at a representative speed and direction of travel. The resulting distributions are shown in Figure 7.12 for each bridge with vehicles travelling in lane at 80 km/h.

Firstly note the similar distribution pattern for each vehicle. The zone of direct load influence (as identified by Bakht and Pinjarkar (1989)) is evident in the resulting DI values, with consistent values obtained (e.g. girders 4 and 5 for travel east for the Dawson River Bridge in Figure 7.12b and the dual peaks observed in the deck units for the Canal Creek Bridge in Figure 7.12a). Note that CR1 and RT2 result in low DI values in these girders in comparison to CR2 and RT1 for Dawson. This highlights the increased likelihood of greater load amplification of these structures in response to steel suspension vehicles.

Peak DI results were restricted predominantly to one girder for the Neerkol Creek Bridge, with results less than zero for girders not predominantly affected by load. The faulty gauge on girder 3 has also limited observations for the superstructure in this instance, however results suggest that dynamic load distribution is sensitive to the number of girders and where direct loading occurs (which agrees with the literature (Bakht & Pinjarkar 1989; Huang, Wang & Shahawy 1993; Kim & Nowak 1997). Greater scatter and increasingly negative DI values was observed where not under direct load (such as girders 1 and 6 where opposite to direction of travel), a phenomenon previously observed by Bakht and Pinjarkar (1989).

Gonzalez (2009) noted that for girder bridges specifically, DI values were more likely to be lower where girders attracted the majority of load, and as such may serve to confirm that current DLA factors are conservative. Based on the results observed in Figure 7.12 showing lower DI values for girders under direct load, this appears to confirm Gonzalez’s observation.

Note that the distribution of DI values varies with direction of travel and vehicle type, which suggests the influence of road profile on results. Greater scatter was observed for Canal Creek results (Figure 7.12a), with CR1 and the air-bag suspension semi-trailer consistently producing elevated DI values across the deck, whereas the elevated results were induced by the steel-suspension semi-trailer travelling in the opposite direction. Similar differences were observed for the Dawson River Bridge, however DI values were relatively consistent for the Neerkol Creek Bridge.

The outlier result recorded in DU8 for ST2 relates to different location to which the maximum static strain was recorded which was different to the recorded peak dynamic strain. This highlights the importance of vehicle location in the quantification of dynamic load amplification. It also raises the question of the sensitivity of the method used to determine dynamic increment, with significant changes in the results observed depending on the selection of peak static and dynamic values. The sensitivity of these values will be discussed further in Section 8.

Figure 7.12: Distribution of DI values determined for each test vehicle travelling at 80 km/h

(a) Canal Creek Bridge, travelling West

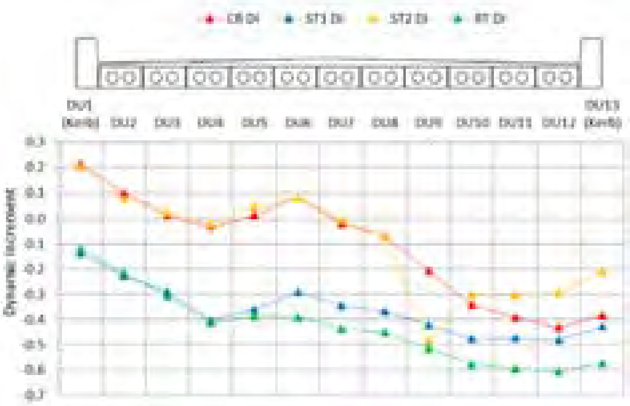

Travelling West

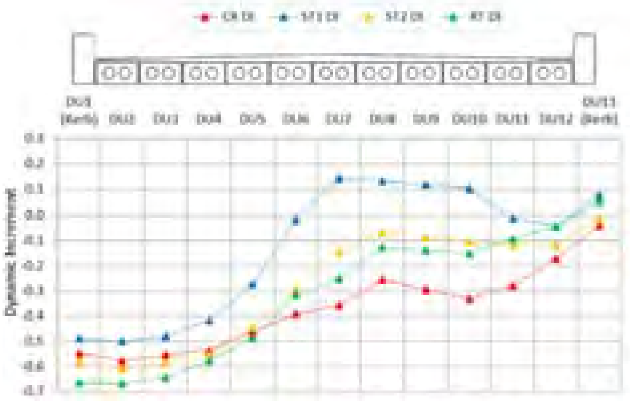

Travelling East

(b) Dawson River Bridge, travelling East

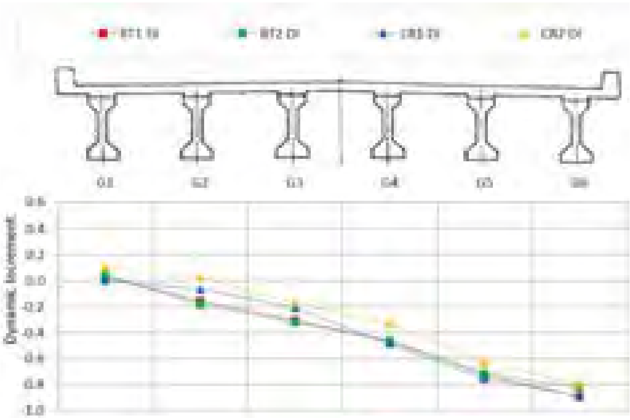

Travelling West

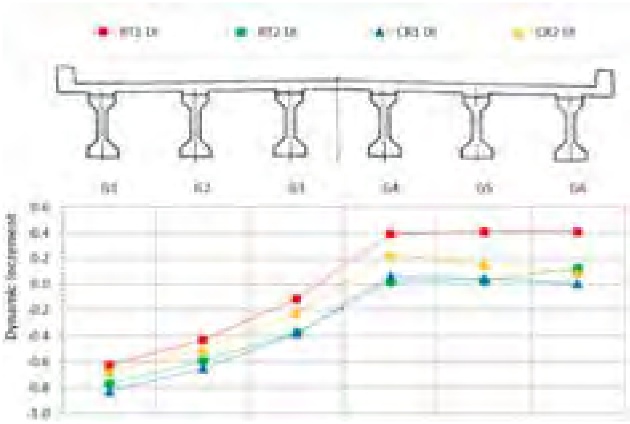

Travelling East

(c) Neerkol Creek Bridge, travelling East

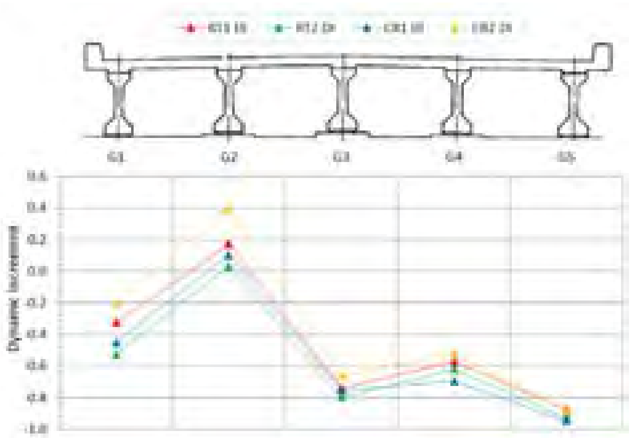

Travelling West

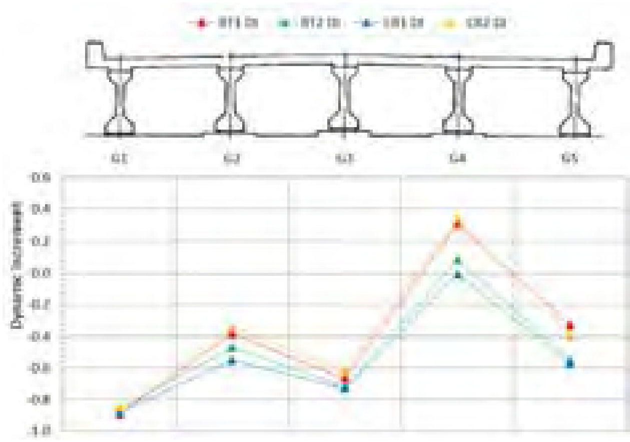

Travelling East

7.6 Influence of the Bridge from the Road Trains

An investigation was conducted into the behaviour relating to frequency response of each of the road trains prior to, during and after the passage of the bridge. Of interest in the data reviewed was the response of the vehicle to the road profile and the influence of the bridge on the response of the bridge. This included a review of acceleration data and subsequent FFT analyses. Representative cases are now discussed for the Dawson River Bridge, and further information can be found in Appendix A for the Neerkol Creek Bridge.

Figure 7.13 and Figure 7.14 show the accelerations measured on the body of RT1 and RT2 respectively for the Dawson River Bridge. From the accelerometer data, the response of each road train to the bridge is distinctly different to the approaching and following road profiles. The vehicle continues to be affected by the dynamic effects of the bridge as it continues on its journey.

The response of RT1 exhibits a greater amplitude and dynamic response than that recorded for the RT2. Also, where significant events were measured for RT2, energy was quickly dissipated with the restoration of the normally subdued dynamic response of this vehicle after crossing the bridge. This highlights the significance of the suspension type and damping condition of the shock absorbers in governing the overall vehicle dynamic response and subsequently the dynamic load imparted to a supporting surface.

The influence of the road profile condition is also evident from the data. Accelerations recorded for the approaches to the bridge for each roadtrain travelling west are less in amplitude than in the alternate direction of travel. The influence of the road profile prior to Abutment 2 for the road trains travelling east was evidently rougher, and notably for RT1, this has set up a significant cyclic and resonant response in this vehicle as it crosses the bridge. Note that this cyclic response was not recorded for the same vehicle travelling west, rather a range of waveforms were recorded above each axle group. For RT2, a discrete, short-lived cyclic event of even greater magnitude was evident. This confirms the observations the greater magnitude of dynamic load amplification measured in the bridge components at such speeds, as well as highlighting the influential nature in road profile condition.

An analysis of the inherent frequency responses for the same runs (via a FFT analysis) highlights similar findings (Figure 7.13 to Figure 7.14). Firstly note the inherent frequency characteristics of the body bounce frequencies of each roadtrain, with FT1 exhibiting a frequency of between 2.5 and 4 Hz, whereas RT2 are between 1.5 and 2.5 Hz. Consistent and greater frequency responses were observed for both roadtrains when crossing the bridge in comparison to road surface travel. Note the shift in frequencies between each vehicle prior to, travelling on and after the bridge. The shifts in frequency responses were also noted in relation to direction of travel, again indicating the influence of the road profile condition, as well as the inherent frequency and structural characteristics and boundary/geometric conditions of the bridge.

It is recommended that further research be carried out to quantify the influences of vehicle frequency characteristics on a structure, as well as the resulting axle loads. Further study on the inherent frequency and axle loading responses of various crane types would also be beneficial.

Figure 7.13: Accelerometer response of RT1 travelling at 80 km/h (Dawson River Bridge)

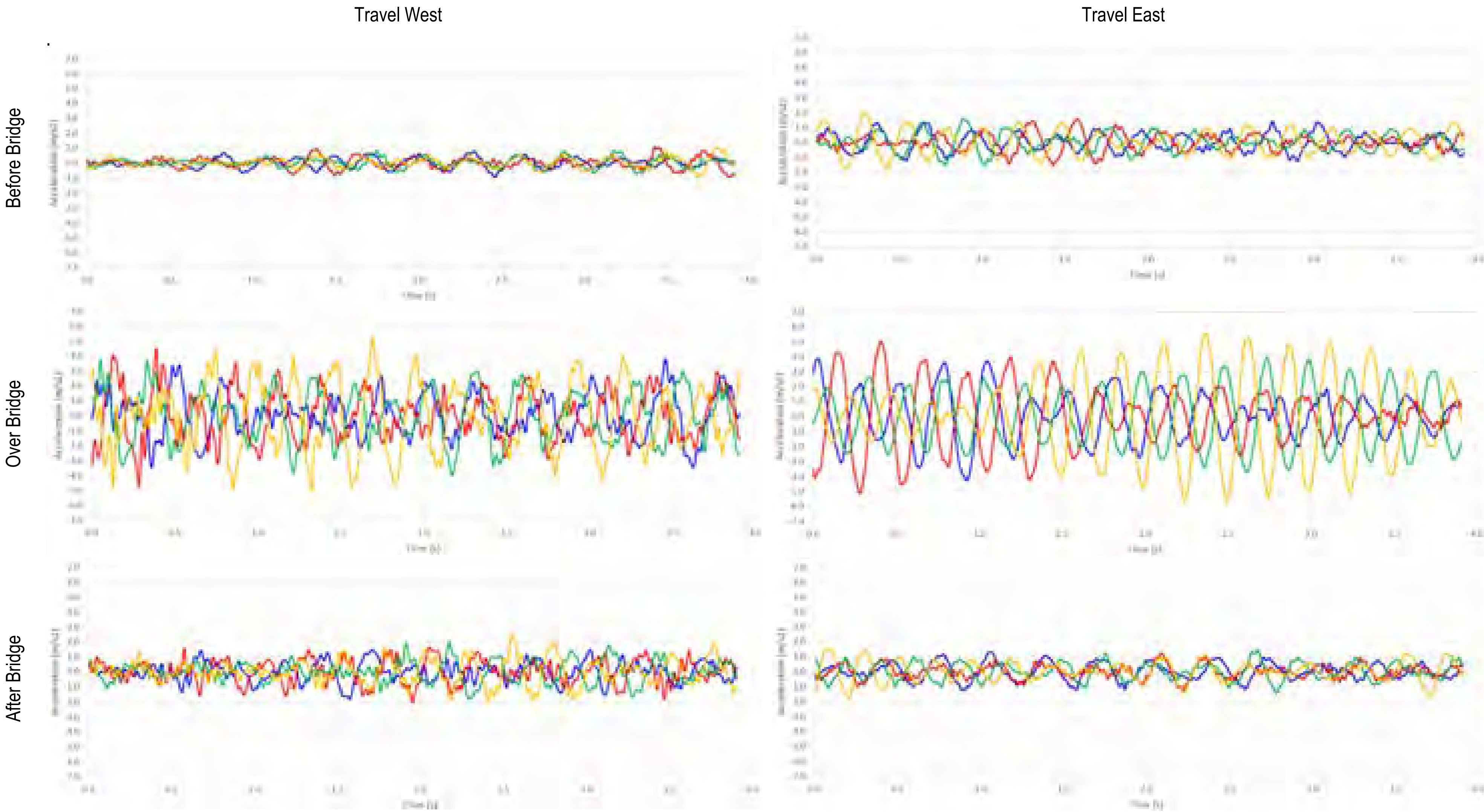

Figure 7.14: Accelerometer response of RT2 travelling at 80 km/h (Dawson River Bridge)

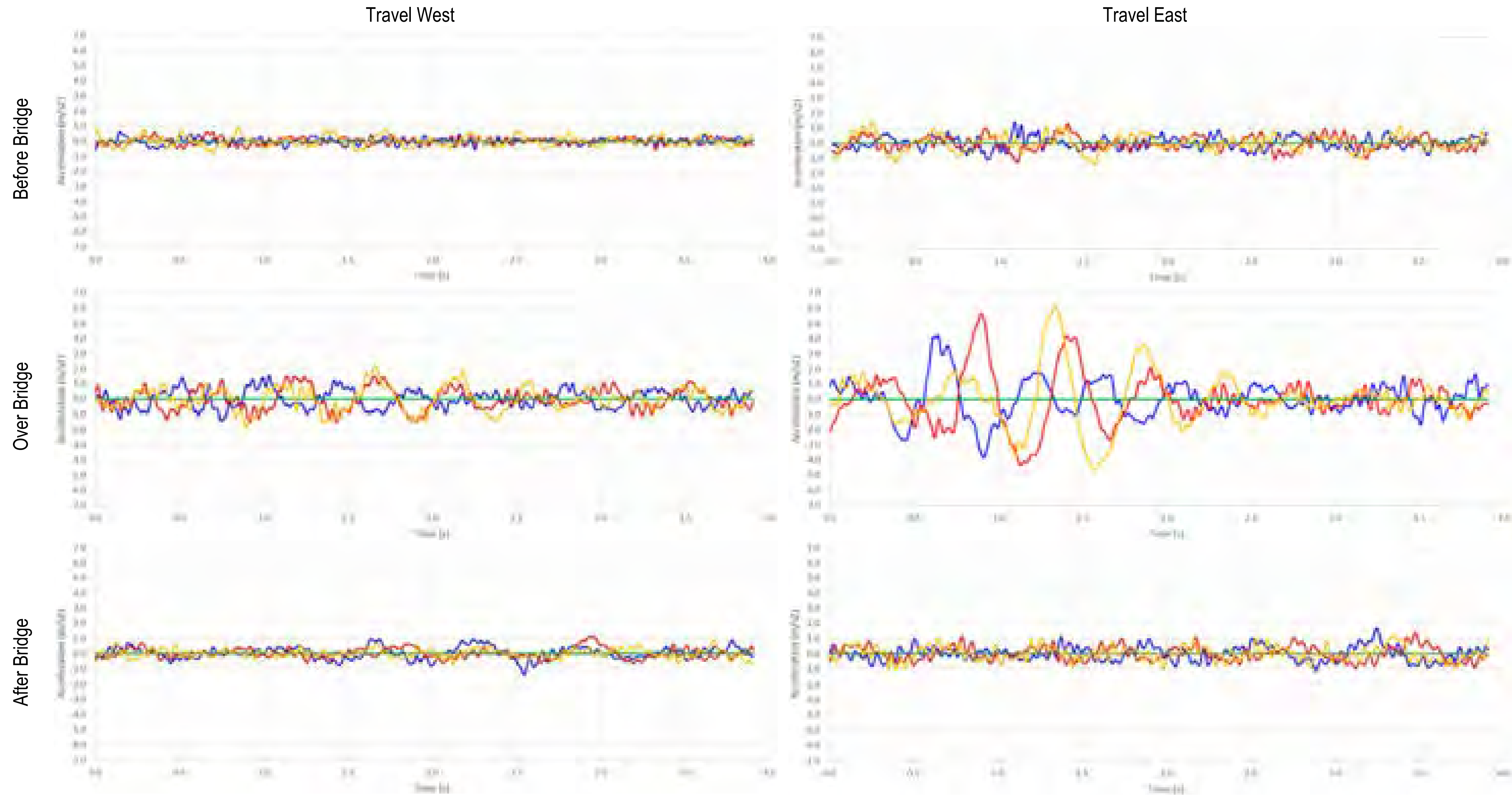

Figure 7.15: FFT analysis of RT1 travelling at 80 km/h (Dawson River Bridge)

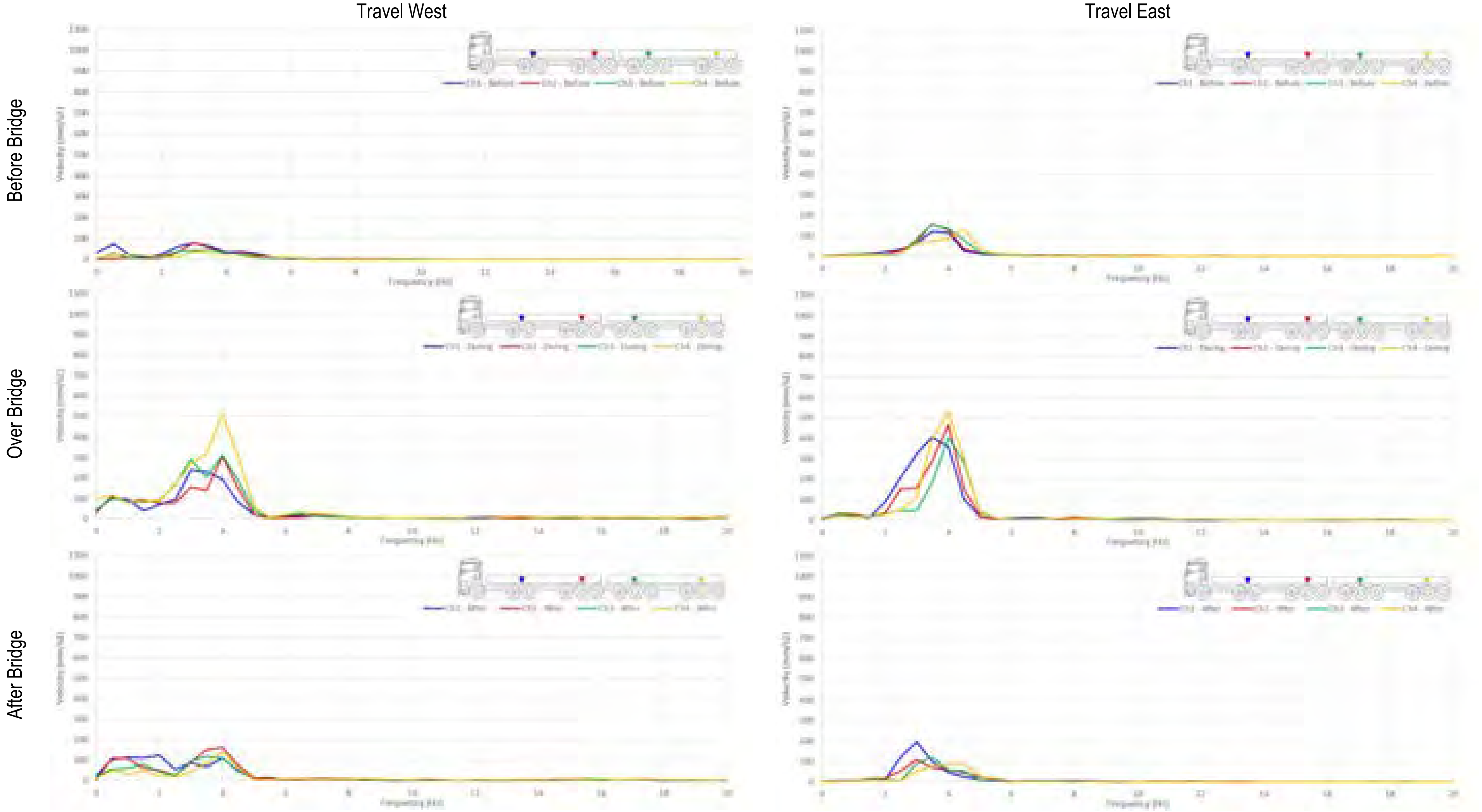

Figure 7.16: FFT analysis of RT2 travelling at 80 km/h (Dawson River Bridge)

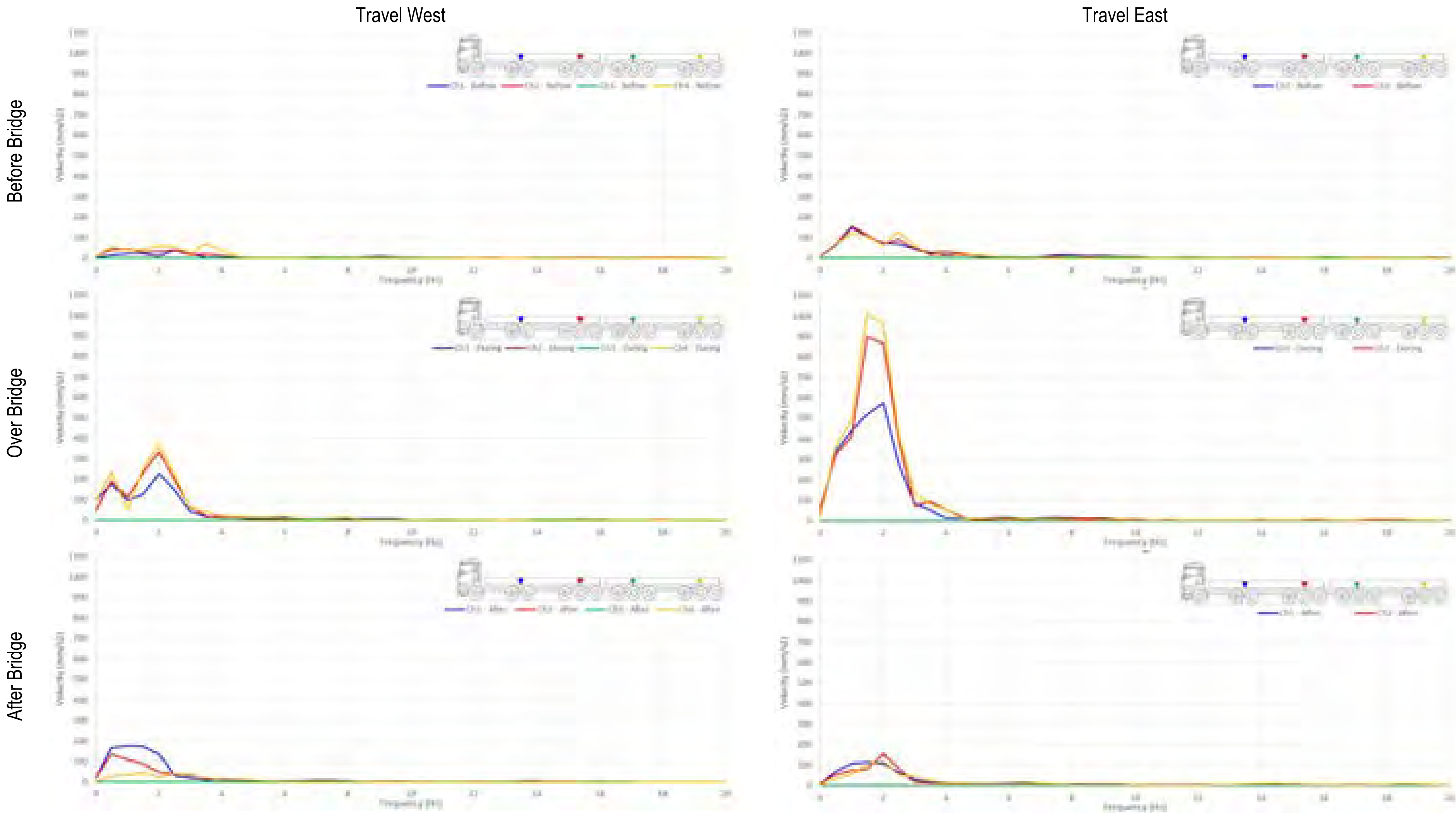

7.7 Relationship between Controlled vs In-service Monitoring

The literature documents that whilst controlled load tests enable an improved understanding of the response of the bridge to specific loading scenarios, it is not highly representative of actual traffic in all cases, and thus in-service dynamic loading a bridge is likely to be less (Caprani 2005; González et al. 2010; Žnidarič et al. 2006). To explore this concept, in-service monitoring data was reviewed for single-vehicle events similar to those recorded for the controlled tests (more detailed information relating to in-service data (such as histograms and peak events) are found in Appendix C). Key events of interest from the in-service data were identified for each bridge (based on waveform patterns, peak strains, likely number of axle groups, speed of vehicle, and dynamic response), and are summarised in Table 7.5 (a) to (c) according to each bridge.

By inspection of the waveforms, the majority of cases for the Canal Creek Bridge were either truck and trailer vehicles or road trains. Some vehicles induced a significant resonant response in the superstructure (such as the 68 $\mu\varepsilon$, 70 $\mu\varepsilon$ and 72 $\mu\varepsilon$ events), whereas others were reasonably discrete (e.g. road train for 69 $\mu\varepsilon$ event). Road train events could also be determined based on data recorded from Dawson and Neerkol bridges, in which the events are more distinct for Dawson than Neerkol. Many significant in-service results appeared to be associated with low loader or permit events, mostly travelling east towards Rockhampton. Some events resulted in resonant responses, at times associated with a particular axle group or end trailer. Peak bending strains on the Neerkol Creek Bridge varied between girders and the soffit of the headstock, with a resonant response often observed for the headstock on several large events.

Of the in-service events, only a handful were reasonably comparable to controlled testing, and the most representative case is shown for the Dawson River Bridge in Figure 7.17. The in-service event, registering a peak bending strain of 72 $\mu\varepsilon$, has distinct similarities to RT1 travelling at 80 km/h when waveforms for mid-span bending strains, headstock deflections and strain distributions are compared. By observation, the reduced deflections recorded for the left headstock cantilever for the in-service event suggest that additional vehicles were likely to have been present on adjacent spans. Strain distributions were similar, with slight discrepancies likely to be attributed to individual axle group loading, the centre of mass for the vehicle, and the transverse location of the vehicle.

Extending the concept of vehicle similarities further, a comparison of DI values was made between RT1 and the in-service event. To make this comparison, the peak static value for RT1 was adopted as the static case for the in-service event, and DI values determined using the actual distribution of strains in each girder at the time where the peak strain value occurred. The resulting DI value comparison is shown in Figure 7.18. Despite the limited girder information (girders 1 and 2 omitted), a similar pattern of DI values is observed between the two vehicles. However, the DI values for the in-service vehicle are lower (peaking at less than 0.3). This may be due to many factors, including the actual loading scenario and concurrent traffic on the bridge at the time of the vehicle passage. However it may suggests that the DI values for in-service traffic may in fact be less than determined for the controlled tests, agreeing with the observations noted in the literature review. International research suggests that vehicle-specific static and dynamic information can be extracted from in-service traffic data (see SAMARIS report (Žnidarič et al. 2006), ARCHES report (González 2009) and others (Cantero et al. 2014; Caprani, O'Brien & McLachlan 2008; Carey et al. 2010; Rattigan et al. 2005; Zhou & Chen 2014). It is recommended that the translation of traffic-specific data to real-life dynamic load amplification data be explored further for application in an Australian context. An investigation comparing dynamic bridge responses to singular and multiple vehicle events under controlled conditions may also be of benefit.

Table 7.5: Summary of heavy vehicle events recorded during in-service monitoring

(a) Canal Creek Bridge

Event timestamp		Peak strain	Direction of travel	Transverse location	Likely vehicle	Likely suspension type	Comment
13h 22m 48s	4 May 2014	60	West	Centre	Road train	Steel leaf	Resonance
23h 53m 12s	5 May 2014	68	West	In lane	Road train	Steel leaf	Resonance, esp. with last few trailers
23h 25m 01s	4 May 2014	69	East	Centre	Road train	Air-bag	
15h 12m 23s	2 May 2014	70	West	Centre	Semi-trailer?	Steel leaf	Resonance
12h 36m 10s	6 May 2014	72	West	Centre	Road train	Steel leaf	Resonance
18h 07m 20s	5 May 2014	77	West	In lane, towards centre	Road train	Steel leaf	
15h 45m 12s	5 May 2014	77	East	In lane, towards centre	Semi-trailer	Air-bag	
17h 06m 25s	4 May 2014	87	West	Centre	Semi-trailer	?	Resonance
17h 23m 21s	4 May 2014	90	West	Centre	Semi-trailer	Air-bag?	

(b) Dawson River Bridge

Event timestamp		Peak strain	Direction of travel	Transverse location	Likely vehicle	Likely suspension type	Comment
21h 00m 32s		68	East	Lane	?	Air-bag?	Resonant response towards front of vehicle
13h 33m 42s		66	East	Lane, outer edge	?	?	Large peak
15h 46m 47s		72	East	Lane	Road train	Steel leaf	Resonance Adjacent spans loaded
17h 18m 12s		73	East	Lane	Road train	steel	
15h 48m 47s		73	East	Lane	?	Air-bag?	
06h 18m 22s		73	East	Lane	?		Significant resonant response; Appears to have induced significant sway response (see headstock)
21h 51m 42s		77	East	Lane	RT?	Steel-leaf	Resonance (end of trailer)
17h 06m 32s		79	East	Lane	Truck and Dog?		
20h 40m 42s		83	East	Lane	?	?	
15h 03m 27s		127	East	Lane	Low loader?	?	Significant load on back axle group

(c) Neerkol Creek Bridge

Peak strain	Direction of travel	Transverse location	Likely vehicle	Likely suspension type	Comment
84	East	Lane	RT	Air-bag?	
87	East	Lane	?		Headstock resonant response
88	East	Lane	Large Crane?	?	
89	East	Lane	?		Long vehicle; HS response greater
90	East	Lane	RT	?	Significant resonant response after passage of vehicle – headstock and superstructure in phase
93	East	Lane	RT	Air-bag?	Torsional effects noted in deflection pattern
98	West	Lane	RT?	Steel?	
101	West	Centre	?	?	Long, heavy vehicle; rapid resonance response; Significant load on headstock
111	West		Crane?	?	Low-frequency resonant response
115	East	Centre	Low Loader?	?	
156	East	In lane, towards centre	Low loader/ HLP	?	Significant event – low-loader (Matches event in Dawson data); HS response greater than girders (also resonant)

Figure 7.17: Comparison between monitoring event and RT1 controlled test run for the Dawson River Bridge

RT1, travelling east at 80 km/h

Event: 72 $\mu\varepsilon$, timestamp: 15h46m47s

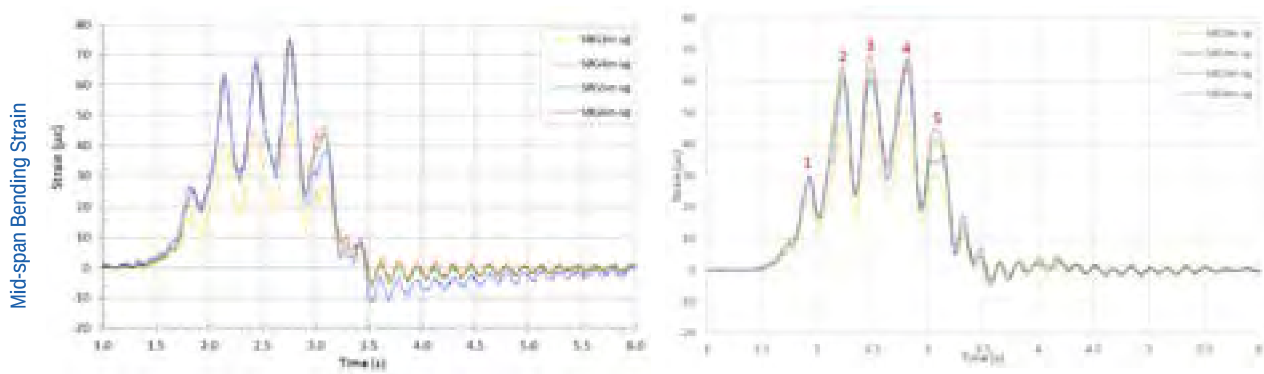

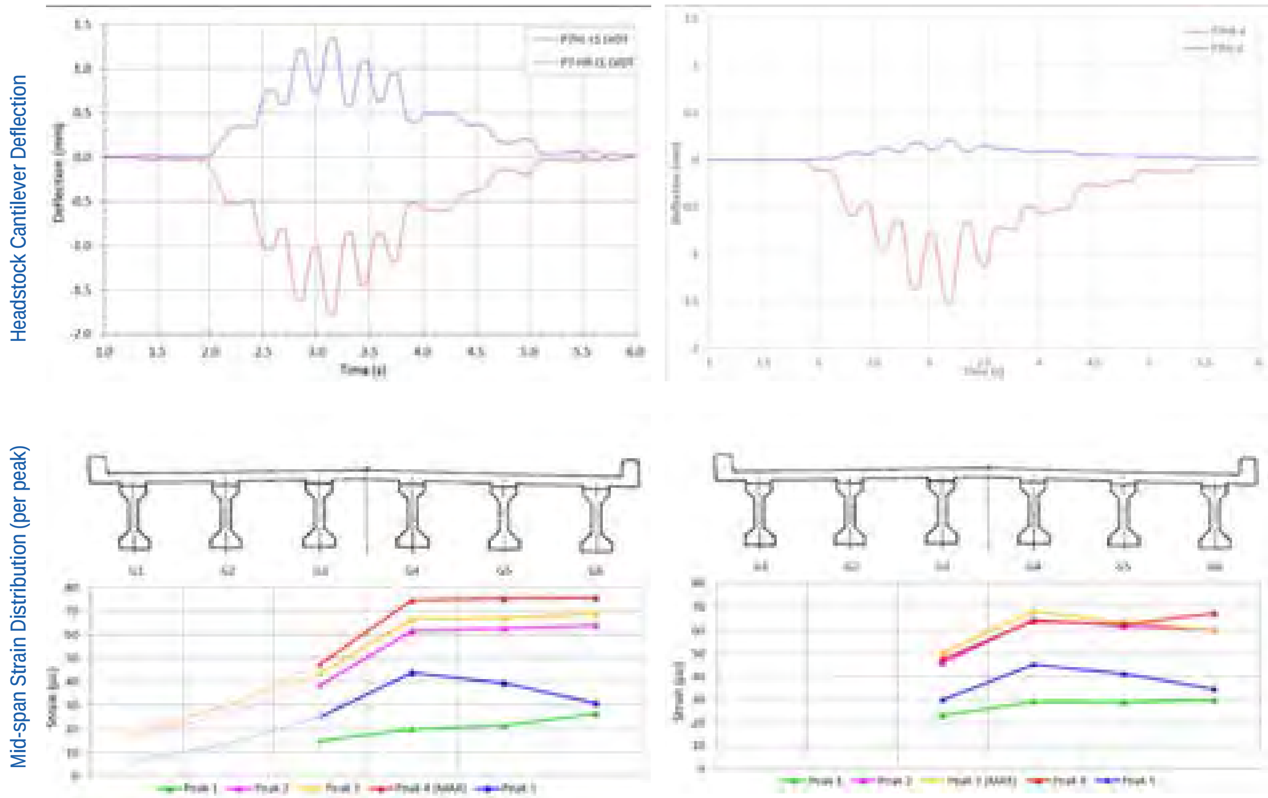

Figure 7.18: Estimated DI distribution for monitoring event (based on RT1 controlled test run)

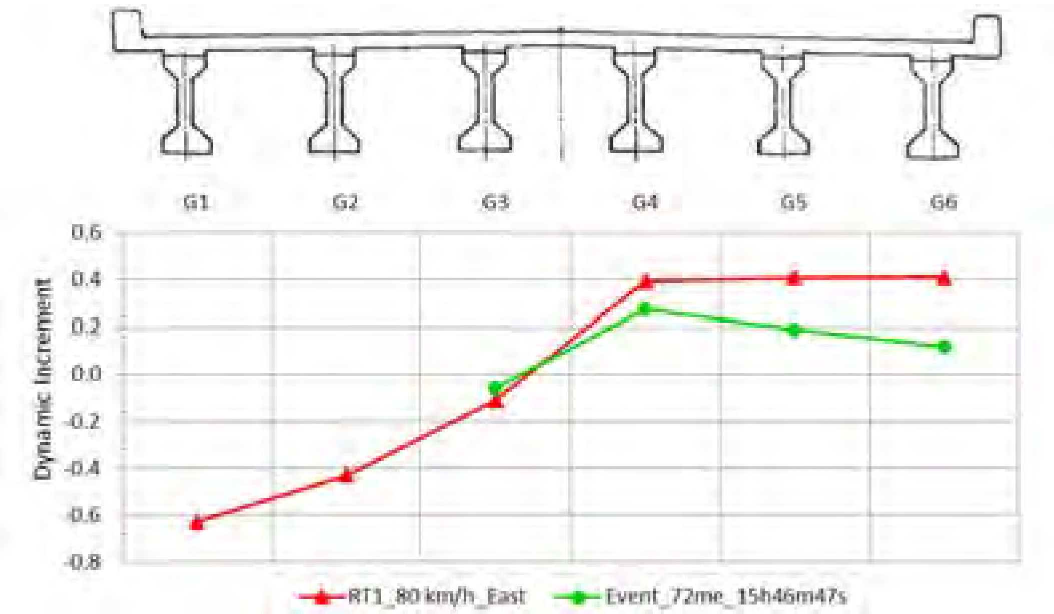

7.8 Summary

In summary, the additional findings discussed in this section are as follows:

- Beat frequencies were observed for the Dawson and Neerkol bridges, which is in keeping with the longer, more flexible prestressed concrete spans and torsional modal response.

- As an extension to this, instances of quasi-resonance were observed between the test vehicle and individual components, and with all components acting harmoniously:
  - elevated DI values were observed in the relevant components in these instances, with significant values greater than DLA of 0.4 recorded for substructure components for some peak runs
  - quasi-resonance occurred at a variety of speeds and irrespective of vehicle type, with instances occurring for the hydro-pneumatic crane and air-bag suspension road train, however most DI peaks were less than 0.4 for these vehicles, and steel suspension vehicles were more likely to yield DI values greater than 0.4
  - the road profile was observed to be influential in promoting quasi-resonance, with the initiation of vehicle response key to driving the bridge response (as previously discussed in Section 5)
  - Dawson River Bridge was found to be more sensitive to quasi resonance across all components, with coincidental features such as inherent frequency response of the headstock cantilevers and the torsion of the deck, the road profile and vehicle type.
- The transverse location of the vehicle was influential on dynamic load distribution and peak mid-span bending strains. This subsequently influenced the determination of DI values, which is reliant on the repeatability of resulting peak values between static and dynamic vehicle runs.
- A review of the distribution of DI values matching the peak DI value recorded for key events was conducted.
  - repeatable patterns were observed between each vehicle and for each direction of travel
  - the condition of the road profile, the vehicle characteristics and the transverse location of the vehicle on the bridge deck were observed to be influential in the resulting DI values.
- A review of road-train accelerometer data obtained during the controlled tests enabled a review of the performance of the vehicle in response to the road profile and the test bridges:
  - bridge-vehicle interactions were demonstrated through this process.
  - the condition of the road profile and the inherent frequency characteristics of the bridge were noted to be influential on the induced response of the vehicle.
  - the vehicle suspension system was found to be influential on the frequency response of the vehicle, with shifts higher or lower depending on the surface being traversed (road or bridge).
- A review of in-service monitoring data in conjunction with controlled test data has identified similar events which may enable the extension of measured DI values to in-service events for selected bridges. It is recommended that this area be explored to investigate the viability and repeatability of the observations made.

8 DISCUSSION

The following sections provide a summary of the key research findings in relation to the project objectives and the specific research gaps identified in Section 2. Following this summary, the implication of these findings are discussed, particularly in relation to individual bridge application, network applications for TMR. Comment on the relationship of these findings to the dynamic load allowance (DLA) factor is provided, with discussion on the sensitivity and accuracy in the determination of the empirically derived dynamic increment values which has historically informed DLA factors. Finally, recommendations are provided for consideration and further action.

8.1 Summary of Findings

The following sections summarise the collective learnings from Section 4 to Section 7.

8.1.1 Superstructure Response

- DI values were on average less than 0.4, irrespective of vehicle type and speed.
- The fundamental frequency response was influential on dynamic response and load amplification.
- However, it was also significantly influenced by body-bounce frequencies of passing vehicle.
- For Dawson and Neerkol bridges, the connection of the girders to the piers appears to have had a significant impact on the torsional modes of the superstructure and substructure both fundamentally and under load.

8.1.2 Substructure Components

- A larger percentage of DI values for substructure components exceeded 0.4 in comparison to superstructure DI values.
- The fundamental frequency responses of the substructure components globally and locally in each direction (vertical, transverse, longitudinal) was influential on the dynamic response and load amplification recorded for these components.
- The longitudinal and transverse rotation of the piers was influential in the vibrational response of the superstructure as a whole.
- Load amplification in substructure components were sensitive to vehicles travelling at elevated speeds and the condition of the road profile.

8.1.3 Vehicle Characteristics

- Conflicting results were noted relating the various vehicle characteristics.
- The vehicle travel speed was found to be influential; however, elevated DI values were more likely to occur at higher speeds when the condition of the road profile was poor.
- The speed of travel influenced the response of the bridge; however, the maximum speed did not always result in peak values. As such, critical speeds were identified for specific bridges and vehicle types, which did not always correlate to maximum travel speed.
- The overall length of the vehicle did not appear to directly influence the repression of the dynamic response of the bridge.
- Conflicting results were noted relating dynamic load amplification and axle groups, vehicle length and gross mass of individual vehicles as defined in the literature.

8.1.4 Vehicle Suspension Types

- The vehicle type had an impact on the response of each bridge.
- Steel suspension vehicles (road train, semi-trailer and crane) were more likely to yield variable DI values with respect to travel speed and direction of travel:
  - they were also more likely to induce greater dynamic response and peak values across all superstructure and substructure components.
- Air-bag suspension road trains and semi-trailers produced consistent DI values lower than 0.4 for superstructure components. However, increasing values recorded for the semi-trailer with increasing speed may suggest require caution in relation to road profile. It has also been previously noted that air-bag suspension systems may result in greater dynamic load amplification if shock absorbers are in a poor condition (Heywood 1995a).
- The air suspension road train induced significant DI values in the columns of both bridges.
- The hydro-pneumatic suspension system of the crane generally induced a more consistent and reduced dynamic response in the bridge regardless of speed or direction of travel.

8.1.5 Vehicle Position

- The transverse location of the vehicle influences the peak distribution of strains in the superstructure components for all bridges.
- The resulting change in distribution was dependent on the differential in track location relating to each girder.
- Load distributions were more sensitive for the PSC girder bridges, with the Neerkol Creek Bridge exhibiting greater variability.
- Varying transverse vehicle location influences the resulting DI value determined for each dynamic test run.

8.1.6 Road Profile

- Load amplification was influenced by the condition of the road profile. For road profiles that were in good condition, DI values tended to be minimal. Where poor conditions or approach settlement existed, DI values tended to increase with increasing vehicle speed.
- Particularly critical on load amplification when combined with high vehicle speeds and for vehicles with steel suspension systems.

8.1.7 Quasi-resonance

- Instances of quasi-resonance were identified for all three bridges:
  - some instances were restricted to vehicle-superstructure matches (such as superstructure components responding to CR1 travelling at 40 km/h on the Dawson River Bridge or the portal frame headstock responding to RT1 and RT2 travelling west at 60 km/h on the Neerkol Creek Bridge)
  - complete matches were observed between all components and the test vehicle (e.g. RT1 travelling east at 80 km/h on the Dawson River Bridge).
- Where frequency matching occurred, amplification of load via elevated DI values was observed; however, in the majority of superstructure cases this did not exceed 0.4. Alternatively, for the same case DI values were greater than 0.4 in substructure components, highlighting their potential sensitivity to dynamic loading.

- For frequency matching to occur, the fundamental frequency characteristics of the bridge as a whole and the individual components (such as the rigid body rotation of the headstock cantilever in the Dawson River Bridge) must closely coincide with the predominant driving frequencies of the vehicle, in particular the body bounce. However, the dynamic behaviour of the vehicle must be enacted, and this is reliant on the condition of the road profile prior to the bridge.
- The body-bounce frequency characteristics of the test vehicles were most influential in driving the frequency matches, especially in relation to the substructure components.
- Quasi-resonance or frequency matching between vehicle and various superstructure and substructure components, partially determined the overall dynamic response and subsequent peak values measured for each of the bridges.

8.2 Application of Results

This research has clearly demonstrated that dynamic response, and ultimately the possibility of load amplification of a bridge, is driven by the interaction between the passing vehicle and the bridge itself. Where conditions of the road surface are poor, this exacerbates the amplification process, highlighting the importance of these three factors acting coincidentally. However, these results need to be reviewed in the light of their practical application to the performance of in-service structures to network vehicles. The following sections explore the applicability of these results.

8.2.1 Review of DI Values

Consideration is given to the complete suite of DI values determined for all controlled load tests. The peak DI values (based on tensile strains) recorded for each vehicle run are summarised in Figure 8.1 to Figure 8.3 for each bridge respectively, whilst the statistical data is presented in Table 8.1. The pie charts highlight the fact that the majority of DI values for superstructure and substructure components were less than the DLA factor of 0.4, which is confirmed by the average values determined for the dataset. For the superstructure components, most are less than 0.2 irrespective of speed, with only the Dawson River Bridge recording 6% of values greater than 0.4. These values were based on the steel suspension road train and crane travelling east at 80 km/h and 60 km/h respectively. The Canal Creek Bridge exhibited the lowest average and standard deviation for all superstructure DI values, and yielded the greatest number of DI values close to or less than 0. This may be indicative of out-of-phase dynamic responses of vehicles to the bridge.

For substructure components, a reduction in the number of values less than 0.2 and an increasing number greater than 0.4 was observed. Approximately 45% of DI values for the Neerkol Creek Bridge exceeded 0.4, with 2% exceeding 1.0. The peak value relates to the air-bag suspension road train travelling at top speed, and the majority of values greater than 0.4 were for various vehicles travelling west.

In relation to the statistical representation of the results (Table 8.1), the standard deviations of the superstructure DI values were relatively consistent (approximately 0.11), but they increased to approximately 0.2 for data relating to the substructure. Consideration was given to these values in relation to 95 % confidence limits for the controlled tests, which have been determined in accordance with normal distribution methods and noted in Table 8.1. For superstructure components, 95% of the peak DI values were likely to be less than 0.3 for all bridges. For substructure components, however, the equivalent 95th percentile value for the Dawson and Neerkol bridges increased to 0.48 and 0.80 respectively. The large standard deviation and low average for the Dawson River Bridge suggests that the majority of the DI values are not likely to go beyond 0.4. Similar conclusions can be made for the Canal Creek Bridge. For the Neerkol Creek

Bridge, however, the combination of these statistics suggests that the DLA of 0.4 is likely to be exceeded in the case of the controlled test data presented.

Table 8.1: Statistical representation of DI values determined for test bridges

	Canal Creek Bridge	Dawson River Bridge		Neerkol Creek Bridge	
	Superstructure	Superstructure	Substructure	Superstructure	Substructure
Count	38	36	72	32	64
Average	0.04	0.11	0.14	0.12	0.38
Standard Deviation	0.10	0.12	0.21	0.11	0.26
5% (1)	–0.13	–0.09	–0.2	–0.06	–0.06
95% (1)	0.21	0.31	0.48 (2)	0.30	8.80 (2)

1 Determined using NORMDIST MS Excel function.

2 Values are highlighted in red if exceeding DLA = 0.4.

Figure 8.1: Distribution of DI values for Canal Creek Bridge

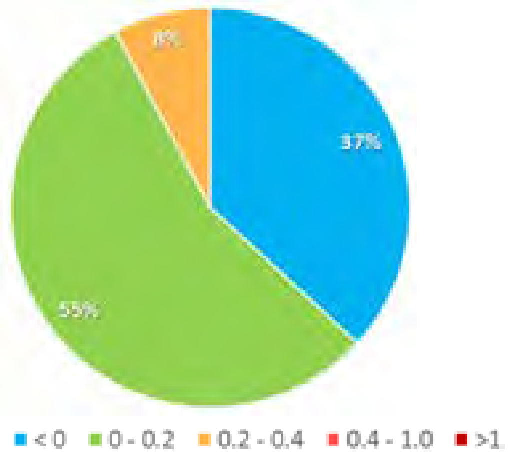

(a) Superstructure

Figure 8.2: Distribution of DI values for the Dawson River Bridge

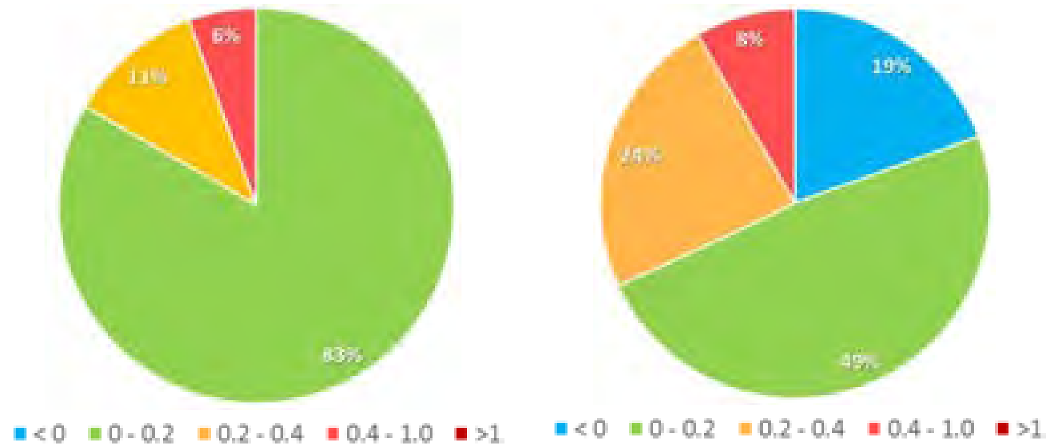

(a) Superstructure

(b) Substructure

Figure 8.3: Distribution of DI values for the Neerkol Creek Bridge

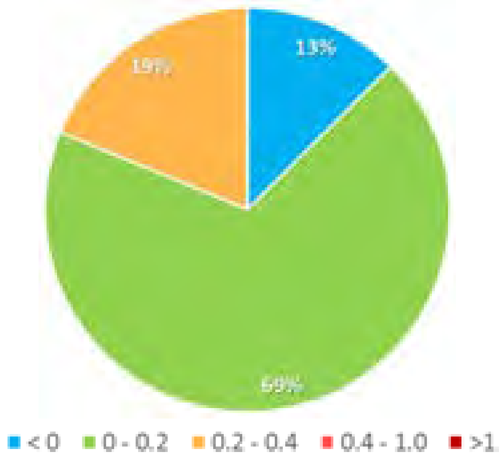

(a) Superstructure

(b) Substructure

8.2.2 Peak Strains

The review of DI values in Section 8.2.1 highlights that the majority of results in response to four different test vehicles were consistently less than the required DLA factor of 0.4 for superstructure components, with most averaging 0.3 or less.

To extend this illustration, Table 8.2 provides a comparison of preliminary theoretical estimates for selected test vehicles, peak strain values and corresponding DI values measured during controlled tests, and the peak strain value recorded during in-service monitoring. The values provided from the theoretical analysis are based on previously developed TMR Tier 1 assessment models for selected test vehicles, with the inclusion of an assumed dynamic load approximation of 0.2 and 0.4 (more detailed information regarding the preliminary analysis is found in Appendix C).

For all superstructure results, actual measured strains were less than those determined theoretically when considering a DLA of 0.4 and 0.2. The reasons for this disparity have not been explored in detail, however it is considered that the following have contributed to these observations:

- modelling assumptions (such as connectivity and material properties)
- the use of HML loading in theoretical assessments and actual GML loading for the Dawson and Neerkol bridges,
- the continuity of the superstructure over the piers due to fixture conditions
- the composite nature of the deck
- the translation of dynamic load laterally due to stiffeners or transverse stressing bars.

The greatest disparity was observed for results obtained for the Canal Creek Bridge, which is a deck unit bridge. It is known that the in-service condition of these structures are not an accurate reflection of the assessment results. These issues are currently being explored via a research program in the concurrent NACoE project S3 '*Deck unit bridge analysis under live load*'.

Substructure results for the Dawson River Bridge had similar differences to the theoretical estimations. For the Neerkol Creek Bridge, however, the headstock values exceeded the estimated values by almost twice. The reasons for this have not been explored; however, it is thought to be related to the cracked condition of the headstock, of which has not been accounted for in the original assessment.

In-service results for the week-long period of monitoring also confirm that significant events that exceeded those relating to the test vehicles were a lower percentage of actual heavy vehicle movements. It is worth noting, however, that several events were found to exhibit quasi-resonance characteristics, with prolonged cyclic loading indicative of resonant behaviour (particularly for the Canal Creek superstructure and the headstock for the Neerkol Creek Bridge – see Section 7).

The corresponding DI values for each peak event recorded for the test vehicle events are shown in Table 8.2. Discrete DI values have been considered in this instance to provide comparison of real-time results in lieu of envelopes. This concept and its implications is explored further in Section 8.3. Note that the majority of results for these events are less than 0.4 for superstructure components, and did not always occur at maximum speeds. For example, consistently elevated results was recorded for CR1 travelling at 40 km/h, suggesting evidence of quasi-resonance (previously discussed in Section 7); however, corresponding superstructure DI values are minimal. Substructure DI values for the Dawson and Neerkol bridges were generally greater than 0.4, which appears to agree well with the increase to theoretical measured in the Neerkol Creek Bridge. On the contrary, peak DI values do not correlate well with the reality of peak strains measured in the columns for the Dawson River Bridge.

Table 8.2: Comparison of preliminary analysis results, measured peak results and corresponding DI values

(a) Canal Creek Bridge

Test Vehicle	Bending strain Comparison ($\mu\varepsilon$)	Superstructure (mid-span)	
		Kerb Unit	Deck Unit [2]
48 t crane	Crack limit ($\mu\varepsilon$) (DLA = 0.4)	278	331
	Peak	97	95
	Speed, Direction of travel	80 km/h, West	60 km/h, West
	Corresponding DI Value	0.21	0.22
HML semi-trailer[1]	Crack Limit (DLA = 0.4)	161	251
	Peak	61	57
	Speed, Direction of travel	40 km/h, West	40 km/h, West
	Corresponding DI Value	0.17	0.11
Peak Recorded In-Service Monitoring Strain		82	92

1 - Maximum results for ST1.

2 - DI value determined using peak static for corresponding deck unit location.

(b) Dawson River Bridge

Test Vehicle	Bending strain Comparison (με)	Superstructure (mid-span)		Headstock (Cantilever)	Column	
		Edge	Inner (2)		Tension	Compression
48 t Crane	Theory (DLA = 0.4)	143	150	27	65	85
	Theory (DLA = 0.2)	123	128	–	–	–
	Peak	83	75	9	30	37
	Speed, Direction of travel	40 km/h, West	40 km/h, West	40 km/h, East	40 km/h, East	40 km/h, East
	Corresponding DI Value	0.12	0.12	0.38	0.09	0.67
HML Road Train (1)	Theory (DLA = 0.4)	129	135	44	92	123
	Theory (DLA = 0.2)	111	116	-	-	-
	Peak	78	75	12	45	51
	Speed, Direction of travel	40 km/h, West	80 km/h, East	80 km/h, East	100 km/h, East	80 km/h, East
	Corresponding DI Value	0.18	0.47	0.85	0.25	0.92
Peak Recorded In-Service Strain		127	118	–	–	–

11 Maximum results for RT1.
12 DI value determined using peak static for corresponding girder group location.

(c) Neerkol Creek Bridge

Test Vehicle	Bending strain Comparison (με)	Superstructure (mid-span)		Headstock (Portal Frame)	Column	
		Edge(2)	Inner		Tension	Compression
48 t crane	Theory (DLA = 0.4)	191	180	35	9	28
	Theory (DLA = 0.2)	163	154	–	–	–
	Peak	55	105	58(1)	12(1)	26(1)
	Speed, Direction of travel	80 km/h, West	80 km/h, West	80 km/h, West	40 km/h, West	40 km/h, West
	Corresponding DI Value	0.41(3)	0.1	0.16	0.09	0.11
HML road train(2)	Theory (DLA = 0.4)	198	169	46	9	38
	Theory (DLA = 0.2)	170	145	–	–	–
	Peak	97	97	76(1)	15	31(1)
	Speed, Direction of travel	80 km/h, West	80 km/h, West	80 km/h, East	60 km/h, West	80 km/h, East
	Corresponding DI Value	0.17 (3)	0.17	0.42	0.85	0.21
Peak Recorded In-Service Strain		116	156	171	32	55

13 Centreline travel.
14 Maximum results for RT1.
15 DI value determined using peak static for corresponding girder group location.

8.2.3 *In-service Traffic Loading*

The in-service traffic data collected for the highways according to bridge location is summarised in Table 8.3. The Canal Creek Bridge experienced the lowest volume of traffic but the greatest percentage of heavy vehicles, indicative of the mining industry that is serviced by the Flinders Highway. There were little differences between the Dawson and the Neerkol bridges in relation to AADT, however during load testing it was observed that Neerkol experienced a greater volume and more frequent vehicle passage.

Table 8.3: Summary of in-service traffic data

	Canal Creek Bridge	Dawson River Bridge	Neerkol Creek Bridge
Statistics obtained for heavy vehicle route	Flinders Highway	Capricorn Highway	Capricorn Highway
AADT	400	3400	3500
% Heavy Vehicles	30	20	23
TMR gazetted route	HML B-Double/road train	GML B-Double/road train	HML B-Double/road train

Source: TMR.

Recently, there has been some discussion in the literature regarding the actual amplification of dynamic load due to in-service traffic. Traditionally, the determination of dynamic increment has been determined from peak events extracted from single vehicle events, mostly test vehicles. This methodology has historically informed the current DLA requirement in the AS 5100 code as well as many other international codes, as discussed in Section 2. However, with an increasing focus on refined bridge assessment procedures, more jurisdictions are seeking to incorporate site or network specific traffic data to better represent the in-service loading existing structures experience.

There is an increasing number of publications that suggest that single vehicle events under controlled conditions represent the upper bound of the dynamic amplification response, and that in reality bridges are subjected to multiple and random vehicle events that are more likely to yield suppressed dynamic load amplification (Broquet et al. 2004; Caprani 2005; Caprani et al. 2008; González 2009; González, Cantero & O'Brien 2011; Hwang & Nowak 1991; Li, Wekezer & Kwasniewski 2008; McLean & Marsh 1998; Nowak et al. 1999; O'Brien et al. 2009; Rattigan et al. 2005; Zhou et al. 2015). This is due to the competing nature of the various vehicle and bridge frequencies experienced by the structure, and that bridges subjected to single vehicle events are more likely to produce quasi-resonance case and subsequent load amplification (Rattigan et al. 2009; Rattigan et al. 2005; Wang, Kang & Jiang 2016). In particular, longer, more flexible structures subject to lower damping levels are more likely to elicit this response (see Section 2).

Whilst the current research explores and isolates the dynamic response and load amplification to controlled vehicle scenarios, including highlighting issues such as quasi-resonance in all bridge components resulting in elevated DI values, it is appreciated that the values determined potentially represent a worst case scenario. The peak in-service strains noted in Section 8.2.2 confirm this notion, with strains less than anticipated from theoretical modelling. As noted in Section 7.7, significant events identified from in-service monitoring was noted to be subjected to additional loading from opposing lanes and contributions from adjacent spans, which contributes to the disruption of dynamic load amplification. The transverse location of the vehicle in-service may also differ to controlled test conditions, which has been observed to influence the magnitude of the dynamic response as discussed in Section 7.4 and Section 7.7.

Several recent international studies have presented findings and recommendations based on numerical simulations which recommend the reduction of DLA for superstructure components where multiple vehicles are present (e.g. Brühwiler & Herwig (2008), Caprani et al. (2008), González et al. (2011), and Li et al. (2008)). Several recent studies also include the analysis of weigh-in-motion (WIM) data to determine appropriate dynamic load amplification allowances for consideration over the life of a structure (Brühwiler & Herwig 2008; Caprani et al. 2008; González, O'Connor & O'Brien 2003; Žnidarič et al. 2006). Other studies have also investigated the extrapolation of bridge in-service monitoring data for application to other structures on a network bases (O'Connor & Pritchard 1984; Pritchard 1982; Pritchard & O'Connor 1984). As the majority of these studies are based on numerical simulations or older research, validation of these solutions would be required via field trials prior to the application of any recommendations.

Consideration is also required for the volume of traffic. In Europe, for example, the majority of structures are subjected to significant traffic volumes and random traffic mixes. Within Australia, and more specifically Queensland, the differences in traffic volumes between rural and urban areas varies significantly. For bridges located in urban areas, increased traffic volumes and a greater variety in traffic loading can be anticipated which may support potential reductions in DLA factors. However for bridges located in rural areas, traffic volumes can be significantly lower and may consist of a higher proportion of heavy vehicles travelling at high speeds (as evidenced by the Canal Creek Bridge). For the latter case, single vehicles are a more likely occurrence, which therefore may be better represented by an upper bound DLA value. Additional in-service considerations are the speed environment, the tendency for vehicles to travel along the centreline if it is a single-vehicle crossing, and the condition of the road profile.

8.2.4 Vehicle Characteristics

The current research clearly suggests that the dynamic response of a bridge (and any resulting load amplification) can be significantly altered based on the dynamic characteristics of the passing vehicle. In particular, steel suspension heavy vehicles have the propensity to induce greater load amplification, especially when travelling at higher speeds and where poor road profile conditions exist. Air-bag suspension and the hydro-pneumatic suspension system are more likely to consistently suppress bridge dynamic responses irrespective of speed and road condition, however results have also indicated that frequency matching is still a possibility, which may lead to load amplification.

For the Dawson and Neerkol bridges, data collected for the two road trains highlight the influence body bounce frequencies play on driving the response of a bridge, and that where these frequencies match natural frequencies of some or all of individual bridge components, load amplification is likely, as demonstrated by superstructure and substructure responses and DI values for RT1 travelling east at 80 km/h. In combination with poor road profile, care needs to be taken when considering DLA factors in these instances.

Despite air-bag suspension vehicles being defined as being 'road friendly' (due to their reduction in the magnitude of peak loads (Chen et al. 2002; Heywood 1995a; Sun 2002)), previous research has identified concerns relating to whether this is equivocal to such systems being 'bridge friendly'. More specifically, the following issues have been documented (Chen et al. 2002; Davis & Bunker 2009; Heywood 1995a; Heywood 1995b; Lambert et al. 2004; OECD 1999):

- where air-bag suspension vehicles exhibit a reduction in damping capability due to deterioration or inefficiencies of the shock absorbers, this may result in increased load amplification
- axle-hop vehicle responses may become more critical in governing the dynamic response and subsequent load amplification especially in short-span bridges
- the accuracy of the claim regarding the load-sharing capability of an air-bag suspension system across a tandem or triaxle group is questioned.

Research using numerical interaction models has suggested that alterations to a vehicle's suspension and damping system may allow control of dynamic loads imparted to a bridge, thus reducing the likelihood of load amplification (Chen et al. 2002; Harris, OBrien & González 2007). Similarly, field trials conducted by Davis and colleagues also investigated the control of dynamic loads and load sharing capabilities in an air-bag suspension vehicle through alterations in air pipe diameters and design (Davis & Bunker 2009; Davis & Bunker 2008). However, this project is predominantly related to vehicle performance and not correlated to bridge responses. These areas may provide opportunities for further investigation in order to restrict load amplification in bridges.

In addition to the vehicles investigated as part of this current study, other vehicle types such as low-loaders and heavy load platforms remains unknown in terms of their influence on the bridge-vehicle interaction process and potential load amplification. Depending on TMR's permit requirements and network issues relating to such vehicles, it is recommended that the dynamic impacts of these vehicles be explored. Similarly, limited research has been conducted within an Australian context on the influence of the inherent dynamic characteristics of 4 and 5-axle hydro-pneumatic cranes on dynamic loading and load amplification on structures.

8.2.5 Road Profile

Through the current research, the condition of the road profile has been shown to be significantly influential on the dynamic response and resulting load amplification experienced by a structure. This concept is well documented in historical and more recent literature (e.g. Austroads (2003), Austroads (2002b), Deng & Phares (2016), González, O'Brien & McGetrick (2010), Holt & Schoorl (1985), Prem & Heywood (2000), and Sun (2003)), and the pending draft of AS 5100.7 allows reductions in DLA to 0.3 where the roughness of the road profile exhibits an IRI of less than 4 mm/km. In reviewing the current research, there is a degree of correlation between IRI values and the amplification measured in each of the test bridges, however there are inconsistencies yet to be clarified in relation to the AS 5100 requirement. For example,

- The length that the IRI is taken over, be it over the length of the entire bridge, or discretised in accordance with approaches and span lengths, is not defined in the current version of AS 5100.7. The value of IRI can vary significantly depending on the interval provided by the relevant authority.
- It does not take into account discrete defects in the road profile over a longer interval (rather, the defect is averaged out, despite the influence that the defect may have physically on the resulting dynamic load application).

It is recommended that further investigation be conducted to correlate actual road profile condition, IRI and resulting dynamic load amplification on structures.

Whilst general road roughness influences are recognised, the presence of approach settlement appears to be the most significant feature that triggers the greatest dynamic response. A number of publications documenting results of field trials confirm the significance of abutment 'bumps' or 'depressions' in dynamic load amplification (Deng & Phares 2016; González et al. 2009; Huffman et al. 2015; Szurgott et al. 2011). These abutment jumps are equivalent to axle hop planks and 'bumps' that have been previously investigated in the literature that excite dynamic effects in vehicles to induce maximum dynamic effects on the supporting structure (Barr et al. 2008; Baumgärtner 1998; Cebon 1986; Heywood 1995b; McGetrick et al. 2013; O'Connor & Pritchard 1985; O'Connor & Pritchard 1984; Senthilvasan et al. 1997).

In all publications, it is recognised that the elimination or reduction of such vehicle obstacles is highly likely to result in a reduction in resulting dynamic loading on a bridge, and thus load amplification. On a practical level, this requires the resurfacing of bridge approaches or the installation or reinstatement of run-on slabs. The effectiveness of the run-on slab is evident in the results for the Neerkol Creek Bridge, where the presence of the slab has reduced vehicle vibrations on the west approach to the bridge however settlement behind the abutment has resulted in an axle-hop scenario which has re-instigated vehicle vibrations, evident in elevated DI values for some test vehicles. By means of an example, the Austrian highway agency acknowledge this issue in relation to their existing bridge stock and now require the installation of a 'drag plate' in the construction of new bridge abutments, due to evidence that it minimises dynamic impact loading as vehicles enter the bridge (Federal Highway Administration (FHWA) 2010).

8.3 Sensitivity Analysis in the Determination of DI Values

The methodology used to determine DI values for the current project has previously been discussed in Section 2 and detailed processes outlined in Appendix A. It is the traditionally used method (Bakht & Pinjarkar 1989; Cantieni et al. 2010; Paultre et al. 1992) of which most bridge design codes are based in their definition of DLA factors.

However during the course of the current project, queries were raised regarding the sensitivity of DI values to the selection of appropriate static and dynamic peak values. The method adopted for the current project involved the calculation of DI values using the maximum strain value measured for any group of superstructure or substructure components and the corresponding absolute peak static strain for the equivalent vehicle run. Variations in DI values could be encountered when considering the following additional scenarios:

- DI values determined using the absolute peak dynamic strain and the corresponding component static strain (not necessarily the maximum static strain for the component group)
- maximum DI value adopted for components directly affected by vehicle loading (which did not necessarily correlate to the peak dynamic strain).

By means of an example, a sensitivity analysis was conducted on DI results from the three bridges, and are presented in Figure 8.4 to Figure 8.5, demonstrating the three different methods to derive DI values. It was found that superstructure results were more sensitive to the selection of static and dynamic strains in the determination of DI values. Observations of this review highlight the similarities between the waveforms, however the most significant point of difference is the magnitude of the peak DI values. Adopting the method of maximum DI value presentation results in significant DI values, which may not be representative of the actual performance of the bridge. However this method does take into account those girders under direct load, and with the variation of vehicle transverse location across the deck, this method may yet yield useful information.

In relation to the determination of DI values for the Canal Creek Bridge, the process of determining the representative DI value for each vehicle run was complicated, with many more variables to consider. To demonstrate these sensitivities, Figure 8.6 highlights the determination of DI values depending on the various dynamic and static strains and inclusions for both kerb and deck units, with the value in pink showing the value reported against for the for the current project. The variability of the DI value depending on the governing parameters is clearly evident, with values ranging between –0.03 to 0.38.

Regarding the transverse location of the vehicle, Section 7.4 highlighted the sensitivity of the dynamic vehicle deviation from original static runs and the inherent changes to DI with those changes. The results from the Canal Creek Bridge (shown in Figure 7.12(a)) exemplify these sensitivities, with peak outliers and evidence of direct wheel loading observed.

Figure 8.4: Sensitivity analysis of DI Values determined for the Dawson River Bridge

(a) Method adopted for report

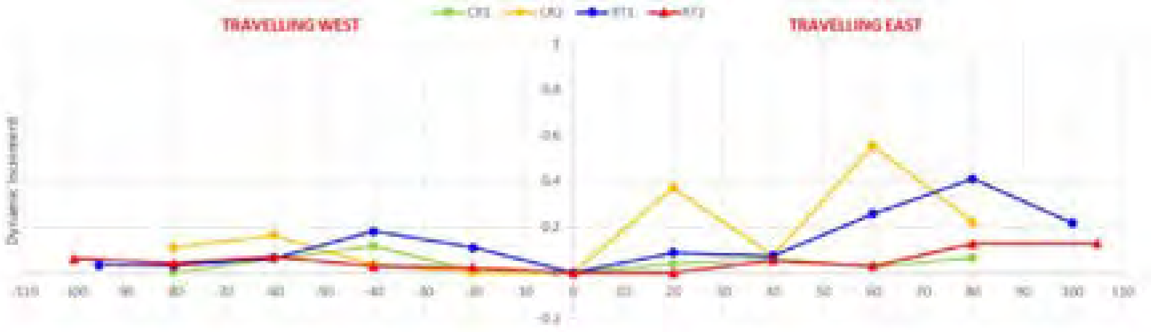

(b) Method using maximum dynamic strain & corresponding static strain

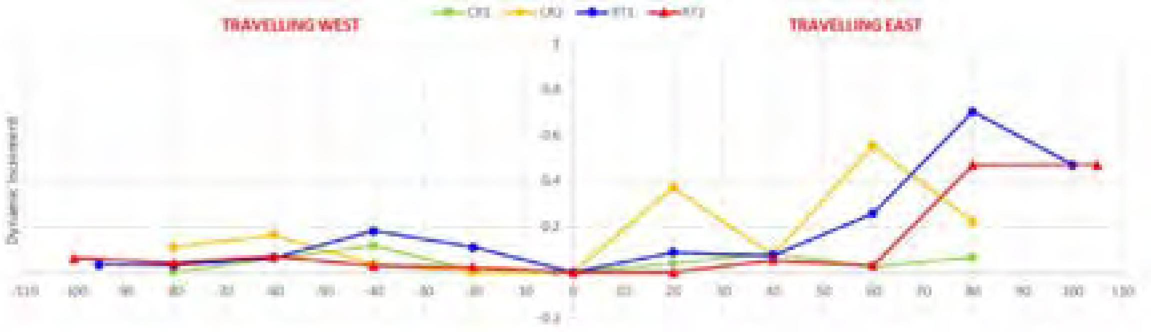

(c) Method using maximum DI value under direct load

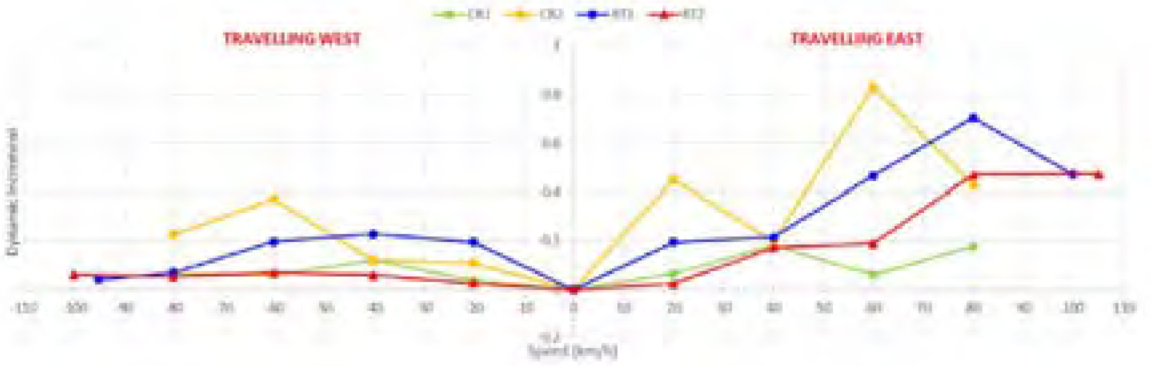

Figure 8.5: Sensitivity analysis of DI Values determined for the Neerkol Creek Bridge

(a) Method adopted for report

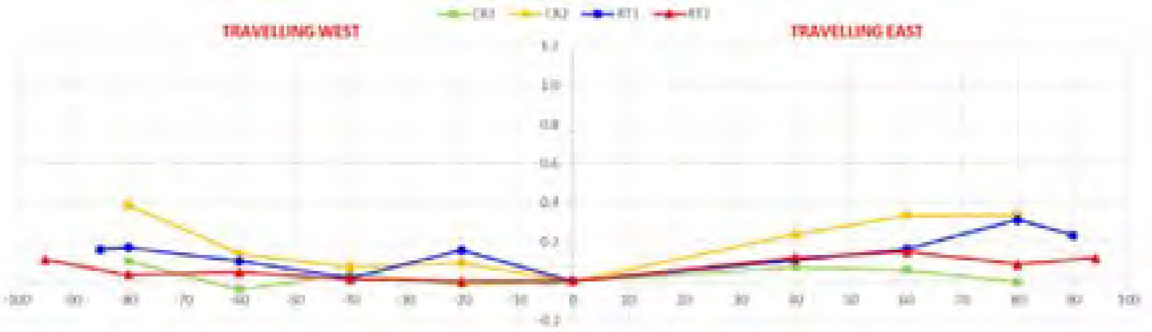

(b) Method using maximum dynamic strain & corresponding static strain

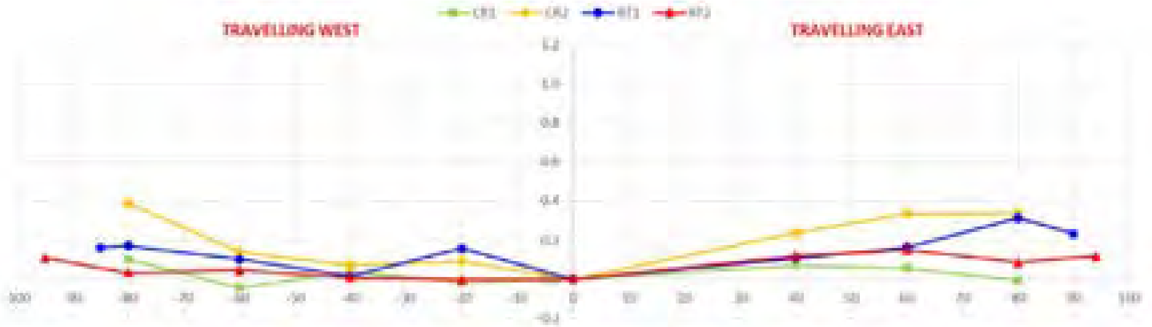

(c) Method using maximum DI value under direct load

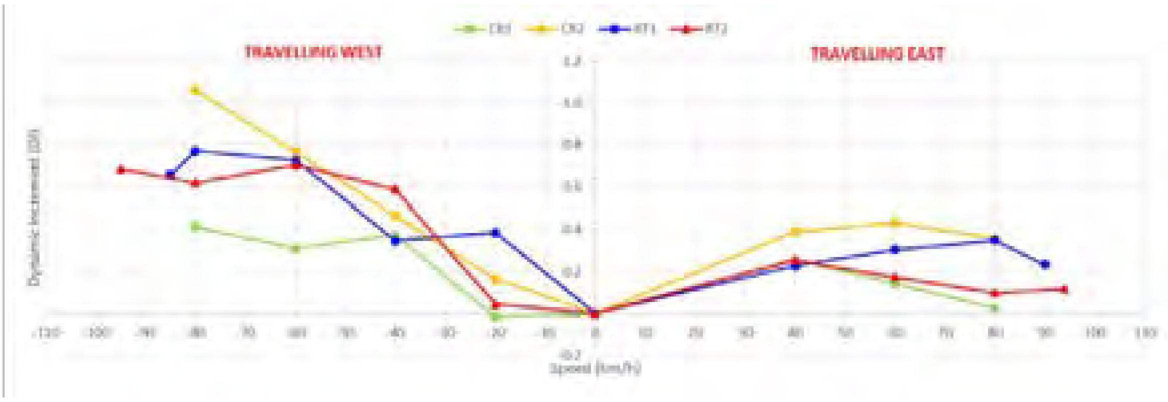

Figure 8.6: DI Values determined for CR1 travelling west at 80 km/h (showing deck units 1 – 8): Canal Creek Bridge

	KU1	DU2	DU3	DU4	DU5	DU6	DU7	DU8
Max Dynamic Strain(με)	96.70	87.30	83.10	77.10	80.70	85.90	81.40	76.50
Static Strain (με) (max per unit)	79.60	73.00	77.90	63.30	58.80	62.10	65.90	55.00
Static Strain (με) (max total Span 1)	79.60	79.60	79.60	79.60	79.60	79.60	79.60	79.60
Static Strain (με) (max unit type)	79.60	77.90	77.90	77.90	77.90	77.90	77.90	77.90
DI (max per unit)	21.48%	19.59%	6.68%	21.80%	37.24%	38.33%	23.52%	39.09%
DI (max per Span 1)	21.48%	9.67%	4.40%	-3.14%	1.38%	7.91%	2.26%	-3.89%
DI (max per unit type)	21.48%	12.07%	6.68%	-1.03%	3.59%	10.27%	4.49%	-1.80%
Ave DI (Group)	24.09%							
Max DI (Group)	38.33%							

These inconsistencies highlight the sensitivity in the determination of DI values, and that the process can be significantly skewed if a consistent approach is not taken. It also flags the potential subjective nature of the process overall, and calls into question how DI values have been determined historically, particularly those that have influenced the derivation of the AS 5100 empirically based DLA factor. As AS 5100.7 permits the adoption of DI values determined from field trials, caution is advised when reviewing absolute values for the amplification of load for individual components or the bridge as a whole. Clear guidelines are required in the determination of DI values to ensure a consistent and representative approach, as well as considering the actual in-service performance of the structure.

The method of calculating the substructure DI values was also scrutinised. Similar methodology was adopted in the determination of all headstock and column DI values for both the Dawson and Neerkol bridges. There is a reasonable degree of confidence in relation to the headstock values, as these represent a pure bending strain relating to direct load application. However, for the case of the columns, tensile and compressive strains were considered in isolation. Larger DI values were typically observed for compressive strains, and the question is asked as to the practical implications of this as there was no evidence of concrete crushing in the vicinity of the strain gauges. Alternatively, lower DI values were noted for tensile strains despite the presence of bending and shear cracks observed in the columns of both bridges. Alternative methods in the determination of DI values may be to consider the total combined effect of the compressive and tensile strains across the cross-sectional area of the columns, with the differences between static and dynamic total strains used in the representation of load amplification. This requires further exploration.

Additional queries raised during this process were:

- the requirement to adopt the absolute maximum dynamic and static strains in the determination of DI values, as these values may not actually occur at the same time, and as such may result in the inclusion of unnecessary conservatism.
- whether actual differences exist between dynamic and static material strengths
- considerations towards ultimate and service limit states when determining the final DI value.

Some of these considerations have been investigated in parametric studies (e.g. (Brühwiler & Herwig 2008; González et al. 2008; Gonzalez et al. 2011), but it is clear that further investigation is required.

8.4 Recommendations

8.4.1 Individual Bridges

Based on this discussion, the following recommendations are made in relation to the three test bridges:

- The results highlight a large degree of variance in DI values, predominantly due to vehicle type, speed and direction of travel. It is also apparent that the inherent frequency characteristics of the bridge and each test vehicle, both independently and in interaction, are influential on the resulting amplification of load. Therefore, a unique DLA factor based on DI values for each bridge and component cannot specifically be recommended based on this research alone.

- A large proportion of superstructure DI values were less than 0.4 irrespective of vehicle speed and direction of travel. Based on 95th percentile estimates using a normal distribution, these values are unlikely to exceed 0.4 for the test vehicles tested. This is supported by the observation that peak measurements for these components did not exceed the theoretical estimates in most cases, as well as the likelihood that multiple vehicles are likely to be traversing these bridges, precluding single vehicle events to which the DI values have been determined.
  - Therefore the reduction of the DLA factor for superstructure components in all three bridges could be considered by TMR for operational considerations for any future structural assessments. The following caveats should be considered for each bridge:
    - Steel suspension vehicles show a greater propensity to yield higher DI values, particularly with increasing speed and where increasingly poor road profile or abutment settlement conditions exist.
    - Consideration should be given to eliminate any road profile irregularities to minimise load amplification.
- The DI values determined for all air-bag suspension vehicles and hydro-pneumatic cranes may support a reduction in superstructure DLA factors for these structures for operational conditions, however caution is recommended where poor road profile conditions and high speed conditions
- If the proposed methodology adopted for determining substructure DI values in the current report is valid, it is recommended that DLA factors <u>not be reduced</u> from the current value of 0.4.
- It is recommended that speed limits for hydro-pneumatic four-axle cranes be investigated for the Dawson River Bridge based on evidence of quasi-resonance for the 48 t crane travelling at 40 km/h during testing.
- For the Dawson River Bridge, cracking at the base of the column (one side only) and across the cantilevered headstock, the sway motion of the pier in general, instances of quasi-resonance and the higher DI values determined during this test, may highlight potential structural deficiencies in the substructure (despite theoretical estimates to the contrary). A detailed structural review of the piers is therefore recommended for comparison against the test measurements contained in this report. This may provide additional information for TMR to determine whether strengthening or other strategies are required.
- For the Neerkol Creek Bridge, the evidence of bending and shear cracking across the headstock, the strong resonant behaviour and low damping capability of the superstructure and substructure, and the high tensile values recorded in the soffit of the headstock compared to the girders (particularly for the large in-service event noted) raise concerns regarding the serviceability and structural capability of the headstocks. A detailed structural review of the headstock and columns is therefore recommended for comparison against the test measurements contained in this report. This may provide additional information for TMR to determine whether strengthening or other strategies are required.

8.4.2 Dynamic Load Allowance Factor

Based on the current research project, the following observations are made for structures of similar construction to those tested in this program:

- A reduction in DLA factor from 0.4 for the substructure in bridge assessments may not be supported on a network level.

- Consideration could be given regarding the potential reduction of the current DLA factor of 0.4 for superstructure components for some vehicle types (such as air-bag suspension vehicles) where operational requirements for access can be adopted. Such reductions have been implemented successfully internationally, and has been adopted in previous Australian bridge design codes when related to fundamental bridge frequencies. However, any recommendation for change would need to be supported by a critical review of all available condition and structural information, analysis results (including natural frequency requirements), and vehicle details.
- Caution is advised where high DI values coincide with poor component condition and theoretical limits that indicate structural deficiencies.
- Caution is recommended when reviewing absolute DI values determined from load tests for the amplification of load for individual components or the bridge as a whole.

8.4.3 Application of Findings across the Network

As shown in the current research, it was noted that whilst similarities were observed between both bridges in terms of fundamental frequency responses (e.g. bending fundamental frequency responses of both bridges were between 4-6 Hz), each bridge exhibited its own unique dynamic characteristics which led to amplification or cancellation of dynamic loads across the superstructure and down to the substructure. The current research also showed that the vehicle characteristics (e.g. speed, mass and unique frequency characteristics) were a dominant factor in the measured response of both bridges.

As such, the direct application of these findings on similar structures remains untested and caution should be exercised when reviewing these results in light of their application to similar structures. It is also noted that the current research focusses on the derivation of DI values based on single test vehicle events, which is not reflective of in-service loading conditions where multiple vehicles with different axle loading, configuration and inherent frequency characteristics travel at various speeds, locations and spacing. Therefore to investigate the applicability of findings from the current research, the following recommendations are suggested:

- a comparative test program on similar structures without pre-existing cracked components to determine the effect of cracking on the measured substructure DI; this would also serve to validate the findings of the current research
- a controlled load test investigating the effects of multiple vehicles on DI
- a review of existing controlled load test data in conjunction with WIM/in-service monitoring data to investigate the applicability and degree of variance (if any) of DI and load amplification or suppression.

In addition, caution is recommended in the interpretation and application of high DI values in individual components where peak strain and deflection measurements do not exceed theoretical values. Where the opposite is true, high DI values and excessive measurements should be reviewed in light of the condition of the structure, current and future traffic conditions and the likely risks associated with amplification of dynamic loads and overloading in relation to the overall performance of the structure and its critical components.

Similarly, caution is also recommended in relation to applying the current research findings to structures of different construction and configurations. To correlate the current findings for similar and dissimilar structures, additional field trials and analysis is recommended.

8.5 Additional Considerations

Further to the discussion points previously presented, the following items are provided for further consideration:

- It is recommended that further research be conducted to investigate the translation of in-service traffic data (derived from WIM data or other similar in-service monitoring methods) to the quantification of dynamic load amplification on existing structures. The following suggestions may assist:
  - conduct a review of historical WIM data to identify traffic loading and movement trends (with particular distinction between urban and rural settings)
  - review international literature to determine appropriate methodologies on how to extract DLA data from WIM data
  - conduct field trials to correlate WIM and controlled test data
  - conduct field trials to investigate multiple vehicle events.
- The influence of expansion joints on inducing greater load amplification was not investigated as part of this study. This has, however, been investigated in the literature due to reasons similar to abutment and road profile obstacles outlined in Section 8.2.5 (Deng, Yan & Zhu 2015; Maljaars et al. 2002). Depending on the condition of TMR’s expansion joint assets, this may require further review.
- Similarly, vehicle braking on a bridge has been known to be influential on dynamic loading, most notably impact loading, with significant amplification recorded for such scenarios (Deng, Wang & He 2015). This is dependent on traffic volume and movements, however some condition and structure critical structures may be at risk of this event.
- Despite the identification of quasi-resonance, the practical implications for in-service bridges remains unknown. Investigations into the probability of such an occurrence, using critical vehicle events and correlating to in-service data, may provide additional clarity on this issue.
- The condition of the structure has not been explored in great detail in this project. However, it is clear that this would be influential on some critical structures. Considerations include bending and shear cracking, foundation movements or settlement, influence on stiffness characteristics locally and globally, and contributions to material properties.
- Current investigations and subsequent determinations are based on the assumption that the bridge performs elastically and is not cracked. It does not consider the implications for serviceability states, fatigue implications or where the structure may potentially be operating under plastic conditions, if the structure ductility permits this. These issues warrant further investigation if further refinement is required in bridge assessment processes.
- Significant work has been conducted in developing and utilising theoretical models to predict bridge-vehicle interactions and resulting dynamic load amplifications. Some success has been achieved with these models, and may provide TMR with an additional tool for refined bridge assessments.

9 CONCLUSIONS

As part of the National Asset Centre of Excellence (NACoE), the Queensland Department of Transport and Main Roads (TMR) and the Australian Road Research Board (ARRB) embarked on a program of research investigating the influences dynamic interactions between bridges and vehicles have on amplification of dynamic loads. TMR recognised that research into this area may afford implementable improvements and refinements to their current bridge assessment procedures, which may ultimately lead to the realisation of economic and strategic benefits if applied across its network of approximately 3 000 bridges and 4 000 major culverts.

The topic is complex, with recognition in the literature that any resulting load amplification can be influenced by numerous parameters, including the inherent dynamic characteristics of the bridge, the vehicle and the condition of the road profile. In addition, a number of areas have been identified by TMR for further exploration, such as the response of structures to longer road trains and hydro-pneumatic all-terrain cranes, the quantified dynamic response of substructure components in comparison to the superstructure, the role of vehicle suspension types, and frequency matching between bridge components and vehicles leading to greater load amplification.

This report presents the current understanding on this topic and identifies research gaps to be explored to TMR’s advantage. The results obtained for this program of research have been presented and discussed, including dynamic structural and vehicle observations obtained from controlled load tests and the in-service monitoring on three bridges and general findings relating to the assessment of structures for dynamic loading.

The research has highlighted the fact that substructure components (such as headstocks and columns) were more likely to yield dynamic increments equal to or greater than superstructure components (e.g. girders). The degree of variation between components was dependent on vehicle type, suspension characteristics, as well as the speed and direction of travel and the transverse location of the test vehicle. The inherent frequency responses of the bridge and the vehicle both influenced the response of each bridge to controlled loads, as did the condition of the road profile leading up to the bridge. Evidence of frequency matching between the vehicles, the superstructure and substructure components resulted in load amplification beyond the Dynamic Load Amplification factor (DLA) of 0.4 in isolated cases.

The majority of the dynamic increment (DI) values determined for superstructure components were less than 0.4, and peak strain values did not exceed anticipated theoretical values. Based on these results, and practices adopted internationally, a reduction in the DLA factor for the superstructure components for these bridges may be viable for operational applications if certain conditions are met. A reduction in the DLA for substructure components is not recommended, however.

It is not clear to what extent the results obtained on the three bridges tested can be extended to other similar bridges as the presence of existing defects/cracks in the substructure may influence these results. Further research would be required to determine whether the research findings should be applied to other similar structures.

REFERENCES

AASHTO 2014, *LRFD Bridge design specification*, 7th edn, American Association of State Highway and Transportation Officials, USA.

AASHTO 2003, *Guide manual for condition evaluation and load and resistance factor rating (LRFR) of highway bridges*, American Association of State Highway and Transportation Officials, USA.

AASHTO 2011, *Manual for bridge evaluation,* 2nd edn, American Association of State Highway and Transportation Officials, USA.

Al-Zaid, RZ & Nowak, AS 1988, 'Fatigue strength of prestressed concrete girder bridges', *Canadian Journal of Civil Engineering*, vol. 15, no. 2, pp. 199–205.

Arun, S, Menon, D & Prasad, AM 2011, 'Simulating the dynamic responses of highway bridges for multiple vehicle presence effects', *International conference on structural engineering construction & management, Kandy, Sri Lanka*.

Austroads 2003, *Dynamic interaction of vehicles and bridges*, AP-T23-03, Austroads, Sydney, NSW.

Austroads 2002a, *Validation of dynamic load models: technical documentation*, AP-T12-02, Austroads, Sydney, NSW.

Austroads 2002b, *Guide to road profile unevenness and bridge damage*, AP-T13-02, Austroads, Sydney, NSW.

Bakht, B & Pinjarkar, SG 1989, 'Dynamic testing of highway bridges: a review', *Transportation Research Record*, no. 1223, pp. 93–100.

Barr, PJ, Halling, MW & Womack, KC 2008, 'Influence of changes in boundary condition on bridge response', *24th US-Japan bridge engineering workshop*, Minneapolis, Minnesota, USA, pp. 185–192.

Baumgärtner, W 1998, 'Bridge-truck interaction: simulation, measurements and load identification', *International symposium on heavy vehicle weights and dimensions, 5th, 1998, Maroochydore, Queensland, Australia,* Conference Organising Committee, Melbourne, Vic, pp. 114–31.

Bez, B, Cantieni, R & Jacquemoud, J 1987, 'Modeling of highway traffic loads in Switzerland', *IABSE Periodica*, vol. 3, pp. 153–68.

Billing, JR 1984, 'Dynamic loading and testing of bridges in Ontario', *Canadian Journal of Civil Engineering*, vol. 11, no. 4, pp. 833–43.

Billing, JR & Agarwal, AC 1990, 'The art and science of dynamic testing of highway bridges', *Proceedings of the developments in short and medium span bridge engineering*, Canadian Society for Civil Engineers, pp. 531–44.

Billing, JR & Green, R 1984, 'Design provisions for dynamic loading of highway bridges', *Transportation Research Board*, no. 950, pp. 94–103.

Brady, SP, O'Brien, EJ & Žnidarič, A 2006, 'Effect of vehicle velocity on the dynamic amplification of a vehicle crossing a simply supported bridge', *Journal of Bridge Engineering,* vol. 11, no. 2.

Broquet, C, Bailey, SF, Fafard, M & Brühwiler, E 2004, 'Dynamic behavior of deck slabs of concrete road bridges', *Journal of Bridge Engineering*, vol. 9, no. 2, pp. 137–46.

Brühwiler, E & Herwig, A 2008, ‘Consideration of dynamic traffic action effects on existing bridges at ultimate limit state', in H-M Koh & D Frangopol (eds), *Bridge maintenance, safety, management, health monitoring and informatics*, Taylor & Francis Group, London, UK, pp. 3675–82.

Cantero, D, Karoumi, R & O’Brien, EJ 2014, 'Maximum total load effects in vehicle-bridge dynamic interaction problems for simply supported structures', *Proceedings of the 9th international conference on structural dynamics (EURODYN 2014), Porto, Portugal*, European Association for Structural dynamics, pp.1169–74.

Cantieni, R 1983, *Dynamic load tests on highway bridges in Switzerland: 60 years’ experience of EMPA,* EMPA, Dubendorf, Switerland.

Cantieni, R, Krebs, W & Heywood, RJ 2010, *Dynamic interaction between vehicle and infrastructure experiment*, EMPA Test Report No. 153’031, EMPA Switzerland & QUT Australia, Dubendorf, Switzerland.

Caprani, CC 2005, 'Probalistic analysis of highway bridge traffic loading', PhD thesis, National University of Ireland.

Caprani, CC, O’Brien, EJ & McLachlan, GJ 2008, 'Characteristic traffic load effects from a mixture of loading events on short to medium span bridges', *Structural Safety*, vol.30, no.5, pp. 394–404.

Cantero, D, Karoumi, R & O’Brien, EJ 2014, 'Maximum total load effects in vehicle-bridge dynamic interaction problems for simply supported structures', A Cunha, E Caetano, P Ribeiro, & G Müller, (eds.) *International conference on structural dynamics*, *EURODYN2014, Faculty of Engineering, Porto, Portugal*, European Association for Structural Dynamics, pp. 1169–1174.

Carey, C, O’Brien, EJ & González, A 2010, 'Dynamic amplification factors for bridges with various boundary conditions', *Bridge & infrastructure research in Ireland 2010, Cork Institute of Technology, September, 2010*, BCRI.

Cebon, D 1986, 'Road damaging effects of dynamic axle loads', *International symposium on heavy vehicle weights and dimensions, Kelowna, British Columbia,* Roads and Transportation Association of Canada, Ontario, Canada.

Chan, THT & O’Connor, C 1990, 'Wheel loads from highway bridge strains: field studies', *Journal of Structural Engineering*, vol.116, no.7, pp. 1751–71.

Chegini, Z & Palermo, A 2014, 'Investigation of the behaviour of small-scale bridge models using shake table tests', *NZSEE conference ‘Towards integrated seismic design’*, New Zealand Society for Earthquake Engineering, Auckland, New Zealand.

Chen, Y, Tan, CA, Bergman, LA & Tsao, TC 2002, 'Smart suspension systems for bridge-friendly vehicles', *SPIE’s 9th annual international symposium on smart structures and materials*, International Society for Optics and Photonics, pp. 52-61.

Constanzi, M & Cebon, D 2006, 'Simulation of damage evolution in a spray sealed road', *9th International symposium on heavy vehicle weights and dimensions*, Taylor and Francis, University Park, Pennsylvania, USA, pp. 892–903.

Davis, LE 2010, 'Heavy vehicle suspensions - testing and analysis', PhD thesis, Queensland University of Technology, Brisbane, QLD.

Davis, LE & Bunker, JM 2008, *Suspension testing of 3 heavy vehicles-methodology and preliminary frequency analysis: report*, Queensland Department of Main Roads, Brisbane, QLD.

Davis, LE & Bunker, JM 2009, *Heavy vehicle suspension testing and analysis – dynamic load sharing*, Queensland Department of Main Roads & Queensland University of Technology, Brisbane, QLD.

Deng, L & Cai, CS 2010, 'Development of dynamic impact factor for performance evaluation of existing multi-girder concrete bridges', *Engineering Structures*, vol.32, no.1, pp. 21–31.

Deng, L, Wang, F & He, W 2015, 'Dynamic impact factors for simply-supported bridges due to vehicle braking', *Advances in Structural Engineering*, vol.18, no.6, pp. 791–802.

Deng, L, Yan, W & Zhu, Q 2015, 'Vehicle impact on the deck slab of concrete box-girder bridges due to damaged expansion joints', *Journal of Bridge Engineering*, vol.21, no.2.

Deng, YJ & Phares, BM 2016, *Investigation of the effect of speed on the dynamic impact factor for bridges with different entrance conditions*, InTrans Project 14-521, Bridge Engineering Center, Iowa State University, USA.

FHWA 2010, *Assuring bridge safety and serviceability in Europe*, FHWA-PL-10-014, Federal Highway Administration (FHWA), Washington, DC, USA.

Frýba, L 1972, *Vibration of solids and structures under moving loads*, Springer, Netherlands.

Gillmann, R 1999, 'Axle Spacing and Load Equivalency Factors', *Transportation Research Record*, 1655, pp. 227-32.

Green, MF & Xie, H 1998, 'Simulating the dynamic response of DIVINE bridges', *International symposium on heavy vehicle weights and dimensions, 5th, 1998, Maroochydore, Queensland, Australia*, Conference Organising Committee, Melbourne, VIC.

González, A 2009a, *Recommendations on dynamic amplification allowance - appendix a: review on dynamic response of bridge to traffic loading*, ARCHES-22-DE10_A, ARCHES.

González, A 2009b, *Recommendations on dynamic amplification allowance - appendix b: vehicle-bridge interaction models*, ARCHES-22-DE10_B, ARCHES.

Gonzalez, A, Cantero, D & O'Brien, EJ 2011, 'Dynamic increment for shear force due to heavy vehicles crossing a highway bridge', *Computers & Structures*, no.89, pp. 2261–2272.

González, A, Dowling, J, O'Brien, EJ & Znidaric, A 2010, 'Experimental determination of dynamic allowance for traffic loading in bridges', *Transportation Research Board 89th Annual Meeting,* TRB, Washington, DC, USA.

González, A, O'Brien, EJ & McGetrick, P 2010, 'Detection of bridge dynamic parameters using an instrumented vehicle', *World conference on structural control and monitoring, 5th, Tokyo, Japan*.

Gonzalez, A, O'Connor, A & O'Brien, EJ 2003, 'An assessment of the influence of dynamic interaction modelling on predicted characteristic load effects in bridges', *Proceedings of the 3rd International conference on current and future trends in bridge design, construction and maintenance*, Thomas Telford Limited, London, UK.

González, A, Rattigan, P, OBrien, EJ & Caprani, C 2008, 'Determination of bridge lifetime dynamic amplification factor using finite element analysis of critical loading scenarios', *Engineering Structures*, vol.30, no.9, pp. 2330–337.

González, A, Cantero, D & O'Brien, EJ 2009, 'The impact of a bump on the response of a bridge to traffic', *Proceedings of the twelfth international conference on civil, structural and environmental engineering computing*, Civil-Comp Ltd, Funchal, Madeira, Portugal.

Harris, NK, O'Brien, EJ & González, A 2007, 'Reduction of bridge dynamic amplification through adjustment of vehicle suspension damping', *Journal of Sound and Vibration*, vol.302, no.3, pp. 471–485.

Heywood, RJ 1995a, *Road-friendly suspensions and short span bridges*, ARR 260, Australian Road Research Board, Vermont South, VIC.

Heywood, RJ 1995b, 'DIVINE Element 6: dynamic bridge testing: short span bridges', *Dynamic loading of heavy vehicles and road wear, Mid-Term Seminar, 1995, Sydney, New South Wales, Australia*, Roads and Traffic Authority (RTA), Sydney, NSW.

Heywood, RJ 1998, 'Hydro-pneumatic crane and tractor semi-trailers: a comparative study of their dynamic effects on a short-span bridge', *5th International Symposium on Heavy Vehicle Weights and Dimensions (HVWD5),* International Forum for Road Transport Technology, Australia, pp. 51–72.

Heywood, RJ 2000, *Dynamic interaction of vehicles and bridges - review of bridge tests & recent research*, 173a, Infratech Systems & Services, Brisbane, QLD.

Heywood, RJ, Roberts, W & Boully, G 2001, 'Dynamic loading of bridges', *Transportation Research Record*, no.1770, pp. 58-66.

Holt, JE & Schoorl, D 1985, 'A theoretical and experimental analysis of the effects of suspension and road profile on bruising in multilayered apple packs', *Journal of Agricultural Engineering Research*, vol.31, no.4, pp. 297–308.

Huang, D, Wang, T & Shahawy, M 1993, 'Impact studies of multigirder concrete bridges', *Journal of Structural Engineering*, vol.119, no.8, pp. 2387-402.

Huffman, JT, Xiao, F, Chen, G & Hulsey, JL 2015, 'Detection of soil-abutment interaction by monitoring bridge response using vehicle excitation', *Journal of Civil Structural Health Monitoring*, vol.5, no.4, pp. 389-95.

Hwang, E-S & Nowak, AS 1991, 'Simulation of dynamic load for bridges', *Journal of Structural Engineering*, vol.117, no.5, pp. 1413–34.

Japan Road Association 2012, *Specifications for highway bridges (set)*, Japan Road Association, Japan.

Kaliyaperumal, G, Imam, B & Righiniotis, T 2011, 'Advanced dynamic finite element analysis of a skew steel railway bridge', *Engineering Structures*, vol.33, no.1, pp. 181-90.

Kim, S & Nowak, AS 1997, 'Load distribution and impact factors for I-girder bridges', *Journal of Bridge Engineering*, vol.2, no.3, pp. 97–104.

Lambert, J, McLean, A & Li, BH 2004, 'Air suspensions: dynamic performance', *Proceedings 8th International symposium on heavy vehicle weights and dimensions, 'Loads, Roads and the Information Highway'*, Johannesburg, South Africa, 11pp.

Li, H, Wekezer, JW & Kwasniewski, L 2008, 'Dynamic response of a highway bridge subjected to moving vehicles', *Journal of Bridge Engineering*, vol.13, no.5, pp. 439-48.

Maljaars, J, Waarts, PH, Leenderts, JS & Hoogvelt, RB 2002, 'Dynamic increment factor in modular expansion joints of bridges under heavy traffic loading', *International symposium on heavy vehicle weights and dimensions, 7th, 2002, Delft, The Netherlands.*

McGetrick, PJ, Kim, C-W, Gonzalez, A & O'Brien, EJ 2013, 'Dynamic axle force and road profile identification using a moving vehicle', *International Journal of Architecture, Engineering and Construction*, pp. 1–16.

McLean, DI & Marsh, ML 1998, *Dynamic impact factors for bridges*, Transportation Research Board, Washington, DC, USA.

Moghimi, H & Ronagh, HR 2008, 'Development of a numerical model for bridge-vehicle interaction and human response to traffic-induced vibration', *Engineering Structures*, vol.30, pp. 3808 -19.

National Association of Australian State Road Authorities 1976, *NAASRA bridge design specification,* 5th edn, Sydney, NSW *(superseded and no longer available).*

Nassif, HH & Nowak, AS 1995, 'Dynamic load spectra for girder bridges', *Transportation Research Board Annual Meeting,* TRB, Washington, DC, USA, pp. 69–83.

Nowak, AS 1993, 'Load model for bridge design code', *Canadian Journal of Civil Engineering*, vol.21, pp. 36–49.

Nowak, AS, Kim, S & Szerszen, MM 1999, 'Dynamic loads for steel girder bridges', *International modal analysis conference, 17th, Kissimmee, Florida,* Society for Experimental Mechanics, USA. pp. 731-37.

NZ Transport Agency 2016, *Bridge manual*, 3rd edn, NZ Transport Agency, Wellington, NZ.

O'Brien, EJ, Li, Y & González, A 2006, 'Bridge roughness index as an indicator of bridge dynamic amplification', *Computers & Structures*, vol.84, no.12, pp. 759-69.

O'Brien, EJ, Rattigan, P, González, A, Dowling, J & Žnidarič, A 2009, 'Characteristic dynamic traffic load effects in bridges', *Engineering Structures*, vol.31, no.7, pp. 1607–12.

O'Connor, C & Pritchard, R 1985, 'Impact studies on small composite girder bridge', *Journal of Structural Engineering*, vol.111, no.3, pp. 641-53.

O'Connor, C & Pritchard, RW 1984, 'Dynamic behaviour of Six Mile Creek bridge', *Metal structures conference, 1983, Brisbane, Australia*, Institution of Engineers, Australia, ACT.

OECD 1999, *Dynamic interaction between vehicle and infrastructure experiment (DIVINE)*, technical report DSTI/DOT/RTR/IR6(98)1/FINAL, OECD, France.

Paultre, P, Chaallal, O & Proulx, J 1992, 'Bridge dynamics and dynamic amplification factors-a review of analytical and experimental findings', *Canadian Journal of Civil Engineering*, vol.19, no.2, pp. 260-78.

Prem, H & Heywood, RJ 2000, *Effects of road profile rehabilitation on dynamic loading of bridges,* ARRB Transport Research, Vermont South, VIC.

Pritchard, RW 1982, 'Service traffic loads on Six Mile Creek bridge, Queensland', MEng thesis, University of Queensland.

Pritchard, RW & O'Connor, C 1984, 'Measurement and prediction of traffic loads on Six Mile Creek bridge', *Australian Road Research*, vol.12, no.2.

Queensland Department of Transport and Main Roads 2011, *Heavy load assessment: project brief for external consultants*, TMR, Brisbane, QLD.

Queensland Department of Transport and Main Roads 2013, *Tier 1 bridge heavy load assessment criteria*, TMR, Brisbane, QLD.

Rattigan, P, Gonzalez, A & O'Brien, EJ 2009, 'Influence of pre-existing vibrations on the dynamic response of medium span bridges', *Canadian Journal of Civil Engineering*, vol.36, no.1, pp. 73-84.

Rattigan, PH, OBrien, EJ & Gonzalez, A 2005, *The dynamic amplification on highway bridges due to traffic flow*, University College Dublin, Ireland.

Senthilvasan, J, Brameld, GH & Thambiratnam, DP 1997, 'Bridge-vehicle interaction in curved box girder bridges', *Computer-Aided Civil and Infrastructure Engineering*, vol.12, no.3, pp. 171-82.

Senthilvasan, J, Thambiratnam, DP & Brameld, GH 2002, 'Dynamic response of a curved bridge under moving truck load', *Engineering Structures*, vol.24, no.10, pp. 1283-93.

Steinauer, B & Ueckermann, A 2002, 'Road roughness and its effects on the infrastructure', *International symposium on heavy vehicle weights and dimensions*, *7th, 2002, Delft, The Netherlands.*

Sweatman, PF, Woodrooffe, J & McFarlane, S 1997, *Improving the interaction between heavy trucks, roads and bridges*, technical paper 973265, SAE, USA.

Sun, L 2002, 'Optimum design of 'road-friendly' vehicle suspension systems subjected to rough pavement surfaces', *Applied Mathematical Modelling*, vol.26, no.5, pp. 635-52.

Sun, L 2003, 'Simulation of pavement roughness and IRI based on power spectral density', *Mathematics and Computers in Simulation*, vol.61, no.2, pp. 77-88.

Szurgott, P, Wekezer, JW, Kwasniewski, L, Siervogel, J & Ansley, M 2011, 'Experimental assessment of dynamic responses induced in concrete bridges by permit vehicles', *Journal of Bridge Engineering*, vol.16, no.1, pp. 108–116.

Wang, L, Kang, X & Jiang, P 2016, 'Vibration analysis of a multi-span continuous bridge subject to complex traffic loading and vehicle dynamic interaction', *KSCE Journal of Civil Engineering*, vol.20, no.1, pp. 323-32.

Zhou, Y & Chen, S 2014, 'Dynamic simulation of a long-span bridge-traffic system subjected to combined service and extreme loads', *Journal of Structural Engineering*, vol.141, no.9.

Zhou, X-Y, Treacy, M, Schmidt, F, Brühwiler, E, Toutlemonde, F & Jacob, B 2015, 'Effect on bridge load effects of vehicle transverse in-lane position: a case study', *Journal of Bridge Engineering*, vol.20, no.12.

Žnidarič, A, O'Brien, E, Casas, JR, O'Connor, A, Wierzbicki, T, Lavrič, I & Kalin, J 2006, *SAMARIS program: Guidance for the optimal assessment of highway structures,* Deliverable SAM-GE-D30 EU 6th framework report, EU.

Australian Standards

AS 5100 Set-2017, *Bridge design set.*

AS 5100.2-2017, *Bridge design: design loads.*

AS 5100.2-2004, *Bridge design: design loads (superseded).*

AS 5100.5-2004, *Bridge design: concrete (superseded).*

AS 5100.7-2017, *Bridge design: bridge assessment.*

AS 5100.8-2017, *Bridge design: Rehabilitation and strengthening of existing bridges.*

SAA HB77 1996, *Australian bridge design code (superseded by AS 5100-2004).*

International Standards

EN 1990-2005, *Eurocode – basis for structural design.*

EN 1991.2-2003, *Eurocode 1: Actions on structures - part 2: traffic loads on bridges.*

BS EN 1991.2-2003, *Eurocode 1. Actions on structures. Traffic loads on bridges*.

CSA S6-2014, *Canadian highway bridge design code*.

JTG D60-2004, *General code for design of highway bridges and culverts (Chinese).*

APPENDIX A SUMMARY OF PEAK RESPONSES

A.1 Canal Creek Bridge

Table A 1: Canal Creek Bridge Summary of Peak Strain Responses (Crawl speed)

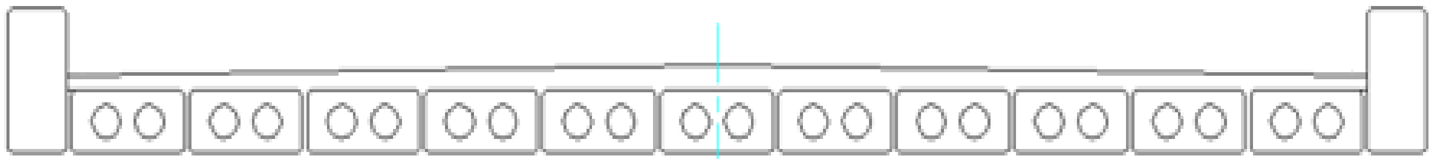

Vehicle	Run #	Location	Travel to	DU1 (kerb) SG1	DU2 SG2	DU3 SG3	DU4 SG4	DU5 SG5	DU6 SG6	DU7 SG7	DU8 SG8	DU9 SG9	DU10 SG10	DU11 SG11	DU12 SG12	DU13 (kerb) SG13	DU7 Span2 SG14	DU1 top SG15	DU1 mid SG16	File name
Crane	01	Centre	Cloncurry	59.00	61.30	61.40	68.10	63.20	62.00	60.60	68.40		45.30	43.80	42.40	45.10	58.90	-123.00	3.24	01-CR_CL_crawl_CC
	07	Lane	Cloncurry	79.60	73.00	77.90	63.30	58.80	62.10	65.90	55.00		35.30	33.10	31.50	33.00	66.40	-136.00	4.80	07-CR_0.6_crawl_CC
	04	Centre	Julia Creek	52.75	49.50	48.96	49.24	65.49	61.23	59.37	62.07		53.16	50.44	51.02	56.46	58.03	-87.80	4.42	04-CR_CL_crawl_JC
	10	Lane	Julia Creek	28.90	27.90	30.40	31.60	38.20	50.00	64.60	61.00		60.80	74.00	71.90	80.00	63.20	-46.70	4.30	10-CR_0.6_crawl_JC
		Maximum strains		79.60	73.00	77.90	68.10	65.49	62.10	65.90	68.40		60.80	74.00	71.90	80.00	66.40	-136.00	4.80	
Semi 1-1 (Steel, 1st Prime Mover)	02	Centre	Cloncurry	42.70	27.00	28.60	31.00	37.90	45.90	42.50	44.00		30.80	28.10	26.00	26.80	38.80	-51.80	1.46	02-ST1_CL_crawl_CC
	08	Lane	Cloncurry	51.60	48.10	51.10	42.30	40.30	44.80	34.90	27.20		16.50	14.30	12.50	12.50	33.70	-89.70	3.16	08-ST1_0.6_crawl_CC
	05	Centre	Julia Creek	27.60	26.30	28.80	32.00	42.10	40.70	40.50	45.10		25.70	23.20	20.90	21.80	41.80	-46.40	3.03	05-ST1_CL_crawl_JC
	11	Lane	Julia Creek	11.60	11.60	13.00	15.70	19.70	28.50	33.80	45.00		39.60	44.80	41.60	45.50	33.60	-28.00	4.04	11-ST1_0.6_crawl_JC
		Maximum strains		51.60	48.10	51.10	42.30	42.10	45.90	42.50	45.10		39.60	44.80	41.60	45.50	41.80	-89.70	4.04	
Semi 1-2 (Steel, 2nd Prime Mover)	71	Centre	Cloncurry	29.04	28.36	30.03	32.08	40.49	44.35	42.23	47.40		30.12	27.00	24.93	26.42	40.53	2.53	0.89	71-ST1_CL_crawl_CC
	73	Lane	Cloncurry	55.07	51.89	56.31	45.10	43.50	46.59	34.02	27.81		16.49	14.48	12.06	11.76	32.19	1.68	1.20	73-ST1_0.6_crawl_CC
	72	Centre	Julia Creek	26.35	25.39	27.20	30.36	36.64	44.67	40.07	42.63		29.14	26.42	24.66	25.40	40.95	4.43	1.11	72-ST1_CL_crawl_JC
	74	Lane	Julia Creek	11.37	12.42	13.38	16.52	20.64	27.04	31.43	44.42		41.21	48.20	46.52	49.95	31.64	4.08	2.74	74-ST1_0.6_crawl_JC
		Maximum strains		55.07	51.89	56.31	45.10	43.50	46.59	42.23	47.40		41.21	48.20	46.52	49.95	40.95	1.68	2.74	
Semi 2 (Air)	03	Centre	Cloncurry	41.10	36.80	37.90	40.20	50.10	48.20	47.60	52.60		30.90	29.00	27.20	27.90	47.30	-72.50	1.50	03-ST2_CL_crawl_CC
	09	Lane	Cloncurry	57.90	54.10	56.50	47.00	45.90	51.20	39.00	32.10		19.90	17.90	15.50	16.30	41.00	-100.00	5.21	09-ST2_0.6_crawl_CC
	06	Centre	Julia Creek	34.30	33.50	34.80	37.20	44.10	56.00	50.20	53.20		38.90	36.90	35.90	37.50	29.20	-59.50	1.58	06-ST2_CL_crawl_JC
	12	Lane	Julia Creek	17.70	17.70	19.30	22.70	27.80	37.10	42.70	55.80		51.60	58.10	57.50	62.40	11.70	0.77	1.59	12-ST2_0.6_crawl_JC
		Maximum strains		57.90	54.10	56.50	47.00	50.10	56.00	50.20	55.80		51.60	58.10	57.50	62.40	47.30	-100.00	5.21	
Road Train	75	Centre	Cloncurry	30.40	29.70	31.50	34.00	43.10	45.70	44.20	49.70		29.40	26.60	24.70	25.60	41.30	-58.20	1.20	75-RT_CL_crawl_CC
	77	Lane	Cloncurry	55.60	52.60	54.10	44.10	43.50	46.00	33.30	26.40		15.40	13.20	11.80	11.50	32.30	-107.00	1.10	77-RT_0.6_crawl_CC
	76	Centre	Julia Creek	31.10	30.70	32.50	33.20	43.30	42.10	40.80	45.00		27.00	25.40	23.70	24.10	42.10	-62.60	1.51	76-RT_CL_crawl_JC
	78	Lane	Julia Creek	11.40	11.20	12.70	14.90	19.40	26.80	31.50	41.10		41.30	47.20	46.60	49.50	31.40	-24.40	1.59	78-RT_0.6_crawl_JC
		Maximum strains		55.60	52.60	54.10	44.10	43.50	46.00	44.20	49.70		41.30	47.20	46.60	49.50	42.10	-107.00	1.59	

Table A 2: Canal Creek Bridge Summary of Peak Strain Responses (10 km/h and 20 km/h speed)

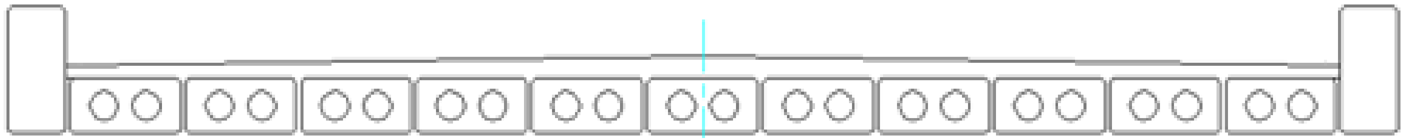

10 km/h				DU1 (kerb)	DU2	DU3	DU4	DU5	DU6	DU7	DU8	DU9	DU10	DU11	DU12	DU13 (kerb)	DU7 Span2	DU1 top	DU1 mid	File name
Vehicle	Run #	Location	Travel to	SG1	SG2	SG3	SG4	SG5	SG6	SG7	SG8	SG9	SG10	SG11	SG12	SG13	SG14	SG15	SG16	
Crane	21	Lane	Cloncurry	85.90	78.20	78.60	63.30	60.10	65.10	68.60	52.60		33.70	32.00	29.00	30.90	65.60	-144.00	4.51	21-CR_0.6_10_CC
	24	Lane	Julia Creek	30.20	29.20	30.50	34.10	40.90	52.20	67.10	65.40		62.70	77.60	78.70	85.00	64.40	-49.80	3.81	24-CR_0.6_10_JC
	Maximum strains			85.90	78.20	78.60	63.30	60.10	65.10	68.60	65.40		62.70	77.60	78.70	85.00	65.60	-144.00	4.51	
Semi 1-1 (Steel, 1st Prime Mover)	22	Lane	Cloncurry	54.10	51.30	53.90	44.40	42.30	46.30	34.90	27.70		16.80	15.10	13.90	14.00	35.30	-90.00	2.86	22-ST1_0.6_10_CC
	25	Lane	Julia Creek	15.10	14.80	15.80	18.90	23.40	30.00	37.40	47.00		41.60	47.20	43.10	47.60	36.70	-25.90	3.03	25-ST1_0.6_10_JC
	Maximum strains			54.10	51.30	53.90	44.40	42.30	46.30	37.40	47.00		41.60	47.20	43.10	47.60	36.70	-90.00	3.03	
Semi 1-1 (Steel, 2nd Prime Mover)	NA	Lane	Cloncurry																	NA
	NA	Lane	Julia Creek																	NA
	Maximum strains																			
Semi 2 (Air)	23	Lane	Cloncurry	58.20	53.60	55.30	46.10	46.20	50.10	38.90	32.40		19.70	18.40	16.30	17.50	40.90	-94.60	3.56	23-ST2_0.6_10_CC
	26	Lane	Julia Creek	16.90	16.80	18.90	21.70	26.90	35.60	40.80	54.00		49.50	56.50	56.90	62.50	38.60	-28.50	2.14	26-ST2_0.6_10_JC
	Maximum strains			58.20	53.60	55.30	46.10	46.20	50.10	40.80	54.00		49.50	56.50	56.90	62.50	40.90	-94.60	3.56	
Road Train	79	Lane	Cloncurry	57.30	54.70	55.50	45.80	44.40	44.30	32.70	26.60		14.80	12.60	11.20	10.70	33.60	-107.00	1.85	79-RT_0.6_10_CC
	80	Lane	Julia Creek	12.80	13.00	14.30	16.80	21.90	30.20	34.90	45.40		43.90	50.00	50.00	54.30	34.70	-24.80	2.28	80-RT_0.6_10_JC
	Maximum strains			57.30	54.70	55.50	45.80	44.40	44.30	34.90	45.40		43.90	50.00	50.00	54.30	34.70	-107.00	2.28	

20 km/h				DU1 (kerb)	DU2	DU3	DU4	DU5	DU6	DU7	DU8	DU9	DU10	DU11	DU12	DU13 (kerb)	DU7 Span2	DU1 top	DU1 mid	File name
Vehicle	Run #	Location	Travel to	SG1	SG2	SG3	SG4	SG5	SG6	SG7	SG8	SG9	SG10	SG11	SG12	SG13	SG14	SG15	SG16	
Crane	56	Centre	Cloncurry	58.30	53.50	52.80	56.60	69.80	65.30	62.10	66.30		52.50	50.20	50.90	55.60	63.10	-102.00	3.29	56-CR_CL_20_CC
	27	Lane	Cloncurry	86.80	80.10	86.30	68.90	65.10	69.70	75.30	60.40	0.00	38.30	35.30	33.60	35.60	64.40	-142.00	4.88	27-CR_0.6_20_CC
	62	Lane	Cloncurry	86.30	80.70	85.00	66.20	62.50	67.10	71.80	57.10	0.00	36.70	33.70	31.50	33.80	68.20	-159.00	4.17	62-CR_0.6_20_CC
	55	Centre	Julia Creek	57.40	53.20	52.40	54.80	71.50	67.60	63.20	64.30		54.50	51.70	52.90	58.40	63.30	-100.00	3.27	55-CR_CL_20_JC
	59	Lane	Julia Creek	35.00	33.80	35.10	38.20	44.90	58.50	71.90	66.10	0.00	63.90	76.50	75.30	85.80	70.40	-65.50	2.97	59-CR_0.6_20_JC
	30	Lane	Julia Creek	31.80	30.30	32.30	35.50	42.50	54.90	68.90	64.90	0.00	63.90	78.30	75.40	83.20	65.90	-52.80	3.36	30-CR_0.6_20_JC
	Maximum strains			86.80	80.70	86.30	68.90	71.50	69.70	75.30	66.30		63.90	78.30	75.40	85.80	70.40	-159.00	4.88	
Semi 1-1 (Steel, 1st Prime Mover)	28	Lane	Cloncurry	55.40	52.40	56.50	47.90	46.10	52.90	40.30	32.10		19.50	17.90	16.40	16.60	40.00	-91.50	2.36	28-ST1a_0.6_20_CC
	31	Lane	Julia Creek	16.40	15.80	17.50	20.00	23.90	33.00	38.00	47.10		42.80	47.50	46.50	51.40	40.40	-28.20	1.85	31-ST1a_0.6_20_JC
	Maximum strains			55.40	52.40	56.50	47.90	46.10	52.90	40.30	47.10		42.80	47.50	46.50	51.40	40.40	-91.50	2.36	
Semi 1-1 (Steel, 2nd Prime Mover)	63	Lane	Cloncurry	49.00	46.10	47.70	45.40	51.10	54.60	48.00	44.50	0.00	27.50	24.70	23.30	25.00	48.50	-89.30	2.31	63-ST1b_0.6_20_CC
	60	Lane	Julia Creek	18.50	17.70	19.20	22.00	27.90	37.60	43.20	50.00	0.00	49.80	50.40	52.90	59.10	26.90	-37.20	1.23	60-ST1b_0.6_20_JC
	Maximum strains			49.00	46.10	47.70	45.40	51.10	54.60	48.00	50.00		49.80	50.40	52.90	59.10	48.50	-89.30	2.31	
Semi 2 (Air)	29	Lane	Cloncurry	58.40	54.60	57.20	49.10	47.60	53.90	41.80	34.00		21.20	19.20	17.80	18.80	44.40	-95.80	2.87	29-ST2_0.6_20_CC
	64	Lane	Cloncurry	59.40	55.60	56.70	48.20	48.00	52.20	39.60	31.90	0.00	19.70	17.40	16.50	17.10	43.70	-107.00	4.04	64-ST2_0.6_20_CC
	32	Lane	Julia Creek	18.30	17.80	18.90	22.20	27.70	36.40	42.80	55.20		49.50	55.20	54.70	60.50	39.80	-30.40	2.17	32-ST2_0.6_20_JC
	61	Lane	Julia Creek	19.20	18.80	20.30	23.20	28.90	37.70	44.70	57.10	0.00	51.00	56.50	55.80	61.80	40.80	-36.60	1.76	61-ST2_0.6_20_JC
	Maximum strains			59.40	55.60	57.20	49.10	48.00	53.90	44.70	57.10		51.00	56.50	55.80	61.80	44.40	-107.00	4.04	
Road Train	81	Lane	Cloncurry	66.60	59.80	57.70	52.50	50.40	47.90	38.70	31.10		18.50	15.80	14.00	13.90	36.90	-118.00	2.00	81-RT_0.6_20_CC
	82	Lane	Julia Creek	13.40	13.40	15.30	18.60	22.70	30.20	35.00	41.40		45.50	47.50	52.70	58.50	34.60	-25.10	1.90	82-RT_0.6_20_JC
	Maximum strains			66.60	59.80	57.70	52.50	50.40	47.90	38.70	41.40		45.50	47.50	52.70	58.50	36.90	-118.00	2.00	

Table A 3: Canal Creek Bridge Summary of Peak Strain Responses (40 km/h and 60 km/h speed)

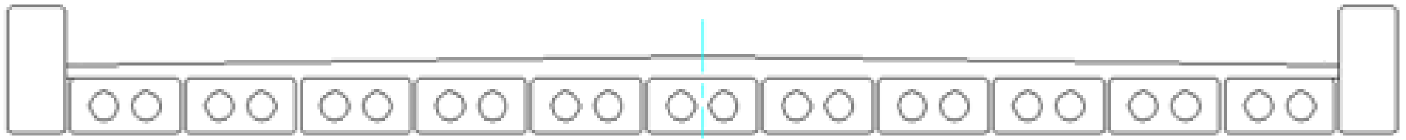

40 km/h				DU1 (kerb)	DU2	DU3	DU4	DU5	DU6	DU7	DU8	DU9	DU10	DU11	DU12	DU13 (kerb)	DU7 Span2	DU1 top	DU1 mid	File name
Vehicle	Run #	Location	Travel to	SG1	SG2	SG3	SG4	SG5	SG6	SG7	SG8	SG9	SG10	SG11	SG12	SG13	SG14	SG15	SG16	
Crane	58	Centre	Cloncurry	66.70	61.40	58.20	64.60	62.30	66.00	63.20	73.40		47.80	47.00	45.80	49.70	66.10	-118.00	3.50	58-CR_CL_40_CC
	33	Lane	Cloncurry	82.10	76.60	73.00	58.00	55.10	58.20	57.00	43.70	0.00	29.80	27.80	26.60	27.60	71.90	-139.00	5.58	33-CR_0.6_40_CC
	68	Lane	Cloncurry	76.80	70.60	75.60	60.10	56.80	61.70	67.90	52.50	0.00	33.30	30.90	29.40	31.30	73.40	-144.00	4.53	68-CR_0.6_40_CC
	57	Centre	Julia Creek	59.40	55.10	55.10	58.10	74.20	67.70	63.70	67.30		54.20	51.20	51.00	55.30	65.50	-103.00	3.21	57-CR_CL_40_JC
	36	Lane	Julia Creek	36.30	34.70	36.30	39.60	47.30	60.10	74.20	70.70	0.00	69.40	84.30	82.80	92.90	68.40	-60.30	4.05	36-CR_0.6_40_JC
	65	Lane	Julia Creek	37.10	35.50	37.10	41.10	50.40	62.70	74.00	69.80	0.00	67.10	78.80	74.30	83.20	75.10	-68.00	3.02	65-CR_0.6_40_JC
	Maximum strains			82.10	76.60	75.60	64.60	74.20	67.70	74.20	73.40		69.40	84.30	82.80	92.90	75.10	-144.00	5.58	
Semi 1-1 (Steel, 1st Prime Mover)	34	Lane	Cloncurry	61.20	57.30	56.90	53.00	55.00	56.70	50.20	43.60		27.50	25.40	23.50	25.40	40.80	-100.00	2.71	34-ST1a_0.6_40_CC
	37	Lane	Julia Creek	16.80	16.20	17.80	19.50	24.50	32.80	40.30	44.80		44.30	44.20	40.30	45.00	38.00	-29.90	1.68	37-ST1a_0.6_40_JC
	Maximum strains			61.20	57.30	56.90	53.00	55.00	56.70	50.20	44.80		44.30	44.20	40.30	45.00	40.80	-100.00	2.71	
Semi 1-1 (Steel, 2nd Prime Mover)	69	Lane	Cloncurry	63.20	59.10	63.90	61.80	59.40	63.30	55.60	46.30	0.00	29.50	26.60	25.80	27.40	45.40	-117.00	2.27	69-ST1b_0.6_40_CC
	66	Lane	Julia Creek	17.30	17.00	17.90	20.30	25.20	33.90	42.90	45.30	0.00	45.10	41.80	38.90	42.90	39.00	-33.40	2.14	66-ST1b_0.6_40_JC
	Maximum strains			63.20	59.10	63.90	61.80	59.40	63.30	55.60	46.30		45.10	41.80	38.90	42.90	45.40	-117.00	2.27	
Semi 2 (Air)	35	Lane	Cloncurry	60.70	55.80	55.90	49.00	48.30	52.60	42.10	34.40		22.00	20.70	19.40	20.60	44.40	-99.70	3.46	35-ST2_0.6_40_CC
	70	Lane	Cloncurry	61.00	56.10	55.70	49.00	48.90	50.80	41.50	35.20	0.00	22.70	21.10	19.60	20.70	44.50	-115.00	3.67	70-ST2_0.6_40_CC
	38	Lane	Julia Creek	22.80	21.60	22.80	25.80	31.70	40.90	48.10	57.50		52.20	56.40	54.50	60.90	47.10	-38.60	2.36	38-ST2_0.6_40_JC
	67	Lane	Julia Creek	21.00	19.70	21.30	24.20	30.00	38.90	45.70	58.20	0.00	52.00	57.90	55.50	62.00	43.80	-41.70	1.89	67-ST2_0.6_40_JC
	Maximum strains			61.00	56.10	55.90	49.00	48.90	52.60	48.10	58.20		52.20	57.90	55.50	62.00	47.10	-115.00	3.67	
Road Train	83	Lane	Cloncurry	65.10	60.70	61.10	54.80	53.40	52.80	44.80	36.50		22.10	19.80	17.70	17.90	36.80	-113.00	2.78	83-RT_0.6_40_CC
	84	Lane	Julia Creek	17.00	17.00	18.60	20.60	25.90	34.20	39.70	44.00		43.60	44.70	45.70	50.50	29.20	-31.30	1.74	84-RT_0.6_40_JC
	Maximum strains			65.10	60.70	61.10	54.80	53.40	52.80	44.80	44.00		43.60	44.70	45.70	50.50	36.80	-113.00	2.78	

60 km/h				DU1 (kerb)	DU2	DU3	DU4	DU5	DU6	DU7	DU8	DU9	DU10	DU11	DU12	DU13 (kerb)	DU7 Span2	DU1 top	DU1 mid	File name
Vehicle	Run #	Location	Travel to	SG1	SG2	SG3	SG4	SG5	SG6	SG7	SG8	SG9	SG10	SG11	SG12	SG13	SG14	SG15	SG16	
Crane	39	Lane	Cloncurry	93.10	86.90	94.70	77.60	72.30	77.80	84.00	69.00		43.00	40.60	38.50	40.60	72.50	-154.00	4.76	39-CR_0.6_60_CC
	42	Lane	Julia Creek	35.20	33.70	35.50	38.90	46.20	60.20	74.60	69.30		68.90	84.40	80.10	88.40	66.40	-60.60	3.13	42-CR_0.6_60_JC
	Maximum strains			93.10	86.90	94.70	77.60	72.30	77.80	84.00	69.30		68.90	84.40	80.10	88.40	72.50	-154.00	4.76	
Semi 1-1 (Steel, 1st Prime Mover)	40	Lane	Cloncurry	50.90	47.60	53.70	46.30	42.50	47.40	39.50	32.30		20.80	19.90	19.10	19.60	48.20	-85.30	2.53	40-ST1a_0.6_60_CC
	43	Lane	Julia Creek	17.80	17.00	18.30	20.50	25.40	33.80	38.30	42.00		40.10	38.50	39.90	43.90	48.00	8.71	2.58	43-ST1a_0.6_60_JC
	Maximum strains			50.90	47.60	53.70	46.30	42.50	47.40	39.50	42.00		40.10	38.50	39.90	43.90	48.20	-85.30	2.58	
Semi 1-1 (Steel, 2nd Prime Mover)	NA	Lane	Cloncurry																	NA
	NA	Lane	Julia Creek																	NA
	Maximum strains																			
Semi 2 (Air)	41	Lane	Cloncurry	62.10	55.70	54.20	49.20	49.10	51.30	43.70	38.80		26.50	24.80	24.00	26.30	44.40	-102.00	3.35	41-ST2_0.6_60_CC
	44	Lane	Julia Creek	21.40	20.10	22.20	25.10	30.80	40.70	47.20	57.20		52.10	55.80	55.40	61.30	47.70	-37.80	2.61	44-ST2_0.6_60_JC
	Maximum strains			62.10	55.70	54.20	49.20	49.10	51.30	47.20	57.20		52.10	55.80	55.40	61.30	47.70	-102.00	3.35	
Road Train	85	Lane	Cloncurry	59.70	54.90	55.70	48.00	45.70	45.50	38.80	32.70		19.20	17.20	16.20	16.30	38.40	-105.00	2.06	85-RT_0.6_60_CC
	86	Lane	Julia Creek	18.70	17.70	19.50	22.00	26.80	36.00	43.00	45.40		47.80	46.50	45.60	49.60	43.60	-32.90	2.87	86-RT_0.6_60_JC
	Maximum strains			59.70	54.90	55.70	48.00	45.70	45.50	43.00	45.40		47.80	46.50	45.60	49.60	43.60	-105.00	2.87	

Table A 4: Canal Creek Bridge Summary of Peak Strain Responses (80 km/h and maximum speed)

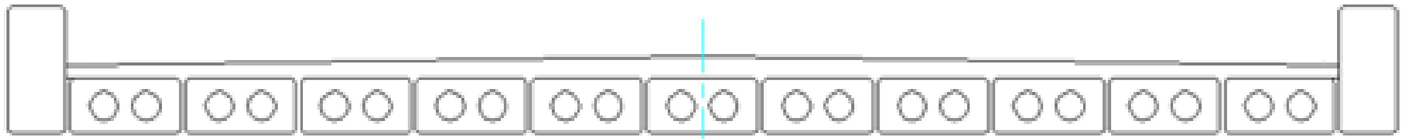

80 km/h				DU1 (kerb)	DU2	DU3	DU4	DU5	DU6	DU7	DU8	DU9	DU10	DU11	DU12	DU13 (kerb)	DU7 Span2	DU1 top	DU1 mid	File name
Vehicle	Run #	Location	Travel to	SG1	SG2	SG3	SG4	SG5	SG6	SG7	SG8	SG9	SG10	SG11	SG12	SG13	SG14	SG15	SG16	
Crane	45	Lane	Cloncurry	96.70	87.30	83.10	77.10	80.70	85.90	81.40	76.50		52.60	49.40	47.00	50.20	66.60	-158.00	4.94	45-CR_0.6_80_CC
	48	Lane	Julia Creek	39.20	37.00	37.90	39.30	46.80	58.70	61.40	62.20		62.80	66.70	67.40	76.60	81.70	-66.20	3.44	48-CR_0.6_80_JC
	Maximum strains			96.70	87.30	83.10	77.10	80.70	85.90	81.40	76.50		62.80	66.70	67.40	76.60	81.70	-158.00	4.94	
Semi 1-1 (Steel, 1st Prime Mover)	46	Lane	Cloncurry	44.60	39.90	37.10	37.80	39.90	41.30	39.40	36.70		27.20	27.20	26.80	29.50	43.60	-75.70	3.41	46-ST1a_0.6_80_CC
	49	Lane	Julia Creek	24.40	22.70	24.40	27.00	33.40	44.60	51.90	51.90		50.10	44.90	43.80	49.70	49.10	-40.40	1.84	49-ST1a_0.6_80_JC
	Maximum strains			44.60	39.90	37.10	37.80	39.90	44.60	51.90	51.90		50.10	44.90	43.80	49.70	49.10	-75.70	3.41	
Semi 1-1 (Steel, 2nd Prime Mover)	NA	Lane	Cloncurry																	NA
	NA	Lane	Julia Creek																	NA
	Maximum strains																			
Semi 2 (Air)	47	Lane	Cloncurry	69.60	62.30	59.20	56.70	60.70	62.50	57.80	53.90		40.50	40.30	41.10	45.90	49.10	-117.00	3.27	47-ST2_0.6_80_CC
	50	Lane	Julia Creek	28.10	27.10	28.40	30.30	36.60	47.20	53.70	59.70		55.80	55.20	55.00	61.60	50.10	-50.90	2.56	50-ST2_0.6_80_JC
	Maximum strains			69.60	62.30	59.20	56.70	60.70	62.50	57.80	59.70		55.80	55.20	55.00	61.60	50.10	-117.00	3.27	
Road Train	87	Lane	Cloncurry	49.10	43.70	38.70	34.20	34.30	36.50	33.00	30.50		23.50	22.90	22.90	24.60	43.30	-85.80	2.38	87-RT_0.6_80_CC
	88	Lane	Julia Creek	17.00	16.70	17.80	20.90	26.10	35.30	44.70	50.70		49.20	48.90	47.50	52.30	51.60	-30.90	1.92	88-RT_0.6_80_JC
	Maximum strains			49.10	43.70	38.70	34.20	34.30	36.50	44.70	50.70		49.20	48.90	47.50	52.30	51.60	-85.80	2.38	

Speed limit				DU1 (kerb)	DU2	DU3	DU4	DU5	DU6	DU7	DU8	DU9	DU10	DU11	DU12	DU13 (kerb)	DU7 Span2	DU1 top	DU1 mid	File name
Vehicle	Run #	Location	Travel to	SG1	SG2	SG3	SG4	SG5	SG6	SG7	SG8	SG9	SG10	SG11	SG12	SG13	SG14	SG15	SG16	
Crane	NA	Lane	Cloncurry																	NA
	NA	Lane	Julia Creek																	NA
	Maximum strains																			
Semi 1-1 (Steel, 1st Prime Mover)	53	Lane	Cloncurry	36.70	34.10	34.60	37.70	44.40	45.20	44.30	47.00		32.20	31.10	31.90	34.60	51.40	-68.00	3.48	53-ST1a_0.6_100_CC
	51	Lane	Julia Creek	30.60	29.10	28.80	30.70	35.50	47.30	45.40	46.20		38.10	36.10	36.70	39.70	60.00	-59.00	2.76	51-ST1a_0.6_100_JC
	Maximum strains			36.70	34.10	34.60	37.70	44.40	47.30	45.40	47.00		38.10	36.10	36.70	39.70	60.00	-68.00	3.48	
Semi 1-1 (Steel, 2nd Prime Mover)	NA	Lane	Cloncurry																	NA
	NA	Lane	Julia Creek																	NA
	Maximum strains																			
Semi 2 (Air)	54	Lane	Cloncurry	74.80	67.80	64.10	59.10	62.80	64.40	59.60	56.30		41.90	41.60	41.40	46.20	48.10	-135.00	4.73	54-ST2_0.6_100_CC
	52	Lane	Julia Creek	23.90	22.90	23.70	25.80	31.50	40.20	46.70	55.90		50.80	55.70	54.30	60.90	49.40	-46.90	1.69	52-ST2_0.6_100_JC
	Maximum strains			74.80	67.80	64.10	59.10	62.80	64.40	59.60	56.30		50.80	55.70	54.30	60.90	49.40	-135.00	4.73	
Road Train	89	Lane	Cloncurry	45.40	41.20	40.80	39.10	43.10	45.50	40.80	37.00		26.40	25.00	24.70	27.50	60.80	-77.50	3.00	89-RT_0.6_88_CC
	90	Lane	Julia Creek	21.80	20.40	22.30	24.10	31.10	42.60	53.00	48.30		51.20	42.70	39.60	43.90	52.50	-34.20	2.17	90-RT_0.6_84_JC
	Maximum strains			45.40	41.20	40.80	39.10	43.10	45.50	53.00	48.30		51.20	42.70	39.60	43.90	60.80	-77.50	3.00	

Table A 5: Canal Creek Bridge Summary of Peak Strain Responses (crawl speed)

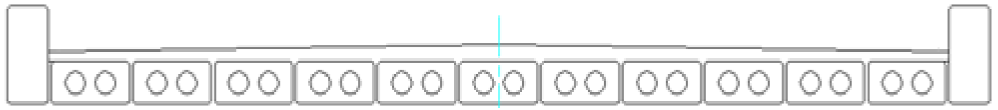

				DU1 (kerb)	DU2	DU3	DU4	DU5	DU6	DU7	DU8	DU9	DU10	DU11	DU12	DU13 (kerb)												
	Run #	**Location**	**Travel to**	LVDT1	LVDT2	LVDT3	LVDT4	LVDT5	LVDT6	LVDT7	LVDT8	LVDT9	LVDT10	LVDT11	LVDT12	LVDT13	LVDT14	LVDT15	LVDT16	LVDT17	LVDT18	LVDT19	LVDT20	LVDT21	LVDT22	LVDT23	LVDT24	File
Crane	01	Centre	Cloncurry	-1.68	-1.84	-2.14	-2.73	-2.92	-3.21	-3.11	-3.03	-2.36	-1.87	-1.50	-1.05	-0.86	-1.14	-1.57	-1.94	-2.06	-1.26	-1.71	-2.32	-0.26	-0.36	-2.95	-2.50	01-CR_CL_crawl_CC
	07	0.6 m from kerb	Cloncurry	-2.12	-2.25	-2.50	-2.93	-2.83	-3.13	-3.01	-2.60	-1.90	-1.47	-1.15	-0.68	-0.47	-1.48	-1.90	-1.92	-2.05	-1.61	-1.96	-2.35	-0.28	-0.35	-3.02	-3.25	07-CR_0.6_crawl_CC
	13	0.3 m from kerb	Cloncurry	-2.63	-2.70	-2.80	-3.01	-2.85	-3.11	-2.66	-2.10	-1.48	-1.11	-0.87	-0.44	-0.27	-1.85	-2.14	-1.93	-1.81	-2.04	-2.19	-2.28	-0.26	-0.29	-2.71	-2.77	13-CR_0.3_crawl_CC
	04	Centre	Julia Creek	-1.21	-1.38	-1.68	-2.28	-2.57	-3.11	-3.13	-3.17	-2.68	-2.21	-1.84	-1.37	-1.10	-0.83	-1.28	-1.74	-2.08	-0.89	-1.35	-2.10	-0.26	-0.35	-3.07	-2.79	04-CR_CL_crawl_JC
	10	0.6 m from kerb	Julia Creek	-0.58	-0.71	-0.94	-1.45	-1.79	-2.45	-3.01	-3.21	-2.87	-2.69	-2.55	-2.19	-2.03	-0.35	-0.71	-1.16	-2.05	-0.41	-0.74	-1.44	-0.28	-0.34	-2.98	-3.09	10-CR_0.6_crawl_JC
	16	0.3 m from kerb	Julia Creek	-0.46	-0.57	-0.75	-1.19	-1.50	-2.09	-2.80	-3.31	-3.04	-2.86	-2.81	-2.58	-2.47	-0.29	-0.61	-0.99	-1.94	-0.31	-0.60	-1.22	-0.29	-0.31	-2.75	-2.79	16-CR_0.3_crawl_JC
	Maximum deflections			**-2.63**	**-2.70**	**-2.80**	**-3.01**	**-2.92**	**-3.21**	**-3.13**	**-3.31**	**-3.04**	**-2.86**	**-2.81**	**-2.58**	**-2.47**	**-1.85**	**-2.14**	**-1.94**	**-2.08**	**-2.04**	**-2.19**	**-2.35**	**-0.29**	**-0.36**	**-3.07**	**-3.25**	**-3.31**
Semi 1-1 (Steel, 1st Prime Mover)	02	Centre	Cloncurry	-0.59	-0.67	-0.77	-1.15	-1.35	-1.71	-1.77	-1.72	-1.38	-1.11	-0.91	-0.64	-0.51	-0.40	-0.58	-0.80	-1.14	-0.40	-0.63	-1.07	-0.12	-0.18	-1.58	-1.36	02-ST1_CL_crawl_CC
	08	0.6 m from kerb	Cloncurry	-1.23	-1.30	-1.47	-1.67	-1.60	-1.76	-1.48	-1.16	-0.83	-0.62	-0.45	-0.22	-0.13	-0.82	-1.06	-1.06	-0.98	-0.93	-1.10	-1.29	-0.09	-0.12	-1.25	-1.90	08-ST1_0.6_crawl_CC
	14	0.3 m from kerb	Cloncurry	-1.63	-1.70	-1.82	-2.06	-1.93	-1.97	-1.43	-1.07	-0.66	-0.46	-0.30	-0.11	-0.02	-1.07	-1.30	-1.27	-0.95	-1.26	-1.42	-1.58	-0.11	-0.12	-1.51	-1.84	14-ST1_0.3_crawl_CC
	05	Centre	Julia Creek	-0.55	-0.60	-0.70	-1.11	-1.28	-1.58	-1.61	-1.53	-1.10	-0.84	-0.62	-0.35	-0.21	-0.32	-0.54	-0.76	-1.05	-0.36	-0.57	-1.02	-0.11	-0.16	-1.85	-1.49	05-ST1_CL_crawl_JC
	11	0.6 m from kerb	Julia Creek	-0.17	-0.22	-0.22	-0.50	-0.69	-0.98	-1.32	-1.62	-1.44	-1.32	-1.21	-0.93	-0.82	-0.08	-0.20	-0.32	-0.89	-0.10	-0.18	-0.51	-0.10	-0.10	-1.52	-1.83	11-ST1_0.6_crawl_JC
	17	0.3 m from kerb	Julia Creek	-0.08	-0.11	-0.08	-0.34	-0.50	-0.77	-1.08	-1.57	-1.52	-1.45	-1.41	-1.16	-1.10	-0.04	-0.15	-0.21	-0.75	-0.06	-0.13	-0.41	-0.08	-0.08	-1.04	-1.68	17-ST1_0.3_crawl_JC
	Maximum deflections			**-1.63**	**-1.70**	**-1.82**	**-2.06**	**-1.93**	**-1.97**	**-1.77**	**-1.72**	**-1.52**	**-1.45**	**-1.41**	**-1.16**	**-1.10**	**-1.07**	**-1.30**	**-1.27**	**-1.14**	**-1.26**	**-1.42**	**-1.58**	**-0.12**	**-0.18**	**-1.85**	**-1.90**	**-2.06**
Semi 1-2 (Steel, 2nd Prime Mover)	71	Centre	Cloncurry	-0.62	-0.73	-0.81	-1.15	-1.34	-1.66	-1.68	-1.58	-1.22	-0.95	-0.73	-0.48	-0.29	-0.38	-0.62	-0.72	-1.07	-0.45	-0.66	-1.08	-0.08	-0.13	-1.55	-1.44	71-ST1b_CL_crawl_CC
	73	0.6 m from kerb	Cloncurry	-1.40	-1.45	-1.50	-1.69	-1.60	-1.68	-1.36	-1.02	-0.68	-0.48	-0.33	-0.15	-0.05	-0.93	-1.14	-0.91	-0.86	-1.11	-1.20	-1.28	-0.08	-0.10	-1.25	-1.21	73-ST1b_0.6_crawl_CC
	72	Centre	Julia Creek	-0.57	-0.67	-0.77	-1.10	-1.27	-1.62	-1.65	-1.60	-1.26	-1.00	-0.81	-0.54	-0.38	-0.36	-0.58	-0.69	-1.07	-0.43	-0.62	-1.01	-0.09	-0.12	-1.55	-1.38	72-ST1b_CL_crawl_JC
	74	0.6 m from kerb	Julia Creek	-0.14	-0.20	-0.20	-0.46	-0.64	-0.95	-1.26	-1.56	-1.43	-1.37	-1.37	-1.17	-1.08	-0.07	-0.18	-0.21	-0.81	-0.11	-0.20	-0.49	-0.08	-0.09	-1.16	-1.05	74-ST1b_0.6_crawl_JC
	Maximum deflections			**-1.40**	**-1.45**	**-1.50**	**-1.69**	**-1.60**	**-1.68**	**-1.68**	**-1.60**	**-1.43**	**-1.37**	**-1.37**	**-1.17**	**-1.08**	**-0.93**	**-1.14**	**-0.91**	**-1.07**	**-1.11**	**-1.20**	**-1.28**	**-0.09**	**-0.13**	**-1.55**	**-1.44**	**-1.69**
Semi 2 (Air)	03	Centre	Cloncurry	-0.90	-1.00	-1.17	-1.62	-1.82	-2.16	-2.18	-1.99	-1.52	-1.20	-0.93	-0.59	-0.43	-0.59	-0.85	-1.12	-1.41	-0.66	-0.96	-1.44	-0.16	-0.22	-2.10	-1.75	03-ST2_CL_crawl_CC
	09	0.6 m from kerb	Cloncurry	-1.46	-1.55	-1.71	-2.02	-1.96	-2.17	-1.82	-1.42	-0.97	-0.71	-0.50	-0.25	-0.13	-1.00	-1.28	-1.29	-1.17	-1.11	-1.35	-1.60	-0.13	-0.18	-1.78	-2.19	09-ST2_0.6_crawl_CC
	15	0.3 m from kerb	Cloncurry	-1.65	-1.72	-1.82	-2.07	-1.95	-1.99	-1.43	-1.07	-0.66	-0.46	-0.30	-0.11	-0.02	-1.11	-1.32	-1.27	-0.95	-1.27	-1.42	-1.58	-0.11	-0.12	-1.51	-1.84	15-ST2_0.3_crawl_CC
	06	Centre	Julia Creek	-0.72	-0.79	-0.93	-1.43	-1.69	-2.19	-2.26	-2.26	-1.76	-1.44	-1.14	-0.75	-0.57	-0.44	-0.72	-1.04	-1.50	-0.48	-0.77	-1.33	-0.17	-0.20	-1.35	-2.62	06-ST2_CL_crawl_JC
	12	0.6 m from kerb	Julia Creek	-0.30	-0.36	-0.42	-0.82	-1.03	-1.44	-1.88	-2.34	-2.08	-1.90	-1.78	-1.41	-1.28	-0.18	-0.36	-0.56	-1.28	-0.23	-0.37	-0.83	-0.16	-0.17	-0.61	-2.22	12-ST2_0.6_crawl_JC
	18	0.3 m from kerb	Julia Creek	-0.15	-0.19	-0.22	-0.54	-0.73	-1.07	-1.47	-2.10	-2.01	-1.90	-1.89	-1.58	-1.51	-0.09	-0.23	-0.37	-1.02	-0.09	-0.23	-0.61	-0.13	-0.14	-1.48	-1.90	18-ST2_0.3_crawl_JC
	Maximum deflections			**-1.65**	**-1.72**	**-1.82**	**-2.07**	**-1.96**	**-2.19**	**-2.26**	**-2.34**	**-2.08**	**-1.90**	**-1.89**	**-1.58**	**-1.51**	**-1.11**	**-1.32**	**-1.29**	**-1.50**	**-1.27**	**-1.42**	**-1.60**	**-0.17**	**-0.22**	**-2.10**	**-2.62**	**-2.62**
Road Train	75	Centre	Cloncurry	-0.68	-0.79	-0.89	-1.24	-1.44	-1.79	-1.76	-1.65	-1.27	-1.01	-0.80	-0.56	-0.40	-0.44	-0.68	-0.81	-1.12	-0.51	-0.72	-1.14	-0.12	-0.15	-1.68	-1.45	75-RT_CL_crawl_CC
	77	Lane	Cloncurry	-1.38	-1.44	-1.49	-1.69	-1.59	-1.70	-1.37	-1.03	-0.69	-0.50	-0.33	-0.24	-0.06	-0.93	-1.13	-0.94	-0.86	-1.10	-1.17	-1.26	-0.08	-0.08	-1.31	-1.13	77-RT_0.6_crawl_CC
	76	Centre	Julia Creek	-0.71	-0.82	-0.92	-1.27	-1.44	-1.75	-1.80	-1.65	-1.24	-0.96	-0.74	-0.46	-0.41	-0.47	-0.69	-0.82	-1.18	-0.51	-0.73	-1.15	-0.11	-0.14	-1.66	-1.46	76-RT_CL_crawl_JC
	78	Lane	Julia Creek	-0.15	-0.24	-0.25	-0.55	-0.72	-1.04	-1.41	-1.69	-1.57	-1.50	-1.43	-1.29	-1.15	-0.10	-0.24	-0.31	-0.94	-0.11	-0.24	-0.56	-0.09	-0.09	-0.99	-1.13	78-RT_0.6_crawl_JC
	Maximum deflections			**-1.65**	**-1.72**	**-1.82**	**-2.07**	**-1.96**	**-2.19**	**-2.26**	**-2.34**	**-2.08**	**-1.90**	**-1.89**	**-1.58**	**-1.51**	**-1.11**	**-1.32**	**-1.29**	**-1.50**	**-1.27**	**-1.42**	**-1.60**	**-0.17**	**-0.22**	**-2.10**	**-2.62**	**-2.62**

Table A 6: Canal Creek Bridge Summary of Peak Strain Responses (10 km/h and 20 km/h speed)

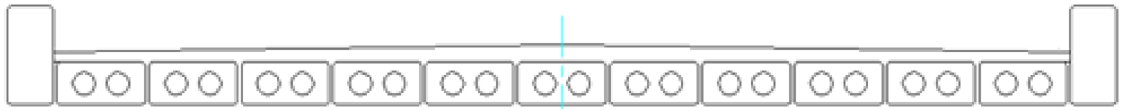

10 km/h				DU1 (kerb)	DU2	DU3	DU4	DU5	DU6	DU7	DU8	DU9	DU10	DU11	DU12	DU13 (kerb)									
Vehicle	**Run #**	**Location**	**Travel to**	LVDT1	LVDT2	LVDT3	LVDT4	LVDT5	LVDT6	LVDT7	LVDT8	LVDT9	LVDT10	LVDT11	LVDT12	LVDT13	LVDT14	LVDT15	LVDT16	LVDT20	LVDT21	LVDT22	LVDT23	LVDT24	File
Crane	21	Lane	Cloncurry	-2.25	-2.42	-2.68	-3.01	-2.93	-3.23	-3.03	-2.50	-1.84	-1.37	-1.04	-0.68	-0.46	-1.59	-2.07	-2.03	-2.41	-0.32	-0.36	-3.09	-2.81	21-CR_0.6_10_CC
	24	Lane	Julia Creek	-0.61	-0.78	-1.02	-1.52	-1.87	-2.51	-3.15	-3.39	-3.07	-2.84	-2.70	-2.35	-2.16	-0.41	-0.80	-1.28	-1.51	-0.35	-0.36	-3.16	-2.93	24-CR_0.6_10_JC
	Maximum deflections			**-0.61**	**-0.78**	**-1.02**	**-1.52**	**-1.87**	**-2.51**	**-3.03**	**-2.50**	**-1.84**	**-1.37**	**-1.04**	**-0.68**	**-0.46**	**-0.41**	**-0.80**	**-1.28**	**-1.51**	**-0.32**	**-0.36**	**-3.09**	**-2.81**	**-3.09**
Semi 1-1 (Steel, 1st Prime Mover)	22	Lane	Cloncurry	-1.27	-1.37	-1.57	-1.78	-1.74	-1.90	-1.59	-1.21	-0.90	-0.67	-0.50	-0.28	-0.17	-0.88	-1.23	-1.22	-1.40	-0.15	-0.12	-1.45	-1.86	22-ST1_0.6_10_CC
	25	Lane	Julia Creek	-0.27	-0.34	-0.40	-0.71	-0.91	-1.25	-1.63	-1.89	-1.71	-1.51	-1.39	-1.12	-0.95	-0.13	-0.34	-0.50	-0.71	-0.16	-0.18	-1.64	-1.88	25-ST1_0.6_10_JC
	Maximum deflections			**-0.27**	**-0.34**	**-0.40**	**-0.71**	**-0.91**	**-1.25**	**-1.59**	**-1.21**	**-0.90**	**-0.67**	**-0.50**	**-0.28**	**-0.17**	**-0.13**	**-0.34**	**-0.50**	**-0.71**	**-0.15**	**-0.12**	**-1.45**	**-1.86**	**-1.86**
Semi 1-1 (Steel, 2nd Prime Mover)	NA	Lane	Cloncurry																						NA
	NA	Lane	Julia Creek																						NA
	Maximum deflections																								
Semi 2 (Air)	23	Lane	Cloncurry	-1.45	-1.56	-1.76	-2.06	-2.05	-2.28	-1.93	-1.50	-1.11	-0.82	-0.58	-0.31	-0.17	-0.97	-1.38	-1.43	-1.73	-0.20	-0.23	-1.96	-2.08	23-ST2_0.6_10_CC
	26	Lane	Julia Creek	-0.28	-0.38	-0.47	-0.83	-1.06	-1.46	-1.95	-2.41	-2.17	-1.94	-1.77	-1.47	-1.27	-0.19	-0.41	-0.63	-0.83	-0.20	-0.18	-1.92	-2.02	26-ST2_0.6_10_JC
	Maximum deflections			**-0.28**	**-0.38**	**-0.47**	**-0.83**	**-1.06**	**-1.46**	**-1.93**	**-1.50**	**-1.11**	**-0.82**	**-0.58**	**-0.31**	**-0.17**	**-0.19**	**-0.41**	**-0.63**	**-0.83**	**-0.20**	**-0.18**	**-1.92**	**-2.02**	**-2.02**
Road Train	79	Lane	Cloncurry	-1.41	-1.49	-1.50	-1.67	-1.58	-1.66	-1.32	-0.98	-0.64	-0.44	-0.28	-0.11	-0.02	-0.96	-1.18	-0.95	-1.25	-0.08	-0.10	-1.44	-1.03	79-RT_0.6_10_CC
	80	Lane	Julia Creek	-0.18	-0.26	-0.29	-0.58	-0.75	-1.11	-1.52	-1.82	-1.69	-1.60	-1.54	-1.30	-1.19	-0.09	-0.27	-0.37	-0.72	-0.10	-0.11	-1.34	-1.17	80-RT_0.6_10_JC
	Maximum deflections			**-0.18**	**-0.26**	**-0.29**	**-0.58**	**-0.75**	**-1.11**	**-1.32**	**-0.98**	**-0.64**	**-0.44**	**-0.28**	**-0.11**	**-0.02**	**-0.09**	**-0.27**	**-0.37**	**-0.72**	**-0.08**	**-0.10**	**-1.34**	**-1.03**	**-1.34**

20 km/h				DU1 (kerb)	DU2	DU3	DU4	DU5	DU6	DU7	DU8	DU9	DU10	DU11	DU12	DU13 (kerb)									File name
Vehicle	**Run #**	**Location**	**Travel to**	LVDT1	LVDT2	LVDT3	LVDT4	LVDT5	LVDT6	LVDT7	LVDT8	LVDT9	LVDT10	LVDT11	LVDT12	LVDT13	LVDT14	LVDT15	LVDT16	LVDT20	LVDT21	LVDT22	LVDT23	LVDT24	
Crane	56	Centre	Cloncurry	-1.33	-1.53	-1.91	-2.55	-2.89	-3.29	-3.34	-3.44	-2.90	-2.31	-1.84	-1.38	-1.06	-0.89	-1.48	-2.02	-2.39	-0.37	-0.40	-3.62	-2.81	56-CR_CL_20_CC
	27	Lane	Cloncurry	-2.19	-2.39	-2.74	-3.14	-3.07	-3.41	-3.35	-2.84	-2.14	-1.62	-1.21	-0.79	-0.59	-1.55	-2.12	-2.17	-2.56	-0.36	-0.41	-3.47	-3.10	27-CR_0.6_20_CC
	62	Lane	Cloncurry	-2.23	-2.39	-2.73	-3.11	-3.07	-3.36	-3.23	-2.73	-2.09	-1.56	-1.16	-0.76	-0.54	-1.52	-2.07	-2.12	-2.50	-0.39	-0.41	-3.35	-2.78	62-CR_0.6_20_CC
	55	Centre	Julia Creek	-1.33	-1.55	-1.96	-2.58	-2.94	-3.40	-3.41	-3.46	-2.99	-2.41	-1.94	-1.51	-1.20	-0.90	-1.49	-2.05	-2.43	-0.39	-0.46	-3.33	-2.89	55-CR_CL_20_JC
	30	Lane	Julia Creek	-0.65	-0.81	-1.06	-1.57	-1.93	-2.61	-3.21	-3.40	-3.09	-2.86	-2.61	-2.22	-2.03	-0.42	-0.84	-1.30	-1.57	-0.35	-0.41	-3.40	-2.92	30-CR_0.6_20_JC
	59	Lane	Julia Creek	-0.76	-0.92	-1.23	-1.75	-2.15	-2.84	-3.40	-3.62	-3.29	-2.99	-2.75	-2.32	-2.05	-0.49	-0.94	-1.42	-1.77	-0.39	-0.45	-3.62	-2.91	59-CR_0.6_20_JC
	Maximum deflections			**-0.65**	**-0.81**	**-1.06**	**-1.57**	**-1.93**	**-2.61**	**-3.21**	**-2.73**	**-2.09**	**-1.56**	**-1.16**	**-0.76**	**-0.54**	**-0.42**	**-0.84**	**-1.30**	**-1.57**	**-0.35**	**-0.40**	**-3.33**	**-2.78**	**-3.33**
Semi 1-1 (Steel, 1st Prime Mover)	28	Lane	Cloncurry	-1.33	-1.43	-1.66	-1.92	-1.89	-2.10	-1.81	-1.43	-1.07	-0.80	-0.58	-0.37	-0.25	-0.93	-1.34	-1.43	-1.55	-0.19	-0.16	-1.65	-2.03	28-ST1a_0.6_20_CC
	31	Lane	Julia Creek	-0.27	-0.36	-0.45	-0.75	-0.96	-1.31	-1.75	-2.04	-1.85	-1.67	-1.48	-1.22	-1.03	-0.16	-0.39	-0.56	-0.73	-0.19	-0.17	-1.76	-1.96	31-ST1a_0.6_20_JC
	Maximum deflections			**-0.27**	**-0.36**	**-0.45**	**-0.75**	**-0.96**	**-1.31**	**-1.75**	**-1.43**	**-1.07**	**-0.80**	**-0.58**	**-0.37**	**-0.25**	**-0.16**	**-0.39**	**-0.56**	**-0.73**	**-0.19**	**-0.16**	**-1.65**	**-1.96**	**-1.96**
Semi 1-1 (Steel, 2nd Prime Mover)	63	Lane	Cloncurry	-1.14	-1.27	-1.58	-1.99	-2.14	-2.39	-2.30	-1.94	-1.49	-1.13	-0.87	-0.55	-0.40	-0.74	-1.14	-1.39	-1.63	-0.24	-0.21	-1.89	-1.31	63-ST1b_0.6_20_CC
	60	Lane	Julia Creek	-0.34	-0.43	-0.53	-0.84	-1.08	-1.48	-1.98	-2.28	-2.12	-1.88	-1.63	-1.34	-1.13	-0.20	-0.44	-0.58	-0.78	-0.21	-0.19	-1.90	-1.04	60-ST1b_0.6_20_JC
	Maximum deflections			**-0.34**	**-0.43**	**-0.53**	**-0.84**	**-1.08**	**-1.48**	**-1.98**	**-1.94**	**-1.49**	**-1.13**	**-0.87**	**-0.55**	**-0.40**	**-0.20**	**-0.44**	**-0.58**	**-0.78**	**-0.21**	**-0.19**	**-1.89**	**-1.04**	**-1.98**
Semi 2 (Air)	29	Lane	Cloncurry	-1.39	-1.51	-1.72	-2.06	-2.05	-2.28	-1.97	-1.54	-1.12	-0.81	-0.58	-0.32	-0.18	-0.91	-1.30	-1.39	-1.67	-0.18	-0.20	-2.05	-2.05	29-ST2_0.6_20_CC
	64	Lane	Cloncurry	-1.41	-1.52	-1.80	-2.05	-2.06	-2.24	-1.85	-1.43	-1.08	-0.80	-0.58	-0.31	-0.18	-0.91	-1.29	-1.41	-1.71	-0.20	-0.21	-2.01	-1.10	64-ST2_0.6_20_CC
	32	Lane	Julia Creek	-0.29	-0.39	-0.50	-0.84	-1.08	-1.50	-2.01	-2.41	-2.16	-1.93	-1.75	-1.47	-1.27	-0.17	-0.43	-0.66	-0.81	-0.20	-0.17	-1.98	-2.02	32-ST2_0.6_20_JC
	61	Lane	Julia Creek	-0.36	-0.45	-0.59	-0.91	-1.18	-1.60	-2.12	-2.49	-2.28	-2.02	-1.77	-1.47	-1.25	-0.24	-0.49	-0.70	-0.91	-0.25	-0.24	-2.01	-1.23	61-ST2_0.6_20_JC
	Maximum deflections			**-0.29**	**-0.39**	**-0.50**	**-0.84**	**-1.08**	**-1.50**	**-1.85**	**-1.43**	**-1.08**	**-0.80**	**-0.58**	**-0.31**	**-0.18**	**-0.17**	**-0.43**	**-0.66**	**-0.81**	**-0.18**	**-0.17**	**-1.98**	**-1.10**	**-1.98**
Road Train	81	Lane	Cloncurry	-1.58	-1.68	-1.74	-1.97	-1.87	-1.95	-1.60	-1.19	-0.82	-0.57	-0.41	-0.20	-0.08	-1.11	-1.35	-1.17	-1.48	-0.11	-0.12	-1.42	-1.20	81-RT_0.6_20_CC
	82	Lane	Julia Creek	-0.22	-0.31	-0.36	-0.66	-0.85	-1.21	-1.62	-1.95	-1.81	-1.73	-1.67	-1.41	-1.33	-0.14	-0.32	-0.43	-0.70	-0.11	-0.12	-1.46	-1.16	82-RT_0.6_20_JC
	Maximum deflections			**-0.22**	**-0.31**	**-0.36**	**-0.66**	**-0.85**	**-1.21**	**-1.60**	**-1.19**	**-0.82**	**-0.57**	**-0.41**	**-0.20**	**-0.08**	**-0.14**	**-0.32**	**-0.43**	**-0.70**	**-0.11**	**-0.12**	**-1.42**	**-1.16**	**-1.60**

A.2 Dawson River Bridge

Table A 7: Dawson River Bridge Summary of Peak Responses

			Girders								Headstock							
			Strain (με)				Deflection (mm)				Strain (με)				Deflection (mm)			
			CR1	RT1	RT2	MAX	CR1	RT1	RT2	MAX	CR1	RT1	RT2	MAX	CR1	RT1	RT2	MAX
		Max - static	65.20	65.98	67.08	67.08	5.20	5.01	4.97	5.20	6.74	7.05	7.95	7.95	1.13	1.47	1.41	1.47
		Max - dynamic	83.35	77.89	71.63	83.35	5.63	6.49	5.59	6.49	9.28	11.79	10.95	11.79	1.26	1.78	1.75	1.78
		Corresponding Speed	40	80	60	80	Max, 40	80	80	80	Max, 40	80	Max	80	60	80	80	80
		Travel	Lane	Lane	Lane	Lane	Lane	Lane	Lane	Lane	Lane	Lane	Lane	Lane	Lane	Lane	Lane	Lane
		Direction	D	R	D	D	R	R	R	R	R	R	R	R	D	R	R	R
Lane/ CL	Direction of travel		CR1	RT1	RT2	MAX	CR1	RT1	RT2	MAX	CR1	RT1	RT2	MAX	CR1	RT1	RT2	MAX
Lane	Duaringa	Max - dynamic	83.35	77.89	71.63	83.35	5.34	5.44	4.95	5.44	5.17	6.19	6.24	6.24	1.26	1.73	1.62	1.73
		static	61.95	65.98	67.08	67.08	4.72	4.64	4.57	4.72	4.88	7.05	6.06	7.05	1.13	1.46	1.19	1.46
		20km/h	75.17	73.19	68.58	75.17	4.87	5.16	4.92	5.16	4.44	5.72	6.24	6.24	1.19	1.64	1.53	1.64
		40km/h	83.35	77.89	68.89	83.35	5.34	5.44	4.80	5.44	5.17	5.78	6.24	6.24	1.13	1.65	1.53	1.65
		60km/h	78.98	70.12	71.63	78.98	4.92	5.03	4.93	5.03	4.59	6.07	6.06	6.07	1.26	1.71	1.59	1.71
		80km/h	74.65	68.06	69.88	74.65	4.59	4.86	4.87	4.87	4.76	6.19	5.97	6.19	1.14	1.65	1.52	1.65
		max	-	68.25	71.17	71.17	-	4.87	4.95	4.95	-	5.81	6.16	6.16	-	1.59	1.62	1.62
Lane	R'hampton	Max - dynamic	69.42	75.53	64.69	75.53	5.63	6.49	5.59	6.49	9.28	11.79	10.95	11.79	1.17	1.78	1.75	1.78
		static	65.20	53.58	57.40	65.20	5.20	5.01	4.97	5.20	6.74	6.37	7.95	7.95	1.05	1.47	1.41	1.47
		20km/h	67.72	58.24	57.34	67.72	5.40	5.52	5.21	5.52	7.01	7.86	8.49	8.49	1.12	1.56	1.49	1.56
		40km/h	69.34	57.48	60.33	69.34	5.63	5.31	5.42	5.63	9.28	9.33	9.49	9.49	1.17	1.55	1.54	1.55
		60km/h	66.93	67.45	59.02	67.45	4.96	5.75	5.17	5.75	7.62	10.04	10.14	10.14	1.17	1.44	1.46	1.46
		80km/h	69.42	75.53	64.59	75.53	4.99	6.49	5.59	6.49	7.86	11.79	10.95	11.79	1.05	1.78	1.55	1.78
		max	-	65.23	64.69	65.23	-	5.67	5.52	5.67	-	10.27	10.90	10.90	-	1.74	1.75	1.75
CL	Duaringa	Max - dynamic	63.99	63.91	58.26	63.99	2.40	3.09	2.62	3.09	4.68	6.09	5.51	6.09	0.10	0.31	0.19	0.31
		static	61.95	56.05	56.13	61.95	2.77	2.54	2.59	2.77	4.57	5.13	5.60	5.60	0.25	0.43	0.09	0.43
		20km/h	-	-	-	0.00	-	-	-	0.00	-	-	-	0.00	-	-	-	0.00
		40km/h	-	-	-	0.00	-	-	-	0.00	-	-	-	0.00	-	-	-	0.00
		60km/h				0.00				0.00				0.00				0.00
		80km/h	63.99	63.91	58.26	63.99	2.40	3.09	2.62	3.09	4.68	6.09	5.31	6.09	0.10	0.31	0.19	0.31
		max	-	-	-	0.00	-	-	-	0.00	-	-	-	0.00	-	-	-	0.00
CL	R'hampton	Max - dynamic	0.00	0.00	0.00	0.00	0.00	0.00	0.00	0.00	0.00	0.00	0.00	0.00	0.00	0.00	0.00	0.00
		static	64.45	50.95	56.09	64.45	2.31	2.32	2.63	2.63	5.11	4.58	5.20	5.20	0.05	0.28	0.26	0.28
		20km/h	-	-	-	0.00	-	-	-	0.00	-	-	-	0.00	-	-	-	0.00
		40km/h	-	-	-	0.00	-	-	-	0.00	-	-	-	0.00	-	-	-	0.00
		60km/h	-	-	-	0.00	-	-	-	0.00	-	-	-	0.00	-	-	-	0.00
		80km/h	-	-	-	0.00	-	-	-	0.00	-	-	-	0.00	-	-	-	0.00
		max	-	-	-	0.00	-	-	-	0.00	-	-	-	0.00	-	-	-	0.00

			Columns								Bearing Compression			
			Strain - Tension (με)				Strain - Compression (με)				Compression			
			CR1	RT1	RT2	MAX	CR1	RT1	RT2	MAX	CR1	RT1	RT2	MAX
		Max - static	27.92	36.02	33.72	36.02	-32.06	-45.92	-38.26	-45.92	-169.04	-183.42	-198.45	-198.45
		Max - dynamic	30.32	44.96	44.70	44.96	-36.65	-51.30	-49.89	-51.30	-178.27	-203.24	-205.20	-205.20
		Corresponding Speed	40	Max	Max	Max	40	80	40	80	20	20	20	20
		Travel	Lane	Lane	Lane	Lane	CL	CL	CL	CL	Lane	Lane	Lane	Lane
		Direction	R	D	D	D	S	R	S	R	D	D	D	D
Lane/ CL	Direction of travel		CR1	RT1	RT2	MAX	CR1	RT1	RT2	MAX	CR1	RT1	RT2	MAX
Lane	Duaringa	Max - dynamic	25.31	34.29	31.47	34.29	-36.65	-50.28	-48.28	-36.65	-178.27	-203.24	-205.20	-205.20
		static	21.24	30.68	24.68	30.68	-32.06	-45.92	-38.26	-32.06	-169.04	-183.42	-198.45	-198.45
		20km/h	21.70	34.21	30.55	34.21	-30.97	-47.59	-44.62	-30.97	-178.27	-201.97	-202.70	-202.70
		40km/h	24.43	31.90	28.77	31.90	-35.53	-45.56	-43.13	-35.53	-176.19	-203.24	-200.32	-203.24
		60km/h	25.31	33.09	31.41	33.09	-36.65	-49.24	-46.14	-36.65	-166.52	-202.77	-201.49	-201.49
		80km/h	20.94	34.29	31.47	34.29	-32.62	-50.28	-44.69	-32.62	-162.28	-185.58	205.05	205.05
		max		32.45	30.91	32.45		-46.49	-48.28	-48.28	-	-197.85	-205.20	-205.20
Lane	R'hampton	Max - dynamic	30.32	44.96	44.70	44.96	-36.29	-51.30	-49.89	-36.29	-169.19	-197.36	-174.03	-197.36
		static	27.92	36.02	33.72	36.02	-21.74	-26.75	-27.65	-21.74	-168.62	-165.52	-177.15	-177.15
		20km/h	26.64	38.88	33.90	38.88	-33.55	-46.70	-42.82	-33.55	-162.11	-178.28	-170.38	-178.28
		40km/h	30.32	38.49	35.07	38.49	-36.29	-46.19	-44.38	-36.29	-169.19	-165.13	-169.13	-169.19
		60km/h	28.64	30.47	32.91	32.91	-34.49	-39.16	-41.01	-34.49	-146.87	-175.86	-162.06	-175.86
		80km/h	26.49	44.31	37.55	44.31	-31.18	-51.30	-42.85	-31.18	-146.80	-197.36	-171.61	-197.36
		max		44.96	44.70	44.96		-50.13	-49.89	-49.89		-177.87	-174.03	-177.87
CL	Duaringa	Max - dynamic	2.59	8.57	2.81	8.57	-8.93	-13.94	-12.94	-8.93	-157.74	-168.31	-189.24	-189.24
		static	3.27	4.21	2.89	4.21	-12.38	-14.56	-10.90	-10.90	-165.48	-158.29	-177.45	-177.45
		20km/h	-	-	-	0.00	-	-	-	0.00	-	-	-	0.00
		40km/h	-	-	-	0.00	-	-	-	0.00	-	-	-	0.00
		60km/h	-	-	-	0.00	-	-	-	0.00	-	-	-	0.00
		80km/h	2.59	8.57	2.81	8.57	-8.93	-13.94	-12.94	-8.93	-157.74	-168.31	-189.24	-189.24
		max	-	-	-	0.00	-	-	-	0.00	-	-	-	0.00
CL	R'hampton	Max - dynamic	0.00	0.00	0.00	0.00	0.00	0.00	0.00	0.00	0.00	0.00	0.00	0.00
		static	4.95	9.52	7.85	9.52	-6.85	-15.28	-11.43	-6.85	159.09	-170.70	-172.99	-172.99
		20km/h	-	-	-	0.00	-	-	-	0.00	-	-	-	0.00
		40km/h	-	-	-	0.00	-	-	-	0.00	-	-	-	0.00
		60km/h	-	-	-	0.00	-	-	-	0.00	-	-	-	0.00
		80km/h	-	-	-	0.00	-	-	-	0.00	-	-	-	0.00
		max	-	-	-	0.00	-	-	-	0.00	-	-	-	0.00

Table A 8: Dawson River Bridge Peak Responses

Sensor type		Strain gauges (με)												Proximity probes (μm)								String potentiometers (mm)				Tilt meters (milli-degrees)			
Location		Pier P7						Span 8 girders, midspan						Span 7 girder end		Span 8 girder end						Pier headstock		Girder midspan		Pier headstock			
Sensor		P7CL-sg	P7CR-sg	P7HLS7-sg	P7HRS7-sg	P7HLS8-sg	P7HRS8-sg	S8G1m-sg	S8G2m-sg	S8G3m-sg	S8G4m-sg	S8G5m-sg	S8G6m-sg	S7G3e-p	S7G4e-p	S8G1e-p	S8G2e-p	S8G3e-p	S8G4e-p	S8G5e-p	S8G6e-p	P7HL-t1	P7-HR-t1	S8G1m-d	S8G6m-d	P7HL-t1	P7-HL-t1	P7-HR-t1	P7-HR-t1
STATIC	Max	62.235	30.676	5.2663	7.2166	7.7409	8.191	100.62	68.491	57.528	65.205	63.933	58.245	22.892	21.222	32.792	13.803	14.319	19.559	25.357	42.887	2.0064	1.6205	0.87286	0.69534	40.985	8.0679	9.6243	44.519
	Min	-55.826	-39.294	-2.3177	-3.6076	-2.4914	-5.3739	-4.5014	-5.438	-6.4012	-8.0364	-11.203	-19.71	-136.92	-151.25	-208.91	-185.7	-198.45	-164.84	-203.85	-241.14	-2.0323	-2.3887	-6.2317	-6.8276	-37.203	-6.1742	-10.413	-37.271
DYNAMIC	Max	44.96	34.289	5.1621	7.579	6.2406	11.793	83.351	74.984	62.653	82.637	78.301	75.531	85.826	47.629	17.868	6.12	7.621	7.17	13.111	34.715	1.4027	1.247	0.96643	0.47245	80.496	19.931	34.869	86.715
	Min	-50.281	-51.303	-3.1816	-2.4427	-3.3101	-4.1583	-8.6597	-8.4262	-8.6303	-7.3242	-9.6446	-17.533	-157.07	-159.39	-165.96	-176.99	-205.2	-197.34	-197.36	-169.55	-1.731	-1.7843	-5.3425	-6.4877	-74.281	-12.221	-19.445	-60.981
01-CR1_CL_CWL_D	Max	3.2173	3.2714	3.0355	4.5667	3.2916	3.3651	41.925	51.373	57.528	61.953	34.332	22.894	6.844	11.44	6.433	3.568	2.821	2.936	2.934	3.093	0.00492	0.062613	0.00629	0.03469	9.6398	5.778	5.3984	5.3151
	Min	-12.383	-2.4086	-1.7945	-1.6733	-2.1484	-3.4249	-3.2446	-3.9175	-3.9422	-3.9969	-2.5383	-5.5261	-116.26	-107.66	-83.467	-105.13	-165.48	-125.06	-87.766	-47.207	-0.2511	-0.00619	-2.7727	-1.8813	-6.1342	-3.8495	-4.3666	-8.6532
01-CR2_CL_CWL_D	Max	4.9472	3.835	3.0796	3.558	3.7603	3.1048	32.956	38.09	45.743	50.996	29.291	21.253	6.441	9.033	3.985	2.687	2.497	2.948	3.288	3.981	0.04487	0.013473	0.05881	0.02314	11.38	6.9177	8.7011	10.28
	Min	-9.0428	-5.025	-1.6504	-1.672	-1.8297	-3.4352	-2.9144	-3.1704	-4.4174	-4.094	-4.1689	-6.4073	-96.259	-98.167	-67.915	-84.813	-138.5	-112.25	-79.912	-48.619	-0.0261	-0.01803	-2.1092	-1.7879	-9.9014	-4.6167	-7.6429	-11.637
01-RT1_CL_CWL_D	Max	4.2081	3.6959	3.0972	4.6199	3.7039	5.1303	30.369	35.463	47.278	56.051	37.204	28.502	6.099	10.788	2.653	2.064	1.412	1.803	2.333	7.897	0.03745	0.006118	0.00938	0.00399	10.751	7.2037	8.5945	15.156
	Min	-6.2019	-14.564	-1.6828	-1.6701	-1.8261	-3.0697	-2.291	-3.3169	-4.2424	-2.6087	-3.0461	-4.7984	-108.6	-125.61	-58.247	-86.436	-158.29	-152.2	-106.57	-63.403	-0.0056	-0.42638	-1.9596	-2.543	-13.6	-4.1313	-5.0906	-8.9418
01-RT2_CL_CWL_D	Max	2.8246	2.8904	2.9901	4.8264	3.9431	5.5979	32.962	38.233	48.997	56.15	38.7	29.99	11.969	14.484	2.217	1.682	1.154	1.407	1.47	4.681	0.00523	0.011313	0.01027	0.00608	6.3937	7.7226	6.8398	10.439
	Min	-6.6854	-10.9	-1.5799	-1.8136	-1.7369	-1.6421	-2.3085	-2.1666	-3.1732	-3.0104	-3.1495	-3.31	-119.33	-127.82	-62.183	-96.518	-177.45	-160.09	-110.63	-64.819	-0.0238	-0.09339	-2.0927	-2.5879	-9.2263	-3.0371	-5.0502	-4.5516
02-CR1_CL_CWL_R	Max	4.1708	4.9511	3.8145	5.1145	3.846	4.4761	36.304	43.21	57.377	64.454	39.163	25.639	9.294	13.137	4.854	4.63	3.411	3.415	4.577	4.915	0.00742	0.00829	0.00705	0.01293	6.883	6.1103	6.2693	6.4006
	Min	-6.8492	-4.2489	-2.1655	-1.6755	-2.144	-2.5139	-2.9865	-4.0701	-4.3026	-3.5558	-3.3974	-6.5512	-113.61	-118.56	-71.246	-93.07	-159.09	-129.79	-94.723	-58.785	-0.0186	-0.04791	-2.306	-2.2441	-6.124	-4.7718	-7.5537	-6.3278
02-CR2_CL_CWL_R	Max	1.3405	4.7371	2.9572	4.3095	3.208	3.9411	28.594	32.852	47.245	52.387	33.221	24.102	9.877	13.251	2.637	2.161	2.482	2.582	2.377	2.417	0.0125	0.006524	0.01276	0.01884	6.3481	6.0977	6.7277	5.5841
	Min	-5.5595	-4.3129	-2.0728	-1.7305	-1.822	-3.2589	-3.3059	-3.2176	-3.6149	-3.1526	-3.4488	-5.9784	-93.123	-100.25	-59.163	-77.139	-127.92	-116.42	-89.523	-61.883	-0.0125	-0.07328	-1.7662	-2.1502	-6.316	-4.3401	-5.7843	-6.4195
02-RT1_CL_CWL_R	Max	3.4439	9.5218	4.0685	4.5714	4.517	4.5821	35.195	37.512	45.867	50.955	32.513	22.774	13.579	14.422	7.411	3.081	2.804	3.292	2.985	3.138	0.01371	0.15042	0.0225	0.14547	14.45	6.1151	7.5153	9.8187
	Min	-15.276	-4.0682	-1.6615	-1.9686	-1.673	-2.0079	-3.7948	-4.2379	-4.493	-2.7246	-3.0569	-4.8457	-128.92	-109.28	-66.889	-96.519	-170.7	-139.81	-94.115	-55.262	-0.2833	-0.00538	-2.3205	-2.0475	-8.0098	-5.2142	-6.0317	-12.724
02-RT2_CL_CWL_R	Max	7.8532	3.8214	3.6942	4.8456	4.9095	5.1978	34.093	37.501	48.69	56.09	37.549	26.31	17.626	15.355	2.153	3.794	4.714	4.506	4.51	5.573	0.18347	0.005356	0.09516	0.00587	9.7172	6.6115	8.4664	10.28
	Min	-5.7268	-11.429	-1.6358	-2.0944	-2.1805	-3.0022	-2.7773	-2.8889	-3.4699	-3.5305	-3.0012	-5.7401	-119.87	-133.74	-65.447	-96.406	-172.99	-156.39	-106.99	-60.227	-0.0055	-0.26214	-2.1208	-2.6271	-9.1018	-6.1742	-7.2316	-8.8375
03-CR1_LA_CWL_D	Max	4.4638	21.237	3.4745	3.0714	4.88	3.6896	74.505	66.916	56.439	40.162	19.762	9.2703	7.582	13.678	17.184	5.48	2.958	1.74	1.861	1.032	0.00952	0.87255	0.00608	0.32629	21.265	6.5659	6.9805	5.5513
	Min	-32.056	-2.0132	-1.9155	-1.6586	-1.61	-2.3004	-2.6147	-4.9736	-4.381	-2.9977	-2.5179	-4.9197	-122.22	-72.022	-150.22	-151.12	-169.04	-90.46	-54.139	-16.168	-1.1305	-0.00555	-4.7229	-0.47771	-7.1032	-3.1813	-4.3775	-20.647
03-CR2_LA_CWL_D	Max	2.5354	19.234	3.5232	2.754	4.2974	1.981	60.282	53.172	46.974	34.076	18.177	8.6949	4.901	9.563	11.888	4.174	3.531	1.803	1.919	1.931	0.00552	0.51522	0.00652	0.2415	20.383	5.9191	6.9811	5.0285
	Min	-27.305	-1.4963	-1.5568	-2.576	-1.7926	-3.059	-3.3081	-5.438	-2.8858	-2.1939	-1.6432	-3.2851	-101.7	-65.137	-125.91	-124.63	-143.67	-78.297	-46.981	-14.169	-0.8055	-0.00588	-3.8365	-0.3945	-5.3892	-3.9571	-3.9169	-20.217
03-RT1_LA_CWL_D	Max	2.0834	30.676	4.8011	3.3914	7.0524	4.6863	65.98	55.816	45.392	34.703	19.256	10.192	2.1	13.606	20.661	8.234	3.881	2.323	1.09	1.067	0.0204	1.0415	0.03156	0.35155	34.263	5.937	8.1509	5.5825
	Min	-45.917	-2.0237	-2.1389	-1.9986	-1.4476	-1.4937	-2.7396	-1.0737	-1.7979	-2.3773	-1.4636	-1.8281	-136.1	-67.894	-134.24	-156.97	-183.42	-86.377	-53.31	-17.933	-1.4606	-0.02629	-4.6444	-0.24345	-5.7887	-3.6402	-6.2531	-30.958
03-RT2_LA_CWL_D	Max	7.1155	24.676	4.2784	3.1028	6.0558	3.31	67.075	57.797	48.772	38.546	20.273	10.218	16.178	10.541	17.892	7.293	3.553	2.354	1.853	0.792	0.09471	0.81418	0.05264	0.27269	24.522	5.6263	6.8669	5.0173
	Min	-38.264	-1.7445	-1.8616	-1.6772	-1.0942	-2.53	-2.5555	-2.3231	-3.0479	-2.8543	-2.8674	-3.4619	-136.92	-76.459	-140.11	-168.21	-198.45	-98.246	-57.147	-17.208	-1.1883	-0.03962	-4.5724	-0.41531	-5.2785	-3.2546	-3.7131	-23.192
04-CR1_LA_CWL_R	Max	27.916	6.8406	2.27	6.4333	3.1226	6.7415	10.417	20.326	34.869	65.205	63.933	58.245	11.122	12.697	2.344	4.317	4.907	2.528	2.626	10.077	0.76709	0.008152	0.38421	0.00488	4.2511	6.499	6.3933	24.338
	Min	-1.6244	-21.739	-1.5	-1.9167	-1.4074	-3.2185	-2.0531	-1.9638	-2.0108	-2.5546	-3.5271	-11.825	-60.678	-131.5	-15.556	-45.883	-88.693	-137.87	-157.37	-168.62	-0.0059	-1.0533	-0.28079	-5.1971	-21.216	-4.0888	-6.2797	-3.8221
04-CR2_LA_CWL_R	Max	19.605	5.1389	2.3194	4.8384	2.1655	4.5992	10.956	17.707	29.558	52.776	48.753	43.422	7.003	12.672	3.039	3.953	3.256	3.521	4.028	10.447	0.47382	0.027814	0.12976	0.0364	9.3836	6.2849	7.8852	17.675
	Min	-3.8954	-18.651	-1.7606	-2.1016	-1.7545	-3.6008	-2.5838	-2.4233	-3.6518	-2.9645	-4.0166	-9.0982	-57.797	-109.83	-20.061	-44.747	-81.044	-117.48	-132.97	-131.45	-0.0742	-0.73869	-0.53824	-3.9866	-16.052	-5.6316	-8.3688	-8.3182
04-RT1_LA_CWL_R	Max	36.022	9.823	2.3477	6.1241	2.9368	6.3673	11.394	19.279	29.923	53.579	51.33	44.342	10.954	12.275	1.651	3.22	3.421	1.518	4.675	19.709	1.1721	0.03644	0.34353	0.01077	11.9	7.0757	8.3817	30.921
	Min	-4.8881	-26.747	-1.7823	-2.0259	-1.9432	-4.0427	-2.2857	-3.2009	-3.987	-3.5713	-6.4204	-13.558	-54.646	-144.82	-25.349	-51.98	-94.379	-149.08	-165.52	-139.49	-0.0259	-1.4677	-0.38847	-5.0052	-26.344	-5.0713	-7.8423	-11.718
04-RT2_LA_CWL_R	Max	33.718	5.909	2.8514	7.1231	3.6467	7.9511	13.761	20.893	33.485	57.295	52.734	43.942	7.593	18.248	4.515	3.771	2.684	1.459	3.053	20.11	0.96724	0.05548	0.2676	0.11527	8.894	8.0679	9.6243	29.662
	Min	-5.5325	-27.651	-1.9786	-1.8769	-1.4833	-1.8089	-2.4887	-3.4566	-3.2345	-2.9655	-4.9764	-12.408	-66.807	-151.25	-26.485	-57.229	-104.92	-164.84	-177.15	-144.19	-0.0788	-1.4125	-0.5434	-4.9717	-25.658	-5.1201	-7.0987	-8.86
05-CR1_KB_CWL_D	Max	3.8835	18.431	4.2359	2.8857	5.4916	2.4468	100.62	68.491	47.989	27.908	11.428	1.8143	5.807	13.171	30.945	9.671	3.161	3.12	2.846	17.715	0.00552	1.3288	0.00787	0.62639	31.037	5.8656	7.356	4.853
	Min	-42.907	-6.2692	-1.7941	-2.1443	-1.7084	-2.6332	-3.4227	-2.289	-3.0706	-2.3716	-2.0124	-3.3157	-124.89	-54.829	-204.96	-164.03	-159.54	-67.68	-29.954	-18.485	-1.7595	-0.00734	-6.1351	-0.00461	-5.4383	-4.7162	-4.698	-28.693
05-CR2_KB_CWL_D	Max	2.0502	15.532	4.2892	3.3658	5.4195	3.2733	75.493	54.411	44.427	27.949	13.544	4.3765	5.324	11.402	19.142	6.935	3.562	2.225	1.861	6.841	0.00645	0.83392	0.01221	0.17486	25.912	6.3347	7.8589	6.3357
	Min	-33.87	-1.6781	-1.6008	-1.5642	-1.1705	-1.4567	-2.9965	-1.3786	-1.3528	-1.6809	-1.8058	-2.5135	-105.28	-51.098	-153.16	-133.56	-141.34	-64.875	-34.539	-15.659	-1.0615	-0.00818	-4.5838	-0.06014	-6.2859	-4.897	-4.7441	-24.942
05-RT1_KB_CWL_D	Max	1.9251	20.236	4.9359	3.3227	7.7409	3.223	88.435	58.35	40.641	26.689	11.786	2.9552	1.913	15.768	28.467	12.159	4.132	1.587	1.106	14.881	0.01017	1.6205	0.07287	0.64233	40.985	5.8914	8.3111	4.3349
	Min	-55.535	-3.0036	-1.9641	-2.0173	-1.5191	-2.057	-2.6754	-1.6601	-1.369	-2.0808	-2.1044	-1.2248	-134.79	-48.032	-196.43	-172.74	-167.67	-64.513	-31.894	-22.419	-1.9988	-0.00826	-6.1391	-0.00767	-5.8669	-3.0748	-4.5179	-37.271
05-RT2_KB_CWL_D	Max	8.6742	20.951	5.2663	3.5465	7.523	3.0421	90.429	60.908	41.998	28.036	11.399	2.4307	17.138	10.874	32.792	13.803	6.444	4.735	4.157	16.25	0.0837	1.4763	0.11728	0.40829	38.977	5.3985	7.3835	5.6332
	Min	-55.826	-2.4992	-1.9737	-2.1935	-2.037	-2.8379	-4.5014	-3.1825	-2.8215	-3.3541	-1.8306	-1.4493	-136.46	-54.726	-208.91	-185.7	-180.46	-69.265	-32.743	-22.85	-2.0323	-0.02871	-6.2317	-0.01871	-5.6856	-3.0758	-3.7485	-33.745
06-CR2_KB_CWL_R	Max	27.265	6.6696	2.1123	5.848	1.9886	4.4782	4.5447	10.288	19.659	44.034	44.737	44.896	9.246	9.149	4.739	9.84	14.319	19.559	25.357	42.887	0.80818	0.067573	0.2678	0.69534	12.828	5.6429	6.1975	23.865
	Min	-6.145	-14.91	-2.3177	-1.502	-2.4914	-4.2218	-2.5053	-4.652	-6.4012	-8.0364	-11.203	-19.094	-44.554	-116.75	-15.661	-25.96	-54.981	-99.741	-125.94	-150.71	-0.0358	-1.0025	-0.0082	-4.4397	-20.76	-5.423	-9.6425	-13.029
06-RT1_KB_CWL_R	Max	62.235	5.5127	2.6958	7.2166	3.4817	8.191	2.6011	11.943	23.083	46.664	53.816	54.165	22.892	10.396	4.679	2.821	3.717	3.416	4.881	29.734	2.0064	0.009677	0.87286	0.00712	12.461	6.5637	8.0895	44.519
	Min	-2.6652	-26.337	-2.0842	-1.7434	-1.6583	-2.429	-2.1789	-2.2474	-3.9771	-4.7061	-7.1545	-18.986	-33.508	-144.3	-23.021	-33.879	-66.983	-135.58	-185.52	-224.37	-0.0046	-2.3887	-0.00814	-6.7559	-37.203	-5.2952	-5.0655	-12.449

Sensor type		Strain gauges (με)												Proximity probes (μm)								String potentiometers (mm)				Tilt meters (milli-degrees)			
Location		Pier P7						Span 8 girders, midspan						Span 7 girder end		Span 8 girder end						Pier headstock		Girder midspan		Pier headstock			
Sensor		P7CL-sg	P7CR-sg	P7HLS7-sg	P7HRS7-sg	P7HLS8-sg	P7HRS8-sg	S8G1m-sg	S8G2m-sg	S8G3m-sg	S8G4m-sg	S8G5m-sg	S8G6m-sg	S7G3e-p	S7G4e-p	S8G1e-p	S8G2e-p	S8G3e-p	S8G4e-p	S8G5e-p	S8G6e-p	P7HL-t1	P7-HR-t1	S8G1m-d	S8G6m-d	P7HL-t1	P7-HL-t1	P7-HR-t1	P7-HR-t1
STATIC	**Max**	**62.235**	**30.676**	**5.2663**	**7.2166**	**7.7409**	**8.191**	**100.62**	**68.491**	**57.528**	**65.205**	**63.933**	**58.245**	**22.892**	**21.222**	**32.792**	**13.803**	**14.319**	**19.559**	**25.357**	**42.887**	**2.0064**	**1.6205**	**0.87286**	**0.69534**	**40.985**	**8.0679**	**9.6243**	**44.519**
	Min	**-55.826**	**-39.294**	**-2.3177**	**-3.6076**	**-2.4914**	**-5.3739**	**-4.5014**	**-5.438**	**-6.4012**	**-8.0364**	**-11.203**	**-19.71**	**-136.92**	**-151.25**	**-208.91**	**-185.7**	**-198.45**	**-164.84**	**-203.85**	**-241.14**	**-2.0323**	**-2.3887**	**-6.2317**	**-6.8276**	**-37.203**	**-6.1742**	**-10.413**	**-37.271**
DYNAMIC	**Max**	**44.96**	**34.289**	**5.1621**	**7.579**	**6.2406**	**11.793**	**83.351**	**74.984**	**62.653**	**82.637**	**78.301**	**75.531**	**85.826**	**47.629**	**17.868**	**6.12**	**7.621**	**7.17**	**13.111**	**34.715**	**1.4027**	**1.247**	**0.96643**	**0.47245**	**80.496**	**19.931**	**34.869**	**86.715**
	Min	**-50.281**	**-51.303**	**-3.1816**	**-2.4427**	**-3.3101**	**-4.1583**	**-8.6597**	**-8.4262**	**-8.6303**	**-7.3242**	**-9.6446**	**-17.533**	**-157.07**	**-159.39**	**-165.96**	**-176.99**	**-205.2**	**-197.34**	**-197.36**	**-169.55**	**-1.731**	**-1.7843**	**-5.3425**	**-6.4877**	**-74.281**	**-12.221**	**-19.445**	**-60.981**
06-RT2_KB_CWL_R	Max	59.465	4.9427	2.435	6.8632	3.3118	7.9754	2.3645	12.014	25.324	50.737	57.04	51.185	11.446	21.222	4.563	4.988	3.296	1.074	3.651	30.256	1.6857	0.16093	0.67801	0.04341	10.47	7.2838	7.1905	41.058
	Min	-5.8853	-25.747	-2.195	-1.6368	-1.7682	-2.9446	-2.9155	-2.2157	-3.1458	-3.9429	-6.0497	-18.145	-45.754	-146.58	-23.237	-36.312	-73.604	-150.03	-203.85	-241.14	-0.2273	-2.0902	-0.06699	-6.8276	-33.749	-5.0267	-8.6665	-11.042
07-CR1_CL_80_D	Max	2.5924	2.3418	2.2566	4.3835	2.9192	4.6833	34.658	41.985	59.258	63.987	39.722	31.653	9.416	12.651	6.26	4.171	6.16	5.518	6.5	10.063	0.00645	0.006219	0.18773	0.25662	8.4717	15.934	17.09	10.59
	Min	-8.9276	-5.7082	-1.7134	-1.8565	-1.5608	-1.9067	-4.1819	-5.3549	-6.0419	-5.9926	-5.208	-6.8765	-106.98	-110.95	-69.54	-83.929	-157.74	-131.18	-91.2	-64.337	-0.0546	-0.10108	-2.1713	-2.3994	-9.9373	-8.0266	-10.556	-7.4703
07-CR2_CL_80_D	Max	4.6467	3.78	2.2449	3.776	4.3331	4.0551	34.559	42.276	48.819	52.464	35.994	28.47	8.393	12.947	8.719	5.119	4.643	4.146	4.703	6.625	0.04678	0.032216	0.1937	0.15681	13.514	13.482	17.208	13.868
	Min	-11.043	-4.82	-2.1351	-2.014	-2.0069	-1.8749	-4.8911	-5.5645	-5.2111	-4.4859	-3.746	-5.09	-108.41	-113.35	-68.581	-91.781	-154.36	-128.35	-90.497	-57.375	-0.0942	-0.00598	-2.1833	-2.1432	-13.074	-9.1508	-10.082	-11.152
07-RT1_CL_60_D	Max	8.5653	5.4812	2.583	4.5552	3.6865	6.0911	35.99	42.527	56.22	63.91	45.085	36.683	9.942	14.522	4.035	3.574	3.393	4.544	5.378	7.213	0.18068	0.061982	0.06945	0.02686	19.332	12.054	16.605	19.307
	Min	-8.8947	-13.939	-1.487	-1.5348	-1.4935	-1.8589	-1.4396	-3.653	-3.6996	-2.1997	-3.1646	-5.1665	-125.36	-136.78	-65.865	-94.526	-168.31	-153.96	-115.12	-72.887	-0.0383	-0.31292	-2.2705	-3.0901	-19.682	-6.9407	-7.8068	-17.576
07-RT2_CL_80_D	Max	2.8086	1.971	2.9746	4.1484	3.4588	5.5107	37.565	41.384	51.335	58.261	40.087	33.242	6.148	10.76	7.274	2.331	2.655	2.956	3.316	5.272	0.00879	0.008781	0.08934	0.05064	12.549	11.613	13.89	7.5744
	Min	-12.941	-7.139	-1.8554	-1.6916	-1.6212	-2.0793	-3.8452	-3.7862	-4.7147	-2.609	-2.0127	-4.4877	-125.65	-122.14	-68.626	-96.569	-189.24	-162.94	-102.08	-61.428	-0.1862	-0.00692	-2.3907	-2.6154	-6.0045	-5.4305	-9.1278	-9.6028
09-CR1_LA_80_D	Max	2.5999	20.942	3.6952	2.8538	4.7563	2.9561	74.646	70.19	60.138	38.999	19.09	9.896	8.308	13.92	12.437	4.872	6.625	7.17	7.743	9.731	0.00597	0.83472	0.32571	0.43079	31.725	19.656	14.321	11.404
	Min	-32.62	-2.7579	-1.6848	-1.5762	-1.8337	-1.9739	-6.4042	-7.2797	-5.6224	-4.1113	-4.3503	-5.704	-116.59	-68.58	-142.26	-137.03	-162.28	-83.43	-46.657	-13.369	-1.137	-0.00448	-4.5863	-0.32721	-11.801	-10.194	-7.0451	-31.532
09-CR2_LA_80_D	Max	6.0549	22.566	3.7875	2.6601	4.1601	3.8875	66.87	62.31	50.855	41.813	22.971	13.488	7.747	12.142	7.709	3.289	2.74	3.202	3.639	5.672	0.0238	0.7716	0.03261	0.21099	59.834	19.931	12.196	17.774
	Min	-34.095	-5.4037	-1.5425	-2.3199	-1.9299	-1.9925	-2.3102	-2.9403	-2.265	-2.1571	-2.6386	-3.8218	-118.75	-80.358	-138.49	-141.31	-171.36	-99.198	-57.061	-18.328	-1.0542	-0.0261	-4.4304	-0.77101	-17.828	-12.221	-9.1572	-53.827
09-RT1_LA_80_D	Max	5.8188	34.289	4.3472	3.8849	6.1896	4.228	68.057	57.858	47.519	37.132	21.122	12.214	7.533	16.502	14.078	6.12	3.825	3.892	3.728	3.87	0.00483	1.2347	0.06916	0.40855	52.761	13.17	10.342	19.42
	Min	-50.281	-4.8012	-1.4328	-1.5951	-1.7604	-1.962	-2.5331	-3.7722	-3.1413	-2.2083	-2.0676	-3.9361	-157.07	-77.898	-138.42	-147.78	-185.58	-91.408	-52.972	-21.93	-1.6502	-0.00537	-4.8578	-0.49145	-16.61	-9.257	-8.6236	-46.872
09-RT2_LA_80_D	Max	2.6599	31.466	4.0209	2.872	5.9698	4.1384	69.877	59.076	51.302	40.257	21.406	12.715	7.039	14.019	15.052	5.215	4.552	4.439	3.662	11.839	0.00596	1.0529	0.15595	0.43987	39.38	14.493	9.5684	10.261
	Min	-44.69	-2.3443	-1.8591	-2.008	-2.0302	-1.6416	-5.0829	-5.9741	-5.8983	-4.1627	-2.6436	-5.5952	-150.36	-76.481	-141.25	-162.69	-205.05	-97.961	-52.538	-22.661	-1.523	-0.00521	-4.873	-0.44513	-10.226	-9.4177	-7.9756	-38.677
10-CR1_LA_80_R	Max	26.494	2.4281	1.6945	6.6588	2.5192	7.8623	14.258	23.97	41.043	69.418	68.302	66.2	12.574	11.141	3.642	3.172	5.139	4.348	6.701	18.271	0.71651	0.006784	0.60183	0.05791	10.477	10.119	22.988	38.921
	Min	-2.1356	-31.182	-1.4755	-1.5912	-1.2608	-1.6477	-4.4616	-4.3598	-4.1374	-3.2319	-3.6376	-7.6498	-59.126	-121.76	-23.458	-49.128	-95.461	-136.25	-146.8	-141.53	-0.0155	-1.0511	-0.55517	-4.9921	-36.189	-7.9314	-13.758	-11.756
10-CR2_LA_80_R	Max	20.538	7.5514	1.9473	5.4695	2.9038	7.2484	17.294	27.488	42.197	64.915	61.735	57.688	9.947	12.966	4.47	3.752	3.224	3.458	7.718	16.381	0.57264	0.093713	0.48597	0.05726	27.905	12.453	27.714	33.394
	Min	-6.5321	-27.569	-1.4227	-1.4805	-1.9762	-2.1116	-4.3864	-4.7124	-4.5834	-3.7054	-4.0149	-7.5118	-76.253	-136.23	-32.93	-63.548	-122.28	-157.14	-158.08	-130.62	-0.1134	-0.87419	-0.86503	-4.7137	-29.582	-11.913	-18.289	-24.158
10-RT1_LA_80_R	Max	44.308	6.4571	2.1768	6.4231	3.9474	11.793	19.904	31.945	48.043	74.519	75.43	75.531	9.815	12.291	4.524	5.156	7.621	6.363	12.037	26.292	1.3454	0.061405	0.66005	0.08433	27.03	11.032	34.869	83.225
	Min	-5.8523	-51.303	-1.8432	-2.1269	-1.6926	-2.2475	-4.4962	-5.0745	-5.437	-5.2215	-7.2801	-11.749	-73.785	-156.51	-39.076	-72.544	-135.38	-197.34	-197.36	-166.81	-0.0526	-1.7843	-0.82395	-6.4877	-67.697	-7.6361	-18.475	-21.2
10-RT2_LA_80_R	Max	37.549	3.8855	1.9473	7.1673	3.8059	10.948	15.099	23.775	36.088	60.826	59.228	64.588	9.954	10.055	3.978	3.131	3.457	2.524	7.189	23.092	1.2056	0.005618	0.51639	0.00378	8.9829	9.3831	17.391	44.599
	Min	-2.4912	-42.855	-1.6227	-2.4427	-1.4841	-2.1323	-2.2107	-2.1847	-2.5519	-2.3036	-4.1523	-9.1616	-67.146	-158.25	-28.322	-54.169	-104.14	-162.78	-171.61	-153.31	-0.0054	-1.5502	-0.44861	-5.5912	-40.448	-4.6867	-13.437	-9.7552
11-RT1_LA_95_D	Max	6.747	32.454	4.0296	3.28	5.8124	4.5048	68.247	58.141	46.707	35.945	19.007	9.7313	6.714	11.826	14.343	4.946	4.449	4.528	4.454	4.971	0.01824	1.1428	0.21743	0.47245	80.496	17.894	13.734	24.257
	Min	-48.493	-6.3861	-2.0604	-2.01	-1.6776	-1.6852	-5.4031	-7.4591	-4.8029	-3.0955	-3.0234	-3.3987	-154.29	-78.574	-139.76	-153.05	-197.85	-87.272	-48.346	-17.229	-1.5888	-0.04984	-4.8746	-0.36455	-18.65	-11.688	-7.3606	-58.345
11-RT2_LA_105_D	Max	2.6887	30.914	4.2847	3.1247	6.1632	3.7517	71.172	61.224	51.127	40.067	21.252	10.747	8.858	13.07	15.154	5.688	1.604	2.034	3.475	4.51	0.00442	1.1708	0.00471	0.36477	54.119	16.882	13.477	15.216
	Min	-48.281	-4.056	-1.8053	-1.5953	-1.9868	-2.1383	-2.0781	-4.2659	-4.3126	-2.5926	-3.7084	-3.9928	-144.54	-71.93	-140.95	-165.61	-205.2	-100.07	-52.025	-19.39	-1.6206	-0.00536	-4.9533	-0.47023	-15.888	-11.77	-7.6237	-49.906
12-RT1_LA_100_R	Max	44.96	4.9086	1.5759	6.6952	3.621	10.271	15.849	27.628	42.861	62.696	62.987	65.226	6.824	9.497	5.028	5.058	6.764	4.019	7.626	18.21	1.2858	0.013691	0.74663	0.16013	24.996	10.574	23.262	86.715
	Min	-4.8496	-50.131	-1.8441	-2.3648	-1.459	-2.5092	-5.2313	-5.172	-4.7787	-4.3136	-4.3727	-9.7337	-66.776	-143.1	-34.772	-59.342	-113.64	-166.08	-177.87	-149.19	-0.0692	-1.7382	-0.54237	-5.6729	-74.281	-6.8154	-17.428	-24.976
12-RT2_LA_105_R	Max	44.704	3.3439	1.4321	7.579	3.3329	10.904	15.412	24.278	38.021	62.839	61.821	64.687	8.493	9.013	4.313	3.168	6.352	4.527	10.17	34.715	1.4027	0.019405	0.70377	0.06839	14.958	8.933	22.072	64.442
	Min	-3.0464	-49.886	-1.7879	-2.031	-1.7471	-2.8358	-4.6577	-3.1816	-4.9491	-3.9211	-4.4794	-11.773	-56.707	-156.39	-36.187	-55.132	-100.25	-159.27	-174.03	-147.09	-0.0094	-1.7542	-0.55923	-5.5186	-54.633	-6.4093	-19.445	-17.776
13-CR1_KB_CWL_R	Max	34.81	6.8463	2.0067	4.6424	2.2542	5.2361	1.9514	11.061	23.103	54.875	57.279	52.53	15.105	10.943	8.586	4.435	5.441	3.839	5.819	10.992	1.3795	0.005417	0.65471	0.00422	4.5936	5.8266	5.3996	32.187
	Min	-6.9497	-39.294	-2.2133	-3.6076	-2.0258	-5.3739	-2.7786	-2.9789	-4.6666	-5.5452	-8.2706	-19.71	-46.395	-134.56	-18.014	-28.765	-67.859	-128.46	-172.08	-214.31	-0.0065	-1.6844	-0.00629	-6.4538	-27.911	-5.0102	-10.413	-4.5882
14-CR1_LA_60_D	Max	4.5554	25.311	4.1756	2.4147	4.5907	3.7758	78.98	68.611	58.251	38.579	19.409	9.7533	9.639	11.215	14.485	4.467	1.678	1.687	2.236	5.239	0.004	0.94932	0.02733	0.41715	37.648	16.07	10.332	7.0476
	Min	-36.645	-3.819	-1.6044	-1.5553	-1.6393	-1.3042	-2.1205	-4.2287	-3.7287	-2.1214	-2.3714	-3.1267	-118.66	-66.385	-153.02	-141.13	-166.52	-84.913	-45.264	-14.461	-1.26	-0.00588	-4.9217	-0.38785	-6.8446	-9.2038	-5.156	-39.193
14-CR2_LA_60_D	Max	5.3479	23.971	3.5728	3.1998	4.6446	3.2506	70.072	69.851	62.653	46.725	23.892	13.267	10.266	10.767	7.47	2.433	1.679	2.116	2.546	3.795	0.03851	0.82073	0.00818	0.30901	63.852	15.833	17.809	16.903
	Min	-35.552	-4.7588	-1.5572	-1.9802	-1.8454	-1.8794	-2.0282	-4.5092	-3.2468	-1.8749	-2.5175	-3.4826	-126.73	-87.233	-136.63	-147.77	-184.52	-102.78	-57.254	-21.805	-1.1645	-0.03797	-4.4408	-0.83499	-17.781	-8.5474	-13.459	-60.981
15-CR1_LA_60_R	Max	28.636	2.0914	1.6386	6.3262	2.8687	7.6238	11.488	20.747	36.96	66.934	64.905	61.312	10.478	10.911	1.606	2.278	2.764	2.683	5.88	18.832	0.85035	0.005149	0.51309	0.02415	10.56	7.5209	18.486	35.281
	Min	-2.104	-34.489	-1.7314	-1.9238	-1.4013	-1.9862	-1.6018	-2.8525	-2.4804	-2.0855	-3.1048	-10.118	-58.722	-129.89	-19.394	-45.922	-87.736	-131.52	-146.82	-146.87	-0.0037	-1.1676	-0.42991	-4.9589	-30.537	-7.547	-14.055	-11.746
15-CR2_LA_60_R	Max	22.627	7.1514	2.1142	5.4182	3.0294	8.6575	20.734	33.025	54.139	82.637	78.301	74.891	9.353	11.852	2.965	2.218	1.708	1.656	4.429	14.254	0.60539	0.12944	0.32989	0.08066	25.122	13.55	26.385	36.972
	Min	-6.9035	-28.469	-1.5658	-1.9818	-1.4006	-2.7125	-2.8057	-3.1953	-3.0615	-2.183	-3.4994	-9.019	-74.347	-137.15	-35.735	-73.782	-134.09	-171.04	-179.77	-169.55	-0.1206	-0.88686	-0.96711	-6.1123	-34.182	-9.6997	-14.195	-26.867

Sensor type		Strain gauges (με)											
Location		Pier P7						Span 8 girders, midspan					
Sensor		P7CL-sg	P7CR-sg	P7HLS7-sg	P7HRS7-sg	P7HLS8-sg	P7HRS8-sg	S8G1m-sg	S8G2m-sg	S8G3m-sg	S8G4m-sg	S8G5m-sg	S8G6m-sg
STATIC	**Max**	**62.235**	**30.676**	**5.2663**	**7.2166**	**7.7409**	**8.191**	**100.62**	**68.491**	**57.528**	**65.205**	**63.933**	**58.245**
	Min	**-55.826**	**-39.294**	**-2.3177**	**-3.6076**	**-2.4914**	**-5.3739**	**-4.5014**	**-5.438**	**-6.4012**	**-8.0364**	**-11.203**	**-19.71**
DYNAMIC	**Max**	**44.96**	**34.289**	**5.1621**	**7.579**	**6.2406**	**11.793**	**83.351**	**74.984**	**62.653**	**82.637**	**78.301**	**75.531**
	Min	**-50.281**	**-51.303**	**-3.1816**	**-2.4427**	**-3.3101**	**-4.1583**	**-8.6597**	**-8.4262**	**-8.6303**	**-7.3242**	**-9.6446**	**-17.533**
16-RT1_LA_60_D	Max	4.8959	33.085	4.0999	2.9003	6.0711	3.487	70.122	61.611	54.038	41.519	22.739	12.749
	Min	-49.244	-4.5952	-1.3401	-2.2297	-2.3389	-2.703	-5.1882	-7.769	-5.6817	-4.011	-4.2806	-5.5714
16-RT2_LA_60_D	Max	3.3678	31.413	5.1621	2.4965	6.0601	4.1512	71.628	58.513	50.753	39.611	20.875	11.225
	Min	-46.142	-2.1969	-1.3279	-2.3335	-1.7299	-2.0388	-2.0724	-4.9274	-4.0874	-2.3987	-2.915	-3.765
17-RT1_LA_60_R	Max	30.472	5.0242	2.24	5.8871	3.0208	10.035	15.683	26.967	43.854	67.449	63.3	59.662
	Min	-5.4976	-39.156	-1.89	-2.0129	-1.9592	-2.3345	-2.3269	-2.9634	-3.8857	-3.1307	-5.87	-13.188
17-RT2_LA_60_R	Max	32.909	2.8601	1.6175	7.1374	3.2382	10.14	14.241	22.266	37.372	59.023	54.422	52.305
	Min	-3.1712	-41.01	-1.4525	-1.9726	-1.4918	-2.3403	-2.4585	-3.584	-4.688	-4.7174	-5.8978	-13.795
18-CR1_LA_40_D	Max	2.762	24.431	4.0795	2.9819	5.17	3.5246	83.351	74.984	61.706	42.886	24.859	17.646
	Min	-35.528	-1.5787	-1.7105	-2.1081	-2.13	-1.7054	-7.0086	-8.4262	-6.4137	-7.3242	-6.6909	-6.5441
18-CR2_LA_40_D	Max	5.8702	24.197	3.6543	2.1473	4.6678	3.0194	62.473	57.842	52.571	38.065	19.346	11.978
	Min	-33.83	-4.3331	-1.4257	-1.9827	-1.5622	-2.0106	-4.0367	-5.6475	-6.6995	-5.4053	-6.5644	-8.5922
18-RT1_LA_40_D	Max	21.868	21.142	3.0584	2.3144	4.5399	2.7681	78.352	65.666	55.231	42.083	23.742	14.135
	Min	-31.112	-16.888	-3.1816	-1.9556	-3.3101	-2.9619	-4.4078	-6.4235	-4.5287	-3.1367	-4.4785	-7.5546
18-RT2_LA_40_D	Max	5.3839	28.768	4.3804	3.0086	6.2406	3.7905	68.892	57.938	51.626	39.122	20.513	9.541
	Min	-43.126	-4.3916	-1.2596	-1.6714	-1.9594	-1.8995	-1.9976	-4.8424	-3.914	-2.1785	-2.4769	-3.189
19-CR1_LA_40_R	Max	30.32	2.5991	2.193	6.0072	2.356	9.275	13.03	20.756	35.337	67.203	69.342	68.824
	Min	-2.5803	-36.291	-2.027	-2.0428	-1.214	-2.045	-8.6597	-8.3138	-6.9225	-4.8872	-5.7181	-14.086
19-CR2_LA_40_R	Max	22.132	3.6979	2.2557	5.3919	2.4209	6.5488	14.287	22.539	35.416	57.111	53.873	50.812
	Min	-3.9283	-28.152	-1.5243	-1.6981	-1.5091	-2.0112	-2.1631	-3.2709	-3.4737	-2.9085	-4.7873	-11.668
19-RT1_LA_40_R	Max	38.488	4.3305	1.9652	6.2137	2.894	9.3323	17.594	23.891	34.83	57.477	56.515	53.907
	Min	-5.1318	-46.19	-1.5148	-2.2363	-1.276	-2.7477	-2.7359	-6.4392	-8.6303	-6.9728	-9.6446	-17.533
19-RT2_LA_40_R	Max	35.066	3.1123	1.6868	6.5395	2.8466	9.4883	12.989	22.196	35.724	60.332	56.139	51.54
	Min	-4.3243	-44.378	-1.3832	-2.3605	-1.3734	-2.7917	-1.6505	-2.9545	-3.4159	-2.5477	-5.0808	-13.1
20-CR1_LA_20_D	Max	4.3954	21.205	4.0992	2.791	4.4392	2.3305	75.169	68.63	58.528	40.821	20.151	9.3108
	Min	-30.365	-3.4045	-2.1308	-1.889	-2.4008	-2.6995	-2.9009	-5.2704	-4.4022	-2.4489	-2.8394	-4.4692
20-CR2_LA_20_D	Max	12.531	12.195	2.64	2.034	3.6928	2.3398	60.729	54.52	49.836	37.55	18.996	9.2521
	Min	-18.409	-9.9947	-2.29	-2.046	-3.0072	-2.3402	-3.1607	-5.3396	-3.9942	-2.7903	-3.1841	-3.9779
20-RT1_LA_20_D	Max	13.123	27.462	3.7309	2.9443	5.4013	3.5444	73.487	63.823	53.646	41.017	20.595	9.4205
	Min	-40.007	-10.718	-1.9091	-1.5357	-1.8387	-2.4856	-2.7729	-7.0574	-5.1142	-3.6534	-3.6551	-4.3695
20-RT2_LA_20_D	Max	8.2652	25.698	4.1833	2.9449	6.0371	3.4139	68.737	54.953	48.8	37.95	19.228	8.5706
	Min	-39.125	-7.0125	-2.1067	-1.0851	-2.0629	-2.1161	-2.4428	-5.5672	-4.1305	-2.4001	-2.8622	-3.6094
21-CR1_LA_20_R	Max	26.639	1.8711	1.9856	5.433	3.0393	7.0065	10.159	20.475	37.136	67.719	66.903	61.29
	Min	-1.4307	-33.549	-1.4344	-2.107	-1.3407	-2.8535	-1.4614	-3.1148	-3.1138	-2.9113	-4.7866	-13.77
21-CR2_LA_20_R	Max	22.753	2.3756	2.0589	4.5013	2.2663	6.8064	15.646	25.381	42.855	72.862	67.547	58.035
	Min	-2.8571	-29.174	-1.5611	-2.1887	-1.8037	-3.0036	-2.3135	-3.3885	-3.2753	-2.3977	-4.0428	-11.135
21-RT1_LA_20_R	Max	38.878	3.3589	1.8207	6.0092	3.1138	7.8617	12.998	22.135	35.762	58.244	56.732	48.4
	Min	-4.1919	-46.701	-2.0593	-2.2908	-1.4662	-4.1583	-2.0519	-3.9146	-4.188	-3.3359	-6.3079	-15.8
21-RT2_LA_20_R	Max	33.897	2.1602	1.7891	6.344	2.7457	8.4877	12.033	20.029	34.093	57.337	53.92	44.334
	Min	-3.2333	-42.82	-1.6409	-1.706	-1.3243	-2.7323	-1.5571	-3.5606	-3.6869	-2.9833	-5.4899	-13.766

Sensor type		Proximity probes (μm)								String potentiometers (mm)				Tilt meters (milli-degrees)			
Location		Span 7 girder end		Span 8 girder end						Pier headstock		Girder midspan		Pier headstock			
Sensor		S7G3e-p	S7G4e-p	S8G1e-p	S8G2e-p	S8G3e-p	S8G4e-p	S8G5e-p	S8G6e-p	P7HL-t1	P7-HR-t1	S8G1m-d	S8G6m-d	P7HL-t1	P7-HL-t1	P7-HR-t1	P7-HR-t1
STATIC	**Max**	**22.892**	**21.222**	**32.792**	**13.803**	**14.319**	**19.559**	**25.357**	**42.887**	**2.0064**	**1.6205**	**0.87286**	**0.69534**	**40.985**	**8.0679**	**9.6243**	**44.519**
	Min	**-136.92**	**-151.25**	**-208.91**	**-185.7**	**-198.45**	**-164.84**	**-203.85**	**-241.14**	**-2.0323**	**-2.3887**	**-6.2317**	**-6.8276**	**-37.203**	**-6.1742**	**-10.413**	**-37.271**
DYNAMIC	**Max**	**85.826**	**47.629**	**17.868**	**6.12**	**7.621**	**7.17**	**13.111**	**34.715**	**1.4027**	**1.247**	**0.96643**	**0.47245**	**80.496**	**19.931**	**34.869**	**86.715**
	Min	**-157.07**	**-159.39**	**-165.96**	**-176.99**	**-205.2**	**-197.34**	**-197.36**	**-169.55**	**-1.731**	**-1.7843**	**-5.3425**	**-6.4877**	**-74.281**	**-12.221**	**-19.445**	**-60.981**
16-RT1_LA_60_D	Max	13.998	21.002	14.804	4.57	2.63	4.308	5.646	7.978	0.00804	1.247	0.11644	0.40688	56.509	10.922	13.726	12.731
	Min	-146.9	-83.098	-140.3	-165.93	-202.77	-103.09	-55.954	-23.422	-1.731	-0.02559	-5.0306	-0.53512	-13.803	-6.1547	-5.1811	-54.131
16-RT2_LA_60_D	Max	10.093	13.56	13.729	4.993	0.91	1.293	1.323	6.164	0.00283	1.1233	0.00395	0.38686	42.29	12.197	9.1615	7.5695
	Min	-145.61	-72.94	-145.67	-164.21	-203.49	-97.407	-50.077	-22.636	-1.5852	-0.00384	-4.9321	-0.53114	-6.9037	-4.7708	-4.2665	-40.686
17-RT1_LA_60_R	Max	10.151	11.464	3.358	4.081	3.834	1.739	6.918	23.97	1.0816	0.004003	0.43009	0.04099	13.378	9.5735	18.141	39.419
	Min	-69.449	-154.24	-31.342	-61.819	-122.47	-175.86	-174.58	-142.53	-0.0044	-1.4394	-0.56191	-5.753	-31.535	-6.5491	-9.991	-11.652
17-RT2_LA_60_R	Max	9.117	9.71	2.561	2.34	4.218	4.103	7.617	25.691	1.0878	0.004012	0.48048	0.00701	5.4626	6.3389	11.897	32.296
	Min	-65.783	-159.39	-29.039	-50.86	-103.48	-160.3	-162.08	-130.61	-0.0052	-1.4631	-0.47752	-5.168	-26.399	-4.4416	-9.1793	-5.9555
18-CR1_LA_40_D	Max	11.425	15.241	17.868	5.977	3.707	3.464	6.349	9.813	0.00408	0.77899	0.26045	0.39766	31.914	10.346	8.1961	3.8511
	Min	-127.28	-76.259	-163.33	-149.72	-176.19	-94.836	-52.751	-24.587	-1.1269	-0.00441	-5.3425	-0.84834	-3.8094	-7.1581	-4.4979	-29.51
18-CR2_LA_40_D	Max	5.603	9.901	9.178	3.296	3.376	3.179	6.04	9.624	0.00907	0.79044	0.12818	0.25875	46.814	10.906	10.446	16.643
	Min	-112.3	-74.599	-129.92	-125.4	-148.42	-83.421	-46.36	-21.776	-1.0769	-0.01976	-4.1298	-0.77025	-16.855	-6.354	-9.782	-44.177
18-RT1_LA_40_D	Max	85.826	47.629	8.635	2.41	4.061	3.628	11.894	19.765	0.44153	0.84698	0.31569	0.26348	41.02	9.9221	9.2351	12.946
	Min	-60.674	-34.071	-165.96	-176.99	-201.94	-98.672	-46.906	-11.435	-1.1915	-0.35692	-5.2613	-0.89152	-10.395	-5.4815	-5.2109	-36.209
18-RT2_LA_40_D	Max	11.138	10.674	14.992	4.851	1.28	1.413	2.088	3.831	0.00332	1.0698	0.02126	0.32704	36.882	7.4737	9.8459	7.0255
	Min	-141.16	-75.126	-142.21	-162.05	-200.32	-95.987	-49.912	-17.969	-1.5277	-0.00681	-4.7987	-0.47096	-7.5963	-4.014	-5.2921	-35.762
19-CR1_LA_40_R	Max	17.501	11.721	7.03	5.962	7.236	5.404	13.111	25.858	0.90777	0.039787	0.96643	0.17622	6.1657	6.9404	11.38	33.774
	Min	-57.399	-134.68	-30.17	-44.938	-88.064	-144.1	-169.19	-168.64	-0.0042	-1.1658	-0.54657	-5.6328	-29.445	-6.8453	-9.6695	-6.8601
19-CR2_LA_40_R	Max	10.442	10.64	3.358	3.223	3.638	3.773	6.035	15.924	0.61668	0.038727	0.32359	0.00423	10.497	8.0624	11.377	31.367
	Min	-60.758	-121.56	-27.842	-48.677	-89.762	-124.03	-134.97	-128.88	-0.0283	-0.85347	-0.67041	-4.4418	-27.61	-4.8508	-7.6263	-9.6507
19-RT1_LA_40_R	Max	10.138	11.909	4.291	4.086	3.703	2.993	10.165	24.909	1.1158	0.028072	0.52313	0.03517	15.708	9.0236	11.383	45.264
	Min	-64.162	-157.59	-34.909	-56.314	-101.6	-151.11	-165.13	-139.29	-0.1092	-1.5501	-0.62787	-5.3088	-37.067	-6.2735	-8.557	-11.06
19-RT2_LA_40_R	Max	9.417	10.991	1.621	1.263	2.051	1.699	5.87	20.948	1.1541	0.012649	0.43793	0.00694	9.4862	7.0347	9.2141	31.516
	Min	-60.083	-157.01	-26.279	-54.437	-104.15	-159	-169.13	-138.05	-0.0039	-1.5422	-0.38307	-5.4171	-26.218	-4.1653	-6.7269	-9.3967
20-CR1_LA_20_D	Max	8.606	11.72	14.637	4.953	2.016	2.089	3.785	5.586	0.00425	0.83426	0.00686	0.33796	25.053	6.2276	6.7624	5.1366
	Min	-121.39	-70.08	-147.66	-147.85	-177.68	-92.111	-47.115	-12.214	-1.1938	-0.00344	-4.8701	-0.51904	-5.4862	-3.3398	-4.7386	-23.157
20-CR2_LA_20_D	Max	55.025	36.813	3.918	1.659	3.187	3.624	5.421	7.424	0.22276	0.40706	0.07059	0.17222	24.813	6.8313	8.7873	12.747
	Min	-67.375	-45.987	-132.98	-134.74	-159.61	-88.976	-44.879	-9.876	-0.6172	-0.18844	-4.0134	-0.65378	-13.754	-4.5386	-7.1237	-21.377
20-RT1_LA_20_D	Max	29.384	13.542	11.484	3.704	1.329	3.095	4.924	8.297	0.10299	1.071	0.01523	0.32311	59.039	8.0536	6.8516	37.172
	Min	-123.02	-68.658	-145.62	-167.6	-201.97	-103.4	-52.176	-13.303	-1.497	-0.13375	-5.1318	-0.49189	-12.309	-8.84	-6.1874	-33.852
20-RT2_LA_20_D	Max	17.366	7.619	12.792	4.418	1.652	3.436	2.602	4.577	0.01733	1.0575	0.00474	0.26275	30.21	6.2558	6.9259	3.9227
	Min	-140.03	-75.981	-141.71	-169.78	-203.15	-96.564	-47.898	-14.223	-1.5127	-0.01367	-4.9213	-0.47825	-5.0699	-2.8692	-4.5391	-27.889
21-CR1_LA_20_R	Max	11.362	11.272	1.152	2.049	2.879	1.64	5.394	19.165	0.82822	0.004489	0.39712	0.00576	4.3571	6.0062	6.5417	27.39
	Min	-60.638	-140.03	-14.948	-45.251	-89.921	-137.76	-162.11	-161.04	-0.0048	-1.1213	-0.31288	-5.3992	-23.34	-3.6124	-4.2313	-3.5697
21-CR2_LA_20_R	Max	9.15	12.325	2.943	3.006	2.665	2.586	3.968	11.767	0.63769	0.005051	0.23104	0.00542	11.581	9.286	17.298	29.828
	Min	-65.05	-127.38	-26.757	-58.894	-111.83	-148.21	-159.73	-153.93	-0.0143	-0.88525	-0.74896	-5.3236	-26.656	-7.0184	-9.4889	-10.054
21-RT1_LA_20_R	Max	9.524	10.871	2.068	2.812	1.756	1.793	5.224	21.403	1.2379	0.051235	0.46513	0.01325	8.8615	8.9877	12.091	40.122
	Min	-60.576	-153.33	-24.432	-55.288	-107.44	-164.21	-178.28	-148.7	-0.0141	-1.5624	-0.44287	-5.5207	-32.111	-3.8716	-9.3469	-8.3981
21-RT2_LA_20_R	Max	9.154	11.434	2.188	2.229	2.486	2.661	6.225	21.127	1.1137	0.010436	0.32741	0.0072	8.4323	6.325	5.8443	30.198
	Min	-63.946	-158.67	-23.212	-51.971	-102.51	-162.04	-170.38	-134.47	-0.0053	-1.4879	-0.45659	-5.2138	-25.52	-3.8898	-6.2017	-7.9629

Sensor type		Velocity																
Location		Pier 7 headstock							Span 8 girder, end	Pier 7 headstock		Span 7 girder, end	Pier 7 headstock		Span 7 girder	Span 8 girders, mid-span		Span 8 girder, end
Sensor		P7HLS8-a z vel	P7HLS8-a x vel	P7HLS8-a y vel	P7HRS8-a y vel	P7HRS8-a x vel	P7HRS8-a z vel	P7HC-a z vel	S8G1e-a z vel	P7HLS7 z vel	P7HC-a x vel	S7G1e-a z vel	P7HC-a y vel	P7HRS7-a z vel	S7G6-a z vel	S8G1m-a z vel	S8G6m-a z vel	S8G6e-a z vel
STATIC	**Max**	**5.7565**	**7.1429**	**7.1131**	**0**	**16.139**	**8.3615**	**0.0024666**	**0.014345**	**1.3855**	**1.2172**	**1.4467**	**1.9067**	**1.5777**	**1.5522**	**24.433**	**9.6055**	**2.1575**
	Min	**-5.2484**	**-8.7847**	**-6.7755**	**0**	**-17.952**	**-9.2548**	**-0.0019104**	**-0.014439**	**-1.4324**	**-1.1795**	**-1.4394**	**-1.7456**	**-1.5787**	**-1.5645**	**-28.261**	**-8.9328**	**-2.697**
DYNAMIC	**Max**	**22.718**	**21.989**	**14.085**	**87.489**	**48.957**	**17.254**	**0.011948**	**0.10378**	**9.5811**	**3.8066**	**10.099**	**10.403**	**11.049**	**8.2708**	**38.05**	**50.973**	**27.105**
	Min	**-21.803**	**-21.404**	**-19.471**	**-112.76**	**-38.289**	**-17.507**	**-0.01128**	**-0.09947**	**-9.7437**	**-4.0788**	**-9.5888**	**-10.552**	**-10.233**	**-9.6367**	**-34.962**	**-41.987**	**-23.59**
01-CR1_CL_CWL_D	Max	0.69594	0.57674	0.7593	0	0.54418	1.2678	0.0004367	0.0066461	0.65657	0.43633	0.63386	0.60689	0.50397	0.47755	1.1569	1.1361	0.53032
	Min	-0.67761	-1.1014	-0.92374	0	-0.62694	-1.1664	-0.00043379	-0.0053252	-0.51344	-0.3115	-0.53833	-0.74354	-0.59725	-0.55399	-1.3136	-1.0863	-0.6403
01-CR2_CL_CWL_D	Max	0.78945	0.93914	0.92275	0	0.55853	0.62434	0.00047875	0.0068617	0.67498	0.41665	0.68129	0.85395	0.77041	0.93309	0.94224	0.89765	0.78497
	Min	-1.4655	-0.81856	-0.82494	0	-0.58272	-0.66114	-0.00058353	-0.0062679	-0.62861	-0.40679	-0.63161	-0.83682	-0.70979	-0.69633	-0.73647	-0.86668	-0.69138
01-RT1_CL_CWL_D	Max	1.4112	0.79505	1.6053	0	1.1588	1.3254	0.002425	0.012125	1.2309	0.5821	1.2195	1.6645	1.3773	1.1102	2.1718	2.8	1.5006
	Min	-1.4325	-0.8229	-1.4308	0	-1.1098	-1.3977	-0.0019104	-0.013826	-1.3594	-0.60128	-1.3988	-1.4844	-1.2465	-1.3236	-2.7127	-2.5623	-1.4267
01-RT2_CL_CWL_D	Max	1.0914	0.98834	0.61807	0	0.88221	0.56889	0.00084673	0.0040943	0.37336	0.2435	0.4131	0.64855	0.57588	0.45558	1.2361	1.0618	0.64229
	Min	-0.95144	-0.53246	-0.64415	0	-0.7833	-0.56702	-0.00060436	-0.0058906	-0.53983	-0.36008	-0.54961	-0.4454	-0.44502	-0.43421	-1.2195	-1.2289	-0.43507
02-CR1_CL_CWL_R	Max	0.84849	0.62448	0.84778	0	0.56205	0.84871	0.00048913	0.0039955	0.46366	0.52752	0.47333	0.56589	0.51291	0.64924	1.0546	1.0051	0.47116
	Min	-0.70744	-0.68917	-0.73333	0	-0.70493	-0.98769	-0.00045194	-0.0048161	-0.4559	-0.43923	-0.47266	-0.5139	-0.40661	-0.7435	-0.9505	-1.2279	-0.49354
02-CR2_CL_CWL_R	Max	2.7142	0.61764	0.59836	0	0.78073	1.3427	0.00048838	0.0055616	0.55888	0.6833	0.5617	0.5639	0.51182	0.46482	1.3142	1.3123	0.4717
	Min	-1.5456	-0.55259	-0.6539	0	-0.87825	-0.70846	-0.00053411	-0.0047897	-0.45369	-0.55324	-0.47152	-0.64513	-0.54884	-0.54605	-1.317	-1.3564	-0.493
02-RT1_CL_CWL_R	Max	2.189	1.5118	1.7171	0	1.3858	1.1829	0.00069301	0.010438	1.0402	0.96481	1.0518	1.486	1.2193	1.1992	1.5249	1.316	1.2363
	Min	-3.2305	-1.3447	-1.3975	0	-1.9243	-1.0566	-0.0010074	-0.011586	-1.2051	-0.82113	-1.2198	-1.3845	-1.2067	-1.1758	-1.5888	-1.5155	-1.2085
02-RT2_CL_CWL_R	Max	3.8746	1.2004	1.2701	0	1.42	1.1642	0.00089823	0.010119	1.0913	1.2054	1.1142	1.3467	1.001	1.0204	1.8633	1.4552	1.1026
	Min	-3.9861	-0.8845	-1.204	0	-1.4639	-1.3172	-0.00095945	-0.01199	-1.312	-1.1795	-1.3185	-1.3321	-1.0668	-1.0424	-1.8471	-1.6026	-1.1622
03-CR1_LA_CWL_D	Max	2.3517	1.0794	5.1551	0	1.2044	4.1691	0.0015469	0.0058841	0.60559	0.33415	0.62409	0.65198	0.52208	0.46972	2.1238	1.0259	0.70697
	Min	-3.4935	-0.77122	-5.453	0	-1.6509	-3.8018	-0.001505	-0.0063989	-0.65105	-0.35786	-0.71544	-0.58887	-0.53832	-0.68335	-2.3901	-1.0868	-0.67016
03-CR2_LA_CWL_D	Max	1.4065	0.92765	1.539	0	1.3445	1.6437	0.00046456	0.0056541	0.57378	0.25338	0.57724	0.75955	0.63487	0.63587	1.8476	0.8568	0.94068
	Min	-1.1074	-0.54456	-2.2513	0	-1.4626	-2.0694	-0.00055253	-0.0058595	-0.60782	-0.25883	-0.61233	-0.68075	-0.56368	-0.57228	-1.8086	-0.79386	-1.3788
03-RT1_LA_CWL_D	Max	1.706	1.6272	1.3345	0	1.4265	3.2588	0.00093917	0.010249	1.0255	0.3386	1.2068	1.0239	0.87241	0.90774	3.548	1.6581	0.92553
	Min	-1.6509	-1.8051	-1.1274	0	-1.8022	-2.396	-0.00089442	-0.0092275	-0.92064	-0.49939	-1.0354	-1.1578	-0.93425	-0.98084	-3.2381	-1.865	-0.94042
03-RT2_LA_CWL_D	Max	2.2786	1.7316	2.1394	0	16.139	6.1282	0.00058528	0.0042685	0.44978	0.44074	0.44616	0.47532	0.33605	0.5892	1.4567	1.1185	1.513
	Min	-1.6007	-1.7244	-2.5855	0	-17.028	-5.8088	-0.00058986	-0.0035887	-0.4134	-0.40788	-0.41479	-0.51184	-0.42406	-0.51481	-1.2303	-1.1515	-1.0301
04-CR1_LA_CWL_R	Max	1.249	5.6493	2.4198	0	3.0906	2.8739	0.0010524	0.0055137	0.52983	0.29437	0.52641	0.44051	0.45251	0.82416	1.2714	1.3709	1.5602
	Min	-1.7657	-4.1487	-2.9392	0	-2.727	-2.707	-0.00045295	-0.0034622	-0.34734	-0.18853	-0.35082	-0.67839	-0.63494	-0.62344	-1.1508	-1.6184	-1.6806
04-CR2_LA_CWL_R	Max	1.6853	2.9513	2.5807	0	2.4505	1.4616	0.0005672	0.010354	1.0699	0.79046	1.0526	1.4513	1.1923	1.1247	1.1854	1.6311	1.2833
	Min	-2.509	-2.1507	-2.0378	0	-2.1889	-1.3907	-0.00070768	-0.011827	-1.225	-0.74885	-1.2618	-1.2693	-1.1306	-1.1469	-1.416	-1.4119	-1.1273
04-RT1_LA_CWL_R	Max	1.6551	3.2856	3.6302	0	13.297	3.7157	0.0021846	0.012292	1.2403	0.96601	1.2683	1.5524	1.2675	1.1931	1.4382	2.3117	1.2107
	Min	-2.3982	-3.7368	-4.2148	0	-17.952	-3.1865	-0.00084081	-0.012893	-1.2505	-0.79849	-1.2386	-1.4805	-1.3003	-1.2939	-1.557	-2.2314	-1.333
04-RT2_LA_CWL_R	Max	3.5757	1.4407	3.057	0	5.3117	2.4408	0.00082713	0.0099102	0.93732	1.2172	0.96753	1.1402	0.93385	0.94738	1.4066	1.2902	1.0422
	Min	-3.7971	-1.7283	-2.6844	0	-7.1394	-2.9793	-0.00092474	-0.0098968	-0.9955	-0.97364	-0.98758	-1.1328	-0.98967	-0.97662	-1.2626	-1.6068	-1.6106
05-CR1_KB_CWL_D	Max	3.9275	4.9309	4.7399	0	4.9652	3.4103	0.001181	0.0053368	0.5635	0.61103	0.55706	0.76136	0.67613	0.62819	1.1851	1.2501	1.0899
	Min	-3.6957	-4.7287	-3.8527	0	-2.8892	-3.4748	-0.0014335	-0.0064428	-0.71265	-0.51919	-0.73296	-0.68777	-0.58844	-0.713	-1.0289	-1.0548	-0.96541
05-CR2_KB_CWL_D	Max	2.0999	1.7245	1.9267	0	3.1359	2.7221	0.00045855	0.0069441	0.70111	0.36263	0.7064	0.74097	0.63968	0.65383	1.3489	0.74082	0.60557
	Min	-2.4017	-1.7891	-2.5917	0	-2.4867	-1.5716	-0.00047032	-0.0064689	-0.61307	-0.33565	-0.62439	-0.81575	-0.67075	-0.66136	-1.5081	-0.8921	-0.79558
05-RT1_KB_CWL_D	Max	3.3144	2.446	6.8426	0	3.9358	2.1861	0.0010293	0.01242	1.0983	0.29405	1.049	1.4248	1.2573	1.2303	3.4077	0.95374	1.2475
	Min	-5.2484	-3.4224	-6.7755	0	-5.7665	-1.7871	-0.0011598	-0.012022	-1.0985	-0.32397	-1.0879	-1.3056	-1.1222	-1.1556	-3.7861	-0.92384	-1.3168
05-RT2_KB_CWL_D	Max	4.5579	5.4767	3.0071	0	6.2276	3.1001	0.0014529	0.0028172	0.2901	0.19533	0.29415	0.29039	0.25124	0.54588	1.141	0.78087	0.89289
	Min	-4.0057	-6.8896	-2.2444	0	-6.1749	-3.1416	-0.0012044	-0.0024332	-0.23508	-0.23707	-0.24098	-0.3576	-0.30564	-0.50956	-1.018	-0.81386	-0.78712
06-CR2_KB_CWL_R	Max	2.1815	2.2843	1.4906	0	4.9488	6.2695	0.001139	0.011431	1.1599	1.0918	1.1436	1.2376	1.0281	1.0026	2.1834	1.8462	2.0061
	Min	-2.9166	-2.6965	-2.0279	0	-5.5121	-6.3058	-0.0013612	-0.010601	-1.1361	-0.93326	-1.1848	-1.3944	-1.1516	-1.1498	-1.8078	-1.6759	-2.697
06-RT1_KB_CWL_R	Max	5.5339	2.7822	3.7341	0	7.0495	4.4235	0.0021124	0.014345	1.3814	0.63084	1.4467	1.9067	1.5777	1.5522	24.433	9.6055	1.5621
	Min	-4.2573	-2.9818	-2.4625	0	-5.829	-3.9213	-0.00077779	-0.014439	-1.4324	-0.54984	-1.4394	-1.7456	-1.5787	-1.5645	-28.261	-8.9328	-1.5061

Sensor type		Velocity																	
Location		Pier 7 headstock							Span 8 girder, end	Pier 7 headstock		Span 7 girder, end	Pier 7 headstock		Span 7 girder	Span 8 girders, mid-span		Span 8 girder, end
Sensor		P7HLS8-a z vel	P7HLS8-a x vel	P7HLS8-a y vel	P7HRS8-a y vel	P7HRS8-a x vel	P7HRS8-a z vel	P7HC-a z vel	S8G1e-a z vel	P7HLS7 z vel	P7HC-a x vel	S7G1e-a z vel	P7HC-a y vel	P7HRS7-a z vel	S7G6-a z vel	S8G1m-a z vel	S8G6m-a z vel	S8G6e-a z vel
STATIC	**Max**	**5.7565**	**7.1429**	**7.1131**	**0**	**16.139**	**8.3615**	**0.0024666**	**0.014345**	**1.3855**	**1.2172**	**1.4467**	**1.9067**	**1.5777**	**1.5522**	**24.433**	**9.6055**	**2.1575**
	Min	**-5.2484**	**-8.7847**	**-6.7755**	**0**	**-17.952**	**-9.2548**	**-0.0019104**	**-0.014439**	**-1.4324**	**-1.1795**	**-1.4394**	**-1.7456**	**-1.5787**	**-1.5645**	**-28.261**	**-8.9328**	**-2.697**
DYNAMIC	**Max**	**22.718**	**21.989**	**14.085**	**87.489**	**48.957**	**17.254**	**0.011948**	**0.10378**	**9.5811**	**3.8066**	**10.099**	**10.403**	**11.049**	**8.2708**	**38.05**	**50.973**	**27.105**
	Min	**-21.803**	**-21.404**	**-19.471**	**-112.76**	**-38.289**	**-17.507**	**-0.01128**	**-0.09947**	**-9.7437**	**-4.0788**	**-9.5888**	**-10.552**	**-10.233**	**-9.6367**	**-34.962**	**-41.987**	**-23.59**
06-RT2_KB_CWL_R	Max	2.2681	6.8503	2.1736	0	7.9219	3.6838	0.0024666	0.013567	1.3855	1.0753	1.3812	1.4991	1.3212	1.367	2.1445	1.5017	2.1575
	Min	-1.9991	-8.7847	-3.1159	0	-7.102	-4.3094	-0.0013454	-0.012308	-1.2314	-0.71496	-1.248	-1.6726	-1.394	-1.3262	-3.1473	-1.3109	-2.2992
07-CR1_CL_80_D	Max	4.7859	4.3851	7.2671	6.9464	2.7705	4.0373	0.0040577	0.020688	1.3999	1.9034	1.6373	1.3625	1.2839	1.8595	13.942	14.75	11.219
	Min	-8.6791	-4.4951	-7.0298	-5.1818	-5.0856	-5.0473	-0.0038135	-0.017379	-1.6926	-1.4674	-1.9098	-1.3333	-1.6392	-1.4134	-18.247	-16.865	-10.23
07-CR2_CL_80_D	Max	5.9241	7.0194	2.8397	3.4065	5.8817	4.5385	0.0069525	0.022809	1.647	2.1357	1.7954	1.6666	1.5525	1.8079	17.864	11.336	3.3191
	Min	-3.3553	-6.1593	-3.5116	-5.1043	-6.1561	-5.0659	-0.0054129	-0.024373	-2.1065	-1.4127	-2.5535	-1.7948	-1.9834	-2.6035	-16.687	-15.568	-3.1916
07-RT1_CL_60_D	Max	6.0425	9.4243	9.0596	7.8887	10.976	5.3621	0.0070153	0.030896	3.1279	2.1074	3.1452	3.5021	2.8747	2.9596	21.073	16.173	11.402
	Min	-5.2351	-8.7258	-11.874	-12.526	-11.091	-5.6848	-0.0056008	-0.028601	-2.8393	-2.3557	-2.8565	-3.7444	-3.1884	-2.4987	-18.56	-17.446	-9.8484
07-RT2_CL_80_D	Max	9.2892	9.7943	5.763	9.6983	5.1491	5.1281	0.0050268	0.027634	2.3932	1.3118	3.1288	1.7602	1.893	4.3834	16.934	18.971	10.101
	Min	-11.047	-8.4218	-6.6006	-19.334	-6.8663	-4.1852	-0.0045089	-0.025362	-2.3685	-1.3272	-2.4619	-1.5591	-2.1709	-2.8126	-17.931	-15.772	-12.24
09-CR1_LA_80_D	Max	15.19	9.5145	6.8142	30.449	22.7	6.6464	0.0050739	0.02114	1.4241	1.6577	2.007	1.0197	1.1048	1.713	20.22	12.22	4.6131
	Min	-11.208	-8.2791	-5.4515	-32.345	-17.689	-7.1754	-0.0035169	-0.019981	-1.6385	-1.5007	-1.6904	-1.0911	-1.1425	-1.7391	-22.955	-12.101	-7.9934
09-CR2_LA_80_D	Max	8.2845	7.9401	6.6426	17.142	14.844	5.0709	0.0072648	0.069017	5.7354	1.8901	5.6482	6.2057	5.2625	4.9475	24.819	11.204	7.8557
	Min	-5.7961	-7.7356	-4.8194	-12.348	-10.119	-6.0686	-0.0062792	-0.064466	-6.0311	-1.4286	-5.6432	-4.39	-3.581	-3.6001	-25.944	-9.4485	-6.9099
09-RT1_LA_80_D	Max	20.375	10.131	12.087	27.554	9.7038	8.8002	0.0079574	0.058302	6.0998	1.6953	8.08	5.6453	5.012	3.5383	27.448	10.143	8.591
	Min	-12.297	-9.8072	-19.471	-51.273	-8.0452	-12.362	-0.0092419	-0.075262	-6.6658	-2.1131	-7.0036	-5.9234	-5.135	-3.4817	-22.487	-9.9614	-6.3704
09-RT2_LA_80_D	Max	20.304	16.336	6.3779	36.166	48.957	6.6913	0.011279	0.05043	4.6548	1.3049	5.8497	2.3356	2.5353	3.3839	20.172	15.174	11.343
	Min	-16.484	-12.472	-8.7413	-39.847	-38.289	-9.3245	-0.0080771	-0.041965	-4.8899	-1.46	-5.8257	-1.9563	-3.1043	-3.6443	-24.712	-15.383	-12.794
10-CR1_LA_80_R	Max	5.6173	6.6887	14.085	13.885	21.685	6.5866	0.0042503	0.020355	1.3635	1.2738	1.2512	0.97361	1.7906	2.1696	15.713	20.355	15.434
	Min	-7.3914	-7.7684	-10.098	-14.217	-26.771	-6.6591	-0.0039085	-0.018103	-1.2826	-1.6828	-1.2865	-0.81088	-1.4773	-2.6286	-15.358	-15.991	-10.922
10-CR2_LA_80_R	Max	5.175	3.9651	7.1203	9.0009	9.274	6.9256	0.0089236	0.03673	3.5717	2.9943	3.8235	4.5653	4.6456	6.4696	13.755	24.567	8.5207
	Min	-4.3282	-3.8932	-4.1069	-7.8064	-7.9869	-4.7101	-0.0062002	-0.033768	-3.4953	-2.9283	-3.4361	-3.8898	-5.6048	-5.7658	-15.677	-33.649	-9.3496
10-RT1_LA_80_R	Max	8.9227	16.872	11.197	23.086	18.535	11.887	0.011948	0.084427	8.3124	3.8066	7.9628	9.7079	11.049	8.2708	18.93	33.27	19.492
	Min	-9.0673	-12.27	-13.991	-33.163	-15.942	-15.436	-0.01128	-0.079146	-7.8224	-4.0788	-7.587	-10.552	-10.233	-7.7848	-21.09	-39.788	-14.147
10-RT2_LA_80_R	Max	9.249	7.1737	5.5495	22.717	20.236	10.388	0.0082353	0.020131	1.8714	1.7013	2.6768	1.4784	4.7067	5.9082	13.704	19.936	16.702
	Min	-7.53	-6.9874	-8.1712	-40.465	-18.655	-12.096	-0.0083647	-0.035185	-3.5401	-1.6268	-4.6681	-1.5946	-3.454	-9.6367	-12.67	-32.018	-14.422
11-RT1_LA_95_D	Max	22.718	21.989	8.2708	18.221	10.885	12.51	0.01026	0.10378	9.5811	2.1879	10.099	9.722	7.9739	6.364	30.61	7.7283	7.7253
	Min	-21.803	-16.663	-13.966	-30.269	-11.858	-12.569	-0.008992	-0.09947	-9.7437	-2.0267	-9.5888	-8.2399	-7.644	-6.5611	-34.778	-9.9342	-9.759
11-RT2_LA_105_D	Max	16.506	10.278	6.1033	33.288	19.168	12.985	0.010246	0.041335	4.4372	2.3017	4.5058	2.8382	3.6824	1.7911	24.009	10.639	14.082
	Min	-16.947	-12.405	-6.4173	-27.888	-18.372	-11.853	-0.0092697	-0.062455	-5.6661	-1.7353	-6.3097	-2.6419	-3.1474	-2.8419	-13.714	-13.644	-16.628
12-RT1_LA_100_R	Max	9.1846	14.601	10.143	20.948	24.159	17.254	0.0099715	0.055645	5.1629	3.3822	5.46	5.1136	5.5783	5.8546	23.476	50.973	11.476
	Min	-8.8685	-15.217	-9.1065	-28.562	-22.015	-17.507	-0.0083668	-0.04959	-4.978	-3.4276	-5.1509	-4.9122	-4.692	-3.5558	-25.782	-29.158	-17.9
12-RT2_LA_105_R	Max	10.198	21.54	13.11	87.489	11.997	13.448	0.0074864	0.035812	2.6293	2.1397	2.3566	1.8314	4.3131	5.1618	21.777	30.587	27.105
	Min	-15.259	-21.404	-6.9147	-112.76	-11.859	-16.739	-0.0081873	-0.038954	-2.8547	-1.8417	-2.8255	-1.8625	-4.2353	-4.7508	-18.12	-35.613	-23.59
13-CR1_KB_CWL_R	Max	5.7565	7.1429	7.1131	0	14.132	8.3615	0.00071532	0.0061429	0.59123	0.64198	0.64273	0.70046	0.56692	1.1208	1.89	1.1102	1.3547
	Min	-4.5576	-4.6243	-5.6684	0	-17.455	-9.2548	-0.0010188	-0.0045144	-0.45079	-0.5972	-0.55451	-0.67001	-0.64976	-0.97085	-1.7274	-1.0681	-1.4879
14-CR1_LA_60_D	Max	6.3774	5.6798	9.5705	24.397	20.432	5.6913	0.003513	0.020638	1.483	1.054	1.5579	1.3671	1.202	2.2518	12.949	9.4548	5.6121
	Min	-6.5171	-5.5237	-6.6025	-25.905	-17.982	-6.7395	-0.0034227	-0.02128	-1.7478	-1.042	-1.9792	-1.1738	-0.93353	-1.1696	-16.975	-8.1821	-4.4124
14-CR2_LA_60_D	Max	7.1474	6.517	9.3274	50.641	10.77	6.925	0.0081139	0.063479	5.8456	1.7382	5.5807	7.3322	6.081	5.8063	21.977	6.6571	3.6214
	Min	-8.5907	-5.0315	-7.1069	-66.682	-10.774	-7.5736	-0.0057779	-0.074966	-6.9616	-1.9217	-6.9529	-5.9937	-5.0732	-4.1468	-21.028	-8.8871	-7.1317
15-CR1_LA_60_R	Max	4.8461	6.9893	4.3131	10.231	6.0324	10.294	0.0029451	0.011401	0.89404	1.2104	0.88252	1.054	1.413	2.477	6.9048	13.094	5.1721
	Min	-6.7192	-4.3849	-5.5625	-12.082	-6.7675	-10.831	-0.0031883	-0.010894	-0.87807	-1.2895	-0.87733	-0.92118	-1.3714	-2.0417	-7.3995	-16.473	-6.0546
15-CR2_LA_60_R	Max	4.3819	5.5248	6.4472	8.448	3.6245	7.4391	0.0085053	0.041539	3.812	3.1666	3.7831	3.99	5.6612	4.5291	16.676	30.352	6.5654
	Min	-4.7596	-3.3631	-6.4589	-11.454	-3.7689	-6.7244	-0.005534	-0.029412	-2.8327	-2.9358	-2.628	-5.2793	-5.6249	-4.5963	-13.326	-41.987	-6.6275

Sensor type		Velocity															
Location		Pier 7 headstock							Span 8 girder, end	Pier 7 headstock		Span 7 girder, end	Pier 7 headstock		Span 7 girder	Span 8 girders, mid-span		Span 8 girder, end
Sensor		P7HLS8-a z vel	P7HLS8-a x vel	P7HLS8-a y vel	P7HRS8-a y vel	P7HRS8-a x vel	P7HRS8-a z vel	P7HC-a z vel	S8G1e-a z vel	P7HLS7 z vel	P7HC-a x vel	S7G1e-a z vel	P7HC-a y vel	P7HRS7-a z vel	S7G6-a z vel	S8G1m-a z vel	S8G6m-a z vel	S8G6e-a z vel
STATIC	**Max**	**5.7565**	**7.1429**	**7.1131**	**0**	**16.139**	**8.3615**	**0.0024666**	**0.014345**	**1.3855**	**1.2172**	**1.4467**	**1.9067**	**1.5777**	**1.5522**	**24.433**	**9.6055**	**2.1575**
	Min	**-5.2484**	**-8.7847**	**-6.7755**	**0**	**-17.952**	**-9.2548**	**-0.0019104**	**-0.014439**	**-1.4324**	**-1.1795**	**-1.4394**	**-1.7456**	**-1.5787**	**-1.5645**	**-28.261**	**-8.9328**	**-2.697**
DYNAMIC	**Max**	**22.718**	**21.989**	**14.085**	**87.489**	**48.957**	**17.254**	**0.011948**	**0.10378**	**9.5811**	**3.8066**	**10.099**	**10.403**	**11.049**	**8.2708**	**38.05**	**50.973**	**27.105**
	Min	**-21.803**	**-21.404**	**-19.471**	**-112.76**	**-38.289**	**-17.507**	**-0.01128**	**-0.09947**	**-9.7437**	**-4.0788**	**-9.5888**	**-10.552**	**-10.233**	**-9.6367**	**-34.962**	**-41.987**	**-23.59**
16-RT1_LA_60_D	Max	6.3732	5.2404	6.9364	41.016	23.529	6.7668	0.0088184	0.068704	6.3077	2.5989	7.1185	4.9703	4.0882	4.9969	24.372	12.755	7.2934
	Min	-5.7485	-7.6122	-7.0961	-46.327	-33.371	-6.4645	-0.0091715	-0.063047	-5.9901	-2.2026	-7.5411	-4.4071	-4.6148	-4.1726	-18.49	-11.211	-4.6553
16-RT2_LA_60_D	Max	20.635	11.739	7.5721	22.856	9.7889	6.7734	0.0079212	0.031296	2.9525	1.4068	4.1722	1.9894	2.218	2.8742	20.219	11.328	4.7564
	Min	-13.018	-8.1665	-5.1002	-25.202	-9.3829	-6.5604	-0.0068299	-0.03259	-3.1622	-0.96707	-3.713	-1.9002	-1.8494	-2.4241	-17.686	-11.424	-4.5905
17-RT1_LA_60_R	Max	12.496	12.212	7.5866	67.782	11.379	8.1533	0.0061797	0.034214	3.1875	2.1625	3.3308	3.1824	4.1821	5.2664	10.412	22.821	13.184
	Min	-9.186	-11.238	-11.462	-63.046	-11.748	-7.2494	-0.0057186	-0.034058	-3.0075	-1.955	-3.2955	-4.1644	-4.5479	-4.957	-9.4591	-27.959	-14.428
17-RT2_LA_60_R	Max	4.9413	15.064	8.8771	22.428	16.779	7.0924	0.0052476	0.023142	1.5665	1.0514	1.5189	1.0303	2.2979	4.5761	13.248	21.836	13.567
	Min	-3.8382	-15.716	-12.017	-25.421	-18.741	-10.026	-0.0047407	-0.019438	-1.3259	-1.1589	-1.4424	-1.1881	-2.3311	-4.0892	-12.585	-19.388	-7.796
18-CR1_LA_40_D	Max	3.6785	9.5074	5.0378	15.034	20.803	11.119	0.0046288	0.039887	2.511	1.5975	2.496	1.8694	1.86	1.9056	28.19	15.107	2.8052
	Min	-3.1594	-12.871	-7.5068	-26.436	-29.521	-7.9108	-0.0045933	-0.028969	-1.9079	-1.3234	-2.4524	-1.8731	-1.6819	-1.5975	-34.127	-15.537	-2.4322
18-CR2_LA_40_D	Max	4.747	7.9691	7.2597	47.618	18.855	6.893	0.0036046	0.024844	1.8416	1.354	2.6829	2.3045	2.0152	2.6031	20.995	10.141	2.1174
	Min	-5.532	-6.1022	-5.4767	-57.986	-19.897	-5.5097	-0.0027951	-0.02655	-2.1216	-1.2574	-2.4408	-2.4579	-1.9487	-2.2702	-19.451	-10.86	-2.6366
18-RT1_LA_40_D	Max	4.7442	4.8373	8.3573	25.694	17.121	4.2639	0.0054574	0.057222	4.2899	2.3152	4.1633	4.0458	3.4016	3.599	38.05	14.279	4.3512
	Min	-4.1113	-4.8646	-8.1341	-12.699	-24.655	-5.6244	-0.0058437	-0.046227	-3.6289	-2.0383	-3.375	-3.2681	-2.8317	-2.8129	-34.962	-14.83	-5.763
18-RT2_LA_40_D	Max	4.2826	7.0474	5.525	40.841	16.048	7.4307	0.0048577	0.022476	1.8628	0.82138	1.9142	1.7723	1.5733	1.8241	10.658	4.9666	3.1858
	Min	-5.3162	-6.951	-4.6489	-25.591	-14.442	-5.751	-0.0052795	-0.028734	-2.1874	-0.93152	-2.3697	-1.8154	-1.404	-1.4889	-11.938	-6.6904	-3.2577
19-CR1_LA_40_R	Max	2.338	4.553	3.4112	22.433	6.9445	3.1729	0.0046443	0.022967	1.4033	1.7694	1.6201	1.6002	1.9557	3.281	23.18	36.323	6.4538
	Min	-2.4667	-4.3601	-3.2235	-20.6	-5.333	-2.8452	-0.0043475	-0.023084	-1.2299	-1.5668	-1.4713	-1.2941	-2.0211	-2.5011	-23.681	-35.447	-6.1576
19-CR2_LA_40_R	Max	2.4484	2.9663	3.0214	15.217	5.2298	3.2825	0.0031467	0.018822	1.8423	1.609	1.6747	2.4082	2.2006	2.0624	12.883	25.877	4.8365
	Min	-1.9639	-2.9524	-2.5871	-9.6254	-6.1473	-2.701	-0.0042609	-0.016388	-1.7018	-1.6524	-1.6029	-2.1913	-2.631	-3.2993	-13.173	-17.429	-5.0556
19-RT1_LA_40_R	Max	4.1073	6.3631	5.9508	15.441	10	5.0569	0.0038904	0.036434	3.0942	1.9848	3.0281	4.0959	3.3753	3.4686	19.222	26.338	6.1987
	Min	-5.2668	-3.9519	-5.2223	-15.807	-9.8582	-7.5794	-0.0044712	-0.032084	-2.829	-1.7437	-2.7909	-3.264	-4.1055	-4.0752	-19.909	-24.239	-6.7578
19-RT2_LA_40_R	Max	3.567	4.38	7.6947	21.022	14.445	3.4954	0.0027346	0.012943	1.1747	0.73347	1.1691	1.2799	1.4858	2.0593	8.089	11.63	4.8568
	Min	-3.2969	-4.1643	-13.326	-35.861	-18.337	-4.1011	-0.0029357	-0.013402	-1.1996	-1.0323	-1.2148	-1.0307	-1.9121	-1.9621	-6.9865	-10.559	-3.587
20-CR1_LA_20_D	Max	2.6353	5.6739	6.7349	20.02	9.8682	3.8005	0.0014695	0.018888	1.8409	0.7195	1.8649	2.6921	2.3575	2.3085	12.223	5.9701	2.5378
	Min	-2.9512	-2.9028	-4.7291	-20.683	-11.964	-3.8489	-0.0016196	-0.031359	-2.7172	-0.72645	-2.5748	-2.6313	-2.0606	-1.9492	-11.636	-5.1892	-2.2239
20-CR2_LA_20_D	Max	3.4031	2.9864	6.9778	9.1616	8.1495	3.1878	0.0029884	0.030887	2.858	0.97358	2.8463	3.0193	2.4433	2.4314	11.854	4.229	2.4037
	Min	-3.2168	-3.9103	-6.873	-8.2295	-6.0608	-3.1029	-0.0034949	-0.029086	-2.7412	-1.1019	-2.7348	-2.7792	-2.4319	-2.3067	-13.241	-4.0918	-2.5068
20-RT1_LA_20_D	Max	9.1071	3.0075	10.572	21.206	20.311	9.0183	0.0047961	0.085226	7.9762	1.5688	7.8453	10.403	9.0494	7.7297	16.03	7.0419	8.4137
	Min	-9.3392	-3.1864	-10.031	-19.442	-26.931	-9.6101	-0.0057629	-0.086169	-8.4078	-1.4822	-8.3309	-9.9257	-8.279	-7.7143	-19.112	-7.5633	-7.5119
20-RT2_LA_20_D	Max	2.6956	2.2722	5.4004	12.094	7.8177	4.0601	0.0015811	0.022987	2.1625	0.64248	2.1159	2.5162	2.17	2.1581	5.2751	3.9534	2.6432
	Min	-3.1595	-2.1866	-7.437	-18.881	-8.3966	-4.6501	-0.0021113	-0.019744	-1.8729	-0.57478	-1.8641	-2.5238	-2.1367	-2.1311	-4.7494	-3.876	-2.424
21-CR1_LA_20_R	Max	2.562	2.5604	7.2945	6.7843	17.149	9.1293	0.0016625	0.013165	1.3244	0.71106	1.2618	1.7758	1.4553	1.5715	4.8562	12.863	1.6769
	Min	-3.5444	-2.7094	-5.183	-10.292	-19.992	-6.2502	-0.0017224	-0.012587	-1.2903	-0.75524	-1.3075	-1.7596	-1.5686	-1.5839	-5.4248	-13.296	-1.6033
21-CR2_LA_20_R	Max	3.9031	3.4041	3.3087	3.7873	5.1247	3.4498	0.0043005	0.02317	2.2774	2.4358	2.2586	2.7398	3.4371	3.3072	7.1632	23.202	4.2833
	Min	-2.7409	-4.0312	-2.8441	-6.5259	-5.0503	-3.3148	-0.0033697	-0.021177	-2.0891	-2.0104	-2.0363	-2.945	-3.3455	-3.1668	-8.6365	-27.624	-3.6253
21-RT1_LA_20_R	Max	4.047	5.8665	5.2242	8.1956	4.0954	5.9385	0.0029047	0.037691	3.7057	2.7416	3.709	4.9775	4.4191	3.1276	7.2352	25.228	4.3431
	Min	-4.9918	-3.7511	-4.7645	-10.444	-5.1903	-8.1547	-0.0031043	-0.042139	-4.0337	-2.7819	-3.9149	-4.6244	-3.8738	-3.901	-8.7274	-20.478	-3.3495
21-RT2_LA_20_R	Max	2.3118	4.5205	4.1956	10.021	28.469	4.0921	0.001692	0.011896	1.1803	0.56105	1.2034	1.5924	1.201	1.8615	3.1846	5.3604	1.2353
	Min	-4.7302	-4.3657	-3.0155	-18.319	-19.921	-4.1532	-0.00156	-0.0119	-1.1137	-0.5196	-1.0828	-1.4622	-1.316	-1.8149	-3.3379	-5.3657	-1.6233

Sensor type		Accelerometers (Converted to Velocity mm/s)																
Location		Pier 7 headstock							Span 8 girder, end	Pier 7 headstock		Span 7 girder, end	Pier 7 headstock		Span 7 girder	Span 8 girders, mid-span		Span 8 girder, end
Sensor		P7HLS8-a z accel	P7HLS8-a x accel	P7HLS8-a y accel	P7HRS8-a y accel	P7HRS8-a x accel	P7HRS8-a z accel	P7HC-a z accel	S8G1e-a z accel	P7HLS7 z accel	P7HC-a x accel	S7G1e-a z accel	P7HC-a y accel	P7HRS7-a z accel	S7G6-a z accel	S8G1m-a z accel	S8G6m-a z accel	S8G6e-a z accel
STATIC	**Max**	**0.28265**	**0.2901**	**0.28465**	**0**	**0.85898**	**0.5979**	**0.00018267**	**0.00031606**	**0.030505**	**0.040125**	**0.033845**	**0.035618**	**0.032631**	**0.045677**	**0.17093**	**0.19219**	**0.1089**
	Min	**-0.20141**	**-0.37695**	**-0.43716**	**0**	**-1.4778**	**-0.63061**	**-0.0001373**	**-0.00033398**	**-0.028467**	**-0.03819**	**-0.029784**	**-0.037557**	**-0.035769**	**-0.059166**	**-0.3227**	**-0.15384**	**-0.084249**
DYNAMIC	**Max**	**0.72264**	**0.69387**	**0.66628**	**4.0075**	**2.1062**	**0.79304**	**0.0014419**	**0.0065634**	**0.71912**	**0.26483**	**0.80834**	**0.25288**	**0.45189**	**0.36907**	**1.6764**	**2.2228**	**0.84419**
	Min	**-0.75541**	**-0.5739**	**-0.63119**	**-3.2513**	**-3.7083**	**-0.93287**	**-0.0012619**	**-0.0058122**	**-0.51934**	**-0.24535**	**-0.60205**	**-0.25259**	**-0.49854**	**-0.44275**	**-1.763**	**-1.8837**	**-0.84249**
01-CR1_CL_CWL_D	Max	0.044991	0.03159	0.027736	0	0.051226	0.055685	0.000026672	0.00014014	0.01407	0.011448	0.013872	0.016148	0.015037	0.013906	0.051251	0.031189	0.018673
	Min	-0.022586	-0.048617	-0.019999	0	-0.046626	-0.12095	-0.000027386	-0.00017689	-0.016635	-0.012758	-0.016742	-0.012294	-0.013802	-0.013915	-0.041856	-0.033001	-0.023965
01-CR2_CL_CWL_D	Max	0.028227	0.031365	0.024384	0	0.027461	0.032585	0.000022741	0.00011857	0.011535	0.011047	0.012388	0.012256	0.011108	0.018696	0.028616	0.031591	0.012196
	Min	-0.062038	-0.017579	-0.023582	0	-0.048676	-0.044359	-0.000016801	-0.0001019	-0.011408	-0.010247	-0.011844	-0.01304	-0.011893	-0.014541	-0.029473	-0.030007	-0.013159
01-RT1_CL_CWL_D	Max	0.036274	0.055687	0.031988	0	0.045586	0.094322	0.000070328	0.00031606	0.030505	0.019009	0.033845	0.027515	0.029072	0.032293	0.089122	0.09208	0.039516
	Min	-0.033157	-0.028144	-0.075641	0	-0.11561	-0.058257	-0.000067327	-0.00028048	-0.024602	-0.018818	-0.027366	-0.031116	-0.029434	-0.028322	-0.090864	-0.092705	-0.031329
01-RT2_CL_CWL_D	Max	0.037387	0.057852	0.026296	0	0.059714	0.059053	0.00005143	0.00024113	0.014901	0.011537	0.022615	0.012938	0.015667	0.018498	0.08069	0.07787	0.023643
	Min	-0.027238	-0.039237	-0.037971	0	-0.061139	-0.033486	-0.000047086	-0.00026719	-0.020771	-0.01451	-0.023489	-0.010382	-0.014652	-0.027169	-0.078877	-0.078395	-0.026814
02-CR1_CL_CWL_R	Max	0.045616	0.033212	0.058573	0	0.047895	0.04315	0.000021563	0.00010988	0.011174	0.01167	0.012875	0.010767	0.010394	0.02909	0.037198	0.053929	0.015239
	Min	-0.038203	-0.027087	-0.033288	0	-0.028109	-0.084736	-0.000022596	-0.000087275	-0.0089695	-0.014236	-0.0096189	-0.0085149	-0.0088059	-0.016994	-0.039305	-0.046761	-0.01648
02-CR2_CL_CWL_R	Max	0.075501	0.020057	0.021835	0	0.034266	0.040125	0.000021563	0.00011393	0.011174	0.017436	0.012875	0.013839	0.012207	0.011801	0.049064	0.052559	0.01309
	Min	-0.032523	-0.030286	-0.025766	0	-0.030011	-0.033162	-0.000022596	-0.00012339	-0.011357	-0.015536	-0.011082	-0.010925	-0.0096606	-0.010931	-0.049777	-0.053363	-0.013036
02-RT1_CL_CWL_R	Max	0.042151	0.076912	0.052445	0	0.12031	0.044648	0.000039586	0.00021885	0.022387	0.025344	0.022387	0.021927	0.022597	0.021303	0.053899	0.050547	0.029368
	Min	-0.10469	-0.055723	-0.050205	0	-0.075292	-0.11072	-0.000046856	-0.0002146	-0.020477	-0.023103	-0.020423	-0.023658	-0.021459	-0.020273	-0.058092	-0.047807	-0.023065
02-RT2_CL_CWL_R	Max	0.13207	0.058523	0.054571	0	0.067358	0.069232	0.000047012	0.00025234	0.026692	0.027994	0.02492	0.029161	0.023656	0.022387	0.0634	0.055052	0.029016
	Min	-0.1182	-0.030232	-0.054149	0	-0.069848	-0.038085	-0.000039242	-0.00027054	-0.027724	-0.031078	-0.028991	-0.029692	-0.024602	-0.025855	-0.07154	-0.053082	-0.049583
03-CR1_LA_CWL_D	Max	0.06207	0.054687	0.18716	0	0.15078	0.3536	0.00011723	0.00018224	0.017466	0.010559	0.019347	0.013842	0.021999	0.019177	0.08041	0.044006	0.023812
	Min	-0.10633	-0.042134	-0.13853	0	-0.13913	-0.15289	-0.00011843	-0.00019735	-0.020539	-0.01009	-0.020827	-0.014192	-0.013957	-0.025782	-0.084935	-0.047781	-0.019633
03-CR2_LA_CWL_D	Max	0.06207	0.051977	0.073173	0	0.1015	0.10306	0.000028037	0.00012078	0.011433	0.0096587	0.011774	0.011146	0.0099293	0.01261	0.052769	0.032307	0.043389
	Min	-0.058982	-0.027059	-0.11797	0	-0.13913	-0.19701	-0.000020621	-0.00016313	-0.01224	-0.0074786	-0.012476	-0.012473	-0.011315	-0.0135	-0.062067	-0.035007	-0.061882
03-RT1_LA_CWL_D	Max	0.068333	0.10451	0.060221	0	0.11613	0.3074	0.000061662	0.00027304	0.02634	0.018662	0.031336	0.023368	0.023544	0.02212	0.12053	0.069788	0.0269
	Min	-0.040089	-0.10763	-0.06	0	-0.12006	-0.21966	-0.000065394	-0.00033398	-0.028467	-0.01596	-0.029784	-0.019611	-0.018817	-0.03597	-0.12355	-0.071147	-0.021168
03-RT2_LA_CWL_D	Max	0.073861	0.081266	0.066579	0	0.71721	0.53709	0.000043359	0.00015703	0.011839	0.011736	0.012954	0.010031	0.0097146	0.019575	0.095697	0.090048	0.063143
	Min	-0.090057	-0.071132	-0.10826	0	-0.66235	-0.20328	-0.000037386	-0.0001436	-0.010476	-0.011755	-0.011096	-0.010895	-0.0088968	-0.02236	-0.10163	-0.086707	-0.045212
04-CR1_LA_CWL_R	Max	0.051597	0.24354	0.083744	0	0.13804	0.21815	0.000093358	0.00011284	0.010763	0.011132	0.015418	0.01558	0.016395	0.03325	0.057456	0.051578	0.063263
	Min	-0.052292	-0.16795	-0.12047	0	-0.21121	-0.31786	-0.00005499	-0.00012019	-0.011737	-0.011984	-0.015217	-0.013485	-0.025653	-0.030037	-0.063408	-0.055123	-0.06703
04-CR2_LA_CWL_R	Max	0.044873	0.1347	0.1353	0	0.28819	0.1377	0.000022655	0.00022657	0.023112	0.018388	0.024503	0.022871	0.025976	0.025479	0.050706	0.060791	0.051089
	Min	-0.10402	-0.077202	-0.087311	0	-0.16915	-0.135	-0.000035901	-0.00018814	-0.020161	-0.020688	-0.02071	-0.026453	-0.022682	-0.021378	-0.046133	-0.05902	-0.028756
04-RT1_LA_CWL_R	Max	0.058876	0.14613	0.11724	0	0.85898	0.17475	0.00017223	0.00021802	0.022211	0.028837	0.023684	0.026949	0.028288	0.036444	0.059521	0.083707	0.047548
	Min	-0.12067	-0.12564	-0.17296	0	-0.73586	-0.20548	-0.00010431	-0.00022997	-0.023304	-0.02309	-0.02316	-0.024475	-0.024337	-0.044874	-0.058021	-0.076811	-0.048387
04-RT2_LA_CWL_R	Max	0.13784	0.10253	0.07469	0	0.38626	0.25933	0.000064118	0.00023615	0.021763	0.040125	0.020962	0.02468	0.024623	0.032936	0.06586	0.07987	0.040709
	Min	-0.16869	-0.11015	-0.141	0	-0.28851	-0.2888	-0.000080339	-0.00025675	-0.022971	-0.03819	-0.022516	-0.022877	-0.020775	-0.025126	-0.069229	-0.071635	-0.077801
05-CR1_KB_CWL_D	Max	0.12639	0.2339	0.24758	0	0.20833	0.22783	0.000084533	0.00016352	0.018499	0.016705	0.018999	0.020087	0.015823	0.022583	0.046642	0.046118	0.044788
	Min	-0.18506	-0.16805	-0.096592	0	-0.29006	-0.25723	-0.00012123	-0.00019677	-0.019213	-0.023787	-0.018284	-0.016541	-0.014765	-0.023733	-0.046608	-0.044719	-0.038459
05-CR2_KB_CWL_D	Max	0.077034	0.086634	0.077552	0	0.1506	0.16409	0.000055335	0.00015644	0.015079	0.011614	0.015048	0.013934	0.012381	0.029145	0.041207	0.036102	0.021683
	Min	-0.07906	-0.11964	-0.12725	0	-0.16349	-0.13037	-0.000039089	-0.00012969	-0.012768	-0.01374	-0.013221	-0.017042	-0.014385	-0.017766	-0.034159	-0.030694	-0.019202
05-RT1_KB_CWL_D	Max	0.13341	0.14047	0.28465	0	0.34069	0.1873	0.00007494	0.00029564	0.027558	0.010728	0.027515	0.035618	0.030933	0.031719	0.12731	0.033157	0.066201
	Min	-0.15311	-0.15111	-0.16882	0	-0.256	-0.14195	-0.000090285	-0.00031233	-0.028456	-0.0088624	-0.02744	-0.037557	-0.032085	-0.041854	-0.089409	-0.037013	-0.032719
05-RT2_KB_CWL_D	Max	0.20113	0.20262	0.10917	0	0.23244	0.2875	0.00011969	0.000086596	0.0095767	0.01289	0.01142	0.0085717	0.0083228	0.018901	0.0455	0.03146	0.038403
	Min	-0.10898	-0.32249	-0.11831	0	-0.3497	-0.27914	-0.000087599	-0.000091729	-0.0093224	-0.010018	-0.011796	-0.0092079	-0.010359	-0.017549	-0.049887	-0.03246	-0.031798
06-CR2_KB_CWL_R	Max	0.078954	0.10724	0.13121	0	0.3884	0.5979	0.000097938	0.00030366	0.029777	0.025071	0.030867	0.030081	0.02927	0.032775	0.065091	0.051742	0.064801
	Min	-0.14489	-0.11449	-0.095062	0	-0.41322	-0.31738	-0.000096703	-0.00024798	-0.026571	-0.023458	-0.026851	-0.032149	-0.027877	-0.041946	-0.056045	-0.054081	-0.084249
06-RT1_KB_CWL_R	Max	0.15297	0.090411	0.16496	0	0.46594	0.51682	0.00016219	0.00026574	0.024941	0.018883	0.023842	0.028745	0.032022	0.040108	0.17093	0.19219	0.051051
	Min	-0.12967	-0.13277	-0.10441	0	-0.50454	-0.3038	-0.00010781	-0.00026539	-0.024891	-0.017709	-0.027736	-0.03197	-0.031425	-0.059166	-0.3227	-0.15384	-0.047002

Sensor type		Accelerometers (Converted to Velocity mm/s)																
Location		Pier 7 headstock							Span 8 girder, end	Pier 7 headstock		Span 7 girder, end	Pier 7 headstock		Span 7 girder	Span 8 girders, mid-span		Span 8 girder, end
Sensor		P7HLS8-a z accel	P7HLS8-a x accel	P7HLS8-a y accel	P7HRS8-a y accel	P7HRS8-a x accel	P7HRS8-a z accel	P7HC-a z accel	S8G1e-a z accel	P7HLS7 z accel	P7HC-a x accel	S7G1e-a z accel	P7HC-a y accel	P7HRS7-a z accel	S7G6-a z accel	S8G1m-a z accel	S8G6m-a z accel	S8G6e-a z accel
STATIC	**Max**	**0.28265**	**0.2901**	**0.28465**	**0**	**0.85898**	**0.5979**	**0.00018267**	**0.00031606**	**0.030505**	**0.040125**	**0.033845**	**0.035618**	**0.032631**	**0.045677**	**0.17093**	**0.19219**	**0.1089**
	Min	**-0.20141**	**-0.37695**	**-0.43716**	**0**	**-1.4778**	**-0.63061**	**-0.0001373**	**-0.00033398**	**-0.028467**	**-0.03819**	**-0.029784**	**-0.037557**	**-0.035769**	**-0.059166**	**-0.3227**	**-0.15384**	**-0.084249**
DYNAMIC	**Max**	**0.72264**	**0.69387**	**0.66628**	**4.0075**	**2.1062**	**0.79304**	**0.0014419**	**0.0065634**	**0.71912**	**0.26483**	**0.80834**	**0.25288**	**0.45189**	**0.36907**	**1.6764**	**2.2228**	**0.84419**
	Min	**-0.75541**	**-0.5739**	**-0.63119**	**-3.2513**	**-3.7083**	**-0.93287**	**-0.0012619**	**-0.0058122**	**-0.51934**	**-0.24535**	**-0.60205**	**-0.25259**	**-0.49854**	**-0.44275**	**-1.763**	**-1.8837**	**-0.84249**
06-RT2_KB_CWL_R	Max	0.10621	0.25255	0.13349	0	0.37678	0.32044	0.00018267	0.00024676	0.026168	0.021244	0.026411	0.029966	0.027386	0.041256	0.038496	0.037476	0.1089
	Min	-0.10242	-0.28357	-0.14495	0	-0.64318	-0.3428	-0.0001373	-0.00025034	-0.025164	-0.023285	-0.024911	-0.029886	-0.025872	-0.047143	-0.043144	-0.03873	-0.071197
07-CR1_CL_80_D	Max	0.39979	0.22477	0.41844	0.35513	0.26342	0.41199	0.00053259	0.001105	0.10825	0.12571	0.13694	0.049255	0.087563	0.083999	0.85382	0.79427	0.40881
	Min	-0.34052	-0.22156	-0.26524	-0.30073	-0.32076	-0.34097	-0.00038516	-0.0012466	-0.081999	-0.19389	-0.10611	-0.049391	-0.084568	-0.088699	-1.2834	-0.83297	-0.26796
07-CR2_CL_80_D	Max	0.26958	0.49209	0.11233	0.21364	0.4211	0.19878	0.00049267	0.0013928	0.11925	0.15302	0.12904	0.051859	0.082649	0.083479	0.69992	0.62024	0.20557
	Min	-0.14232	-0.34163	-0.11853	-0.29528	-0.2595	-0.16161	-0.0004855	-0.0011356	-0.10379	-0.24535	-0.1031	-0.067548	-0.079492	-0.088437	-0.81662	-0.53221	-0.18892
07-RT1_CL_60_D	Max	0.19932	0.27484	0.38283	0.33027	0.38424	0.39971	0.00049785	0.0014323	0.13183	0.11	0.19436	0.066153	0.11216	0.11111	0.69602	0.63715	0.37295
	Min	-0.24799	-0.31565	-0.50057	-0.84793	-0.80113	-0.32715	-0.00039053	-0.0011571	-0.10634	-0.21506	-0.1444	-0.080522	-0.11401	-0.10907	-0.81794	-0.79226	-0.40165
07-RT2_CL_80_D	Max	0.40711	0.36599	0.47179	0.45082	0.21051	0.27167	0.00059046	0.0028042	0.18815	0.15009	0.23295	0.071852	0.18594	0.15502	1.4022	1.2604	0.3701
	Min	-0.56434	-0.41249	-0.32744	-0.78651	-0.27069	-0.23791	-0.00048352	-0.0025987	-0.19079	-0.19547	-0.20894	-0.094186	-0.21099	-0.1387	-1.3423	-1.2215	-0.46675
09-CR1_LA_80_D	Max	0.35448	0.44994	0.29865	1.3927	1.1199	0.4161	0.00059079	0.0029867	0.15852	0.12168	0.17823	0.063897	0.096446	0.079642	0.94029	0.49662	0.21051
	Min	-0.56938	-0.38937	-0.3196	-2.086	-1.8341	-0.3229	-0.00061095	-0.0022466	-0.19423	-0.18166	-0.2243	-0.04897	-0.088426	-0.068784	-1.0668	-0.53417	-0.27756
09-CR2_LA_80_D	Max	0.40096	0.39486	0.17083	0.65893	0.53745	0.22087	0.00062629	0.0027093	0.19638	0.14325	0.19918	0.12482	0.098191	0.087065	0.61313	0.41058	0.16306
	Min	-0.31866	-0.32896	-0.14364	-0.60814	-0.97648	-0.21553	-0.00052329	-0.0018393	-0.18053	-0.22586	-0.22048	-0.10382	-0.13154	-0.11885	-0.88507	-0.37486	-0.18238
09-RT1_LA_80_D	Max	0.70117	0.69387	0.54981	1.5619	0.49603	0.458	0.0011119	0.0052918	0.40849	0.10599	0.46015	0.21583	0.21554	0.12152	0.92652	0.56902	0.2002
	Min	-0.75541	-0.41718	-0.44518	-2.4102	-0.6375	-0.53638	-0.00096991	-0.0042825	-0.39562	-0.16932	-0.42064	-0.16432	-0.22647	-0.20517	-0.97231	-0.52864	-0.30244
09-RT2_LA_80_D	Max	0.72264	0.37859	0.45855	1.6849	1.7808	0.36823	0.0014419	0.0065634	0.71912	0.15278	0.80834	0.1228	0.3029	0.17315	1.4117	1.2975	0.41943
	Min	-0.50837	-0.46377	-0.36202	-1.9359	-3.7083	-0.65617	-0.0012619	-0.0049938	-0.51934	-0.21557	-0.60205	-0.11223	-0.33027	-0.19662	-1.763	-1.2417	-0.50978
10-CR1_LA_80_R	Max	0.28731	0.33646	0.38552	0.68472	1.892	0.4425	0.00033213	0.0011016	0.069909	0.18194	0.081969	0.041391	0.23087	0.13651	0.78814	1.3392	0.555
	Min	-0.25476	-0.27703	-0.47116	-1.1849	-1.1936	-0.36106	-0.00033653	-0.001354	-0.096934	-0.15788	-0.081082	-0.032036	-0.16843	-0.14022	-0.91075	-0.87851	-0.47971
10-CR2_LA_80_R	Max	0.23091	0.21182	0.20896	0.50412	0.47038	0.63524	0.00039693	0.001129	0.10402	0.25152	0.11118	0.089223	0.23896	0.18975	0.58686	0.83681	0.50822
	Min	-0.18192	-0.32237	-0.18411	-0.54804	-0.78175	-0.31155	-0.00060475	-0.00118	-0.096819	-0.19465	-0.11245	-0.073161	-0.22882	-0.13855	-0.60332	-1.1377	-0.60191
10-RT1_LA_80_R	Max	0.54371	0.31454	0.66628	1.0535	0.89946	0.54319	0.00091543	0.0025139	0.23469	0.22709	0.2189	0.22521	0.41226	0.35174	1.1967	1.2667	0.59491
	Min	-0.40375	-0.44665	-0.54156	-1.5911	-1.6203	-0.85463	-0.0010678	-0.0031371	-0.29543	-0.20494	-0.3184	-0.23223	-0.47964	-0.39173	-1.0029	-1.6741	-0.55986
10-RT2_LA_80_R	Max	0.3281	0.22631	0.32743	1.1732	1.4424	0.49784	0.00066025	0.0028644	0.29302	0.25725	0.38708	0.099808	0.42054	0.29266	1.0179	1.3999	0.66941
	Min	-0.28185	-0.30104	-0.34726	-0.8987	-0.87648	-0.57014	-0.0010385	-0.0026367	-0.27271	-0.14784	-0.38115	-0.094389	-0.4662	-0.44275	-1.2801	-1.8837	-0.84249
11-RT1_LA_95_D	Max	0.59087	0.55252	0.4519	1.1329	0.45191	0.75907	0.00080437	0.0051794	0.50581	0.13519	0.5438	0.25288	0.39284	0.17398	1.4177	0.47599	0.35052
	Min	-0.69405	-0.40129	-0.63119	-0.74963	-0.6403	-0.67005	-0.001182	-0.0049129	-0.47428	-0.239	-0.53996	-0.25252	-0.29335	-0.20757	-1.2756	-0.48369	-0.40324
11-RT2_LA_105_D	Max	0.70842	0.61301	0.32798	1.3187	0.78607	0.57861	0.0012273	0.0056235	0.58401	0.16665	0.6138	0.108	0.29432	0.092141	1.4129	0.58164	0.52748
	Min	-0.69928	-0.5739	-0.38935	-1.1385	-1.5585	-0.7372	-0.0011748	-0.0058122	-0.5071	-0.22845	-0.56928	-0.13797	-0.23002	-0.14218	-1.0675	-0.61539	-0.43336
12-RT1_LA_100_R	Max	0.41011	0.41809	0.30942	0.92579	1.6751	0.79304	0.00087981	0.0038263	0.32293	0.163	0.30163	0.14765	0.29721	0.21771	1.6764	2.2228	0.50158
	Min	-0.29552	-0.49587	-0.30085	-0.79918	-1.322	-0.93287	-0.0009414	-0.0029709	-0.20925	-0.17383	-0.26935	-0.1382	-0.33414	-0.14858	-1.4515	-1.3898	-0.59653
12-RT2_LA_105_R	Max	0.50492	0.63646	0.39115	4.0075	0.87681	0.78545	0.00086588	0.0036883	0.25591	0.26483	0.25199	0.107	0.45189	0.36907	1.3315	1.6775	0.84419
	Min	-0.41263	-0.53913	-0.30702	-3.2513	-0.81984	-0.62377	-0.00090476	-0.0029854	-0.24386	-0.21065	-0.23521	-0.092802	-0.49854	-0.18273	-1.36	-1.6505	-0.622
13-CR1_KB_CWL_R	Max	0.28265	0.2901	0.24982	0	0.85015	0.53573	0.00005637	0.00019106	0.017333	0.021986	0.021359	0.018623	0.032631	0.045677	0.068938	0.048594	0.050239
	Min	-0.20141	-0.37695	-0.43716	0	-1.4778	-0.63061	-0.000060615	-0.00016527	-0.016408	-0.022698	-0.020579	-0.015209	-0.035769	-0.046507	-0.075907	-0.051686	-0.078959
14-CR1_LA_60_D	Max	0.41402	0.27433	0.40479	1.2029	0.90699	0.37506	0.00045187	0.0022651	0.10203	0.096724	0.10211	0.047617	0.055119	0.098707	1.1308	0.57043	0.17352
	Min	-0.26773	-0.29687	-0.30965	-0.99178	-1.0762	-0.2885	-0.00021302	-0.00099643	-0.10279	-0.14452	-0.12764	-0.032904	-0.044811	-0.085328	-0.89637	-0.6522	-0.13568
14-CR2_LA_60_D	Max	0.31633	0.35427	0.18046	1.9686	0.70444	0.7134	0.00062096	0.00267	0.17207	0.13429	0.18157	0.1342	0.12581	0.15374	0.72825	0.30213	0.11584
	Min	-0.21507	-0.36636	-0.23864	-1.5302	-1.1071	-0.34171	-0.00038336	-0.0014326	-0.12552	-0.17892	-0.12391	-0.13132	-0.14305	-0.095176	-0.49459	-0.24807	-0.16621
15-CR1_LA_60_R	Max	0.19556	0.28675	0.12582	0.53056	0.43104	0.41612	0.00031123	0.00061614	0.052556	0.1362	0.052341	0.033999	0.18411	0.080279	0.6019	0.7374	0.1398
	Min	-0.20048	-0.26983	-0.24696	-0.35041	-0.70033	-0.36037	-0.00028685	-0.00062007	-0.043047	-0.090889	-0.047628	-0.030523	-0.11639	-0.11491	-0.56573	-0.85231	-0.18749
15-CR2_LA_60_R	Max	0.15508	0.19425	0.32711	0.42432	0.30927	0.4338	0.00031432	0.00085181	0.067104	0.20318	0.069705	0.081863	0.1287	0.11049	0.59681	0.93532	0.18579
	Min	-0.10485	-0.15471	-0.19041	-0.27869	-0.22031	-0.2152	-0.00042941	-0.0010708	-0.080829	-0.10718	-0.084909	-0.10356	-0.17694	-0.14624	-0.55189	-1.1358	-0.24333

Sensor type		Accelerometers (Converted to Velocity mm/s)																
Location		Pier 7 headstock							Span 8 girder, end	Pier 7 headstock		Span 7 girder, end	Pier 7 headstock		Span 7 girder	Span 8 girders, mid-span		Span 8 girder, end
Sensor		P7HLS8-a z accel	P7HLS8-a x accel	P7HLS8-a y accel	P7HRS8-a y accel	P7HRS8-a x accel	P7HRS8-a z accel	P7HC-a z accel	S8G1e-a z accel	P7HLS7 z accel	P7HC-a x accel	S7G1e-a z accel	P7HC-a y accel	P7HRS7-a z accel	S7G6-a z accel	S8G1m-a z accel	S8G6m-a z accel	S8G6e-a z accel
STATIC	**Max**	**0.28265**	**0.2901**	**0.28465**	**0**	**0.85898**	**0.5979**	**0.00018267**	**0.00031606**	**0.030505**	**0.040125**	**0.033845**	**0.035618**	**0.032631**	**0.045677**	**0.17093**	**0.19219**	**0.1089**
	Min	**-0.20141**	**-0.37695**	**-0.43716**	**0**	**-1.4778**	**-0.63061**	**-0.0001373**	**-0.00033398**	**-0.028467**	**-0.03819**	**-0.029784**	**-0.037557**	**-0.035769**	**-0.059166**	**-0.3227**	**-0.15384**	**-0.084249**
DYNAMIC	**Max**	**0.72264**	**0.69387**	**0.66628**	**4.0075**	**2.1062**	**0.79304**	**0.0014419**	**0.0065634**	**0.71912**	**0.26483**	**0.80834**	**0.25288**	**0.45189**	**0.36907**	**1.6764**	**2.2228**	**0.84419**
	Min	**-0.75541**	**-0.5739**	**-0.63119**	**-3.2513**	**-3.7083**	**-0.93287**	**-0.0012619**	**-0.0058122**	**-0.51934**	**-0.24535**	**-0.60205**	**-0.25259**	**-0.49854**	**-0.44275**	**-1.763**	**-1.8837**	**-0.84249**
16-RT1_LA_60_D	Max	0.42359	0.44402	0.36581	1.5727	2.1062	0.45229	0.00064427	0.0021177	0.19545	0.13373	0.25676	0.11288	0.13596	0.15039	1.0603	0.63955	0.26037
	Min	-0.39741	-0.37158	-0.31223	-1.647	-2.2347	-0.47612	-0.00058666	-0.0029386	-0.22946	-0.1728	-0.28512	-0.12329	-0.14176	-0.13014	-0.82865	-0.6902	-0.22403
16-RT2_LA_60_D	Max	0.46123	0.28311	0.36581	1.1077	0.89003	0.45225	0.00067489	0.0030964	0.30185	0.10396	0.32127	0.060733	0.14403	0.19594	1.369	0.71196	0.22589
	Min	-0.43903	-0.37158	-0.31603	-1.5421	-1.1316	-0.55277	-0.0008113	-0.0024752	-0.25799	-0.1241	-0.36629	-0.076159	-0.13986	-0.13495	-1.3903	-0.87314	-0.16276
17-RT1_LA_60_R	Max	0.48692	0.43173	0.44102	2.7531	1.2575	0.3278	0.00040651	0.0015098	0.12115	0.16897	0.12376	0.098775	0.23228	0.15888	0.66884	1.0235	0.43167
	Min	-0.23303	-0.52725	-0.31645	-2.4167	-0.82393	-0.40709	-0.00046629	-0.0019211	-0.13637	-0.11133	-0.14062	-0.10893	-0.2256	-0.15542	-0.65547	-0.7348	-0.44126
17-RT2_LA_60_R	Max	0.20301	0.42848	0.36582	0.85559	1.4444	0.54066	0.00041639	0.0018559	0.14339	0.13008	0.14708	0.072237	0.18394	0.18452	0.86791	1.3298	0.47946
	Min	-0.24096	-0.49155	-0.43498	-1.7066	-0.63885	-0.51044	-0.00045405	-0.001897	-0.12624	-0.12461	-0.17344	-0.06353	-0.21934	-0.22566	-1.0447	-1.2778	-0.35895
18-CR1_LA_40_D	Max	0.15473	0.34154	0.22586	0.85399	1.8941	0.52086	0.00019219	0.0014113	0.086575	0.07179	0.090455	0.059855	0.052698	0.053288	1.2976	0.73338	0.13935
	Min	-0.16112	-0.36444	-0.38946	-1.1599	-1.3131	-0.45387	-0.00019555	-0.0013146	-0.07822	-0.088708	-0.091503	-0.048592	-0.060751	-0.056362	-1.3399	-0.56502	-0.15483
18-CR2_LA_40_D	Max	0.31105	0.34963	0.52271	1.6269	2.0598	0.47533	0.00029554	0.0014869	0.072895	0.080656	0.072501	0.04383	0.055251	0.067644	0.93369	0.41109	0.080977
	Min	-0.19094	-0.23072	-0.37332	-1.7411	-0.91362	-0.69521	-0.00015264	-0.0010502	-0.074974	-0.11584	-0.096006	-0.048085	-0.057188	-0.056066	-0.93441	-0.4181	-0.083897
18-RT1_LA_40_D	Max	0.33341	0.21758	0.22234	0.98514	1.051	0.26399	0.00039689	0.0022743	0.14998	0.11255	0.15843	0.081665	0.094881	0.087594	1.2992	0.5671	0.14742
	Min	-0.25829	-0.21506	-0.32913	-0.99164	-0.89915	-0.34526	-0.00032498	-0.001825	-0.17874	-0.13866	-0.18167	-0.11651	-0.10169	-0.092733	-1.351	-0.58869	-0.18046
18-RT2_LA_40_D	Max	0.27874	0.43776	0.43469	1.684	1.169	0.34335	0.00048935	0.0027823	0.16128	0.082044	0.16974	0.039313	0.10776	0.112	0.6886	0.36478	0.16274
	Min	-0.24449	-0.32101	-0.28253	-1.3232	-1.166	-0.42017	-0.0004873	-0.0021182	-0.17634	-0.093512	-0.18162	-0.059905	-0.11782	-0.13011	-0.69246	-0.40873	-0.12828
19-CR1_LA_40_R	Max	0.1132	0.24167	0.24195	1.3064	0.41492	0.31719	0.0002428	0.00083657	0.048763	0.088251	0.052383	0.049089	0.088073	0.10306	0.96767	1.4525	0.28079
	Min	-0.16163	-0.13959	-0.21053	-0.73273	-0.38081	-0.25793	-0.00023289	-0.00084928	-0.045077	-0.094482	-0.062484	-0.046179	-0.092362	-0.10996	-0.93881	-1.5087	-0.22059
19-CR2_LA_40_R	Max	0.14105	0.16519	0.15588	0.88944	0.70301	0.24169	0.00018203	0.00065456	0.053326	0.13608	0.043829	0.057811	0.10462	0.085189	0.52929	0.64092	0.1572
	Min	-0.16547	-0.13283	-0.15833	-0.45708	-0.48805	-0.23235	-0.00017653	-0.00072122	-0.051809	-0.08258	-0.043394	-0.045921	-0.062981	-0.069304	-0.57226	-0.92056	-0.13617
19-RT1_LA_40_R	Max	0.18869	0.36878	0.21989	0.91735	0.83351	0.22704	0.0003009	0.0010963	0.083924	0.13361	0.090283	0.094059	0.15904	0.13208	0.76773	1.056	0.20948
	Min	-0.16571	-0.21425	-0.29353	-0.81386	-1.0474	-0.38296	-0.00028587	-0.0011283	-0.092822	-0.11365	-0.090624	-0.098855	-0.16869	-0.17269	-0.87313	-1.0042	-0.20895
19-RT2_LA_40_R	Max	0.2322	0.25971	0.40413	0.7445	1.477	0.35301	0.00030885	0.00094156	0.092711	0.12092	0.092168	0.049428	0.15043	0.15107	0.35608	0.81336	0.18958
	Min	-0.2483	-0.17135	-0.60292	-1.2203	-1.2684	-0.39209	-0.00031155	-0.0010349	-0.08838	-0.086234	-0.088291	-0.055501	-0.17973	-0.14925	-0.48799	-0.62279	-0.23674
20-CR1_LA_20_D	Max	0.12341	0.40714	0.38076	0.89589	0.79969	0.40875	0.0001441	0.00072785	0.063697	0.031012	0.059962	0.056552	0.052546	0.053321	0.39544	0.23472	0.07515
	Min	-0.13819	-0.16467	-0.29288	-0.90331	-0.69592	-0.25883	-0.000088613	-0.00070414	-0.058165	-0.032072	-0.057487	-0.064159	-0.055057	-0.05425	-0.43565	-0.24589	-0.059394
20-CR2_LA_20_D	Max	0.13468	0.12725	0.34365	0.34185	0.53578	0.13398	0.00013384	0.00072247	0.06525	0.028898	0.066457	0.069931	0.063005	0.060426	0.32628	0.15843	0.061882
	Min	-0.14438	-0.26018	-0.37667	-0.43568	-0.54601	-0.17074	-0.00016447	-0.0008577	-0.081381	-0.034181	-0.076157	-0.061872	-0.054472	-0.051036	-0.24915	-0.13204	-0.064562
20-RT1_LA_20_D	Max	0.29322	0.26734	0.25353	1.0407	1.385	0.24545	0.00025449	0.0024689	0.24315	0.048517	0.23814	0.24661	0.22876	0.24315	0.48446	0.25372	0.27708
	Min	-0.25973	-0.21959	-0.28513	-0.80551	-1.2927	-0.32392	-0.00027473	-0.0024642	-0.22977	-0.058614	-0.22582	-0.25259	-0.21379	-0.19755	-0.61909	-0.24106	-0.25579
20-RT2_LA_20_D	Max	0.15137	0.26739	0.22806	0.92329	0.63792	0.26663	0.00020476	0.00079959	0.075402	0.028717	0.079768	0.058509	0.068932	0.052972	0.26023	0.23344	0.08436
	Min	-0.15689	-0.12304	-0.33685	-0.80659	-0.38771	-0.40289	-0.00021312	-0.00086269	-0.093049	-0.031258	-0.098485	-0.062424	-0.05907	-0.057429	-0.24339	-0.2307	-0.091032
21-CR1_LA_20_R	Max	0.12956	0.14961	0.21853	0.34053	1.2638	0.39148	0.000083706	0.00034758	0.032624	0.033239	0.032246	0.050077	0.048185	0.050393	0.22686	0.4964	0.078818
	Min	-0.10044	-0.1247	-0.14281	-0.65157	-1.2792	-0.49525	-0.000088328	-0.00031535	-0.03308	-0.027906	-0.033134	-0.036426	-0.048961	-0.050474	-0.21875	-0.4685	-0.068003
21-CR2_LA_20_R	Max	0.17831	0.15977	0.12367	0.42248	0.34431	0.12729	0.00018264	0.00049307	0.046738	0.046666	0.045555	0.055807	0.095812	0.070137	0.26793	0.50572	0.088211
	Min	-0.098095	-0.37113	-0.074561	-0.54977	-0.49339	-0.22882	-0.0001699	-0.0005153	-0.050928	-0.054258	-0.048243	-0.059705	-0.067362	-0.060631	-0.23056	-0.5238	-0.097316
21-RT1_LA_20_R	Max	0.17144	0.16651	0.17047	0.55822	0.25189	0.62249	0.00018945	0.001126	0.10595	0.073465	0.10442	0.11465	0.12299	0.099646	0.26425	0.75522	0.1101
	Min	-0.21758	-0.22854	-0.21346	-0.4636	-0.32813	-0.44317	-0.00020675	-0.0010962	-0.10476	-0.078758	-0.10219	-0.12218	-0.13156	-0.10019	-0.27653	-0.52665	-0.1436
21-RT2_LA_20_R	Max	0.14639	0.22717	0.18775	0.5136	1.2047	0.15024	0.00021482	0.00039153	0.036929	0.045196	0.039254	0.04346	0.10215	0.080928	0.18449	0.24679	0.069268
	Min	-0.20092	-0.16131	-0.18	-1.057	-1.6899	-0.29655	-0.0001831	-0.00042356	-0.042106	-0.039774	-0.045681	-0.042134	-0.064913	-0.053959	-0.16753	-0.21426	-0.079242

A.3 Neerkol Creek Bridge

Table A 9: Neerkol Creek Bridge Summary of Peak Responses

			Girders								Headstock				Columns								Bearing Compression			
			Strain (με)				Deflection (mm)				Strain (με)				Strain - Tension (με)				Strain - Compression (με)				Compression (μm)			
			CR1	RT1	RT2	MAX	CR1	RT1	RT2	MAX	CR1	RT1	RT2	MAX	CR1	RT1	RT2	MAX	CR1	RT1	RT2	MAX	CR1	RT1	RT2	MAX
		Max - static	95.53	83.18	86.84	95.53	-6.44	-6.70	-7.10	-7.10	49.74	64.77	59.47	64.77	13.11	17.20	13.79	17.20	-23.59	-31.26	-27.52	-31.26	-294.00	-331.00	-352.58	-352.58
		Max - dynamic	105.26	97.33	96.37	105.26	-7.13	-7.58	-7.09	-7.58	57.83	75.46	74.52	75.46	11.72	14.88	14.39	14.88	-26.12	-31.26	-30.36	-31.26	-294.87	-355.60	-342.60	-355.60
		Corresponding Speed (km/h)	80	80	MAX	80	40	80	80	80	80	80	40	80	40	60	60	80	40	80	40	80	40	80	60	80
		Travel	Lane	Lane	Lane	Lane	CL	CL	CL	CL	CL	CL	CL	CL	CL	Lane	Lane	CL	CL	CL	CL	CL	Lane	Lane	Lane	Lane
		Direction	S	S	S	S	R	R	S	R	S	R	S	R	S	S	S	R	S	R	S	R	R	R	R	R
Lane/ CL	Direction of travel		CR1	RT1	RT2	MAX	CR1	RT1	RT2	MAX	CR1	RT1	RT2	MAX	CR1	RT1	RT2	MAX	CR1	RT1	RT2	MAX	CR1	RT1	RT2	MAX
Lane	Stanwell	*Max - dynamic*	105.26	97.33	96.37	105.26	-5.69	-6.48	-6.67	-6.67	42.40	57.99	59.34	59.34	10.21	14.88	14.39	14.88	-23.17	-30.55	-28.96	-30.55	-245.29	-309.64	-295.19	-309.64
		static	95.53	83.18	86.84	95.53	-5.71	-5.37	-5.80	-5.80	33.30	36.96	37.70	37.70	6.55	8.03	9.64	9.64	-21.57	-24.24	-23.27	-24.24	-245.42	-257.50	-278.62	-278.62
		20 km/h	93.95	96.24	86.59	96.24	-4.93	-6.43	-5.41	-6.43	32.78	42.25	39.56	42.25	7.45	8.69	8.62	8.69	-17.18	-21.00	-19.90	-21.00	-245.29	-309.64	-268.98	-309.64
		40 km/h	99.32	84.40	87.51	99.32	-5.69	-6.07	-6.06	-6.07	42.40	50.80	50.40	50.80	10.21	12.70	12.34	12.70	-22.75	-25.85	-26.42	-26.42	-235.24	-271.25	-277.61	-277.61
		60 km/h	91.31	91.63	90.85	91.63	-5.19	-6.48	-6.18	-6.48	40.02	57.99	59.34	59.34	8.72	14.88	14.39	14.88	-23.17	-30.55	-28.96	-30.55	-234.01	-301.94	-287.99	-301.94
		80 km/h	105.26	97.33	89.56	105.26	-5.50	-6.04	-6.29	-6.29	40.26	56.70	59.28	59.28	9.89	12.77	12.08	12.77	-20.31	-27.90	-28.11	-28.11	-229.18	-262.29	-283.08	-283.08
		max	-	96.54	96.37	96.54	-	-5.90	-6.67	-6.67	-	55.81	53.59	55.81	-	12.39	12.25	12.39	-	-25.71	-25.86	-25.86	-229.00	-260.97	-295.19	-295.19
Lane	Rockhampton	*Max - dynamic*	82.81	86.57	74.97	86.57	-5.65	-6.91	-6.52	-6.91	44.94	66.89	60.28	66.89	11.02	12.51	12.68	12.68	-19.32	-24.70	-22.87	-24.70	-294.87	-355.60	-342.60	-355.60
		static	77.24	65.99	65.20	77.24	-5.73	-5.65	-6.07	-6.07	38.97	40.42	39.40	40.42	11.32	9.18	6.33	11.32	-18.89	-19.68	-16.95	-19.68	-294.00	-331.00	-352.58	-352.58
		20 km/h	-	-	-	0.00	-	-	-	0.00	-	-	-	0.00	-	-	-	0.00	-	-	-	0.00	-	-	-	0.00
		40 km/h	82.81	73.02	73.02	82.81	-5.65	-6.29	-6.32	-6.32	39.51	51.34	53.82	53.82	9.50	10.27	11.28	11.28	-17.98	-21.64	-22.87	-22.87	-294.87	-335.02	-336.62	-336.62
		60 km/h	81.53	76.69	74.97	81.53	-5.56	-6.42	-6.41	-6.42	44.94	66.89	57.54	66.89	10.17	12.51	10.63	12.51	-18.27	-24.70	-22.73	-24.70	-283.95	-334.00	-342.60	-342.60
		80 km/h	76.72	86.57	70.77	86.57	-5.50	-6.91	-6.45	-6.91	44.92	56.41	60.28	60.28	11.02	10.81	10.78	11.02	-19.32	-21.86	-22.27	-22.27	-277.69	-355.60	-339.77	-355.60
		max	-	81.39	72.84	81.39	-	-6.87	-6.52	-6.87	-	55.46	59.00	59.00	-	8.60	12.68	12.68	-	-18.88	-22.36	-22.36	-273.92	-350.94	-333.83	-350.94
CL	Stanwell	*Max - dynamic*	76.73	68.85	70.79	76.73	-6.67	-7.00	-7.09	-7.09	57.83	72.30	74.52	74.52	11.72	13.82	13.28	13.82	-26.12	-28.66	-30.36	-30.36	-278.82	-324.22	-331.86	-331.86
		static	77.88	61.94	68.17	77.88	-6.44	-6.70	-7.10	-7.10	49.74	64.77	59.47	64.77	10.74	17.20	13.79	17.20	-23.59	-31.26	-27.52	-31.26	-280.91	-320.71	-338.37	-338.37
		20 km/h	-	-	-	0.00	-	-	-	0.00	-	-	-	0.00	-	-	-	0.00	-	-	-	0.00	-	-	-	0.00
		40 km/h	76.73	64.31	68.45	76.73	-6.67	-6.79	-7.02	-7.02	56.43	68.87	74.52	74.52	11.72	13.82	13.28	13.82	-26.12	-28.66	-30.36	-30.36	-278.82	-318.10	-331.83	-331.83
		60 km/h	-	-	-	0.00	-	-	-	0.00	-	-	-	0.00	-	-	-	0.00	-	-	-	0.00	-	-	-	0.00
		80 km/h	76.23	68.85	70.79	76.23	-6.30	-7.00	-7.09	-7.09	57.83	72.30	71.40	72.30	10.96	11.59	12.94	12.94	-23.87	-27.58	-29.42	-29.42	-264.32	-324.22	-331.86	-331.86
		max	-	-	-	0.00	-	-	-	0.00	-	-	-	0.00	-	-	-	0.00	-	-	-	0.00	-	-	-	0.00
CL	Rockhampton	*Max - dynamic*	80.48	83.71	72.41	83.71	-7.13	-7.58	-7.00	-7.58	55.54	75.46	72.66	75.46	11.32	13.31	13.42	13.42	-23.43	-31.26	-28.34	-31.26	-286.38	-327.46	-342.40	-342.40
		static	73.45	64.97	69.87	73.45	-6.40	-6.43	-6.78	-6.78	49.14	53.01	57.25	57.25	13.11	9.92	12.87	13.11	-22.87	-25.87	-25.72	-25.87	-291.22	-330.60	-350.18	-350.18
		20 km/h	-	-	-	0.00	-	-	-	0.00	-	-	-	0.00	-	-	-	0.00	-	-	-	0.00	-	-	-	0.00
		40 km/h	80.48	70.48	72.41	80.48	-7.13	-6.80	-7.00	-7.13	55.12	68.12	70.48	70.48	11.32	12.87	13.23	13.23	-23.43	-28.91	-28.34	-28.91	-286.38	-327.46	-342.40	-342.40
		60 km/h	-	-	-	0.00	-	-	-	0.00	-	-	-	0.00	-	-	-	0.00	-	-	-	0.00	-	-	-	0.00
		80 km/h	75.05	83.71	72.04	83.71	-6.41	-7.58	-6.88	-7.58	55.54	75.46	72.66	75.46	10.99	13.31	12.49	13.31	-21.61	-31.26	-26.72	-31.26	-268.41	-326.77	-339.74	-339.74
		max	-	77.37	70.21	77.37	-	-7.22	-6.90	-7.22	-	70.11	69.60	70.11	-	10.96	13.42	13.42	-	-25.93	-27.19	-27.19	-261.86	-320.86	-337.69	-337.69

Table A 10: Neerkol Creek Bridge Peak Responses

Sensor type		Strain gauges (με)												Proximity probes (μm)									Deflection (mm)	Tilt meters (milli-degrees)			
Location		Span 1 girders, mid-span					Pier 7 columns				Pier 7 headstock			Span 2 girders, end			Span 1 girders, end						Girder midspan	Pier headstock			
Sensor/Time (s)		S1G5m	S1G4m	S1G3m	S1G2m	S1G1m	P7CRO	P7CRI	P7CLI	P7CLO	P7HS1	P7HS2	soffit	S2G5e-p	S2G3e-p	S2G1e-p	S1G5e-p	S1G4e-p	S1G3e-p	S1G2e-p	S1G1e-p		LVDT	tilt RHS rot x	tilt RHS rot y	tilt C rot y	tilt LHS rot y
STATIC	**Max**	**38.455**	**77.236**	**26.088**	**95.526**	**39.202**	**17.201**	**3.6811**	**11.685**	**16.231**	**22.455**	**6.8264**	**64.769**	**71.936**	**17.655**	**62.278**	**7.13**	**19.991**	**17.685**	**17.972**	**78.032**		**0.17883**	**42.13**	**12.282**	**8.6676**	**10.759**
	Min	**-9.2452**	**-6.3936**	**-5.454**	**-4.2773**	**-10.598**	**-6.6687**	**-10.939**	**-31.255**	**-7.3493**	**-8.1343**	**-3.8644**	**-15.593**	**-44.264**	**-326.86**	**-32.789**	**-246.47**	**-352.58**	**-350.18**	**-348.93**	**-48.893**		**-7.1026**	**-24.67**	**-12.94**	**-10.059**	**-10.955**
DYNAMIC	**Max**	**48.392**	**86.573**	**31.355**	**108.66**	**66.217**	**14.88**	**5.0317**	**13.208**	**13.815**	**26.345**	**4.8238**	**75.456**	**83.679**	**38.669**	**71.239**	**49.469**	**62.201**	**53.781**	**52.785**	**88.012**		**1.4032**	**38.709**	**29.393**	**15.54**	**21.274**
	Min	**-25.015**	**-24.107**	**-9.9839**	**-17.449**	**-26.226**	**-8.7797**	**-13.432**	**-31.256**	**-7.7773**	**-9.3824**	**-3.4384**	**-15.523**	**-62.059**	**-325.22**	**-35.496**	**-271.23**	**-355.6**	**-342.4**	**-340.54**	**-52.73**		**-7.5789**	**-40.926**	**-23.065**	**-15.358**	**-19.25**
01-CR1_CL_CWL_S	Max	22.934	58.361	26.088	77.882	24.223	10.719	3.4175	7.9446	10.74	17.626	3.3457	49.735	29.399	15.405	31.855	4.557	19.278	14.287	14.089	39.509		0.01857	12.425	12.282	8.6676	10.759
	Min	-5.4961	-5.0294	-4.8318	-2.2177	-6.197	-4.1214	-8.1325	-23.585	-4.3999	-8.1343	-3.4843	-11.335	-3.601	-266.8	-9.145	-133.14	-230.02	-280.91	-280.01	-5.791		-6.4414	-9.036	-5.3855	-4.7134	-4.0506
01-CR2_CL_CWL_S	Max	21.139	49.671	21.592	61.36	20.819	10.946	3.2179	10.361	12.403	18.485	3.4724	45.2	24.325	12.692	28.615	5.454	19.991	15.444	15.092	32.518		0.00506	24.026	12.271	7.5965	9.3206
	Min	-3.731	-4.2688	-3.758	-2.7203	-5.4711	-5.1137	-7.5921	-23.849	-5.7873	-2.8946	-2.5476	-6.7703	-5.175	-234.31	-9.385	-117.55	-205.01	-249.46	-248.71	-6.682		-5.3389	-24.67	-12.94	-10.059	-10.955
01-RT1_CL_CWL_S	Max	25.641	56.72	21.565	61.942	21.024	17.201	3.6811	11.685	16.231	22.455	3.4831	64.769	26.537	17.655	31.348	3.584	12.414	9.794	9.755	33.911		0.17883	42.13	8.0109	6.0518	6.9595
	Min	-4.9386	-5.2597	-5.435	-2.7483	-5.5662	-6.6687	-10.939	-31.255	-7.3493	-7.1454	-2.2369	-11.961	-3.163	-304.44	-8.452	-149.92	-269.09	-320.71	-319.84	-5.289		-6.7042	-21.879	-9.4974	-7.1912	-8.9386
01-RT2_CL_CWL_S	Max	22.317	53.047	21.406	68.166	20.772	13.789	2.0578	7.5007	10.975	20.529	3.2671	59.467	28.15	16.941	31.985	2.624	16.212	12.93	12.868	37.66		0.00535	11.817	6.5143	3.0484	5.4996
	Min	-3.8528	-5.5327	-4.974	-2.424	-6.2085	-3.4313	-10.232	-27.519	-6.0351	-7.7211	-2.8629	-15.593	-3.15	-326.86	-9.615	-142.28	-261.89	-338.37	-337.23	-6.44		-7.1026	-8.928	-3.1331	-2.5086	-3.0739
02-CR1_CL_CWL_R	Max	21.87	60.209	25.245	73.445	22.403	13.11	2.459	5.1737	10.996	16.565	3.2996	49.141	26.17	10.388	32.922	2.905	10.728	10.28	10.24	32.173		0.03425	12.829	2.3578	3.6084	2.3144
	Min	-6.2405	-5.0605	-5.1053	-2.1455	-6.2871	-1.5805	-7.661	-22.866	-4.3741	-5.5145	-3.5804	-9.5194	-3.63	-260.51	-11.278	-136.9	-234.87	-291.22	-290.06	-2.527		-6.4018	-4.6781	-4.8986	-5.4066	-3.5427
02-CR2_CL_CWL_R	Max	21.258	52.376	21.69	64.2	20.433	9.9291	1.2952	2.9646	9.2452	14.24	3.7472	39.688	22.824	10.729	29.667	4.185	15.372	13.187	13.082	31.388		0.02319	11.902	4.0844	3.5357	3.4204
	Min	-2.3217	-3.1237	-2.6997	-2.1002	-4.0871	-2.3709	-7.6548	-20.715	-3.0148	-3.41	-3.5428	-5.442	-6.876	-218.67	-13.433	-119.01	-201.93	-248.81	-248.22	-4.612		-5.4528	-4.7639	-4.6891	-3.9473	-4.484
02-RT1_CL_CWL_R	Max	22.078	51.093	20.652	64.969	19.746	9.9159	1.2268	4.1527	8.572	17.119	2.9246	53.006	21.622	13.481	32.227	3.637	11.539	12.398	12.138	33.158		0.02292	17.497	1.664	2.4498	1.5707
	Min	-4.7419	-5.007	-4.4783	-2.1108	-4.9544	-3.9741	-10.643	-25.867	-6.328	-6.6208	-3.8454	-10.434	-6.278	-292.22	-15.173	-138.06	-256.36	-330.6	-329.46	-2.442		-6.4291	-2.7859	-5.5316	-3.8092	-4.6982
02-RT2_CL_CWL_R	Max	21.836	53.08	21.19	69.867	22.299	12.868	1.7151	3.5476	10.584	17.549	2.7747	57.253	22.614	13.018	34.789	5.688	17.908	15.821	15.973	37.967		0.02585	12.981	4.4377	2.7262	4.4102
	Min	-2.0635	-3.7101	-3.7603	-2.2232	-4.5711	-4.2922	-9.5649	-25.722	-4.0856	-6.7914	-3.1153	-8.5569	-4.386	-313.28	-15.811	-139.21	-265.49	-350.18	-348.93	-3.333		-6.7841	-3.6252	-3.1391	-3.7388	-3.0464
03-CR1_LA_CWL_S	Max	9.0456	32.291	21.188	95.526	39.202	6.5522	1.8801	4.317	6.3211	12.495	2.3322	33.295	5.678	12.799	62.278	4.736	17.925	13.78	13.589	78.032		0.00569	11.014	5.0251	6.3841	4.705
	Min	-3.9344	-4.3086	-5.1918	-3.2141	-10.598	-6.0678	-5.9699	-21.573	-4.7589	-6.4549	-3.7878	-9.9147	-3.922	-236.8	-30.322	-72.664	-156.58	-245.42	-244.71	-40.968		-5.7133	-3.947	-4.8193	-3.5749	-3.5289
03-CR2_LA_CWL_S	Max	10.593	27.976	16.654	78.29	32.149	6.0372	1.2845	4.7834	3.2517	10.401	3.1889	26.602	2.852	11.398	58.511	4.699	16.335	14.485	14.419	65.807		0.00738	9.1696	7.1207	4.2786	5.7045
	Min	-1.7375	-3.4438	-3.8256	-2.48	-8.5614	-4.1528	-6.3455	-16.807	-4.6683	-4.2886	-2.9411	-5.5979	-7.448	-201.1	-32.789	-61.901	-130.87	-204.71	-203.48	-48.893		-4.6136	-9.963	-9.0433	-6.7064	-7.1818
03-RT1_LA_CWL_S	Max	9.9196	28.659	15.936	83.184	31.811	8.0325	1.5599	7.1236	5.8115	13.286	3.574	36.961	4.131	15.468	57.134	4.597	16.497	14.604	14.541	63.352		0.0392	14.2	5.3573	4.0837	4.2667
	Min	-2.3004	-5.3614	-5.454	-3.3159	-10.269	-5.9075	-8.2901	-24.236	-4.1585	-5.7238	-2.256	-10.029	-4.669	-255.03	-29.466	-67.903	-151.2	-257.5	-256.26	-33.948		-5.3678	-11.064	-4.1105	-2.5833	-2.6967
03-RT2_LA_CWL_S	Max	9.2204	31.54	15.636	86.843	29.16	9.637	2.4824	7.2186	3.3557	12.663	3.1356	37.695	3.02	16.978	58.124	5.706	19.312	17.685	17.972	62.878		0.00602	10.668	4.1702	3.2147	4.619
	Min	-1.4996	-5.1705	-3.9839	-4.2773	-7.4303	-1.503	-7.0576	-23.271	-4.9143	-6.5868	-3.8644	-12.265	-4.28	-274.52	-29.976	-72.094	-161.19	-278.62	-277.63	-34.722		-5.802	-6.5612	-3.0333	-1.7563	-2.1814
04-CR1_LA_CWL_R	Max	38.455	77.236	21.624	39.079	9.6102	7.8312	2.0359	3.7967	11.32	14.61	6.8264	38.974	71.936	8.728	9.438	5.619	17.597	13.31	12.767	4.508		0.00427	11.497	3.351	3.7504	3.2859
	Min	-9.2452	-6.3936	-4.9756	-3.0312	-3.7698	-4.2588	-9.0841	-18.893	-3.9304	-3.7998	-3.4436	-8.1061	-44.264	-223.07	-7.962	-218.48	-294	-246.79	-245.73	-2.292		-5.7297	-3.7408	-5.5848	-4.7666	-2.9584
04-CR2_LA_CWL_R	Max	32.112	62.872	17.885	34.207	9.931	4.734	2.7111	3.9135	8.1516	10.31	3.0166	29.712	56.296	6.385	7.925	4.268	14.007	10.478	10.403	2.878		0.03549	15.749	2.6714	2.8766	2.4917
	Min	-6.8079	-5.0978	-3.7351	-2.3428	-2.479	-2.556	-5.5589	-14.597	-2.6384	-2.9002	-2.8834	-5.5077	-42.704	-190.72	-8.275	-187.63	-253.09	-215.92	-215	-2.722		-4.8675	-7.151	-4.9352	-3.7654	-2.4244
04-RT1_LA_CWL_R	Max	33.513	65.993	17.104	40.898	10.046	5.9029	2.1642	4.4101	9.1767	12.429	4.0629	40.419	53.727	9.462	8.503	7.13	17.297	13.804	13.851	4.657		0.03202	17.905	2.0745	2.8832	1.3027
	Min	-3.8566	-4.8366	-2.7456	-1.6623	-1.3337	-3.4471	-8.4758	-19.68	-3.7333	-2.7908	-2.2371	-6.1114	-26.573	-236.84	-7.397	-232.77	-331	-273.9	-272.75	-3.243		-5.65	-8.9683	-3.7994	-3.1278	-2.5472
04-RT2_LA_CWL_R	Max	32.878	65.203	17.934	44.459	9.5582	4.7515	1.9934	3.1244	6.3314	11.767	2.9183	39.4	52.998	11.323	9.118	6.128	17.023	13.34	13.283	5.451		0.03098	10.301	2.0948	1.9297	1.5054
	Min	-2.3421	-5.897	-1.9159	-1.7106	-1.4718	-2.6385	-9.1866	-16.946	-4.5786	-3.4426	-3.3817	-5.1202	-28.402	-258.28	-31.982	-246.47	-352.58	-295.56	-294.32	-1.749		-6.069	-3.1229	-3.1969	-3.0723	-2.2359
05-CR1_CL_40_S	Max	27.532	64.52	29.574	76.733	31.893	9.8643	2.9346	5.4233	11.718	22.002	2.4434	56.429	27.001	10.919	34.398	5.715	18.344	15.384	15.156	36.417		0.02631	13.514	6.3388	5.431	7.8564
	Min	-6.878	-4.3701	-4.3462	-3.0868	-7.6168	-2.8657	-7.9254	-26.117	-4.7617	-5.3581	-2.9266	-7.9709	-2.999	-262.98	-7.102	-142.48	-230.86	-278.82	-277.24	-4.683		-6.6687	-5.3435	-6.344	-4.231	-5.9409
05-CR2_CL_40_S	Max	25.211	52.427	23.304	62.675	25.257	10.124	1.9926	6.6613	10.98	17.529	4.282	46.15	24.568	8.618	30.817	11.119	24.605	23.432	22.913	29.925		0.48235	17.47	8.2255	4.7731	6.8184
	Min	-8.9291	-7.7228	-5.5664	-7.745	-11.733	-4.7164	-7.7474	-23.719	-3.8598	-4.9105	-1.498	-6.5703	-4.532	-237.88	-7.783	-127.08	-224.9	-262.27	-260.89	-9.575		-5.4207	-14.668	-5.741	-3.7729	-5.0066
05-RT1_CL_40_S	Max	29.715	59.171	24.857	64.307	26.898	11.731	3.4288	6.7056	13.815	24.941	3.3235	68.865	32.168	14.698	34.786	6.015	18.893	14.502	14.41	32.661		0.01056	18.503	9.8311	7.0855	7.3576
	Min	-7.5947	-6.3792	-6.0528	-3.7827	-7.9215	-4.8589	-10.981	-28.664	-4.4851	-8.2186	-2.1065	-13.035	-4.832	-299.1	-6.514	-148.38	-263.81	-318.1	-315.99	-5.539		-6.7894	-9.9122	-7.2841	-6.2665	-9.3331
05-RT2_CL_40_S	Max	25.308	55.491	24.637	68.453	29.221	13.211	2.6138	6.002	13.278	26.345	3.8656	74.521	28.921	11.828	35.583	3.623	19.167	15.07	14.883	38.459		0.00588	16.173	7.1571	5.1799	5.9339
	Min	-5.6522	-4.8691	-5.1427	-3.8568	-8.2791	-4.3794	-11.576	-30.358	-4.4416	-6.9947	-2.0244	-10.859	-1.579	-320.17	-6.417	-140.08	-254.23	-331.83	-330.22	-6.441		-7.0181	-8.7837	-5.2104	-3.9461	-6.3099
06-CR1_CL_40_R	Max	30.125	68.488	30.206	80.481	34.366	11.318	2.3416	4.2719	9.8262	19.077	4.0804	55.12	33.532	18.611	32.35	11.543	19.098	15.421	15.241	39.413		0.2073	13.136	6.8696	4.0898	5.8278
	Min	-9.0148	-6.7825	-4.9638	-4.1187	-9.1438	-2.1517	-9.0484	-23.428	-3.7238	-5.9129	-1.9296	-9.3203	-3.968	-257.69	-9.75	-149.06	-242.1	-286.38	-284.76	-4.287		-7.1307	-4.3144	-7.6304	-5.2152	-5.7993
06-CR2_CL_40_R	Max	24.032	56.678	25.94	74.828	31.942	11.602	1.3434	5.3973	9.4779	20.631	2.2675	54.988	28.043	11.551	39.998	7.854	21.388	18.013	17.557	36.942		0.19675	28.654	12.177	7.4227	9.4893
	Min	-8.0576	-7.0318	-4.5197	-4.3825	-9.798	-4.3482	-10.517	-22.593	-5.0121	-4.709	-2.9825	-8.0017	-4.557	-265.55	-12.702	-129.85	-222.01	-283.99	-282.34	-4.258		-6.1362	-22.288	-7.9088	-6.5053	-8.0854
06-RT1_CL_40_R	Max	24.569	52.635	23.968	70.477	32.849	12.867	3.3622	10.543	10.962	24.018	3.5289	68.124	24.261	20.645	40.96	6.222	18.179	17.943	17.698	40.805		0.20208	20.406	8.1322	5.0442	6.6108
	Min	-11.781	-6.5954	-5.692	-5.393	-12.831	-4.3526	-10.088	-28.907	-5.9885	-9.3824	-2.2411	-15.086	-4.639	-299.56	-14.84	-131.38	-240.62	-327.46	-325.7	-5.695		-6.8049	-9.5245	-11.161	-7.1418	-8.0103
06-RT2_CL_40_R	Max	22.957	53.848	24.442	72.406	29.207	13.231	2.3997	5.6922	10.888	24.204	3.1206	70.48	24.734	10.243	34.931	5.266	16.181	15.003	14.865	38.173		0.00491	14.803	5.4639	4.4216	5.3391
	Min	-6.2828	-4.842	-4.7675	-2.6838	-8.2925	-4.1393	-11.01	-28.338	-5.3019	-7.1865	-2.7694	-12.37	-2.266	-303.66	-12.569	-139.83	-254.12	-342.4	-340.54	-3.227		-6.9991	-8.1175	-6.451	-3.7674	-6.3271

Sensor type		Strain gauges (με)											
Location		Span 1 girders, mid-span					Pier 7 columns				Pier 7 headstock		
Sensor/Time (s)		S1G5m	S1G4m	S1G3m	S1G2m	S1G1m	P7CRO	P7CRI	P7CLI	P7CLO	P7HS1	P7HS2	soffit
STATIC	Max	38.455	77.236	26.088	95.526	39.202	17.201	3.6811	11.685	16.231	22.455	6.8264	64.769
	Min	-9.2452	-6.3936	-5.454	-4.2773	-10.598	-6.6687	-10.939	-31.255	-7.3493	-8.1343	-3.8644	-15.593
DYNAMIC	Max	48.392	86.573	31.355	108.66	66.217	14.88	5.0317	13.208	13.815	26.345	4.8238	75.456
	Min	-25.015	-24.107	-9.9839	-17.449	-26.226	-8.7797	-13.432	-31.256	-7.7773	-9.3824	-3.4384	-15.523
07-CR1_LA_40_S	Max	12.024	33.121	24.503	99.322	53.887	10.21	2.2729	4.483	6.2921	16.906	3.6216	42.398
	Min	-4.1862	-4.1286	-4.3169	-2.4082	-13.973	-3.4698	-7.1071	-22.747	-2.8079	-4.7636	-1.8584	-7.5623
07-CR2_LA_40_S	Max	10.114	29.567	20.114	83.937	47.1	8.5907	2.9404	7.0761	5.8368	13.383	3.6403	32.515
	Min	-6.4161	-5.0433	-3.7061	-3.8934	-11.68	-4.5093	-6.5496	-19.514	-3.7832	-4.3871	-2.4897	-6.3248
07-RT1_LA_40_S	Max	15.241	36.521	19.311	84.397	42.874	12.703	3.1727	7.3748	7.9249	18.36	3.6118	50.795
	Min	-4.3587	-6.839	-5.0793	-5.2134	-14.756	-4.3071	-8.8073	-25.845	-2.8651	-5.1499	-1.8782	-9.5747
07-RT2_LA_40_S	Max	11.054	34.102	19.475	87.51	46.341	12.344	2.9161	5.6363	6.2254	18.713	3.4018	50.397
	Min	-3.7564	-4.1778	-4.7451	-3.2098	-13.859	-4.2962	-8.3239	-26.424	-3.3946	-5.1469	-2.2582	-9.3726
08-CR1_LA_40_R	Max	48.392	82.807	21.923	35.641	12.036	5.3168	2.7379	4.3687	9.499	14.351	4.0154	39.511
	Min	-9.588	-4.8733	-3.887	-3.1292	-5.634	-2.3432	-7.4321	-17.981	-2.941	-4.0689	-1.9946	-6.5686
08-CR2_LA_40_R	Max	44.665	77.694	23.834	42.091	13.855	7.5909	2.4852	4.3444	9.941	16.996	3.0282	45.506
	Min	-8.5349	-6.4262	-3.7857	-4.409	-8.4449	-2.9191	-8.6448	-19.046	-4.659	-3.5535	-2.4018	-7.3641
08-RT1_LA_40_R	Max	41.13	73.022	20.273	44.937	16.079	6.9548	2.5618	5.4692	10.272	16.158	2.9259	51.338
	Min	-11.04	-6.668	-4.7373	-2.1727	-3.2407	-2.9152	-10.108	-21.641	-4.6882	-5.1617	-2.2741	-9.5319
08-RT2_LA_40_R	Max	41.261	73.021	20.968	41.737	12.5	7.1032	2.109	4.5355	11.275	16.625	3.253	53.821
	Min	-9.5595	-6.499	-4.6115	-2.3726	-3.9702	-2.9868	-10.281	-22.865	-4.1446	-5.6448	-2.177	-10.129
09-CR1_LA_60_S	Max	10.021	30.826	21.948	91.311	51.367	8.7167	2.5427	4.3485	6.9478	15.605	3.3991	40.018
	Min	-3.3286	-2.8141	-4.6521	-2.1394	-14.382	-2.8033	-6.1973	-23.172	-2.4322	-5.245	-1.7909	-6.5216
09-CR2_LA_60_S	Max	13.482	35.575	23.754	89.175	56.74	11.105	2.7583	6.9524	8.236	17.624	3.6087	43.727
	Min	-3.3176	-3.735	-3.9262	-2.7651	-12.09	-3.7852	-6.8817	-22.318	-3.614	-4.5765	-2.4013	-7.0328
09-RT1_LA_60_S	Max	12.444	38.767	21.843	91.632	54.887	14.88	5.0317	13.208	9.8227	21.76	3.6685	57.994
	Min	-3.286	-3.7726	-4.5367	-3.5979	-15.483	-8.7797	-9.9083	-30.552	-7.7773	-6.4798	-2.2215	-10.176
09-RT2_LA_60_S	Max	11.555	35.03	21.33	90.849	49.702	14.393	3.2155	7.5243	7.0051	21.647	3.258	59.338
	Min	-4.6549	-4.5999	-5.1599	-3.7114	-16.498	-5.3071	-9.2345	-28.956	-3.3749	-6.8931	-2.642	-10.582
10-CR1_LA_60_R	Max	43.913	81.528	24.348	36.278	11.618	6.4074	1.9316	3.9626	10.167	13.985	3.3703	44.935
	Min	-11.217	-5.4023	-3.7825	-2.1018	-3.5321	-2.3626	-7.8184	-18.267	-3.0927	-4.4353	-1.7697	-6.3346
10-CR2_LA_60_R	Max	45.999	83.916	24.925	41.446	13.954	7.6988	2.6914	6.2218	10.525	16.189	3.3897	43.768
	Min	-10.691	-6.574	-4.4051	-3.7844	-7.9357	-2.6512	-8.5886	-19.728	-4.1446	-3.5914	-2.1503	-7.8524
10-RT1_LA_60_R	Max	39.744	76.69	22.3	45.368	16.035	10.478	3.1985	7.0148	12.507	23.373	3.2935	66.886
	Min	-13.076	-8.3999	-5.8399	-5.1923	-9.3452	-3.8322	-13.432	-24.695	-5.5629	-6.7071	-1.8365	-12.304
10-RT2_LA_60_R	Max	38.601	74.965	20.817	42.519	13.702	8.2347	3.0158	4.9075	10.631	16.997	3.1147	57.541
	Min	-11.679	-7.2647	-5.5029	-1.9808	-4.8783	-2.0153	-10.814	-22.732	-4.5088	-6.5732	-2.3653	-11.879
11-CR1_CL_80_S	Max	21.396	60.851	28.239	76.233	29.073	9.7942	2.5408	6.2701	10.956	19.801	3.4322	57.828
	Min	-9.0239	-8.1591	-5.9714	-6.2569	-11.347	-2.9858	-8.4792	-23.87	-3.4136	-7.0193	-1.9878	-11.352
11-CR2_CL_80_S	Max	27.419	69.058	29.391	75.997	30.25	10.849	2.7214	4.9376	9.4532	20.122	4.185	52.453
	Min	-7.7908	-6.052	-4.6987	-3.4331	-8.5098	-3.4105	-8.3986	-21.822	-2.9868	-5.6383	-2.115	-8.7267
11-RT1_CL_80_S	Max	25.09	61.032	26.458	68.845	28.888	10.736	4.2196	9.661	11.591	24.331	3.486	72.299
	Min	-9.8502	-7.9082	-6.7324	-5.0147	-9.6417	-6.5837	-11.46	-27.579	-5.129	-6.4593	-2.234	-12.621
11-RT2_CL_80_S	Max	24.414	56.473	25.432	70.785	32.201	12.408	3.6004	6.4177	12.936	24.689	4.0224	71.399
	Min	-7.7859	-6.3771	-7.0185	-3.4246	-9.359	-4.0224	-9.7496	-29.422	-3.8441	-7.3514	-1.9376	-13.571
12-CR1_CL_80_R	Max	22.686	63.143	29.135	75.053	29.24	10.989	2.2708	4.3997	9.5154	18.777	3.3692	55.543
	Min	-8.5937	-4.5071	-4.8447	-2.7074	-8.7804	-3.0609	-9.0692	-21.61	-3.0946	-5.6826	-2.3508	-11.017
12-CR2_CL_80_R	Max	25.15	69.632	31.355	85.017	32.369	11.483	2.5436	6.0474	9.803	22.142	4.8238	61.575
	Min	-9.69	-7.8981	-5.6851	-6.5931	-11.031	-2.4573	-9.3264	-23.973	-4.157	-6.108	-1.9462	-10.375
12-RT1_CL_80_R	Max	23.023	60.103	28.397	83.707	36.332	11.588	2.5242	7.1437	13.309	24.741	4.1129	75.456
	Min	-9.4968	-9.7669	-6.3126	-8.5233	-14.548	-3.6223	-10.886	-31.256	-4.9913	-7.7092	-2.1371	-13.034
12-RT2_CL_80_R	Max	23.007	54.576	24.783	72.04	29.678	12.493	3.3491	5.7525	10.019	24.267	3.6381	72.657
	Min	-8.3828	-5.134	-5.7374	-2.7198	-8.6816	-3.8871	-10.161	-26.718	-3.0609	-8.2926	-1.9019	-12.873

Sensor type		Proximity probes (μm)								Deflection (mm)	Tilt meters (milli-degrees)			
Location		Span 2 girders, end			Span 1 girders, end					Girder midspan	Pier headstock			
Sensor/Time (s)		S2G5e-p	S2G3e-p	S2G1e-p	S1G5e-p	S1G4e-p	S1G3e-p	S1G2e-p	S1G1e-p	LVDT	tilt RHS rot x	tilt RHS rot y	tilt C rot y	tilt LHS rot y
STATIC	Max	71.936	17.655	62.278	7.13	19.991	17.685	17.972	78.032	0.17883	42.13	12.282	8.6676	10.759
	Min	-44.264	-326.86	-32.789	-246.47	-352.58	-350.18	-348.93	-48.893	-7.1026	-24.67	-12.94	-10.059	-10.955
DYNAMIC	Max	83.679	38.669	71.239	49.469	62.201	53.781	52.785	88.012	1.4032	38.709	29.393	15.54	21.274
	Min	-62.059	-325.22	-35.496	-271.23	-355.6	-342.4	-340.54	-52.73	-7.5789	-40.926	-23.065	-15.358	-19.25
07-CR1_LA_40_S	Max	6.284	12.046	67.547	6.599	18.443	15.558	15.32	80.543	0.0072	9.0529	8.1109	5.9311	7.8616
	Min	-5.516	-232.55	-27.753	-68.701	-146.76	-235.24	-234.08	-41.757	-5.6918	-5.5057	-5.7982	-4.4689	-6.766
07-CR2_LA_40_S	Max	5.802	8.931	63.588	10.773	16.555	16.323	16.061	70.418	0.16671	17.666	5.3375	3.8823	7.0024
	Min	-8.098	-205.67	-28.212	-61.727	-129.95	-220.28	-218.64	-42.982	-4.7893	-8.742	-5.7793	-4.7657	-6.6458
07-RT1_LA_40_S	Max	7.619	11.748	57.204	10.105	22.826	19.353	19.284	60.425	0.03929	19.294	6.5882	5.4913	8.7277
	Min	-3.081	-263.45	-21.796	-84.195	-168.87	-271.25	-269.92	-25.675	-6.0667	-10.949	-7.5546	-6.4397	-10.184
07-RT2_LA_40_S	Max	5.563	11.105	61.399	6.431	20.63	15.894	15.672	68.03	0.00447	14.051	6.3196	4.5977	7.4248
	Min	-3.637	-272.1	-24.401	-70.169	-157.37	-277.61	-275.93	-29.27	-6.0565	-3.2866	-4.3744	-3.1383	-6.5214
08-CR1_LA_40_R	Max	82.961	10.552	9.456	11.513	21.733	13.785	13.723	4.918	0.05865	11.922	8.2652	3.4672	5.1712
	Min	-51.539	-210.75	-7.544	-231.49	-294.87	-231.52	-230.28	-7.882	-5.6493	-6.6726	-7.1845	-4.2338	-4.5099
08-CR2_LA_40_R	Max	76.271	12.025	13.393	10.464	25.474	18.492	18.234	7.936	0.11408	24.419	15.533	9.5604	10.783
	Min	-39.429	-224.07	-9.707	-211.04	-287.83	-249.71	-248.47	-7.664	-5.9579	-16.346	-10.294	-6.6126	-7.0751
08-RT1_LA_40_R	Max	56.705	11.212	17.498	8.325	21.676	15.829	15.701	9.297	0.0412	19.529	10.265	6.103	7.2354
	Min	-18.895	-242.79	-7.802	-238.07	-335.02	-280.87	-279.3	-7.303	-6.2948	-9.9125	-11.51	-7.472	-9.5781
08-RT2_LA_40_R	Max	57.402	8.425	12.233	6.422	19.584	16.24	16.039	5.915	0.00592	12.115	7.7749	4.3793	4.8913
	Min	-20.798	-251.38	-7.467	-239.48	-336.62	-280.86	-279.36	-4.085	-6.3231	-5.3841	-6.0554	-3.4017	-3.5002
09-CR1_LA_60_S	Max	5.939	11.265	68.574	4.907	18.079	15.986	15.848	81.126	0.02026	13.283	7.8666	7.1071	9.9776
	Min	-5.361	-231.03	-26.926	-64.293	-142.42	-234.01	-232.35	-46.974	-5.1887	-3.8052	-7.6494	-6.7589	-10.689
09-CR2_LA_60_S	Max	6.922	12.138	66.47	6.089	19.975	17.629	17.727	83.24	0.08009	25.093	14.627	12.676	17.883
	Min	-4.878	-260.66	-33.83	-73.511	-153.02	-253.57	-251.97	-36.16	-5.5189	-20.713	-14.444	-12.638	-17.652
09-RT1_LA_60_S	Max	7.011	12.047	60.765	6.07	21.466	17.458	17.39	73.215	0.00695	38.709	10.819	9.8017	13.545
	Min	-5.489	-265.55	-20.735	-80.53	-174.53	-301.94	-299.51	-27.285	-6.4821	-40.926	-13.952	-10.524	-14.766
09-RT2_LA_60_S	Max	6.762	12.338	63.87	5.844	20.159	20.506	20.01	67.935	0.02035	14.588	8.5732	7.1773	10.37
	Min	-4.238	-282.86	-26.63	-70.156	-156.24	-287.99	-285.79	-30.965	-6.1757	-12.392	-7.9643	-6.5657	-10.667
10-CR1_LA_60_R	Max	74.37	6.27	8.733	6.828	19.651	13.284	13.106	4.496	0.0519	13.95	12.213	6.3946	6.108
	Min	-44.03	-217.23	-5.467	-216.67	-283.95	-231.02	-229.69	-4.504	-5.5591	-7.2217	-9.6414	-6.1644	-5.87
10-CR2_LA_60_R	Max	81.439	9.61	11.704	8.435	22.887	15.719	15.619	4.971	0.20286	21.197	16.256	9.2121	9.1374
	Min	-51.261	-232.69	-8.596	-223.86	-294.51	-241.78	-240.78	-7.329	-5.9071	-14.089	-14.005	-9.1159	-8.6475
10-RT1_LA_60_R	Max	65.505	27.836	15.666	7.999	21.098	15.334	15.352	8.334	0.18264	31.383	23.318	12.454	11.042
	Min	-22.195	-297.56	-13.734	-234.3	-334	-284.87	-283.05	-6.666	-6.4244	-21.502	-15.91	-9.1055	-11.247
10-RT2_LA_60_R	Max	57.396	9.504	11.291	6.024	18.5	13.45	13.309	8.324	0.00634	11.93	10.484	5.7507	5.8174
	Min	-21.704	-255.7	-7.809	-235.08	-342.6	-286.25	-284.59	-5.876	-6.4137	-4.4038	-7.5262	-4.6643	-5.321
11-CR1_CL_80_S	Max	28.62	19.445	31.701	12.887	30.585	29.576	28.548	36.039	0.27389	14.094	17.703	13.533	17.353
	Min	-6.08	-270.86	-6.099	-122.41	-212.12	-264.32	-262.65	-4.161	-6.3001	-7.2771	-12.6	-7.1453	-9.7069
11-CR2_CL_80_S	Max	26.001	23.26	33.485	8.691	24.266	23.992	24.062	27.851	0.21938	16.1	18.264	13.72	18.418
	Min	-7.599	-260.44	-9.815	-153.51	-253.03	-279.11	-277.44	-6.149	-6.8966	-11.442	-13.369	-9.109	-12.211
11-RT1_CL_80_S	Max	35.219	17.685	31.483	10.392	28.274	22.378	21.651	33.28	0.03957	23.286	18.675	12.182	14.164
	Min	-6.481	-323.82	-6.317	-151.71	-262.33	-324.22	-321.75	-6.42	-6.9984	-20.545	-16.671	-11.403	-12.693
11-RT2_CL_80_S	Max	28.734	10.283	38.357	11.205	23.587	21.041	20.479	36.83	0.01634	15.738	12.552	9.3795	11.485
	Min	-3.266	-325.22	-5.843	-140.79	-249.81	-331.86	-329.22	-6.97	-7.0907	-9.2738	-9.5282	-6.2975	-7.8869
12-CR1_CL_80_R	Max	32.216	14.338	29.427	7.132	21.434	17.59	17.409	31.15	0.09125	7.2644	19.961	13.164	15.735
	Min	-2.384	-253.66	-9.473	-132.77	-225.87	-268.41	-266.29	-3.05	-6.4087	-3.9646	-13.667	-8.901	-9.9669
12-CR2_CL_80_R	Max	24.513	22.643	34.956	13.465	21.92	19.672	19.296	33.099	0.51273	16.424	20.172	13.461	16.279
	Min	-7.787	-258.16	-13.444	-142.43	-224.18	-284.83	-282.8	-5.301	-6.8893	-13.524	-14.329	-11.13	-13.808
12-RT1_CL_80_R	Max	26.407	21.646	38.623	15.313	21.306	20.333	19.965	43.197	0.37412	22.381	17.187	13.879	15.421
	Min	-5.093	-298.75	-16.077	-136.79	-250.19	-326.77	-324.54	-6.603	-7.5789	-15.932	-23.065	-15.358	-19.25
12-RT2_CL_80_R	Max	29.697	8.679	35.165	8.258	20.726	18.856	18.833	34.742	0.00606	14.659	10.74	7.6277	10.954
	Min	-2.003	-302.42	-10.735	-150.64	-257.67	-339.74	-337.77	-4.358	-6.8789	-8.3662	-10.217	-7.1123	-9.809

Sensor type		Strain gauges (με)												Proximity probes (μm)								Deflection (mm)	Tilt meters (milli-degrees)			
Location		Span 1 girders, mid-span					Pier 7 columns				Pier 7 headstock			Span 2 girders, end			Span 1 girders, end					Girder midspan	Pier headstock			
Sensor/Time (s)		S1G5m	S1G4m	S1G3m	S1G2m	S1G1m	P7CRO	P7CRI	P7CLI	P7CLO	P7HS1	P7HS2	soffit	S2G5e-p	S2G3e-p	S2G1e-p	S1G5e-p	S1G4e-p	S1G3e-p	S1G2e-p	S1G1e-p	LVDT	tilt RHS rot x	tilt RHS rot y	tilt C rot y	tilt LHS rot y
STATIC	**Max**	**38.455**	**77.236**	**26.088**	**95.526**	**39.202**	**17.201**	**3.6811**	**11.685**	**16.231**	**22.455**	**6.8264**	**64.769**	**71.936**	**17.655**	**62.278**	**7.13**	**19.991**	**17.685**	**17.972**	**78.032**	**0.17883**	**42.13**	**12.282**	**8.6676**	**10.759**
	Min	**-9.2452**	**-6.3936**	**-5.454**	**-4.2773**	**-10.598**	**-6.6687**	**-10.939**	**-31.255**	**-7.3493**	**-8.1343**	**-3.8644**	**-15.593**	**-44.264**	**-326.86**	**-32.789**	**-246.47**	**-352.58**	**-350.18**	**-348.93**	**-48.893**	**-7.1026**	**-24.67**	**-12.94**	**-10.059**	**-10.955**
DYNAMIC	**Max**	**48.392**	**86.573**	**31.355**	**108.66**	**66.217**	**14.88**	**5.0317**	**13.208**	**13.815**	**26.345**	**4.8238**	**75.456**	**83.679**	**38.669**	**71.239**	**49.469**	**62.201**	**53.781**	**52.785**	**88.012**	**1.4032**	**38.709**	**29.393**	**15.54**	**21.274**
	Min	**-25.015**	**-24.107**	**-9.9839**	**-17.449**	**-26.226**	**-8.7797**	**-13.432**	**-31.256**	**-7.7773**	**-9.3824**	**-3.4384**	**-15.523**	**-62.059**	**-325.22**	**-35.496**	**-271.23**	**-355.6**	**-342.4**	**-340.54**	**-52.73**	**-7.5789**	**-40.926**	**-23.065**	**-15.358**	**-19.25**
13-CR1_LA_80_S	Max	8.6505	30.191	23.745	105.26	55.412	9.8935	2.172	5.2903	4.7656	16.102	3.4396	40.264	7.304	13.602	65.404	13.774	25.604	24.715	24.077	83.77	0.11872	10.945	11.746	11.01	17.878
	Min	-5.7795	-5.8787	-5.5852	-3.7103	-15.598	-2.2565	-6.098	-20.31	-3.6144	-4.508	-2.3404	-7.0762	-6.496	-226.1	-35.496	-59.826	-138.3	-229.18	-227.72	-52.73	-5.5043	-7.6817	-11.521	-7.8216	-11.963
13-CR2_LA_80_S	Max	11.641	38.094	26.88	108.66	66.217	11.268	2.7274	5.6233	4.5067	17.929	4.1418	43.14	6.395	14.393	70.508	10.879	23.078	24.234	23.796	88.012	0.1579	16.995	13.302	12.319	19.692
	Min	-5.4294	-4.9958	-5.0603	-5.927	-17.253	-3.4116	-7.8126	-22.127	-4.5833	-5.1609	-3.1582	-7.1601	-7.005	-239.31	-30.292	-77.021	-169.92	-262.87	-261.2	-29.588	-6.5991	-16.137	-11.097	-11.84	-17.608
13-RT1_LA_80_S	Max	10.964	36.347	21.649	97.326	56.329	12.768	4.0448	8.3968	5.4305	20.265	3.675	56.695	9.825	30.844	71.239	16.832	30.837	27.014	26.906	75.224	0.24002	18.172	14.458	13.046	20.978
	Min	-6.5363	-7.9231	-5.9709	-5.6936	-14.901	-3.9717	-8.5652	-27.903	-4.1895	-7.8649	-1.925	-12.575	-10.575	-267.76	-32.561	-72.868	-155.86	-262.29	-260.29	-27.476	-6.042	-15.96	-14.814	-12.925	-17.596
13-RT2_LA_80_S	Max	10.523	35.671	19.689	89.564	47.223	12.076	1.7032	7.0352	6.6361	20.877	3.8049	59.277	11.147	9.92	59.642	22.107	25.034	21.718	21.687	67.747	0.00447	12.759	11.169	9.2905	14.341
	Min	-5.2569	-5.2592	-6.0611	-4.666	-15.887	-6.0444	-9.9568	-28.105	-3.6339	-7.2526	-2.9051	-11.513	-4.053	-284.98	-25.658	-72.593	-161.57	-283.08	-281.01	-30.553	-6.2885	-6.8596	-9.3944	-8.5225	-12.496
14-CR1_LA_60_R	Max	35.082	76.72	22.18	36.463	11.685	3.6303	2.3942	4.1782	11.022	12.592	2.8461	44.92	72.254	4.225	6.498	8.295	23.006	15.686	15.696	3.633	0.06292	16.857	13.98	6.9678	6.6483
	Min	-10.998	-7.2402	-4.5896	-2.4168	-4.8447	-3.2397	-7.5658	-19.322	-3.1779	-3.9284	-2.2839	-7.0501	-45.746	-219.88	-3.302	-211.51	-277.69	-233.31	-231.8	-4.967	-5.5031	-9.3491	-12.088	-7.4432	-7.1277
14-CR2_LA_80_R	Max	39.006	84.139	24.298	41.212	11.485	5.5538	2.4057	5.1578	11.178	17.63	2.9203	51.614	62.392	21.036	10.523	7.436	20.243	13.058	12.846	4.293	0.00514	16.068	24.225	12.232	12.098
	Min	-11.224	-5.9114	-4.4016	-3.0682	-5.4947	-2.2062	-8.6743	-21.722	-3.8923	-4.5703	-1.9797	-8.7064	-41.908	-213.76	-15.477	-212.66	-279.06	-236.74	-235.05	-7.107	-6.0589	-13.992	-15.704	-9.6615	-9.1886
14-RT1_LA_80_R	Max	45.245	86.573	22.006	47.917	16.871	6.0446	3.4509	7.4127	10.81	16.949	2.9328	56.41	59.94	18.472	12.034	49.469	62.201	53.781	52.785	9.409	1.4032	21.469	15.232	9.7449	10.238
	Min	-25.015	-24.107	-9.9839	-14.433	-14.689	-2.8254	-11.279	-21.857	-4.7902	-6.9805	-3.3072	-14.37	-29.66	-248.53	-9.866	-271.23	-355.6	-285.02	-282.71	-13.991	-6.9058	-10.808	-19.372	-12.049	-12.859
14-RT2_LA_80_R	Max	33.103	70.774	19.705	43.512	13.13	6.0716	2.5479	5.9532	10.784	17.479	3.4454	60.283	58.643	8	11.784	7.239	20.028	15.437	15.441	4.003	0.04478	10.916	13.338	7.492	7.3679
	Min	-12.397	-9.7263	-5.9354	-3.5476	-6.3696	-3.0084	-10.172	-22.267	-4.1056	-5.6714	-2.0346	-11.707	-23.657	-249.6	-5.916	-238.26	-339.77	-291.86	-289.56	-7.897	-6.4522	-6.4885	-11.604	-6.587	-6.9095
15-CR1_LA_80_S	Max	8.7106	30.474	21.455	101.98	51.673	8.9814	2.5719	3.7351	4.9226	16.079	2.9978	41.859	7.554	12.188	65.946	17.7	29.552	28.603	28.208	81.297	0.2689	12.599	12.775	10.483	17.05
	Min	-6.8994	-7.1056	-5.9955	-5.477	-15.727	-3.9586	-6.6981	-21.045	-2.5874	-4.8205	-2.1922	-6.5411	-7.146	-225.11	-33.554	-59.5	-138.85	-229	-227.39	-52.503	-5.4641	-8.1681	-11.16	-6.5989	-10.472
15-CR2_LA_80_S	Max	10.947	39.378	24.608	102.85	60.877	10.825	2.5752	5.2938	5.3285	19.219	4.511	44.467	7.492	18.963	63.354	11.244	23.63	24.543	24.376	80.243	0.17957	18.746	15.204	13.525	21.274
	Min	-4.6628	-4.7915	-5.172	-5.7813	-16.013	-3.3254	-8.3948	-21.236	-3.7015	-4.8206	-2.549	-8.9133	-6.708	-241.14	-23.646	-78.356	-169.77	-257.36	-255.62	-26.957	-6.3844	-16.783	-11.187	-9.3285	-14.369
15-RT1_LA_85_S	Max	10.04	35.323	20.316	96.539	52.667	12.392	4.368	8.8522	6.0518	19.376	3.7241	55.806	11.921	38.669	70.447	17.273	28.937	25.63	24.626	70.793	0.18546	16.518	13.958	13.057	21.066
	Min	-6.1096	-7.2173	-5.9543	-4.4206	-14.223	-4.238	-9.202	-25.708	-3.2182	-7.034	-1.8159	-12.914	-10.979	-267.93	-30.253	-71.527	-153.16	-260.97	-258.87	-24.607	-5.8995	-15.419	-15.088	-13.019	-18.003
15-RT2_LA_95_S	Max	11.732	38.803	19.622	96.369	49.123	12.253	2.0294	6.0876	6.6094	19.541	3.3975	53.587	8.768	9.216	60.846	12.548	25.626	23.605	23.079	67.047	0.05593	12.69	14.415	11.773	18.728
	Min	-4.8483	-6.3874	-5.3376	-6.481	-17.537	-3.9674	-9.4106	-25.862	-3.8906	-6.8092	-2.4425	-10.863	-7.432	-275.18	-26.954	-82.852	-170.67	-295.19	-293.32	-25.453	-6.6681	-9.9186	-14.019	-12.712	-19.032
16-CR1_LA_80_R	Max	37.661	79.047	19.741	34.265	10.688	3.761	2.9482	4.4394	8.6575	12.502	3.073	39.67	75.641	12.272	7.542	8.496	21.582	14.755	14.757	5.092	0.37422	7.7424	22.129	12.127	11.323
	Min	-15.429	-11.283	-5.5587	-5.3947	-7.4921	-2.419	-7.5918	-15.521	-3.6625	-3.8485	-2.127	-8.0796	-62.059	-203.13	-9.358	-222	-273.92	-213.55	-212.24	-11.808	-5.2488	-5.467	-15.57	-8.9775	-8.2666
16-CR2_LA_80_R	Max	35.314	73.456	20.044	44.191	16.388	5.9998	2.6016	5.0753	10.682	15.527	3.1461	48.598	83.679	24.087	11.256	15.879	30.646	21.921	21.589	6.949	0.26122	16.863	29.393	15.54	13.18
	Min	-14.006	-11.734	-5.426	-6.0886	-9.6722	-3.0902	-7.9384	-19.305	-3.9776	-4.6134	-2.9239	-7.6025	-43.921	-262.21	-12.744	-226.12	-309.15	-260.38	-258.41	-12.551	-6.2558	-14.183	-20.255	-12.661	-11.656
16-RT1_LA_90_R	Max	37.084	81.393	20.36	44.961	13.989	7.913	3.5134	6.829	8.5965	16.452	4.0269	55.459	56.301	26.727	53.762	29.821	40.555	46.476	45.787	13.116	1.1394	15.197	19.313	11.166	9.9192
	Min	-18.096	-19.677	-8.8499	-17.449	-18.201	-3.227	-11.537	-18.881	-4.8335	-6.8177	-2.3931	-12.201	-31.499	-264.27	-10.938	-266.08	-350.94	-280.22	-278.31	-13.184	-6.8746	-9.9652	-19.965	-12.788	-14.791
16-RT2_LA_94_R	Max	30.817	72.838	19.699	45.755	12.828	6.7156	2.8471	8.0149	12.675	20.212	3.9083	58.996	58.177	25.787	14.12	9.386	20.468	16.952	16.253	5.772	0.18279	10.92	23.399	13.707	13.621
	Min	-13.973	-11.662	-6.4507	-5.6947	-5.9216	-3.2744	-11.673	-22.355	-4.2746	-6.1984	-2.7417	-13.494	-26.623	-276.01	-8.58	-238.01	-333.83	-284.05	-282.15	-7.028	-6.5242	-7.5402	-18.893	-10.433	-11.719
18-CR1_LA_20_S	Max	6.4089	29.128	16.874	93.948	33.513	7.452	2.7258	5.051	5.2876	9.4496	3.0719	32.777	5.9207	10.161	59.19	6.125	19.625	16.756	16.584	69.064	0.0042611	10.853	4.4859	5.5637	4.9092
	Min	-3.1211	-6.0721	-5.1363	-3.9518	-10.857	-4.168	-5.4342	-17.179	-3.7424	-4.5204	-3.0581	-7.4731	-3.5365	-228.53	-22.019	-68.114	-146.34	-245.29	-243.73	-35.32	-4.9346	-8.8712	-3.0347	-2.6356	-4.132
18-CR2_LA_20_S	Max	6.3587	27.6	14.694	85.459	37.442	7.5673	2.4287	4.9744	5.9348	10.53	3.3298	32.727	3.2297	9.2303	55.242	4.8489	17.855	16.088	15.944	73.398	0.0054167	19.55	8.1584	5.4495	8.1746
	Min	-3.1213	-6.5698	-4.426	-4.0409	-10.118	-3.4727	-5.7813	-16.616	-5.1552	-4.0302	-1.9202	-7.5131	-4.7623	-220.94	-23.3	-64.194	-133.6	-222.56	-221.29	-38.18	-4.7462	-18.006	-7.2202	-6.4109	-7.2677
18-RT1_LA_20_S	Max	14.043	39.667	16.452	96.241	41.694	8.6862	3.556	8.6739	5.6002	11.334	3.5	42.252	9.8421	11.836	55.58	24.603	41.178	34.992	34.86	63.27	0.45336	21.755	14.036	9.5485	12.791
	Min	-10.667	-13.953	-9.8079	-10.779	-26.226	-5.8338	-7.564	-20.996	-4.2598	-7.2061	-2.22	-13.338	-8.5839	-285.47	-19.767	-101.76	-195.21	-309.64	-307.15	-28.329	-6.4328	-14.696	-10.572	-7.1303	-9.3144
18-RT2_LA_20_S	Max	6.4146	28.506	12.625	86.588	30.469	8.6166	2.9931	5.3488	4.2643	11.611	3.4794	39.559	6.2711	9.7849	56.885	10.638	21.916	20.025	20.051	57.938	0.0038889	13.329	4.8595	3.8657	6.0057
	Min	-4.1354	-7.8841	-5.3046	-5.8621	-11.271	-5.0634	-6.6969	-19.901	-2.4757	-4.6088	-2.0006	-9.5914	-3.4525	-271.49	-23.389	-69.149	-149.33	-268.98	-267.26	-27.135	-5.4078	-5.6934	-3.3889	-2.1324	-3.3536
19-CR1_CL_80_R	Max	18.503	57.589	24.239	70.689	25.539	9.1377	2.5294	5.6611	9.2743	16.545	3.6356	53.874	29.268	11.715	30.657	11.822	21.972	19.345	18.976	30.557	0.3852	7.9918	20.659	14.408	18.105
	Min	-10.787	-8.5509	-7.291	-5.681	-13.791	-3.3823	-8.2806	-20.869	-4.4457	-5.9048	-1.9644	-12.686	-3.832	-256.19	-6.743	-124.68	-215.13	-261.86	-260.02	-4.343	-5.9978	-4.4246	-13.974	-9.1432	-10.252
19-CR2_CL_80_R	Max	21.037	67.047	27.066	87.187	31.159	10.245	2.6174	5.2699	9.8967	20.163	3.2465	58.496	22.347	21.983	34.062	16.361	25.337	25.149	24.673	33.316	0.51664	14.319	21.242	13.749	17.473
	Min	-9.9734	-10.753	-7.3044	-8.8227	-10.691	-2.4252	-7.8226	-23.88	-3.5333	-5.5371	-3.2335	-10.124	-7.953	-256.82	-13.038	-142.94	-221.76	-278.45	-276.53	-4.384	-6.9254	-13.725	-12.197	-9.1307	-12.258
19-RT1_CL_90_R	Max	18.812	57.765	23.957	77.371	28.851	10.962	3.1945	6.9371	10.772	22.946	3.623	70.107	25.958	17.524	37.156	16.021	23.297	23.94	23.293	36.392	0.5782	18.613	16.661	12.363	15.447
	Min	-10.478	-12.915	-7.6928	-9.4594	-14.089	-3.9284	-11.215	-25.933	-5.1278	-7.9042	-2.037	-15.523	-4.342	-290.18	-11.444	-136.38	-248.6	-320.86	-318.61	-6.908	-7.2188	-14.216	-18.27	-12.617	-16.42
19-RT2_CL_94_R	Max	16.473	54.874	20.377	70.205	25.802	13.419	3.147	5.7977	10.967	20.732	3.4516	69.599	27.944	15.212	36.775	8.783	23.31	20.812	20.391	30.595	0.01652	17.663	15.216	11.068	14.618
	Min	-7.317	-8.5657	-5.5533	-4.0052	-9.2385	-2.5808	-10.093	-27.192	-4.4629	-7.7579	-3.4384	-13.361	-2.956	-304.39	-11.425	-141.02	-255.09	-337.69	-335.21	-5.105	-6.8965	-11.356	-14.527	-9.1581	-12.653

Sensor type		Velocity															
Location		Span 1 girders, end			Span 1 girders, mid-span		Span 2 girders, end			Pier 7 headstock			Pier 1 headstock				
Sensor/Time (s)		S1G2e-a vel	S1G3e-a vel	S1G4e-a vel	S1G3m vel	S1G5m vel	S2G2e-a vel	S2G3e-a vel	S2G4e-a vel	P7 HS1-a z vel	P7 HS2-a z vel	P7 HC-a x vel	P1H RHS-a x vel	P1H RHS-a z vel	P1H LHS-a x vel	P1H LHS-a y vel	P1H LHS-a z vel
STATIC	**Max**	**0**	**1.4032**	**0**	**9.3336**	**9.0774**	**14.204**	**0**	**0**	**0.38182**	**0.4495**	**2.5622**	**14.148**	**6.3326**	**2.5891**	**4.3384**	**0.15781**
	Min	**0**	**-1.6263**	**0**	**-10.656**	**-8.3944**	**-10.174**	**0**	**0**	**-0.44159**	**-0.4827**	**-2.5544**	**-12.254**	**-6.8999**	**-2.6129**	**-4.4923**	**-0.15393**
DYNAMIC	**Max**	**26.199**	**8.3469**	**30.734**	**52.181**	**61.875**	**36.298**	**45.082**	**41.815**	**5.7287**	**5.2527**	**6.0197**	**6.346**	**9.0174**	**5.3241**	**6.6129**	**2.1538**
	Min	**-23.272**	**-9.466**	**-49.248**	**-56.231**	**-63.324**	**-38.632**	**-29.024**	**-32.21**	**-7.2631**	**-6.4158**	**-5.768**	**-7.5538**	**-5.2826**	**-5.7157**	**-8.1065**	**-2.5429**
01-CR1_CL_CWL_S	Max	0	0.98	0	2.9486	2.6218	1.2472	0	0	0.17742	0.18867	0.8785	1.0304	0.47103	0.86243	1.8091	0.09574
	Min	0	-0.9887	0	-2.5047	-2.5731	-1.5278	0	0	-0.19144	-0.21434	-1.0177	-1.1339	-0.49548	-1.148	-1.7337	-0.083283
01-CR2_CL_CWL_S	Max	0	1.4032	0	6.3926	6.0682	0.39721	0	0	0.34779	0.373	2.2648	1.7245	0.30269	2.2555	4.3182	0.12578
	Min	0	-1.204	0	-5.8073	-4.7864	-0.35552	0	0	-0.33968	-0.34785	-2.0476	-1.2497	-0.239	-1.9722	-4.4923	-0.11778
01-RT1_CL_CWL_S	Max	0	0.96921	0	9.3336	9.0774	0.64717	0	0	0.38182	0.4495	2.5622	2.8613	0.54901	2.5891	4.3384	0.15781
	Min	0	-1.3303	0	-10.656	-8.3944	-0.58532	0	0	-0.44159	-0.4827	-2.5544	-2.9448	-0.57657	-2.6129	-4.2451	-0.15393
01-RT2_CL_CWL_S	Max	0	1.1056	0	1.4779	1.477	0.41033	0	0	0.19514	0.21867	0.4632	0.61182	0.50334	0.44902	1.795	0.094955
	Min	0	-0.93154	0	-1.4883	-1.564	-0.64061	0	0	-0.26029	-0.24196	-0.51753	-0.64459	-0.85371	-0.4433	-1.8612	-0.10612
02-CR1_CL_CWL_R	Max	0	1.1244	0	2.5599	2.5829	0.52372	0	0	0.15752	0.16861	0.54373	0.74714	0.16591	0.51085	0.99103	0.082187
	Min	0	-0.9579	0	-2.3289	-2.7219	-0.72543	0	0	-0.16027	-0.17243	-0.64795	-0.72504	-0.21888	-0.62172	-1.0369	-0.083853
02-CR2_CL_CWL_R	Max	0	0.79456	0	5.3908	5.0177	0.69973	0	0	0.19475	0.16204	0.7861	0.81294	0.15347	0.72747	0.91957	0.076682
	Min	0	-0.78282	0	-5.5542	-4.8723	-0.51631	0	0	-0.182	-0.21551	-0.66491	-0.76067	-0.16624	-0.67627	-0.99789	-0.07882
02-RT1_CL_CWL_R	Max	0	1.1571	0	4.4765	4.7106	0.86384	0	0	0.23994	0.19765	0.86381	0.96717	0.25697	0.79602	0.88122	0.083169
	Min	0	-1.3666	0	-5.0561	-5.9344	-0.61369	0	0	-0.21464	-0.23104	-0.66303	-0.8199	-0.1585	-0.64353	-0.83085	-0.1015
02-RT2_CL_CWL_R	Max	0	0.94707	0	1.5909	1.5521	1.1566	0	0	0.1711	0.12644	0.35502	0.32074	0.24233	0.3197	0.47053	0.081989
	Min	0	-1.2072	0	-1.4998	-1.8251	-0.74915	0	0	-0.16306	-0.15957	-0.27371	-0.28256	-0.15306	-0.29012	-0.46063	-0.084419
03-CR1_LA_CWL_S	Max	0	0.84035	0	1.9802	2.9062	0.44472	0	0	0.13647	0.14997	0.9017	0.99231	0.10464	0.87725	0.97819	0.083603
	Min	0	-1.0854	0	-2.3371	-3.0957	-0.41328	0	0	-0.1552	-0.19055	-0.77239	-0.89143	-0.1051	-0.69034	-0.96695	-0.065878
03-CR2_LA_CWL_S	Max	0	0.96119	0	3.0048	2.7668	0.39607	0	0	0.16368	0.214	1.55	1.6557	0.13894	1.4935	1.817	0.088167
	Min	0	-1.0345	0	-3.2799	-2.7933	-0.3492	0	0	-0.15848	-0.21288	-1.2318	-1.2949	-0.13857	-1.3236	-2.3023	-0.087508
03-RT1_LA_CWL_S	Max	0	1.2969	0	2.4711	2.7586	0.60442	0	0	0.21123	0.24742	1.4232	1.7347	0.22515	1.3764	2.6614	0.08693
	Min	0	-0.98788	0	-2.5884	-2.8211	-0.62787	0	0	-0.23172	-0.25097	-1.4336	-1.8531	-0.17956	-1.3756	-2.575	-0.090672
03-RT2_LA_CWL_S	Max	0	1.2369	0	0.90395	2.2149	0.45193	0	0	0.26034	0.26684	0.46653	0.67276	0.11926	0.50329	1.1683	0.11047
	Min	0	-1.1838	0	-0.87155	-2.5293	-0.59741	0	0	-0.22973	-0.27622	-0.45567	-0.60524	-0.15934	-0.50574	-1.4257	-0.10036
04-CR1_LA_CWL_R	Max	0	0.91381	0	2.2361	4.1074	0.43648	0	0	0.18999	0.17588	0.45586	0.45309	6.3326	0.43731	0.69158	0.090543
	Min	0	-0.75823	0	-2.2876	-3.9543	-0.31032	0	0	-0.18885	-0.20519	-0.43017	-0.43476	-6.8999	-0.43761	-0.89595	-0.072852
04-CR2_LA_CWL_R	Max	0	1.2326	0	3.0093	4.5438	14.204	0	0	0.18327	0.16691	0.44671	14.148	2.4131	0.55834	2.2289	0.077416
	Min	0	-1.6263	0	-2.7442	-4.6618	-10.174	0	0	-0.18724	-0.23229	-0.5505	-12.254	-2.0971	-0.54803	-2.002	-0.080209
04-RT1_LA_CWL_R	Max	0	0.8907	0	2.5389	5.654	3.5846	0	0	0.16511	0.17183	0.42004	2.5013	1.6849	0.48225	2.4539	0.073015
	Min	0	-0.84551	0	-2.0977	-4.4217	-2.4059	0	0	-0.18297	-0.17327	-0.48614	-1.7236	-2.5495	-0.46497	-1.588	-0.081737
04-RT2_LA_CWL_R	Max	0	0.97327	0	0.97876	1.4577	1.1443	0	0	0.13	0.15812	0.19792	0.40177	0.13872	0.1953	0.50831	0.072497
	Min	0	-0.96191	0	-0.96544	-1.2134	-0.8227	0	0	-0.11688	-0.13626	-0.16621	-0.39395	-0.22252	-0.18424	-0.51902	-0.083167
05-CR1_CL_40_S	Max	3.7395	2.5963	3.0373	20.09	21.94	3.7671	2.7898	1.9758	1.0393	0.79422	2.4816	1.7186	0.52875	1.3488	1.3204	0.31208
	Min	-3.0758	-1.7868	-3.9383	-18.466	-22.22	-3.4176	-4.2589	-2.6566	-0.77051	-0.94709	-1.6877	-1.3899	-0.5765	-1.2251	-1.4651	-0.35046
05-CR2_CL_40_S	Max	2.5241	3.83	3.3754	29.509	35.911	2.3287	2.2127	3.1259	1.6889	1.0818	1.6437	2.0603	0.62423	1.9324	2.9562	0.50237
	Min	-2.8679	-2.4544	-2.7612	-26.045	-36.666	-1.9735	-2.8495	-6.5304	-1.0207	-0.96797	-2.1215	-2.4242	-0.87661	-1.9364	-3.184	-0.39479
05-RT1_CL_40_S	Max	5.4556	3.6531	4.8083	25.102	23.079	4.2347	4.7809	4.8777	1.7148	1.7003	2.8138	3.3942	1.0361	2.932	1.8633	0.55675
	Min	-5.9144	-3.0679	-4.0397	-29.699	-24.048	-3.9088	-6.4802	-4.6984	-2.0702	-1.7843	-3.3138	-3.2779	-0.97857	-3.1943	-2.3618	-0.75174
05-RT2_CL_40_S	Max	5.1025	3.4899	4.9631	18.389	12.664	3.4169	4.613	3.7934	2.1905	1.9514	2.1346	1.7249	0.89987	1.6259	2.0563	0.77188
	Min	-3.5026	-2.8678	-4.3891	-14.279	-15.411	-3.7957	-5.5026	-5.092	-2.0917	-1.838	-1.6226	-2.1075	-1.748	-1.7006	-2.0946	-0.68802
06-CR1_CL_40_R	Max	3.397	3.4104	3.8334	38.576	22.872	3.4709	4.9108	4.1152	1.4242	1.5572	2.2182	2.9483	1.0129	2.0362	1.4252	0.46779
	Min	-3.1075	-2.5899	-3.2511	-27.852	-32.644	-3.3552	-6.9209	-4.3159	-1.1041	-1.0126	-1.9055	-2.6835	-0.54485	-1.7219	-1.1342	-0.46606
06-CR2_CL_40_R	Max	3.735	2.4679	3.4202	28.286	29.115	2.4249	3.3244	2.9473	1.3624	1.6252	2.0287	2.6966	0.76293	2.2144	4.5551	0.48356
	Min	-3.3258	-2.5262	-3.6217	-38.88	-30.559	-2.9363	-3.794	-4.2953	-1.5281	-1.7781	-2.6314	-3.0138	-0.57	-2.2894	-4.3275	-0.39468
06-RT1_CL_40_R	Max	4.8584	3.3553	6.0098	36.22	40.093	5.3377	7.1362	5.8718	1.768	1.9056	2.7556	3.4592	1.082	2.2308	3.7325	0.56861
	Min	-5.4282	-3.2904	-5.6943	-36.749	-41.692	-8.5445	-7.8575	-4.6396	-1.7211	-1.6203	-2.7461	-4.1919	-1.139	-2.1456	-3.0079	-0.52801
06-RT2_CL_40_R	Max	4.861	3.1452	4.8634	12.758	11.083	4.626	4.0535	5.5734	2.0864	2.0777	1.6031	1.4298	0.97857	1.5081	2.0401	0.5559
	Min	-3.2698	-2.9994	-4.2374	-11.4	-10.826	-6.0747	-4.7872	-6.3772	-2.2745	-2.0852	-1.8235	-1.3832	-0.95356	-1.4364	-1.6611	-0.6484

Sensor type		Velocity														
Location		Span 1 girders, end			Span 1 girders, mid-span		Span 2 girders, end			Pier 7 headstock			Pier 1 headstock				
Sensor/Time (s)		S1G2e-a vel	S1G3e-a vel	S1G4e-a vel	S1G3m vel	S1G5m vel	S2G2e-a vel	S2G3e-a vel	S2G4e-a vel	P7 HS1-a z vel	P7 HS2-a z vel	P7 HC-a x vel	P1H RHS-a x vel	P1H RHS-a z vel	P1H LHS-a x vel	P1H LHS-a y vel	P1H LHS-a z vel
STATIC	**Max**	**0**	**1.4032**	**0**	**9.3336**	**9.0774**	**14.204**	**0**	**0**	**0.38182**	**0.4495**	**2.5622**	**14.148**	**6.3326**	**2.5891**	**4.3384**	**0.15781**
	Min	**0**	**-1.6263**	**0**	**-10.656**	**-8.3944**	**-10.174**	**0**	**0**	**-0.44159**	**-0.4827**	**-2.5544**	**-12.254**	**-6.8999**	**-2.6129**	**-4.4923**	**-0.15393**
DYNAMIC	**Max**	**26.199**	**8.3469**	**30.734**	**52.181**	**61.875**	**36.298**	**45.082**	**41.815**	**5.7287**	**5.2527**	**6.0197**	**6.346**	**9.0174**	**5.3241**	**6.6129**	**2.1538**
	Min	**-23.272**	**-9.466**	**-49.248**	**-56.231**	**-63.324**	**-38.632**	**-29.024**	**-32.21**	**-7.2631**	**-6.4158**	**-5.768**	**-7.5538**	**-5.2826**	**-5.7157**	**-8.1065**	**-2.5429**
07-CR1_LA_40_S	Max	3.9349	1.8138	2.157	14.005	10.333	4.9324	3.4069	2.9157	1.0383	0.69725	1.9569	2.0181	0.34138	1.9605	1.6087	0.39084
	Min	-3.754	-1.9085	-2.5813	-10.031	-7.3987	-6.2463	-2.7794	-2.5605	-0.96188	-0.83463	-1.5196	-1.97	-0.3091	-1.7313	-1.4045	-0.31674
07-CR2_LA_40_S	Max	2.6257	2.0939	2.2009	23.999	18.726	3.1537	3.0181	1.8888	1.1311	0.8485	2.4506	2.067	0.31277	2.2466	3.0784	0.51647
	Min	-2.9916	-1.9398	-2.1331	-22.387	-19.246	-4.7438	-5.3202	-1.6326	-0.9932	-0.86553	-2.0043	-2.1773	-0.30603	-2.0837	-2.2716	-0.30938
07-RT1_LA_40_S	Max	6.7546	2.3728	4.5045	21.206	20.943	5.3762	5.0926	4.2302	1.7759	1.8922	2.7851	2.1541	0.57347	3.0292	2.6718	0.59713
	Min	-3.6132	-2.7147	-5.0105	-22.642	-25.724	-4.7806	-6.0677	-5.0245	-1.4183	-1.1438	-1.7101	-2.1157	-0.59716	-1.9324	-2.612	-0.47467
07-RT2_LA_40_S	Max	4.5755	3.9977	3.2828	8.501	7.9587	5.6017	4.4605	2.7	2.6328	1.6149	1.8574	1.3988	0.62485	2.1572	1.7647	1.0625
	Min	-5.161	-3.4562	-2.9932	-10.835	-8.4226	-4.7697	-3.9193	-2.7704	-2.4854	-2.3682	-1.3524	-1.5484	-0.63449	-1.7965	-2.3042	-0.86061
08-CR1_LA_40_R	Max	2.2523	2.0134	2.7703	11.02	26.888	2.1652	3.3379	4.8151	0.65893	0.85824	1.5209	2.342	1.5697	1.4835	2.4304	0.1979
	Min	-2.6389	-1.1835	-3.1592	-10.181	-28.456	-1.9848	-3.6609	-3.44	-0.57633	-0.66312	-1.7139	-2.5732	-0.67398	-1.9241	-1.9513	-0.25632
08-CR2_LA_40_R	Max	3.215	1.9962	4.4259	23.685	34.855	2.0525	3.7776	4.943	1.4791	1.4634	2.8255	3.3377	1.4802	2.6919	3.9886	0.46481
	Min	-2.5393	-2.6189	-5.2355	-25.934	-37.929	-2.3517	-3.1857	-4.1148	-1.4563	-1.3541	-2.6834	-3.4228	-0.91212	-2.8453	-4.6494	-0.31151
08-RT1_LA_40_R	Max	4.2248	1.9782	5.7553	24.314	29.079	2.7191	4.5385	3.9912	1.0883	1.0973	2.6707	2.4712	0.96282	3.2505	2.636	0.42865
	Min	-3.0686	-2.1053	-5.4858	-24.299	-23.194	-2.9176	-3.576	-3.8182	-1.1698	-1.1681	-3.2994	-4.2569	-0.9059	-2.8585	-2.3967	-0.4356
08-RT2_LA_40_R	Max	3.7159	2.9877	5.0338	12.989	15.995	3.169	5.9185	7.2681	1.9736	1.9052	1.9419	2.4852	1.388	1.2976	2.2219	0.60282
	Min	-2.9174	-2.2822	-6.7679	-12.271	-15.001	-3.0155	-5.3806	-5.3524	-1.8503	-1.6809	-1.6314	-2.2756	-1.3466	-1.2191	-1.9525	-0.53328
09-CR1_LA_60_S	Max	6.08	3.3705	3.8063	9.2803	8.3264	8.2925	9.0041	4.777	1.8186	1.1497	2.602	1.7516	1.1754	2.4517	1.4462	0.75813
	Min	-7.3441	-2.1615	-3.6288	-10.642	-6.7296	-6.7798	-6.4465	-4.4005	-1.136	-1.2387	-1.6566	-1.7121	-1.0961	-2.1891	-1.8196	-0.3672
09-CR2_LA_60_S	Max	4.4132	4.437	2.7021	29.655	22.261	4.7719	4.698	3.598	2.5785	2.1261	3.6486	3.1402	0.62965	3.1768	3.952	0.90945
	Min	-4.3378	-3.1394	-2.8436	-31.58	-22.82	-7.4676	-5.7984	-2.5501	-1.6885	-1.7957	-3.1054	-3.0244	-0.58046	-3.5024	-3.8801	-0.4503
09-RT1_LA_60_S	Max	9.9387	4.3084	4.183	24.755	11.592	8.3942	9.4465	5.4261	2.5717	2.5586	2.8905	2.8564	1.0692	3.1472	6.4462	1.1558
	Min	-7.2812	-3.1766	-4.6392	-26.402	-12.45	-10.887	-8.4521	-10.554	-2.1044	-1.6868	-2.8295	-3.4174	-1.2166	-4.2493	-8.1065	-0.89592
09-RT2_LA_60_S	Max	10.467	5.0447	6.5424	23.817	16.932	6.1758	6.5972	4.9352	3.9577	3.6199	2.7612	2.0609	1.1655	3.0596	2.4733	1.3264
	Min	-10.48	-5.1081	-5.0575	-21.093	-14.564	-6.9507	-7.8916	-6.5567	-3.7945	-3.2704	-2.3805	-1.9645	-1.0546	-2.4405	-3.0476	-1.3003
10-CR1_LA_60_R	Max	3.2252	1.7283	10.266	10.355	10.576	7.0869	6.3807	13.657	0.98679	1.0532	1.6689	2.2762	1.5597	1.0042	1.7441	0.30064
	Min	-4.4706	-3.0004	-13.564	-6.4755	-6.8493	-6.0521	-7.1053	-16.898	-1.6811	-0.86499	-2.145	-3.892	-1.6785	-1.1738	-2.0694	-0.47105
10-CR2_LA_60_R	Max	2.5632	2.8217	3.9022	23.28	31.893	2.1153	3.948	9.4676	1.7433	1.6642	2.2711	3.1936	0.93192	2.0716	3.4419	0.38993
	Min	-3.1201	-2.7087	-3.5599	-34.051	-38.88	-3.2967	-3.394	-6.5531	-1.4178	-1.4951	-2.4724	-4.5498	-2.2921	-1.7887	-3.8998	-0.47399
10-RT1_LA_60_R	Max	4.3973	4.9611	14.16	32.445	30.424	5.9251	7.6262	19.111	3.512	3.596	3.4148	5.1956	2.2556	2.9903	6.6129	0.83015
	Min	-4.5207	-4.6926	-12.682	-40.748	-48.916	-4.9072	-8.738	-10.728	-3.2735	-3.469	-4.0621	-7.5538	-2.4546	-3.7779	-5.9133	-0.95119
10-RT2_LA_60_R	Max	6.851	4.3651	9.9043	22.834	20.889	4.8778	6.1231	8.3355	3.1012	2.4426	1.7395	2.3826	1.5771	1.5812	1.8062	0.61552
	Min	-4.9835	-4.2549	-8.9671	-19.253	-22.415	-5.9919	-6.9371	-7.2185	-3.128	-3.3598	-2.1974	-3.1115	-1.9363	-1.3299	-2.5962	-0.73477
11-CR1_CL_80_S	Max	5.8584	3.0437	9.2697	26.436	21.785	6.182	7.2291	7.185	1.4797	1.7589	4.5026	3.1843	0.85211	2.8435	2.6155	0.50278
	Min	-5.2386	-3.8333	-27.857	-34.631	-20.949	-6.491	-9.9084	-7.5874	-2.1576	-1.6446	-3.0288	-2.8579	-1.068	-2.339	-2.1669	-0.66737
11-CR2_CL_80_S	Max	5.8369	6.1867	8.1579	43.786	33.233	5.2419	7.5635	8.8505	2.9578	3.1252	3.9676	4.4896	1.0622	4.1014	2.7532	0.81947
	Min	-7.7788	-5.6585	-5.0327	-44.081	-31.92	-5.7896	-6.9394	-12.061	-3.2233	-2.9004	-3.7157	-4.2137	-1.3309	-3.6612	-2.7541	-0.87901
11-RT1_CL_80_S	Max	14.144	3.7748	10.484	29.951	25.624	8.4801	12.443	17.431	2.7653	3.1784	3.624	4.0897	2.1635	3.2253	5.014	1.0256
	Min	-9.823	-4.117	-12.371	-29.156	-27.986	-12.199	-11.833	-11.744	-3.2832	-3.6015	-3.5162	-4.1172	-1.9137	-3.107	-5.3461	-0.87507
11-RT2_CL_80_S	Max	15.789	6.0642	11.753	39.971	30.424	9.6838	15.01	13.702	4.0564	3.5712	2.3402	3.9066	2.0649	2.4362	2.9323	1.1818
	Min	-11.771	-6.3313	-11.185	-43.086	-31.729	-11.094	-15.619	-15.487	-4.263	-4.4099	-2.6639	-3.5053	-3.1369	-2.6406	-3.6899	-1.2587
12-CR1_CL_80_R	Max	8.8049	3.4055	6.8103	30.168	24.851	7.8718	11.321	7.0825	2.0414	1.5161	2.5623	3.3127	1.6543	2.578	1.7118	0.52939
	Min	-6.6745	-3.1258	-7.7022	-31.831	-27.837	-7.5576	-7.6911	-7.5326	-1.848	-1.8721	-3.9717	-2.2462	-1.3366	-2.7139	-1.3858	-0.5453
12-CR2_CL_80_R	Max	7.6144	3.7841	4.4592	48.464	26.157	7.912	5.4619	5.1384	2.5256	2.1871	3.712	3.8144	1.9506	3.4772	2.58	0.65156
	Min	-6.3137	-4.5344	-4.4227	-56.231	-40.55	-6.9118	-9.5356	-7.8546	-3.0849	-2.0378	-5.768	-5.665	-3.6329	-4.7257	-2.759	-0.71984
12-RT1_CL_80_R	Max	9.2346	4.5704	13.28	48.346	23.15	12.056	16.004	11.312	2.7005	2.668	6.0197	6.346	1.5503	5.0522	4.9702	1.0677
	Min	-12.356	-5.3592	-13.685	-43.642	-25.271	-10.657	-18.034	-12.681	-3.1938	-2.9348	-5.5779	-5.4149	-3.127	-4.911	-4.8635	-0.96958
12-RT2_CL_80_R	Max	9.4193	6.5778	13.493	35.14	26.951	9.3701	12.112	11.246	4.496	4.1494	2.6943	3.0506	2.8717	2.5443	3.3522	1.1315
	Min	-13.735	-6.1273	-15.444	-27.753	-27.568	-12.976	-13.111	-15.55	-4.1212	-4.7702	-3.049	-3.209	-2.9647	-2.7304	-2.4693	-1.2255

Sensor type		Velocity														
Location		Span 1 girders, end			Span 1 girders, mid-span		Span 2 girders, end			Pier 7 headstock			Pier 1 headstock			
Sensor/Time (s)		S1G2e-a vel	S1G3e-a vel	S1G4e-a vel	S1G3m vel	S1G5m vel	S2G2e-a vel	S2G3e-a vel	S2G4e-a vel	P7 HS1-a z vel	P7 HS2-a z vel	P7 HC-a x vel	P1H RHS-a x vel	P1H RHS-a z vel	P1H LHS-a x vel	P1H LHS-a y vel	P1H LHS-a z vel
STATIC	Max	0	1.4032	0	9.3336	9.0774	14.204	0	0	0.38182	0.4495	2.5622	14.148	6.3326	2.5891	4.3384	0.15781
	Min	0	-1.6263	0	-10.656	-8.3944	-10.174	0	0	-0.44159	-0.4827	-2.5544	-12.254	-6.8999	-2.6129	-4.4923	-0.15393
DYNAMIC	Max	26.199	8.3469	30.734	52.181	61.875	36.298	45.082	41.815	5.7287	5.2527	6.0197	6.346	9.0174	5.3241	6.6129	2.1538
	Min	-23.272	-9.466	-49.248	-56.231	-63.324	-38.632	-29.024	-32.21	-7.2631	-6.4158	-5.768	-7.5538	-5.2826	-5.7157	-8.1065	-2.5429
13-CR1_LA_80_S	Max	8.2025	2.5177	4.61	20.679	18.456	12.276	10.894	7.2308	1.456	1.32	3.6534	3.0803	1.0315	3.6588	2.5125	0.84755
	Min	-8.5652	-2.2093	-6.3675	-27.543	-17.162	-11.103	-12.411	-6.8947	-1.4952	-1.7908	-3.3429	-3.2327	-1.015	-4.2007	-2.1585	-0.51002
13-CR2_LA_80_S	Max	4.372	4.6985	4.4074	43.659	20.371	9.9384	10.946	5.1761	2.9306	3.3656	2.739	3.248	1.0925	3.2772	4.3614	1.1774
	Min	-7.26	-5.2227	-3.5854	-40.279	-16.582	-6.5305	-9.8405	-4.0152	-2.7718	-2.4492	-2.7501	-3.6867	-0.75923	-3.1137	-4.2165	-0.84575
13-RT1_LA_80_S	Max	15.489	4.4511	7.3235	25.32	14.82	14.801	18.497	13.178	3.338	3.5802	4.8908	5.907	1.4797	5.1075	3.7037	1.1725
	Min	-17.545	-5.044	-9.7366	-26.525	-14.262	-17.186	-10.681	-10.727	-3.1262	-2.8687	-5.1731	-6.1926	-1.2247	-5.2052	-4.1991	-1.2587
13-RT2_LA_80_S	Max	13.213	8.3469	7.8472	25.87	17.029	16.142	11.697	12.215	5.7287	5.0522	2.7509	2.2433	2.446	3.19	2.7458	2.1538
	Min	-11.513	-9.466	-10.378	-24.615	-13.33	-14.472	-14.667	-8.1955	-7.2631	-6.4158	-2.7331	-3.8663	-3.0425	-3.3445	-3.0488	-2.5429
14-CR1_LA_60_R	Max	5.074	1.8095	6.0612	8.2161	10.597	4.6985	8.1431	13.549	0.88593	0.90936	1.5529	2.6865	1.0585	0.88589	1.9085	0.34219
	Min	-3.8819	-2.7518	-8.076	-7.0849	-8.893	-5.4695	-7.8333	-10.943	-1.5663	-0.93055	-2.0716	-3.8458	-2.2266	-1.0249	-1.7698	-0.4487
14-CR2_LA_80_R	Max	4.5	3.2185	11.632	28.73	37.779	4.7412	6.825	10.125	2.754	2.2666	4.3329	4.6978	1.2667	3.8691	2.7302	0.50183
	Min	-4.1565	-4.224	-12.318	-33.84	-51.221	-7.7649	-6.9623	-9.797	-3.5182	-3.2284	-5.4612	-6.2462	-2.9827	-4.2383	-2.8091	-0.80163
14-RT1_LA_80_R	Max	8.3467	3.8144	14.832	48.536	61.875	6.2003	11.92	30.65	2.9293	2.9025	4.6985	4.6087	9.0174	4.2633	4.9412	0.90404
	Min	-8.5388	-4.6512	-27.796	-50.821	-63.324	-10.349	-9.9267	-14.548	-2.8999	-3.1394	-4.1343	-5.14	-4.0784	-4.6383	-4.0098	-0.90924
14-RT2_LA_80_R	Max	6.6382	5.4898	13.867	20.409	15.441	8.5034	11.224	13.423	3.5072	3.6056	2.0049	3.5875	2.3411	2.0669	3.0085	1.2829
	Min	-6.9576	-5.3702	-20.62	-15.61	-17.227	-10.196	-9.3427	-11.997	-3.7924	-3.3105	-2.7581	-4.2735	-5.2826	-2.0073	-2.5791	-1.1518
15-CR1_LA_80_S	Max	7.3254	3.1834	6.0877	22.129	21.683	9.4492	8.1189	5.0803	1.5062	1.4204	3.5711	3.0235	0.79691	3.5144	2.0298	0.85702
	Min	-7.853	-3.823	-5.9924	-30.25	-20.889	-7.8791	-10.499	-6.5375	-1.7942	-1.8102	-3.1023	-3.169	-1.0641	-3.5003	-2.6585	-0.55627
15-CR2_LA_80_S	Max	7.4693	5.7713	4.5793	40.057	20.13	8.9984	10.131	8.4608	3.0908	3.6569	2.9753	3.9414	1.4108	3.1225	3.7888	1.1887
	Min	-8.7733	-5.7917	-4.3948	-38.313	-16.79	-6.254	-11.264	-4.9597	-2.6864	-2.4809	-2.6218	-3.6668	-0.97775	-3.1181	-3.9926	-0.8212
15-RT1_LA_85_S	Max	23.171	4.6511	6.4689	24.813	14.905	15.021	18.844	11.472	3.1649	3.2027	5.0056	6.0958	1.6735	5.3241	3.608	1.2593
	Min	-16.969	-5.3155	-9.0152	-22.333	-14.599	-11.629	-16.687	-10.446	-3.1461	-2.9905	-5.3704	-7.041	-1.6409	-5.7157	-4.615	-1.3428
15-RT2_LA_95_S	Max	23.187	4.7259	14.011	28.452	18.922	36.298	40.366	18.423	3.1847	3.4587	3.6135	4.0277	2.5471	4.3891	4.8941	1.4977
	Min	-23.272	-6.5147	-23.028	-27.369	-23.342	-38.632	-29.024	-23.48	-4.0019	-3.5456	-3.2603	-3.532	-2.3213	-4.3742	-4.0803	-1.6825
16-CR1_LA_80_R	Max	5.0061	2.8165	10.184	18.593	26.879	4.9435	8.9144	10.692	1.5151	1.9072	2.7657	3.5589	1.4619	2.7277	2.0844	0.45836
	Min	-5.7296	-1.9393	-17.701	-18.878	-23.921	-6.6467	-8.719	-13.596	-1.3326	-1.3639	-3.5505	-4.5706	-1.6113	-2.4876	-2.4245	-0.46283
16-CR2_LA_80_R	Max	2.9444	2.9347	4.475	31.116	33.085	3.3313	3.7957	7.6979	2.1057	1.7471	4.0863	4.9693	1.8	3.9121	4.0439	0.54533
	Min	-3.735	-4.3729	-5.0968	-47.594	-43.006	-4.4014	-6.8158	-5.9865	-2.8511	-2.4453	-3.5689	-5.0763	-1.8448	-3.5692	-3.8931	-0.69871
16-RT1_LA_90_R	Max	12.177	3.8638	13.523	43.306	59.131	8.662	12.545	18.725	3.0137	3.2661	4.3632	5.2573	2.9687	4.8998	4.6481	0.78406
	Min	-11.979	-3.6819	-20.793	-43.574	-58.921	-8.0341	-12.125	-19.998	-3.2988	-3.4196	-4.3576	-6.7687	-4.6015	-4.8418	-3.8541	-0.87246
16-RT2_LA_94_R	Max	21.569	5.9582	30.734	25.75	20.139	14.501	24.044	41.815	5.3569	5.2527	3.8294	5.7271	4.5734	4.3544	4.862	1.5454
	Min	-18.308	-6.2965	-49.248	-21.152	-23.323	-34.813	-23.648	-32.21	-3.8876	-3.7433	-4.7522	-5.9761	-4.1146	-3.8174	-3.5753	-0.91951
18-CR1_LA_20_S	Max	4.3623	0.98479	2.2548	14.095	9.6933	1.9262	2.4832	1.9705	0.51457	0.43648	1.2453	1.4166	0.22384	1.3565	2.3476	0.26216
	Min	-13.723	-1.2259	-2.3177	-11.478	-10.228	-2.913	-3.7349	-1.5509	-0.43194	-0.39131	-1.2163	-1.381	-0.29523	-1.6198	-4.9608	-0.23855
18-CR2_LA_20_S	Max	2.3606	1.6839	2.5273	17.688	10.189	1.4205	4.0404	1.5298	0.99732	0.86698	1.7202	1.7118	0.32005	1.552	3.8105	0.38007
	Min	-2.0818	-1.4787	-1.967	-19.109	-12.817	-4.5728	-1.6689	-1.2713	-1.0014	-0.97133	-1.4899	-1.8436	-0.35233	-1.8961	-3.6497	-0.38726
18-RT1_LA_20_S	Max	4.0914	3.0029	3.1898	52.181	43.291	2.1161	2.1541	1.8627	1.2826	1.0943	4.595	5.9988	0.69152	4.6441	3.702	0.679
	Min	-4.429	-3.1274	-3.8813	-53.338	-42.365	-2.1043	-2.1025	-2.0653	-1.3779	-1.0833	-4.2258	-5.8797	-0.88913	-4.199	-4.3653	-0.5574
18-RT2_LA_20_S	Max	4.0858	1.6406	2.7955	10.795	12.787	1.6307	2.2523	1.7717	0.96419	0.97499	1.239	1.4828	0.37434	1.3616	1.7218	0.53452
	Min	-6.7655	-1.9406	-2.4592	-11.775	-14.657	-2.4777	-2.0018	-1.721	-1.1541	-0.99826	-1.3562	-1.3092	-0.29013	-1.283	-1.2737	-0.35976
19-CR1_CL_80_R	Max	7.6901	3.8228	6.9067	35.163	26.763	7.2932	9.3534	8.7571	1.9542	1.7029	2.7872	2.3363	2.0763	1.9004	1.3765	0.50449
	Min	-6.1309	-4.1126	-5.6365	-34.827	-27.479	-9.4597	-9.5633	-9.4644	-1.7995	-1.8664	-4.1357	-2.7393	-1.3738	-2.6343	-1.5572	-0.50522
19-CR2_CL_80_R	Max	6.8096	3.8365	6.8999	49.482	28.526	4.9332	7.779	7.1449	2.329	2.2674	4.2014	4.5373	1.3799	3.5451	3.0605	0.62464
	Min	-7.937	-4.4402	-7.8656	-55.716	-44.645	-4.9458	-6.1106	-7.5096	-2.8962	-1.9324	-5.6559	-6.7826	-1.5555	-4.5868	-2.8273	-0.64486
19-RT1_CL_90_R	Max	14.928	4.5406	13.186	46.747	28.899	11.95	16.706	29.148	3.0414	2.8823	4.7607	4.6266	1.8935	4.7765	3.8205	1.0409
	Min	-12.014	-4.4175	-14.744	-40.3	-28.069	-16.578	-20.112	-14.976	-2.5471	-2.6201	-4.5602	-4.9932	-2.2611	-3.9094	-4.0738	-0.96872
19-RT2_CL_94_R	Max	26.199	4.8225	29.954	21.688	16.044	29.827	45.082	24.092	3.2374	3.5197	3.1374	3.5737	2.2385	2.4719	4.5998	1.0185
	Min	-21.169	-6.35	-29.936	-26.427	-17.298	-26.696	-24.856	-13.863	-4.0114	-3.9205	-3.3153	-4.5729	-2.2604	-2.409	-4.5539	-0.87375

Sensor type		Accelerometers (Velocity-mm/s)															
Location		Span 1 girders, end			Span 1 girders, mid-span		Span 2 girders, end			Pier 7 headstock			Pier 1 headstock				
Sensor/Time (s)		S1G2e-a accel	S1G3e-a accel	S1G4e-a accel	S1G3m accel	S1G5m accel	S2G2e-a accel	S2G3e-a accel	S2G4e-a accel	P7 HS1-a z accel	P7 HS2-a z accel	P7 HC-a x accel	P1H RHS-a x accel	P1H RHS-a z accel	P1H LHS-a x accel	P1H LHS-a y accel	P1H LHS-a z accel
STATIC	**Max**	**0**	**0.066887**	**0**	**0.26995**	**0.23605**	**0.44159**	**0**	**0**	**0.027819**	**0.025272**	**0.073416**	**0.64042**	**0.18073**	**0.071329**	**0.078368**	**0.01184**
	Min	**0**	**-0.060226**	**0**	**-0.31672**	**-0.26701**	**-0.6949**	**0**	**0**	**-0.026104**	**-0.024729**	**-0.06617**	**-0.48868**	**-0.24753**	**-0.068324**	**-0.076279**	**-0.01085**
DYNAMIC	**Max**	**2.1692**	**1.1053**	**2.3005**	**2.8364**	**1.9551**	**2.1835**	**2.2288**	**1.7383**	**0.71572**	**0.61169**	**0.55782**	**0.62874**	**0.82366**	**0.39811**	**0.50115**	**0.21555**
	Min	**-1.6624**	**-0.89637**	**-3.1768**	**-2.7702**	**-2.0462**	**-1.7773**	**-1.8208**	**-1.9459**	**-0.72459**	**-0.64818**	**-0.5564**	**-0.52483**	**-0.42666**	**-0.5727**	**-0.61175**	**-0.28721**
01-CR1_CL_CWL_S	Max	0	0.049803	0	0.089355	0.098799	0.066452	0	0	0.018521	0.022355	0.025797	0.036486	0.0181	0.026325	0.033366	0.0116
	Min	0	-0.048612	0	-0.1109	-0.088825	-0.073345	0	0	-0.018937	-0.024185	-0.033901	-0.037218	-0.015416	-0.032331	-0.033008	-0.01085
01-CR2_CL_CWL_S	Max	0	0.045478	0	0.14991	0.11474	0.014527	0	0	0.012315	0.013279	0.045787	0.058281	0.011958	0.044006	0.072006	0.0057475
	Min	0	-0.050672	0	-0.14935	-0.10795	-0.026557	0	0	-0.010907	-0.011699	-0.041349	-0.031403	-0.015351	-0.039566	-0.070963	-0.0053574
01-RT1_CL_CWL_S	Max	0	0.053513	0	0.26995	0.23605	0.04144	0	0	0.027819	0.025272	0.073416	0.082379	0.021829	0.071329	0.077037	0.01184
	Min	0	-0.050572	0	-0.31672	-0.26701	-0.030857	0	0	-0.01974	-0.021162	-0.06617	-0.069513	-0.025796	-0.068324	-0.076279	-0.0098999
01-RT2_CL_CWL_S	Max	0	0.051207	0	0.074954	0.08237	0.021126	0	0	0.02091	0.023456	0.020126	0.02934	0.027973	0.02036	0.034562	0.0086395
	Min	0	-0.057813	0	-0.091706	-0.066204	-0.022663	0	0	-0.026104	-0.024729	-0.023195	-0.021218	-0.040522	-0.024553	-0.038038	-0.0080897
02-CR1_CL_CWL_R	Max	0	0.047087	0	0.10208	0.071014	0.03546	0	0	0.01095	0.011521	0.017299	0.022947	0.01181	0.017983	0.022566	0.0056137
	Min	0	-0.050867	0	-0.070186	-0.095594	-0.040348	0	0	-0.010541	-0.010695	-0.022126	-0.022064	-0.012521	-0.0216	-0.03127	-0.0051544
02-CR2_CL_CWL_R	Max	0	0.051123	0	0.1166	0.10827	0.03125	0	0	0.0069421	0.0071935	0.018085	0.02569	0.008458	0.015768	0.020486	0.0048914
	Min	0	-0.04738	0	-0.14138	-0.14337	-0.023577	0	0	-0.0079342	-0.007149	-0.018956	-0.021154	-0.021309	-0.017052	-0.031472	-0.0045754
02-RT1_CL_CWL_R	Max	0	0.049075	0	0.15648	0.15452	0.028862	0	0	0.014093	0.015186	0.020954	0.024881	0.015759	0.021534	0.027567	0.0063434
	Min	0	-0.057937	0	-0.14025	-0.16529	-0.016857	0	0	-0.01231	-0.011061	-0.020175	-0.029696	-0.0099263	-0.02197	-0.039809	-0.0060412
02-RT2_CL_CWL_R	Max	0	0.050428	0	0.070556	0.06764	0.032768	0	0	0.012939	0.013063	0.010845	0.016288	0.013684	0.010659	0.011364	0.0059777
	Min	0	-0.05041	0	-0.076983	-0.076354	-0.015523	0	0	-0.01343	-0.013166	-0.010416	-0.015291	-0.0079101	-0.010862	-0.017299	-0.0053561
03-CR1_LA_CWL_S	Max	0	0.042046	0	0.06561	0.10573	0.024633	0	0	0.018619	0.018851	0.025954	0.033197	0.010655	0.02043	0.018509	0.0079505
	Min	0	-0.048499	0	-0.070059	-0.098721	-0.030391	0	0	-0.017461	-0.019857	-0.02354	-0.02809	-0.010517	-0.022388	-0.026866	-0.0069772
03-CR2_LA_CWL_S	Max	0	0.066887	0	0.091875	0.10116	0.013233	0	0	0.010384	0.011001	0.037244	0.037967	0.010076	0.038573	0.047247	0.0045653
	Min	0	-0.047187	0	-0.077646	-0.093291	-0.017032	0	0	-0.0093902	-0.010208	-0.03192	-0.041292	-0.012007	-0.03437	-0.036666	-0.00447
03-RT1_LA_CWL_S	Max	0	0.048962	0	0.089633	0.091918	0.035209	0	0	0.018478	0.018244	0.042808	0.056756	0.012468	0.036392	0.052081	0.0086541
	Min	0	-0.050937	0	-0.08737	-0.09537	-0.026153	0	0	-0.020009	-0.018881	-0.035526	-0.045085	-0.022864	-0.036227	-0.058143	-0.008682
03-RT2_LA_CWL_S	Max	0	0.05364	0	0.049086	0.094248	0.032953	0	0	0.023882	0.023868	0.018679	0.021591	0.010562	0.019454	0.02607	0.0096428
	Min	0	-0.050114	0	-0.056702	-0.083677	-0.02585	0	0	-0.023201	-0.022965	-0.019854	-0.021657	-0.01137	-0.019684	-0.027632	-0.0093257
04-CR1_LA_CWL_R	Max	0	0.057132	0	0.089994	0.14144	0.019259	0	0	0.014929	0.014167	0.013494	0.014623	0.18073	0.013552	0.017308	0.0060599
	Min	0	-0.049185	0	-0.076633	-0.15045	-0.017937	0	0	-0.015908	-0.01544	-0.011965	-0.01268	-0.24753	-0.012218	-0.027386	-0.0063581
04-CR2_LA_CWL_R	Max	0	0.052053	0	0.10127	0.14794	0.44159	0	0	0.013163	0.0078564	0.013675	0.64042	0.050504	0.013577	0.06203	0.0054064
	Min	0	-0.045079	0	-0.097629	-0.14519	-0.6949	0	0	-0.01725	-0.011776	-0.013172	-0.48868	-0.059856	-0.015467	-0.046954	-0.0051013
04-RT1_LA_CWL_R	Max	0	0.049074	0	0.10395	0.16975	0.1068	0	0	0.0097561	0.010176	0.017397	0.0778	0.02704	0.012578	0.078368	0.0063725
	Min	0	-0.047456	0	-0.088543	-0.15834	-0.035345	0	0	-0.010148	-0.0093236	-0.012409	-0.026127	-0.078287	-0.012501	-0.025713	-0.0055771
04-RT2_LA_CWL_R	Max	0	0.048758	0	0.045892	0.070819	0.036682	0	0	0.011532	0.012595	0.012605	0.01193	0.0070461	0.0084566	0.012123	0.0049116
	Min	0	-0.060226	0	-0.052684	-0.053203	-0.016646	0	0	-0.011676	-0.012645	-0.0094733	-0.018231	-0.012916	-0.0081181	-0.011862	-0.0053125
05-CR1_CL_40_S	Max	0.27525	0.19493	0.27576	0.8865	0.88099	0.16439	0.31002	0.2742	0.085312	0.10957	0.17014	0.12708	0.054126	0.098331	0.059234	0.025759
	Min	-0.21695	-0.25738	-0.22515	-0.97013	-0.89695	-0.17282	-0.28186	-0.21392	-0.077329	-0.074168	-0.26603	-0.1252	-0.053213	-0.13016	-0.088166	-0.025767
05-CR2_CL_40_S	Max	0.17601	0.18055	0.17585	0.82996	1.1871	0.17132	0.11313	0.3975	0.10119	0.092723	0.1865	0.11299	0.034628	0.12145	0.067112	0.031103
	Min	-0.27961	-0.31484	-0.30894	-0.98372	-1.0618	-0.15858	-0.091023	-0.51022	-0.12625	-0.088882	-0.28932	-0.10774	-0.03207	-0.15606	-0.066345	-0.03566
05-RT1_CL_40_S	Max	0.3488	0.38036	0.45961	1.125	0.93661	0.32978	0.53732	0.4861	0.19447	0.22292	0.17531	0.17659	0.088813	0.1539	0.11244	0.061051
	Min	-0.3168	-0.34956	-0.37468	-0.97123	-0.87079	-0.33159	-0.49575	-0.47303	-0.1807	-0.20805	-0.27733	-0.24701	-0.088019	-0.19558	-0.11641	-0.079364
05-RT2_CL_40_S	Max	0.47813	0.28226	0.52045	0.99062	0.69436	0.41474	0.5372	0.59439	0.19804	0.22063	0.15486	0.1748	0.12296	0.15015	0.13057	0.071499
	Min	-0.42481	-0.40482	-0.43786	-1.1095	-0.79165	-0.43644	-0.48645	-0.39481	-0.21397	-0.1806	-0.24319	-0.23195	-0.17422	-0.16403	-0.12388	-0.077138
06-CR1_CL_40_R	Max	0.20169	0.14727	0.20542	1.311	1.157	0.14854	0.19708	0.20667	0.079238	0.082985	0.15512	0.12804	0.067299	0.10697	0.05999	0.030388
	Min	-0.17909	-0.14986	-0.18202	-1.4443	-1.1002	-0.1868	-0.26454	-0.41872	-0.071267	-0.098229	-0.14402	-0.13476	-0.058853	-0.10828	-0.068087	-0.027658
06-CR2_CL_40_R	Max	0.20484	0.29073	0.18675	1.0195	1.0187	0.16416	0.26582	0.25393	0.14338	0.1086	0.23644	0.083392	0.045853	0.17442	0.09487	0.037285
	Min	-0.304	-0.14235	-0.1705	-1.0186	-0.94561	-0.20544	-0.31824	-0.14258	-0.087486	-0.10443	-0.19959	-0.12934	-0.034615	-0.1426	-0.09196	-0.028637
06-RT1_CL_40_R	Max	0.41365	0.41463	0.37142	1.475	1.1294	0.26506	0.4435	0.38742	0.20941	0.17221	0.26317	0.2058	0.079487	0.20185	0.096551	0.05543
	Min	-0.41387	-0.24957	-0.38603	-1.2404	-1.2743	-0.28357	-0.51033	-0.46143	-0.17346	-0.15682	-0.19693	-0.16589	-0.07725	-0.17114	-0.12597	-0.062685
06-RT2_CL_40_R	Max	0.32981	0.32591	0.44097	0.71181	0.55603	0.25188	0.45665	0.51658	0.22894	0.20955	0.22253	0.14151	0.080331	0.20589	0.098979	0.073879
	Min	-0.28212	-0.27452	-0.42583	-0.8046	-0.5724	-0.32489	-0.43446	-0.58875	-0.22072	-0.21092	-0.15347	-0.15327	-0.09902	-0.12618	-0.12669	-0.070917

Sensor type		Accelerometers (Velocity-mm/s)															
Location		Span 1 girders, end			Span 1 girders, mid-span		Span 2 girders, end			Pier 7 headstock			Pier 1 headstock				
Sensor/Time (s)		S1G2e-a accel	S1G3e-a accel	S1G4e-a accel	S1G3m accel	S1G5m accel	S2G2e-a accel	S2G3e-a accel	S2G4e-a accel	P7 HS1-a z accel	P7 HS2-a z accel	P7 HC-a x accel	P1H RHS-a x accel	P1H RHS-a z accel	P1H LHS-a x accel	P1H LHS-a y accel	P1H LHS-a z accel
STATIC	**Max**	**0**	**0.066887**	**0**	**0.26995**	**0.23605**	**0.44159**	**0**	**0**	**0.027819**	**0.025272**	**0.073416**	**0.64042**	**0.18073**	**0.071329**	**0.078368**	**0.01184**
	Min	**0**	**-0.060226**	**0**	**-0.31672**	**-0.26701**	**-0.6949**	**0**	**0**	**-0.026104**	**-0.024729**	**-0.06617**	**-0.48868**	**-0.24753**	**-0.068324**	**-0.076279**	**-0.01085**
DYNAMIC	**Max**	**2.1692**	**1.1053**	**2.3005**	**2.8364**	**1.9551**	**2.1835**	**2.2288**	**1.7383**	**0.71572**	**0.61169**	**0.55782**	**0.62874**	**0.82366**	**0.39811**	**0.50115**	**0.21555**
	Min	**-1.6624**	**-0.89637**	**-3.1768**	**-2.7702**	**-2.0462**	**-1.7773**	**-1.8208**	**-1.9459**	**-0.72459**	**-0.64818**	**-0.5564**	**-0.52483**	**-0.42666**	**-0.5727**	**-0.61175**	**-0.28721**
07-CR1_LA_40_S	Max	0.24012	0.13408	0.1748	0.68706	0.49738	0.31691	0.30637	0.19478	0.065649	0.11455	0.17083	0.072992	0.038229	0.15406	0.066052	0.029664
	Min	-0.26694	-0.22118	-0.1473	-0.62138	-0.45973	-0.31159	-0.23717	-0.1725	-0.085396	-0.074073	-0.23698	-0.084171	-0.031994	-0.21232	-0.046069	-0.037678
07-CR2_LA_40_S	Max	0.3688	0.16469	0.1551	1.0414	0.74487	0.42543	0.33797	0.12367	0.089808	0.10176	0.19215	0.13733	0.034405	0.16867	0.093778	0.051413
	Min	-0.34584	-0.30306	-0.149	-1.1464	-0.72344	-0.37038	-0.44421	-0.10726	-0.12428	-0.071967	-0.23922	-0.10909	-0.029288	-0.30864	-0.083969	-0.044574
07-RT1_LA_40_S	Max	0.63479	0.27949	0.23278	0.69853	0.8952	0.64568	0.46001	0.2537	0.17918	0.17482	0.13214	0.13767	0.078019	0.18705	0.10137	0.051516
	Min	-0.40748	-0.27722	-0.21239	-0.80637	-0.83982	-0.33936	-0.33797	-0.26479	-0.12864	-0.17443	-0.23232	-0.14362	-0.065329	-0.30065	-0.10134	-0.057535
07-RT2_LA_40_S	Max	0.41972	0.23938	0.29852	0.65701	0.52615	0.66573	0.48342	0.22035	0.20184	0.18985	0.16222	0.13199	0.071676	0.21088	0.10377	0.096161
	Min	-0.45521	-0.48993	-0.29251	-0.6743	-0.45053	-0.38723	-0.40265	-0.28334	-0.27594	-0.23519	-0.21439	-0.13575	-0.070296	-0.28845	-0.12964	-0.10409
08-CR1_LA_40_R	Max	0.17972	0.14063	0.29879	0.51044	1.2352	0.14678	0.19724	0.36725	0.072591	0.0593	0.15294	0.27609	0.14602	0.085336	0.07867	0.024497
	Min	-0.18907	-0.095612	-0.28159	-0.52421	-0.99954	-0.19746	-0.20455	-0.41	-0.068746	-0.075143	-0.14582	-0.19915	-0.064371	-0.099771	-0.081485	-0.02683
08-CR2_LA_40_R	Max	0.13032	0.22537	0.50637	0.69862	0.9997	0.11182	0.26137	0.34261	0.09613	0.095793	0.20988	0.28796	0.16358	0.10754	0.10714	0.029639
	Min	-0.15409	-0.12307	-0.42239	-0.5307	-0.9429	-0.17859	-0.29004	-0.52654	-0.075778	-0.088086	-0.20297	-0.25485	-0.071509	-0.082398	-0.17111	-0.035079
08-RT1_LA_40_R	Max	0.2168	0.18637	0.4728	0.81348	0.79264	0.30365	0.34945	0.49737	0.11734	0.13491	0.21669	0.32657	0.089206	0.14908	0.099818	0.047644
	Min	-0.24652	-0.19311	-0.57249	-0.82637	-0.95966	-0.28504	-0.44027	-0.54062	-0.14089	-0.15897	-0.18779	-0.26297	-0.083591	-0.12135	-0.10635	-0.057346
08-RT2_LA_40_R	Max	0.24636	0.2867	0.63645	0.82198	1.2313	0.30521	0.71708	0.51917	0.22624	0.23143	0.23953	0.30924	0.11809	0.13004	0.14755	0.075627
	Min	-0.25699	-0.32089	-0.38703	-1.0054	-0.9596	-0.29299	-0.4313	-0.58639	-0.22016	-0.17655	-0.14437	-0.19928	-0.11061	-0.10906	-0.16104	-0.070574
09-CR1_LA_60_S	Max	0.63634	0.35829	0.36209	0.49574	0.28822	1.035	0.60996	0.49996	0.21528	0.14124	0.22896	0.1923	0.095207	0.21245	0.10749	0.076775
	Min	-0.6177	-0.35564	-0.41409	-0.51957	-0.35286	-1.0417	-0.62038	-0.36899	-0.18982	-0.13459	-0.32882	-0.23304	-0.09694	-0.3923	-0.13078	-0.083047
09-CR2_LA_60_S	Max	0.31186	0.3715	0.25862	1.1543	0.93905	0.67658	0.74364	0.36765	0.18439	0.22206	0.28972	0.15593	0.060492	0.26022	0.095322	0.068306
	Min	-0.59207	-0.51207	-0.24678	-1.1081	-0.76851	-0.69622	-0.59161	-0.25396	-0.18475	-0.16236	-0.46532	-0.26058	-0.11291	-0.49184	-0.09671	-0.088287
09-RT1_LA_60_S	Max	0.66032	0.38781	0.48002	1.0577	0.67506	1.0667	0.73294	0.5623	0.28608	0.23685	0.23487	0.28637	0.12344	0.24829	0.17058	0.12329
	Min	-0.75487	-0.39771	-0.4208	-0.93635	-0.44042	-0.66033	-0.56895	-0.42189	-0.24779	-0.26159	-0.31222	-0.28728	-0.11134	-0.37293	-0.17351	-0.11741
09-RT2_LA_60_S	Max	0.8753	0.55472	0.4907	1.828	1.0311	0.85656	0.77413	0.44979	0.44485	0.39067	0.22333	0.18102	0.12672	0.27397	0.14119	0.13246
	Min	-0.63121	-0.46843	-0.48175	-1.6306	-0.96383	-0.62405	-0.59265	-0.54121	-0.34814	-0.29286	-0.32311	-0.22998	-0.10614	-0.44437	-0.14258	-0.13637
10-CR1_LA_60_R	Max	0.39978	0.36718	0.70033	0.52346	0.48783	0.62282	0.78578	1.2026	0.2101	0.13372	0.24808	0.45859	0.18417	0.12228	0.18014	0.058431
	Min	-0.36331	-0.29685	-0.94982	-0.54024	-0.45987	-0.6954	-0.65928	-1.0501	-0.19585	-0.13947	-0.21587	-0.41449	-0.17979	-0.12397	-0.13731	-0.057668
10-CR2_LA_60_R	Max	0.20698	0.47896	0.53319	0.82975	0.9118	0.16466	0.28551	0.75737	0.27684	0.12345	0.3068	0.41811	0.10675	0.14461	0.11136	0.05952
	Min	-0.24821	-0.35117	-0.41693	-0.8246	-0.95309	-0.31174	-0.59832	-0.90476	-0.23139	-0.14397	-0.22748	-0.43197	-0.16498	-0.16575	-0.19722	-0.0597
10-RT1_LA_60_R	Max	0.46054	0.37907	1.0609	1.2607	1.4579	0.35599	0.50762	1.7383	0.2781	0.2473	0.27458	0.45884	0.20531	0.16764	0.161	0.10205
	Min	-0.56323	-0.50946	-0.60777	-1.3954	-1.1552	-0.35968	-0.51772	-1.1996	-0.3798	-0.27826	-0.23921	-0.35985	-0.16528	-0.11953	-0.22433	-0.11125
10-RT2_LA_60_R	Max	0.36872	0.51307	1.0849	1.5878	1.547	0.35853	0.63445	0.74156	0.36254	0.28259	0.25695	0.41098	0.22753	0.14214	0.16201	0.085122
	Min	-0.39698	-0.53118	-1.0037	-1.9332	-1.5719	-0.55319	-0.54224	-0.6873	-0.40104	-0.37324	-0.18966	-0.29183	-0.17764	-0.12708	-0.13616	-0.084514
11-CR1_CL_80_S	Max	0.51612	0.43643	1.0265	1.8788	1.1845	0.59929	1.0166	0.74177	0.22267	0.24713	0.35704	0.23854	0.14807	0.1916	0.30839	0.072674
	Min	-0.54235	-0.63253	-2.6659	-1.8911	-1.116	-0.81217	-1.3943	-0.95549	-0.2955	-0.21921	-0.5564	-0.40421	-0.14279	-0.33871	-0.13799	-0.07206
11-CR2_CL_80_S	Max	0.55117	0.65623	0.53507	2.0711	1.5702	0.3379	0.87361	1.2149	0.30977	0.35319	0.34418	0.19026	0.1147	0.16252	0.12346	0.09492
	Min	-0.43535	-0.59342	-0.62676	-1.6736	-1.4375	-0.37648	-0.61682	-1.2044	-0.24395	-0.32625	-0.54253	-0.4014	-0.11205	-0.33586	-0.10802	-0.095819
11-RT1_CL_80_S	Max	1.1465	0.46849	0.90186	1.4347	1.0686	1.4573	1.3576	1.1605	0.3131	0.45996	0.34048	0.26508	0.17442	0.18491	0.16667	0.12931
	Min	-1.1552	-0.407	-1.0264	-1.5724	-0.83699	-1.0108	-1.4632	-1.1936	-0.31008	-0.29556	-0.44939	-0.49746	-0.24806	-0.32205	-0.1764	-0.11133
11-RT2_CL_80_S	Max	0.99389	0.59663	0.81056	2.8364	1.8551	1.5788	1.4463	1.346	0.46037	0.57652	0.28732	0.24006	0.31568	0.26594	0.20142	0.16018
	Min	-0.82388	-0.80856	-0.85327	-2.7702	-1.9099	-0.88833	-0.86865	-1.3956	-0.49585	-0.45596	-0.41425	-0.47592	-0.24761	-0.31416	-0.23693	-0.14806
12-CR1_CL_80_R	Max	0.7464	0.59114	0.84713	1.8861	1.5668	0.6743	0.88466	0.76828	0.36008	0.18657	0.45786	0.40695	0.17956	0.29345	0.13071	0.10676
	Min	-0.55866	-0.3446	-1.1215	-2.0221	-1.4136	-0.91394	-1.0725	-0.88455	-0.26765	-0.25237	-0.32725	-0.1943	-0.1897	-0.2427	-0.17498	-0.08303
12-CR2_CL_80_R	Max	0.51975	0.59168	0.51516	1.7836	1.5407	0.41146	0.52407	0.51453	0.27717	0.24253	0.55782	0.44428	0.14356	0.39811	0.10586	0.080239
	Min	-0.48419	-0.33635	-0.3626	-1.7846	-1.6454	-0.44242	-0.54284	-0.47325	-0.22995	-0.23976	-0.27695	-0.33758	-0.25943	-0.17652	-0.096627	-0.071576
12-RT1_CL_80_R	Max	0.79246	0.48184	1.3433	2.3935	1.2903	1.1755	1.2457	1.2919	0.31286	0.34606	0.34456	0.33274	0.22768	0.2569	0.16599	0.15303
	Min	-1.0518	-0.45975	-0.8411	-2.0107	-1.3593	-1.5282	-1.8208	-1.3581	-0.32569	-0.34203	-0.34006	-0.33374	-0.30434	-0.24077	-0.16054	-0.13808
12-RT2_CL_80_R	Max	0.81595	0.67826	0.91643	2.1832	1.9551	0.8833	0.94521	0.89573	0.41706	0.48695	0.46562	0.40756	0.22931	0.36142	0.23171	0.17115
	Min	-0.75577	-0.82619	-1.8858	-2.3497	-1.8724	-0.70356	-1.1744	-1.1229	-0.53315	-0.51852	-0.22937	-0.23979	-0.27453	-0.18905	-0.23028	-0.14846

Sensor type		Accelerometers (Velocity-mm/s)															
Location		Span 1 girders, end			Span 1 girders, mid-span		Span 2 girders, end			Pier 7 headstock			Pier 1 headstock				
Sensor/Time (s)		S1G2e-a accel	S1G3e-a accel	S1G4e-a accel	S1G3m accel	S1G5m accel	S2G2e-a accel	S2G3e-a accel	S2G4e-a accel	P7 HS1-a z accel	P7 HS2-a z accel	P7 HC-a x accel	P1H RHS-a x accel	P1H RHS-a z accel	P1H LHS-a x accel	P1H LHS-a y accel	P1H LHS-a z accel
STATIC	**Max**	**0**	**0.066887**	**0**	**0.26995**	**0.23605**	**0.44159**	**0**	**0**	**0.027819**	**0.025272**	**0.073416**	**0.64042**	**0.18073**	**0.071329**	**0.078368**	**0.01184**
	Min	**0**	**-0.060226**	**0**	**-0.31672**	**-0.26701**	**-0.6949**	**0**	**0**	**-0.026104**	**-0.024729**	**-0.06617**	**-0.48868**	**-0.24753**	**-0.068324**	**-0.076279**	**-0.01085**
DYNAMIC	**Max**	**2.1692**	**1.1053**	**2.3005**	**2.8364**	**1.9551**	**2.1835**	**2.2288**	**1.7383**	**0.71572**	**0.61169**	**0.55782**	**0.62874**	**0.82366**	**0.39811**	**0.50115**	**0.21555**
	Min	**-1.6624**	**-0.89637**	**-3.1768**	**-2.7702**	**-2.0462**	**-1.7773**	**-1.8208**	**-1.9459**	**-0.72459**	**-0.64818**	**-0.5564**	**-0.52483**	**-0.42666**	**-0.5727**	**-0.61175**	**-0.28721**
13-CR1_LA_80_S	Max	0.95603	0.36301	0.55996	1.3922	1.0405	1.0725	1.0992	0.56423	0.22754	0.24234	0.32558	0.18875	0.11767	0.31539	0.17953	0.10716
	Min	-0.70338	-0.38795	-0.67878	-1.2798	-0.94231	-1.0861	-1.0678	-0.63009	-0.20183	-0.15994	-0.511	-0.26406	-0.13044	-0.5727	-0.24606	-0.1069
13-CR2_LA_80_S	Max	0.42417	0.4772	0.3488	1.3208	0.88999	0.90538	0.90331	0.48195	0.2635	0.41039	0.3128	0.25189	0.15821	0.25772	0.13911	0.11638
	Min	-0.50324	-0.4629	-0.36437	-1.4699	-0.7928	-0.68782	-0.68549	-0.58132	-0.30629	-0.34498	-0.37857	-0.41148	-0.10226	-0.52629	-0.12007	-0.094246
13-RT1_LA_80_S	Max	1.1552	0.47525	0.75723	1.0107	0.63851	1.1238	0.8782	0.68857	0.28411	0.33356	0.25129	0.30443	0.18232	0.26221	0.24518	0.16259
	Min	-1.157	-0.55789	-0.79831	-1.035	-0.67456	-1.3568	-1.2799	-0.8116	-0.34996	-0.32843	-0.40961	-0.36188	-0.18185	-0.4597	-0.18656	-0.15729
13-RT2_LA_80_S	Max	1.1319	1.1053	0.73711	2.0007	0.97726	0.89487	1.3275	0.86984	0.71572	0.5662	0.47225	0.35383	0.26828	0.35269	0.24225	0.21555
	Min	-1.0092	-0.89637	-1.0423	-1.8829	-1.1141	-0.93119	-1.0384	-0.71423	-0.72459	-0.64818	-0.33066	-0.25187	-0.31719	-0.50618	-0.21988	-0.28721
14-CR1_LA_60_R	Max	0.46789	0.351	0.90223	0.40534	0.42322	0.65609	0.86826	1.0341	0.2005	0.11162	0.24204	0.50795	0.24776	0.12022	0.15151	0.048346
	Min	-0.56343	-0.24383	-0.98422	-0.50968	-0.47727	-0.599	-0.9225	-0.96091	-0.16953	-0.09947	-0.20778	-0.32568	-0.24109	-0.11457	-0.18577	-0.047198
14-CR2_LA_80_R	Max	0.33419	0.4839	1.0819	1.4098	1.3957	0.3019	0.63844	0.69978	0.35802	0.2613	0.35844	0.56104	0.23224	0.24112	0.11737	0.11295
	Min	-0.36735	-0.45608	-1.1919	-1.1315	-1.3135	-0.33859	-0.67156	-1.0537	-0.31354	-0.27917	-0.29589	-0.45248	-0.30007	-0.1728	-0.099815	-0.074292
14-RT1_LA_80_R	Max	0.62576	0.43024	1.3834	1.6913	1.955	0.74147	0.87384	1.2997	0.3033	0.293	0.26457	0.50235	0.82366	0.19895	0.3951	0.12973
	Min	-0.57579	-0.43908	-1.7926	-2.0413	-1.9938	-0.75192	-0.86045	-1.604	-0.31837	-0.34914	-0.22964	-0.32409	-0.42666	-0.14784	-0.61175	-0.16415
14-RT2_LA_80_R	Max	0.59918	0.47229	1.1808	1.3508	1.1518	0.70436	1.1326	1.2322	0.36903	0.34686	0.2725	0.51141	0.27527	0.17736	0.20371	0.13506
	Min	-0.62236	-0.51602	-3.1768	-1.5269	-1.0881	-0.74744	-1.0716	-1.725	-0.38434	-0.34841	-0.29449	-0.35864	-0.41117	-0.17902	-0.25188	-0.13742
15-CR1_LA_80_S	Max	0.73598	0.4682	0.66226	1.5554	1.1226	1.0627	1.1751	0.50959	0.28052	0.27071	0.33178	0.23469	0.10258	0.2819	0.185	0.10131
	Min	-0.78168	-0.45971	-0.64192	-1.4787	-1.0719	-0.77873	-0.84404	-0.50554	-0.20989	-0.17137	-0.4746	-0.27534	-0.1305	-0.50649	-0.12073	-0.098278
15-CR2_LA_80_S	Max	0.56257	0.47668	0.3203	1.4917	0.77885	0.6306	1.0437	0.6884	0.29601	0.43225	0.3336	0.21552	0.14656	0.23564	0.18131	0.12114
	Min	-0.4227	-0.60064	-0.45264	-1.352	-0.80552	-0.45461	-0.41029	-0.36111	-0.32316	-0.34693	-0.41885	-0.40532	-0.11755	-0.47771	-0.13409	-0.099741
15-RT1_LA_85_S	Max	2.1692	0.53171	0.52486	1.0646	0.67023	1.5111	1.6993	0.83781	0.27521	0.28947	0.26896	0.27356	0.16362	0.2657	0.24681	0.19593
	Min	-1.5335	-0.47934	-0.62817	-1.1837	-0.91123	-1.3144	-1.3276	-0.89186	-0.37496	-0.33159	-0.39257	-0.29401	-0.20134	-0.41985	-0.22649	-0.17101
15-RT2_LA_95_S	Max	1.7643	0.613	0.92873	1.3519	0.94594	1.8325	2.2288	1.3021	0.46281	0.4284	0.22963	0.25198	0.24877	0.27421	0.24861	0.20329
	Min	-1.6624	-0.73431	-1.0777	-1.3026	-0.96354	-1.4771	-1.3839	-1.1302	-0.51766	-0.4872	-0.37241	-0.34804	-0.21473	-0.41044	-0.26487	-0.20398
16-CR1_LA_80_R	Max	0.76236	0.28355	1.2059	1.3746	1.3436	0.77049	0.77727	1.4583	0.23564	0.14859	0.36347	0.60723	0.18136	0.20263	0.16039	0.093306
	Min	-0.8308	-0.33873	-1.0809	-1.1394	-1.1694	-0.86739	-0.71222	-0.88768	-0.25424	-0.27678	-0.25451	-0.4867	-0.19042	-0.17423	-0.13214	-0.08689
16-CR2_LA_80_R	Max	0.20736	0.33348	0.68304	1.1294	1.1587	0.22361	0.43676	0.5475	0.19142	0.1392	0.39405	0.62874	0.16681	0.22128	0.183	0.043766
	Min	-0.19206	-0.25141	-0.69008	-1.3831	-1.2007	-0.36515	-0.41161	-0.66016	-0.1108	-0.14142	-0.17068	-0.24291	-0.15554	-0.16039	-0.13802	-0.042694
16-RT1_LA_90_R	Max	1.0426	0.45827	1.3841	1.5393	1.5971	0.6886	1.1144	1.2262	0.30633	0.34909	0.27002	0.56844	0.3639	0.21332	0.50115	0.10142
	Min	-1.1719	-0.58271	-2.6546	-1.492	-2.0462	-1.1257	-1.1613	-1.9459	-0.30975	-0.27444	-0.2353	-0.52483	-0.40164	-0.20573	-0.26037	-0.081626
16-RT2_LA_94_R	Max	0.91635	0.62997	2.3005	1.4222	1.0927	0.89919	1.5185	1.7067	0.60179	0.61169	0.42987	0.6135	0.28909	0.27238	0.34689	0.15205
	Min	-1.0301	-0.56605	-2.1831	-1.7579	-1.261	-1.7773	-1.703	-1.9252	-0.43002	-0.43336	-0.29129	-0.48625	-0.37315	-0.2543	-0.24216	-0.15184
18-CR1_LA_20_S	Max	0.59446	0.071171	0.13773	0.44716	0.30001	0.15873	0.19597	0.13708	0.039661	0.02985	0.055353	0.043972	0.016055	0.052087	0.22473	0.015842
	Min	-1.2717	-0.11131	-0.13129	-0.42192	-0.30954	-0.26923	-0.3206	-0.12262	-0.056874	-0.03949	-0.057483	-0.044575	-0.026829	-0.053612	-0.40034	-0.028181
18-CR2_LA_20_S	Max	0.13423	0.070722	0.11212	0.41402	0.30051	0.21395	0.32799	0.17922	0.056044	0.06569	0.061946	0.069128	0.038966	0.046006	0.064483	0.027111
	Min	-0.13264	-0.11882	-0.12465	-0.52129	-0.36574	-0.41373	-0.18709	-0.071621	-0.080731	-0.04256	-0.05462	-0.054199	-0.040557	-0.043087	-0.080892	-0.036024
18-RT1_LA_20_S	Max	0.21134	0.15126	0.18114	1.5468	1.2489	0.14829	0.16694	0.11711	0.087763	0.083855	0.15216	0.1829	0.044899	0.14942	0.14245	0.045239
	Min	-0.40832	-0.22447	-0.15898	-1.4524	-1.112	-0.18419	-0.17637	-0.10319	-0.14323	-0.091055	-0.1585	-0.1604	-0.055475	-0.22739	-0.12814	-0.061711
18-RT2_LA_20_S	Max	0.2104	0.14175	0.14928	0.69843	0.52292	0.15428	0.16515	0.098436	0.087837	0.098661	0.098557	0.066679	0.034494	0.083499	0.097084	0.037087
	Min	-0.41369	-0.14687	-0.17679	-0.75561	-0.50495	-0.23157	-0.19957	-0.12838	-0.1075	-0.10393	-0.085848	-0.05923	-0.038701	-0.081759	-0.052123	-0.045133
19-CR1_CL_80_R	Max	0.71811	0.47145	0.62199	2.1472	1.8206	0.76216	1.1376	0.82273	0.23736	0.20047	0.44852	0.37926	0.17058	0.18699	0.098402	0.085164
	Min	-0.73347	-0.36341	-0.68622	-2.4172	-1.6282	-0.8178	-1.3045	-1.0509	-0.19936	-0.26209	-0.35549	-0.32367	-0.14982	-0.15459	-0.12722	-0.069867
19-CR2_CL_80_R	Max	0.6774	0.63802	0.44044	1.8116	1.4027	0.56975	0.7466	0.56977	0.23668	0.21335	0.52183	0.39523	0.14929	0.27865	0.16586	0.068246
	Min	-0.57592	-0.30487	-0.62934	-2.0267	-1.648	-0.38266	-0.6206	-0.51696	-0.19225	-0.19236	-0.25354	-0.20918	-0.13919	-0.14926	-0.13827	-0.083498
19-RT1_CL_90_R	Max	1.2306	0.49094	1.2737	2.4034	1.4816	0.94917	1.4729	1.0239	0.32812	0.29637	0.42899	0.33637	0.22905	0.27778	0.16857	0.16385
	Min	-1.353	-0.44297	-0.97104	-2.2415	-1.364	-1.201	-1.3237	-1.5515	-0.31448	-0.39674	-0.29447	-0.28602	-0.19352	-0.2213	-0.16975	-0.13582
19-RT2_CL_94_R	Max	0.93387	0.72789	1.5229	1.8153	1.0489	2.1835	1.8889	1.1082	0.49531	0.41914	0.41722	0.40371	0.25852	0.28178	0.29168	0.12635
	Min	-1.0939	-0.70588	-1.3363	-1.8139	-1.3673	-1.2519	-1.5501	-1.2456	-0.52622	-0.55933	-0.28312	-0.39071	-0.31429	-0.26361	-0.24882	-0.16086

APPENDIX B DYNAMIC INCREMENT DATA

B.1 Summary of Methodology

To determine the magnitude of dynamic load amplification on the superstructure and substructure, the DI was calculated for various structural components for the test vehicles at various speeds in both travel directions using the following equation:

$$DI = \frac{A_{dynamic} - A_{static}}{A_{static}} .100 \ [\%] \qquad 2$$

where

DI	=	Dynamic Increment
$A_{dynamic}$	=	the peak dynamic response (strain or deflection) in the structural component due to a test vehicle at an elevated speed
A_{static}	=	the peak static response (strain or deflection) in the same component due to the same test vehicle at crawl speed, corresponding to the direction and transverse location of vehicle travel

A representative DI value was determined for each component for each run and vehicle required for comparison (i.e. girders, headstock and column). This was achieved using the following methodology:

- Peak values measured from all strain and deflection sensors for both static and dynamic runs were determined for each vehicle and direction of travel.
  - Peak values were cross-referenced against the transverse location of wheel loads for each vehicle for both static and dynamic cases
  - Consideration was given to actual waveforms to confirm coincidence of peak values between static and dynamic runs
  - For the column, peak tensile strains and the corresponding compression strains (and vice versa) were considered
- DI values for individual components were determined using Equation 2 from peak values determined previously
- The representative DI value for each run and component group (e.g. girders, headstock, columns) was selected from the maximum of DI values previously determined. This representative value was determined based on the following rationale:
  - Only components directly affected by vehicle loading per run were considered (e.g. girder sensors registering peak values in one lane only were considered)
  - The transverse position of the vehicle was taken into consideration when reviewing static and dynamic peak values.
- DI values were determined using an automated excel spreadsheet. Values were then reviewed on an individual basis for accuracy and rationality.

DI value determination for the Canal Creek Bridge is shown in Figure B 1, Dawson River Bridge is shown in Figure B 2 and Table B 1, and for Neerkol Creek Bridge Figure B 3 and Table B 2.

Full DI value determinations follow.

Figure B 1: Determination of DI values for various components & vehicle travel (Canal Creek Bridge)

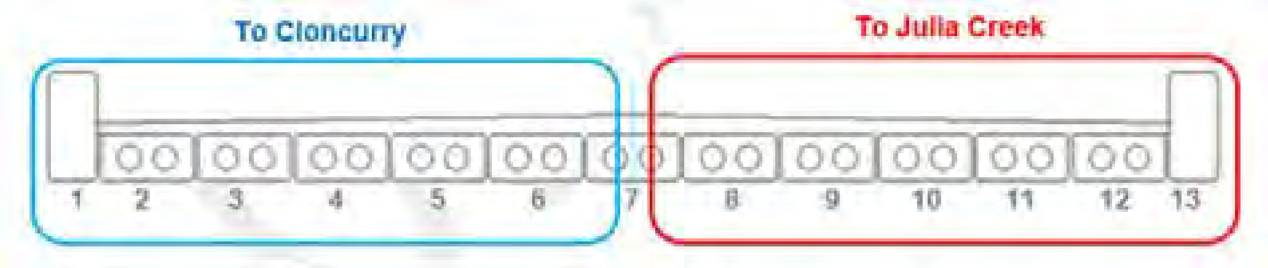

Figure B 2: Determination of DI values for various components & vehicle travel (Dawson River Bridge)

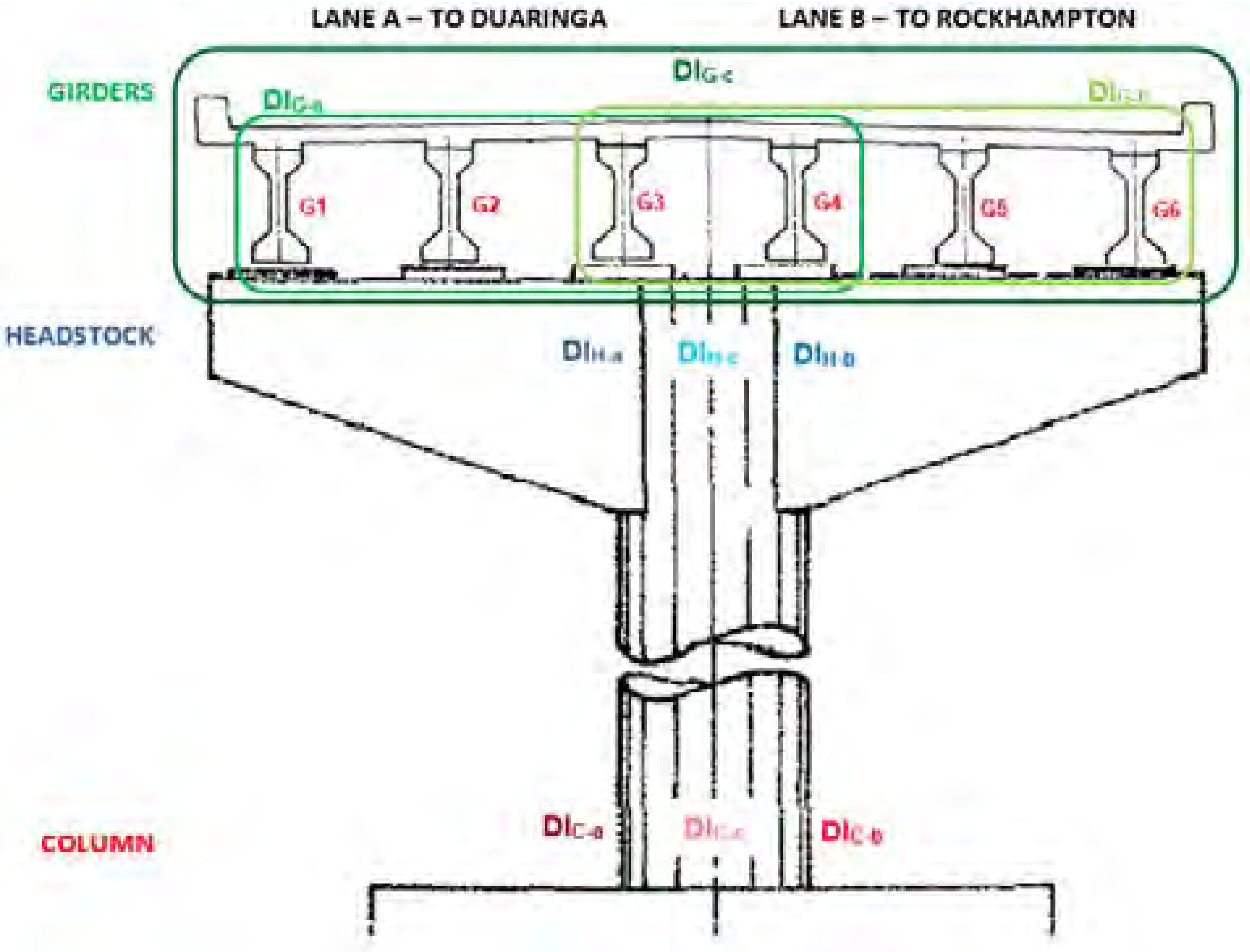

Table B 1: Determination of DI Values for each component group (Dawson River Bridge)

Group Component	Transverse Location	DI Value Notation	DI Value Determination	DI Value Determined from Unit Measurement
Girders	Lane A (to Duaringa)	$DI_{G\text{-}a}$	Max DI [Girders(1-4)]	▪ Bending strain,
	Lane B (to Rockhampton)	$DI_{G\text{-}b}$	Max DI [Girders(3-6)]	▪ Deflection
	Centreline	$DI_{G\text{-}c}$	Max DI [Girders(all)]	
Headstock	Lane A (to Duaringa)	$DI_{H\text{-}a}$	DI [Headstock(L)]	▪ Bending strain,
	Lane B (to Rockhampton)	$DI_{H\text{-}b}$	DI [Headstock(R)]	▪ Deflection
	Centreline	$DI_{H\text{-}c}$	Max DI [Headstock(L + R)]	
Columns	Lane A (to Duaringa)	$DI_{C\text{-}a\text{-}t}$	DI [Headstock(R)] - tension	▪ Bending strain,
		$DI_{C\text{-}a\text{-}c}$	DI [Headstock(L)] - compression	▪ Deflection
	Lane B (to Rockhampton)	$DI_{C\text{-}b\text{-}t}$	DI [Headstock(R)] - tension	
		$DI_{C\text{-}b\text{-}c}$	DI [Headstock(L)] - compression	
	Centreline	$DI_{C\text{-}c\text{-}t}$	DI [Headstock(R)] - tension	
		$DI_{C\text{-}c\text{-}c}$	DI [Headstock(L)] - compression	

Figure B 3: Determination of DI values for various components & vehicle travel (Neerkol Creek Bridge)

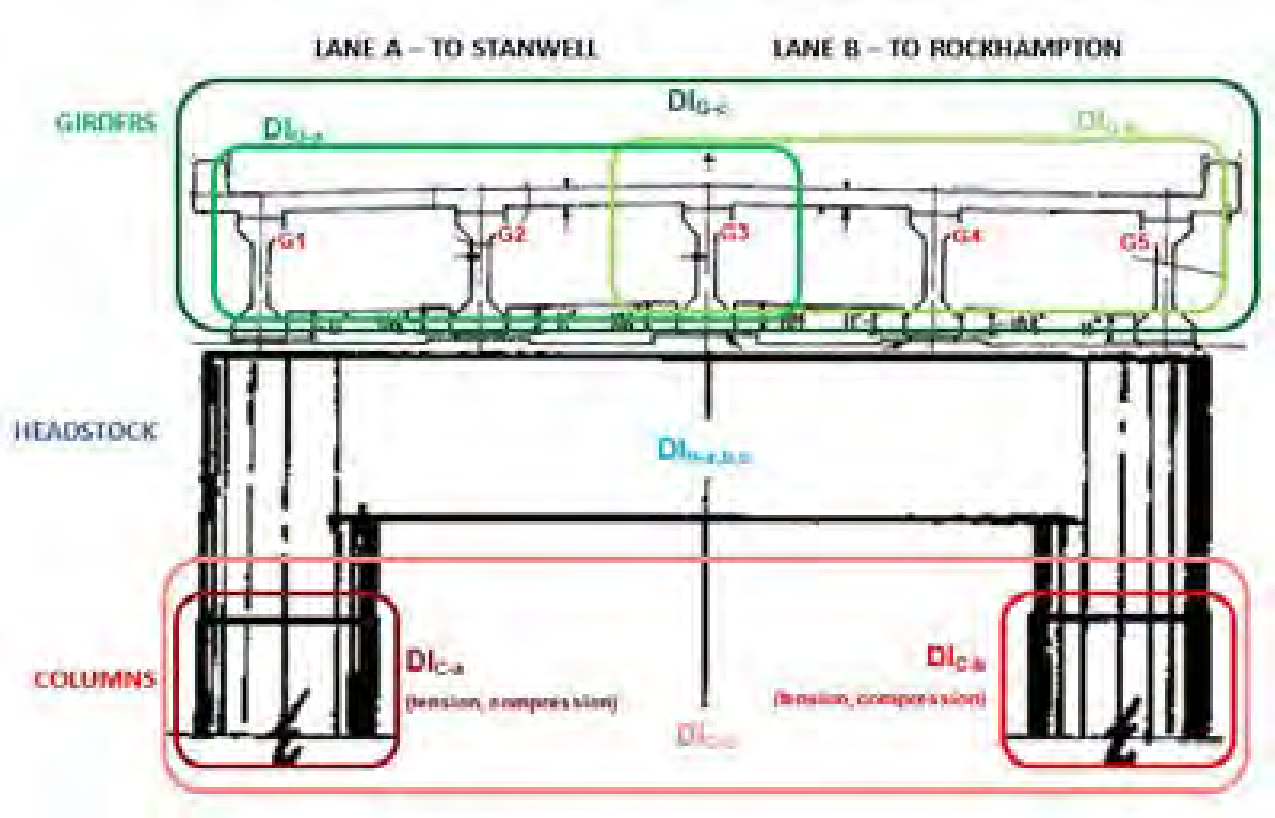

Table B 2: Determination of DI Values for each component group (Neerkol Creek Bridge)

Group Component	Transverse Location	DI Value Notation	DI Value Determination	DI Value Determined from Unit Measurement
Girders	Lane A (to Duaringa)	$DI_{G\text{-}a}$	Max DI [Girders(1-3)]	▪ Bending strain, ▪ Deflection (girder G3 only)
	Lane B (to Rockhampton)	$DI_{G\text{-}b}$	Max DI [Girders(3-5)]	
	Centreline	$DI_{G\text{-}c}$	Max DI [Girders(all)]	
Headstock	Lane A (to Duaringa)	$DI_{H\text{-}a}$	Max DI [Headstock(S1, S2 & soffit)]	▪ Bending strain
	Lane B (to Rockhampton)	$DI_{H\text{-}b}$		
	Centreline	$DI_{H\text{-}c}$		
Columns	Lane A (to Duaringa)	$DI_{C\text{-}a\text{-}t}$ $DI_{C\text{-}a\text{-}c}$	DI [Column(L)] - tension DI [Column(L)] - compression	▪ Bending strain
	Lane B (to Rockhampton)	$DI_{C\text{-}b\text{-}t}$ $DI_{C\text{-}b\text{-}c}$	DI [Column(R)] - tension DI [Column (L)] - compression	
	Centreline	$DI_{C\text{-}c\text{-}t}$ $DI_{C\text{-}c\text{-}c}$	DI [Column (both)] - tension DI [Column (both)] - compression	

B.2 Canal Creek Bridge

B.2.1 *Summary of DI Values*

Table B 3: Canal Creek Bridge DI Summary – Crane 1 (CR1)

						Lane (To Cloncurry)				Centre					Lane (To Julia Creek)			
Speed(km/h)	Run #	Position	Direction to								Strain gauges							
10	21	Lane	Cloncurry	Run #		sg1	sg2	sg3	sg4	sg5	sg6	sg7	sg8	sg9	sg10	sg11	sg12	sg13
					Max Dynamic Strain(µε)	85.90	[illegible]	78.60	[illegible]	60.10	[illegible]	68.60	52.60	0.00	33.70	32.00	29.00	30.90
Input static data				7	Static Strain (µε) (max per unit)	79.60	73.00	77.90	63.30	58.80	62.10	65.90	55.00		35.30	33.10	31.50	33.00
					Static Strain (µε) (max total Span 1)	79.60	79.60	79.60	79.60	79.60	79.60	79.60	79.60		79.60	79.60	79.60	79.60
					Static Strain (µε) (max unit type)	79.60	77.90	77.90	77.90	77.90	77.90	77.90	77.90		77.90	77.90	77.90	79.60
					DI (max per unit)	7.91%	7.12%	0.90%	0.00%	2.21%	4.83%	4.10%	-4.36%		-4.53%	-3.32%	-7.94%	-6.36%
					DI (max per Span 1)	7.91%	-1.76%	-1.26%	-20.48%	-24.50%	-18.22%	-13.82%	-33.92%		-57.66%	-59.80%	-63.57%	-61.18%
					DI (max per unit type)	7.91%	0.39%	0.90%	-18.74%	-22.85%	-16.43%	11.94%	-32.48%		-56.74%	-58.92%	-62.77%	-61.18%
					Ave DI (Group)	4.51%												
					Max DI (Group)	7.91%												
20	30	Lane	Cloncurry		Max Dynamic Strain(µε)	[illegible]	80.70	[illegible]	66.20	62.50	67.10	71.80	57.10	0.00	36.70	33.70	31.50	33.80
				7	Static Strain (µε) (max per unit)	79.60	73.00	77.90	63.30	58.80	62.10	65.90	55.00		35.30	33.10	31.50	33.00
					Static Strain (µε) (max total Span 1)	79.60	79.60	79.60	79.60	79.60	79.60	79.60	79.60		79.60	79.60	79.60	79.60
					Static Strain (µε) (max unit type)	79.60	77.90	77.90	77.90	77.90	77.90	77.90	77.90		77.90	77.90	77.90	79.60
					DI (max per unit)	8.42%	10.55%	9.11%	4.58%	6.29%	8.05%	8.95%	3.82%		3.97%	1.81%	0.00%	2.42%
					DI (max per Span 1)	8.42%	1.38%	6.78%	-16.88%	-21.48%	-15.70%	-9.80%	-28.27%		-53.89%	-57.66%	-60.43%	-57.54%
					DI (max per unit type)	8.42%	3.59%	9.11%	-15.02%	-19.77%	-13.86%	-7.83%	-26.70%		-52.89%	-56.74%	-59.56%	-57.54%
					Ave DI (Group)	7.99%												
					Max DI (Group)	10.55%												
40	65	Lane	Cloncurry		Max Dynamic Strain(µε)	82.10	76.60	73.00	58.00	55.10	58.20	57.00	43.70	0.00	29.80	27.80	26.60	27.60
				7	Static Strain (µε) (max per unit)	79.60	73.00	77.90	63.30	58.80	62.10	65.90	55.00		35.30	33.10	31.50	33.00
					Static Strain (µε) (max total Span 1)	79.60	79.60	79.60	79.60	79.60	79.60	79.60	79.60		79.60	79.60	79.60	79.60
					Static Strain (µε) (max unit type)	79.60	77.90	77.90	77.90	77.90	77.90	77.90	77.90		77.90	77.90	77.90	79.60
					DI (max per unit)	3.14%	4.93%	-6.29%	-8.37%	-6.29%	-6.28%	-13.51%	-20.55%		-15.58%	-16.01%	-15.56%	-16.36%
					DI (max per Span 1)	3.14%	-3.77%	-8.29%	-27.14%	-30.78%	-26.88%	-28.39%	-45.10%		-62.56%	-65.08%	-66.58%	-65.33%
					DI (max per unit type)	3.14%	-1.67%	-6.29%	-25.55%	-29.27%	-25.29%	-26.83%	-43.90%		-61.75%	-64.31%	-65.85%	-65.33%
					Ave DI (Group)	-4.87%												
					Max DI (Group)	4.93%												
60	39	Lane	Cloncurry		Max Dynamic Strain(µε)	[illegible]	86.90	94.70	77.60	72.30	77.80	84.00	69.00	0.00	43.00	40.60	38.50	40.60
				7	Static Strain (µε) (max per unit)	79.60	73.00	77.90	63.30	58.80	62.10	65.90	55.00		35.30	33.10	31.50	33.00
					Static Strain (µε) (max total Span 1)	79.60	79.60	79.60	79.60	79.60	79.60	79.60	79.60		79.60	79.60	79.60	79.60
					Static Strain (µε) (max unit type)	79.60	77.90	77.90	77.90	77.90	77.90	77.90	77.90		77.90	77.90	77.90	79.60
					DI (max per unit)	[illegible]	19.04%	21.57%	22.59%	22.96%	25.28%	27.47%	25.45%		21.81%	22.66%	22.22%	23.03%
					DI (max per Span 1)	16.96%	9.17%	18.97%	-2.51%	-9.17%	-2.26%	5.53%	-13.32%		-45.98%	-48.99%	-51.63%	-48.99%
					DI (max per unit type)	16.96%	11.55%	21.57%	-0.39%	-7.19%	-0.13%	7.83%	-11.42%		-44.80%	-47.88%	-50.58%	-48.99%
					Ave DI (Group)	22.27%												
					Max DI (Group)	27.47%												
80	45	Lane	Cloncurry		Max Dynamic Strain(µε)	96.70	87.90	83.00	77.10	80.70	[illegible]	[illegible]	76.10	0.00	52.60	49.40	47.00	50.20
				7	Static Strain (µε) (max per unit)	79.60	73.00	77.90	63.30	58.80	62.10	65.90	55.00		35.30	33.10	31.50	33.00
					Static Strain (µε) (max total Span 1)	79.60	79.60	79.60	79.60	79.60	79.60	79.60	79.60		79.60	79.60	79.60	79.60
					Static Strain (µε) (max unit type)	79.60	77.90	77.90	77.90	77.90	77.90	77.90	77.90		77.90	77.90	77.90	79.60
					DI (max per unit)	21.48%	19.59%	6.68%	21.80%	37.24%	38.33%	28.52%	39.09%		49.01%	49.24%	49.21%	52.12%
					DI (max per Span 1)	21.48%	9.67%	1.00%	-3.14%	1.38%	7.91%	2.26%	-3.89%		-38.92%	-37.94%	-40.95%	-36.93%
					DI (max per unit type)	21.48%	12.07%	6.68%	-1.03%	3.59%	10.27%	4.49%	-1.80%		-32.48%	-36.59%	-39.67%	-36.93%
					Ave DI (Group)	24.09%												
					Max DI (Group)	38.53%												

10		24 Lane	Julia Creek		Max Dynamic Strain(µε)	30.20	29.20	30.50	34.10	40.90	32.20	67.10	65.40	0.00	62.70	77.60	75.80	85.00
Input static data				7	Static Strain (µε) (max per unit)	28.90	27.90	30.40	31.60	38.20	50.00	64.60	61.00		60.80	74.00	71.90	80.00
					Static Strain (µε) (max total Span 1)	80.00	80.00	80.00	80.00	80.00	80.00	80.00	80.00		80.00	80.00	80.00	80.00
					Static Strain (µε) (max unit type)	80.00	74.00	74.00	74.00	74.00	74.00	74.00	74.00		74.00	74.00	74.00	80.00
					DI (max per unit)	4.50%	4.66%	0.33%	7.91%	7.07%	4.40%	3.87%	7.21%		3.13%	4.86%	5.46%	[illegible]
					DI (max per Span 1)	-62.25%	-63.50%	-61.88%	-57.38%	-48.88%	-34.75%	-16.13%	-18.25%		-21.63%	-3.00%	-1.63%	6.25%
					DI (max per unit type)	-62.25%	-60.54%	-58.78%	-53.92%	-44.73%	-29.46%	-9.32%	-11.62%		-15.27%	3.86%	6.55%	6.25%
					Ave DI (Group)							6.33%						
					Max DI (Group)							9.46%						
20		62 Lane	Julia Creek		Max Dynamic Strain(µε)	35.00	33.80	35.10	38.20	44.90	58.50	71.90	66.10	0.00	63.90	76.50	75.30	85.80
				10	Static Strain (µε) (max per unit)	28.90	27.90	30.40	31.60	38.20	50.00	64.60	61.00		60.80	74.00	71.90	80.00
					Static Strain (µε) (max per unit)	80.00	80.00	80.00	80.00	80.00	80.00	80.00	80.00		80.00	80.00	80.00	80.00
					Static Strain (µε) (max total Span 1)	80.00	74.00	74.00	74.00	74.00	74.00	74.00	74.00		74.00	74.00	74.00	80.00
					Static Strain (µε) (max unit type)	80.00	74.00	74.00	74.00	74.00	74.00	74.00	74.00		74.00	74.00	74.00	80.00
					DI (max per unit)	21.11%	21.15%	15.46%	20.89%	17.54%	17.00%	11.30%	8.36%		5.10%	3.38%	4.73%	[illegible]
					DI (max per Span 1)	-63.88%	-62.30%	-58.92%	-57.30%	-48.38%	-32.43%	-12.70%	-17.57%		-17.84%	0.00%	-2.84%	0.00%
					DI (max per unit type)	-63.88%	-62.30%	-58.92%	-57.30%	-48.38%	-32.43%	-12.70%	-17.57%		-17.84%	0.00%	-2.84%	0.00%
					Ave DI (Group)							6.69%						
					Max DI (Group)							11.30%						
40		68 Lane	Julia Creek	10	Max Dynamic Strain(µε)	37.10	35.50	37.10	41.10	50.40	62.70	74.00	69.80	0.00	67.10	78.80	74.30	[illegible]
					Static Strain (µε) (max per unit)	28.90	27.90	30.40	31.60	38.20	50.00	64.60	61.00		60.80	74.00	71.90	80.00
					Static Strain (µε) (max total Span 1)	80.00	80.00	80.00	80.00	80.00	80.00	80.00	80.00		80.00	80.00	80.00	80.00
					Static Strain (µε) (max unit type)	80.00	74.00	74.00	74.00	74.00	74.00	74.00	74.00		74.00	74.00	74.00	80.00
					DI (max per unit)	28.37%	27.24%	22.04%	30.06%	31.94%	25.40%	14.55%	14.43%		10.36%	6.49%	3.34%	[illegible]
					DI (max per Span 1)	-53.63%	-55.63%	-53.63%	-48.63%	-37.00%	-21.63%	-7.50%	-12.75%		-16.13%	-1.50%	-7.13%	4.00%
					DI (max per unit type)	-53.63%	-52.03%	-49.86%	-44.46%	-31.89%	-15.27%	0.00%	-5.68%		-9.32%	6.49%	0.41%	4.00%
					Ave DI (Group)							8.86%						
					Max DI (Group)							14.55%						
60		42 Lane	Julia Creek	10	Max Dynamic Strain(µε)	35.20	33.70	35.50	38.90	46.20	60.20	74.60	69.30	0.00	68.90	84.40	80.10	88.40
					Static Strain (µε) (max per unit)	28.90	27.90	30.40	31.60	38.20	50.00	64.60	61.00		60.80	74.00	71.90	80.00
					Static Strain (µε) (max total Span 1)	80.00	80.00	80.00	80.00	80.00	80.00	80.00	80.00		80.00	80.00	80.00	80.00
					Static Strain (µε) (max unit type)	80.00	74.00	74.00	74.00	74.00	74.00	74.00	74.00		74.00	74.00	74.00	80.00
					DI (max per unit)	21.80%	20.79%	16.78%	23.10%	20.94%	20.40%	15.48%	13.61%		13.32%	14.05%	11.40%	[illegible]
					DI (max per Span 1)	-56.00%	-57.88%	-55.63%	-51.38%	-42.25%	-24.75%	-6.75%	-13.38%		-13.88%	5.50%	0.12%	10.50%
					DI (max per unit type)	-56.00%	-54.46%	-52.03%	-47.43%	-37.57%	-18.65%	0.81%	-6.35%		-6.89%	14.05%	8.24%	10.50%
					Ave DI (Group)							11.06%						
					Max DI (Group)							15.48%						
80		48 Lane	Julia Creek	10	Max Dynamic Strain(µε)	39.20	37.00	37.90	39.30	46.80	58.70	61.40	62.20	0.00	62.80	66.70	67.40	76.60
					Static Strain (µε) (max per unit)	28.90	27.90	30.40	31.60	38.20	50.00	64.60	61.00		60.80	74.00	71.90	80.00
					Static Strain (µε) (max total Span 1)	80.00	80.00	80.00	80.00	80.00	80.00	80.00	80.00		80.00	80.00	80.00	80.00
					Static Strain (µε) (max unit type)	80.00	74.00	74.00	74.00	74.00	74.00	74.00	74.00		74.00	74.00	74.00	80.00
					DI (max per unit)	35.64%	32.62%	24.67%	24.37%	22.51%	17.40%	-4.95%	1.97%		3.29%	-9.86%	-6.26%	[illegible]
					DI (max per Span 1)	-51.00%	-53.75%	-52.63%	-50.88%	-41.50%	-26.63%	-23.25%	-22.25%		-21.50%	-16.63%	-15.75%	-4.25%
					DI (max per unit type)	-51.00%	-50.00%	-48.78%	-46.89%	-36.76%	-20.68%	-17.03%	-15.95%		-15.14%	-9.86%	-8.92%	-4.25%
					Ave DI (Group)							-3.35%						
					Max DI (Group)							3.29%						

Table B 4: Canal Creek Bridge DI Summary – Semi-Trailer 1 (ST1)

							Lane (To Cloncurry)						Centre			Lane (To Julia Creek)			
													Strain gauges						
Speed(km/h)	Run #	Position	Direction to	Run #			sg1	sg2	sg3	sg4	sg5	sg6	sg7	sg8	sg9	sg10	sg11	sg12	sg13
10	22	Lane	Cloncurry	Run #			sg1	sg2	sg3	sg4	sg5	sg6	sg7	sg8	sg9	sg10	sg11	sg12	sg13
						Max Dynamic Strain(με)	54.10	51.30	53.90	44.40	42.30	46.30	34.90	27.70		16.80	15.10	13.90	14.00
Input static data					8	Static Strain (με) (max per unit)	51.60	48.10	51.10	42.30	40.30	44.80	34.90	27.20		16.50	14.30	12.50	12.50
						Static Strain (με) (max total Span 1)	51.60	51.60	51.60	51.60	51.60	51.60	51.60	51.60		51.60	51.60	51.60	51.60
						Static Strain (με) (max unit type)	51.60	51.10	51.10	51.10	51.10	51.10	51.10	51.10		51.10	51.10	51.10	51.60
						DI (max per unit)	4.84%	6.65%	5.48%	4.96%	4.96%	3.35%	0.00%	1.84%		1.82%	5.59%	11.20%	12.00%
						DI (max per Span 1)	4.84%	-0.58%	4.46%	-13.95%	-18.02%	-10.27%	-32.36%	-46.32%		-67.44%	-70.74%	-73.06%	-72.87%
						DI (max per unit type)	4.84%	0.39%	5.48%	-13.11%	-17.22%	-9.39%	-31.70%	-45.79%		-67.12%	-70.45%	-72.80%	-72.87%
						Ave DI (Group)	5.04%												
						Max DI (Group)	6.65%												
20	28	Lane	Cloncurry			Max Dynamic Strain(με)	55.40	52.40	56.50	47.90	46.10	52.90	40.30	32.10		19.50	17.90	16.40	16.60
					8	Static Strain (με) (max per unit)	51.60	48.10	51.10	42.30	40.30	44.80	34.90	27.20		16.50	14.30	12.50	12.50
						Static Strain (με) (max total Span 1)	51.60	51.60	51.60	51.60	51.60	51.60	51.60	51.60		51.60	51.60	51.60	51.60
						Static Strain (με) (max unit type)	51.60	51.10	51.10	51.10	51.10	51.10	51.10	51.10		51.10	51.10	51.10	51.60
						DI (max per unit)	7.36%	8.94%	10.57%	13.24%	14.39%	18.08%	15.47%	18.01%		18.18%	25.17%	31.20%	32.80%
						DI (max per Span 1)	7.36%	1.55%	9.50%	-7.17%	-10.66%	2.52%	-21.90%	-37.79%		-62.21%	-65.31%	-68.22%	-67.83%
						DI (max per unit type)	7.36%	2.54%	10.57%	-6.26%	-9.78%	3.52%	-21.14%	-37.18%		-61.84%	-64.97%	-67.91%	-67.83%
						Ave DI (Group)	12.10%												
						Max DI (Group)	18.08%												
40	34	Lane	Cloncurry			Max Dynamic Strain(με)	61.20	57.30	56.90	53.00	55.00	56.70	50.20	43.60		27.50	25.40	23.50	25.40
					8	Static Strain (με) (max per unit)	51.60	48.10	51.10	42.30	40.30	44.80	34.90	27.20		16.50	14.30	12.50	12.50
						Static Strain (με) (max total Span 1)	51.60	51.60	51.60	51.60	51.60	51.60	51.60	51.60		51.60	51.60	51.60	51.60
						Static Strain (με) (max unit type)	51.60	51.10	51.10	51.10	51.10	51.10	51.10	51.10		51.10	51.10	51.10	51.60
						DI (max per unit)	18.60%	19.13%	11.35%	25.10%	36.48%	26.56%	43.84%	60.29%		66.67%	77.62%	88.00%	103.20%
						DI (max per Span 1)	18.60%	11.05%	10.27%	2.71%	6.59%	9.88%	-2.71%	-15.50%		-46.71%	-50.78%	-54.46%	-50.78%
						DI (max per unit type)	18.60%	12.13%	11.35%	3.72%	7.63%	10.96%	-1.76%	-14.68%		-46.18%	-50.29%	-54.01%	-50.78%
						Ave DI (Group)	22.90%												
						Max DI (Group)	36.48%												
60	40	Lane	Cloncurry			Max Dynamic Strain(με)	50.90	47.60	53.70	46.30	42.50	47.40	39.50	32.30		20.80	19.90	19.10	19.60
					8	Static Strain (με) (max per unit)	51.60	48.10	51.10	42.30	40.30	44.80	34.90	27.20		16.50	14.30	12.50	12.50
						Static Strain (με) (max total Span 1)	51.60	51.60	51.60	51.60	51.60	51.60	51.60	51.60		51.60	51.60	51.60	51.60
						Static Strain (με) (max unit type)	51.60	51.10	51.10	51.10	51.10	51.10	51.10	51.10		51.10	51.10	51.10	51.60
						DI (max per unit)	-1.36%	-1.04%	5.09%	9.46%	5.46%	5.80%	13.18%	18.75%		26.06%	39.16%	52.80%	56.80%
						DI (max per Span 1)	-1.36%	-7.75%	4.07%	-10.27%	-17.64%	-8.14%	-23.45%	-37.40%		-59.69%	-61.43%	-62.98%	-62.02%
						DI (max per unit type)	-1.36%	-6.85%	5.09%	-9.39%	-16.83%	-7.24%	-22.70%	-36.79%		-59.30%	-61.06%	-62.62%	-62.02%
						Ave DI (Group)	3.90%												
						Max DI (Group)	9.46%												
80	46	Lane	Cloncurry			Max Dynamic Strain(με)	44.60	39.90	37.10	37.80	39.90	41.30	39.40	36.70		27.20	27.20	26.80	29.50
					8	Static Strain (με) (max per unit)	42.70	27.00	28.60	31.00	37.90	45.90	42.50	44.00	37.40	30.80	28.10	26.00	26.80
						Static Strain (με) (max total Span 1)	45.90	45.90	45.90	45.90	45.90	45.90	45.90	45.90		45.90	45.90	45.90	45.90
						Static Strain (με) (max unit type)	42.70	45.90	45.90	45.90	45.90	45.90	45.90	45.90		45.90	45.90	45.90	42.70
						DI (max per unit)	4.45%	47.78%	29.72%	21.94%	5.28%	-10.02%	-7.29%	-16.59%		-11.69%	-3.20%	3.08%	10.07%
						DI (max per Span 1)	-2.83%	-13.07%	-19.17%	-17.65%	-13.07%	-10.02%	-14.16%	-20.04%		-40.74%	-40.74%	-41.61%	-35.73%
						DI (max per unit type)	4.45%	-13.07%	-19.17%	-17.65%	-13.07%	-10.02%	-14.16%	-20.04%		-40.74%	-40.74%	-41.61%	-30.91%
						Ave DI (Group)	16.52%												
						Max DI (Group)	47.78%												
100	51	Lane	Cloncurry			Max Dynamic Strain(με)	36.70	34.10	34.60	37.70	44.40	45.20	44.30	47.00		32.20	31.10	31.90	34.60
					8	Static Strain (με) (max per unit)	42.70	27.00	28.60	31.00	37.90	45.90	42.50	44.00	37.40	30.80	28.10	26.00	26.80
						Static Strain (με) (max total Span 1)	45.90	45.90	45.90	45.90	45.90	45.90	45.90	45.90		45.90	45.90	45.90	45.90
						Static Strain (με) (max unit type)	42.70	45.90	45.90	45.90	45.90	45.90	45.90	45.90		45.90	45.90	45.90	42.70
						DI (max per unit)	-14.05%	26.30%	20.98%	21.61%	17.15%	-1.53%	4.24%	6.82%		4.55%	10.68%	22.69%	29.10%
						DI (max per Span 1)	-20.04%	-25.71%	-24.62%	-17.86%	-3.27%	-1.53%	-3.49%	2.40%		-29.85%	-32.24%	-30.50%	-24.62%
						DI (max per unit type)	-14.05%	-25.71%	-24.62%	-17.86%	-3.27%	-1.53%	-3.49%	2.40%		-29.85%	-32.24%	-30.50%	-18.97%
						Ave DI (Group)	11.74%												
						Max DI (Group)	26.30%												

10	25 Lane	Julia Creek		Max Dynamic Strain(με)	15.10	14.80	15.80	18.90	23.40	30.00	37.40	47.00		[illegible]	[illegible]	[illegible]	[illegible]
Input static data			11	Static Strain (με) (max per unit)	11.60	11.60	13.00	15.70	19.70	28.50	33.80	[illegible]		[illegible]	[illegible]	[illegible]	[illegible]
				Static Strain (με) (max total Span 1)	45.50	45.50	45.50	45.50	45.50	45.50	45.50	45.50		45.50	45.50	45.50	45.50
				Static Strain (με) (max unit type)	45.50	45.00	45.00	45.00	45.00	45.00	45.00	45.00		45.00	45.00	45.00	45.50
				DI (max per unit)	30.17%	27.59%	21.54%	20.38%	18.78%	5.26%	10.65%	4.44%		5.05%	5.36%	3.61%	4.62%
				DI (max per Span 1)	-66.81%	-67.47%	-65.27%	-58.46%	-48.57%	-34.07%	-17.80%	3.30%		-8.57%	5.74%	-5.27%	4.62%
				DI (max per unit type)	-66.81%	-67.11%	-64.89%	-58.00%	-48.00%	-33.33%	-16.89%	4.44%		-7.56%	4.89%	-4.22%	4.62%
				Ave DI (Group)								4.61%					
				Max DI (Group)								5.36%					
20	51 Lane	Julia Creek		Max Dynamic Strain(με)	16.40	15.80	17.50	20.00	23.90	33.00	38.00	47.10		42.80	47.50	46.50	51.40
			11	Static Strain (με) (max per unit)	11.60	11.60	13.00	15.70	19.70	28.50	33.80	45.00		39.60	44.80	41.60	45.50
				Static Strain (με) (max total Span 1)	45.50	45.50	45.50	45.50	45.50	45.50	45.50	45.50		45.50	45.50	45.50	45.50
				Static Strain (με) (max unit type)	45.50	45.00	45.00	45.00	45.00	45.00	45.00	45.00		45.00	45.00	45.00	45.50
				DI (max per unit)	41.38%	36.21%	34.62%	27.39%	21.32%	15.79%	12.43%	4.67%		8.08%	6.03%	11.78%	12.97%
				DI (max per Span 1)	-74.51%	-74.51%	-71.43%	-65.49%	-56.70%	-37.36%	-25.71%	-1.10%		-12.97%	-1.54%	-8.57%	0.00%
				DI (max per unit type)	-74.51%	-74.22%	-71.11%	-65.11%	-56.22%	-36.67%	-24.89%	0.00%		-12.00%	-0.44%	-7.56%	0.00%
				Ave DI (Group)								8.70%					
				Max DI (Group)								12.97%					
40	37 Lane	Julia Creek		Max Dynamic Strain(με)	16.80	16.20	17.80	19.50	24.50	32.80	40.30	[illegible]		[illegible]	[illegible]	[illegible]	[illegible]
			11	Static Strain (με) (max per unit)	11.60	11.60	13.00	15.70	19.70	28.50	33.80	45.00		39.60	44.80	41.60	45.50
				Static Strain (με) (max total Span 1)	45.50	45.50	45.50	45.50	45.50	45.50	45.50	45.50		45.50	45.50	45.50	45.50
				Static Strain (με) (max unit type)	45.50	45.00	45.00	45.00	45.00	45.00	45.00	45.00		45.00	45.00	45.00	45.50
				DI (max per unit)	44.83%	39.66%	36.92%	24.20%	24.37%	15.09%	19.23%	-0.44%		11.87%	-1.34%	-3.33%	-1.10%
				DI (max per Span 1)	-63.08%	-64.40%	-60.88%	-57.14%	-46.15%	-27.91%	-11.43%	-1.54%		-2.64%	-2.88%	-11.43%	-1.10%
				DI (max per unit type)	-63.08%	-64.00%	-60.44%	-56.67%	-45.56%	-27.11%	-10.44%	-0.44%		-1.56%	-1.78%	-10.44%	-1.10%
				Ave DI (Group)								1.17%					
				Max DI (Group)								11.87%					
60	45 Lane	Julia Creek		Max Dynamic Strain(με)	17.80	17.00	18.30	20.50	25.40	33.80	38.30	42.00		40.10	38.50	39.90	[illegible]
			11	Static Strain (με) (max per unit)	11.60	11.60	13.00	15.70	19.70	28.50	33.80	45.00		39.60	44.80	41.60	45.50
				Static Strain (με) (max total Span 1)	45.50	45.50	45.50	45.50	45.50	45.50	45.50	45.50		45.50	45.50	45.50	45.50
				Static Strain (με) (max unit type)	45.50	45.00	45.00	45.00	45.00	45.00	45.00	45.00		45.00	45.00	45.00	45.50
				DI (max per unit)	53.45%	46.55%	40.77%	30.57%	28.93%	18.60%	13.31%	-6.67%		1.26%	-14.06%	-4.09%	-3.52%
				DI (max per Span 1)	-60.88%	-62.64%	-59.78%	-54.95%	-44.18%	-25.71%	-15.82%	-7.69%		-11.87%	-15.38%	-12.31%	-3.52%
				DI (max per unit type)	-60.88%	-62.22%	-59.33%	-54.44%	-43.56%	-24.89%	-14.89%	-6.67%		-10.89%	-14.44%	-11.33%	-3.52%
				Ave DI (Group)								-5.41%					
				Max DI (Group)								1.26%					
80	49 Lane	Julia Creek		Max Dynamic Strain(με)	24.40	22.70	24.40	27.00	33.40	44.60	51.90	51.90		50.10	44.90	43.80	49.70
			11	Static Strain (με) (max per unit)	11.60	11.60	13.00	15.70	19.70	28.50	33.80	45.00	0.00	39.60	44.80	41.60	45.50
				Static Strain (με) (max total Span 1)	45.50	45.50	45.50	45.50	45.50	45.50	45.50	45.50		45.50	45.50	45.50	45.50
				Static Strain (με) (max unit type)	45.50	45.00	45.00	45.00	45.00	45.00	45.00	45.00		45.00	45.00	45.00	45.50
				DI (max per unit)	110.34%	95.69%	87.69%	71.97%	69.54%	56.49%	53.55%	15.33%		26.52%	0.22%	5.29%	9.23%
				DI (max per Span 1)	-46.37%	-50.11%	-46.37%	-40.66%	-26.59%	-1.98%	14.07%	14.07%		10.11%	-1.32%	-3.74%	9.23%
				DI (max per unit type)	-46.37%	-49.56%	-45.78%	-40.00%	-25.78%	-0.89%	15.33%	15.33%		11.33%	-0.22%	-2.67%	9.23%
				Ave DI (Group)								11.32%					
				Max DI (Group)								26.52%					
100	53 Lane	Julia Creek		Max Dynamic Strain(με)	30.60	29.10	28.80	30.70	35.50	47.30	45.40	46.20		38.10	36.10	36.70	39.70
			11	Static Strain (με) (max per unit)	11.60	11.60	13.00	15.70	19.70	28.50	33.80	45.00	42.30	39.60	44.80	41.60	45.50
				Static Strain (με) (max total Span 1)	45.50	45.50	45.50	45.50	45.50	45.50	45.50	45.50		45.50	45.50	45.50	45.50
				Static Strain (με) (max unit type)	45.50	45.00	45.00	45.00	45.00	45.00	45.00	45.00		45.00	45.00	45.00	45.50
				DI (max per unit)	163.79%	150.86%	121.54%	95.54%	80.20%	65.96%	34.32%	2.67%		-3.79%	-19.42%	-11.78%	-12.75%
				DI (max per Span 1)	-32.75%	-36.04%	-36.70%	-32.53%	-21.98%	3.96%	-0.22%	1.54%		-16.26%	-20.66%	-19.34%	-12.75%
				DI (max per unit type)	-32.75%	-35.33%	-36.00%	-31.78%	-21.11%	5.11%	0.89%	2.67%		-15.33%	-19.78%	-18.44%	-12.75%
				Ave DI (Group)								-9.01%					
				Max DI (Group)								2.67%					

Table B 5: Dawson River Bridge DI Summary – Semi-trailer 2 (ST2)

						Lane (To Cloncurry)					Centre				Lane (To Julia Creek)		
											Strain gauges						
Speed(km/h)	Run #	Position	Direction to	Run #	sg1	sg2	sg3	sg4	sg5	sg6	sg7	sg8	sg9	sg10	sg11	sg12	sg13
10	23	Lane	Cloncurry	Run #	sg1	sg2	sg3	sg4	sg5	sg6	sg7	sg8	sg9	sg10	sg11	sg12	sg13
				Max Dynamic Strain(µε)	58.20	53.60	55.30	46.10	46.20	50.10	38.90	32.40		19.70	18.40	16.30	17.50
Input static data				9 Static Strain (µε) (max per unit)	57.90	54.10	56.50	47.00	45.90	51.20	39.00	32.10		19.90	17.90	15.50	16.30
				Static Strain (µε) (max total Span 1)	57.90	57.90	57.90	57.90	57.90	57.90	57.90	57.90		57.90	57.90	57.90	57.90
				Static Strain (µε) (max unit type)	57.90	56.50	56.50	56.50	56.50	56.50	56.50	56.50		56.50	56.50	56.50	57.90
				DI (max per unit)	0.52%	-0.92%	-2.12%	-1.91%	0.65%	-2.15%	-0.26%	0.93%		-1.01%	2.79%	5.16%	7.36%
				DI (max per Span 1)	0.52%	-7.43%	-4.49%	-20.38%	-20.21%	-13.47%	-32.82%	-44.04%		-65.98%	-68.22%	-71.85%	-69.78%
				DI (max per unit type)	0.52%	-5.13%	-2.12%	-18.41%	-18.23%	-11.33%	-31.15%	-42.65%		-65.13%	-67.43%	-71.15%	-69.78%
				Ave DI (Group)	-0.99%												
				Max DI (Group)	0.65%												
20	54	Lane	Cloncurry	Max Dynamic Strain(µε)	59.40	55.60	56.70	48.20	48.00	52.20	39.60	31.90	0.00	19.70	17.40	16.50	17.10
	can be 29			9 Static Strain (µε) (max per unit)	57.90	54.10	56.50	47.00	45.90	51.20	39.00	32.10		19.90	17.90	15.50	16.30
				Static Strain (µε) (max total Span 1)	57.90	57.90	57.90	57.90	57.90	57.90	57.90	57.90		57.90	57.90	57.90	57.90
				Static Strain (µε) (max unit type)	57.90	56.50	56.50	56.50	56.50	56.50	56.50	56.50		56.50	56.50	56.50	57.90
				DI (max per unit)	2.59%	2.77%	0.35%	2.55%	4.58%	1.95%	1.54%	-0.62%		-1.01%	-2.79%	6.45%	4.91%
				DI (max per Span 1)	2.59%	3.97%	-2.07%	-16.75%	-17.10%	-9.84%	-31.61%	-44.91%		-65.98%	-69.95%	-71.50%	-70.47%
				DI (max per unit type)	2.59%	-1.59%	0.35%	-14.69%	-15.04%	-7.61%	-29.91%	-43.54%		-65.13%	-69.20%	-70.80%	-70.47%
				Ave DI (Group)	2.47%												
				Max DI (Group)	4.58%												
40	70	Lane	Cloncurry	Max Dynamic Strain(µε)	61.00	56.10	55.70	49.00	48.90	50.80	41.50	35.20	0.00	22.70	21.10	19.60	20.70
	can be 35			9 Static Strain (µε) (max per unit)	57.90	54.10	56.50	47.00	45.90	51.20	39.00	32.10		19.90	17.90	15.50	16.30
				Static Strain (µε) (max total Span 1)	57.90	57.90	57.90	57.90	57.90	57.90	57.90	57.90		57.90	57.90	57.90	57.90
				Static Strain (µε) (max unit type)	57.90	56.50	56.50	56.50	56.50	56.50	56.50	56.50		56.50	56.50	56.50	57.90
				DI (max per unit)	5.35%	3.70%	-1.42%	4.26%	6.54%	-0.78%	6.41%	9.66%		14.07%	17.88%	26.45%	26.99%
				DI (max per Span 1)	5.35%	-3.11%	-3.80%	-15.37%	-15.54%	-12.26%	-28.32%	-39.21%		-60.79%	-63.56%	-66.15%	-64.25%
				DI (max per unit type)	5.35%	-0.71%	-1.42%	-13.27%	-13.45%	-10.09%	-26.55%	-37.70%		-59.82%	-62.65%	-65.31%	-64.25%
				Ave DI (Group)	2.94%												
				Max DI (Group)	6.54%												
60	41	Lane	Cloncurry	Max Dynamic Strain(µε)	62.10	55.70	54.20	49.20	49.10	51.30	43.70	38.80		26.50	24.80	24.00	26.30
				9 Static Strain (µε) (max per unit)	57.90	54.10	56.50	47.00	45.90	51.20	39.00	32.10		19.90	17.90	15.50	16.30
				Static Strain (µε) (max total Span 1)	57.90	57.90	57.90	57.90	57.90	57.90	57.90	57.90		57.90	57.90	57.90	57.90
				Static Strain (µε) (max unit type)	57.90	56.50	56.50	56.50	56.50	56.50	56.50	56.50		56.50	56.50	56.50	57.90
				DI (max per unit)	7.25%	2.96%	-4.07%	4.68%	6.97%	0.20%	12.05%	20.87%		33.17%	38.55%	54.84%	61.35%
				DI (max per Span 1)	7.25%	-3.80%	-6.39%	-15.03%	-15.20%	-11.40%	-24.53%	-32.99%		-54.23%	-57.17%	-58.55%	-54.58%
				DI (max per unit type)	7.25%	-1.42%	-4.07%	-12.92%	-13.10%	-9.20%	-22.65%	-31.33%		-53.10%	-56.11%	-57.52%	-54.58%
				Ave DI (Group)	3.00%												
				Max DI (Group)	7.25%												
80	47	Lane	Cloncurry	Max Dynamic Strain(µε)	69.60	62.30	59.20	56.70	60.70	62.50	57.80	53.90		40.50	40.30	41.10	45.90
				9 Static Strain (µε) (max per unit)	57.90	54.10	56.50	47.00	45.90	51.20	39.00	32.10		19.90	17.90	15.50	16.30
				Static Strain (µε) (max total Span 1)	57.90	57.90	57.90	57.90	57.90	57.90	57.90	57.90		57.90	57.90	57.90	57.90
				Static Strain (µε) (max unit type)	57.90	56.50	56.50	56.50	56.50	56.50	56.50	56.50		56.50	56.50	56.50	57.90
				DI (max per unit)	20.21%	15.16%	4.78%	20.64%	32.24%	22.07%	48.21%	67.91%		103.52%	125.14%	165.16%	181.60%
				DI (max per Span 1)	20.21%	7.60%	2.25%	-2.07%	4.84%	7.94%	-0.17%	-6.91%		-30.05%	-30.40%	-29.02%	-20.73%
				DI (max per unit type)	20.21%	10.27%	4.78%	0.35%	7.43%	10.62%	2.30%	-4.60%		-28.32%	-28.67%	-27.26%	-20.73%
				Ave DI (Group)	19.18%												
				Max DI (Group)	32.24%												
100	34	Lane	Cloncurry	Max Dynamic Strain(µε)	74.80	67.80	64.10	59.10	62.80	64.40	59.60	56.30	0.00	41.90	41.60	41.40	46.20
				9 Static Strain (µε) (max per unit)	57.90	54.10	56.50	47.00	45.90	51.20	39.00	32.10		19.90	17.90	15.50	16.30
				Static Strain (µε) (max total Span 1)	57.90	57.90	57.90	57.90	57.90	57.90	57.90	57.90		57.90	57.90	57.90	57.90
				Static Strain (µε) (max unit type)	57.90	56.50	56.50	56.50	56.50	56.50	56.50	56.50		56.50	56.50	56.50	57.90
				DI (max per unit)	29.19%	25.32%	13.45%	25.74%	36.82%	25.78%	52.82%	75.39%		110.55%	132.40%	167.10%	183.44%
				DI (max per Span 1)	29.19%	17.10%	10.71%	2.07%	8.46%	11.23%	2.94%	-2.76%		-27.63%	-28.15%	-28.50%	-20.21%
				DI (max per unit type)	29.19%	20.00%	13.45%	4.60%	11.15%	13.98%	5.49%	-0.35%		-25.84%	-26.37%	-26.73%	-20.21%
				Ave DI (Group)	26.05%												
				Max DI (Group)	36.82%												

								Lane (To Cloncurry)			Centre				Lane (To Julia Creek)		
											Strain gauges						
Speed(km/h)	Run #	Position	Direction to	Run #		sg1	sg2	sg3	sg4	sg5	sg6	sg7	sg8	sg9	sg10	sg11	sg12	sg13
30	26	Lane	Julia Creek		Max Dynamic Strain(με)	16.90	16.80	18.90	21.70	26.90	35.60	40.80	54.00		49.50	56.50	56.70	62.50
Input static data				12	Static Strain (με) (max per unit)	17.70	17.70	19.30	22.70	27.80	37.10	42.70	55.80		51.60	58.10	57.50	62.40
					Static Strain (με) (max total Span 1)	62.40	62.40	62.40	62.40	62.40	62.40	62.40	62.40		62.40	62.40	62.40	62.40
					Static Strain (με) (max unit type)	62.40	58.10	58.10	58.10	58.10	58.10	58.10	58.10		58.10	58.10	58.10	62.40
					DI (max per unit)	-4.52%	-5.08%	-2.07%	-4.41%	-3.24%	-4.04%	-4.45%	-3.23%		-4.07%	-2.75%	-1.04%	0.16%
					DI (max per Span 1)	-72.92%	-73.08%	-69.71%	-65.22%	-56.89%	-42.95%	-34.62%	-13.46%		-20.67%	-9.46%	-8.81%	0.16%
					DI (max per unit type)	-72.92%	-71.08%	-67.47%	-62.65%	-53.70%	-38.73%	-29.78%	-7.06%		-14.40%	2.75%	-2.07%	0.16%
					Ave DI (Group)								-2.19%					
					Max DI (Group)								0.16%					
20	61	Lane	Julia Creek		Max Dynamic Strain(με)	19.20	18.80	20.30	23.20	28.90	37.70	44.70	57.10	0.00	[illegible]	56.50	[illegible]	61.80
	can be 32			12	Static Strain (με) (max per unit)	17.70	17.70	19.30	22.70	27.80	37.10	42.70	55.80		51.60	58.10	57.50	62.40
					Static Strain (με) (max total Span 1)	62.40	62.40	62.40	62.40	62.40	62.40	62.40	62.40		62.40	62.40	62.40	62.40
					Static Strain (με) (max unit type)	62.40	58.10	58.10	58.10	58.10	58.10	58.10	58.10		58.10	58.10	58.10	62.40
					DI (max per unit)	8.47%	6.21%	5.18%	2.20%	3.96%	1.62%	4.68%	2.33%		-1.16%	-2.75%	-2.96%	-0.96%
					DI (max per Span 1)	-69.23%	-69.87%	-67.47%	-62.82%	-53.69%	-39.58%	-28.37%	-8.49%		-18.27%	-9.46%	-10.58%	-0.96%
					DI (max per unit type)	-69.23%	-67.64%	-65.06%	-60.07%	-50.26%	-35.11%	-23.06%	-1.72%		-12.22%	-2.75%	-3.96%	-0.96%
					Ave DI (Group)								-1.10%					
					Max DI (Group)								2.33%					
40	67	Lane	Julia Creek	12	Max Dynamic Strain(με)	21.00	19.70	21.30	24.20	30.00	38.90	45.70	58.20	0.00	52.00	57.90	55.50	62.00
	can be 38				Static Strain (με) (max per unit)	17.70	17.70	19.30	22.70	27.80	37.10	42.70	55.80		51.60	58.10	57.50	62.40
					Static Strain (με) (max total Span 1)	62.40	62.40	62.40	62.40	62.40	62.40	62.40	62.40		62.40	62.40	62.40	62.40
					Static Strain (με) (max unit type)	62.40	58.10	58.10	58.10	58.10	58.10	58.10	58.10		58.10	58.10	58.10	62.40
					DI (max per unit)	18.64%	11.30%	10.36%	6.61%	7.91%	4.85%	7.03%	4.30%		0.78%	-0.34%	-3.48%	-0.64%
					DI (max per Span 1)	-66.35%	-68.43%	-65.87%	-61.22%	-51.92%	-37.66%	-26.76%	-6.73%		-16.67%	-7.21%	-11.06%	-0.64%
					DI (max per unit type)	-66.35%	-66.09%	-63.34%	-58.35%	-48.36%	-33.05%	-21.34%	0.17%		-10.50%	-0.34%	-4.48%	-0.64%
					Ave DI (Group)								0.12%					
					Max DI (Group)								4.30%					
60	44	Lane	Julia Creek	12	Max Dynamic Strain(με)	21.40	20.10	22.20	25.10	30.80	40.70	47.20	57.20		[illegible]	[illegible]	[illegible]	[illegible]
					Static Strain (με) (max per unit)	17.70	17.70	19.30	22.70	27.80	37.10	42.70	55.80		51.60	58.10	57.50	62.40
					Static Strain (με) (max total Span 1)	62.40	62.40	62.40	62.40	62.40	62.40	62.40	62.40		62.40	62.40	62.40	62.40
					Static Strain (με) (max unit type)	62.40	58.10	58.10	58.10	58.10	58.10	58.10	58.10		58.10	58.10	58.10	62.40
					DI (max per unit)	20.90%	13.56%	15.03%	10.57%	10.79%	9.70%	10.54%	2.51%		0.97%	-3.96%	-3.65%	-1.76%
					DI (max per Span 1)	-65.71%	-67.79%	-64.42%	-59.78%	-50.64%	-34.78%	-24.36%	-8.33%		-16.51%	-10.58%	-11.22%	-1.76%
					DI (max per unit type)	-65.71%	-65.40%	-61.79%	-56.80%	-46.99%	-29.95%	-18.76%	-1.55%		-10.33%	-3.96%	-4.65%	-1.76%
					Ave DI (Group)								-1.18%					
					Max DI (Group)								2.51%					
80	50	Lane	Julia Creek	12	Max Dynamic Strain(με)	28.10	27.10	28.40	30.30	36.60	47.20	53.70	59.70		[illegible]	[illegible]	[illegible]	[illegible]
					Static Strain (με) (max per unit)	17.70	17.70	19.30	22.70	27.80	37.10	42.70	55.80		51.60	58.10	57.50	62.40
					Static Strain (με) (max total Span 1)	62.40	62.40	62.40	62.40	62.40	62.40	62.40	62.40		62.40	62.40	62.40	62.40
					Static Strain (με) (max unit type)	62.40	58.10	58.10	58.10	58.10	58.10	58.10	58.10		58.10	58.10	58.10	62.40
					DI (max per unit)	58.76%	53.11%	47.15%	33.48%	31.65%	27.22%	25.76%	6.99%		8.14%	-4.99%	-4.35%	-1.28%
					DI (max per Span 1)	-54.97%	-56.57%	-54.49%	-51.44%	-41.35%	-24.36%	-13.94%	-4.33%		-10.58%	-11.54%	-11.86%	-1.28%
					DI (max per unit type)	-54.97%	-53.36%	-51.12%	-47.85%	-37.01%	-18.76%	-7.57%	2.75%		-3.96%	-4.99%	-5.34%	-1.28%
					Ave DI (Group)								0.90%					
					Max DI (Group)								8.14%					
100	52	Lane	Julia Creek	12	Max Dynamic Strain(με)	23.90	22.90	23.70	25.80	31.50	40.20	46.70	[illegible]	0.00	[illegible]	[illegible]	[illegible]	[illegible]
					Static Strain (με) (max per unit)	17.70	17.70	19.30	22.70	27.80	37.10	42.70	55.80		51.60	58.10	57.50	62.40
					Static Strain (με) (max total Span 1)	62.40	62.40	62.40	62.40	62.40	62.40	62.40	62.40		62.40	62.40	62.40	62.40
					Static Strain (με) (max unit type)	62.40	58.10	58.10	58.10	58.10	58.10	58.10	58.10		58.10	58.10	58.10	62.40
					DI (max per unit)	35.03%	29.38%	22.80%	13.66%	13.31%	8.36%	9.37%	0.18%		-1.55%	-4.13%	-5.57%	-2.40%
					DI (max per Span 1)	-61.70%	-63.30%	-62.02%	-58.65%	-49.52%	-35.58%	-25.16%	-10.42%		-18.59%	-10.74%	-12.98%	-2.40%
					DI (max per unit type)	-61.70%	-60.59%	-59.21%	-55.59%	-45.78%	-30.81%	-19.62%	-3.79%		-12.56%	-4.13%	-6.54%	-2.40%
					Ave DI (Group)								-2.69%					
					Max DI (Group)								0.18%					

Table B 6: Dawson River Bridge DI Summary – Roadtrain 1(RT1)

						Lane (To Cloncurry)						Centre			Lane (To Julia Creek)			
Speed(km/h)	Run #	Position	Direction to									Strain gauges						
Speed(km/h)	Run #	Position	Direction to	Run #		sg1	sg2	sg3	sg4	sg5	sg6	sg7	sg8	sg9	sg10	sg11	sg12	sg13
10	79	Lane	Cloncurry	Run #	Max Dynamic Strain(με)	57.30	54.70	55.50	45.80	44.40	44.30	32.70	26.60	0.00	14.80	12.60	11.20	10.70
Input static data				77	Static Strain (με) (max per unit)	55.60	52.60	54.10	44.10	43.50	46.00	33.30	26.40	20.90	15.40	13.20	11.80	11.50
					Static Strain (με) (max total Span 1)	55.60	55.60	55.60	55.60	55.60	55.60	55.60	55.60		55.60	55.60	55.60	55.60
					Static Strain (με) (max unit type)	55.60	54.10	54.10	54.10	54.10	54.10	54.10	54.10		54.10	54.10	54.10	55.60
					DI (max per unit)	3.06%	3.99%	2.59%	3.85%	2.07%	-3.70%	-1.80%	0.76%		-3.90%	-4.55%	-5.08%	-6.96%
					DI (max per Span 1)	3.06%	-1.62%	-0.18%	-17.63%	-20.14%	-20.32%	-41.19%	-52.16%		-73.38%	-77.34%	-79.86%	-80.76%
					DI (max per unit type)	3.06%	1.11%	2.59%	-15.34%	-17.93%	-18.11%	-39.56%	-50.83%		-72.64%	-76.71%	-79.30%	-80.76%
					Ave DI (Group)	3.11%												
					Max DI (Group)	3.99%												
20	81	Lane	Cloncurry		Max Dynamic Strain(με)	66.60	59.80	57.70	52.50	50.40	47.90	38.70	31.10	0.00	18.50	15.80	14.00	13.90
				77	Static Strain (με) (max per unit)	55.60	52.60	54.10	44.10	43.50	46.00	33.30	26.40		15.40	13.20	11.80	11.50
					Static Strain (με) (max total Span 1)	55.60	55.60	55.60	55.60	55.60	55.60	55.60	55.60		55.60	55.60	55.60	55.60
					Static Strain (με) (max unit type)	55.60	54.10	54.10	54.10	54.10	54.10	54.10	54.10		54.10	54.10	54.10	55.60
					DI (max per unit)	19.78%	13.69%	6.65%	19.05%	15.86%	4.13%	16.22%	17.80%		20.13%	19.70%	18.64%	20.87%
					DI (max per Span 1)	19.78%	7.55%	3.78%	-5.58%	-9.35%	-13.85%	-30.40%	-44.06%		-66.73%	-71.58%	-74.82%	-75.00%
					DI (max per unit type)	19.78%	10.54%	6.65%	-2.96%	-6.84%	-11.46%	-28.47%	-42.51%		-65.80%	-70.79%	-74.12%	-75.00%
					Ave DI (Group)	15.01%												
					Max DI (Group)	19.78%												
40	83	Lane	Cloncurry		Max Dynamic Strain(με)	65.10	60.70	61.10	54.80	53.40	52.80	44.80	36.50	0.00	22.10	19.80	17.70	17.90
				77	Static Strain (με) (max per unit)	55.60	52.60	54.10	44.10	43.50	46.00	33.30	26.40		15.40	13.20	11.80	11.50
					Static Strain (με) (max total Span 1)	55.60	55.60	55.60	55.60	55.60	55.60	55.60	55.60		55.60	55.60	55.60	55.60
					Static Strain (με) (max unit type)	55.60	54.10	54.10	54.10	54.10	54.10	54.10	54.10		54.10	54.10	54.10	55.60
					DI (max per unit)	17.09%	15.40%	12.94%	24.26%	22.76%	14.78%	34.53%	38.26%		43.51%	50.00%	50.00%	55.65%
					DI (max per Span 1)	17.09%	9.17%	9.89%	-1.44%	-3.96%	-5.04%	-19.42%	-34.35%		-60.25%	-64.39%	-68.17%	-67.81%
					DI (max per unit type)	17.09%	12.20%	12.94%	1.29%	-1.29%	-2.40%	-17.19%	-32.53%		-59.15%	-63.40%	-67.28%	-67.81%
					Ave DI (Group)	18.49%												
					Max DI (Group)	24.26%												
60	85	Lane	Cloncurry		Max Dynamic Strain(με)	59.70	54.90	55.70	48.00	45.70	45.50	38.80	32.70	0.00	19.20	17.20	16.20	16.30
				77	Static Strain (με) (max per unit)	55.60	52.60	54.10	44.10	43.50	46.00	33.30	26.40		15.40	13.20	11.80	11.50
					Static Strain (με) (max total Span 1)	55.60	55.60	55.60	55.60	55.60	55.60	55.60	55.60		55.60	55.60	55.60	55.60
					Static Strain (με) (max unit type)	55.60	54.10	54.10	54.10	54.10	54.10	54.10	54.10		54.10	54.10	54.10	55.60
					DI (max per unit)	7.37%	4.37%	2.96%	8.84%	5.06%	-1.09%	16.52%	23.86%		24.68%	30.30%	37.29%	41.74%
					DI (max per Span 1)	7.37%	-1.26%	0.18%	-13.67%	-17.81%	-18.17%	-30.22%	-41.19%		-65.47%	-69.06%	-70.86%	-70.68%
					DI (max per unit type)	7.37%	1.48%	2.96%	-11.28%	-15.53%	-15.90%	-28.28%	-39.56%		-64.51%	-68.21%	-70.06%	-70.68%
					Ave DI (Group)	5.72%												
					Max DI (Group)	8.84%												
80	87	Lane	Cloncurry		Max Dynamic Strain(με)	49.10	43.70	38.70	34.20	34.30	36.50	33.00	30.50	0.00	23.50	22.90	22.90	24.60
				77	Static Strain (με) (max per unit)	55.60	52.60	54.10	44.10	43.50	46.00	33.30	26.40		15.40	13.20	11.80	11.50
					Static Strain (με) (max total Span 1)	55.60	55.60	55.60	55.60	55.60	55.60	55.60	55.60		55.60	55.60	55.60	55.60
					Static Strain (με) (max unit type)	55.60	54.10	54.10	54.10	54.10	54.10	54.10	54.10		54.10	54.10	54.10	55.60
					DI (max per unit)	-11.69%	-16.92%	-28.47%	-22.45%	-21.15%	-20.65%	-0.90%	15.53%		52.60%	73.48%	94.07%	113.91%
					DI (max per Span 1)	-11.69%	-21.40%	-30.40%	-38.49%	-38.31%	-34.35%	-40.65%	-45.14%		-57.73%	-58.81%	-58.81%	-55.76%
					DI (max per unit type)	-11.69%	-19.22%	-28.47%	-36.78%	-36.60%	-32.53%	-39.00%	-43.62%		-56.56%	-57.67%	-57.67%	-55.76%
					Ave DI (Group)	-20.14%												
					Max DI (Group)	-11.69%												
88	89	Lane	Cloncurry		Max Dynamic Strain(με)	45.40	41.20	40.90	39.10	43.10	45.50	40.80	37.00	0.00	26.40	25.00	24.70	27.50
				77	Static Strain (με) (max per unit)	55.60	52.60	54.10	44.10	43.50	46.00	33.30	26.40		15.40	13.20	11.80	11.50
					Static Strain (με) (max total Span 1)	55.60	55.60	55.60	55.60	55.60	55.60	55.60	55.60		55.60	55.60	55.60	55.60
					Static Strain (με) (max unit type)	55.60	54.10	54.10	54.10	54.10	54.10	54.10	54.10		54.10	54.10	54.10	55.60
					DI (max per unit)	-18.35%	-21.67%	-24.38%	-11.34%	-0.92%	-1.09%	22.52%	40.15%		71.43%	89.39%	109.32%	139.13%
					DI (max per Span 1)	-18.35%	-25.90%	-26.62%	-29.68%	-22.48%	-18.17%	-26.62%	-33.45%		-52.52%	-55.04%	-55.58%	-50.54%
					DI (max per unit type)	-18.35%	-23.84%	-24.38%	-27.73%	-20.33%	-15.90%	-24.58%	-31.61%		-51.20%	-53.79%	-54.34%	-50.54%
					Ave DI (Group)	-15.37%												
					Max DI (Group)	-0.92%												

								Lane (To Cloncurry)				Centre				Lane (To Julia Creek)		
Speed(km/h)	Run #	Position	Direction to									Strain gauges						
Speed(km/h)	Run #	Position	Direction to	Run #		sg1	sg2	sg3	sg4	sg5	sg6	sg7	sg8	sg9	sg10	sg11	sg12	sg13
10	80	Lane	Julia Creek		Max Dynamic Strain(με)	12.80	13.00	14.30	16.80	21.90	30.20	34.90	45.40	0.00	43.00	50.00	50.00	54.30
Input static data				78	Static Strain (με) (max per unit)	11.40	11.20	12.70	14.90	19.40	26.80	31.50	41.10	41.20	41.30	47.20	46.60	49.50
					Static Strain (με) (max total Span 1)	49.50	49.50	49.50	49.50	49.50	49.50	49.50	49.50		49.50	49.50	49.50	49.50
					Static Strain (με) (max unit type)	49.50	47.20	47.20	47.20	47.20	47.20	47.20	47.20		47.20	47.20	47.20	49.50
					DI (max per unit)	12.28%	16.07%	12.60%	12.75%	12.89%	12.69%	10.79%	10.46%		6.20%	5.93%	7.30%	9.70%
					DI (max per Span 1)	-74.14%	-73.74%	-71.11%	-66.06%	-55.76%	-38.99%	-29.49%	-8.28%		-11.31%	1.01%	1.01%	9.70%
					DI (max per unit type)	-74.14%	-72.46%	-69.70%	-64.41%	-53.60%	-36.02%	-26.06%	-3.81%		-6.99%	5.93%	5.93%	9.70%
					Ave DI (Group)								7.94%					
					Max DI (Group)								10.46%					
20	82	Lane	Julia Creek		Max Dynamic Strain(με)	13.40	13.40	15.30	18.60	22.70	30.20	35.00	41.90	0.00	48.50	47.50	51.70	58.50
				78	Static Strain (με) (max per unit)	11.40	11.20	12.70	14.90	19.40	26.80	31.50	41.10		41.30	47.20	46.60	49.50
					Static Strain (με) (max per unit)	49.50	49.50	49.50	49.50	49.50	49.50	49.50	49.50		49.50	49.50	49.50	49.50
					Static Strain (με) (max total Span 1)	49.50	47.20	47.20	47.20	47.20	47.20	47.20	47.20		47.20	47.20	47.20	49.50
					Static Strain (με) (max unit type)	80.00	74.00	74.00	74.00	74.00	74.00	74.00	74.00		74.00	74.00	74.00	80.00
					DI (max per unit)	17.54%	19.64%	20.47%	24.83%	17.01%	12.69%	11.11%	0.73%		10.17%	0.64%	11.09%	18.18%
					DI (max per Span 1)	-76.97%	-76.27%	-73.09%	-68.43%	-58.90%	-43.22%	-33.26%	-12.92%		-12.50%	0.00%	-1.27%	0.00%
					DI (max per unit type)	-85.75%	-84.86%	-82.84%	-79.86%	-73.78%	-63.78%	-57.43%	-44.46%		-44.19%	-36.22%	-37.03%	-38.13%
					Ave DI (Group)								13.81%					
					Max DI (Group)								18.18%					
40	84	Lane	Julia Creek	78	Max Dynamic Strain(με)	17.00	17.00	18.60	20.60	25.90	34.20	39.70	46.00	0.00	44.00	46.70	45.70	50.50
					Static Strain (με) (max per unit)	11.40	11.20	12.70	14.90	19.40	26.80	31.50	41.10		41.30	47.20	46.60	49.50
					Static Strain (με) (max total Span 1)	49.50	49.50	49.50	49.50	49.50	49.50	49.50	49.50		49.50	49.50	49.50	49.50
					Static Strain (με) (max unit type)	49.50	47.20	47.20	47.20	47.20	47.20	47.20	47.20		47.20	47.20	47.20	49.50
					DI (max per unit)	49.12%	51.79%	46.46%	38.26%	33.51%	27.61%	26.03%	7.06%		5.57%	-5.30%	-1.93%	2.02%
					DI (max per Span 1)	-65.66%	-65.66%	-62.42%	-58.38%	-47.68%	-30.91%	-19.80%	-11.11%		-11.92%	-9.70%	-7.68%	2.02%
					DI (max per unit type)	-65.66%	-63.98%	-60.59%	-56.36%	-45.13%	-27.54%	-15.89%	-6.78%		-7.63%	-5.30%	-3.18%	2.02%
					Ave DI (Group)								1.48%					
					Max DI (Group)								7.06%					
60	86	Lane	Julia Creek	78	Max Dynamic Strain(με)	18.70	17.70	19.50	22.00	26.80	36.00	43.00	45.80	0.00	47.60	46.50	45.60	49.60
					Static Strain (με) (max per unit)	11.40	11.20	12.70	14.90	19.40	26.80	31.50	41.10		41.30	47.20	46.60	49.50
					Static Strain (με) (max total Span 1)	49.50	49.50	49.50	49.50	49.50	49.50	49.50	49.50		49.50	49.50	49.50	49.50
					Static Strain (με) (max unit type)	49.50	47.20	47.20	47.20	47.20	47.20	47.20	47.20		47.20	47.20	47.20	49.50
					DI (max per unit)	64.04%	58.04%	53.54%	47.65%	38.14%	34.33%	36.51%	10.46%		15.74%	-1.48%	-2.15%	0.20%
					DI (max per Span 1)	-62.22%	-64.24%	-60.61%	-55.56%	-45.86%	-27.27%	-13.13%	-8.28%		-3.43%	-6.06%	-7.88%	0.20%
					DI (max per unit type)	-62.22%	-62.50%	-58.69%	-53.39%	-43.22%	-23.73%	-8.90%	-3.81%		1.27%	-1.48%	-3.39%	0.20%
					Ave DI (Group)								4.55%					
					Max DI (Group)								15.74%					
80	88	Lane	Julia Creek	78	Max Dynamic Strain(με)	17.00	16.70	17.80	20.90	26.10	35.30	44.70	50.70	0.00	49.30	48.90	47.50	52.30
					Static Strain (με) (max per unit)	11.40	11.20	12.70	14.90	19.40	26.80	31.50	41.10		41.30	47.20	46.60	49.50
					Static Strain (με) (max total Span 1)	49.50	49.50	49.50	49.50	49.50	49.50	49.50	49.50		49.50	49.50	49.50	49.50
					Static Strain (με) (max unit type)	49.50	47.20	47.20	47.20	47.20	47.20	47.20	47.20		47.20	47.20	47.20	49.50
					DI (max per unit)	49.12%	49.11%	40.16%	40.27%	34.54%	31.72%	41.90%	23.36%		19.11%	3.60%	1.93%	5.66%
					DI (max per Span 1)	-65.66%	-66.26%	-64.04%	-57.78%	-47.27%	-28.69%	-9.70%	2.42%		-0.61%	-1.21%	-4.04%	5.66%
					DI (max per unit type)	-65.66%	-64.62%	-62.29%	-55.72%	-44.70%	-25.21%	-5.30%	7.42%		4.24%	3.60%	0.64%	5.66%
					Ave DI (Group)								10.74%					
					Max DI (Group)								23.36%					
84	90	Lane	Julia Creek	78	Max Dynamic Strain(με)	21.00	20.40	22.30	24.10	31.10	42.60	51.00	48.30	0.00	51.20	42.70	39.60	43.80
					Static Strain (με) (max per unit)	11.40	11.20	12.70	14.90	19.40	26.80	31.50	41.10		41.30	47.20	46.60	49.50
					Static Strain (με) (max total Span 1)	49.50	49.50	49.50	49.50	49.50	49.50	49.50	49.50		49.50	49.50	49.50	49.50
					Static Strain (με) (max unit type)	49.50	47.20	47.20	47.20	47.20	47.20	47.20	47.20		47.20	47.20	47.20	49.50
					DI (max per unit)	91.23%	82.14%	75.59%	61.74%	60.31%	58.96%	68.25%	17.52%		23.97%	-9.53%	-15.02%	-11.31%
					DI (max per Span 1)	-55.96%	-58.79%	-54.95%	-51.31%	-37.17%	-13.94%	7.07%	-2.42%		3.43%	-13.74%	-20.00%	-11.31%
					DI (max per unit type)	-55.96%	-56.78%	-52.75%	-48.94%	-34.11%	-9.75%	12.29%	2.33%		8.47%	-9.53%	-16.10%	-11.31%
					Ave DI (Group)								1.12%					
					Max DI (Group)								23.97%					

B.2.2 DI Graph – Mid-span of Girders

Lane travel

Figure B 4: DI – girder mid-span bending strains (lane travel)

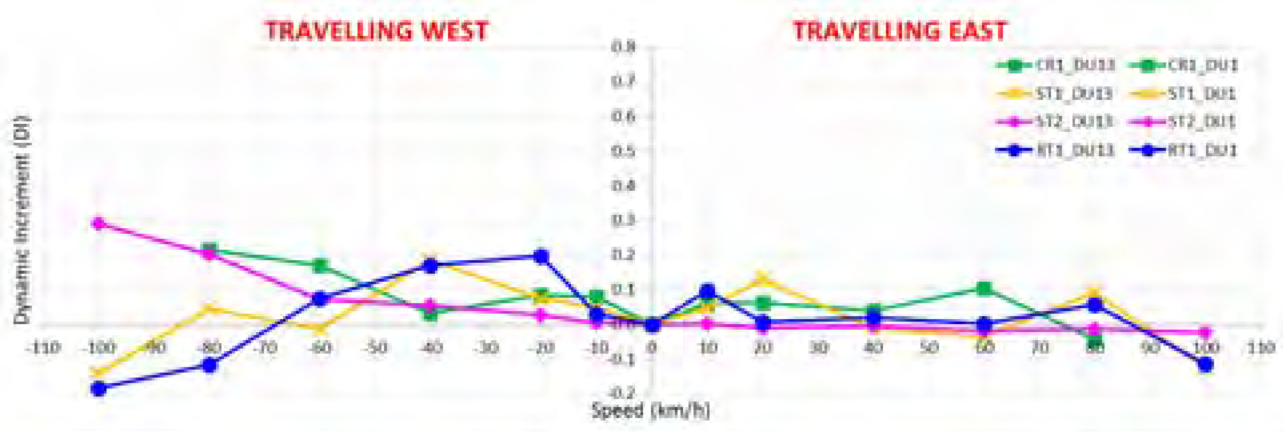

B.3 Dawson River Bridge

B.3.1 Summary of DI Values

Table B 7: Dawson River Bridge DI Summary – Crane 1 (CR1)

			GIRDERS							HEADSTOCK				
		MAX	83.35	74.98	61.71	69.42	69.34	68.82	[illegible]	4.31	8.66	5.17	9.28	9.28
		MAX DI	0.17	0.18	0.18	0.07	0.26	0.60	[illegible]	0.24	0.04	0.08	0.39	0.39
Position	To	Speed	G1	G2	G3	G4	G5	G6	Max	P7HLS7	P7HRS7	P7HLS8	P7HRS8	Max
CL	D	Static	41.92	51.37	57.53	61.95	34.33	22.89	61.95	3.04	4.57	3.29	3.37	4.57
		20	–	–	–	–	–	–	0.00	–	–	–	–	0.00
		DI	–	–	–	–	–	–	0.00	–	–	–	–	0.00
		40	–	–	–	–	–	–	0.00	–	–	–	–	0.00
		DI	–	–	–	–	–	–	0.00	–	–	–	–	0.00
		60	–	–	–	–	–	–	0.00	–	–	–	–	0.00
		DI	–	–	–	–	–	–	0.00	–	–	–	–	0.00
		80	34.68	41.98	59.26	63.99	39.72	31.65	63.99	3.28	4.38	2.92	4.68	4.68
		DI	-0.17	-0.18	0.03	0.00	0.13	0.38	0.033	-0.26	-0.04	-0.11	0.39	0.39
CL	R	Static	36.50	43.21	57.08	64.45	39.18	25.64	64.45	3.81	5.11	3.85	4.48	5.11
		20	–	–	–	–	–	–	0.00	–	–	–	–	0.00
		DI	–	–	–	–	–	–	0.00	–	–	–	–	0.00
		40	–	–	–	–	–	–	0.00	–	–	–	–	0.00
		DI	–	–	–	–	–	–	0.00	–	–	–	–	0.00
		60	–	–	–	–	–	–	0.00	–	–	–	–	0.00
		DI	–	–	–	–	–	–	0.00	–	–	–	–	0.00
		80	–	–	–	–	–	–	0.00	–	–	–	–	0.00
		DI	–	–	–	–	–	–	0.00	–	–	–	–	0.00
Lane	D	Static	74.50	65.92	56.44	40.16	19.76	9.27	74.50	3.47	3.07	4.88	3.69	4.88
		20	75.17	68.76	58.50	40.85	20.11	9.14	75.17	4.31	2.80	4.44	2.34	4.44
		DI	0.01	0.03	0.04	0.02	0.02	-0.01	0.009	0.24	-0.09	-0.09	-0.37	-0.09
		40	83.35	74.98	61.71	42.89	24.86	17.65	83.35	4.08	2.98	5.17	3.52	5.17
		DI	0.12	0.13	0.09	0.07	0.26	0.90	0.119	0.18	-0.03	0.06	-0.05	0.06
		60	78.98	68.61	58.25	38.58	19.41	9.75	78.98	4.18	2.41	4.59	3.78	4.59
		DI	0.06	0.03	0.03	-0.04	-0.02	0.05	0.060	0.20	-0.21	-0.06	0.02	-0.06
		80	74.65	70.19	60.14	39.00	19.06	9.90	74.65	3.70	2.85	4.78	2.96	4.78
		DI	0.00	0.05	0.07	-0.03	-0.03	0.07	0.002	0.07	-0.07	-0.02	-0.20	-0.02
Lane	R	Static	10.42	20.33	54.87	65.20	63.93	58.24	65.20	2.27	8.43	5.12	8.74	8.74
		20	10.16	20.48	57.14	67.72	66.90	61.29	67.72	1.99	5.43	3.04	7.01	7.01
		DI	-0.03	0.01	0.07	0.04	0.05	0.05	0.039	-0.12	-0.16	-0.03	0.04	0.04
		40	13.03	20.76	55.34	67.20	69.34	68.82	69.34	2.19	6.01	2.38	9.28	9.28
		DI	0.25	0.02	0.01	0.03	0.08	0.18	0.062	-0.04	-0.07	-0.14	0.18	0.38
		60	11.49	20.75	56.98	66.93	64.81	61.31	66.93	1.64	6.53	2.87	7.62	7.62
		DI	0.10	0.02	0.06	0.03	0.02	0.05	0.027	-0.28	-0.02	-0.08	0.13	0.13
		80	14.26	23.87	41.04	69.42	68.30	66.10	69.42	1.68	8.66	2.52	7.86	7.86
		DI	0.37	0.18	0.18	0.06	0.07	0.14	0.065	-0.26	0.04	-0.19	0.12	0.17

			COLUMN						GIRDER DEFLECTION			HEADSTOCK DEFLECTION			BEARING COMPRESSION						
			C	T	C	T	T	C													
		MAX	-56.65	30.32	-36.29	25.51	[illegible]	[illegible]	5.34	5.63	5.63	1.26	1.17	1.26	-183.05	-151.12	-179.27	-144.10	-169.19	-168.64	-178.3
		MAX DI	0.59	0.09	1.37	0.19	0.19	0.67	2.45	0.78	0.19	0.19	0.60	0.60	0.04	0.07	0.08	0.05	0.08	0.52	0.06
Position	To	Speed	P7CL		P7CR		Max	Min	SB01	SB06	Max	P7HL	P7HR	Max	SBG1	SBG2	SBG3	SBG4	SBG5	SBG6	Max
CL	D	Static	-12.38	3.22	-2.41	3.17	3.37	-12.38	2.77	1.88	2.77	0.25	0.06	0.25	-83.47	-105.13	-165.48	-125.06	-87.77	-47.21	-165.48
		20	–	–	–	–	0.00	0.00	–	–	0.00	–	–	0.00	–	–	–	–	–	–	0.00
		DI	–	–	–	–	-1.00	-1.00	–	–	0.00	–	–	0.00	–	–	–	–	–	–	
		40	–	–	–	–	0.00	0.00	–	–	0.00	–	–	0.00	–	–	–	–	–	–	0.00
		DI	–	–	–	–	-1.00	-1.00	–	–	0.00	–	–	0.00	–	–	–	–	–	–	
		60	–	–	–	–	0.00	0.00	–	–	0.00	–	–	0.00	–	–	–	–	–	–	0.00
		DI	–	–	–	–	-1.00	-1.00	–	–	0.00	–	–	0.00	–	–	–	–	–	–	
		80	-8.93	2.59	-5.71	2.34	2.59	-8.93	2.17	2.40	2.40	0.05	0.10	0.10	-69.54	-83.93	-157.74	-131.18	-91.20	-64.34	-157.74
		DI	-0.08	-0.20	1.37	-0.28	-0.20	-0.28	-0.22	0.28	0.28	0.60	0.60	0.60	-0.17	-0.27	-0.05	-0.05	0.04	0.38	-0.05
CL	R	Static	-8.85	4.17	-4.25	4.95	4.95	-8.85	2.81	1.24	2.81	0.03	0.05	0.05	-71.25	-93.07	-159.09	-129.79	-94.72	-58.79	-159.09
		20	–	–	–	–	0.00	0.00	–	–	0.00	–	–	0.00	–	–	–	–	–	–	0.00
		DI	–	–	–	–	-1.00	-1.00	–	–	0.00	–	–	0.00	–	–	–	–	–	–	
		40	–	–	–	–	0.00	0.00	–	–	0.00	–	–	0.00	–	–	–	–	–	–	0.00
		DI	–	–	–	–	-1.00	-1.00	–	–	0.00	–	–	0.00	–	–	–	–	–	–	
		60	–	–	–	–	0.00	0.00	–	–	0.00	–	–	0.00	–	–	–	–	–	–	0.00
		DI	–	–	–	–	-1.00	-1.00	–	–	0.00	–	–	0.00	–	–	–	–	–	–	
		80	–	–	–	–	0.00	0.00	–	–	0.00	–	–	0.00	–	–	–	–	–	–	0.00
		DI	–	–	–	–	-1.00	-1.00	–	–	0.00	–	–	0.00	–	–	–	–	–	–	
Lane	D	Static	-52.06	4.46	-2.03	21.24	21.24	-52.06	4.72	0.48	4.72	1.13	0.87	1.13	-150.12	-151.12	-169.04	-90.46	-54.14	-16.17	-169.04
		20	-50.97	3.79	-2.91	21.70	21.70	-50.97	4.87	0.52	4.87	1.19	0.83	1.19	-148.09	-148.32	-178.27	-92.95	-47.88	-13.28	-178.27
		DI	-0.05	-0.15	0.43	0.01	0.01	-0.05	-0.03	0.09	0.03	0.05	-0.03	0.05	-0.01	-0.03	0.05	-0.03	-0.12	-0.17	0.05
		40	-55.53	2.76	-1.58	24.43	24.43	-55.53	5.34	0.85	5.34	1.13	0.78	1.13	-163.03	-169.71	-176.19	-84.84	-52.75	-24.59	-176.19
		DI	0.11	-0.38	-0.23	0.15	0.15	0.11	0.13	0.78	0.13	0.00	-0.11	0.00	0.09	-0.01	0.04	0.05	-0.03	0.52	0.04
		60	-56.65	4.56	-3.82	25.11	25.11	-56.65	4.92	0.41	4.81	1.26	0.95	1.26	-153.00	-141.13	-186.52	-84.01	-45.26	-14.48	-186.52
		DI	0.16	0.02	0.90	0.18	0.18	0.14	0.04	-0.12	0.04	0.11	0.09	0.11	0.01	-0.07	-0.01	-0.08	-0.16	-0.11	-0.01
		80	-52.62	2.60	-2.78	20.94	20.94	-52.62	4.59	0.43	4.59	1.14	0.83	1.14	-142.26	-137.03	-162.28	-83.43	-46.66	-13.37	-162.28
		DI	0.01	-0.42	0.37	-0.01	-0.01	0.01	-0.03	-0.10	-0.03	0.01	-0.05	0.01	-0.05	-0.09	-0.04	-0.08	-0.14	-0.17	-0.04
Lane	R	Static	-1.82	27.92	-21.74	6.84	27.92	-21.74	0.28	5.20	5.20	0.77	1.05	1.05	-15.56	-45.88	-88.69	-137.87	-157.37	-168.42	-168.42
		20	-1.63	26.64	-33.55	1.87	26.64	-33.55	0.40	5.40	5.40	0.83	1.12	1.12	-14.95	-45.25	-89.92	-137.76	-162.11	-161.04	-162.11
		DI	-0.12	-0.05	0.54	-0.73	-0.05	0.54	-0.42	0.04	0.04	0.08	0.05	0.08	-0.04	-0.01	0.01	0.00	0.03	-0.04	0.03
		40	-2.58	30.32	-36.29	2.60	30.32	-36.29	0.97	5.63	5.63	0.91	1.17	1.17	-30.17	-44.94	-88.06	-144.10	-169.19	-168.64	-169.19
		DI	0.59	-0.09	0.67	-0.62	0.09	0.67	2.45	0.08	0.08	0.19	0.11	0.11	0.44	-0.02	-0.01	0.05	0.08	0.00	0.08
		60	-2.10	28.64	-34.49	2.09	28.64	-34.49	0.51	4.96	4.96	0.85	1.17	1.17	-19.39	-45.92	-87.74	-131.52	-146.82	-146.87	-146.87
		DI	0.50	-0.03	0.59	-0.69	0.03	0.59	0.83	-0.09	-0.05	0.11	0.11	0.11	0.25	0.00	-0.01	-0.05	-0.07	-0.13	-0.13
		80	-2.14	26.48	-31.18	2.43	26.48	-31.18	0.60	4.99	4.99	0.72	1.05	1.05	-23.48	-49.15	-95.48	-156.25	-146.80	-141.53	-146.80
		DI	0.51	-0.05	0.43	-0.64	-0.05	0.43	1.14	-0.04	-0.04	-0.06	0.00	0.00	0.51	0.07	0.08	-0.01	-0.01	-0.16	-0.07

Table B 8: Dawson River Bridge DI Summary – Crane 2 (CR2))

			GIRDERS							HEADSTOCK				
		MAX	70.07	69.85	62.65	82.64	78.82	74.89	82.64	3.79	5.47	4.67	8.66	8.66
		MAX DI	0.81	0.84	0.80	0.55	0.59	0.60	0.55	0.14	0.14	0.31	0.88	[illegible]
Position	To	Speed	G1	G2	G3	G4	G5	G6	Max	P7HS17	P7HR57	P7HS58	P7HR58	Max
CL	0	Static	52.98	38.09	45.74	51.05	29.29	21.25	51.00	3.08	3.56	3.76	3.10	3.76
		20	–	–	–	–	–	–	0.00	–	–	–	–	0.00
		DI	–	–	–	–	–	–	0.00	–	–	–	–	0.00
		40	–	–	–	–	–	–	0.00	–	–	–	–	0.00
		DI	–	–	–	–	–	–	0.00	–	–	–	–	0.00
		60	–	–	–	–	–	–	0.00	–	–	–	–	0.00
		DI	–	–	–	–	–	–	0.00	–	–	–	–	0.00
		80	54.59	42.28	48.82	52.48	35.99	28.47	52.48	2.24	3.78	4.33	4.06	4.33
		DI	0.05	0.11	0.07	0.09	0.23	0.34	0.029	-0.27	0.06	0.15	0.31	0.15
CL	9	Static	28.59	32.85	47.25	52.39	33.22	34.10	52.39	2.94	4.31	3.21	3.94	4.31
		20	–	–	–	–	–	–	0.00	–	–	–	–	0.00
		DI	–	–	–	–	–	–	0.00	–	–	–	–	0.00
		40	–	–	–	–	–	–	0.00	–	–	–	–	0.00
		DI	–	–	–	–	–	–	0.00	–	–	–	–	0.00
		60	–	–	–	–	–	–	0.00	–	–	–	–	0.00
		DI	–	–	–	–	–	–	0.00	–	–	–	–	0.00
		80	–	–	–	–	–	–	0.00	–	–	–	–	0.00
		DI	–	–	–	–	–	–	0.00	–	–	–	–	0.00
Lane	0	Static	60.29	52.97	46.88	55.82	18.19	8.82	60.29	3.11	2.80	4.14	2.07	4.14
		20	60.36	54.42	49.60	37.78	19.46	9.58	60.36	3.61	2.25	4.30	2.85	4.30
		DI	0.00	0.03	0.08	0.12	0.07	0.09	0.001	0.09	-0.18	0.04	0.38	0.04
		40	62.47	57.84	52.57	38.08	19.35	11.98	62.47	3.65	2.15	4.67	3.01	4.67
		DI	0.04	0.09	0.12	0.13	0.06	0.36	0.036	0.10	-0.23	0.13	0.46	0.13
		60	70.07	69.85	62.65	46.73	23.89	13.27	70.07	3.57	3.20	4.64	3.25	4.64
		DI	0.16	0.32	0.34	0.39	0.31	0.50	0.162	0.08	0.14	0.12	0.57	0.12
		80	66.87	62.51	50.85	41.85	22.97	13.46	66.87	3.79	2.66	4.18	3.89	4.18
		DI	0.11	0.18	0.08	0.24	0.28	0.51	0.109	0.14	-0.05	0.05	0.88	0.00
Lane	9	Static	10.85	17.90	30.00	53.15	48.40	45.04	53.15	2.61	4.97	2.32	4.92	4.97
		20	15.65	25.58	42.85	72.86	67.55	58.03	72.86	2.06	4.50	2.27	6.81	6.81
		DI	0.44	0.42	0.43	0.37	0.37	0.29	0.371	-0.21	-0.09	-0.02	0.38	0.38
		40	14.29	22.54	35.42	57.11	53.87	50.61	57.11	2.26	3.39	2.42	6.55	6.55
		DI	0.01	0.09	0.58	0.07	0.09	0.13	0.075	-0.13	-0.06	0.04	0.33	0.33
		60	20.73	33.02	54.14	82.64	78.50	74.89	82.64	2.11	5.42	3.05	8.66	8.66
		DI	0.91	0.84	0.80	0.55	0.58	0.66	0.555	-0.19	0.09	0.31	0.76	0.76
		80	17.28	27.49	43.20	64.92	61.75	57.69	64.92	1.95	5.47	2.90	7.25	7.25
		DI	-0.59	0.54	0.41	0.22	0.28	0.28	0.211	-0.15	0.10	0.05	0.47	0.47

			COLUMN						GIRDER DEFLECTION			HEADSTOCK DEFLECTION			BEARING COMPRESSION						
			C	T	C	T	T	C													
		MAX	-35.55	23.75	-29.17	24.20	24.20	-35.55	4.44	6.11	6.11	1.16	0.89	1.16	-138.49	-147.77	-184.52	-171.04	-179.77	-169.55	-184.5
		MAX DI	0.77	0.55	2.94	0.47	0.29	0.55	0.69	1.10	0.55	1.01	0.44	1.01	0.79	0.85	0.85	0.44	0.55	0.64	0.55
Position	To	Speed	P7I3		P7C8		Max	Min	SB01	SB06	Max	P7HS	P7HR	Max	SB01	SB02	SB03	SB04	SB05	SB06	Max
CL	0	Static	-9.04	4.95	-5.03	3.84	4.95	-9.04	2.11	1.79	2.11	0.04	0.02	0.04	-67.92	-84.81	-158.50	-112.35	-79.91	-48.62	-158.50
		20	–	–	–	–	0.00	0.00	–	–	0.00	–	–	0.00	–	–	–	–	–	–	0.00
		DI	–	–	–	–	-1.00	-1.00	–	–	0.00	–	–	0.00	–	–	–	–	–	–	
		40	–	–	–	–	0.00	0.00	–	–	0.00	–	–	0.00	–	–	–	–	–	–	0.00
		DI	–	–	–	–	-1.00	-1.00	–	–	0.00	–	–	0.00	–	–	–	–	–	–	
		60	–	–	–	–	0.00	0.00	–	–	0.00	–	–	0.00	–	–	–	–	–	–	0.00
		DI	–	–	–	–	-1.00	-1.00	–	–	0.00	–	–	0.00	–	–	–	–	–	–	
		80	-8.93	2.59	-5.71	2.04	2.59	-8.93	2.18	2.14	2.18	0.09	0.03	0.09	-68.58	-91.78	-154.36	-128.35	-90.50	-57.38	-154.36
		DI	-0.01	-0.48	0.14	-0.89	-0.48	-0.01	0.03	-0.20	-0.20	1.01	0.46	1.01	0.01	0.06	0.11	0.14	0.13	0.18	0.11
CL	9	Static	-5.58	1.34	-4.31	4.74	4.74	-5.58	1.77	2.15	2.15	0.01	0.07	0.07	-59.18	-77.14	-127.92	-116.43	-89.52	-61.88	-127.92
		20	–	–	–	–	0.00	0.00	–	–	0.00	–	–	0.00	–	–	–	–	–	–	0.00
		DI	–	–	–	–	-1.00	-1.00	–	–	0.00	–	–	0.00	–	–	–	–	–	–	
		40	–	–	–	–	0.00	0.00	–	–	0.00	–	–	0.00	–	–	–	–	–	–	0.00
		DI	–	–	–	–	-1.00	-1.00	–	–	0.00	–	–	0.00	–	–	–	–	–	–	
		60	–	–	–	–	0.00	0.00	–	–	0.00	–	–	0.00	–	–	–	–	–	–	0.00
		DI	–	–	–	–	-1.00	-1.00	–	–	0.00	–	–	0.00	–	–	–	–	–	–	
		80	–	–	–	–	0.00	0.00	–	–	0.00	–	–	0.00	–	–	–	–	–	–	0.00
		DI	–	–	–	–	-1.00	-1.00	–	–	0.00	–	–	0.00	–	–	–	–	–	–	
Lane	0	Static	-27.00	3.90	-1.57	18.75	18.75	-27.00	3.84	0.39	3.84	0.81	0.52	0.81	-125.66	-124.55	-143.55	-77.62	-46.30	-15.32	-143.55
		20	-26.84	4.10	-3.44	18.75	18.75	-26.84	4.08	0.58	4.08	0.85	0.60	0.85	-129.06	-133.84	-161.40	-90.54	-47.85	-14.32	-161.40
		DI	-0.01	0.05	1.81	0.00	0.00	-0.01	0.06	0.47	0.06	0.06	0.16	0.06	0.03	0.08	0.13	0.17	0.03	0.08	0.13
		40	-33.83	5.87	-4.53	24.20	24.20	-33.83	4.13	0.77	4.13	1.08	0.79	1.08	-129.92	-125.40	-148.42	-83.42	-46.36	-21.78	-148.42
		DI	0.25	0.51	2.18	0.29	0.29	0.25	0.08	0.45	0.08	0.14	0.53	0.34	0.03	0.01	0.04	0.07	0.00	0.64	0.04
		60	-35.55	5.35	-4.76	22.97	22.97	-35.55	4.44	0.83	4.44	1.16	0.82	1.16	-136.65	-147.77	-184.52	-102.78	-57.25	-21.80	-184.52
		DI	0.32	0.37	2.47	0.28	0.28	0.32	0.16	1.10	0.16	0.44	0.59	0.44	0.09	0.19	0.29	0.32	0.24	0.64	0.29
		80	-34.09	6.05	-5.40	22.57	22.57	-34.09	4.43	0.77	4.43	1.05	0.77	1.05	-138.49	-141.31	-171.36	-99.20	-57.06	-18.55	-171.36
		DI	0.26	0.55	2.94	0.20	0.20	0.26	0.15	0.95	0.15	0.30	0.49	0.30	0.10	0.14	0.20	0.28	0.23	0.28	0.10
Lane	9	Static	-3.89	19.81	-18.65	5.15	19.81	-18.65	0.57	3.94	3.94	0.58	0.66	0.66	-20.00	-44.70	-81.04	-118.81	-135.09	-131.45	-135.09
		20	-2.86	23.75	-29.17	2.38	23.75	-29.17	0.75	5.32	5.32	0.64	0.89	0.89	-26.78	-58.89	-111.85	-148.21	-159.75	-152.93	-159.75
		DI	-0.28	0.16	0.56	-0.54	0.16	0.56	0.31	0.35	0.35	0.10	0.35	0.35	0.34	0.32	0.38	0.35	0.18	0.17	0.18
		40	-3.93	22.13	-28.15	3.70	22.13	-28.15	0.67	4.44	4.44	0.62	0.85	0.85	-27.84	-48.68	-89.76	-124.07	-134.97	-128.88	-134.97
		DI	0.01	0.13	0.51	-0.28	0.13	0.51	0.17	0.13	0.13	0.73	0.29	0.29	0.39	0.09	0.11	0.04	0.00	-0.02	0.00
		60	-6.90	22.63	-28.47	7.25	22.63	-28.47	0.87	6.11	6.11	0.61	0.89	0.89	-35.73	-73.78	-134.09	-171.04	-179.77	-169.55	-179.77
		DI	0.77	0.13	0.51	0.59	0.15	0.55	0.69	0.55	0.55	0.10	0.35	0.35	0.79	0.85	0.65	0.44	-0.81	0.28	0.55
		80	-6.53	20.54	-27.97	7.55	20.54	-27.97	0.87	4.71	4.71	0.57	0.87	0.87	-32.93	-63.55	-122.28	-157.14	-158.08	-150.62	-158.08
		DI	0.08	0.05	0.48	0.47	0.05	0.48	0.50	0.19	0.19	0.38	0.32	0.32	0.69	0.42	0.51	0.32	1.17	-0.02	0.17

Table B 9: Dawson River Bridge DI Summary – Road Train 1 (RT1)

			GIRDERS							HEADSTOCK					COLUMN						GIRDER DEFLECTION			HEADSTOCK DEFLECTION			BEARING COMPRESSION						
															C	T	C	T	T	C													
		MAX	77.89	66.13	56.22	74.52	75.43	75.53	77.89	4.80	6.70	7.05	11.79	11.79	-50.28	44.94	-81.30	34.29	44.94	-81.30	5.44	6.49	6.49	1.73	1.78	1.78	-158.48	-173.75	-203.24	-197.34	-197.36	-166.81	-203.2
		MAX DI	0.75	0.66	0.61	0.39	0.47	0.70	0.41	-0.05	0.14	0.34	0.85	0.85	1.36	2.57	2.16	0.48	2.04	0.92	1.10	1.11	0.80	0.90	0.21	0.21	0.54	0.40	0.43	0.32	0.19	0.31	0.192
Position	To	Speed	G1	G2	G3	G4	G5	G6	Max	P7HLS7	P7HRS7	P7HLS8	P7HRS8	Max	P7CL		P7CR		Max	Min	SBG1	SBG6	Max	P7HL	P7HR	Max	SBG1	SBG2	SBG3	SBG4	SBG5	SBG6	Max
DL	D	Static	30.37	35.46	47.28	56.05	37.20	28.50	56.05	3.10	4.63	3.70	5.13	5.13	-4.20	4.21	-14.06	3.70	4.21	-14.06	1.96	2.04	2.04	0.04	0.43	0.43	-58.25	-86.44	-158.29	-162.20	-106.57	-43.40	-162.20
		20	-	-	-	-	-	-	0.00	-	-	-	-	0.00	-	-	-	-	0.00	0.00	-	-	0.00	-	-	0.00	-	-	-	-	-	-	0.00
		DI	-	-	-	-	-	-	0.00	-	-	-	-	0.00	-	-	-	-	0.00	0.00	-	-	0.00	-	-	0.00	-	-	-	-	-	-	
		40	-	-	-	-	-	-	0.00	-	-	-	-	0.00	-	-	-	-	0.00	0.00	-	-	0.00	-	-	0.00	-	-	-	-	-	-	0.00
		DI	-	-	-	-	-	-	0.00	-	-	-	-	0.00	-	-	-	-	0.00	0.00	-	-	0.00	-	-	0.00	-	-	-	-	-	-	
		60	-	-	-	-	-	-	0.00	-	-	-	-	0.00	-	-	-	-	0.00	0.00	-	-	0.00	-	-	0.00	-	-	-	-	-	-	0.00
		DI	-	-	-	-	-	-	0.00	-	-	-	-	0.00	-	-	-	-	0.00	0.00	-	-	0.00	-	-	0.00	-	-	-	-	-	-	
		80	35.99	42.53	56.22	63.91	45.09	38.68	63.91	2.50	4.56	3.69	6.08	6.08	-8.89	8.57	-13.94	5.48	8.57	-13.94	2.27	3.09	3.09	0.18	0.31	0.31	-65.86	-94.53	-168.31	-153.96	-116.12	-72.89	-168.31
		DI	0.18	0.20	0.19	0.14	0.21	0.19	0.140	-0.17	-0.01	0.00	0.19	0.18	0.43	1.04	0.04	0.48	1.04	-0.04	0.16	0.12	0.22	3.50	-0.28	-0.28	0.13	0.09	0.06	0.01	0.09	0.16	0.06
		100	-	-	-	-	-	-	0.00	-	-	-	-	0.00	-	-	-	-	0.00	0.00	-	-	0.00	-	-	0.00	-	-	-	-	-	-	0.00
		DI	-	-	-	-	-	-	0.00	-	-	-	-	0.00	-	-	-	-	0.00	0.00	-	-	0.00	-	-	0.00	-	-	-	-	-	-	
DL	F	Static	35.20	37.61	46.87	50.95	32.51	21.77	50.95	4.07	4.57	4.62	4.56	4.56	-15.28	3.44	-4.07	9.52	9.52	-15.28	2.32	2.06	2.32	0.38	0.16	0.38	-66.89	-96.62	-170.70	-128.81	-94.11	-56.26	-170.70
		20	-	-	-	-	-	-	0.00	-	-	-	-	0.00	-	-	-	-	0.00	0.00	-	-	0.00	-	-	0.00	-	-	-	-	-	-	0.00
		DI	-	-	-	-	-	-	0.00	-	-	-	-	0.00	-	-	-	-	0.00	0.00	-	-	0.00	-	-	0.00	-	-	-	-	-	-	
		40	-	-	-	-	-	-	0.00	-	-	-	-	0.00	-	-	-	-	0.00	0.00	-	-	0.00	-	-	0.00	-	-	-	-	-	-	0.00
		DI	-	-	-	-	-	-	0.00	-	-	-	-	0.00	-	-	-	-	0.00	0.00	-	-	0.00	-	-	0.00	-	-	-	-	-	-	
		-	-	-	-	-	-	-	0.00	-	-	-	-	0.00	-	-	-	-	0.00	0.00	-	-	0.00	-	-	0.00	-	-	-	-	-	-	0.00
		DI	-	-	-	-	-	-	0.00	-	-	-	-	0.00	-	-	-	-	0.00	0.00	-	-	0.00	-	-	0.00	-	-	-	-	-	-	
		80	-	-	-	-	-	-	0.00	-	-	-	-	0.00	-	-	-	-	0.00	0.00	-	-	0.00	-	-	0.00	-	-	-	-	-	-	0.00
		DI	-	-	-	-	-	-	0.00	-	-	-	-	0.00	-	-	-	-	0.00	0.00	-	-	0.00	-	-	0.00	-	-	-	-	-	-	
		90	-	-	-	-	-	-	0.00	-	-	-	-	0.00	-	-	-	-	0.00	0.00	-	-	0.00	-	-	0.00	-	-	-	-	-	-	0.00
		DI	-	-	-	-	-	-	0.00	-	-	-	-	0.00	-	-	-	-	0.00	0.00	-	-	0.00	-	-	0.00	-	-	-	-	-	-	
Lane	D	Static	65.98	55.82	45.39	34.70	19.26	10.19	65.98	4.80	3.39	7.05	4.69	7.05	-45.92	2.06	-2.02	30.68	30.68	-45.92	4.64	0.39	4.64	1.46	1.04	1.46	-134.24	-156.97	-183.42	-66.38	-53.11	-17.93	-183.42
		20	73.19	64.82	54.21	41.27	21.01	10.26	73.19	4.15	2.81	5.72	4.00	5.72	-47.59	5.54	-3.97	34.21	34.21	-47.59	5.56	0.46	5.16	1.64	1.21	1.64	-142.62	-166.55	-201.97	-104.77	-55.49	-18.19	-201.97
		DI	0.11	0.16	0.19	0.19	0.09	0.01	0.109	-0.14	-0.17	-0.19	-0.15	-0.19	0.04	1.69	0.97	0.12	0.12	0.04	0.21	0.21	0.11	0.12	0.16	0.12	0.06	0.06	0.10	0.11	0.04	0.01	0.10
		40	77.89	66.13	55.74	42.16	23.98	14.58	77.89	4.35	2.89	5.78	3.56	5.78	-45.56	7.42	-4.33	31.90	31.90	-45.56	5.44	0.74	5.44	1.65	1.21	1.65	-158.48	-173.75	-203.24	-86.55	-50.26	-17.31	-203.24
		DI	0.18	0.18	0.23	0.22	0.24	0.43	0.181	-0.09	-0.15	-0.18	-0.24	-0.18	-0.01	2.87	1.31	0.04	0.04	-0.01	0.17	1.11	0.17	0.13	0.16	0.13	0.18	0.11	0.11	0.30	-0.06	0.03	0.11
		60	70.12	61.63	54.04	41.92	22.74	12.75	70.12	4.10	2.90	6.07	3.49	6.07	-49.24	4.90	-4.60	33.09	33.09	-49.24	5.03	0.54	5.03	1.73	1.28	1.73	-140.30	-165.93	-202.77	-103.09	-55.95	-23.42	-202.77
		DI	0.06	0.10	0.19	0.21	0.18	0.25	0.063	-0.15	-0.14	-0.14	-0.26	-0.14	0.07	1.36	1.28	0.08	0.08	0.07	0.08	0.04	0.08	0.16	0.23	0.18	0.05	0.06	0.11	0.19	0.05	0.31	0.11
		80	68.08	57.86	47.92	37.13	21.12	12.21	68.08	4.35	3.88	6.19	4.73	6.19	-50.28	5.82	-4.80	34.29	34.29	-50.28	4.88	0.49	4.88	1.65	1.28	1.65	-138.42	-147.78	-185.58	-91.43	-62.87	-21.93	-185.58
		DI	0.03	0.04	0.06	0.07	0.10	0.20	0.032	-0.09	0.14	-0.12	-0.20	-0.12	0.09	1.80	1.38	0.12	0.12	0.09	0.05	0.40	0.05	0.13	0.18	0.13	0.03	-0.06	0.01	0.08	-0.01	0.22	0.01
		90	68.29	58.14	46.72	35.95	19.01	9.73	68.25	4.03	3.28	5.81	4.50	5.81	-48.49	6.75	-6.39	32.45	32.45	-48.49	4.87	0.47	4.87	1.59	1.14	1.59	-109.75	-153.08	-187.85	-87.27	-48.03	-17.23	-187.85
		DI	0.03	0.04	0.03	0.04	-0.01	-0.09	0.034	-0.16	-0.03	-0.18	-0.04	-0.18	0.06	2.28	2.16	0.06	0.06	0.06	0.05	0.24	0.05	0.09	0.10	0.09	0.04	-0.02	0.08	0.01	-0.09	-0.04	0.08
Lane	R	Static	11.39	19.28	29.92	53.58	53.33	44.34	53.58	2.35	6.12	2.84	6.37	6.37	-4.89	36.02	-26.75	9.82	36.02	-26.75	0.39	5.01	5.01	1.17	1.47	1.47	-25.38	-51.98	-94.38	-149.08	-165.52	-139.49	-165.52
		20	13.00	22.14	35.76	58.24	56.73	48.40	58.24	1.82	6.01	3.11	7.86	7.86	-4.19	38.88	-46.70	3.26	38.88	-46.70	0.47	5.52	5.52	1.24	1.56	1.56	-24.43	-55.29	-107.44	-164.21	-178.28	-148.70	-178.28
		DI	0.14	0.15	0.20	0.09	0.11	0.09	0.087	-0.23	-0.02	0.09	0.23	0.23	-0.14	0.08	0.75	-0.66	0.08	0.75	0.21	0.10	0.10	0.06	0.06	0.06	-0.04	0.06	0.14	0.10	0.08	0.07	0.08
		40	17.58	23.89	34.83	57.40	56.52	53.31	57.40	1.97	6.21	2.89	9.33	9.33	-5.13	38.49	-46.19	4.32	38.49	-46.19	0.63	5.31	5.31	1.12	1.55	1.55	-34.91	-56.31	-101.60	-151.11	-165.13	-139.29	-165.13
		DI	0.54	0.24	0.16	0.07	0.10	0.11	0.071	-0.16	0.01	-0.01	0.46	0.46	0.05	0.07	0.73	-0.56	0.07	0.73	0.62	0.06	0.06	-0.04	0.05	0.05	0.38	0.08	0.08	0.01	0.00	0.00	0.00
		60	15.68	26.97	43.85	67.45	63.30	59.66	67.45	2.24	5.89	3.01	10.04	10.04	-5.50	30.47	-39.16	5.02	30.47	-39.16	0.84	5.75	5.75	1.08	1.44	1.44	-31.38	-63.82	-112.47	-175.88	-174.58	-142.53	-175.88
		DI	0.38	0.40	0.47	0.26	0.23	0.35	0.259	-0.05	-0.04	0.03	0.58	0.58	0.12	-0.15	0.46	-0.49	-0.15	0.46	0.44	0.15	0.15	-0.08	-0.02	-0.02	0.24	0.23	0.19	0.18	0.05	0.02	0.18
		80	19.90	31.95	48.04	74.52	75.43	75.53	75.53	2.18	4.42	3.86	11.79	11.79	-5.05	44.31	-81.30	6.46	44.31	-81.30	0.82	6.49	6.49	1.35	1.78	1.78	-39.08	-72.94	-135.38	-197.34	-197.36	-166.81	-197.36
		DI	0.75	0.66	0.61	0.39	0.47	0.70	0.410	-0.07	0.08	0.36	0.85	0.85	0.03	0.23	0.92	-0.34	0.23	0.92	1.10	0.30	0.30	0.15	0.13	0.21	0.54	0.40	0.43	0.32	0.19	0.20	0.19
		100	15.85	27.83	42.86	62.70	62.99	65.23	65.23	1.58	6.70	3.62	10.27	10.27	-4.85	44.94	-60.13	4.91	44.94	-60.13	0.76	5.67	5.67	1.29	1.74	1.74	-34.77	-58.94	-113.84	-166.06	-177.87	-149.28	-177.87
		DI	0.39	0.40	0.43	0.17	0.18	0.47	0.217	-0.33	0.09	0.23	0.60	0.61	0.01	0.25	0.87	-0.50	0.25	0.87	0.92	0.13	0.13	0.10	0.18	0.18	0.07	0.14	0.20	0.11	0.07	0.07	0.07

Table B 10: Dawson River Bridge DI Summary – Road Train 2 (RT2)

			GIRDERS							HEADSTOCK					COLUMN						GIRDER DEFLECTION			HEADSTOCK DEFLECTION			BEARING COMPRESSION						
															C	T	C	T	T	C													
		MAX	77.89	66.23	56.22	74.52	75.40	75.53	77.89	4.80	6.70	7.05	11.79	11.79	-50.28	44.96	-51.30	34.29	44.96	-51.30	5.44	6.49	6.49	1.73	1.78	1.78	-158.40	-173.75	-203.24	-197.34	-197.36	-166.81	-203.2
		MAX DI	0.75	0.66	0.61	0.39	0.47	0.70	0.41	-0.05	0.14	0.34	0.85	0.85	1.96	2.57	2.16	0.46	3.04	-0.92	1.10	1.11	0.35	0.50	0.21	0.21	0.54	0.40	0.43	0.32	0.19	0.31	0.192
Position	To	Speed	G1	G2	G3	G4	G5	G6	Max	P7HS17	P7HR17	P7HL58	P7HS08	Max	P7C1		P7C8		Max	Min	SBG1	SBG6	Max	P7HL	P7HR	Max	SBG1	SBG2	SBG3	SBG4	SBG5	SBG6	Max
CL	D	Static	50.37	35.48	47.28	56.05	37.20	28.90	56.05	3.10	4.62	3.70	5.10	5.13	-4.20	4.21	-14.56	3.70	4.21	-14.56	1.96	2.54	2.54	0.04	0.43	0.43	-50.25	-88.44	-158.29	-152.20	-106.87	-43.40	-158.29
		20	-	-	-	-	-	-	0.00	-	-	-	-	0.00	-	-	-	-	0.00	0.00	-	-	0.00	-	-	0.00	-	-	-	-	-	-	0.00
		DI	-	-	-	-	-	-	0.00	-	-	-	-	0.00	-	-	-	-	0.00	0.00	-	-	0.00	-	-	0.00	-	-	-	-	-	-	
		40	-	-	-	-	-	-	0.00	-	-	-	-	0.00	-	-	-	-	0.00	0.00	-	-	0.00	-	-	0.00	-	-	-	-	-	-	0.00
		DI	-	-	-	-	-	-	0.00	-	-	-	-	0.00	-	-	-	-	0.00	0.00	-	-	0.00	-	-	0.00	-	-	-	-	-	-	
		60	-	-	-	-	-	-	0.00	-	-	-	-	0.00	-	-	-	-	0.00	0.00	-	-	0.00	-	-	0.00	-	-	-	-	-	-	0.00
		DI	-	-	-	-	-	-	0.00	-	-	-	-	0.00	-	-	-	-	0.00	0.00	-	-	0.00	-	-	0.00	-	-	-	-	-	-	
		80	35.99	42.53	56.22	63.91	45.09	55.61	63.91	2.58	4.58	3.69	6.09	6.09	-8.85	3.57	-13.94	5.48	8.57	-13.94	2.27	3.09	3.09	0.18	0.31	0.31	-65.86	-94.53	-148.31	-153.96	-116.12	-72.89	-168.81
		DI	0.19	0.20	0.18	0.14	0.21	0.19	0.140	-0.27	-0.01	0.00	0.19	0.19	-0.43	1.04	-0.04	-0.48	1.04	-0.04	0.16	0.22	0.22	0.60	-0.28	-0.28	0.13	0.09	0.06	0.01	0.08	0.15	0.06
		100	-	-	-	-	-	-	0.00	-	-	-	-	0.00	-	-	-	-	0.00	0.00	-	-	0.00	-	-	0.00	-	-	-	-	-	-	0.00
		DI	-	-	-	-	-	-	0.00	-	-	-	-	0.00	-	-	-	-	0.00	0.00	-	-	0.00	-	-	0.00	-	-	-	-	-	-	
CL	R	Static	35.20	37.51	40.87	50.95	32.51	22.77	50.95	4.07	4.57	4.52	4.58	4.58	-15.28	3.44	-4.07	9.52	9.52	-15.28	2.32	2.05	2.32	0.28	0.25	0.28	-66.89	-96.52	-170.70	-139.81	-94.11	-55.28	-170.70
		20	-	-	-	-	-	-	0.00	-	-	-	-	0.00	-	-	-	-	0.00	0.00	-	-	0.00	-	-	0.00	-	-	-	-	-	-	0.00
		DI	-	-	-	-	-	-	0.00	-	-	-	-	0.00	-	-	-	-	0.00	0.00	-	-	0.00	-	-	0.00	-	-	-	-	-	-	
		40	-	-	-	-	-	-	0.00	-	-	-	-	0.00	-	-	-	-	0.00	0.00	-	-	0.00	-	-	0.00	-	-	-	-	-	-	0.00
		DI	-	-	-	-	-	-	0.00	-	-	-	-	0.00	-	-	-	-	0.00	0.00	-	-	0.00	-	-	0.00	-	-	-	-	-	-	
		60	-	-	-	-	-	-	0.00	-	-	-	-	0.00	-	-	-	-	0.00	0.00	-	-	0.00	-	-	0.00	-	-	-	-	-	-	0.00
		DI	-	-	-	-	-	-	0.00	-	-	-	-	0.00	-	-	-	-	0.00	0.00	-	-	0.00	-	-	0.00	-	-	-	-	-	-	
		80	-	-	-	-	-	-	0.00	-	-	-	-	0.00	-	-	-	-	0.00	0.00	-	-	0.00	-	-	0.00	-	-	-	-	-	-	0.00
		DI	-	-	-	-	-	-	0.00	-	-	-	-	0.00	-	-	-	-	0.00	0.00	-	-	0.00	-	-	0.00	-	-	-	-	-	-	
		90	-	-	-	-	-	-	0.00	-	-	-	-	0.00	-	-	-	-	0.00	0.00	-	-	0.00	-	-	0.00	-	-	-	-	-	-	0.00
		DI	-	-	-	-	-	-	0.00	-	-	-	-	0.00	-	-	-	-	0.00	0.00	-	-	0.00	-	-	0.00	-	-	-	-	-	-	
Lane	D	Static	65.98	55.82	45.39	34.70	19.26	10.19	65.98	4.80	3.39	7.05	4.69	7.05	-45.92	2.08	-2.02	30.68	30.68	-45.92	4.64	0.39	4.64	1.46	1.04	1.46	-194.24	-155.97	-183.42	-66.38	-53.11	-17.93	-183.42
		20	73.19	64.82	54.21	41.27	21.01	10.26	73.19	4.15	2.81	5.72	4.00	5.72	-47.59	5.54	-3.97	34.21	34.21	-47.59	5.16	0.48	5.16	1.64	1.21	1.64	-142.82	-168.55	-201.97	-104.77	-55.49	-18.19	-201.97
		DI	0.11	0.16	0.19	0.19	0.09	0.01	0.109	-0.14	-0.17	-0.19	-0.15	-0.19	0.04	1.66	0.97	0.12	0.11	0.04	0.11	0.21	0.11	0.12	0.16	0.12	0.06	0.08	0.07	0.12	0.04	0.05	0.10
		40	77.89	66.23	56.74	42.16	23.98	14.58	77.89	4.39	2.89	5.78	3.56	5.78	-45.56	7.42	-4.33	31.90	31.90	-45.56	5.44	0.74	5.44	1.65	1.25	1.65	-158.48	-173.75	-203.24	-99.55	-60.26	-17.31	-203.24
		DI	0.18	0.08	0.23	0.22	0.25	0.48	0.181	-0.09	-0.15	-0.18	-0.24	-0.18	-0.01	2.57	1.13	0.04	0.04	-0.01	0.17	1.11	0.17	0.13	0.16	0.13	0.18	0.11	0.11	0.15	-0.06	0.03	0.11
		60	70.12	61.61	54.09	41.52	22.74	12.75	70.12	4.10	2.90	6.07	3.49	6.07	-49.24	4.90	-4.60	33.09	33.09	-49.24	5.05	0.54	5.05	1.73	1.25	1.73	-140.30	-165.93	-202.77	-103.09	-55.95	-23.42	-202.77
		DI	0.08	0.10	0.18	0.20	0.18	0.25	0.063	-0.15	-0.14	-0.14	-0.25	-0.14	0.07	1.36	1.28	0.09	0.08	0.07	0.09	0.54	0.09	0.16	0.20	0.18	0.06	0.06	0.11	0.19	0.05	0.31	0.11
		80	68.06	57.86	47.52	37.13	21.12	12.21	68.06	4.35	3.66	6.19	4.23	6.19	-50.28	5.82	-4.80	34.29	34.29	-50.28	4.86	0.49	4.86	1.65	1.23	1.65	-138.47	-147.78	-185.58	-91.41	-52.87	-21.93	-185.58
		DI	0.03	0.04	0.06	0.07	0.10	0.20	0.032	-0.09	0.14	-0.12	-0.20	-0.12	0.09	1.80	1.38	0.12	0.12	0.09	0.05	0.40	0.05	0.13	0.18	0.13	0.05	-0.06	0.01	0.08	-0.01	0.22	0.01
		95	68.25	58.14	46.72	35.95	19.01	9.73	68.25	4.03	3.28	5.81	4.50	5.81	-48.49	6.75	-4.39	32.45	32.45	-48.49	4.87	0.47	4.87	1.58	1.14	1.58	-109.76	-151.08	-197.85	-87.27	-48.05	-17.23	-197.85
		DI	0.09	0.04	0.03	0.04	-0.01	-0.05	0.034	-0.16	-0.03	-0.18	-0.04	-0.18	0.06	2.25	2.16	0.06	0.06	0.06	0.05	0.34	0.05	0.09	0.10	0.09	0.04	-0.03	0.08	0.01	-0.09	-0.04	0.08
Lane	R	Static	11.39	19.28	29.92	53.58	51.03	44.34	53.58	2.35	6.12	2.84	6.37	6.37	-4.09	36.02	-26.75	9.82	36.02	-26.75	0.39	5.01	5.01	1.17	1.47	1.47	-25.35	-51.90	-94.38	-149.08	-165.92	-139.49	-165.92
		20	13.00	22.14	35.76	58.24	56.73	48.40	58.24	1.82	6.01	3.11	7.56	7.56	-4.19	38.88	-46.70	3.36	38.88	-46.70	0.47	5.52	5.52	1.24	1.56	1.56	-24.43	-55.29	-107.44	-164.21	-178.28	-148.70	-178.28
		DI	0.14	0.15	0.20	0.09	0.11	0.09	0.087	-0.23	-0.02	0.06	0.19	0.19	-0.14	0.08	0.75	-0.66	0.08	0.75	0.21	0.10	0.10	0.06	0.06	0.06	-0.04	0.06	0.14	0.10	0.06	0.07	0.06
		40	17.58	23.89	34.83	57.40	56.52	53.91	57.40	1.97	6.21	2.09	9.32	9.32	-5.13	38.49	-46.19	4.33	38.49	-46.19	0.63	3.31	5.21	1.12	1.55	1.55	-34.91	-56.01	-101.60	-151.11	-165.13	-139.29	-165.13
		DI	0.54	0.24	0.16	0.07	0.10	0.22	0.078	-0.16	0.01	-0.02	0.46	0.46	0.05	0.07	0.73	-0.56	0.07	0.73	0.62	0.04	-0.06	-0.04	0.06	0.05	0.38	0.08	0.08	0.01	0.00	0.00	0.00
		60	15.68	26.97	43.85	67.45	63.80	59.68	67.45	2.24	5.89	3.02	10.04	10.04	-5.90	30.47	-39.16	5.02	30.47	-39.16	0.56	5.75	5.75	1.08	1.44	1.44	-31.59	-63.82	-112.47	-175.88	-174.58	-142.53	-175.88
		DI	0.38	0.40	0.47	0.26	0.25	0.35	0.259	-0.08	-0.04	0.09	0.58	0.58	0.12	-0.23	0.46	-0.49	-0.15	0.46	0.44	0.15	0.15	-0.08	-0.02	-0.02	0.24	0.19	0.00	0.18	0.05	0.02	0.18
		80	19.90	31.95	48.04	74.52	75.40	75.53	75.53	2.18	6.42	3.95	11.79	11.79	-5.85	44.31	-51.30	6.46	44.31	-51.30	0.82	6.49	6.49	1.35	1.78	1.78	-29.08	-72.94	-135.38	-197.34	-197.36	-166.81	-197.36
		DI	0.75	0.66	0.61	0.39	0.47	0.70	0.410	-0.07	0.05	0.39	0.85	0.85	0.20	0.23	0.92	-0.34	0.23	0.92	1.10	0.30	0.30	0.15	0.21	0.21	0.54	0.40	0.43	0.32	0.19	0.31	0.19
		100	15.80	27.83	41.86	62.70	62.99	65.21	65.21	1.58	6.70	3.42	10.27	10.27	-4.85	44.96	-50.13	4.91	44.96	-50.13	0.76	5.67	5.67	1.28	1.74	1.74	-34.77	-58.94	-113.64	-166.08	-177.87	-149.29	-177.87
		DI	0.39	0.60	0.61	0.17	0.22	0.47	0.212	-0.33	0.08	0.11	0.61	0.61	-0.01	0.25	0.87	-0.10	0.25	0.87	0.92	0.17	0.16	0.30	0.18	0.18	0.17	0.04	0.20	0.11	0.07	0.03	0.07

B.3.2 DI Graph – Mid-span of Girders

Lane travel

Figure B 5: DI – Girder Mid-span Bending Strains (Lane Travel)

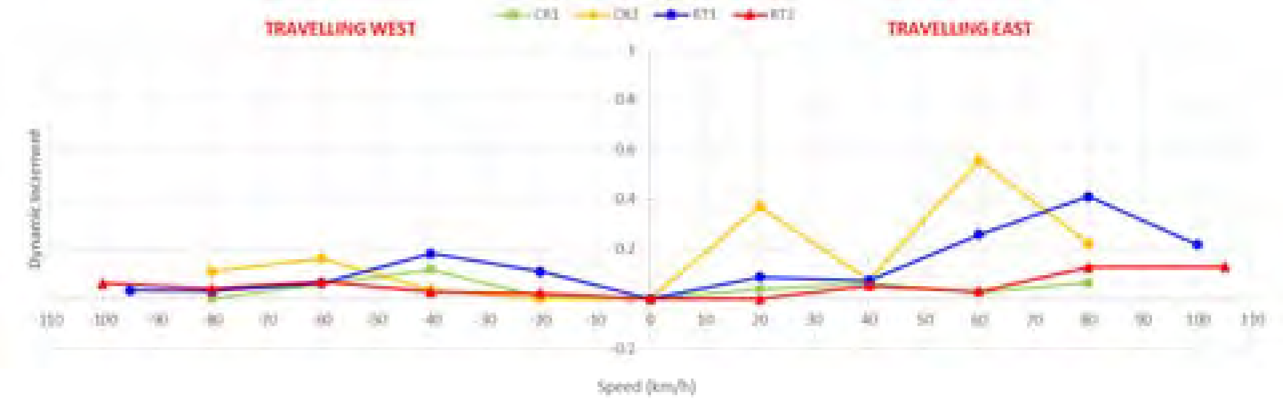

Figure B 6: DI – Girder Mid-span Deflections (Lane Travel)

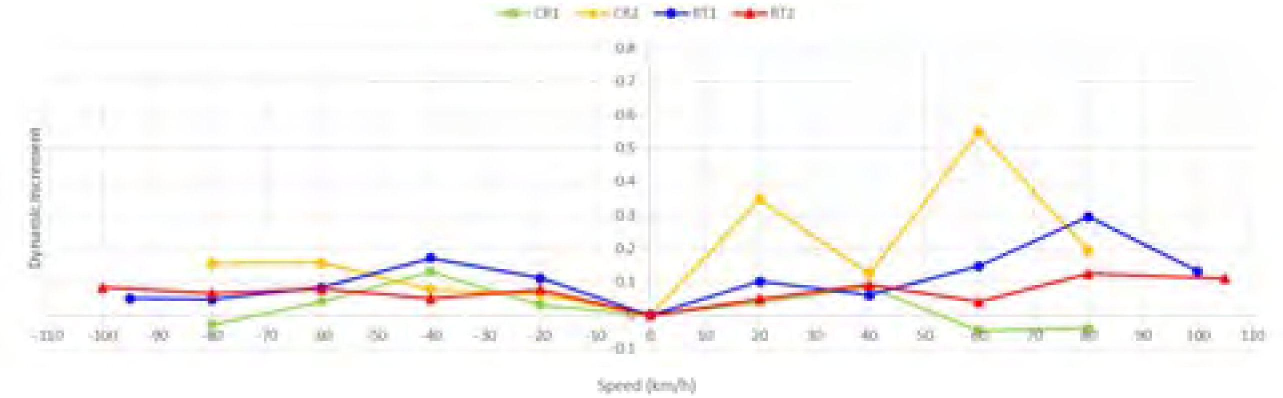

B.3.3 DI Graph – Headstock

Lane travel

Figure B 7: DI – Headstock Bending Strains (Lane Travel)

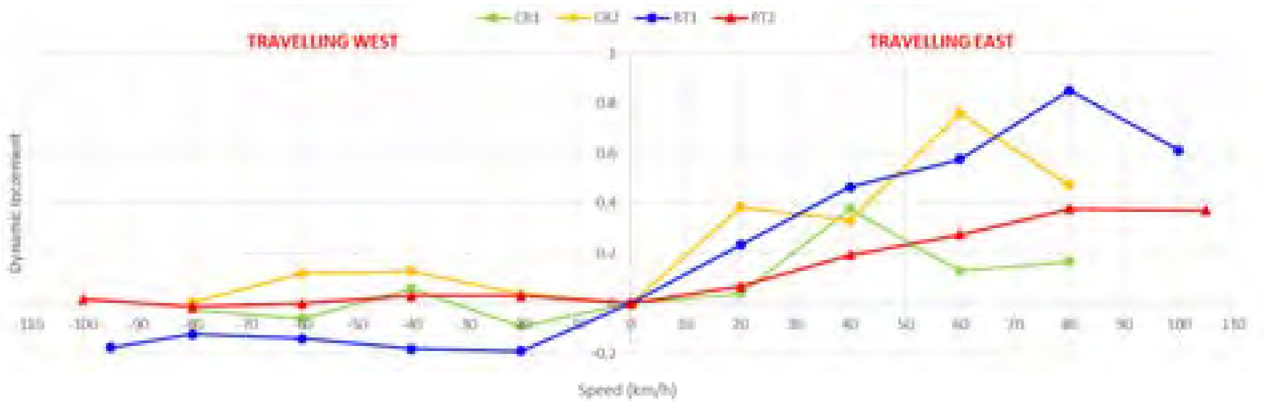

Figure B 8: DI – Headstock Cantilever Deflections (Lane Travel)

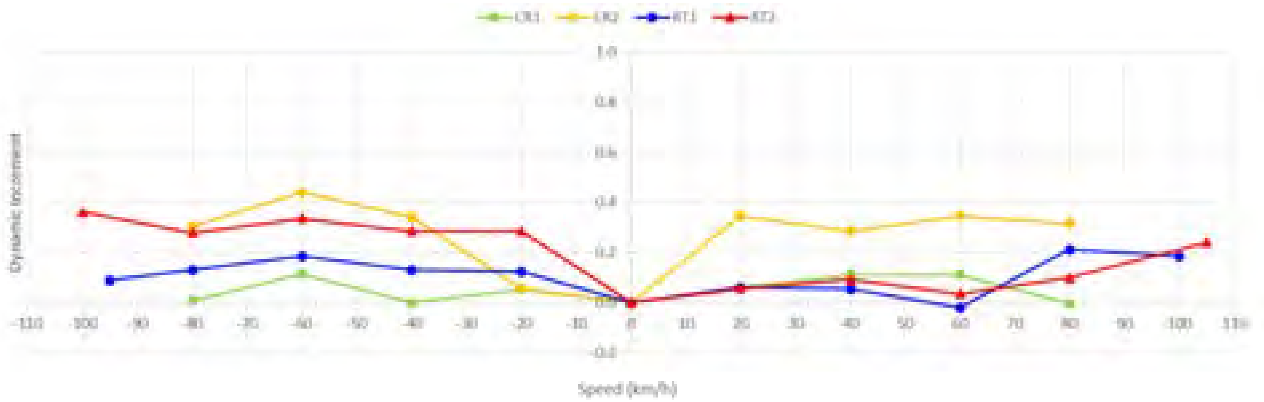

B.3.4 DI Graph – Column

Lane travel

Figure B 9: DI – Column Tensile Strains (Lane Travel)

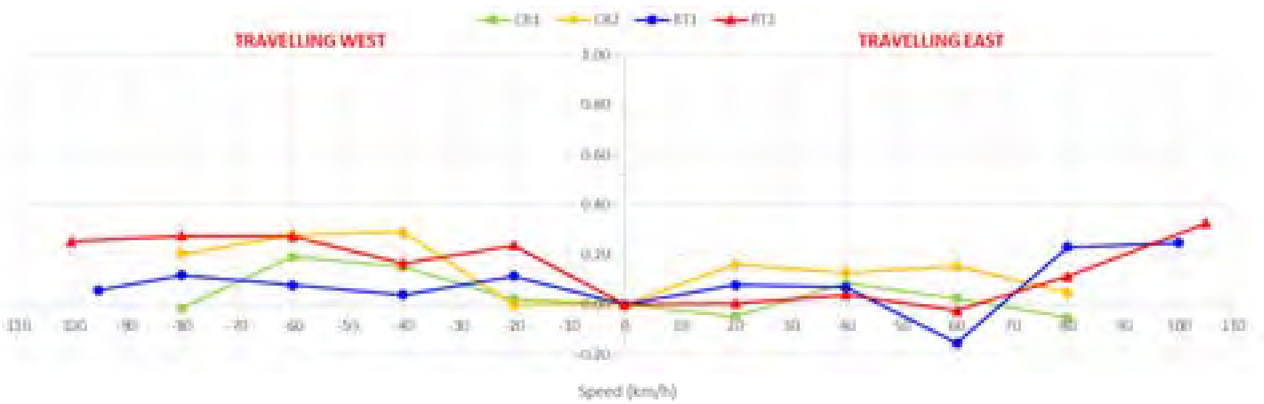

Figure B 10: DI – Column Compression Strains (Lane Travel)

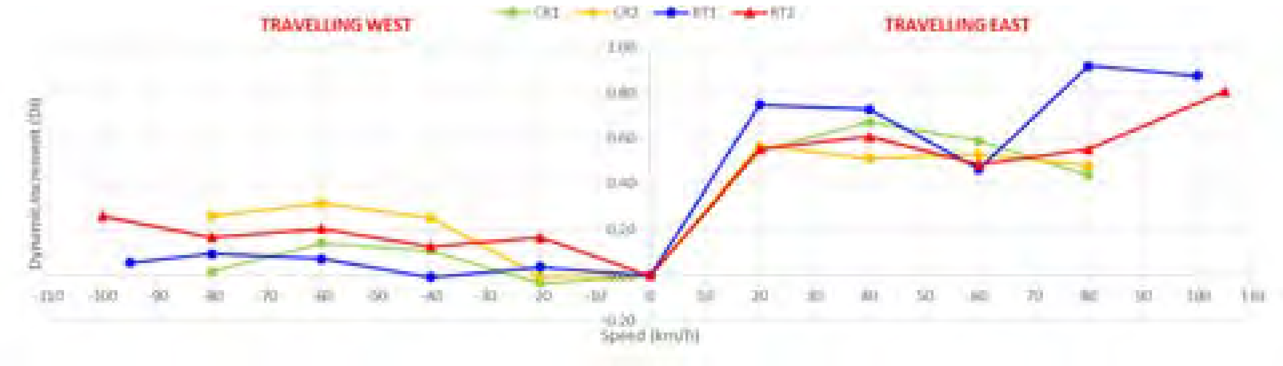

B.4 Neerkol Creek Bridge

B.4.1 Summary of DI Values

Table B 11: Neerkol Creek Bridge DI Summary – Crane 1 (CR1)

			GIRDERS						HEADSTOCK			
		MAX	48.59	82.81	30.21	105.26	55.41	105.26	22.00	6.85	57.83	57.83
		MAX DI	0.38	0.14	0.20	0.10	0.53	0.10	0.35	0.55	0.27	0.27
Position	To	Speed	G5	G4	G3	G2	G1	Max	P1HS1	P1HS2	P1HUm	Max
CL	S	Static	22.93	58.36	26.09	77.88	24.22	77.88	17.63	3.55	49.74	49.74
		20	–	–	–	–	–	0.00	–	–	–	0.00
		DI	–	–	–	–	–	0.00	–	–	–	0.00
		40	27.53	64.52	29.57	76.73	31.89	76.73	22.00	2.44	56.43	56.43
		DI	0.20	0.11	0.13	-0.01	0.31	-0.015	0.25	-0.27	0.13	0.13
		60	–	–	–	–	–	0.00	–	–	–	0.00
		DI	–	–	–	–	–	0.00	–	–	–	0.00
		80	21.40	60.85	28.24	76.23	29.07	76.23	19.80	3.43	57.83	57.83
		DI	-0.07	0.04	0.08	-0.02	0.20	-0.021	0.12	-0.03	0.16	0.16
CL	R	Static	21.87	60.21	25.25	73.45	22.40	73.45	16.57	3.30	49.14	49.14
		20	–	–	–	–	–	0.00	–	–	–	0.00
		DI	–	–	–	–	–	0.00	–	–	–	0.00
		40	30.13	68.49	30.21	80.48	34.37	80.48	19.08	4.08	55.12	55.12
		DI	0.38	0.14	0.20	0.10	0.53	0.096	0.15	0.24	0.12	0.12
		60	–	–	–	–	–	0.00	–	–	–	0.00
		DI	–	–	–	–	–	0.00	–	–	–	0.00
		80	22.69	63.14	29.14	75.05	29.24	75.05	18.78	3.37	55.54	55.54
		DI	0.04	0.05	0.15	0.02	0.31	0.022	0.13	0.02	0.13	0.13
Lane	S	Static	9.05	32.29	21.19	95.53	39.20	95.53	12.50	2.33	33.30	33.30
		20	6.41	29.13	16.87	93.95	33.51	93.95	9.45	3.07	32.78	32.78
		DI	-0.29	-0.10	-0.20	-0.02	-0.15	-0.017	-0.24	0.32	-0.02	-0.02
		40	12.02	33.12	24.50	99.32	53.86	99.32	16.91	3.62	42.40	42.40
		DI	0.33	0.03	0.16	0.04	0.37	0.040	0.35	0.55	0.27	0.27
		60	10.02	30.83	21.95	91.31	51.37	91.31	15.61	3.40	40.02	40.02
		DI	0.11	-0.05	0.04	-0.04	0.31	-0.044	0.25	0.46	0.20	0.20
		80	8.65	30.19	23.75	105.26	55.41	105.26	16.10	3.44	40.26	40.26
		DI	-0.04	-0.07	0.12	0.10	0.41	0.102	0.29	0.47	0.21	0.21
Lane	R	Static	38.46	77.24	21.62	39.08	9.61	77.24	14.61	6.85	38.97	38.97
		20	–	–	–	–	–	0.00	–	–	–	0.00
		DI	–	–	–	–	–	0.00	–	–	–	0.00
		40	48.59	82.81	21.92	35.64	12.04	82.81	14.35	4.02	39.51	39.51
		DI	0.26	0.07	0.01	-0.09	0.25	0.072	-0.02	-0.41	0.01	0.01
		60	43.91	81.53	24.35	36.28	11.62	81.53	13.99	3.37	44.94	44.94
		DI	0.14	0.06	0.13	-0.07	0.21	0.056	-0.04	-0.51	0.15	0.15
		80	35.08	76.72	22.18	36.46	11.69	76.72	12.59	2.85	44.92	44.92
		DI	-0.09	-0.01	0.03	-0.07	0.21	-0.007	-0.14	-0.58	0.15	0.15

			COLUMN						GIRDER DEFLECTION		BEARING COMPRESSION					
			T	C	C	T	T	C								
		MAX	13.11	-9.08	-26.12	11.72	13.11	-26.12	-7.13	-7.13	-294.00	-294.87	-291.22	-290.06	-52.73	-294.87
		MAX DI	0.56	0.19	0.11	0.10	0.56	0.11	0.11	0.11	0.09	0.03	0.00	0.00	2.44	0.70
Position	To	Speed	P1CRO	P1CRI	P1CLI	P1CLO	Max	Min	S1G3m	Max	S1G5	S1G4	S1G3	S1G2	S1G1	Max
CL	S	Static	10.72	-8.13	-23.59	10.74	10.74	-23.59	-6.44	-6.44	-133.14	-230.02	-280.91	-280.01	-5.79	-280.91
		20	–	–	–	–	0.00	0.00	–	0.00	–	–	–	–	–	0.00
		DI	–	–	–	–	0.00	0.00	–	0.00	–	–	–	–	–	0.00
		40	9.86	-7.93	-26.12	11.72	11.72	-26.12	-6.67	-6.67	-142.48	-230.86	-278.82	-277.24	-4.68	-278.82
		DI	-0.08	-0.03	0.11	0.09	0.09	0.11	0.04	0.04	0.07	0.00	-0.01	-0.01	-0.19	0.07
		60	–	–	–	–	0.00	0.00	–	0.00	–	–	–	–	–	0.00
		DI	–	–	–	–	0.00	0.00	–	0.00	–	–	–	–	–	0.00
		80	9.79	-8.48	-23.87	10.96	10.96	-23.87	-6.30	-6.30	-122.41	-212.12	-264.32	-262.65	-4.16	-264.32
		DI	-0.09	0.04	0.01	0.02	0.02	0.01	-0.02	-0.02	-0.08	-0.08	-0.06	-0.06	-0.28	-0.06
CL	R	Static	13.11	-7.66	-22.87	11.00	13.11	-22.87	-6.40	-6.40	-136.90	-234.87	-291.22	-290.06	-2.53	-291.22
		20	–	–	–	–	0.00	0.00	–	0.00	–	–	–	–	–	0.00
		DI	–	–	–	–	0.00	0.00	–	0.00	–	–	–	–	–	0.00
		40	11.32	-9.05	-23.43	9.83	11.32	-23.43	-7.13	-7.13	-149.06	-242.10	-286.38	-284.76	-4.29	-286.38
		DI	-0.14	0.18	0.02	-0.11	-0.14	0.02	0.11	0.11	0.09	0.03	-0.02	-0.02	0.70	0.70
		60	–	–	–	–	0.00	0.00	–	0.00	–	–	–	–	–	0.00
		DI	–	–	–	–	0.00	0.00	–	0.00	–	–	–	–	–	0.00
		80	10.99	-9.07	-21.61	9.52	10.99	-21.61	-6.41	-6.41	-132.77	-225.87	-268.41	-266.29	-3.05	-268.41
		DI	-0.16	0.18	-0.05	-0.13	-0.16	-0.05	0.00	0.00	-0.03	-0.04	-0.08	-0.08	0.21	0.21
Lane	S	Static	6.55	-5.97	-21.57	6.32	6.55	-21.57	-5.71	-5.71	-72.66	-156.58	-245.42	-244.71	-40.97	-245.42
		20	7.45	-5.43	-17.18	5.29	7.45	-17.18	-4.93	-4.93	-68.11	-146.34	-245.29	-243.73	-35.32	-245.29
		DI	0.14	-0.09	-0.20	-0.16	0.14	-0.20	-0.14	-0.14	-0.06	-0.07	0.00	0.00	-0.14	0.00
		40	10.21	-7.11	-22.75	6.29	10.21	-22.75	-5.69	-5.69	-68.70	-146.76	-235.24	-234.08	-41.76	-235.24
		DI	0.56	0.19	0.05	0.00	0.56	0.05	0.00	0.00	-0.05	-0.06	-0.04	-0.04	0.02	0.02
		60	8.72	-6.20	-23.17	6.95	8.72	-23.17	-5.19	-5.19	-64.29	-142.42	-234.01	-232.55	-46.97	-234.01
		DI	0.33	0.04	0.07	0.10	0.33	0.07	-0.09	-0.09	-0.12	-0.09	-0.05	-0.05	0.15	0.15
		80	9.89	-6.10	-20.31	4.77	9.89	-20.31	-5.50	-5.50	-59.83	-138.30	-229.18	-227.72	-52.73	-229.18
		DI	0.51	0.02	-0.06	-0.25	0.51	-0.06	-0.04	-0.04	-0.18	-0.12	-0.07	-0.07	0.29	0.29
Lane	R	Static	7.83	-9.08	-18.89	11.32	11.32	-18.89	-5.73	-5.73	-294.00	-294.00	-246.79	-245.73	-2.29	-294.00
		20	–	–	–	–	0.00	0.00	–	0.00	–	–	–	–	–	0.00
		DI	–	–	–	–	0.00	0.00	–	0.00	–	–	–	–	–	0.00
		40	5.32	-7.43	-17.98	9.50	9.50	-17.98	-5.65	-5.65	-231.49	-294.87	-231.52	-230.28	-7.88	-294.87
		DI	-0.32	-0.18	-0.05	-0.16	-0.16	-0.05	-0.01	-0.01	-0.21	0.00	-0.06	-0.06	2.44	0.00
		60	6.41	-7.82	-18.27	10.17	10.17	-18.27	-5.56	-5.56	-216.67	-283.95	-231.02	-229.69	-4.50	-283.95
		DI	-0.18	-0.14	-0.03	-0.10	-0.10	-0.03	-0.03	-0.03	-0.26	-0.03	-0.06	-0.07	0.97	-0.03
		80	5.63	-7.57	-19.32	11.02	11.02	-19.32	-5.50	-5.50	-211.51	-277.69	-233.31	-231.80	-4.97	-277.69
		DI	-0.34	-0.17	0.02	-0.03	-0.03	0.02	-0.04	-0.04	-0.28	-0.06	-0.05	-0.06	1.17	-0.05

Table B 12: Neerkol Creek Bridge DI Summary – Crane 2 (CR2)

			GIRDERS						HEADSTOCK				COLUMN						GIRDER DEFLECTION		BEARING COMPRESSION					
													T	C	C	T	T	C								
		MAX	46.00	84.14	31.36	108.66	66.22	108.66	22.14	4.82	61.58	61.58	11.60	-10.52	-23.97	12.40	12.40	-23.97	-6.90	-6.90	-223.86	-294.51	-284.83	-282.80	-48.89	-294.51
		MAX DI	0.43	0.39	0.61	0.89	1.06	0.39	0.72	0.30	0.74	0.74	0.87	0.56	0.49	1.55	0.87	0.49	0.45	0.45	0.31	0.50	0.28	0.28	1.82	0.43
Position	To	Speed	G5	G4	G3	G2	G1	Max	P1HS1	P1HS2	P1HSm	Max	P1CRO	P1CRI	P1CLI	P1CLO	Max	Min	S1G5m	Max	S1G5	S1G4	S1G3	S1G2	S1G1	Max
CL	S	Static	21.14	49.87	21.59	61.36	20.82	61.36	18.49	3.47	45.20	45.20	10.95	-7.59	-23.85	12.40	12.40	-23.85	-5.34	-5.34	-117.55	-205.01	-249.46	-248.71	-6.68	-249.46
		20	–	–	–	–	–	0.00	–	–	–	0.00	–	–	–	–	0.00	0.00	–	0.00	–	–	–	–	–	0.00
		DI	–	–	–	–	–	0.00	–	–	–	0.00	–	–	–	–	0.00	0.00	–	0.00	–	–	–	–	–	0.00
		40	25.21	52.43	23.30	62.68	25.26	62.68	17.58	4.28	46.15	46.15	10.12	-7.75	-23.72	10.98	10.98	-23.72	-5.42	-5.42	-127.08	-224.90	-262.27	-260.89	-9.58	-262.27
		DI	0.19	0.06	0.08	0.02	0.21	0.021	-0.05	0.23	0.00	0.02	-0.08	0.02	-0.01	-0.11	-0.11	-0.01	0.02	0.02	0.08	0.10	0.05	0.05	0.43	0.43
		60	–	–	–	–	–	0.00	–	–	–	0.00	–	–	–	–	0.00	0.00	–	0.00	–	–	–	–	–	0.00
		DI	–	–	–	–	–	0.00	–	–	–	0.00	–	–	–	–	0.00	0.00	–	0.00	–	–	–	–	–	0.00
		80	27.42	69.06	29.39	76.00	30.25	76.00	20.12	4.19	52.45	52.45	10.85	-8.40	-21.82	9.45	10.85	-21.82	-6.90	-6.90	-155.51	-253.03	-279.11	-277.44	-6.15	-279.11
		DI	0.30	0.39	0.36	0.24	0.45	0.239	0.09	0.21	0.15	0.16	-0.01	0.11	-0.08	-0.24	-0.01	-0.08	0.29	0.29	0.31	0.23	0.12	0.12	-0.08	0.31
CL	R	Static	21.26	52.58	21.69	64.20	20.43	64.20	14.24	3.75	39.69	39.69	9.93	-7.65	-20.72	9.25	9.93	-20.72	-5.45	-5.45	-119.01	-201.93	-248.81	-248.22	-4.61	-248.81
		20	–	–	–	–	–	0.00	–	–	–	0.00	–	–	–	–	0.00	0.00	–	0.00	–	–	–	–	–	0.00
		DI	–	–	–	–	–	0.00	–	–	–	0.00	–	–	–	–	0.00	0.00	–	0.00	–	–	–	–	–	0.00
		40	24.03	56.68	25.94	74.83	31.94	74.83	20.63	2.27	54.99	54.99	11.60	-10.52	-22.59	9.48	11.60	-22.59	-6.14	-6.14	-129.85	-222.01	-283.99	-282.34	-4.28	-283.99
		DI	0.13	0.08	0.20	0.17	0.56	0.166	0.45	-0.39	0.39	0.38	0.17	0.37	0.09	0.03	0.17	0.09	0.13	0.13	0.08	0.10	0.14	0.14	-0.08	0.14
		60	–	–	–	–	–	0.00	–	–	–	0.00	–	–	–	–	0.00	0.00	–	0.00	–	–	–	–	–	0.00
		DI	–	–	–	–	–	0.00	–	–	–	0.00	–	–	–	–	0.00	0.00	–	0.00	–	–	–	–	–	0.00
		80	25.15	69.63	31.36	85.02	32.37	85.02	22.14	4.82	61.58	61.58	11.48	-9.33	-23.97	9.80	11.48	-23.97	-6.89	-6.89	-147.43	-224.18	-284.83	-282.80	-5.30	-284.83
		DI	0.18	0.33	0.45	0.32	0.58	0.324	0.55	0.29	0.55	0.55	0.16	0.22	0.16	0.06	0.16	0.16	0.26	0.26	0.20	0.11	0.14	0.14	0.15	0.20
Lane	S	Static	10.59	27.98	16.65	78.29	32.15	78.29	10.40	3.19	26.60	26.60	6.04	-6.35	-16.81	3.25	6.04	-16.81	-4.61	-4.61	-61.90	-130.87	-204.71	-205.48	-48.89	-204.71
		20	8.36	27.60	14.69	85.46	37.44	85.46	10.53	3.33	32.73	32.73	7.57	-5.78	-16.62	5.93	7.57	-16.62	-4.75	-4.75	-64.19	-133.60	-222.56	-221.29	-38.18	-222.56
		DI	-0.40	-0.01	-0.12	0.09	0.16	0.092	0.01	0.04	0.23	0.23	0.25	-0.09	-0.01	0.83	0.25	-0.01	0.05	0.05	0.04	0.02	0.09	0.08	-0.22	0.09
		40	10.11	29.57	20.11	83.94	47.10	83.94	13.38	3.64	32.52	32.52	8.59	-6.55	-19.51	5.84	8.59	-19.51	-4.79	-4.79	-61.75	-129.95	-220.28	-218.64	-42.98	-220.28
		DI	-0.05	0.06	0.21	0.07	0.47	0.072	0.29	0.14	0.22	0.22	0.42	0.03	0.16	0.79	0.42	0.16	0.04	0.04	0.00	-0.01	0.08	0.07	-0.12	0.08
		60	13.48	35.58	23.75	89.18	56.74	89.18	17.62	3.61	43.73	43.73	11.11	-6.88	-22.32	8.24	11.11	-22.32	-5.52	-5.52	-73.51	-153.03	-253.57	-251.97	-36.16	-253.57
		DI	0.27	0.27	0.43	0.14	0.76	0.139	0.69	0.13	0.64	0.64	0.84	0.08	0.33	1.53	0.84	0.33	0.20	0.20	0.19	0.17	0.24	0.24	-0.26	0.24
		80	11.64	38.09	26.88	108.66	66.22	108.66	17.93	4.14	43.14	43.14	11.27	-7.81	-22.13	4.51	11.27	-22.13	-6.60	-6.60	-77.02	-169.93	-262.87	-261.20	-29.59	-262.87
		DI	0.10	0.36	0.61	0.89	1.06	0.388	0.72	0.10	0.62	0.62	0.87	0.23	0.32	0.39	0.87	0.32	0.43	0.43	0.24	0.30	0.28	0.28	-0.39	0.30
Lane	R	Static	32.11	62.87	17.89	34.21	9.93	62.87	10.31	3.02	29.71	29.71	4.75	-5.56	-14.60	8.15	8.15	-14.60	-4.87	-4.87	-187.63	-253.09	-215.92	-215.00	-2.72	-253.09
		20	–	–	–	–	–	0.00	–	–	–	0.00	–	–	–	–	0.00	0.00	–	0.00	–	–	–	–	–	0.00
		DI	–	–	–	–	–		–	–	–	0.00	–	–	–	–	0.00	0.00	–	0.00	–	–	–	–	–	0.00
		40	44.67	77.69	23.83	42.09	13.86	77.69	17.00	3.03	45.51	45.51	7.59	-8.64	-19.05	9.94	9.94	-19.05	-5.96	-5.96	-211.04	-287.83	-249.71	-248.47	-7.86	-287.83
		DI	0.09	0.24	0.33	0.23	0.40	0.236	0.65	0.00	0.53	0.53	0.60	0.56	0.50	0.22	0.22	0.50	0.22	0.22	0.12	0.14	0.16	0.16	1.82	0.16
		60	46.00	83.92	24.93	41.45	13.95	83.92	18.19	3.39	43.77	43.77	7.70	-8.59	-19.73	10.53	10.53	-19.73	-5.91	-5.91	-223.86	-294.51	-241.78	-240.78	-7.35	-294.51
		DI	0.43	0.33	0.39	0.21	0.41	0.335	0.57	0.12	0.47	0.47	0.63	0.55	0.35	0.29	0.29	0.35	0.21	0.21	0.18	0.18	0.12	0.12	1.69	0.19
		80	39.01	84.14	24.50	41.21	11.49	84.14	17.63	2.92	51.61	51.61	5.55	-8.67	-21.72	11.18	11.18	-21.72	-6.06	-6.06	-212.66	-279.06	-236.74	-235.05	-7.11	-279.06
		DI	0.21	0.34	0.36	0.20	0.08	0.338	0.71	-0.03	0.74	0.74	0.17	0.56	0.49	0.87	0.37	0.49	0.24	0.24	0.23	0.10	0.10	0.09	1.61	0.13

Table B 13: Neerkol Creek Bridge DI Summary – Road Train 1 (RT1)

			GIRDERS						HEADSTOCK				COLUMN						GIRDER DEFLECTION		BEARING COMPRESSION					
													T	C	C	T	T	C								
		MAX	45.25	86.57	38.40	97.33	56.33	97.33	24.94	4.11	75.46	75.46	17.20	-13.43	-31.26	16.21	17.20	-31.26	-7.58	-7.58	-271.23	-355.60	-330.60	-329.46	-33.95	-355.60
		MAX DI	0.56	0.38	0.38	0.29	0.84	0.31	0.88	0.41	0.65	0.65	0.65	0.58	0.26	0.89	0.89	0.26	0.22	0.22	0.50	0.29	0.20	0.20	3.31	1.83
Position	To	Speed	G5	G4	G3	G2	G1	Max	P1HS1	P1HS2	P1HSUm	Max	P1CRO	P1CRI	P1CLI	P1CLO	Max	Min	S103m	Max	S105	S104	S103	S102	S101	Max
CL	S	Static	25.64	56.72	21.57	61.94	21.02	61.94	22.46	3.48	64.77	64.77	17.20	-10.94	-31.26	16.23	17.20	-31.26	-6.70	-6.70	-349.92	-299.09	-320.71	-319.84	-5.29	-320.71
		20	–	–	–	–	–	0.00	–	–	–	0.00	–	–	–	–	0.00	0.00	–	0.00	–	–	–	–	–	0.00
		DI	–	–	–	–	–	0.00	–	–	–	0.00	–	–	–	–	0.00	0.00	–	0.00	–	–	–	–	–	0.00
		40	29.72	59.17	24.86	64.31	26.90	64.31	24.94	3.32	68.87	68.87	11.73	-10.98	-28.66	13.82	13.82	-28.66	-6.79	-6.79	-148.38	-263.81	-318.10	-315.99	-5.34	-318.10
		DI	0.16	0.04	0.15	0.04	0.28	0.038	0.11	-0.05	0.06	0.06	-0.32	0.00	-0.08	-0.15	-0.15	-0.08	0.01	0.01	-0.01	-0.02	-0.01	-0.01	0.05	0.05
		60	–	–	–	–	–	0.00	–	–	–	0.00	–	–	–	–	0.00	0.00	–	0.00	–	–	–	–	–	0.00
		DI	–	–	–	–	–	0.00	–	–	–	0.00	–	–	–	–	0.00	0.00	–	0.00	–	–	–	–	–	0.00
		80	25.09	61.03	26.46	68.85	28.89	68.85	24.55	3.49	72.30	72.30	10.74	-11.48	-27.58	11.59	11.59	-27.58	-7.00	-7.00	-151.71	-262.55	-324.22	-321.75	-6.42	-324.22
		DI	-0.02	0.08	0.23	0.11	0.37	0.111	0.08	0.00	0.12	0.12	-0.38	0.05	-0.12	-0.23	-0.29	-0.12	0.04	0.04	0.01	-0.03	0.01	0.02	0.21	0.21
		–	–	–	–	–	–	0.00	–	–	–	0.00	–	–	–	–	0.00	0.00	–	0.00	–	–	–	–	–	0.00
		DI	–	–	–	–	–	0.00	–	–	–	0.00	–	–	–	–	0.00	0.00	–	0.00	–	–	–	–	–	0.00
CL	R	Static	22.08	51.09	20.65	64.97	19.75	64.97	17.12	2.92	53.01	53.01	9.92	-10.64	-25.87	8.57	9.92	-25.87	-6.43	-6.43	-138.06	-256.56	-330.60	-329.46	-2.44	-330.60
		20	–	–	–	–	–	0.00	–	–	–	0.00	–	–	–	–	0.00	0.00	–	0.00	–	–	–	–	–	0.00
		DI	–	–	–	–	–	0.00	–	–	–	0.00	–	–	–	–	0.00	0.00	–	0.00	–	–	–	–	–	0.00
		40	24.57	52.64	23.97	70.48	32.85	70.48	24.02	3.53	68.12	68.12	12.87	-10.09	-28.91	10.96	12.87	-28.91	-6.80	-6.80	-131.58	-240.62	-327.46	-325.70	-5.70	-327.46
		DI	0.11	0.03	0.16	0.08	0.66	0.085	0.40	0.21	0.29	0.29	0.30	-0.05	0.12	0.28	0.30	0.12	0.06	0.06	-0.05	-0.06	0.01	-0.01	1.33	1.33
		–	–	–	–	–	–	0.00	–	–	–	0.00	–	–	–	–	0.00	0.00	–	0.00	–	–	–	–	–	0.00
		DI	–	–	–	–	–	0.00	–	–	–	0.00	–	–	–	–	0.00	0.00	–	0.00	–	–	–	–	–	0.00
		80	23.02	60.10	38.40	83.71	36.33	83.71	24.74	4.11	75.46	75.46	11.59	-10.89	-31.26	13.31	13.31	-31.26	-7.58	-7.58	-136.79	-250.19	-326.77	-324.54	-6.60	-326.77
		DI	0.04	0.18	0.38	0.29	0.84	0.288	0.45	0.41	0.42	0.42	0.17	0.02	0.21	0.55	0.55	0.21	0.18	0.18	-0.01	-0.02	-0.01	-0.01	1.70	1.70
		90	18.81	57.77	23.96	77.37	28.85	77.37	22.95	3.62	70.11	70.11	10.96	-11.22	-25.93	10.77	10.96	-25.93	-7.22	-7.22	-136.38	-248.60	-320.86	-318.63	-6.91	-320.86
		DI	-0.15	0.13	0.16	0.19	0.46	0.191	0.34	0.24	0.32	0.32	0.11	0.05	0.00	0.26	0.11	0.00	0.12	0.12	-0.01	-0.03	-0.03	-0.03	1.83	1.83
Lane	S	Static	9.92	28.66	15.94	83.18	31.81	83.18	13.29	3.57	36.96	36.96	8.03	-8.29	-24.24	5.81	8.03	-24.24	-5.37	-5.37	-67.90	-151.20	-257.50	-256.26	-33.95	-33.95
		20	14.04	39.47	16.45	96.24	41.69	96.24	11.33	3.50	42.25	42.25	8.69	-7.56	-21.00	5.60	8.69	-21.00	-6.43	-6.43	-101.76	-195.21	-309.64	-307.35	-28.33	-28.33
		DI	0.42	0.38	0.03	0.16	0.31	0.157	-0.15	-0.02	0.14	0.14	0.08	-0.09	-0.13	-0.04	0.08	-0.13	0.20	0.20	0.50	0.29	0.20	0.20	-0.17	0.29
		40	15.24	36.52	19.33	84.40	42.87	84.40	18.36	3.61	50.80	50.80	12.70	-8.81	-25.85	7.92	12.70	-25.85	-6.07	-6.07	-84.20	-168.87	-271.25	-269.92	-25.68	-25.68
		DI	0.54	0.27	0.21	0.01	0.35	0.015	0.38	0.01	0.37	0.37	0.58	0.06	0.07	0.36	0.58	0.07	0.13	0.13	0.24	0.12	0.05	0.05	-0.24	0.12
		60	12.44	38.77	21.84	91.63	54.89	91.63	21.76	3.67	57.98	57.98	14.88	-9.91	-30.55	9.82	14.88	-30.55	-6.48	-6.48	-80.53	-174.53	-301.94	-299.51	-27.29	-27.29
		DI	0.25	0.35	0.37	0.10	0.73	0.102	0.64	0.03	0.57	0.57	0.85	0.20	0.26	0.69	0.85	0.26	0.21	0.21	0.19	0.15	0.17	0.17	-0.20	0.17
		80	10.96	36.35	21.65	97.33	56.33	97.33	20.27	3.68	56.70	56.70	12.77	-8.57	-27.90	5.43	12.77	-27.90	-6.04	-6.04	-72.87	-155.86	-262.29	-260.29	-27.48	-27.48
		DI	0.11	0.27	0.36	0.17	0.77	0.170	0.53	0.03	0.53	0.53	0.59	0.03	0.15	-0.07	0.59	0.15	0.13	0.13	0.07	0.03	0.02	0.02	-0.19	0.03
		85	10.04	35.32	20.32	96.54	52.67	96.54	19.38	3.72	55.81	55.81	12.39	-9.20	-25.71	6.05	12.39	-25.71	-5.90	-5.90	-71.53	-153.16	-260.97	-258.87	-24.61	-24.61
		DI	0.01	0.23	0.27	0.16	0.66	0.161	0.48	0.04	0.51	0.51	0.54	0.11	0.08	0.04	0.54	0.06	0.10	0.10	0.05	0.01	0.01	0.01	-0.29	0.01
Lane	R	Static	33.51	65.99	17.10	40.90	10.05	65.99	12.43	4.06	40.42	40.42	5.90	-8.48	-19.68	9.18	9.18	-19.68	-5.65	-5.65	-232.77	-331.00	-279.90	-272.75	-3.24	-331.00
		20	–	–	–	–	–	0.00	–	–	–	0.00	–	–	–	–	0.00	0.00	–	0.00	–	–	–	–	–	0.00
		DI	–	–	–	–	–	0.000	–	–	–	0.00	–	–	–	–	0.00	0.00	–	0.00	–	–	–	–	–	0.00
		40	41.13	73.02	20.27	44.94	16.08	73.02	16.16	2.93	51.34	51.34	6.95	-10.11	-21.64	10.27	10.27	-21.64	-6.29	-6.29	-238.07	-335.02	-280.87	-279.30	-7.30	-335.02
		DI	0.23	0.11	0.19	0.10	0.60	0.107	0.30	-0.28	0.27	0.27	0.18	0.19	0.10	0.12	0.12	0.10	0.11	0.11	0.02	0.01	0.00	0.02	1.25	0.03
		60	39.74	76.69	22.30	45.37	16.04	76.69	23.37	3.29	66.80	66.80	10.48	-13.43	-24.70	12.51	12.51	-24.70	-6.42	-6.42	-234.30	-334.00	-284.87	-283.05	-6.67	-334.00
		DI	0.19	0.16	0.30	0.11	0.60	0.162	0.88	-0.19	0.65	0.65	0.78	0.58	0.25	0.36	0.36	0.25	0.14	0.14	0.01	0.01	0.04	0.04	1.06	0.04
		80	45.25	86.57	22.01	47.92	16.87	86.57	16.95	2.93	56.41	56.41	6.04	-11.28	-21.86	10.81	10.81	-21.86	-6.91	-6.91	-271.23	-355.60	-285.02	-282.71	-13.99	-355.60
		DI	0.56	0.41	0.29	0.17	0.68	0.312	0.38	-0.29	0.40	0.40	0.02	0.35	0.21	0.28	0.18	0.11	0.22	0.22	0.17	0.07	0.04	0.04	3.32	0.17
		90	37.08	81.39	20.96	44.96	13.99	81.39	16.45	4.03	55.46	55.46	7.91	-11.54	-18.88	8.60	8.60	-18.88	-6.87	-6.87	-266.08	-350.94	-280.22	-278.31	-13.18	-350.94
		DI	0.11	0.25	0.19	0.10	0.39	0.253	0.32	-0.01	0.37	0.37	0.34	0.36	-0.04	-0.06	-0.06	-0.04	0.22	0.22	0.14	0.06	0.03	0.02	3.07	0.14

Table B 14: Neerkol Creek Bridge DI Summary – Road Train 2 (RT2

			GIRDERS						HEADSTOCK				COLUMN						GIRDER DEFLECTION		BEARING COMPRESSION					
													T	C	C	T	T	C								
		MAX	41.26	74.97	29.57	96.37	49.70	96.37	24.69	4.02	72.66	72.66	14.39	-11.67	-29.42	12.94	14.39	-29.42	-7.10	-7.10	-246.47	-352.58	-350.18	-348.93	-34.72	-352.58
		MAX DI	0.27	0.23	0.38	0.18	0.73	0.15	0.72	0.34	0.57	0.57	0.73	0.41	0.35	1.09	1.09	0.35	0.15	0.15	0.15	0.06	0.06	0.06	3.53	0.53
Position	To	Speed	G5	G4	G3	G2	G1	Max	P1HS1	P1HS2	P1HSm	Max	P1CRO	P1CRI	P1CLI	P1CLO	Max	Min	S1G3m	Max	S1G5	S1G4	S1G3	S1G2	S1G1	Max
CL	5	Static	22.52	55.05	21.41	68.17	20.77	68.17	20.53	5.27	59.47	59.47	13.79	-10.23	-27.52	10.98	13.79	-27.52	-7.10	-7.10	-342.28	-261.89	-338.37	-337.23	-6.44	-338.37
		20	-	-	-	-	-	0.00	-	-	-	0.00	-	-	-	-	0.00	0.00	-	0.00	-	-	-	-	-	0.00
		DI	-	-	-	-	-	0.00	-	-	-	0.00	-	-	-	-	0.00	0.00	-	0.00	-	-	-	-	-	0.00
		40	27.53	64.52	29.57	76.73	31.89	76.73	22.00	2.44	56.43	56.43	9.85	-7.93	-26.12	11.72	11.72	-26.12	-6.67	-6.67	-342.48	-230.86	-278.82	-277.24	-4.68	-278.82
		DI	0.20	0.22	0.38	0.18	0.54	0.126	0.07	-0.23	-0.05	-0.05	-0.28	-0.23	-0.05	0.07	0.07	-0.05	-0.06	-0.06	0.00	-0.12	-0.18	-0.18	-0.27	0.00
		60	-	-	-	-	-	0.00	-	-	-	0.00	-	-	-	-	0.00	0.00	-	0.00	-	-	-	-	-	0.00
		DI	-	-	-	-	-	0.00	-	-	-	0.00	-	-	-	-	0.00	0.00	-	0.00	-	-	-	-	-	0.00
		80	24.41	56.47	25.43	70.79	32.20	70.79	24.69	4.02	71.40	71.40	12.41	-9.75	-29.42	12.94	12.94	-29.42	-7.09	-7.09	-340.79	-249.83	-331.86	-329.22	-6.97	-331.86
		DI	0.09	0.08	0.19	0.04	0.55	0.038	0.20	0.23	0.20	0.20	-0.83	-0.09	0.07	0.18	0.18	0.07	0.00	0.00	-0.01	-0.08	-0.02	-0.02	0.08	0.08
		-	-	-	-	-	-	0.00	-	-	-	0.00	-	-	-	-	0.00	0.00	-	0.00	-	-	-	-	-	0.00
		DI	-	-	-	-	-	0.00	-	-	-	0.00	-	-	-	-	0.00	0.00	-	0.00	-	-	-	-	-	0.00
CL	8	Static	21.84	53.08	21.19	69.87	22.30	69.87	17.55	2.77	57.25	57.25	12.87	-9.56	-25.72	10.58	12.87	-25.72	-6.78	-6.78	-139.21	-265.49	-350.18	-348.93	-5.55	-350.18
		20	-	-	-	-	-	0.00	-	-	-	0.00	-	-	-	-	0.00	0.00	-	0.00	-	-	-	-	-	0.00
		DI	-	-	-	-	-	0.00	-	-	-	0.00	-	-	-	-	0.00	0.00	-	0.00	-	-	-	-	-	0.00
		40	22.96	53.85	24.44	72.41	28.21	72.41	24.20	3.12	70.48	70.48	13.25	-11.01	-28.54	10.89	13.25	-28.54	-7.00	-7.00	-139.85	-254.12	-342.40	-340.54	-5.23	-342.40
		DI	0.05	0.01	0.15	0.04	0.31	0.036	0.38	0.12	0.23	0.23	0.03	0.15	0.10	0.03	0.03	0.10	0.03	0.03	0.00	-0.04	-0.02	-0.02	-0.03	0.00
		-	-	-	-	-	-	0.00	-	-	-	0.00	-	-	-	-	0.00	0.00	-	0.00	-	-	-	-	-	0.00
		DI	-	-	-	-	-	0.00	-	-	-	0.00	-	-	-	-	0.00	0.00	-	0.00	-	-	-	-	-	0.00
		80	23.01	54.58	24.78	72.04	29.68	72.04	24.27	3.64	72.66	72.66	12.49	-10.16	-26.72	10.02	12.49	-26.72	-6.88	-6.88	-150.64	-257.67	-339.74	-337.77	-4.36	-339.74
		DI	0.06	0.03	0.17	0.03	0.33	0.031	0.38	0.31	0.27	0.27	-0.03	0.06	0.04	-0.05	-0.03	0.04	0.01	0.01	0.08	-0.03	-0.03	-0.03	0.31	0.31
		94	16.47	54.87	20.38	70.21	25.80	70.21	20.73	3.45	69.60	69.60	13.42	-10.09	-27.19	10.97	13.42	-27.19	-6.90	-6.90	-141.02	-255.09	-337.89	-335.21	-5.11	-337.89
		DI	-0.25	0.03	-0.04	0.00	0.16	0.005	0.18	0.24	0.22	0.22	0.04	0.06	0.06	0.04	0.04	0.06	0.03	0.03	0.01	-0.04	-0.04	-0.04	0.53	0.53
Lane	5	Static	9.22	31.54	15.64	86.84	29.16	86.84	12.66	3.14	37.70	37.70	9.64	-7.06	-23.27	5.36	9.64	-23.27	-5.80	-5.80	-72.09	-161.19	-278.62	-277.63	-34.72	-34.72
		20	6.41	28.51	13.63	86.59	30.47	86.59	11.65	3.48	39.56	39.56	8.62	-6.70	-19.95	4.26	8.62	-19.95	-5.41	-5.41	-69.15	-149.33	-268.98	-267.26	-27.14	-27.14
		DI	-0.30	-0.10	-0.19	0.00	0.04	-0.003	-0.08	0.11	0.05	0.05	-0.11	-0.05	-0.14	0.27	-0.11	-0.14	-0.07	-0.07	-0.04	-0.07	-0.03	-0.04	-0.22	-0.03
		40	11.05	34.10	19.48	87.51	48.34	87.51	18.71	3.40	50.40	50.40	12.34	-8.12	-26.42	6.21	12.34	-26.42	-6.06	-6.06	-70.17	-157.87	-277.61	-275.93	-29.27	-29.27
		DI	0.20	0.08	0.25	0.01	0.59	0.008	0.48	0.08	0.34	0.34	0.28	0.16	0.14	0.86	0.28	0.14	0.04	0.04	-0.03	-0.02	0.00	-0.01	-0.16	0.00
		60	11.56	35.01	21.33	90.85	49.70	90.85	21.65	3.26	59.34	59.34	14.39	-9.23	-28.96	7.01	14.39	-28.96	-6.18	-6.18	-70.16	-156.24	-287.99	-285.79	-30.97	-30.97
		DI	0.25	0.11	0.36	0.05	0.73	0.046	0.71	0.04	0.57	0.57	0.49	0.31	0.24	1.09	0.49	0.24	0.06	0.06	-0.03	-0.03	0.03	0.03	-0.11	0.03
		80	10.52	35.67	19.69	89.56	47.22	89.56	20.88	3.80	59.28	59.28	12.08	-9.96	-28.11	6.64	12.08	-28.11	-6.29	-6.29	-72.59	-161.57	-285.08	-283.01	-30.55	-30.55
		DI	0.14	0.13	0.26	0.03	0.62	0.031	0.65	0.21	0.57	0.57	0.25	0.41	0.21	0.98	0.25	0.21	0.08	0.08	0.01	0.00	0.02	0.01	-0.12	0.02
		95	11.73	38.80	19.62	96.37	49.12	96.37	19.54	3.40	53.59	53.59	12.25	-9.41	-25.86	6.61	12.25	-25.86	-6.67	-6.67	-82.85	-170.67	-296.19	-293.32	-25.45	-25.45
		DI	0.27	0.23	0.25	0.11	0.68	0.110	0.54	0.08	0.42	0.42	0.27	0.33	0.11	0.97	0.27	0.11	0.15	0.15	0.15	0.06	0.06	0.06	-0.27	0.06
Lane	8	Static	32.88	65.20	17.93	44.46	9.56	65.20	11.77	2.92	39.40	39.40	4.75	-9.19	-16.95	6.33	6.33	-16.95	-6.07	-6.07	-246.47	-352.58	-295.56	-294.32	-1.75	-352.58
		20	-	-	-	-	-	0.00	-	-	-	0.00	-	-	-	-	0.00	0.00	-	0.00	-	-	-	-	-	0.00
		DI	-	-	-	-	-	0.000	-	-	-	0.00	-	-	-	-	0.00	0.00	-	0.00	-	-	-	-	-	0.00
		40	41.26	73.02	20.97	41.74	12.50	73.02	16.63	3.25	53.82	53.82	7.10	-10.28	-22.87	11.28	11.28	-22.87	-6.52	-6.52	-239.48	-336.62	-280.86	-279.36	-4.09	-336.62
		DI	0.25	0.12	0.17	-0.06	0.31	0.120	0.41	0.11	0.37	0.37	0.49	0.12	0.35	0.78	0.78	0.35	0.08	0.04	-0.03	-0.05	-0.05	-0.05	1.34	-0.03
		60	38.60	74.97	20.82	42.52	13.70	74.97	17.00	3.11	57.54	57.54	8.25	-10.81	-22.73	10.63	10.63	-22.73	-6.41	-6.41	-235.08	-342.60	-286.25	-284.59	-5.88	-342.60
		DI	0.17	0.15	0.16	-0.04	0.43	0.150	0.44	0.07	0.46	0.46	0.73	0.18	0.34	0.68	0.68	0.34	0.06	0.06	-0.05	-0.03	-0.03	-0.03	2.36	-0.03
		80	38.10	70.77	19.71	43.51	15.13	70.77	17.48	3.45	60.28	60.28	6.07	-10.17	-22.27	10.78	10.78	-22.27	-6.45	-6.45	-238.26	-339.77	-291.88	-288.56	-7.90	-339.77
		DI	0.03	0.09	0.10	-0.01	0.37	0.085	0.49	0.18	0.55	0.55	0.28	0.11	0.31	0.70	0.70	0.31	0.06	0.06	-0.03	-0.04	-0.02	-0.02	3.51	-0.03
		94	30.82	72.84	19.70	45.76	12.83	72.84	20.21	3.91	59.00	59.00	6.72	-11.67	-22.36	12.68	12.68	-22.36	-6.52	-6.52	-238.01	-333.85	-284.05	-282.15	-7.03	-333.85
		DI	-0.06	0.12	0.10	0.03	0.34	0.117	0.72	0.34	0.50	0.50	0.41	0.27	0.32	1.00	1.00	0.32	0.08	0.08	-0.03	-0.05	-0.04	-0.04	3.53	-0.05

B.5 DI Graph – Mid-span of Girders

B.5.1 Lane Travel

Figure B 11: DI – Girder Mid-span Bending Strains (Lane Travel)

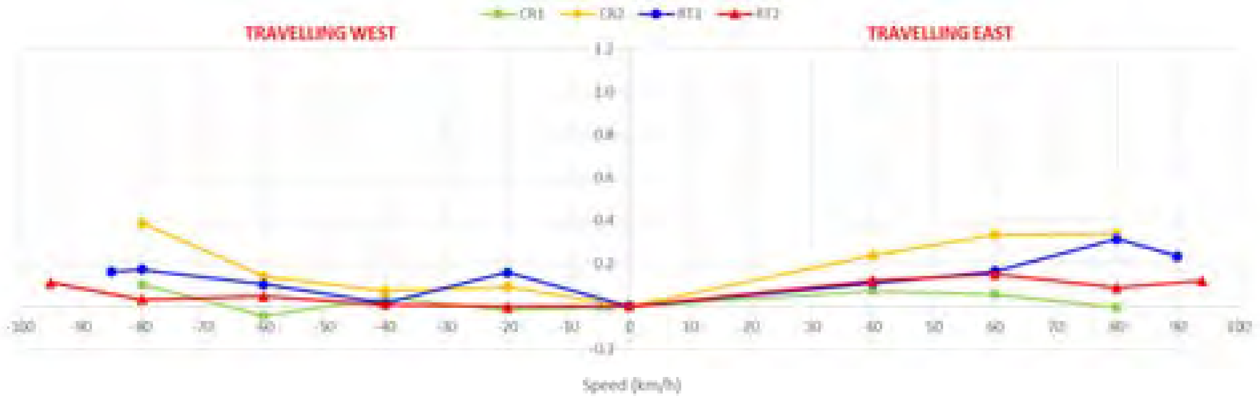

Figure B 12: DI – Girder Mid-span Deflections (Lane Travel)

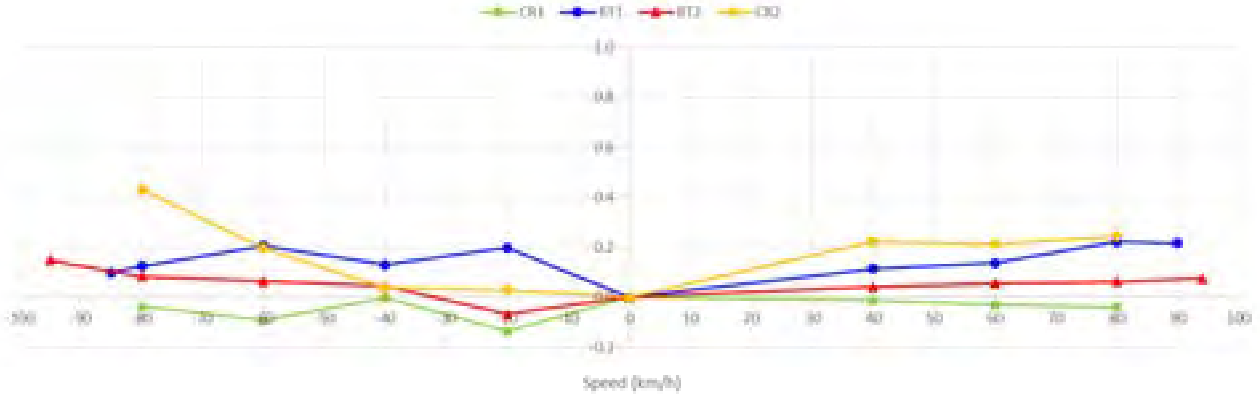

B.5.2 DI Graph – Headstock

Lane travel

Figure B 13: DI – Headstock Bending Strains (Lane Travel)

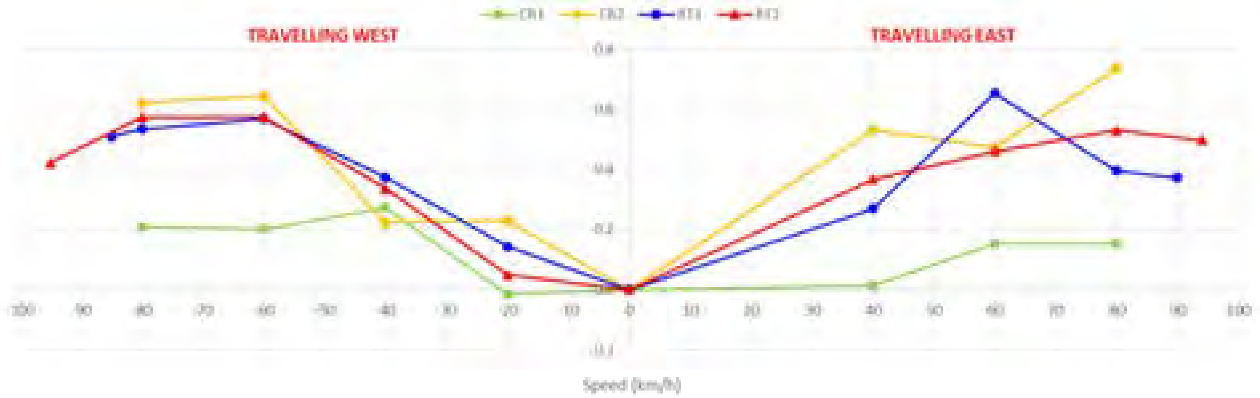

B.5.3 DI Graph – Columns

Lane travel

Figure B 14: DI – Column Tensile Strains (Lane Travel)

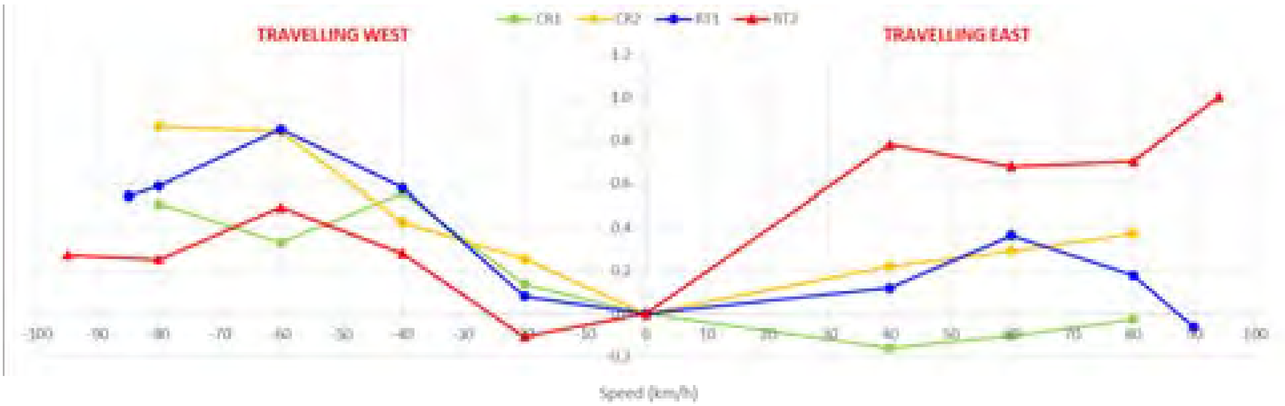

Figure B 15: DI – Column Compression Strains (Lane Travel)

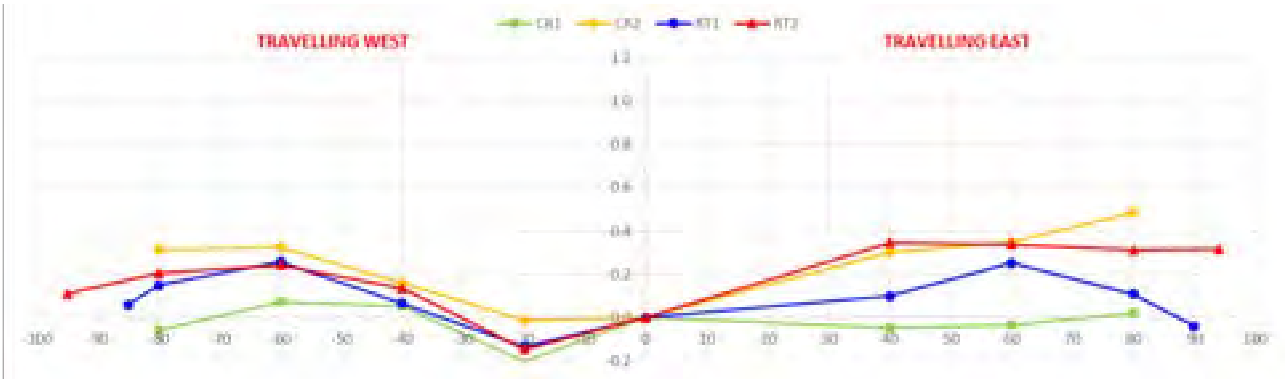

APPENDIX C IN-SERVICE MONITORING

C.1 Introduction/Background

The following sections provide a summary of in-service monitoring data collected for each test bridge. Full details regarding in-service monitoring data can be found in SLR Consulting Reports.

C.2 Setup and Monitoring Summary

To gain an understanding of the performance of each bridge under in-service conditions, a program of continuous monitoring was conducted. The monitoring priorities included:

- peak mid-span girder strains and deflections
- peak strains and deflections of substructure elements
- traffic statistics of vehicles using each bridge, i.e. count, mix of traffic, trends in traffic movement
- identification of any risks posed to each bridge due to high-load traffic events.

In-service monitoring took place at the completion of controlled testing for each bridge, as shown in Table C 1.

Full instrumentation was used for Canal Creek Bridge and Neerkol Creek Bridge. A selection of sensors were used for in-service monitoring of Dawson River Bridge (four channels for bending strains, four channels for deflection, see Figure 3.25).

At the completion of all in-service monitoring, all instrumentation was removed from both bridges.

Figure C 1: Instrumentation selected for in-service monitoring – Dawson River Bridge

Source: ARRB Group Ltd

Table C 1: In-Service monitoring dates

	In-Service Monitoring
Canal Creek Bridge	2-8 May 2014
Dawson River Bridge	14-19 May 2015
Neerkol Creek Bridge	15-20 May 2015

C.3 Canal Creek Bridge

Section 6.2 and Appendix C of the SLR Consulting report provides information on the number of heavy vehicle events recorded during the monitoring period. Histogram plots for each gauge were presented in logical bin sizes, i.e. strains were typically grouped into 5 $\mu\varepsilon$ lots.

Table C 2 shows the recorded number of heavy vehicle events based on the strain data collected for SG6 (the strain gauge most likely under a wheel line of random traffic). A total of 1413 events were recorded, with 562 events greater than 10 $\mu\varepsilon$.

Table C 2: Recorded number of heavy vehicle crossing events

Logging period	Total number of extracted events	Number of events greater than 5 $\mu\varepsilon$ on SG6	Number of events greater than 10 $\mu\varepsilon$ on SG6
Friday, 2 May 2014[1]	211	167	78
Saturday, 3 May 2014	236	183	86
Sunday, 4 May 2014	265	219	97
Monday, 5 May 2014	287	248	120
Tuesday, 6 May 2014	358	294	150
Wednesday 7 May 2014[2]	56	42	31
Total	1413	1153	562

Notes: 1 – approximately 13 hours of data recorded; 2 – approximately 7 hours of data recorded.

Figure C 2 presents an example of the number of heavy vehicle crossing events recorded in a 24 hour period on 6 May. It shows two large vehicle events, one with a strain value of **83 $\mu\varepsilon$** and another with a strain value of **98 $\mu\varepsilon$**. These values are similar to the strains induced by the 48 t crane used for the controlled tests.

Refer to Appendix C of the SLR report for the presentation of data recorded for other strain gauges.

Figure C 2: Count of number of heavy vehicle crossing events on 6 May 2014

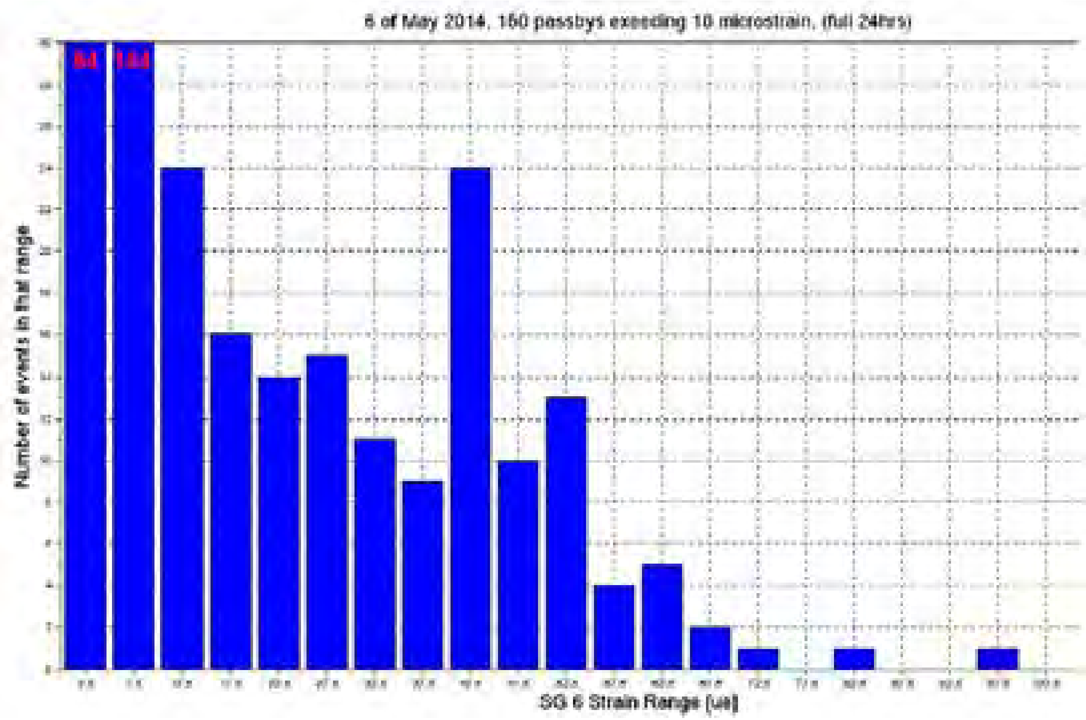

Source: SLR Consulting.

Appendix F of the SLR Consulting report provides scatter plots for the deflection data recorded during the monitoring. The maximum deflection recorded for a kerb unit was **2.4 mm** (on DU1) and for a deck unit was **4.5 mm** (on DU7).

Similarly, Appendix G of the SLR Consulting report presents scatter plots for the strain data recorded during the in-service monitoring. From this data, the maximum strain recorded for a kerb unit was **95 $\mu\varepsilon$** (on DU1) and for a deck unit was **89 $\mu\varepsilon$** (on DU7).

Figure C 3 and Figure C 4 show the scatter plots for the mid-span deflection and strain recorded for deck unit DU7 respectively. Only a small number of events recorded induced large deflections and strains comparable to the maximum values induced by the 48 t test crane in the controlled load tests (3.30 mm deflection and 96 $\mu\varepsilon$ strain).

The monitoring data captured did not indicate emerging patterns from seasonal effects, the preferred direction of travel, or the preference for larger vehicles to travel during low-volume traffic periods.

Figure C 3: Scatter plot for the mid-span deflections of deck unit DU7

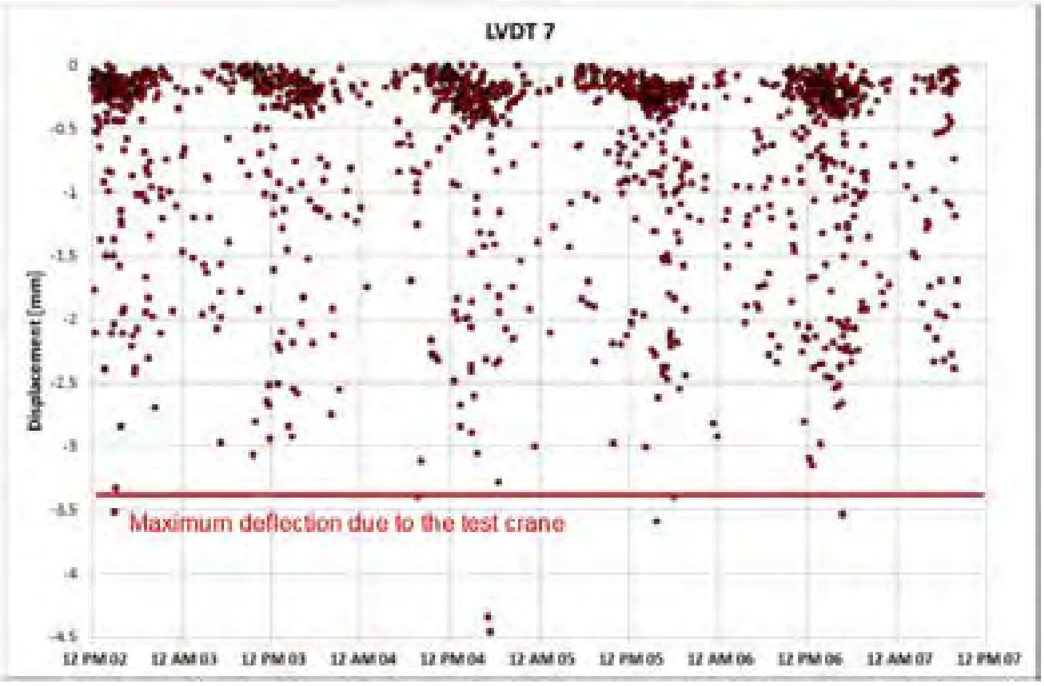

Source: Based on SLR Consulting graph.

Figure C 4: Scatter plot for the mid-span strains of deck unit DU7

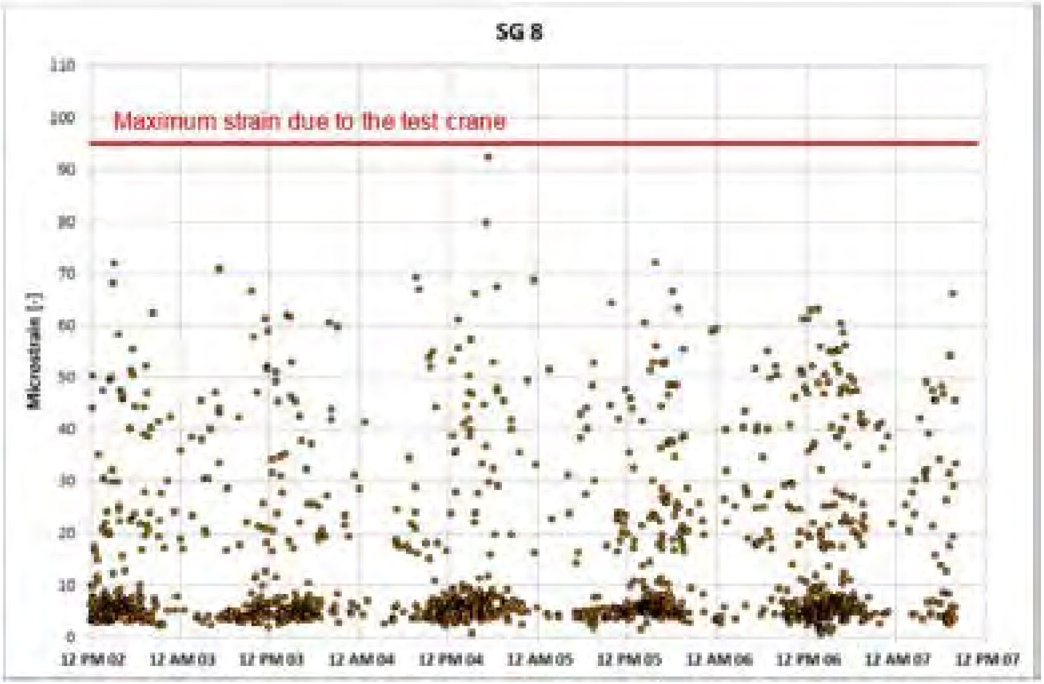

Source: Based on SLR Consulting graph.

In general, the following features were observed from the in-service monitoring data:

- Peak values recorded were similar to those obtained in the controlled tests. This indicates a low risk of excessively large heavy vehicle events crossing the bridge during its service life.
- The predominant number of traffic events induced strains of less than 20 $\mu\varepsilon$.

- High vibration events were recorded.
- Due to the short period of monitoring, the data captured did not provide emerging patterns from seasonal effects or direction of travel.

Figure C 5: Resulting strain waveform based on 90 $\mu\varepsilon$ peak event recorded for DU7

Figure C 6: Resulting deflection waveform based on 90 $\mu\varepsilon$ peak event recorded for DU7

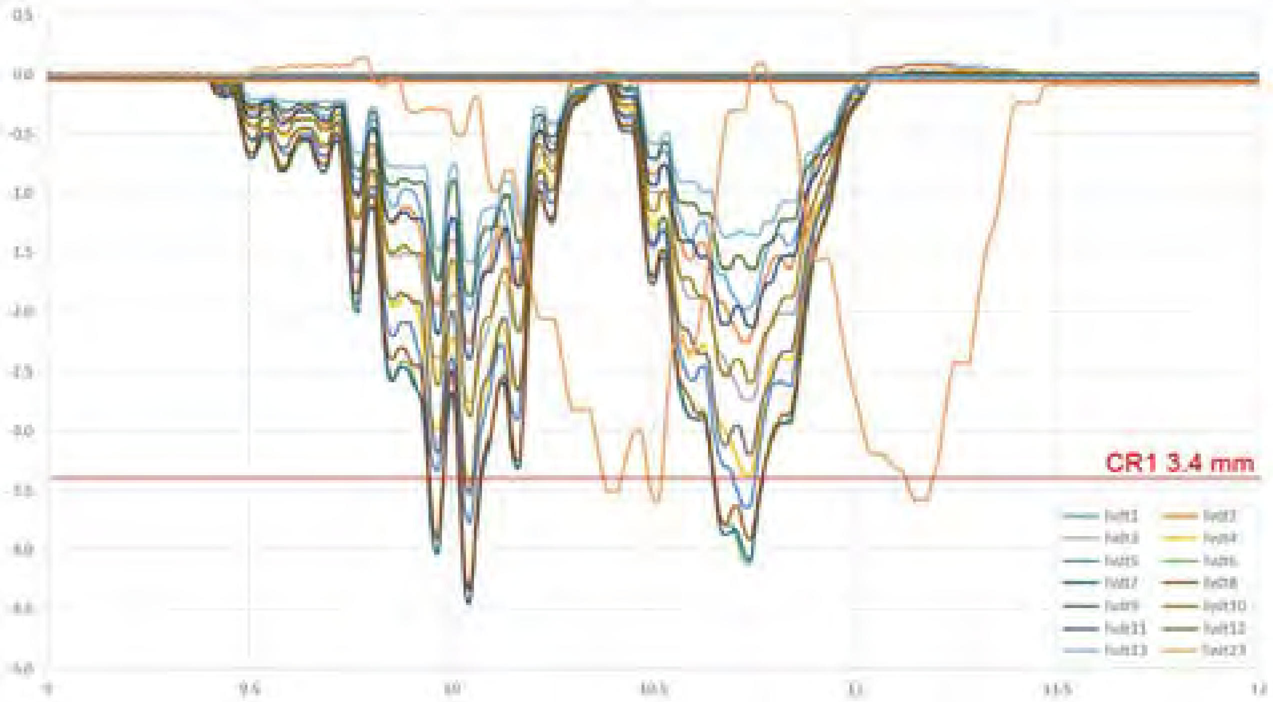

Figure C 7: Distribution of strain across girders based on 90 με peak event recorded for DU7

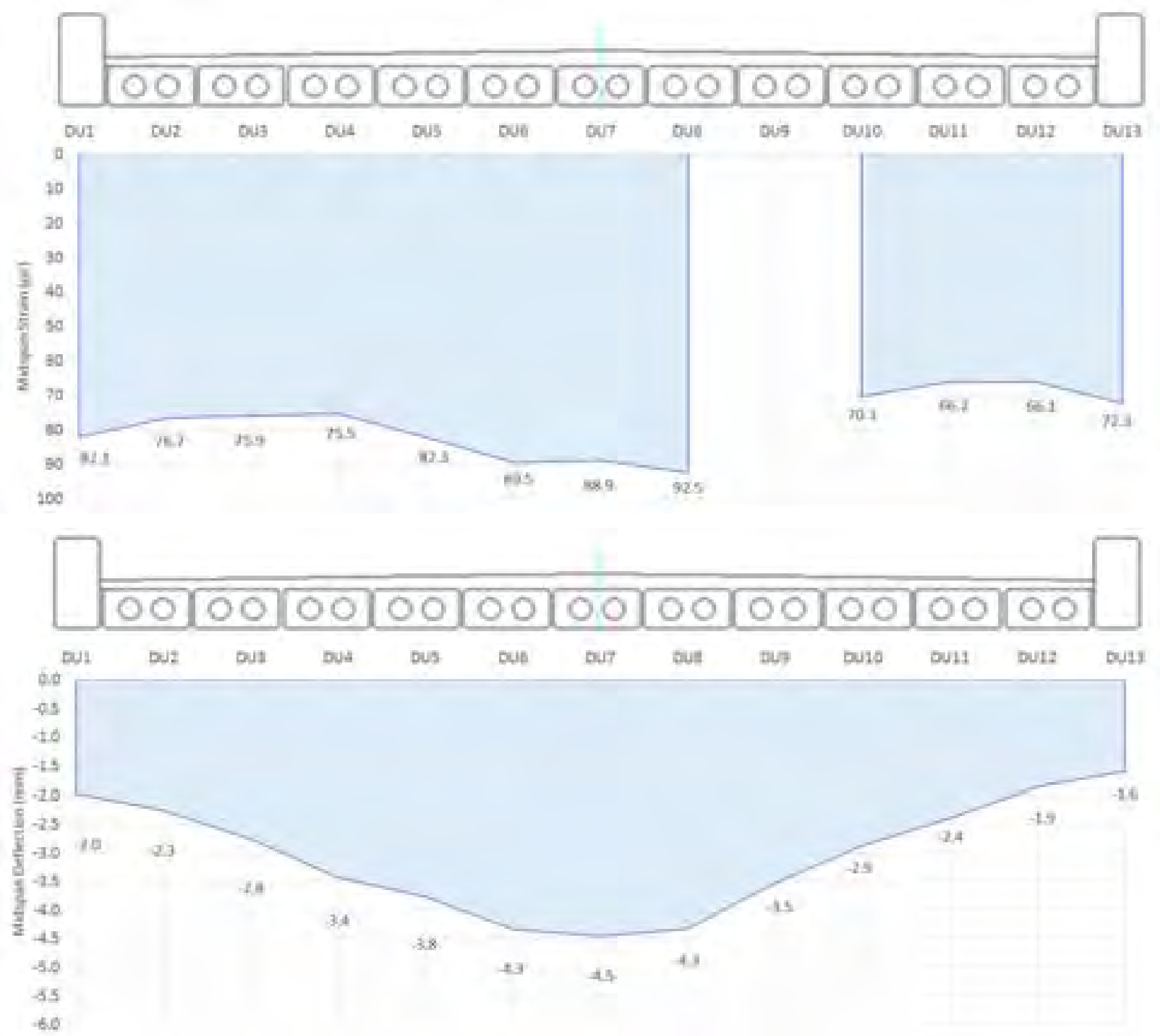

C.4 Dawson River Bridge

Continuous monitoring for Dawson River Bridge took place from Thursday 14 May to Tuesday 19 May 2015. A reduced 8-channel instrumentation set-up was in place for the task, with the priority placed on lane travel to Rockhampton due to the load amplification observed in the controlled tests.

Over 2000 events were recorded, with 260 of the greatest events extracted and reviewed in more detail. These events were based on strains greater than 50 με measured in girder strain gauge S8G4m-sg.

Histograms of all events recorded are shown in Figure C 8 overlaid with peak strains measured in girders for controlled tests. This demonstrates that only two large events produced load effects greater than the peak strain measured for the known test vehicles (83 με). This event, recorded during the monitoring period, is shown in Figure C 9 and Figure C 10, with a peak strain of 123 με in girder G6 and peak headstock deflection of 2.7 mm recorded. The distribution of strains across the girders is shown in Figure C 11. A similar result observed in the continuous monitoring data for Neerkol Creek Bridge approximately two hours later suggests that this load was travelling towards Rockhampton at approximately 60 km/h and was likely to be travelling under a permit. In addition, diurnal effects were observed in the data, with girders hogging with increasing temperature.

Figure C 8: Histogram of events recorded for mid-span bending strains recorded for girder G6

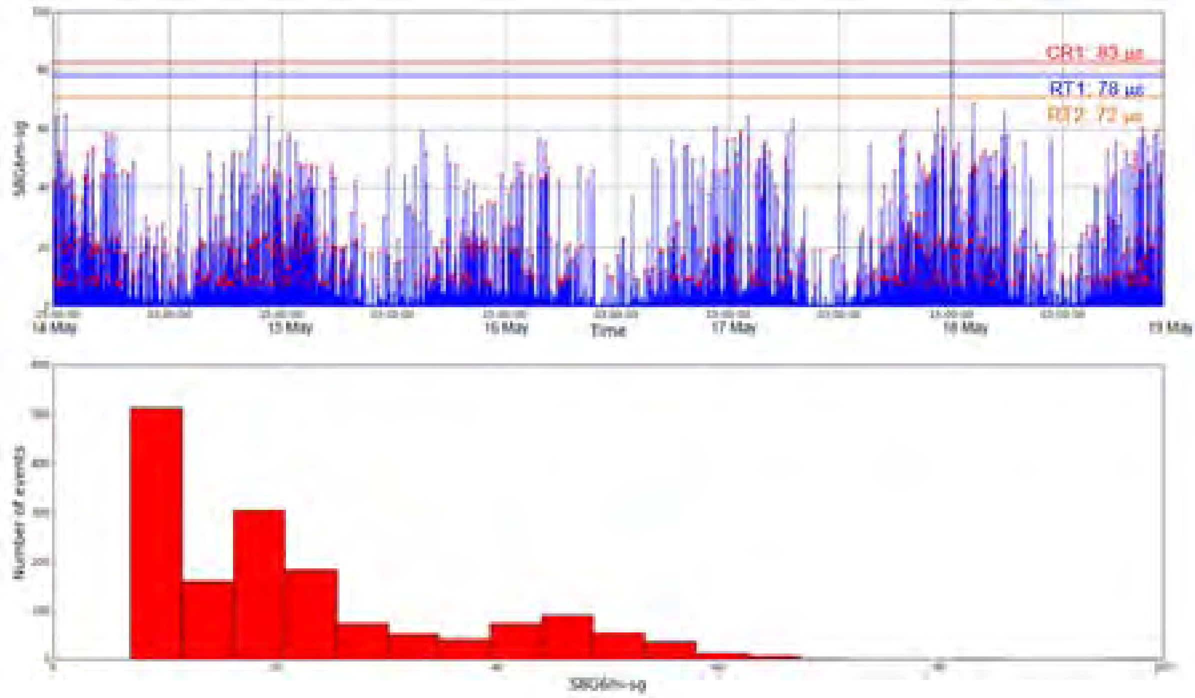

Source: SLR Consulting Dawson River Bridge Load Tests report

Figure C 9: Resulting strain waveform based on 123 με peak event recorded for girder G6

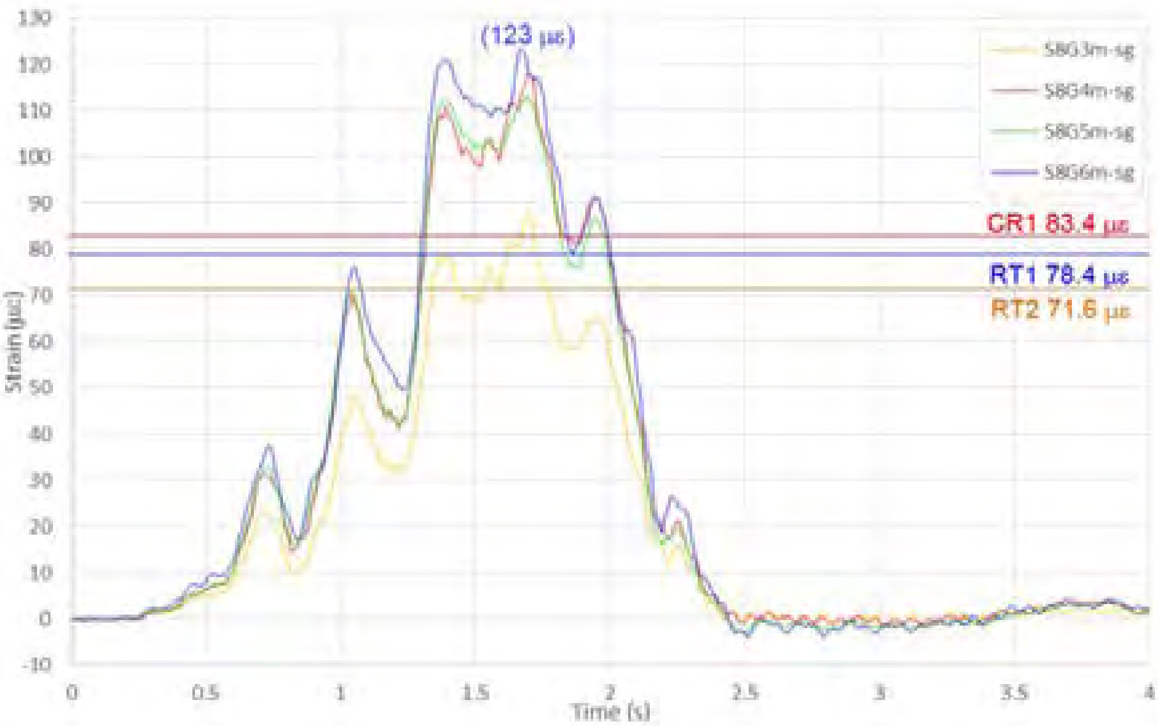

Figure C 10: Resulting deflection waveform based on 123 $\mu\varepsilon$ peak event recorded for girder G6

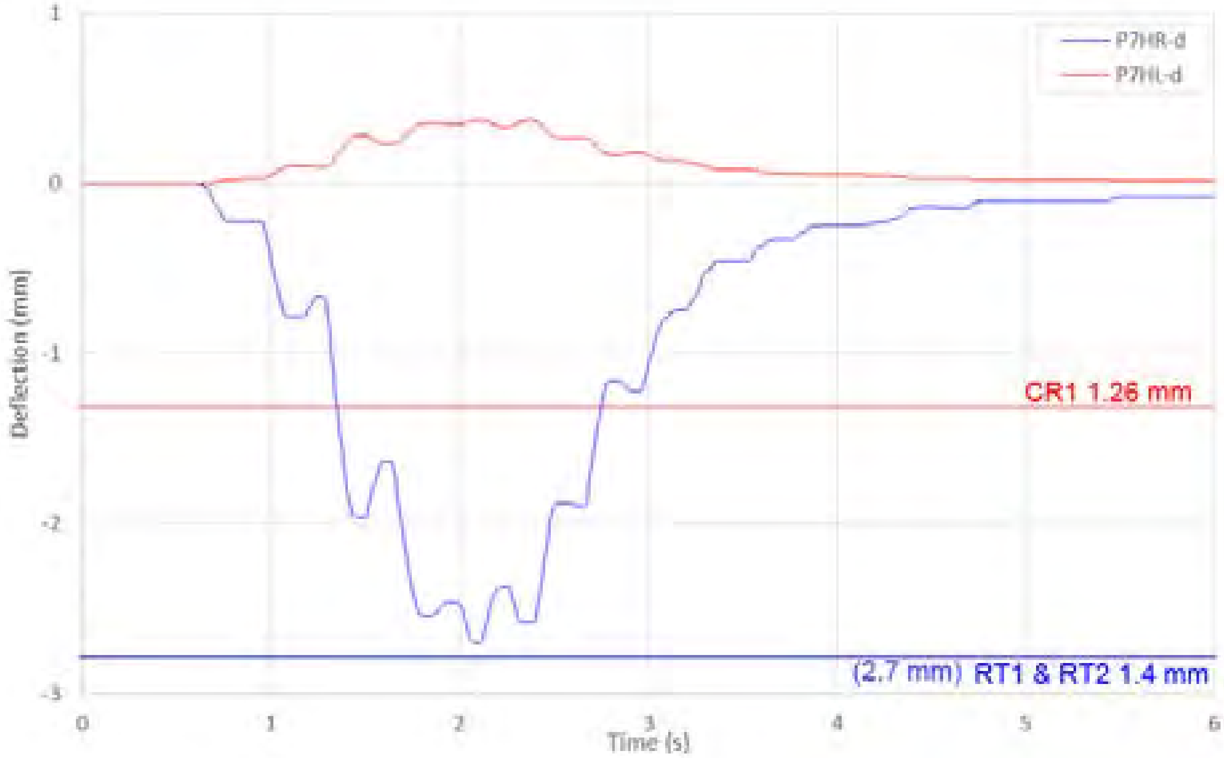

Figure C 11: Distribution of strain across girders for 123 $\mu\varepsilon$ peak event recorded for girder G6

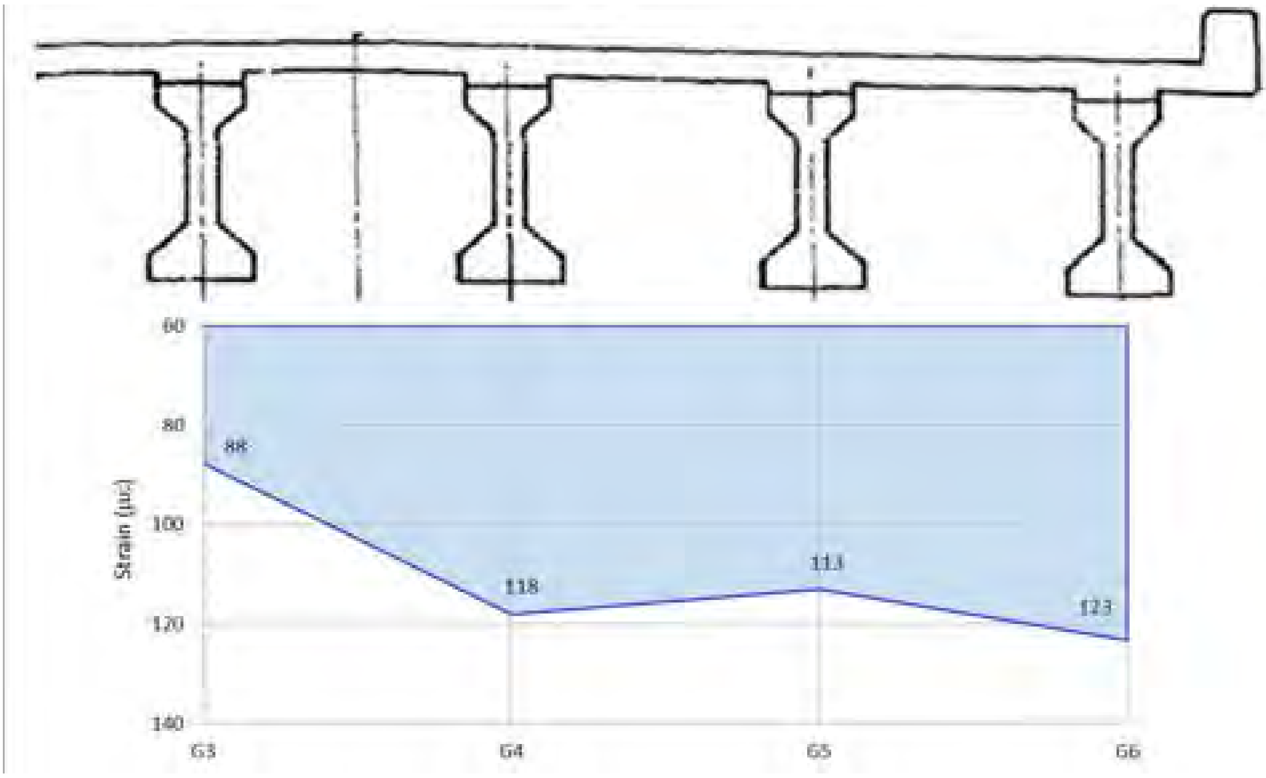

C.5 Neerkol Creek Bridge

Continuous monitoring for Neerkol Creek Bridge took place from Friday 15 May to Wednesday 20 May 2015. Over 2000 events were recorded, with 264 of the greatest events extracted and reviewed in more detail (these events were based on deflections greater than 4 mm measured in girder G3 S1G3m-d).

Histograms of all events recorded are shown in Figure C 12, overlaid with peak deflections measured for girder G3 for controlled tests. Several events exceed these controlled test measurements. One notable event reached 13 mm in girder G3, corresponding to a peak girder mid-span bending strain of 156 με in girder G4 and 171 με in the headstock soffit. The corresponding girder and headstock strain and deflection waveforms are shown in Figure C 13 and

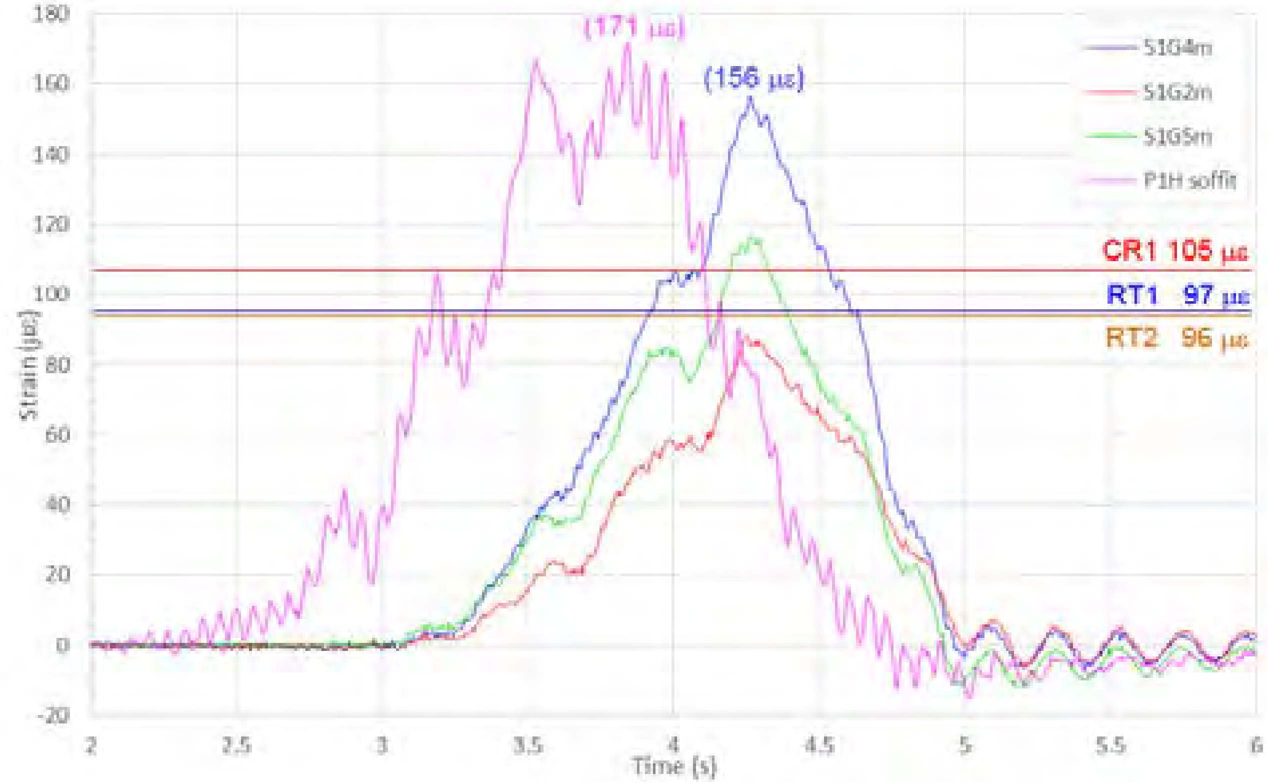

Figure C 14 respectively. The distribution of strains and the performance of the bearings across the girders during this event are shown in

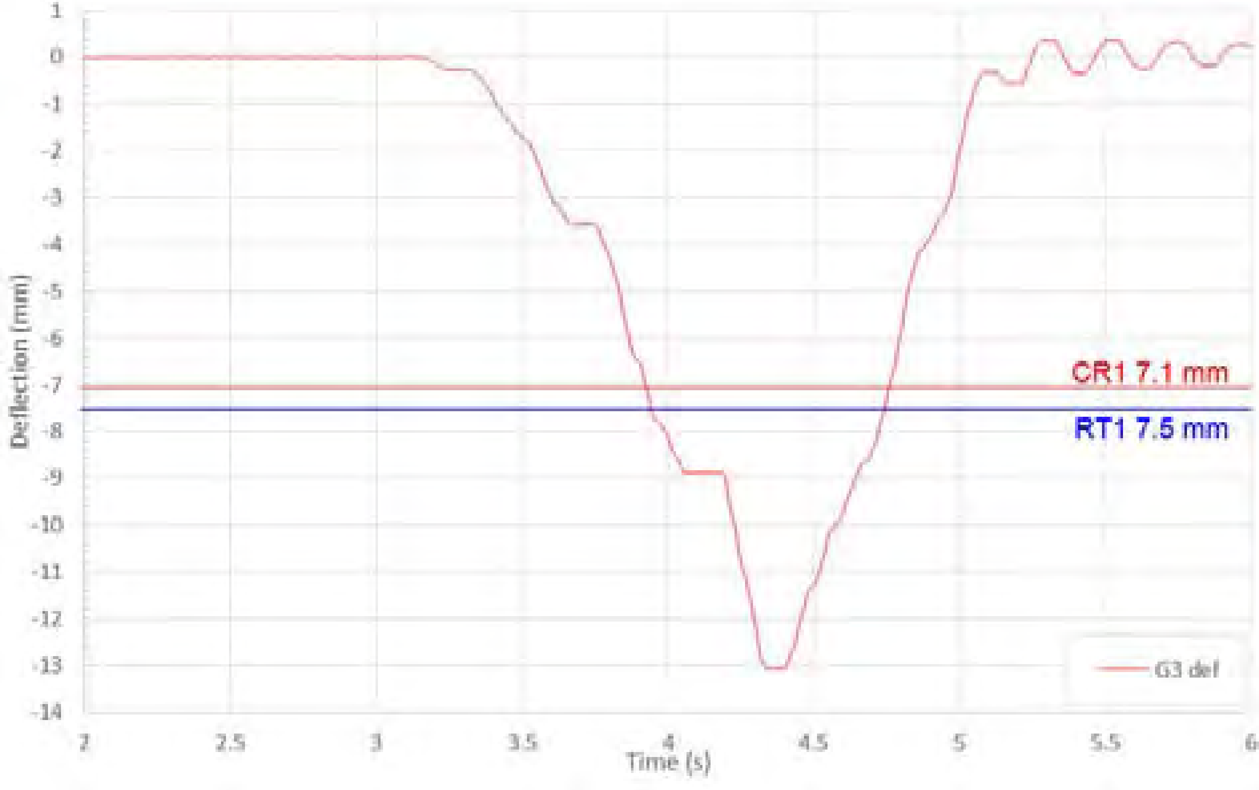

Figure C 15 and

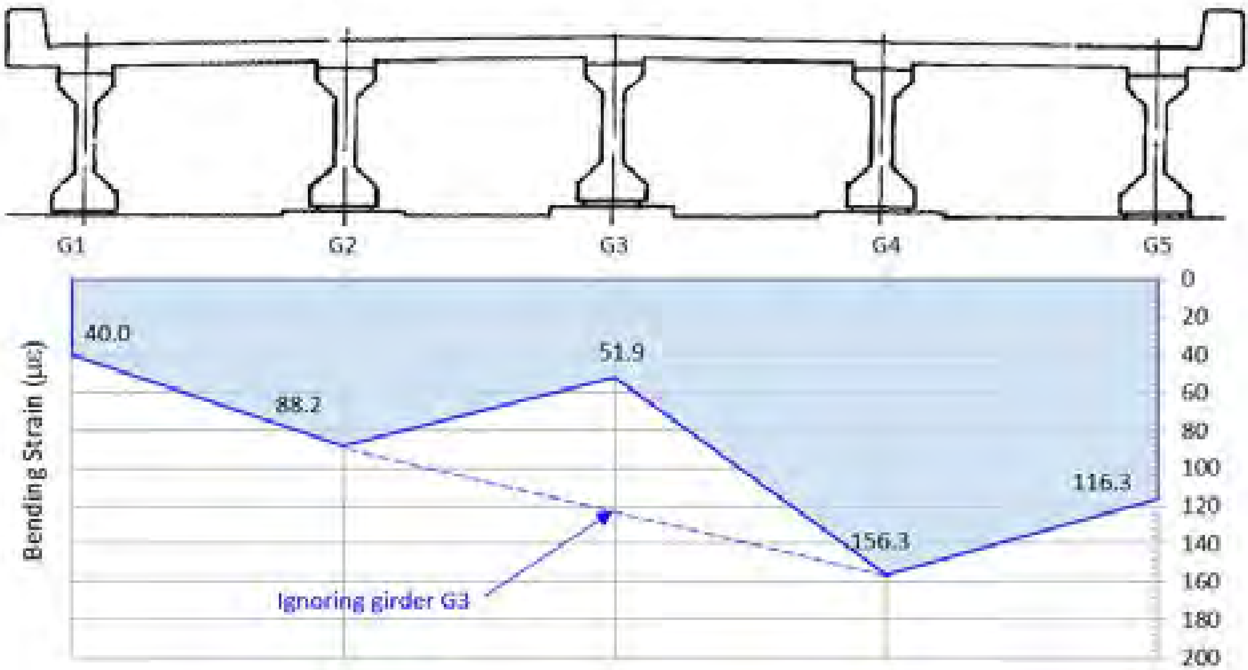

Figure C 16 respectively. Based on the peak event recorded for girder G3 and the load distribution observed in

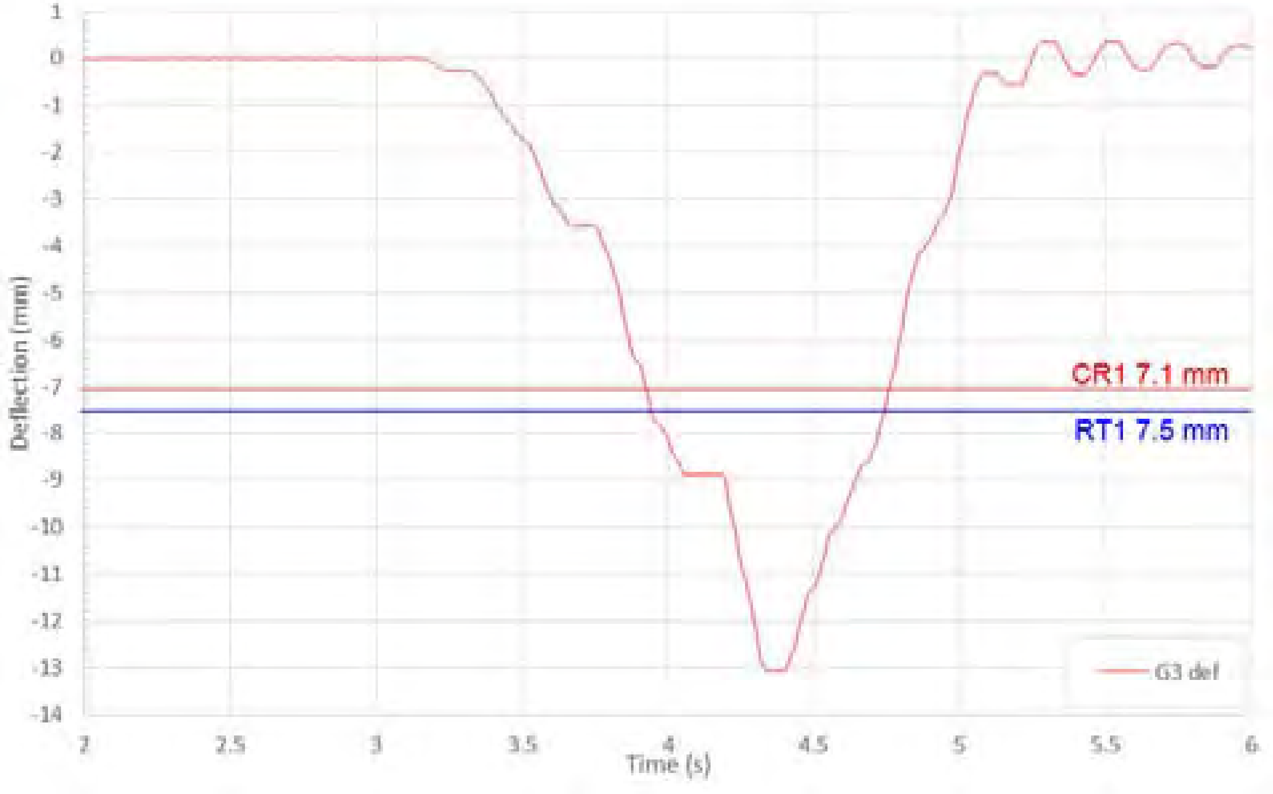

Figure C 15 and

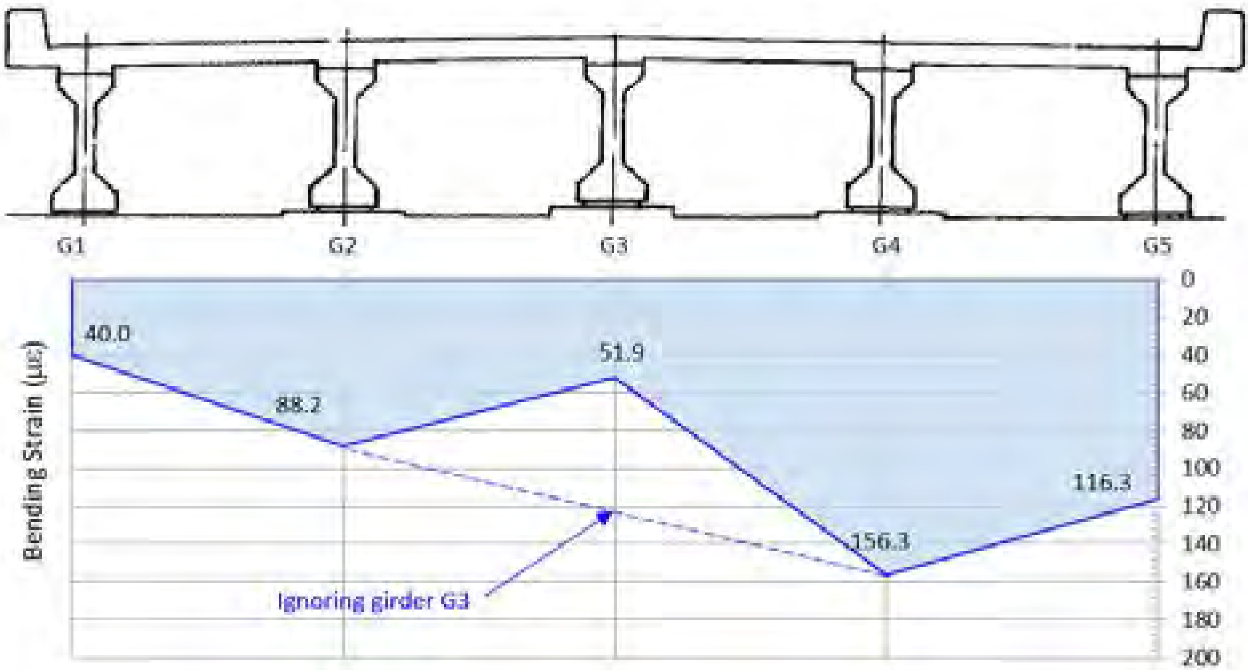

Figure C 16, the deflections for adjacent girders were likely to be greater than 13 mm. Note also the significant peak response of the headstock compared to the girders for this example, as well as the amplified cyclic response.

Based on the data, this load was travelling close to the lane width towards Rockhampton and is a likely match for the large event captured at Dawson River Bridge. Diurnal effects were observed in the data, with girders hogging with increasing temperature.

Figure C 12: Histogram of events recorded for mid-span deflections recorded for girder G3

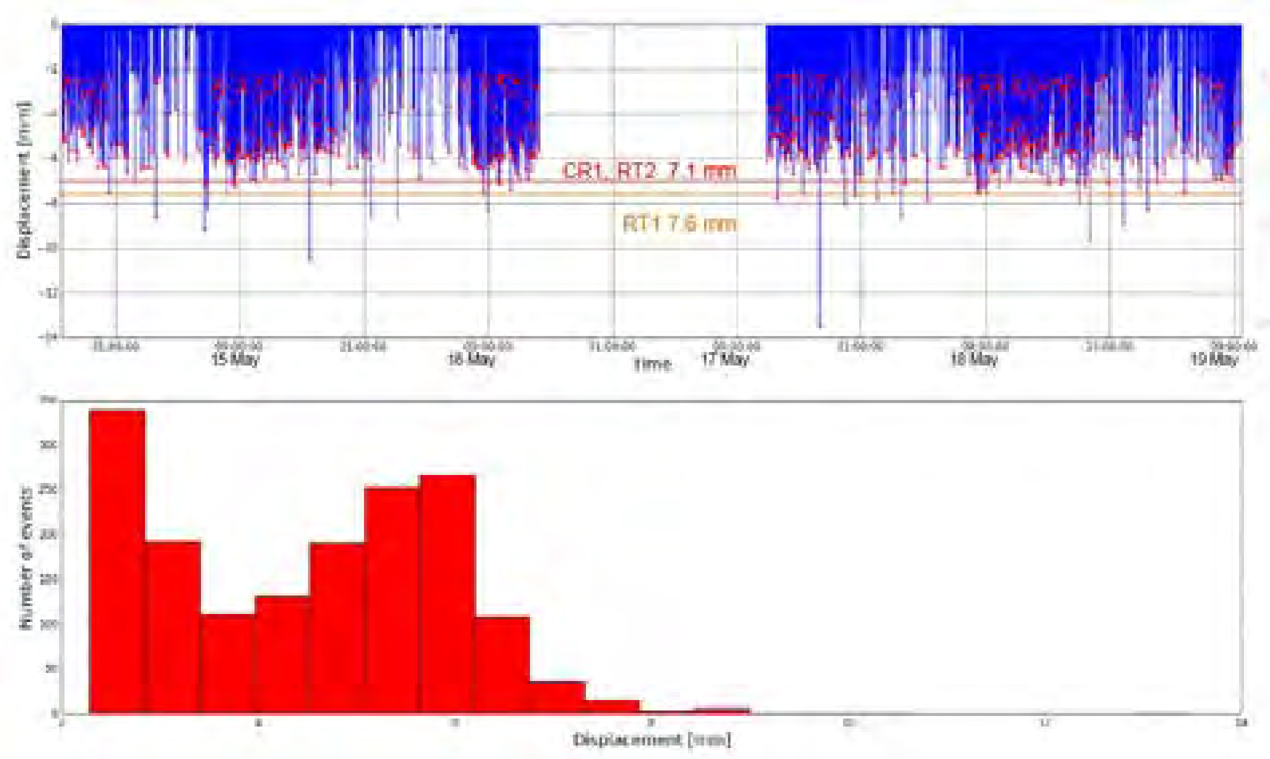

Source: SLR Consulting Neerkol Creek Bridge Load Tests report.

Figure C 13: Resulting strain waveform based on 13 mm peak event recorded for girder G3

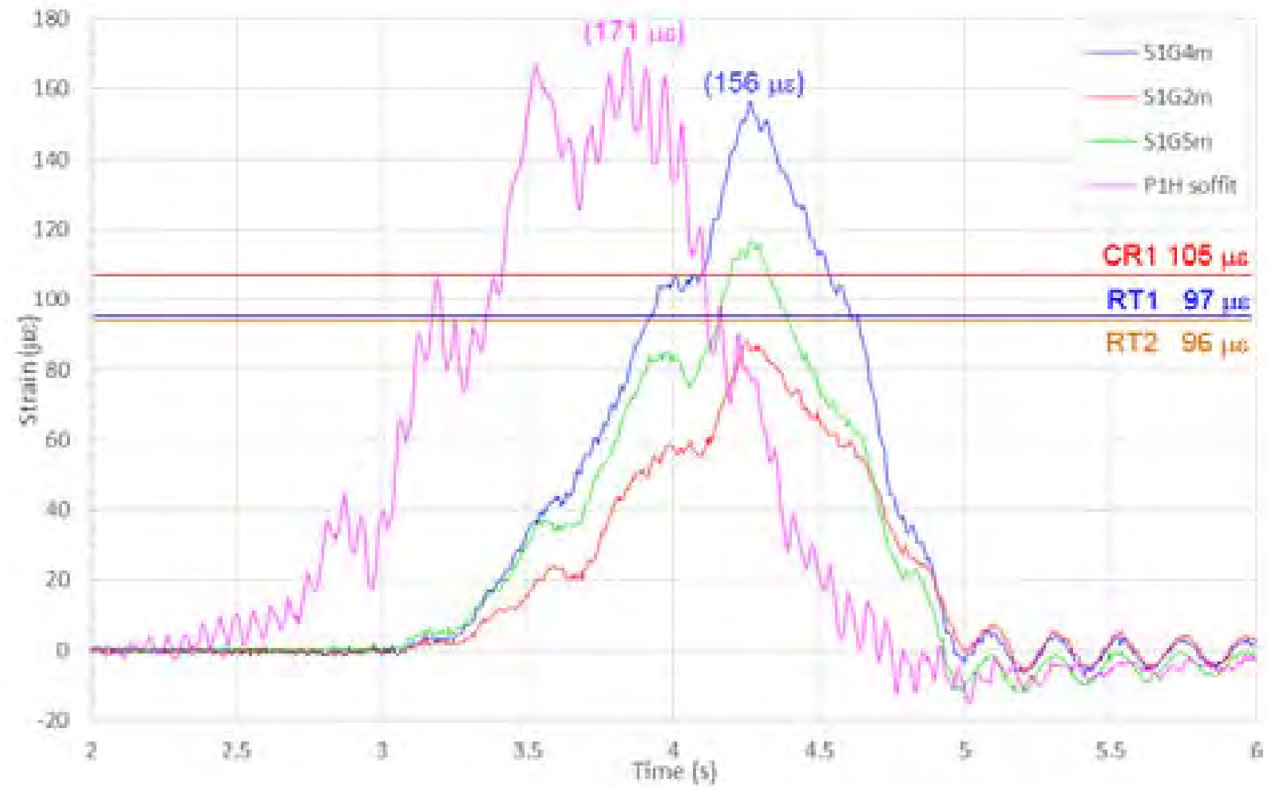

Figure C 14: Resulting deflection waveform based on 13 mm peak event recorded for girder G3

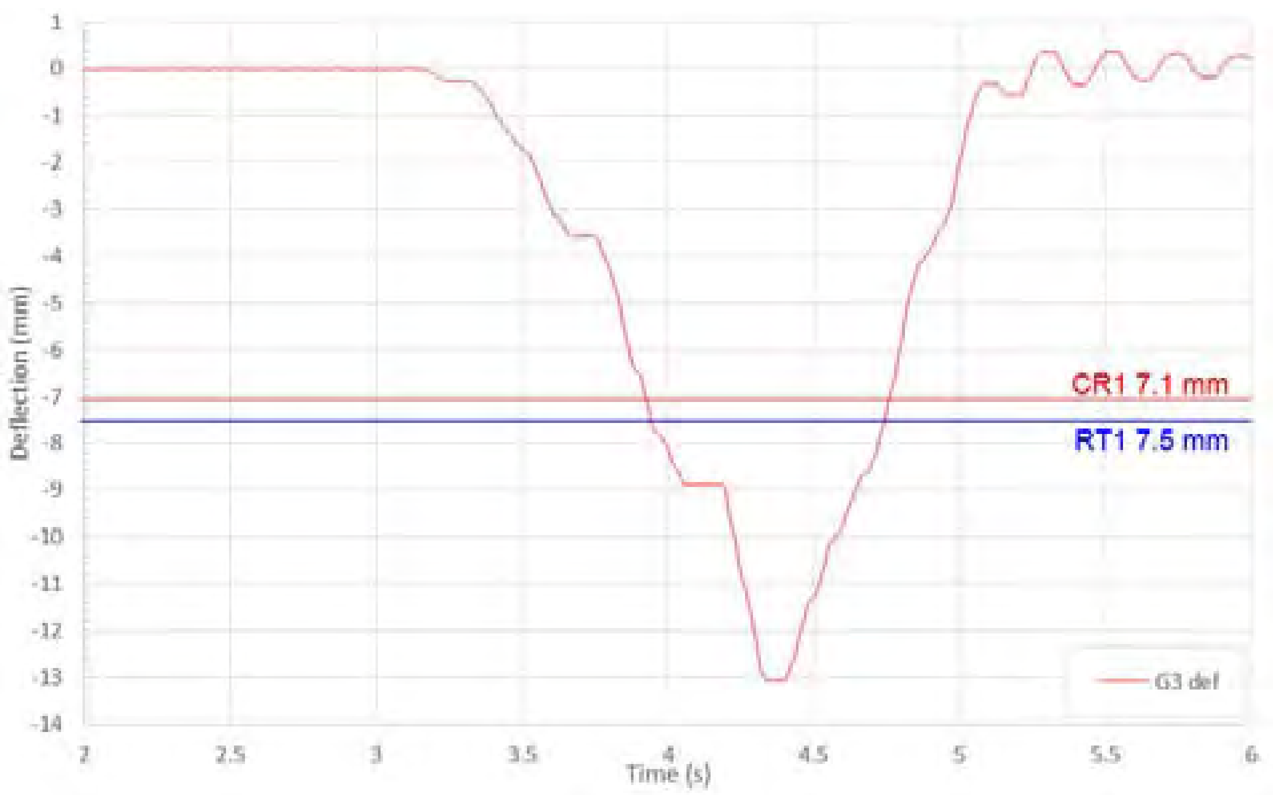

Figure C 15: Distribution of strain across girders for 13 mm peak event recorded for girder G3

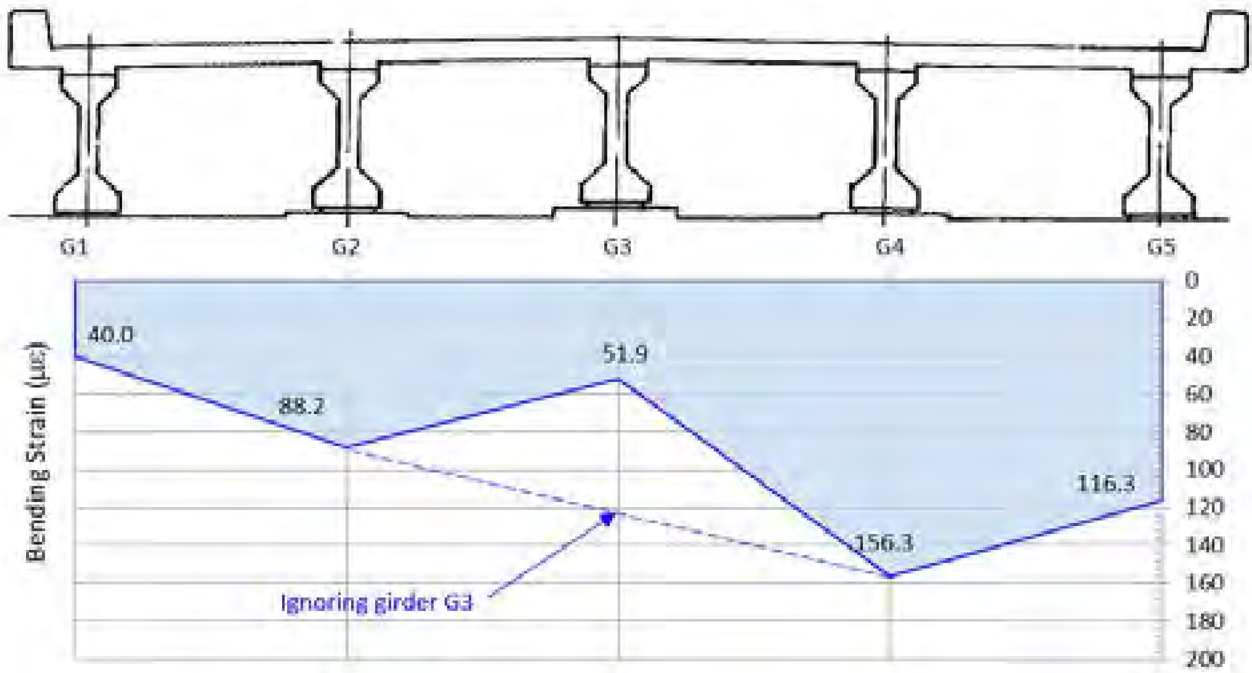

Figure C 16: Bearing compression across pier P1 for 13 mm peak event recorded for girder G3

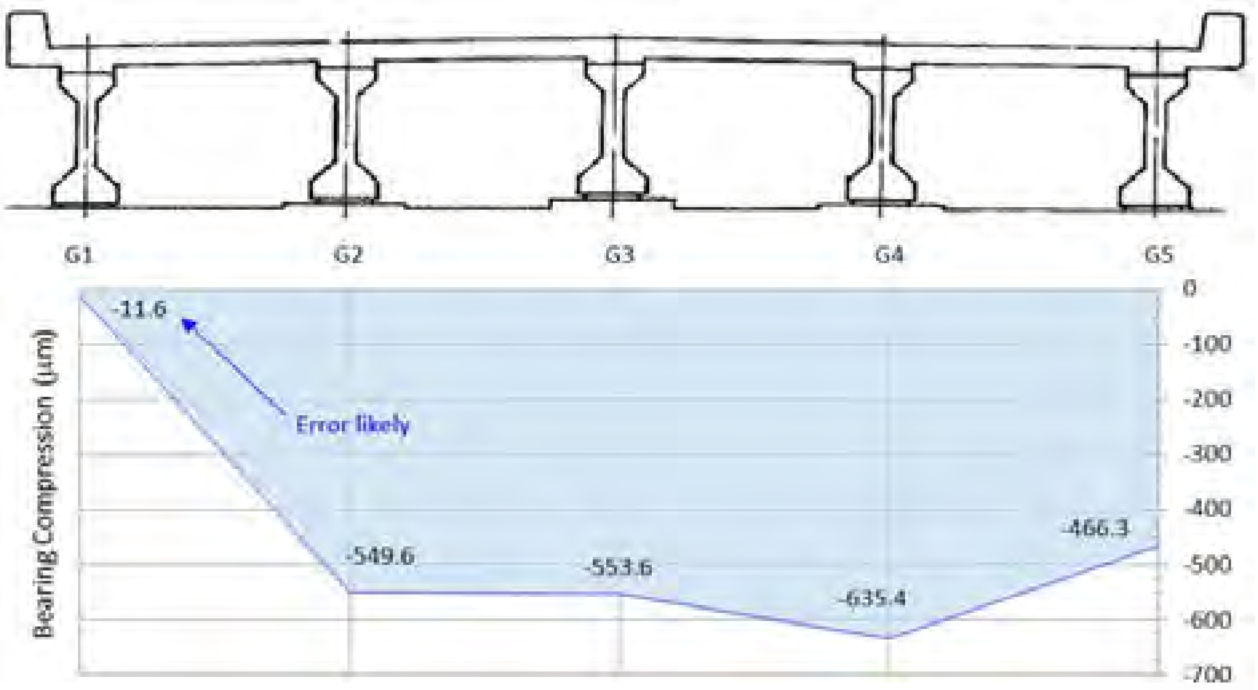

APPENDIX D HISTORICAL INFORMATION/PREVIOUS LOAD TESTS

D.1 Background

The focus of the current project is centred on conducting a load test on a nominated structure with various representative vehicles, with the aim of making recommendations regarding the applicability of the current DLA factor specified by TMR in the assessment of existing structures. However, the results obtained for an individual structure may not be transferable or directly applicable across the whole of the TMR bridge network due to the number of factors that influence the amplification of dynamic loads.

To provide a more informed approach regarding dynamic amplification of vehicle loading, a review of experimental data (based on actual dynamic responses of structures to heavy vehicles) was undertaken. Over the last few decades, a significant number of bridge load tests have been conducted, with particular focus on dynamic load amplification. The majority of these tests have been initiated by the asset owner in response to the advent of increased regulatory mass limits and identified structural deficiencies, the deterioration in condition of older structures, and the large percentage of older timber structures requiring management before replacement. While these individual reports reside with relevant jurisdictions and are traditionally used to inform asset management and maintenance procedures and strategies, holistically a database of combined national information does not exist, to the best of the author's knowledge.

The collation and review of these reports would provide an invaluable reference for TMR and other road jurisdictions in the management of their infrastructure networks. By reviewing and summarising dynamic load amplifications, data trends may be identified which may result in identifying general expectations for bridge dynamic responses according to bridge and vehicle characteristics and road condition. This would be required to take place in conjunction with a review of all relevant network and condition information, and the application of sound engineering judgement. Specific benefits of this review may include:

- the elimination or reduction in the number of load tests required due to the application of empirical knowledge
- the reduction of DLA factors for different vehicle types
- ownership of an extensive international and national bridge performance database with the ability to filter bridges based on structural and vehicle characteristics, materials, and road condition.

Therefore, previous load test reports recording dynamic load amplifications have been collated and reviewed from various national and international jurisdictions. This has included a variety of structures, vehicle types, construction materials, and road profiles. The following sections provide details on the process of obtaining this information, the data capture priorities, jurisdictions that participated in this study, the list of structures reviewed, and the processing and interpretation of the data captured. The main deliverable from this study is the provision of a historical load test database. It also provides for the capture and collation of historical load test data in a document which can be referenced in future, reducing the risk of valuable data and information being lost over time.

D.2 Collation of Data

D.2.1 Background and Literature Review

A number of approaches were adopted to obtain relevant load test reports from various sources. These included:

- requesting information from relevant jurisdictions (national and international)
- conducting a literature search using internal and external search engines and libraries
- the utilisation of knowledge from Dr. Wayne Roberts and Dr. Rob Heywood, previously of Infratech Systems and Services (bridge instrumentation and monitoring contractors).

D.2.2 Response to Survey

Requests for agreement and the provision of relevant information via a survey were sent in November 2013 to the Austroads Bridge Task Force and various international contacts previously contacted in relation to the Austroads project AT 1537 'Bridge Management using Performance Models'.

The following responses were obtained:

Table D 1: Recorded response to issued survey of participants

	International	National
Number of requests sent	TOTAL 141 USA 87 Canada 12 UK 12 Ireland 4 Switzerland 4 Japan 3 France 2 Germany 2 Taiwan 2 Denmark 2 Scotland 2 UAE 1 Spain 1 South Africa 1 Korea 1 Middle East 1 Netherlands 1 Italy 1 Finland 1 Croatia 1	TOTAL 9 QLD NSW VIC TAS SA WA NT ACT NZ
	International	National
Number of responses	12	6

	International	National
	Florida Croatia FHWA New Jersey Canada Saskatchewan Alberta Oklahoma Ohio Ireland Louisiana France South Africa	QLD VIC TAS WA NZ NT
Number of acceptances for participation	8 Ontario, Canada (4 reports obtained) Ohio, US (12 reports obtained) South Africa (4 reports obtained) Saskatchewan, Canada Alberta, Canada Louisiana, US Oklahoma, US Florida, US France	5 QLD (32 reports obtained) WA (5 reports obtained) TAS (17 reports obtained) VIC NT

Of the contacts that responded, the majority were willing to participate in the study and share information. Nationally, the majority of reports were received from QLD, WA and Tasmania, with reports from NSW and SA still pending at the time of this report. Of the reports received from international jurisdictions, only a small number were relevant for the current study.

D.2.3 Literature Review

A significant number of publications were identified and reviewed for information specific to dynamic load amplification. Publications were obtained from a variety of sources, namely:

- transportation research records
- conference proceedings (e.g. Austroads Bridge Conference)
- technical and research papers from journals and publications
- research reports from research institutions and universities
- theses (national and international).

In addition, the review of several significant research reports of similar topic yielded a number of bridges with specific dynamic amplification factors already identified. These reports included:

- OECD – DIVINE Project, Element 6 reports (Barella and Cantieni, 1995; Cantieni et al., 2010; OECD, 1999)
- several additional reports by Cantieni (1983, 1984, 1992)

- several reports by Billing (1982; 1984; 1990)
- a review conducted by Paultre et al (1992).

Previous research by Heywood et al (2000) has also provided a database of dynamic increment test data for various bridges in Australia and Switzerland (as an extension to the DIVINE Project). Whilst thorough, additional data is still required to further validate the findings of this research (as recommended by the authors). The omission of the relationship between DI and structure type, additional vehicle characteristics, and road condition would also improve the validity of this research. This data has been incorporated into the current project work.

D.2.4 Data Capture

Reports and publications collated from information sources outlined in Section D.2.1 were reviewed and a series of bridges were shortlisted for further data interrogation and interpretation. The selection criteria for inclusion in the review process were the following:

- short to medium span length, varying in stiffness and natural frequency
- reports containing information regarding impact factors, dynamic increment, or dynamic amplification factors (or at least the ability to calculate the dynamic increment based on strain or deflection data)
- information pertaining to influencing factors (such as road roughness, construction material, structure type, vehicle suspension characteristics) was considered desirable for inclusion.
- variations in vehicle speed and vehicle type
- unusual or significantly complex structure types were omitted.

Each report varied in details provided, including vehicle configurations, suspension and shock absorber types, vehicle masses, the number of test runs, and a vast amount of information was collated. Information was subsequently streamlined into a single Excel database, containing all critical dynamic information pertaining to each bridge.

The following information was extracted from the load test reports obtained.

- asset information: bridge name, location, road, and asset owner
- construction information: date of construction, bridge geometry and configuration details, number of spans, super and substructure details, and predominant structural material
- bridge dynamic characteristic: first fundamental natural frequency and damping capabilities
- bridge condition
- road condition
- vehicle details: vehicle type, axle configuration, gross vehicle mass, maximum axle load, and suspension type
- load test details: number of tests, direction of travel of vehicles, speed increments, lateral location of vehicles during test, and the inducement of axle hop
- dynamic test results: dynamic increment (DI) calculated, identification of peak or average DI value, location and speed of corresponding peak DI value, notation of unusual results, and strain or deflection-based DI calculation.

Information regarding the first fundamental frequency and damping characteristics was limited in the majority of reports. Where frequency information was not available, and other geometric information was available, the first fundamental frequency was approximated using the relationship shown in Equation 6, based on the length of the bridge span load tested (Heywood 2000). This was to improve the number of data points available for analysis in Section D.3.

$$Frequency, f = \frac{L}{100} \qquad (3)$$

where

f	=	first fundamental frequency, in hertz (Hz)
L	=	length of the test span, in metres (m)

Both peak and average DI values were captured in the database, where such information existed. The method adopted in the majority of reports to calculate DI was based on the formula shown in Equation 4, however in some instances dynamic load amplification was represented by an Impact Factor (Equation 5). Peak DI values were based on either maximum strain or deflection values from individual locations or units (i.e. girders), or as a total value recorded for the entire span or bridge per speed increment. An overall peak DI value was identified in the database for each bridge. Similarly, peak values for vehicle and suspension types were noted.

$$Dynamic\ Increment\ (DI) = \frac{\left(A_{dynamic} - A_{static}\right)}{A_{static}} \qquad (4)$$

where

$A_{dynamic}$	=	maximum dynamic strain or deflection
A_{static}	=	maximum static strain or deflection

$$Impact\ Factor\ (IF) = \frac{A_{dynamic}}{A_{static}} \qquad (5)$$

where

$A_{dynamic}$	=	maximum dynamic strain or deflection
A_{static}	=	maximum static strain or deflection

Data was subsequently checked for consistency and cleansed accordingly to prepare for the following stage of data interpretation, as discussed in Section D.3.

Table D 2: List of bridges selected for review (international)

Bridge name	Bridge details	City/suburb	State	Country	Jurisdiction	Year constructed	Total length (m)	Span length (m)
#MEG-124-6.78	1 span prestressed concrete box girder bridge	Meigs County	OHIO	USA	OHIO	1994	13.72	13.72
Berlin Research Bridge	2 span prestressed concrete (+ fibreglass) girder bridge	Berlin	NA	Germany	NA	-	50.60	25.30
Bumbu Bridge	2 span beam & slab bridge	Lae	NA	PNG	NA	1969	48.00	24.00
Deibuel Bridge	3 span concrete box girder bridge	near Baar (Canton Zug)	NA	Switzerland	EMPA	-	110.30	41.00
D'Hanis Bridge	12 span timber bridge	D'Hanis	Texas	USA	NA	1940	50.50	4.62
Foss Bridge	3 span concrete box girder bridge	NA	NA	Switzerland	NA	-	79.00	31.00
Gariep bridge	15 span concrete beam & slab bridge	Gariep Dam	Northern Cape Province	South Africa	Dept. Water Affairs	1969-1970	210.00	14.00
Sort Bridge	5 span prestressed concrete box girder bridge	Airolo	NA	Switzerland	NA	-	258.80	69.95
Uphapee Creek	7 span concrete beam & slab bridge	Macon County	AB	USA	AB	-	243.20	34.70
Vanderkloof bridge	15 span concrete beam & slab bridge	Gariep Dam	Northern Cape Province	South Africa	Dept. Water Affairs	-	195.00	13.00

Table D 3: List of bridges selected for review (national)

Bridge name	Bridge details	City/suburb	State	Jurisdiction	Year constructed	Total length (m)	Span length (m)
Blythe River Bridge	3 span concrete beam & slab bridge	Burnie	TAS	DIER	-	71.90	20.10
Bridge 631	31 span timber bridge	Toodyay	WA	MRWA	1950	190.00	6.00
Bridge No. 172	2 span timber bridge	Harvey	WA	MRWA	-	11.90	6.20
Bridge No. 4157	3 span timber + concrete bridge	York	WA	MRWA	-	18.90	6.30
Bridge No. 941	1 span timber bridge	Maddington	WA	MRWA	-	8.40	8.40
Brush Creek Bridge	4 span timber bridge	Texas	QLD	TMR	1949	36.45	8.70
Brushy Plains Rivulet	3 span concrete beam & slab bridge	Buckland	TAS	DIER	1972	72.00	23.70
Bullock Head Creek Bridge	2 span concrete beam & slab bridge	Wacol	QLD	TMR	1920s	13.40	6.70
Bulloo River Bridge	3 span concrete beam & slab bridge	Thargomindah	QLD	TMR	1930	27.43	9.14
Burdekin River Bridge	10 span steel truss bridge	Ayr	QLD	TMR	1957	1103.00	76.00
Burrum River Bridge	10 span concrete beam & slab bridge	Hervey Bay	QLD	Hervey Bay CC	1920	94.50	9.45
Camerons Creek Bridge	4 span concrete deck unit bridge	Newcastle	NSW	RMS	-	36.00	9.14
Chiltern Beechworth Overpass	5 span steel + concrete beam & slab bridge	NA	VIC	VicRoads	-	32.00	6.40
Consuelo Overflow No. 1	3 span prestressed concrete deck unit bridge	Rolleston	QLD	TMR	1987	33.00	11.00
Coxs River Bridge	4 span steel + concrete beam & slab bridge	Wallerawang	NSW	RMS	1945	46.10	11.52
Cromarty Creek Bridge	3 span timber bridge	Newcastle	NSW	RMS	-	24.40	9.00
Don River Bridge	3 span concrete beam & slab bridge	Don	TAS	DIER	1940	30.20	12.20
Glendon Brook Bridge	Not available	NA	NSW	RMS	-	NA	Unknown
Inglis River Bridge	2 span concrete beam & slab bridge	Wynyard	TAS	DIER	1973	50.00	24.47

Bridge name	Bridge details	City/suburb	State	Jurisdiction	Year constructed	Total length (m)	Span length (m)
Kennedy Bridge	1 span steel truss bridge	Bundaberg	QLD	TMR	1899	52.00	51.80
Lawsons Creek Bridge	1 span concrete beam & slab bridge	Lithgow	NSW	RMS	-	24.00	23.30
Maranoa River Bridge	9 span steel + concrete beam & slab bridge	Mitchell	QLD	TMR	1956	123.22	13.72
Maroochy River Bridge	14 span prestressed concrete deck unit bridge	Bli Bli	QLD	TMR	1957	166.20	11.90
North Esk River Bridge	1 span prestressed concrete truss bridge	Corra Linn	TAS	DIER	-	31.12	31.00
Paroo River Bridge	5 span concrete beam & slab bridge	Paroo Shire	QLD	TMR	1928	45.72	9.14
Shannon River Bridge No. 1	2 span steel + concrete beam & slab bridge	Miena	TAS	DIER	1938	28.59	Unknown
Shannon River Bridge No. 2	2 span steel + concrete beam & slab bridge	Miena	TAS	DIER	1938	28.59	Unknown
Sorell Causeway Bridge	34 span prestressed concrete girder bridge	Midway Point	TAS	DIER	1957	436.00	12.80
South Esk River Bridge	3 span steel + concrete beam & slab bridge	Fingal	TAS	DIER	-	97.50	42.70
Ward River Bridge	6 span steel + concrete beam & slab bridge	Charleville	QLD	TMR	1963	82.06	13.59
Yarriambiack Creek Bridge	3 span concrete beam & slab bridge	Dimboola	-	-	1927-	-	8.20

D.3 Data Observations and Trends

D.3.1 General Observations

Assessment of the collated data involved the division of data into discrete categories when compared to DI values, allowing trends in data to be identified.

DI values were reviewed against the following categories:

- bridge stiffness characteristics (first fundamental frequency)
- bridge construction type
- structure-critical bridge material type (superstructure)
- vehicle type
- vehicle speed
- vehicle suspension type
- road profile.

Data is presented visually in the form of charts for clarity, focussed predominantly on the relationship between DI value and the first fundamental frequency of the bridge or span. It includes the research previously conducted by Heywood et al (2000), which reflects the above-mentioned categories.

Overall observations of the data after interpretation yield the following trends:

- The majority of DI values were calculated using either peak strains or deflections.
- DI values varied for the same event depending on the use of maximum strain or deflection transducer measurements.
- It was not always clear how DI values were calculated, particularly when referenced in a published article. The use of global (i.e. overall span) or local (i.e. individual girders) maximum or average values was not always specified, leading to an assumption within the database. This may lead to an inaccurate representation of DI (e.g. Paroo River Bridge).

A summary of DI data is presented in Figure D 1. It shows the peak dynamic increment obtained for each bridge against the corresponding fundamental natural frequency. The data presentation is inclusive, making no allowances for structure or vehicle characteristics. The DLA factor of 0.4 adopted by AS 5100 and by TMR is also highlighted. A wide scatter of the data is observed with no immediate trend. Scatter appears to increase with increasing frequency.

The majority of DI values fall below 0.7, with less than 10 bridges recording a peak DI greater than 1. The accuracy of the outlier DI value of 1.5 (at 15 Hz) is questionable, with limited data and background information from the actual report for Paroo River Bridge. Additional outlier DI values (1.09, 1.1, and 1.25) belong to a family of timber bridges with the exception of the deck unit bridge Cameron's Creek Bridge, achieving a DI of 1.4 (at 11.3 Hz). These observations will be discussed further in Section D.4.

Data points are observed to cluster between 2-5 Hz and 8-15 Hz. Data outliers also tend towards these frequency ranges. It has been previously observed that these ranges are consistent with body-bounce and axle-hop frequencies expected for heavy vehicles (Heywood 2000). Where bridge frequencies are similar to these values, frequency matching, or quasi-resonance, is expected which will lead to dynamic amplification, a fact evidenced by the DI values recorded.

To determine whether there are additional data trends and to expand on these initial observations, data has been further interrogated according to structure type, material type, vehicle characteristics, and road profile, which is discussed in the following sections. Note that the following data does not include the data obtained from Heywood (2000).

Figure D 1: Peak DI versus bridge natural frequency (all data)

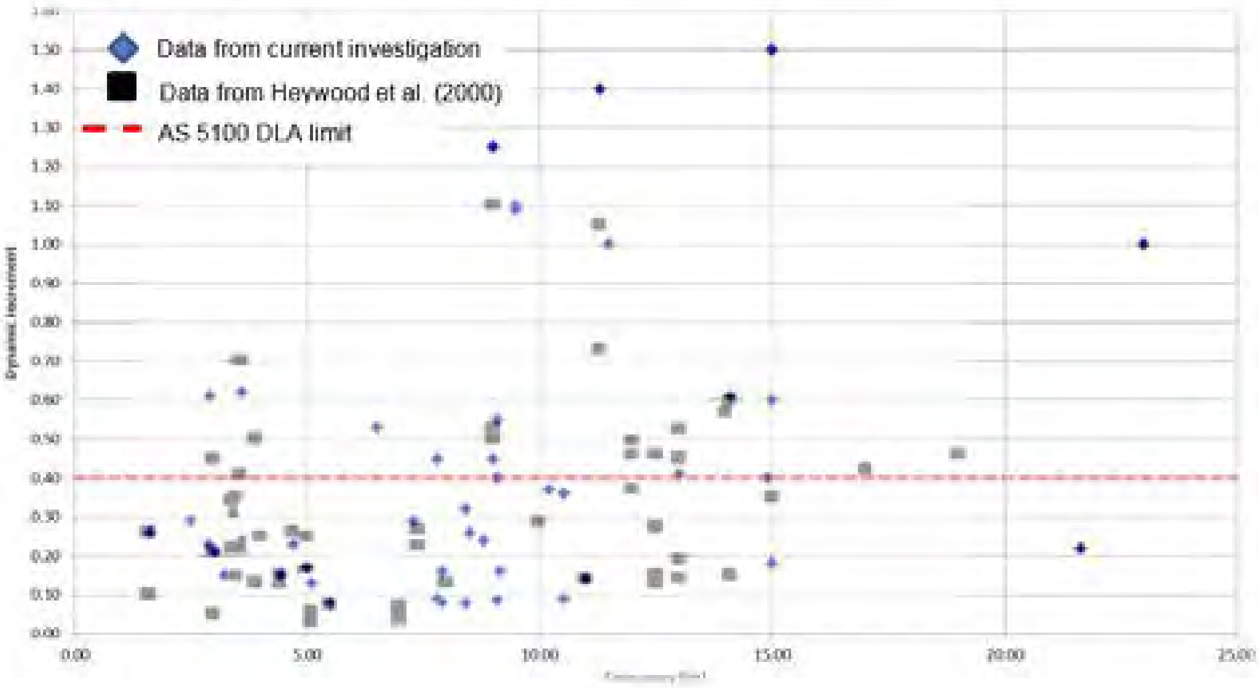

D.3.2 Dynamic Increment vs Structure Type

Figure D 1: has been altered to reflect the common structure types that were encountered during data analysis. This is shown in Figure D 2. Structure types were identified based on the configuration of the superstructure. Six types were identified:

- Beam and slab: I- or T-girders with a deck overlay, predominantly continuous over supports
- Deck unit: series of rectangular units transversely stressed to form a slab deck
- Timber
- Box girder
- Truss
- Girder – no deck overlay, but upper flange of girders form deck after transverse stressing.

Referring to Figure D 2, data scatter was wide for most structure types. Initial trends show that timber structures generally yielded greater DI values (in excess of 0.4) whereas box girder structures are more likely to result in a lower DI (less than 0.4). Recorded responses for deck unit and beam/slab structures were varied, with the majority of structures yielding a DI of 0.6 or less. DI values appeared to increase with increasing frequency. Only a limited number of trusses were included within this dataset, with DI results ranging between 0.2 and 0.6 at similar fundamental frequencies.

A number of outliers were observed in this data. The outlier for the deck unit bridge Cameron's Creek (1.4 at 11.3 Hz) is a possible example of frequency matching between the structure and the vehicle axle hop characteristics. Similarly, the relatively low DI recorded for the timber D'Hanis Rail Bridge (0.22 at 21.65 Hz) is indicative of the vehicle loading and profile over this structure. Bulloo

River Bridge returned a significant peak DI value of 1.0 (at 23 Hz); however the methodology behind the calculation of this value is unknown.

Burdet et al. (1995) has published similar data reviewing structure type versus span length, as shown in Figure D 3, based on European data. It does not include information on DI. Note that the majority of investigated structures are greater than 20 m in span, which is the opposite of findings across Australia's bridge network collectively.

Figure D 2: Peak dynamic increment versus bridge natural frequency (bridge type)

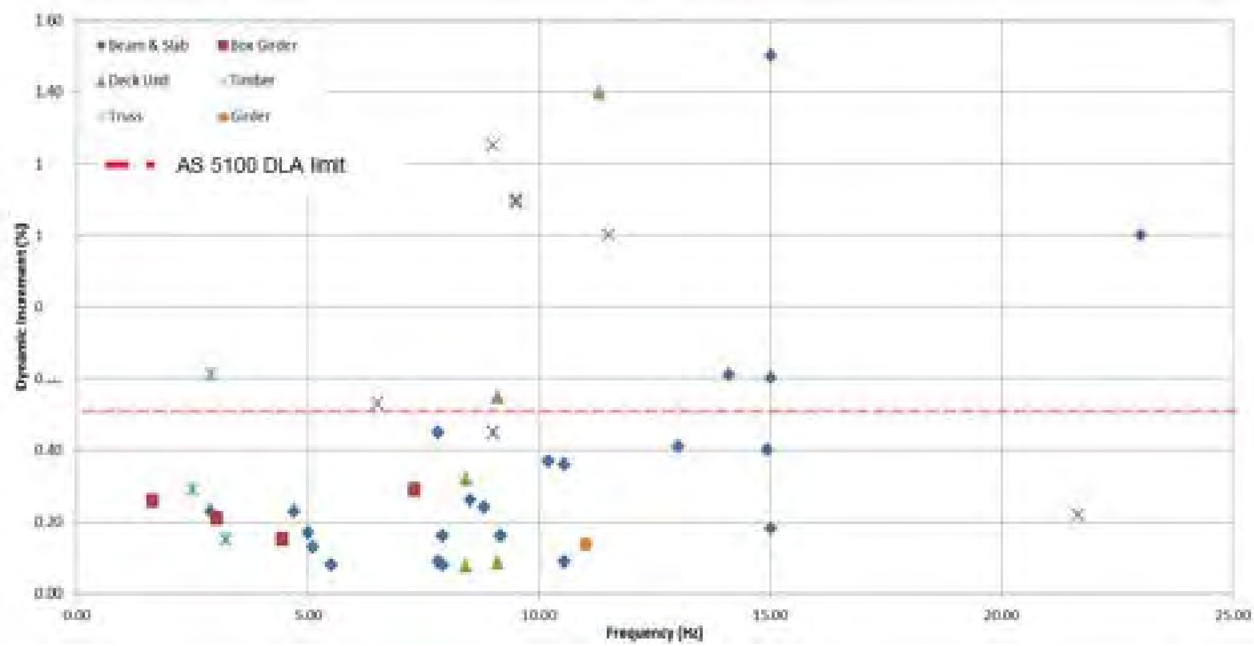

Figure D 3: Natural frequency of different bridge types as a function of bridge span

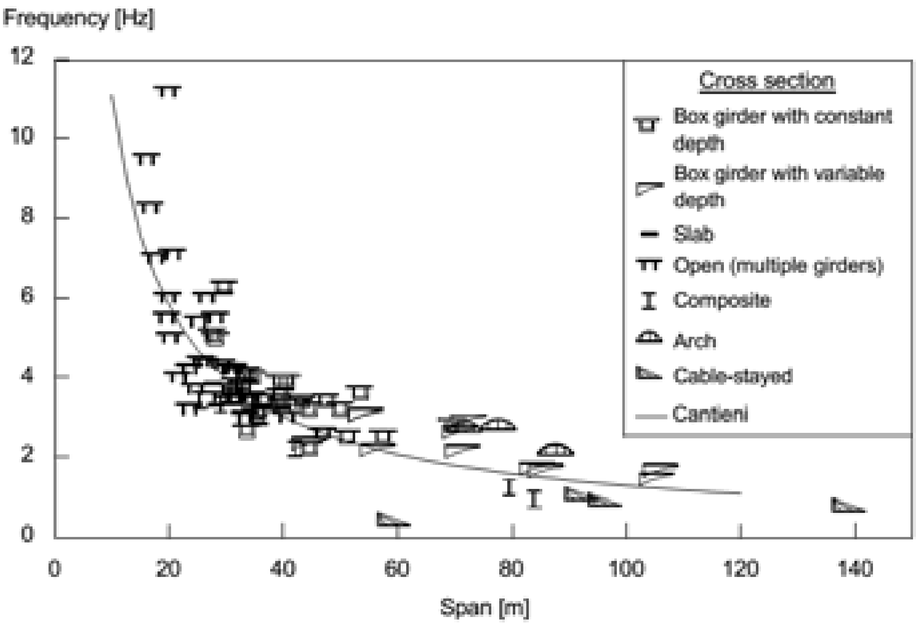

Source: Burdet et al. (1995).

D.3.3 Dynamic Increment vs Structure Material

As an extension to structure type, DI values were reviewed against the predominant superstructure material. Bridges were divided into 5 predominant material types:

- concrete – includes reinforced and superstructure combinations between reinforced and prestressed concrete for beam-slab structure types
- steel and concrete – accounts for steel and in situ concrete combinations (typical for beam-slab structure types)
- prestressed concrete – for superstructures comprised entirely of prestressed concrete
- steel – where the entire superstructure comprises steel (effectively every steel truss structure)
- timber.

The results are shown in Figure D 4. DI results for timber and steel materials mimic those recorded for timber and truss structure types respectively. Results for prestressed concrete and steel/concrete material types are all less than 0.6 regardless of frequency, with the majority less than 0.4.

Concrete structures show greater data scatter, with values ranging from 0.05 to 1.5 across a diverse frequency range. A division of DI response was observed, with the majority of structures less than 10 Hz fundamental frequency yielding DI values less than 0.4, subsequently increasing with increasing frequency, peaking at 15 Hz.

Figure D 4: Peak dynamic increment versus bridge natural frequency (material type)

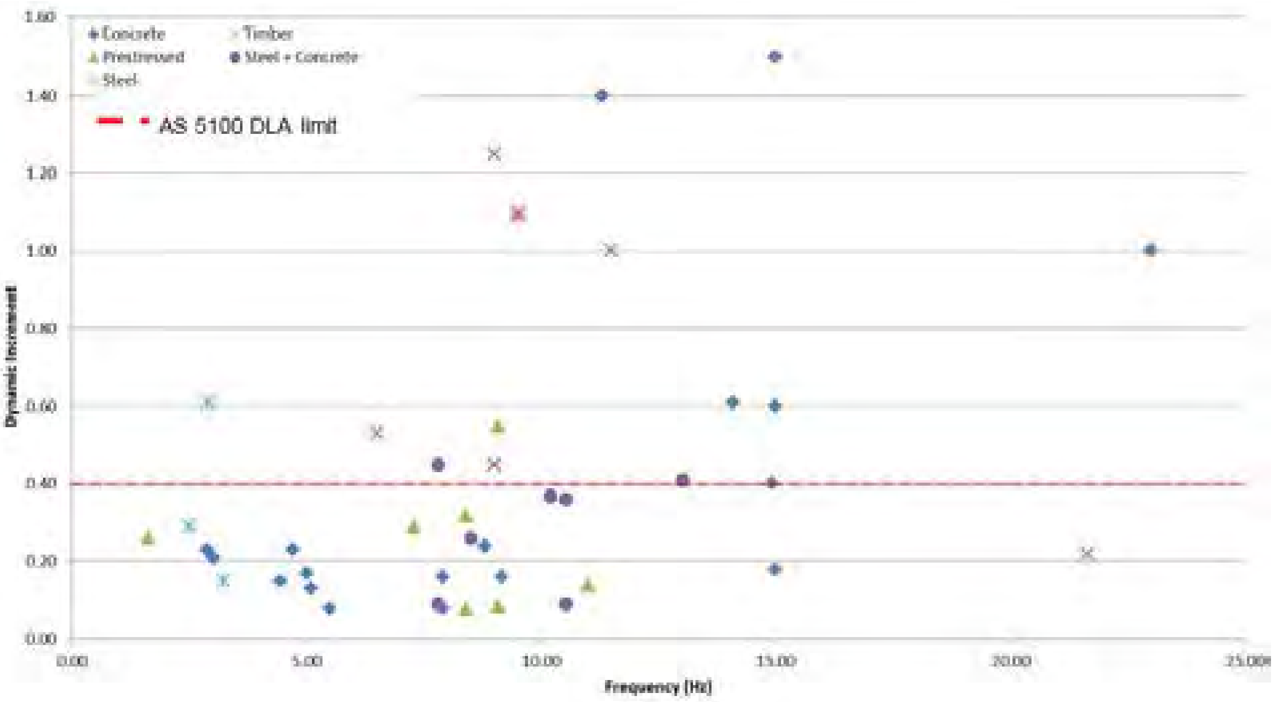

Trends in superstructure material type have been reviewed previously by Heywood (2000), and the results for peak DI values are summarised in Table D 4. These are in general agreement with the observations made in this document.

Table D 4: Summary of DI information for superstructure material types captured by Heywood (2000)

Superstructure material type	DI information
Reinforced concrete	▪ Data clusters at 3-4 Hz, 11-14 Hz ▪ Wide range of peak DI values
Prestressed concrete	▪ Data clusters < 5 Hz and at 11 Hz ▪ For f < 5 Hz, peak DI less than 0.4 ▪ Peak DI values ranged between 0.15 and 1.05
Steel & reinforced concrete	▪ Wide frequency range of data ▪ All peak DI values less than 0.5 ▪ No DI peak/frequency matching trends observed
Steel	▪ All peak DI values less than 0.5, less than 10 Hz frequency ▪ All peak DI values less than 0.5 ▪ Maximum DI 0.45
Timber	▪ Data clusters around 3.5 Hz and between 7-10 Hz ▪ Majority of results less than 0.6 ▪ Maximum DI of 1.1

Source: Heywood (2000).

D.3.4 Dynamic Increment vs Vehicle Type

The peak dynamic response of each bridge to each test vehicle is summarised in Figure D 5. Data clusters of DI values are once again evident at frequencies between 2.5-5 Hz, and 8-15 Hz. Both rigid and semi-trailer vehicle types exhibited DI values mostly less than 0.4 and 0.6 at 2-5 Hz and 8-15 Hz respectively. Low loaders induced a significant dynamic response (0.5 – 1.25), whereas cranes and locomotives consistently produced DI values less than 0.4 and 0.2 respectively.

Data was further interrogated for the influence of vehicle suspension types. The data shown in Figure D 5 has been reconfigured to highlight the varying responses of structures to different vehicle suspension systems (presented in Figure D 6). Most notable is the structural dynamic response to semi-trailers with air or steel suspension. For air-suspension semi-trailers, the majority of DI values were less than 0.4 for all frequencies, with the exception of those between 8-12 Hz (including one outlier value of 1.4 at 11.3 Hz for Cameron's Creek Bridge). Similar results were observed for all rigid vehicles with air-suspension.

Data was more scattered and extreme for steel-suspension semi-trailers, particularly with increasing frequency. Note that the peak in DI values between a frequency range of 8-15 Hz is attributable to steel-suspension vehicle types only (with the one exception of the air-suspension semi-trailer, attributable to a depression adjacent to the abutment in the lane of travel). As identified previously in Figure D 5, the pneumatic suspension system of the cranes has resulted in low DI values.

Figure D 5: Peak dynamic increment versus bridge natural frequency (vehicle type)

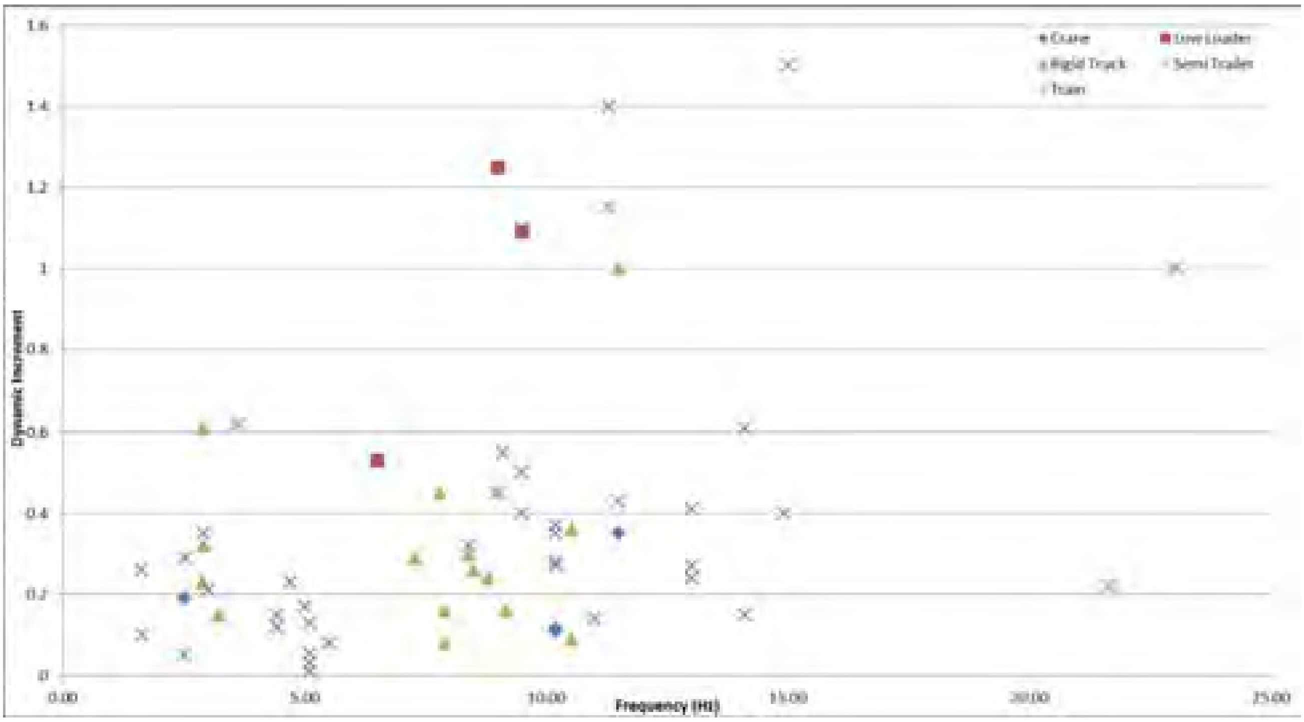

Figure D 6: Peak dynamic increment versus bridge natural frequency (suspension type)

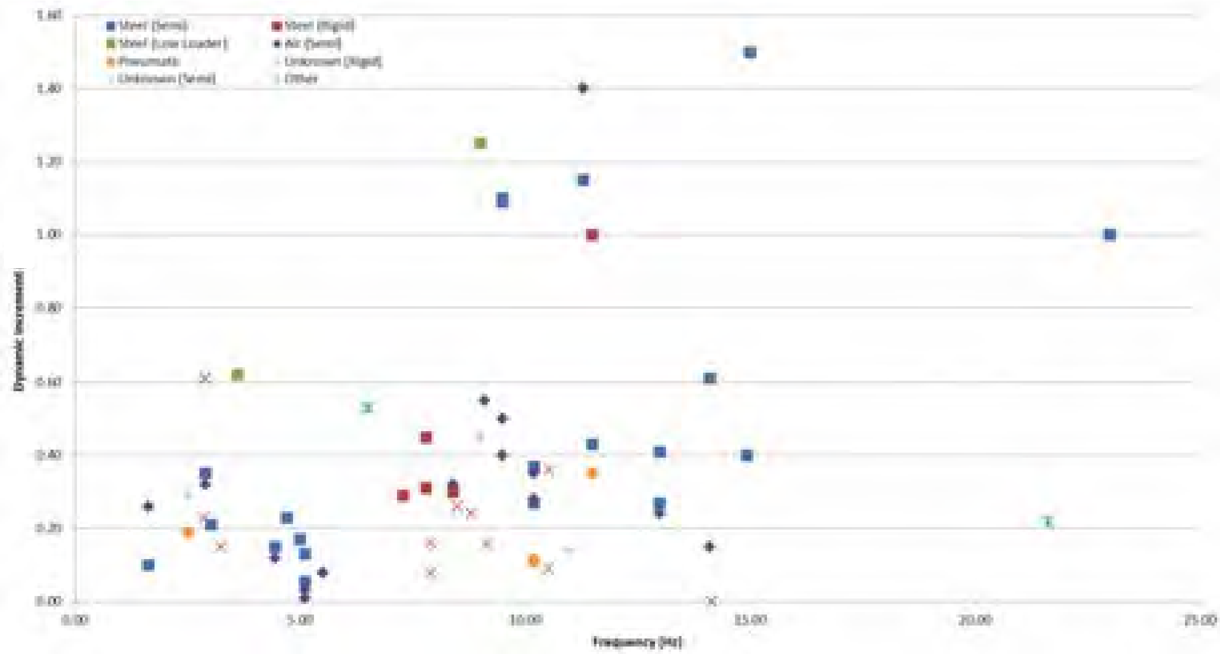

D.3.5 *Dynamic Increment vs Vehicle Speed*

A significant amount of information exists within the database regarding the dynamic responses of bridges to varying speed. Data has been represented graphically comparing the DI value with speeds ranging between 0 and 100 km/h (according to vehicle type, Figure D 7) and fundamental frequency (according to speed, Figure D 8). Significant data scatter is evident, with no obvious trend amongst vehicle types and speed. However a number of features observed in the data are discussed.

The following observations are made in relation to Figure D 7:

- Scatter in DI values increases with increasing speed for most vehicles, in particular semi-trailers.
- For semi-trailers, peak DI values tend to increase with increasing speed. Values appear to peak between 60 and 80 km/h. The DI peak of 1.4 at 40 km/h produced at Paroo River Bridge is likely to be erroneous and should not be considered.
- There is a small trend showing the greater likelihood of rigid vehicles producing a negative DI value for lower speeds (less than 60 km/h).
- For low-loader vehicle types, DI values are generally low (< 0.2) for speeds less than 60 km/h, but increase significantly with speed.
- For cranes, the majority of DI values remain consistently less than 0.2 (with the exception of one value of 0.35) regardless of speed with similar observations made for locomotives).

Figure D 7: Peak dynamic increment versus vehicle speed (vehicle type)

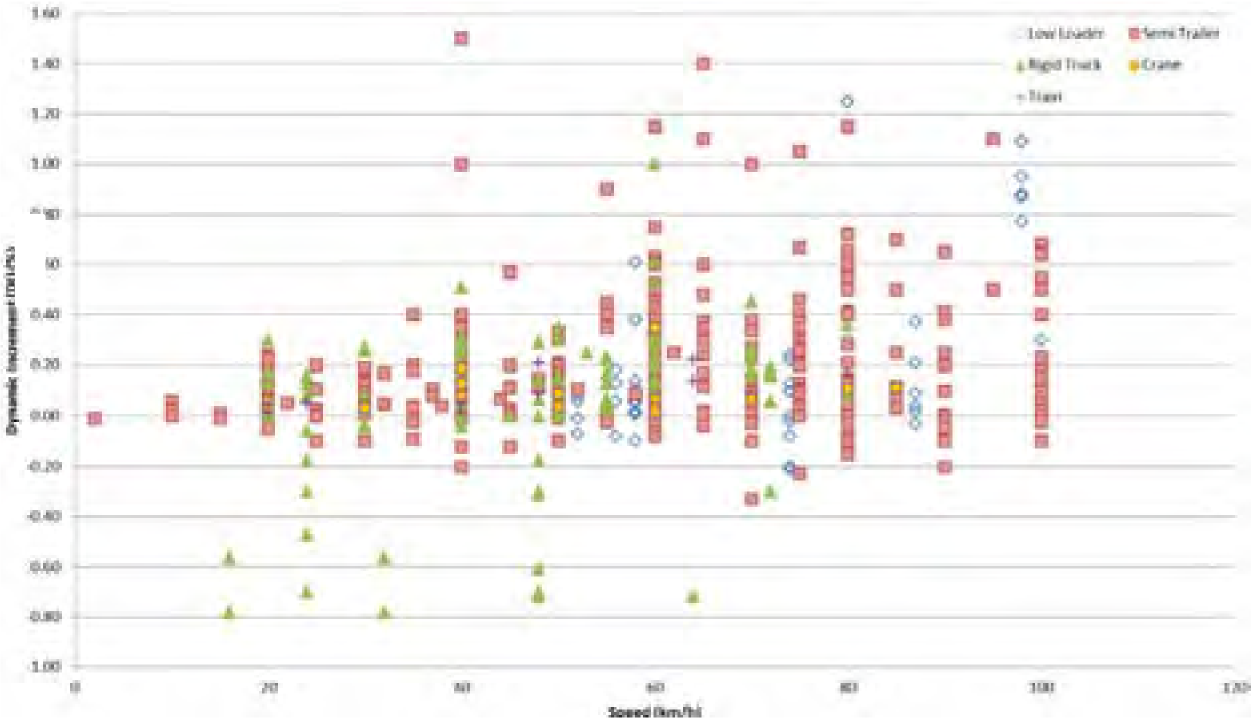

The following observations are made in relation to Figure D 8:

- DI values are generally low (less than 0.4) and produce less scatter at speeds less than 40 km/h.
- Significant scatter in DI values is observed where frequencies are approximately 8-15 Hz and 22 Hz for speeds greater than 40 km/h.
- Peak DI values appear to occur between 60 and 80 km/h.
- DI values significantly vary across all frequency ranges where speeds are greater than 80 km/h. DI values are more consistently high at high speeds where frequencies are between 8-15 Hz.

Figure D 8: Peak dynamic increment versus fundamental bridge frequency (speed increment)

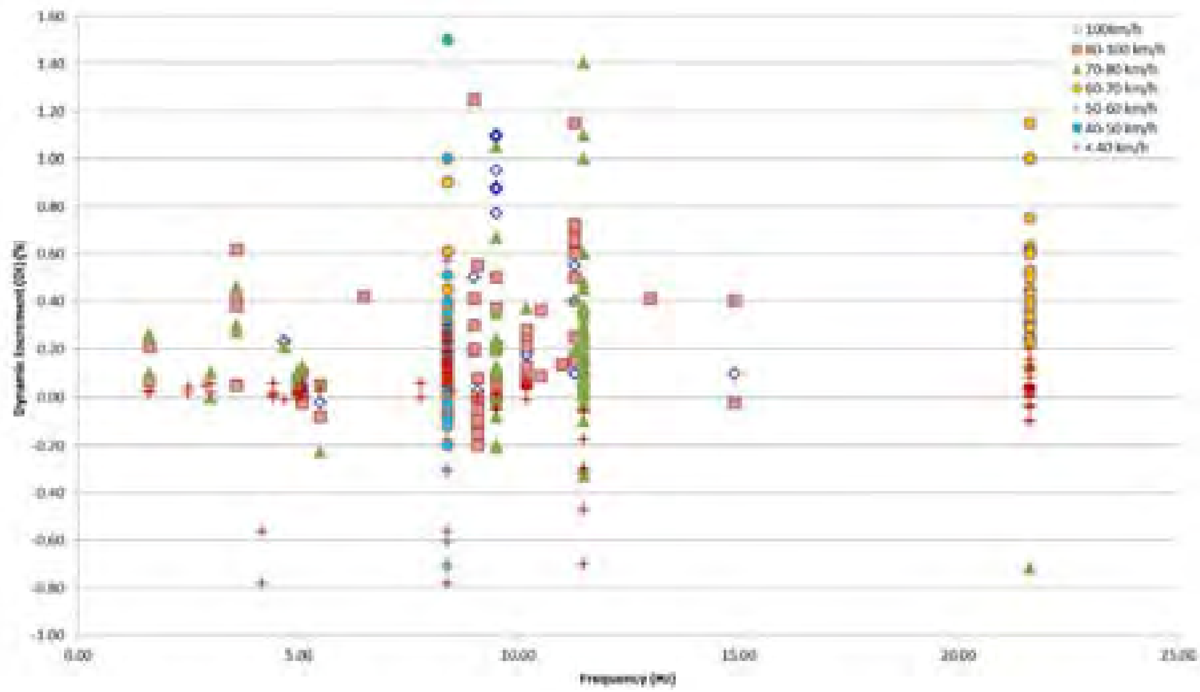

D.3.6 Dynamic Increment vs Vehicle Mass

Gross vehicle mass is known to influence the dynamic response of structures, with previous research showing dynamic effects tend to reduce with increasing mass (Heywood, 2000; Kim and Nowak, 1997). Vehicle loads were captured in the current database and are shown in Figure D 9 for DI vs gross vehicle mass (GVM). Data has been divided into mass and vehicle groups, distinguishing between different vehicle types such as low-loaders and cranes in comparison with articulated semi-trailers and rigid vehicles.

High dynamic responses were recorded for vehicles with GVM greater than 50 t, with DI values in excess of 1. Peak DI values were mostly less than 0.4 for vehicles with GVM between 45-50 t, with the exception of low loaders with all values greater than 0.4. Note the peak value for Cameron Creek Bridge (DI 1.4 at 11.3 Hz), which corresponds to a Higher Mass Limit (HML) air suspension semi-trailer. Minimal difference existed between the dynamic response for low loaders and semi-trailers/rigid vehicles in regard to dynamic response.

There is considerable scatter of data for DI values recorded for semi-trailer/rigid vehicles with GVM ranging between 30 and 45 t. Increasing DI values occur more regularly for semi-trailer/rigid vehicles with GVM between 40 and 45 t at frequencies between 8-15 Hz, suggesting an optimal load case. Low DI values (i.e. less than 0.4) exist for cranes regardless of load.

Individual axle group loads are also known to be influential on the dynamic structural response (Austroads 2003), which may not directly correspond to maximum vehicle mass. This data is captured in Figure D 10, showing peak DI values for maximum axle group load per vehicle for vehicle type (where this has been noted in the reports). As seen in Figure D 9, large axle group loads (greater than 30 t) produce a greater dynamic response. Large data scatter exists for semi-trailers and rigid vehicles with varying axle group loads. DI values tended to be less than 0.4 for semi-trailer/rigid vehicles with axle group loads between 20-30 t and 15-20 t where bridge frequencies were 5 Hz or less, whereas DI values increased from 8 Hz to 15 Hz. DI value for vehicles with low axle loads (< 15 t) typically resulted in DI values less than 0.6. Cranes again produced DI values less than 0.4 despite increased axle group loads.

Figure D 9: Peak dynamic increment versus fundamental bridge frequency (gross mass of vehicle (t))

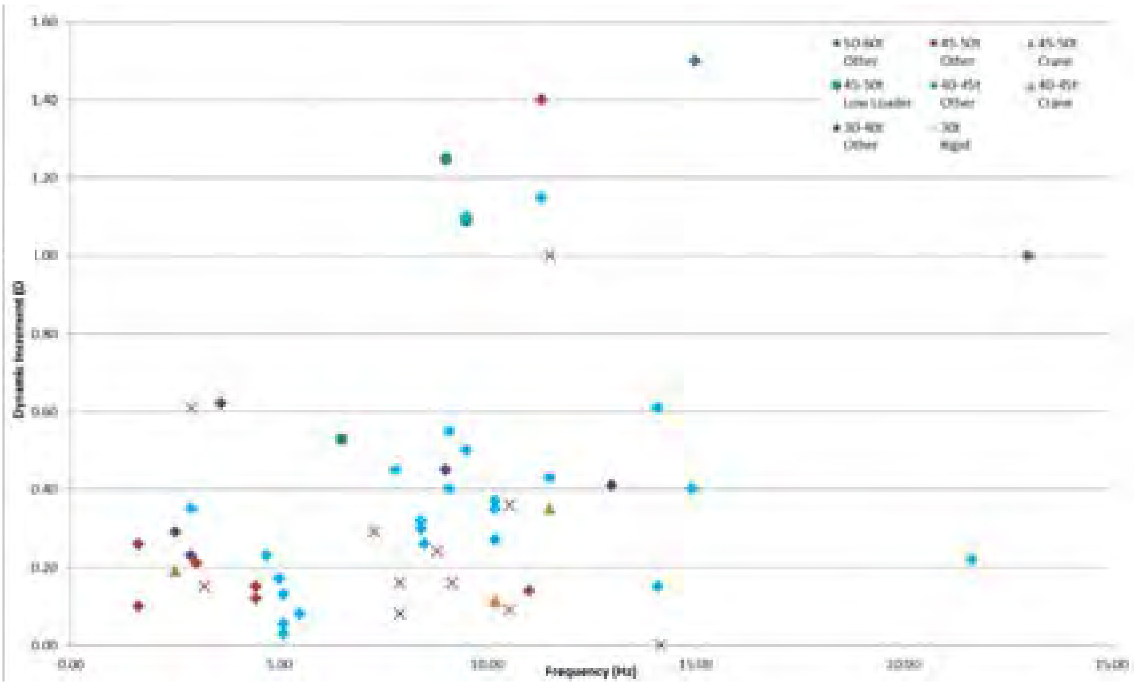

Figure D 10: Peak dynamic increment versus fundamental bridge frequency (maximum axle load (t))

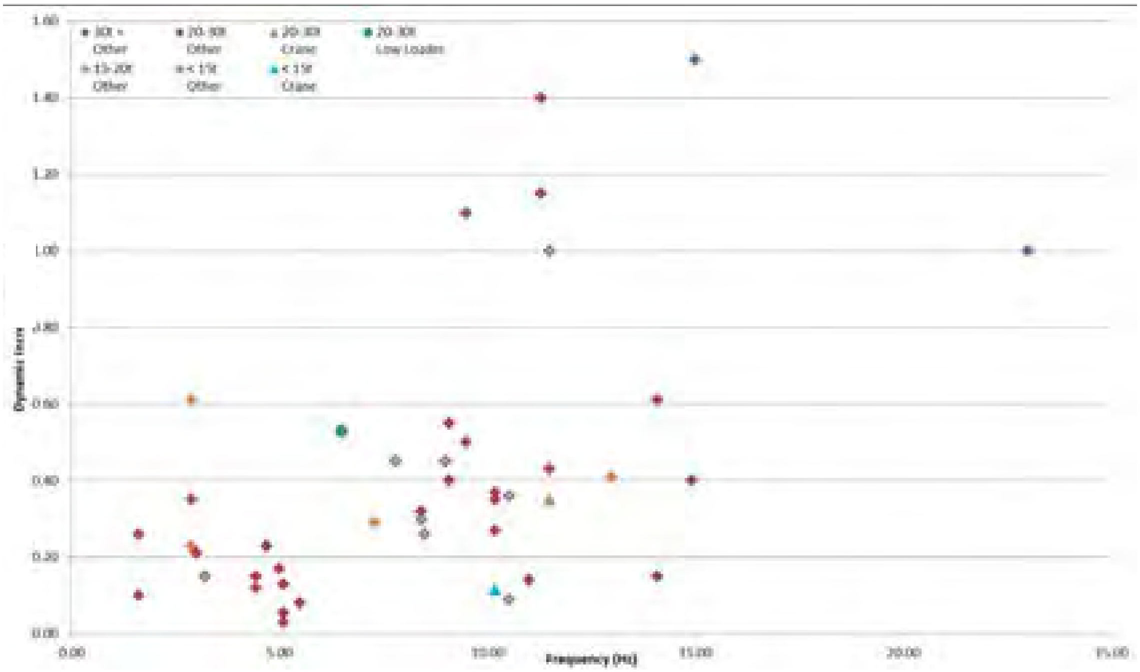

D.3.7 Dynamic Increment vs Road Profile

Several publications highlight the influential nature of the pavement condition on the dynamic effect of wheel loads on the supporting structure (Austroads, 2003; Cantieni et al., 2010; OECD, 1999). Therefore where descriptions on the condition of the road approaches were available, these were included in the review process and are shown in Figure D 11. Based on the current (limited) information, the trends are inconsistent with the current literature. At low frequencies, bridges with road approaches in good condition returned a low DI value (less than 0.3). Roads in poor condition returned more elevated DI values of between 0.5-0.6. However several outliers where road approaches were in average to good condition resulted in large dynamic responses, with DI values greater than 1. It should be noted that the use of axle hop planks (to induce maximum dynamic effect from vehicles on the bridge) did not feature in these results.

With the exception of minor inconsistencies noted in a small number of reports regarding actual road condition, there is an obvious need for further investigation in this area. The volume of evidence that supports the critical nature of the pavement surface condition suggests that the data reflected in this report requires more rigorous review before final conclusions are drawn. Reasons for the disparity in data may be due to the limited information presented in the reports regarding road condition and the lack of formal information regarding the profile over abutments, where the majority of maximum dynamic effects are produced in reality and may be responsible for the DI values observed. The influence of frequency matching between different vehicle types and bridge fundamental frequency may override these results, a factor which is evident in all data to date which falls in the frequency range between 8-15 Hz.

Figure D 11: Peak dynamic increment versus fundamental bridge frequency (road profile)

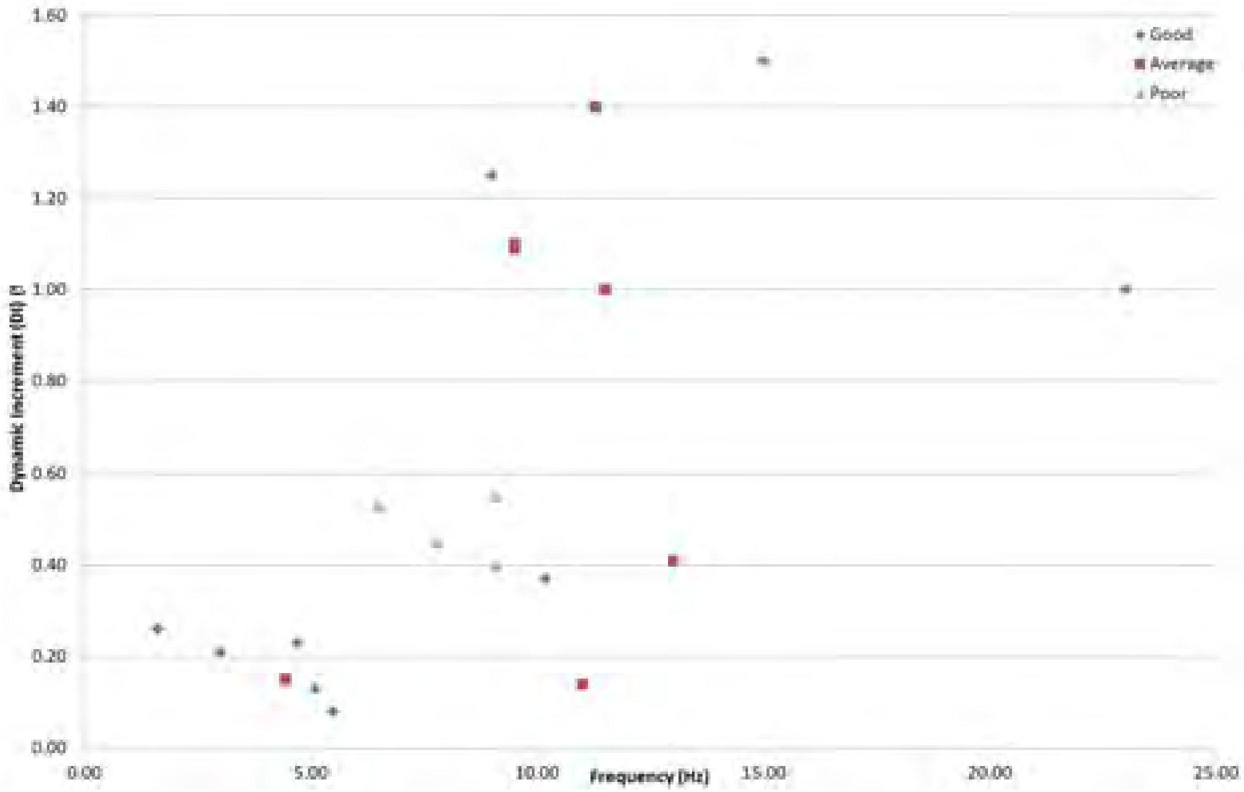

D.4 Discussion

D.4.1 Summary of General Trends

A wide scatter of dynamic data exists across various bridge fundamental frequencies. Whilst there are no clear trends in the data, a number of observations can be made based on the current data set:

- A significant number of structures did not subscribe to the 0.4 DLA limit currently specified in TMR literature.
- Amplification of DI values (indicating frequency matching between test bridges and vehicles) is evident at vehicle axle-hop frequencies (8-15 Hz) and, to a lesser degree, at body-bounce frequencies (1.5-3 Hz).

- Cranes produce DI values less than 0.4, regardless of weight (up to 48 t) and speed.
- Vehicles with steel suspension are more likely to result in elevated DI values where frequency matching occurs.
- Vehicles with air suspension are more likely to result in lower DI values (less than 0.4), unless frequency matching occurs between 8-12 Hz.
- DI values are typically less than 0.4 where speeds are less than 40 km/h.
- Dynamic responses are more likely to peak at speeds between 60-80 km/h.
- Timber structures and materials generally yield greater dynamic responses.
- Deck unit structures yield lower dynamic responses.
- Steel and concrete structures typically yielded peak DI values less than 0.5.
- The largest gross vehicle mass yielded the highest DI value, but similarly large DI values were also produced at masses between 30-50 t. There is no immediate evidence to suggest that larger masses induce lower dynamic responses.
- Anecdotal evidence suggests that road profiles are influential on the magnitude of DI, however further data interrogation is required.
- There is a lack of information relating to the dynamic effects of road trains.

Comment also is required on the derivation of the dynamic increment value. Whilst the majority of the reports have derived DI based on Equation 4, the specific input of peak dynamic and static was found to be relatively subjective. Methodologies range from the use of averaged or ultimate maximum peak DI values per span or per group of girders to peak values. The implementation of static values ranged from global to individual maximums achieved by the bridge during testing. There is also the inconsistency of deriving DI values from strain or deflection peaks, of which the latter has previously been found to be less accurate and yet this seems to be the most common method.

The method of calculation (based on Equation 4) should also be queried. The current method has been recommended by Bakht and Pinjarkar (1989) after conducting a review of various methods. Significant DI values have been recorded previously, however such values can be achieved despite very low or insignificant strains or deflections being achieved. This overestimation can change the resulting outcome considerably, potentially leading to excessive or unnecessary structural or economic recommendations. The calculation of negative DI values provides further evidence that a revision of these methodologies is needed.

The current results also highlight the inconsistencies between the current DLA recommendations in AS 5100 and TMR standards. Figure D 12 shows the combined results of the current review, Heywood (2000) and Swiss findings from Cantieni. The solid line identifies the limits currently adopted by Swiss authorities. Whilst there is a trend in the current data to follow the Swiss model at low frequencies, there are obvious deficiencies for structures between 8-15 Hz. This requires further investigation and additional data to support these initial findings.

Figure D 12: Combined dynamic increment versus fundamental bridge frequency (current results + Heywood + Cantieni from the DIVINE project)

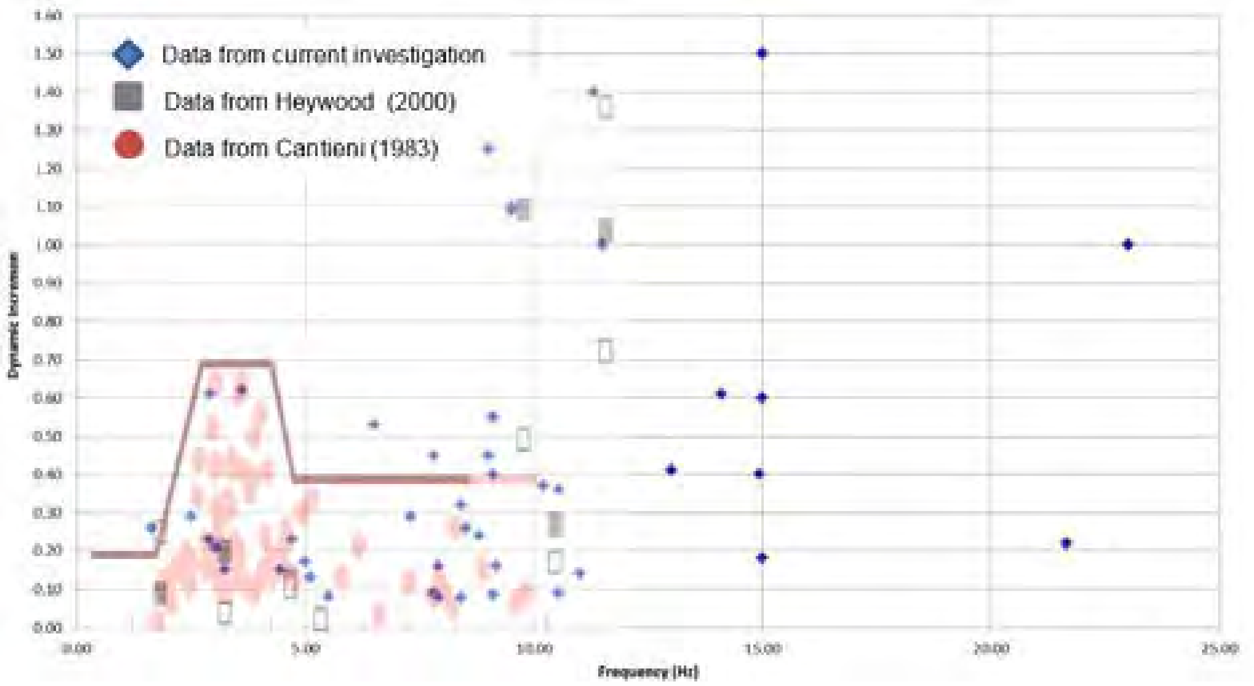

D.5 Future Improvements

To improve or further validate the findings in this report, the following recommendations for further research are suggested:

- More data from other jurisdictions (nationally and internationally) are required to improve the statistical base of data. This would include obtaining raw data from sources such as Cantieni and Heywood in relation to previous work conducted for the DIVINE Element 6 project.
- A more detailed review into the accuracy and relevance of the current DLA limits is required.
- A review into the relevance of the current method for calculating dynamic increment is required.
- More research is required regarding the influence of axle-hop, body bounce, frequency matching, and vehicle suspension types on the dynamic effects induced in bridges.
- More data is to be obtained regarding the dynamic influence of road trains.
- Additional information regarding pavement condition over abutments is required to be included in the database.
  - Further verification is required regarding the influence of pavement condition on dynamic amplification.